CHARACTERISATION OF GENETIC AND EPIGENETIC ABERRATIONS IN PAEDIATRIC HIGH GRADE GLIOMA

PRASANNA CHANNATHODIYIL, MSc

A thesis submitted in fulfilment of the requirements of the University of Wolverhampton for the degree of Doctor of Philosophy

Brain Tumour Research Centre
Research Institute in Healthcare Sciences
Faculty of Science and Engineering
University of Wolverhampton

April 2016

DECLARATION

This work or any part thereof has not previously been presented in any form to the University or to any other body whether for the purposes of assessment, publication or for any other purpose (unless otherwise stated). Save for any express acknowledgments, reference and/or bibliographies cited in the work, I can confirm that the intellectual content of the work is the result of my own efforts and no other person.

The right of Prasanna Channathodiyil to be identified as an author of this work is asserted in accordance with ss.77 and 78 of the Copyright, Designs and Patents Act 1988. At this date copyright is owned by the author.

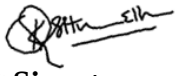

Signature

Date: 18th April 2016

ACKNOWLEDGEMENTS

I would like to express my deepest gratitude to my supervisor, Prof. Tracy Warr for offering me this opportunity to pursue my PhD degree. Her tremendous support and guidance has the major role in the successful completion of this project and the writing of this thesis. Working with her has been an amazing experience.

I am immensely grateful to my co-supervisor, Dr. Mark Morris for his valuable suggestions and constant encouragement that have always been truly inspiring. Learning with him was so much fun and I wholeheartedly thank him for being so kind and friendly. I have deep appreciation for Prof. John Darling for his vital suggestions and valuable support.

My sincere gratitude goes to Prof. Weiguang Wang for providing me an opportunity to work with him during my MSc project that I believe has contributed to a great extent in securing a PhD degree at this University. I owe you a lot, thank you! I am grateful to Dr. Angel Armesilla for his encouragement and friendly conversations. Thanks to Dr. Sarah Brown, Dr.Sarah Jones, Dr.John Howl and Dr.Ian Nicholl for their help and support.

I would like to thank the members of my research group, Dr. Katherine Karakoula, Dr. Farzana Rowther, Dr. Hoda Kardooni, Dr. Anushree Singh and Lawrence Eagles, and colleagues at the University, Dr. Rajendra Pangeni, Sheela Pokherel, Dr. Shawna Bolton, Dr. Raji Kilari, Dr. Peng Liu and Dr. Patricia Tawari for their help and encouragement over the last few years. PhD at the University of Wolverhampton has become an unforgettable experience.

I am thankful to the lab manager, Dr. Angie Williams, and the laboratory technicians, Keith Holding, Henrik Townsend, Balbir Bains, Andy Brook and Clare Murcott for the technical support. I truly appreciate Ramanjit Kaur for her impeccable efforts in taking care of all the research administration works.

I am grateful to The Brain tumour charity and The Ethan Perkins Trust (UK) for funding this project. I also extend my thanks to the collaborators in this project at

Imperial College, London and at Nottingham University. Special thanks to Dr. Nelofer Syed for providing antibodies and drugs.

I am grateful to all my friends outside the University, for their love and encouragement. Special mention goes to Sathishkumar Kurusamy, Karthik Kannappan, Priya Kannappan, Ram Kumar, Saravanan Nagarajan, Kalai Vanan, Neelakandan Bhojan, Manikandan, Jisha, Uma Maheswari, Jithendran Sasidharan, Ranjith Paulson, Jon Yarsley, Julian Hobson, Toye Anifalaje, Bunmi Anifalaje, Dr.Jayan, Dr.Reji, Dr.George Alapatt and my friends from the organisation, Tamil People in UK.

On a personal note, I would love to thank my parents, Mrs. Dakshayani Kizhakkekkara and Mr. Vasudevan Channathodiyil who are always ready to go that extra mile to see the smile on my face. I am grateful to my siblings, Pradeep and Priya for being their constant source of love and support. Thanks to Anu chechy and Renju ettan for their encouragement. Most importantly, I thank Vinu for his love and support over the last 12 years. This wouldn't have been possible without your help. Thank you!

DEDICATION

To my parents...

"The most beautiful thing we can experience is the mysterious. It is the source of all true art and science."

– Albert Einstein

ABSTRACT

Paediatric high grade glioma (HGG), including diffuse intrinsic pontine glioma (DIPG) are highly aggressive tumours with no effective cures. Lack of understanding of the molecular biology of these tumours, in part due to lack of well-characterised pre-clinical models, is a great challenge in the development of novel therapies. Analysis of paired cell culture/biopsy samples in this study revealed that paediatric HGG short-term cell cultures retain many of the tumour characteristics *in vivo*. Using a genome-wide approach, copy number, gene and miRNA expression, and methylation changes were characterised in 17 paediatric HGG-derived short-term cell cultures including 3 from DIPG. The majority of the genomic changes were unique from those arising in adult HGG. Approximately 65% (11/17) of paediatric HGG short-term cell cultures had balanced genetic profiles resembling normal karyotypes. The most frequent copy number gain and loss were detected at 14q11.2 (~94%) and 8p11.23-p11.22 (~59%), respectively. *H3F3A* (K27M) mutation was present in 2/17 (~12%) cases and concurrent loss of *CDKN2A* and *BRAFV600E* in 1/17 (~6%) case. Genes involved in reelin/PI3K signaling (*DAB1*), RTK signaling (*PTPRE*), and arginine biosynthesis (*ASS1* and *ASL*) were frequently deregulated by methylation in these tumours. The anti-growth and anti-migratory properties of *DAB1* and *PTPRE* were demonstrated *in vitro.* Preliminary investigations validated the therapeutic potential of ADI-PEG20 (arginine depletion), and PI-103 (PI3K/mTOR inhibition) in a subset of paediatric HGG short-term cell cultures. This study has identified novel genetic and epigenetic changes in paediatric HGG that may, following further validation, be translated into potential biomarkers and/or therapeutic targets.

TABLE OF CONTENTS

Chapter 8

LIST OF TABLES

LIST OF FIGURES

ABBREVIATIONS

5-AZA	5’-AZA-2’-deoxycytidine
5mC	5-methylcytosine
aCGH	Array comparitive genomic hybridisation
ACVR1	Activin receptor type I
ADC	Arginine decarboxylase
ADI	Arginine deiminase
AGO	Argonaute protein
AID	Activation-induced cytidinedeaminase
ALL	Acute lymphoblastic leukemia
ALT	Alternative lengthening of telomeres
AML	Acute myeloid leukemia
ANOVA	Analysis of variance
APOBEC1	Apolipoprotein B mrna-editing enzyme 1
ASNS	Asparagine synthetase
ATCC	American type culture collection
ATRX	A-thalassemia/mental retardation syndrome protein
BBB	Blood/brain barrier
B-CLL	B cell chronic lymphocytic leukemia
BMP	Bone morphogenetic protein
CBS	Circular binary segmentation
CBTRUS	Central brain tumour registry of the United States

CCG	Children’s cancer group
CCNU	Chloroethyl-cyclohexylnitrosourea
CDS	Coding sequences
CFS	Common fragile site
CGI	Cpg islands
CNA	Copy number alteration
CNS	Central nervous system
CNV	Copy number variation
CoBRA	Combined bisulfite restriction analysis
CpG	Cytosine-guanosinedinucleotides
CRINET	Cribriform neuroepithelial tumours
DAXX	Death domain associated protein
DGCR8	Digeorge syndrome critical region 8
DIPG	Diffuse intrinsic pontine glioma
DLRS	Derivative log ratio spread
DMEM	Dulbecco’s modified Eagle medium
DMSO	Dimethyl sulfoxide
DNA	Deoxyribonucleic acid
DNMT	DNA methyltransferases
DTT	Dithiothreitol
ECM	Extracellular Matrix
EDTA	Ethylenediaminetetraacetic acid
EFS	Event free survival

EGFR	Epidermal growth factor receptor
eIF5A-2	Eukaryotic translation initiation factor 5A-2
EMT	Epithelial-mesenchymal transition
ER	Estrogen receptor
ERAD	Endoplasmic reticulum-associated protein degradation
ERK	Extracellular signal regulating kinase
ESCC	Esophageal squamous cell carcinoma
FCS	Foetal calf serum
FDR	False discovery rate
FFPE	Formalin-fixed paraffin embedded
FOP	Fibrodysplasia ossificans progressive
GBM	Glioblastoma multiforme
GISTIC	Genomic identification of significant targets in cancer
GO	Gene ontology
HBSS	Hanks' buffered salt solution
HCC	Hepatocellular carcinoma
HDACs	Histone deacetylases
HEPES	4-(2-hydroxyethyl)-1-piperazineethanesulfonic acid)
HGG	High grade glioma
Hh	Hedgehog
HK2	Hexokinase 2
hNPCs	Human neural progenitor cells
ICGC	International cancer genome consortium

IDH1	Isocitrate dehydrogenase 1
INO80	Inositol requiring 80
ISWI	Imitation SWI
KEGG	Kyoto encyclopedia of genes and genomes
LINE	Long interspersed nuclear element
MGMT	O6-methylguanine-DNA-methyltransferase
miRNA	Microrna
mRNA	Messenger ribonucleic acid
MSP	Methylation specific PCR
MTT	3-(4,5-dimethylthiazol-2-yl)-2,5-diphenyl-2H-tetrazolium bromide
NCBI	National Centre for Biotechnology Information
NF-kB	Nuclear factor kappa b
NHA	Normal human astrocytes
NTRK	Neurotrophic tyrosine receptor kinase
NuRD	Nucleosome remodelling and deacetylation
OCT	Ornithine carbamyltransferase
OD	Optical density
ORF	Open reading frame
OSCC	Oropharyngeal squamous cell carcinoma
PBS	Phosphate buffered saline
PCA	Principal component analysis
PCGP	Paediatric cancer genome project
PCNA	Proliferating cell nuclear antigen

PCR	Polymerase chain reaction
PDGFRA	Platelet-derived growth factor receptor α
PI3K	Phosphoinositide 3-kinase
PIP2	Phosphatidylinositol-4,5-diphosphate
PIP3	Phosphatidylinositol-3,4,5 -triphosphate
PRC2	Polycomb repressive complex 2
PVD	Polyvinylidene difluoride
QC	Quality control
Q-PCR	Quantitative reverse transcription PCR
RCC	Renal cell carcinoma
RISC	RNA-induced silencing complex
RNA	Ribonucleic acid
RT	Radiotherapy
RT-PCR	Reverse transcription PCR
SAM	S-adenosylmethionine
SFK	Src family of kinases
siRNA	Small interfering RNA
siRNA	Small interfering RNA
Smo	Smoothened
SRB	Sulforhodamine
STAC	Significance testing for aberrant copy number
S-TRAIL	Secretable tumour necrosis factor apoptosis-inducing ligand
SW1/SNF	Switching defective/sucrose non-fermenting

TCGA	The cancer genome atlas
TET	Ten-eleven translocation
TF	Transcription factor
TIC	Tumour initiating cells
TIF	Tagged image file
TMZ	Temozolomide
TSS	Transcription start site
T-UCRs	Transcribed ultra conserved regions
UTR	Untranslated region
WHO	World health organisation

CHAPTER 1

Introduction

1.1 Cancer

1.1.1 Incidence and overview

Cancer has emerged as a major health issue affecting people all over the world irrespective of their age, gender and socioeconomic background and accounts for one in seven deaths worldwide (Siegel et al., 2015). As per the GLOBOCAN database, the global cancer incidence and mortality rates in 2012 were estimated at 14.1 and 8.2 million cases respectively (Ferlay et al., 2014). With almost no immediate likelihood for effective control, annual cancer-related deaths are projected to hit nearly 13 million as early as 2030 (American Cancer Society, 2015).

Cancer is a heterogeneous group of diseases, characterised by cells with unchecked proliferative potential that can originate in almost any part of the body, and often undergo metastatic spread to distant parts (Stratton et al., 2009). The malignant transformation of a cell is a multi-step process during which it acquires several properties capacitating it to grow and divide uncontrollably. These malignant traits, described by Hanahan and Weinberg as 'hallmarks of cancer' include the ability of cells to resist programmed cell death (apoptosis), override growth inhibitory signals, replicate limitlessly, proliferate uncontrollably, form new blood vessels (angiogenesis), reprogram metabolic machinery to meet the energy requirements of the growing tumour, evade destruction by the host immune cells, invade the surrounding tissues and metastasise to other organs in the body (Hanahan and Weinberg, 2011). In line with Darwinian principles, populations of cells that stably acquire and retain these oncogenic traits throughout several generations possess

growth superiority over normal cells in the local tissue environment and are selected for clonal expansion (Greaves and Maley, 2012).

1.1.2 Cancer as a disease of the genome

Cancer has long been understood to develop as a consequence of genomic disruptions such as mutations, copy number changes, deletions, insertions and non-homologous recombination (Hanahan and Weinberg, 2011). The first evidence of genetic mutation in a cancer-related gene emerged from the identification of G>T amino acid substitution (glycine to valine) in codon 12 of *HRAS* (Reddy et al., 1982). Since then, several sequencing efforts including the large scale project initiated by the International Cancer Genome Consortium (ICGC) have enabled the identification of a vast array of mutations in key genes in more than 50 different cancer types (International network of cancer genome projects, 2010). Most of these mutations are considered as 'passengers' while only few of them, called 'drivers', actually contribute to oncogenic progression. Cancer cells often acquire DNA-repair defects resulting in an increase in mutation rate (Puente et al., 2011; Grasso et al., 2012). Research in the past decade has underscored the significance of additional and/or complementary mechanisms of gene silencing which do not involve changes to the primary DNA sequence. These changes, such as DNA methylation and post translational histone modifications, collectively called 'epigenetic' changes are stable and heritable and suitable for the persistent acquisition of malignant traits during the evolutionary process (Baylin and Jones, 2011).

Recently, studies have revealed that genetic and epigenetic changes work in cooperation with each other to cause stable phenotypic changes (You and Jones,

2012; Timp and Feinberg, 2013). For example, mutations in epigenetic regulators have been identified in renal cell carcinoma (RCC), rhabdoid tumours, bladder cancer, hepatocellular carcinoma (HCC), and adult and paediatric brain tumours (Versteege et al., 1998; Gui et al., 2011; Varela et al., 2011; Fujimoto et al., 2012; Sturm et al., 2012; Wu et al., 2012). Similarly, epigenetic inactivation has been reported in DNA repair genes like *MLH1*, *BRCA1, MGMT* and *WRN* (Herman et al., 1998; Esteller et al, 2000; Hedenfalk et al., 2001; Agrelo et al., 2006) elevating mutation rates and contributing to genomic instability. Thus it is becoming increasingly apparent that cancer is a manifestation of both genetic and epigenetic changes in the cells.

1.2 Brain tumours

The annual age-adjusted worldwide incidence of primary brain and CNS tumours is 3.4 per 100,000 people with a mortality rate of more than two-thirds (2.5 per 100,000 people per year) (Central Brain Tumour Registry of the United States (CBTRUS), (www.cbtrus.org/factsheet/factsheet.html). The world annual incidence of brain and CNS tumours in children is lower than in adults with a rate of 1.1 per 100,000 people per year (Ostrom et al., 2015). However, brain and central nervous system (CNS) tumours are the second most frequent malignancy in children, just after leukaemia (CRUK). These tumours account for 24.5% of all tumours in those 0–14 years of age and 8.9% in those 15–24 years of age. Moreover, CNS tumours are the most common cause of cancer-related deaths in both the 0-14 year and the 15-24 year age groups.

1.3 Paediatric glioma

Glioma represent a heterogeneous group of neuroepithelial tumours originating from mature glial cells or their less differentiated precursor cells in the CNS and are the most common type of CNS tumours across all age groups (Louis et al., 2007). Glioma in children share histopathological features with those in adults and can be categorised into various sub types based on the World Health Organisation (WHO) classification system (Louis et al., 2007). Based on their presumed cells of origin, the major sub types of glioma include astrocytoma, oligodendroglioma and oligoastrocytoma (Louis et al., 2007).

1.3.1 Major clinical subgroups of paediatric glioma

The majority of glioma arising in children are astrocytomas, which can be further classified into two broad clinical categories called 'low grade' (Grades I and II) and 'high grade' (Grades III and IV) on the basis of a set of defined histological characteristics such as cellularity, mitotic activity, nuclear atypia and microvascular proliferation (Louis et al., 2007). The assessment of histopathological identities of tumour tissues and the assignment of malignancy grades have been historically incorporated into routine diagnosis of glioma to estimate the degree of their malignant behaviour and to predict clinical outcomes.

1.3.1.1 Low grade glioma (LGG)

LGG are the most prevalent CNS tumour in children (30-50%). These tumours are generally less aggressive and show considerable response to therapy with a 5-year

survival rate of 85%. The two most common histologies include pilocytic astrocytoma (PA) (WHO Grade I) and diffuse astrocytoma (WHO Grade II) (Sievert and Fisher, 2009).

Pilocytic astrocytomas (PA)

PA are the most prevalent glial neoplasm of childhood occurring predominantly within the cerebellum and less frequently in the optic tract, the hypothalamus and the brain stem (Penman et al., 2015). These are benign tumours with slow growth and often show good response to surgical resection (Sievert and Fisher, 2009). They appear relatively well-circumscribed, usually with a cystic component within and around the tumour tissue (Collins et al., 2015). Typical histopathological features of these tumours include low to moderate cellularity with densely fibrillated regions that are enriched with Rosenthal fibres consisting of long bipolar processes, as well as with loosely textured areas consisting of multipolar cells (Collins et al., 2015). The presence of microcysts and eosinophilic granules are common. Mitotic figures are rarely encountered.

Diffuse astrocytoma

Unlike PA, diffuse astrocytoma are less prevalent in children and occur largely in the supratentorial compartment, deep midline structures and the cervicomedullary region (Sievert and Fisher, 2009). These tumours are characterised by their ability to diffusely infiltrate normal structures of the brain, a property that limits the complete resection of these tumours contributing to worse outcomes than PA (Fisher et al.,

2008). They exhibit moderate cellularity with limited or no mitoses. Vascular proliferation and necrosis are mostly absent (Louis et al., 2007).

1.3.1.2 High grade glioma (HGG)

Unlike malignant glioma in adults, HGG in children rarely progress from LGG; the low-grade to high grade transformation in children and adults occur at a rate of 7% and 50% respectively. HGG in children include anaplastic astrocytoma (Grade III), Glioblastoma multiforme (GBM) (Grade IV) and DIPG (Grade III and IV) (Louis et al., 2007).

Anaplastic astrocytoma

Anaplastic astrocytoma show higher cellularity than the low grade tumours with more evident nuclear pleomorphism and higher number of mitotic figures. They are diffusely infiltrative lesions presented with cytological and nuclear atypia (Louis et al, 2007). Necrosis and microvascular proliferation is usually absent (Collins, 2014).

Glioblastoma multiforme (GBM)

Morphologically, GBM cells are polygonal to spindle-shaped presented with features such as acidophilic cytoplasm, oval or elongated nuclei with irregular nuclear membrane, and hyperchromatic chromatin (Schultz et al., 2005). These cells have increased nuclear to cytoplasmic ratio and also show moderate nuclear polymorphism. Necrotic foci are one of the most distinguishing features of GBM; areas of necrosis may be large, focused toward the central area of the tumour, or small, surrounded by pseudopalisading areas (Kleihues and Sobin, 2000). They also

possess high cellularity and high mitotic activity with florid patterns of microvascular proliferation.

Diffuse intrinsic pontine glioma (DIPG)

DIPG originate in the brainstem and are the leading cause of brain tumour-related deaths in children (Jansen et al, 2012; Broniscer et al, 2013; Buczkowicz and Hawkins, 2015). These tumours are highly diffuse in nature and infiltrate the normal neural structures of the pons, often extending to neighbouring parts of the brain; one-third of DIPGs show leptomeningeal dissemination and subventricular spread (Sethi et al., 2010; Caretti et al., 2014). These tumours present with intra-tumour histologic heterogeneity with features of Grade II or III occurring in a Grade IV specimen (Figure 1.1) (Buczkowicz et al., 2014). Thus diagnoses of DIPG based on biopsy are highly challenging owing to the presence of histopathological differences within the tumour specimens.

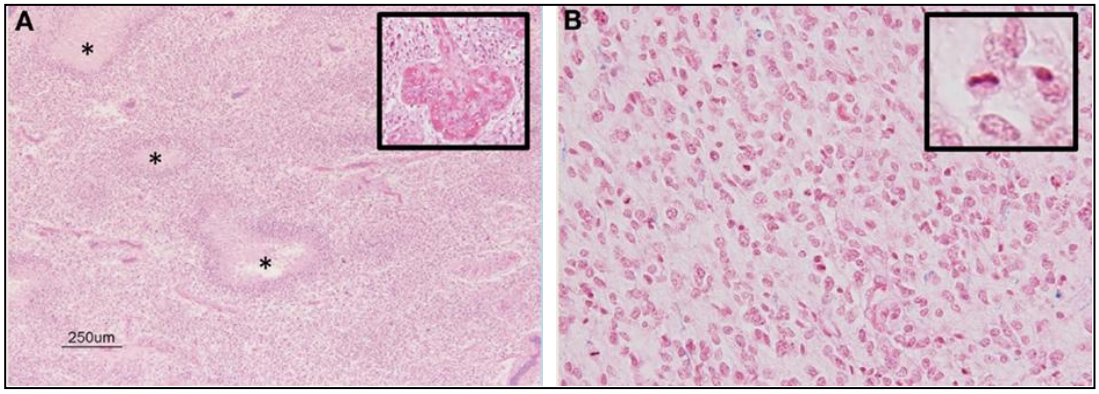

Figure 1.1 Histopathology of DIPG. A. DIPG with features of Grade IV GBM with pseudopalisading necrosis (*) and microvascular proliferation (inset). **B.** Section of DIPG with features of Grade III such as cellularity, nuclear atypia, pleomorphism and mitotic activity (inset) (Buczkowicz et al., 2014).

1.4 Epidemiology and aetiology of paediatric HGG

Although HGG are common in adults, they are a rare occurrence in children accounting for approximately 8-12% of all CNS neoplasms in this population (Bondy et al., 2008; Fangusaro, 2012). Childhood HGG are predominantly located within the supratentorium, with around 30-50% of these diagnosed in the cerebrum and the remaining mainly within the thalamus, hypothalamus, third ventricle, and basal ganglia (Wolff et al, 2004). Approximately 10% of paediatric HGG are located within the brainstem with majority of the cases diagnosed in children aged 6-8 years (Jones et al, 2012). Infratentorial glioma that are located within regions outside the brainstem are relatively rare in children with the ones within the cerebellum accounting only about 5% of all paediatric HGG (Karremann et al., 2013). Despite differences in the prevalence and preferential locations in the brain, childhood and adult HGG share similar clinical aggressiveness and contribute to significant amount of mortality among patients with brain tumours (Jones et al., 2012).

The causes of paediatric CNS tumours, including HGG are not fully understood. However, several factors have been identified that could increase the susceptibility to tumour development in children. The contributions of rare genetic conditions have been identified to be associated with 10% of HGG development. The most common amongst them is Neurofibromatosis type 1, a condition in which the lack of neurofibromin and the consequent loss of Ras regulation results from germline mutations in *NF-1* (Ward and Gutmann, 2005; Rosenfeld et al., 2009). In addition, Li-Fraumeni syndrome, resulting from mutations in the *TP53* gene (Lane, 1992), has also been documented as a risk factor for HGG transformation in children; altered

p53 levels lead to loss of control of cell proliferation escalating the chance of malignant transformation (Varley, 2003; Melean et al., 2004). A well-established factor associated with HGG is a previous exposure to ionizing radiation during treatment of other malignancies, such as the most frequent cancer type in children, acute lymphoblastic leukemia.

1.5 Current therapy for paediatric HGG

The existing standard therapeutic regimen for high grade glioma in children involves a combination of surgery, focal radiotherapy and chemotherapy. However, there has been no notable improvement in the survival of children with HGG; the 2-year survival rates for supratentorial HGG remains <30% and for DIPG is <10% (MacDonald et al., 2011; Jones and Baker, 2014).

1.5.1 Surgery

The extent of maximal safe resection is considered the most valuable prognostic factor in children with high grade glioma (Bucci et al., 2004; Qaddoumi et al., 2009). In the Children's Cancer Group (CCG)-945 trial on HGG patients (172 children of age 18 months to 21 years) randomised to surgery, radiation and chemotherapy, the patients who underwent >90% resection had better survival rates (both progression free and overall survival) compared to those who did not (Finlay et al., 1995). Based on this, the initial choice of treatment for a child with newly diagnosed HGG involves maximal surgical excision of the tumour mass without damaging normal brain structures which helps to ease intracranial pressures and improve the symptoms. Surgery also provides biopsy material for further tumour analysis and

disease follow-up. However, the choice of surgery is mainly dependent on the location of the tumour and the degree of involvement of normal brain. Resection is impractical for the treatment of DIPG owing to its diffuse and infiltrative pattern of growth involving normal neural structures of the brainstem (Vanan and Eisenstat, 2015).

1.5.2 Radiotherapy

Radiotherapy (RT) plays critical roles in the management of HGG as adjuvant therapy to surgery. As malignant glioma often has an irregular border and involves infiltration of normal brain, absolute excision of the tumour is not achievable. Focal RT around the tumour bed is the routine practice in order to achieve maximal eradication of the residual tumour cells and target local recurrence of the tumour. The standard radiation dose for children with newly diagnosed HGG ranges from 50-60 Gy administered in daily fractions of about 180-200 cGy over a course of 6 weeks. As a standalone approach, RT is the gold standard of treatment for inoperable brain tumours and plays vital roles in the treatment of DIPG. Despite several advancements in RT, the potential toxic effects of X-rays on the developing brain restrict its use among children below 3 years of age (Dufour et al., 2006; Sanders et al., 2007). In older children, RT has been associated undesirable late effects such as cognitive delay, restrictive lung disease leading to respiratory failure or increased susceptibility to secondary neoplasms (Jakacki et al., 1995; Neglia et al., 2006).

1.5.3 Chemotherapy

The first and the only substantial evidence in support of chemotherapy emerged from the CCG-943 trial in which the patients who received combination chemotherapy with prednisone, chloroethyl-cyclohexylnitrosourea (CCNU or lomustine), and vincristine (PCV regimen) in addition to post-operative RT reported better 5-year EFS (46% over 18%) than those who were treated with RT only (Sposto et al., 1989). Subsequent studies which investigated the efficacy of intensive chemotherapy including the CCG-945 trial failed to establish convincing roles for chemotherapy in providing survival advantage for children with HGG (Wolff et al., 2010). Although there is not enough evidence for the benefits of chemotherapy in the treatment of paediatric HGG, it is widely accepted as adjuvant and/or concomitant therapy in conjunction with surgery and RT for both newly diagnosed and recurrent HGG in this patient group.

The improved survival rates in adult GBM after the addition of temozolomide (TMZ) to radiotherapy led to the initiation of similar trials in the paediatric population (Stupp et al., 2005). However, the use of TMZ as concomitant and adjuvant chemotherapy in addition to radiotherapy in children did not show remarkable improvement in their survival rates over the reports from the historic CCG-945 study (Cohen et al., 2011). The lack of response was found to be correlated with the expression status of O-6-Methylguanine DNA-Methyltransferase (MGMT); the patients with MGMT overexpression had a 2-year EFS rate of only 5% while those without MGMT overexpression had 17%. Nevertheless, it continues to be used in the current standard treatment in combination with radiotherapy probably due to the ease

of administration of the drug (oral), relatively low toxicity and lack of more efficient therapies.

1.6 Molecular biology of paediatric HGG

The low frequency of HGG incidence in children and the difficulty in obtaining clinical samples for research are some of the key obstacles to the understanding of the molecular mechanisms underlying the biology of HGG in children. In addition, early stage investigations in paediatric HGG were based on a candidate gene approach with frequently altered genes in adult HGG. Increased biopsy procedures and the advancement in high-throughput molecular biology techniques over the last few years have resulted in some improvement in our knowledge of these tumours. Large scale collaborative efforts of the ICGC and the Paediatric Cancer Genome Project (PCGP) (St. Jude Children's Research Hospital and Washington University) have begun to provide intriguing insights into the distinct biology underpinning these tumours (Downing et al., 2012).

1.6.1 RTK/Ras/Raf/PI3K pathway alterations

Dysregulated growth factor signalling by receptor tyrosine kinases (RTKs) and abnormalities in the downstream pathways including activation of mitogen activated protein kinase (MAPK) and phosphatidylinositol 3 kinase (PI3K) pathways are the most common events in adult HGGs (Cancer Genome Atlas Research Network, 2008). Genetic aberrations in these pathways are found in paediatric HGG, albeit with differing frequencies to those found in adults.

Alterations in receptor tyrosine kinases (RTKs)

Members of the RTK group of kinases are cell surface receptors which are activated by extracellular molecules like growth factors, hormones and cytokines (Krause and van Etten, 2005). The extracellular domains of RTKs possess binding sites that can interact with specific ligands and are also involved in receptor dimerisation required for the activation of intrinsic tyrosine kinase activity. Upon binding to the ligand, these receptors are autophosphorylated triggering the activation of Ras and induction of Raf, which can further activate the MEK/ERK1/2 and MAP3K pathways. RTK-autophosphorlyation can also activate the PI3K complex leading to the activation of Akt and mTOR (Cancer Genome Atlas Research Network, 2008). All these networks contribute to signalling events essential for cellular growth, proliferation, differentiation and migration.

Aberrant RTK signaling is one of the major mechanisms by which tumour cells escape the normal regulatory control on growth and proliferation, and the different mechanisms of RTK deregulation such as receptor amplification, mutation or overexpression or chromosomal translocation contribute to the development of various types of cancers (Rusten et al., 2007; Abella et al., 2009). Epidermal growth factor receptor (EGFR) is the most predominantly altered RTK in adult HGG, with copy number alterations and mutations in the gene found in approximately 60-85% of GBM (Brennan et al., 2013). EGFRVIII, the most common EGFR variant generated by deletions of exons 2-7 is also frequently altered in adult HGG (Wong et al., 1992; Pollack et al., 2006). In contrast, *EGFR* amplification and *EGFRVIII* over

expression occur at relatively low frequencies in paediatric HGG and DIPG (Bax et al., 2009).

PDGFRA, encoding platelet-derived growth factor receptor-α is the most common target of amplification and/or activating mutation in paediatric HGG and DIPG (Paugh et al., 2010; Zarghooni et al., 2010; Puget et al., 2012). While amplification of *PDGFRA* is a common event in paediatric glioma (14%, 48 of 351 cases), it is relatively rare in adult HGG (10.6%, 22 of 206 cases) (Jones et al., 2012). The amplification of *PDGFRA* was more frequent in the irradiation-induced subset of tumours suggesting a potential role of this gene in tumour initiation (Paugh et al., 2010). Additionally, *PDGFRA* mutants were shown to induce glioma formation in mouse models, these murine-derived glioma displayed gene expression profiles characteristic of human diffuse HGGs (Paugh et al., 2013). In the same study, none of the samples carried deletions of exons 8 and 9 that were previously reported in adult HGG, hinting that there is a distinct mutational spectrum conferring tumourigenic activity to PDGFRA in a paediatric setting. *PDGFRA* overexpression, associated with or without amplification is also common in paediatric HGG.

v-raf murine sarcoma viral oncogene homologue B1 (BRAF) pathway

BRAF, with serine threonine kinase activity is a component of the RAS/RAF/MEK/ERK kinase cascade of the MAPK pathway and contributes to regulation of key cellular functions like proliferation, survival and metabolism. BRAFV600E, the most common BRAF alteration is a point mutation involving amino acid substitution of valine with glutamic acid at position 600 resulting in constitutive activation of MAPK pathway.

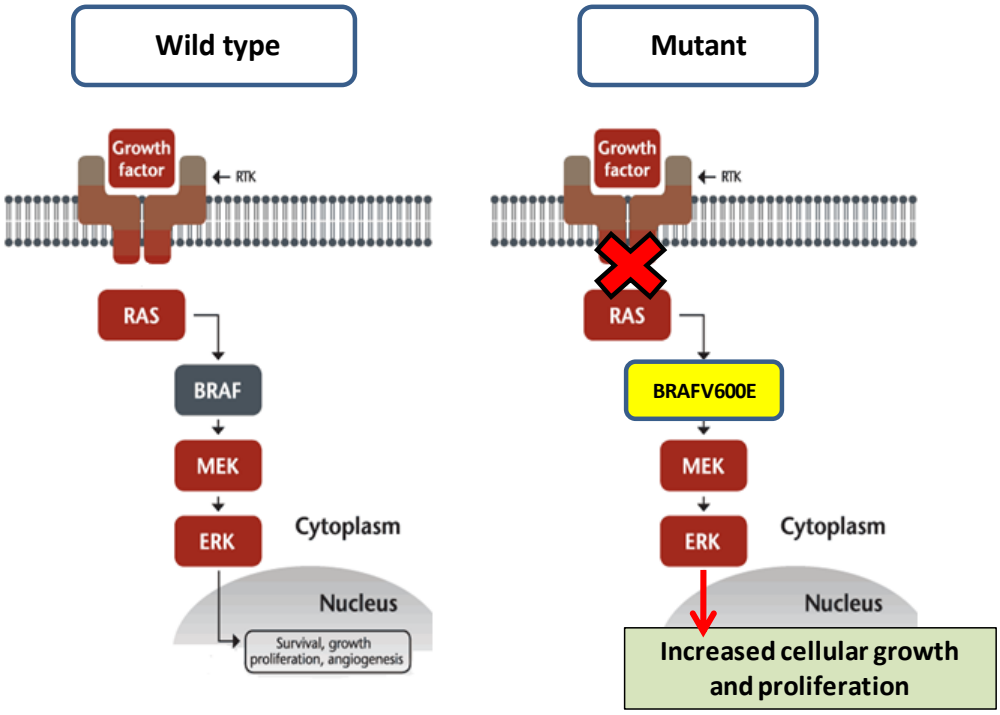

Figure 1.2 BRAF/MEK/ERK pathway. BRAF participates in signal transduction by growth factor signaling. In normal cells, this pathway regulates growth and proliferation in response to extracellular signals received from growth factors. In *BRAFV600E*-mutant cells, the pathway is constitutively active and need not receive growth factor stimulation leading to uncontrolled proliferation.

This mutation is found in several cancers including a small proportion of paediatric low grade glioma. A study by Schiffman and colleagues (2010) identified BRAFV600E mutation in 10% (5/20 Grades III and IV) of paediatric HGG, with 3 of 5 cases harbouring homozygous deletions of *CDKN2A*. A subsequent study on the incidence of BRAFV600E in larger patient cohorts reported significantly higher frequencies of mutations in paediatric GBM accounting for 16.6% (6/36) versus 7.7% (3/39) found in adult GBM (Dahiya et al., 2013). Anatomically, these mutations are observed to be limited to the cortical regions of the brain; no mutations have been reported to date in DIPG.

PI3K/Akt pathway alterations

Mutations, amplifications and deletions affecting the PI3K complex itself as well as its downstream effectors occur in adult and paediatric HGG, albeit at differing frequencies. In adult HGG, mutation rates in the catalytically active subunit (PIK3CA/p110α) and the regulatory subunit (PI3KR1) of PI3K occur at a frequency of 7-21% and 6-11% respectively (Parsons et al., 2008). In paediatric HGG including DIPG, mutations in PIK3R1 occur at a similar frequency as in adults (5-12%). Interestingly, mutations in PIK3CA are less frequent in supratentorial HGG (5%) but more frequent in DIPG (15-25%) (Broderick et al., 2004; Gallia et al., 2006; Grill et al., 2011; Buczkowicz et al., 2014; Strum et al., 2014), indicating a location dependent selection for mutations in this pathway. The feedback regulation of the PI3K pathway is mediated by phosphatase and tensin homolog (PTEN) that causes dephosphorylation of PIP3 and consequent inhibition of Akt activation. Mutations in PTEN are found in about 25-40% of adult HGGs while they occur at a very low rate in paediatric HGG (5-15%) (Pollack et al., 2006; Zarghooni et al., 2010; Barrow et al., 2011; Schwartzentruber et al, 2012; Brennan et al., 2013). Nevertheless, overexpression of Akt and its association with poor prognosis are commonly found in paediatric malignant glioma (Pollack et al., 2010).

1.6.2 RB and p53 pathway alterations

The p53 and RB pathways act in concert with each other to regulate cell division in the G1 phase of the cell cycle. In response to mitogenic stimuli, RB protein undergoes phosphorylation by the cyclin dependent kinase complex (CDK4 or CDK6 coupled with CCND1/2/3) and releases E2F1 transcription factor which then

promotes transcription of genes required for G1/S transition, a process kept under check by the tumour suppressor proteins p16/p14^{ARF} (CDKN2A) and p21^{Cip1}. Under conditions of stress like DNA damage, ARF protein activates p53 by degradation of MDM2, this enables it to inhibit the cell cycle progression or to promote apoptosis. Mutations in TP53 are more common in paediatric HGG than adult HGG, with relatively higher frequencies of occurrence reported in DIPGs than in non-brainstem HGGs (Sung et al., 2000; Grill et al., 2012; Wu et al., 2014). Homozygous deletions of CDKN2A are mostly confined to non-brainstem HGG and mainly absent in DIPGs. The amplification of CDK4/6 or CCND1/2/3 has been found in about 30% of DIPG (Zarghooni et al., 2010; Paugh et al., 2011; Puget et al., 2012; Warren et al., 2012). TP53 mutations occur at higher frequency in children >3 years than younger children (Pollack et al., 2001).

1.6.3 Activin A receptor type I (*ACVR1*)

ACVR1, also known as activin receptor-like kinase II (*ALK2*) encoding bone morphogenetic protein (BMP) receptor type I is involved in the transduction of extracellular signals from BMP protein (Attisano et al., 1993). Recent genome-wide studies have identified mutations in *ACVR1* in paediatric HGG, exclusively in DIPG (range: 20-32%) (Buckowicz et al., 2014; Taylor et al., 2014). This gain-of-function mutation encodes amino acid substitutions in the kinase domain or the adjacent GS (glycine/serine-rich) inhibitory domain of ACVR1. BMP-ACVR1 binding initiates phosphorylation and activation of SMAD transcription factors such as SMAD1, SMAD5 or SMAD8 which further activate growth-promoting genes like *ID1*, *ID2* and *ID3* (Buckowicz et al., 2014; Fontebasso et al., 2014) (Figure 1.3).

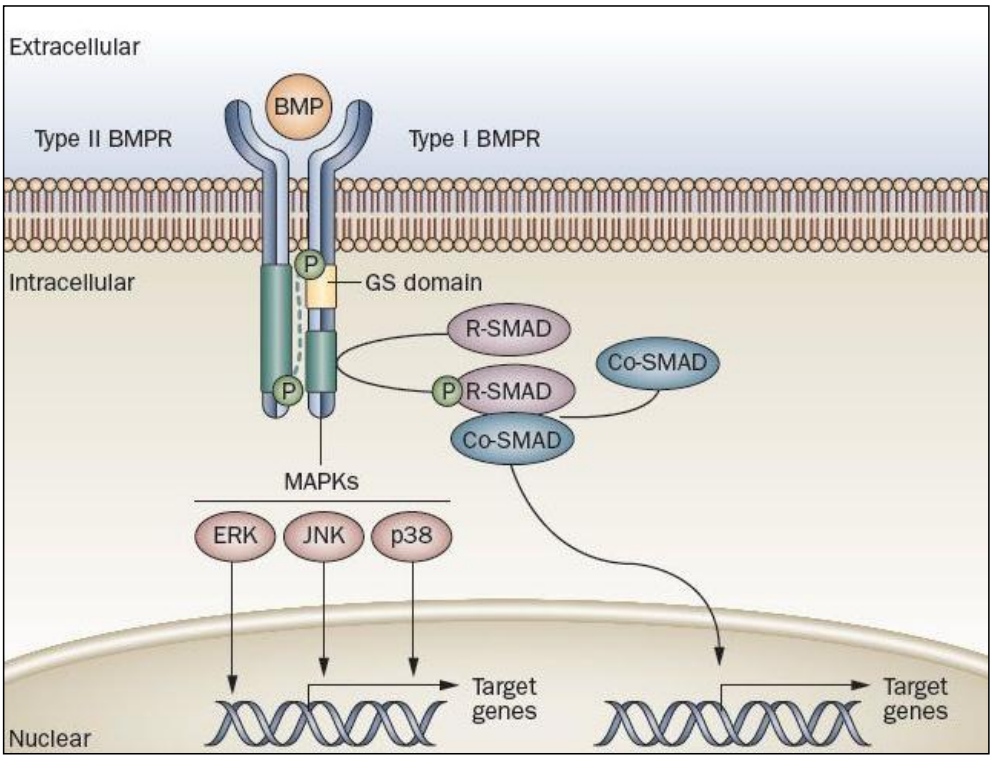

Figure 1.3 BMP signaling pathway. Binding of BMP to ACVR1 (Type I BMPR) triggers phosphorylation of SMAD proteins resulting in activation of growth-promoting genes like *ID1*, *ID2* and *ID3* (Shore and Kaplan, 2010).

Some of the somatic *ACVR1* mutations identified in DIPG resemble germline *ACVR1* mutations described in fibrodysplasia ossificans progressiva (FOP), a disease associated with abnormal formation of bone without any identified link to cancer predisposition. This indicates that *ACVR1* may not have tumour initiating potential in DIPG but may offer growth advantage in the context of other mutations (Jones and Baker, 2014).

1.6.4 Isocitrate dehydrogenase 1 (IDH1) mutations

IDH1, encoding the metabolic enzyme isocitrate dehydrogenase catalyses the production of α-ketoglutarate (KG) from the substrate isocitrate via oxidative decarboxylation. It is the principal source of NADPH in the brain protecting it from oxidative stress (Bleeker et al., 2010). By modulating insulin secretion, *IDH1* plays important roles in determining cellular responses to glucose concentrations (Guay et al., 2013). Recurrent mutations in *IDH1* in GBM were first identified in 2008 as part of the TCGA project when 5 of 6 secondary adult GBM had mutated IDH1 with no mutation in 16 primary GBM included in the cohort. This identification was further supported by studies thereafter in larger sample numbers suggestive of its potential role as an early event in tumourigenesis in adult glioma (Horbinski et al., 2009). Large scale sequencing studies in paediatric HGG reported that IDH1 mutations have no significant role in the paediatric setting. Only 4/32 cases (12.5%) had IDH1 mutations; mutations in IDH2 have not been recorded.

1.6.5 Chromosomal alterations in paediatric HGG

Paediatric HGG exhibit a unique set of CNAs and at lower incidence rates in comparison to their adult counterparts. For instance, the most frequent chromosomal abnormality in adult GBM, the concurrent gain of chromosome 7 and loss of chromosome 10q (83-85%), is far less commonly seen in children than adult HGG (13-19% and 16-38%, respectively) (Maher et al., 2006; Bax et al., 2010; Paugh et al., 2010; Brennan et al., 2013; Sturm et al., 2014). Gain of 1q and loss of 16q are the most frequent CNAs in paediatric HGG (Rickert et al., 2001; Bax et al., 2010). The other major abnormalities consistently found in paediatric HGG at low frequencies

include regions of gains at 1p, 2q, and 21q and losses at 6q, 4q, and 11q (Wong et al., 2006; Bax et al., 2010; Paugh et al., 2010). To add to the complexity of the genomic profiles of paediatric HGG, a subset of paediatric HGG do not possess large scale chromosomal imbalances; 2 independent studies led by Paugh et al. (2010) and Barrow et al. (2011) reported no major chromosomal aberrations in 15/78 (19%) and 5/38 (13%) patients respectively. The notable similarities in CNAs exhibited by a proportion of paediatric and adult HGG include 13q and 14q losses.

The expression of chimeric genes involving the C-terminal kinase domain from the neurotrophic tyrosine receptor kinase (*NTRK*) family members (*NTRK1*, *NTRK2* and *NTRK3*) with N-terminal tails of a number of genes has been recently documented in paediatric HGG, especially in infants. This report, based on a small cohort of 10 patients also demonstrated the oncogenic potential of 2 of the fusion genes, *TPM3-NTRK1* and *BTBD1-NTRK3* by implanting into Tp53-null mice which resulted in HGG formation *in vivo* (Wu et al., 2014).

1.6.6 Gene expression profiling

Integration of copy number and gene expression studies in paediatric HGG have revealed molecular sub-groups within these tumours, which share similarities and differences with those previously identified in adult HGG (proliferative, proneural and mesenchymal). A study by Paugh et al. (2010) identified 3 major sub groups in paediatric HGG – HC1, HC2 and HC3. The HC1 subgroup was associated with amplification of *PDGFRA/PGFRB*, gain of 1q and overexpression of genes involved in cell cycle regulation; HC2 subgroup was associated with gain of 1q and overexpression of genes involved in neuronal differentiation, while HC3 was

associated with overexpression of genes involved in cellular matrix-receptor interactions and cell adhesion (Faury et al., 2007; Paugh et al., 2010).

1.7 Role of epigenetics in cancer

1.7.1 The concept of epigenetics

The concept of epigenetics was first introduced in the early 1940s by Conrad Hal Waddington to study the causal interactions between genes and their products that result in a particular phenotype (Goldberg et al, 2007). Our knowledge on the significance of epigenetic processes in the biology of healthy and disease states has come a long way since then and it is now increasingly understood that they have immense potential to fine-tune the mechanisms of decoding the genetic blueprint of cells (Feinberg and Tycko, 2004; Rodriguez-Paredes and Esteller, 2011). The term 'epigenetics' refers to stable and heritable phenotypic changes in a cell that are not accompanied by changes in the primary DNA sequence and are primarily mediated by DNA methylation, histone modification and non-coding RNAs (Bernstein et al., 2007; Goldberg et al., 2007). These epigenetic mechanisms are well coordinated in normal cells and are essential for the establishment and stable propagation of appropriate patterns of gene expression during normal developmental processes (Berdasco and Estellar, 2010). Disruptions in such regulatory control lead to abnormal expression of genes and altered signalling pathways, which are common events in cancers (Sharma et al., 2010).

1.7.2 DNA methylation

1.7.2.1 Principles of DNA methylation

DNA methylation, the most widely investigated of all known epigenetic mechanisms (Esteller, 2007; Jones and Baylin, 2007), typically involves the covalent transfer of a methyl group ($-CH_3$) from S-adenosylmethionine (SAM) to the 5'carbon on the cytosine (C) moieties within the cytosine-guanosinedinucleotides (CpGs), resulting in the formation of 5-methylcytosine (5mC) (Baylin and Jones, 2011). CpG sites are distributed across the genome, with a small proportion of them clustered in distinct regions called 'CpG islands' (CGIs) and are defined as approximately 500 bp long regions with GC content of 55% and an observed-to-expected CpG ratio of 0.65 (Takai and Jones, 2002). CGIs preferentially span gene promoters, the transcription start sites (TSSs), and/or first exons and cover approximately 60% of human gene promoters (Tsai and Baylin, 2011). They are most commonly found in the promoter regions of housekeeping genes as well as up to 40% of tissue-specific genes and are normally unmethylated (Hackenberg et al., 2010). The remaining small proportions of CGIs are associated with transcription inactivation essential for X-chromosome inactivation (Riggs et al., 1975), genomic imprinting (Li et al, 1993; Zhang et al., 1993), and tissue-specific differentiation (Okano et al, 1999; Esteller, 2007). DNA methylation is also vital for the maintenance of chromosomal stability by preventing the transcription of potentially harmful regions of the genome containing repeat elements, viral inserts and transposable elements (Bird, 2002; Herman and Baylin, 2003).

1.7.2.2 Enzymes involved in the regulation of DNA methylation

The process of DNA methylation is tightly regulated by the activities of two groups of enzymes, which add and remove methyl groups called DNA methyltransferases (DNMTs) and DNA demethylases respectively (Jeltsch and Jurkowska, 2014). The DNMT family includes DNMT1, DNMT3 (DNMT3A, DNMT3B) and DNMT3L (Herman and Baylin, 2003). DNMT3A and DNMT3B, called *de novo* methyltransferases, can function independent of replication and initiate methylation at CpG sites on unmethylated and/or hemimethylated DNA (Okano et al., 1999). On the other hand, DNMT1 called the maintenance methyltransferase, acts during replication and has about 10-40 fold preference for hemi-methylated DNA (Bashtrykov et al., 2012). The recruitment of DNMT1 to the replication fork and to hemimethylated DNA are mediated by proliferating cell nuclear antigen (PCNA) and the ubiquitin-like containing PHD and RING finger domain protein 1 (Uhrf1 protein) respectively (Chuang et al., 1997). However, several studies in recent years have challenged the stringent functional classification of DNMTs.

In addition to their role as *de novo* methyltransferases, the DNMT3 family of enzymes have been identified to have considerable maintenance methylation activity found at repeat elements, this activity occurs both independently of, and in cooperation with, DNMT1 (Liang et al., 2002; Chen et al., 2003). It has also been found that efficient *de novo* methylation occurs as a result of the combined efforts of DNMT3 and DNMT1; DNMT3 can generate methylated CpG sites in only one of the strands of DNA due to their preferences for flanking sequences (Handa and Jeltsch, 2005) as well as their nature of binding to DNA that supports methylation of

neighbouring CpG sites in a single binding only resulting in the generation of hemi-methylated strands that act as substrates for DNMT1. The third member, DNMT3L lacks catalytic activity, but can enhance the methyltransferase activities of the other members in the family in a context-dependent fashion (Hata et al., 2002; Jurkowska et al., 2011; Neri et al., 2013).

DNA methylation can also be influenced by the activities of DNA demethylases which include ten-eleven translocation (TET) dioxygenases, activation-induced cytidinedeaminase (AID) and apolipoprotein B mRNA-editing enzyme 1 (APOBEC1) (Tahiliani et al., 2009; De Carvalho et al., 2010, Ito et al., 2010). The TET family of enzymes consisting of TET 1, TET 2 and TET 3 are involved in the catalyses of oxidation of 5-methylcytosine to 5-hydroxymethylcytosine, which is further deaminated to form cytosine by the AID and APOBEC1 proteins(Kohli and Zhang, 2013; Pastor et al., 2013).

1.7.2.3 Mechanisms of DNA methylation-mediated gene silencing

The exact mechanisms of how the information represented by DNA methylation is interpreted to bring about gene silencing are not completely clear. Two main models have been proposed. Firstly, the physical position of the methyl group of a CpG in the major groove of DNA can directly block the binding of transcription factors (TFs) (Hervouet et al., 2009). TFs such as c-Myc/Myn, CREB/ATF, E2F and NFκB have recognition sites containing CpG sites and are inhibited by methylation (Allis et al., 2007). The second mechanism involves the participation of a group of proteins, called methyl-CpG-binding proteins (MBPs) that can bind to methylated CpGs causing hindrance to the binding of TFs. These proteins have also been associated

with histone deacetylases activity and contribute to maintenance of silent chromatin. Three families of MBPs have been identified. The first group that contains methyl-CpG binding domains (MBDs) contributes to transcription repression through the action of its four main members - MeCP2, MBD1, MBD2 and MBD3. The second group consists of proteins that lack MBDs, but have specialised zinc finger domains to detect methylated DNA; these include zinc finger and BTB domain-containing protein 4 (ZBTB4), ZBTB33/kaiso, and ZBTB38. The third group includes the SET and RING-associated (SRA) domain proteins such as inverted CCAAT box-binding protein of 90 kDa (ICBP90) (Unoki et al, 2004).

1.7.2.4 DNA methylation in cancer

Altered methylation patterns in the genome manifested as global hypomethylation and/or region-specific hypermethylation are common events in cancers. As the basal methylation levels vary with tissue-types, 'hypo' or 'hyper' methylation of DNA in a particular cancer is a relative measure of the amounts of DNA methylation with respect to methylation levels in their corresponding normal tissues (Ehrlich et al., 1982). The global changes in DNA methylation in normal and tumour cells is illustrated in Figure 1.4.

Although genome-wide DNA hypomethylation was one of the first epigenetic alterations to be identified in malignant cells, this phenomenon remains largely understudied. Global reduction in methylation can have potentially undesirable cellular consequences associated with different stages of cancer development and has been reported in several cancers including GBM in adults (Cadieux et al., 2006). Hypomethylation is associated with transcriptional activation of protooncogenes,

some of which include HRAS in melanoma, cyclinD2 and maspin in gastric cancer, and MN/CA9 in renal cell carcinoma. Notably, hypomethylation can lead to genomic instability and mitotic recombination resulting in deletions and translocations, and the reactivation of various transposable elements (such as long interspersed nuclear elements (LINEs) and Alu repeats), viral oncogenes, and/or growth-related imprinted genes like *IGF2* (Ehrlich, 2009).

Unlike global hypomethylation, localised DNA hypermethylation has been extensively investigated in cancers (Sharma et al., 2010). Promoter-specific DNA hypermethylation in cancer cells can turn off tumour suppressor genes and is as prevalent as mutational events in cancer development (Jones et al., 2002). DNA hypermethylation can contribute to tumourigenesis by causing transcription inactivation of a wide array of genes involved various cellular processes such as cell cycle, apoptosis, angiogenesis, metastasis, and metabolism (Herman and Baylin, 2003). Some of these genes are classic tumour suppressors such as *RB* in retinoblastomas and *VHL* (associated with von Hippel-Lindau disease) in renal cell cancers (Herman et al, 1994), while others act as transcription factors, the silencing of which in turn affect the expression of numerous other genes controlled by them. Hypermethylation can also disrupt the levels of DNA repair genes (eg: *MLH1* and *BRCA1*) reducing the capacity of cells to repair genomic errors thereby increasing their vulnerability to malignant transformation (Esteller, 2009).

Identification of hypermethylated genes can serve as a powerful tool for early detection of tumours (eg: *GSTP1* in prostate cancer) and for predicting response to therapy (eg: *MGMT* predict response to DNA-alkylation agents like TMZ in GBM

patients). The reversible property of DNA methylation has also led to the development of demethylating therapy for some cancers such as acute myeloid leukemia (AML) (Momparler et al., 2014).

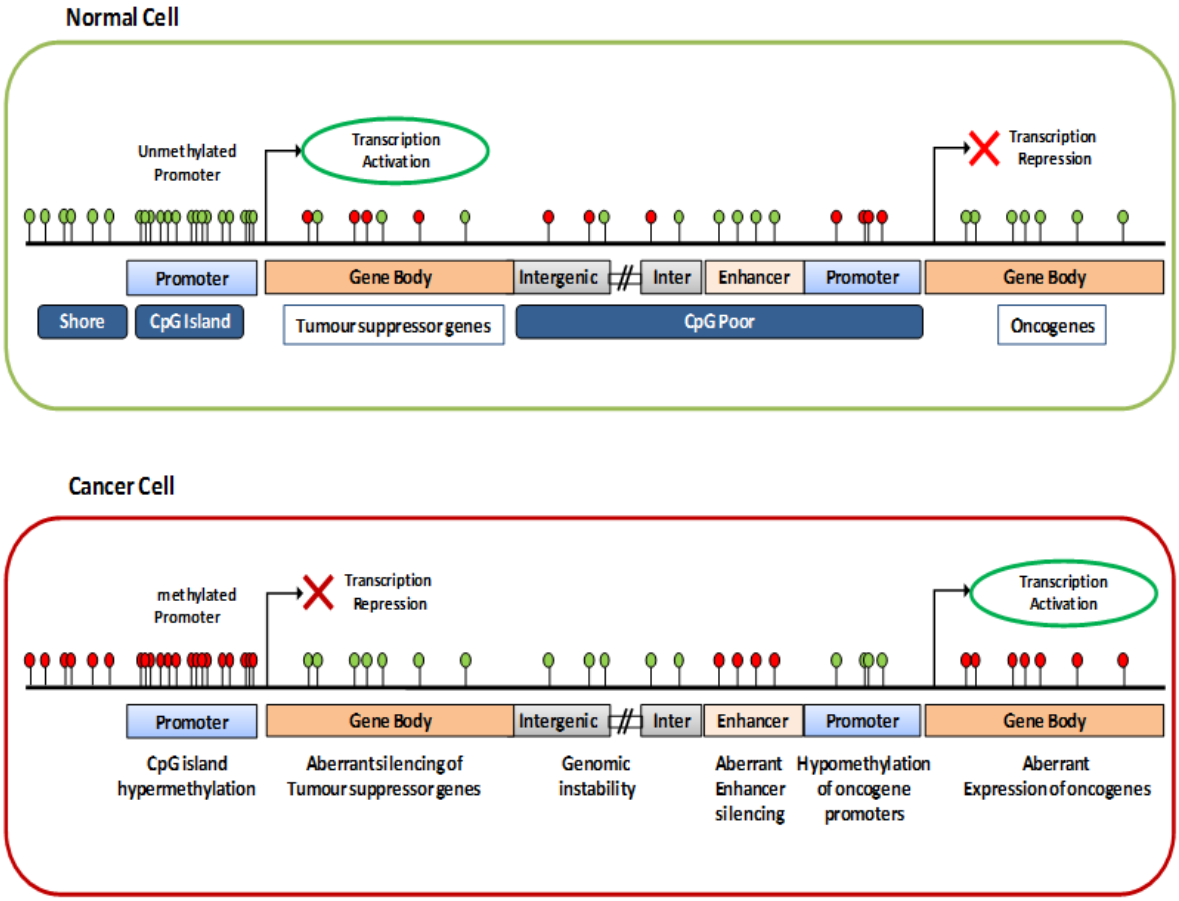

Figure 1.4 Global changes in DNA methylation in normal and tumour cells. In normal cells the CpG islands in active promoters are unmethylated allowing the transcription of genes. Aberrant methylation of promoter CpG islands often occurs in coding regions in tumour cells. This leads to aberrant silencing of tumour suppressor genes in tumour cells.

1.7.3 Histone modifications

1.7.3.1 Principles of histone modifications

Eukaryotic chromatin is made of repeating units of nucleosomes, each composed of roughly 147 base pairs of DNA coiled around an octameric core, containing two units each of four types of histone proteins - H2A, H2B, H3 and H4 (Luger et al., 1997; Cutter and Hayes, 2015). The amino acid moieties of these core histones, predominantly the ones located in the N-terminal tails, can undergo dynamic chemical modifications such as lysine acetylation, lysine and arginine methylation, lysine ubiquitylation, lysine sumoylation, serine/threonine/tyrosine phosphorylation and arginine citrullination (Kouzarides et al., 2007; Bannister and Kouzarides, 2011). In addition, several less common modifications have been identified in the past few years, which include lysine crotonylation, tyrosine hydroxylation, lysine butyrylation, lysine propionylation and serine/threonine *O*-GlcNAcylation (Chen et al., 2007; Fujiki et al., 2011; Tan et al., 2011). These modifications, either singly or in combination, play decisive roles in the establishment of 'active' (euchromatin) versus 'silent' (heterochromatin) chromatin domains in the genome and coordinate the execution of crucial DNA-based biological functions like transcription, replication and repair (Kouzarides et al., 2007). The functional consequences of these modifications depend on the nature of the modification, and the type and number of amino acid residues involved in the process (Sharma et al., 2010). For instance, acetylation of lysine is associated with transcriptional activation where as methylation of lysine may result in activation (as in case of trimethylation of lysine 4

on histone H3 (H3K4me3)) or repression (as in cases of trimethylation of H3K9 (H3K9me3) and H3K27 (H3K27me3)) of transcription.

Recent studies have unravelled some of the layers of complexity in the ways histone modifications operate in cells. These new findings suggest the involvement of cross talk between the combinations of modifications occurring in a context-dependent manner, making it difficult to predict an exact causal relationship between a particular modification and its biological response in the cell (Lee et al., 2010; Rothbart and Strahl, 2014). In normal cells, these modifications work under extreme coordination to establish specific patterns in particular cell types. For instance, in embryonic stem (ES) cells, there occurs a state of 'bivalency' defined by the co-existence of permissive (H3K4Me3) and repressive (H3K27Me3) histone marks in the promoter regions of genes involved in developmental events (Bernstein et al., 2006). This is regulated by the antagonistic effects of the Trithorax and Polycomb group of proteins which favour the activating and repressive marks respectively resulting in the commitment of stem and/or progenitor cells into specific lineages. On the other hand, this bivalency is lost in differentiated cells enabling them to maintain their cell fates over several generations (Mikkelsen et al., 2007).

1.7.3.2 Enzymatic regulation of histone modifications

Post-translational histone modifications are regulated by enzymes that catalyse either deposition of specific chemical moieties, called chromatin 'writers' (such as histone acetylases (HATs)) or their removal, called 'erasers' (such as histone deacetylases (HDACs)). The resulting modified structure can turn on the recruitment of effector proteins called 'readers', with specialised domains that can bind to such structures

and initiate specific chromatin-associated downstream events (Jenuwein, 2001). While the 'writers' and 'erasers' can impose a direct effect on histone-DNA binding by altering electrostatic charges on the amino acid residues as observed in case of lysine acetylation (Shogren-Knaak et al., 2006) and arginine citrullination (Christophorou et al., 2014), the 'readers' alter chromatin structure by various indirect mechanisms as in case of bromodomain (Dhalluin et al., 1999). In addition to the core histone proteins, non-allelic variants of histones such as H3.3 and H2A.Z also engage in posttranslational modifications and can modulate gene activity by non- covalently altering nucleosome stability as well as by protecting regions of DNA against methylation (Talbert and Henikoff, 2010).

Modifications in the histone/histone variants can interact with chromatin remodelling enzyme complexes and alter the positioning and stability of nucleosomes. There are currently four major sub families of chromatin remodelling enzyme complexes: switching defective/sucrose non-fermenting (SW1/SNF) family, the imitation SWI (ISWI) family, the nucleosome remodelling and deacetylation (NuRD)/Mi-2/ chromodomain helicase DNA binding (CHD) family, and the inositol requiring 80 (INO80) (Wang et al., 2007).

1.7.4 Histone mutations in paediatric HGG

1.7.4.1 H3.3/H3.1 mutations

The investigation of paediatric HGG at the global genomic level has identified novel mutations in the histone modification machinery and the histone proteins themselves. Two independent studies on paediatric GBM and DIPG in 2012 (Schwartzentruber et

al., 2012; Wu et al., 2012) reported the first evidence for tumourigenesis associated with direct mutation of histones. Mutations were identified within *H3F3A* and *HIST1H3B* genes encoding histone variant proteins H3.3 and H3.1 respectively. H3.1 is synthesised in synthetic phase and is deposited only during DNA replication, and H3.3 is present throughout the cell cycle and is incorporated at all phases of the cell cycle (Ahmad and Henikoff 2002). These mutations lead to amino acid substitutions at 2 important residues within the N-terminal histone tail involving replacement of lysine with methionine at position 27 (K27M) and glycine with arginine (G34R) or with valine at position 34 (G34V). These mutations were found to have associations with specific anatomical regions in the brain; K27M mutations were mainly detected in H3F3A and had high frequency of occurrence in DIPG samples (78%) while G34R/G34V mutations exclusively found in H3F3A were largely restricted to tumours found in cerebral hemispheres.

Dysregulation of the histone modification machinery is a common event during malignant transformation affecting the recruitment of transcription factors and patterns of gene expression. The repressive histone mark, H3K27Me3 essential to inhibit the expression of genes that oppose normal development and differentiation has been observed to be globally reduced in *H3F3A* (K27M)-mutant paediatric HGG and DIPG (Bender et al., 2013). This reduction was associated with inappropriate recruitment of the polycomb repressive complex 2 (PRC2) to the mutant H3.3 and inhibition of the enzymatic activity of the H3K27me3-establishing methyltransferase EZH2. The overall survival of DIPG patients with *H3F3A* (K27M) mutations was reduced compared to their wild type counterparts (Khuong-Quang et al., 2012).

1.7.4.2 H3.3/ATRX/DAXX pathway alterations

Interestingly, the roles of histone modifications in gliomagenesis in children have been further cemented by the identification of mutations in the chromatin remodelling complex *ATRX/DAXX* alone and in conjunction with H3.3 and TP53 mutations. *ATRX* mutations have been detected in 31% of samples with all of them harbouring the G34R/V H3.3 mutation. In some cases, these mutations were detected along with *TP53* mutations suggesting the contribution to the molecular biology of these tumours of the interconnection between these pathways.

Death domain associated protein (DAXX) forms highly specific, stable complexes with H3.3 and functions as histone chaperons in cooperation with α-thalassemia/mental retardation syndrome protein (ATRX) aiding the deposition of H3.3, preferentially at repetitive heterochromatic regions such as telomeric and pericentric DNA repeats, and ribosomal repeat sequences (Tang et al., 2004; Lewis et al., 2010). Mutations in the *H3.3/ATRX/DAXX/TP53* network results in the incorporation of mutant H3.3 and the consequent presence of a telomere maintenance mechanism called alternative lengthening of telomeres (ALT) which do not require the involvement of telomerase. Mutations in *TP53* have also been demonstrated to have a connection with ALT leading to enhanced lengthening of telomeres that confers uncontrolled proliferative ability to cells (Heaphy et al., 2015).

1.7.4.3 Mutations in histone modifiers and chromatin remodelers

Recently, Fontebasso and colleagues (2013) identified loss-of-function mutation in *SETD2* in approximately 15% (11/73) of paediatric HGG and 8% (5/65) of adult

HGG. This mutation was exclusively found in HGG arising in the cerebral cortex. *SETD2* encodes H3K36 trimethyltransferase which catalyses the trimethylation of lysine residues of histone H3 at position 36 (Edmunds et al., 2008) and the mutation in the gene was associated with decreased levels of H3K36Me3 histone marks. H3K36Me3 has dual roles in activation as well as repression of transcription and regulates various processes in the cell such as DNA replication and repair.

1.7.4 Non-coding RNAs

Non-coding RNAs were once thought as non-functioning products of 'junk DNA'; today they are known as crucial biological participants in the regulation of gene expression (Ling et al., 2015). These encompass a class of RNAs, ranging from small to long ncRNAs, including micro RNAs (miRNAs), PIWI-interacting RNAs (piRNAs), small nucleolar RNAs (snoRNAs), large intergenic non-coding RNAs (lincRNAs) and transcribed ultra conserved regions (T-UCRs).

1.7.4.1 Overview

The best studied among the non-coding RNAs are miRNAs, which are small RNAs of approximately 18-24 nucleotides in length capable of mediating diverse cellular processes essential for normal mammalian development and tissue homeostasis (Vidigal and Ventura, 2015). Each miRNA has in its 5'end a set of nucleotides (particularly nucleotides 2-8), called the 'seed' and can bind to corresponding sequences ('seed site') on 3'UTR regions of specific messenger RNA (mRNA) targets through complementary base pairing (Lewis et al., 2003; Saito, 2015), resulting in mRNA degradation and/or translational repression. In addition to

3’UTRs, miRNAs can also target 5’UTR regions (Lee et al., 2009), other non-coding RNAs and even proteins. More than 1000 human miRNAs have been discovered to date; some miRNAs have unique specificity for their targets, whereas others can affect hundreds of targets, suggesting that miRNAs may exert control on the expression of the vast majority of the protein coding genes.

1.7.4.2 Biogenesis of miRNAs

The majority of miRNAs are transcribed in the nucleus from miRNA genes (canonical pathway) and about 30% of them from introns of protein-coding genes (non-canonical pathway). The transcription of miRNA genes is mediated by RNA polymerase II, resulting in long primary transcripts (pri-miRNAs) which are then capped at the 5’end and polyadenylated at the 3’ end (Lee et al., 2004). Pri-miRNAs are processed by the microprocessor complex consisting of RNA polymerase III/Drosha and the RNA binding protein, DiGeorge syndrome critical region 8 (DGCR8). Drosha splices pri-miRNAs to yield ~60-70 nucleotide-long hair-pin shaped precursor miRNAs (pre-miRNAs) (Lee et al., 2003). In the non-canonical pathway, pre-miRNAs are generated in splicing events followed by a DROSHA/DICER-independent process involving the lariat-debranching enzyme. Pre-miRNAs, thus produced, are bound to a nuclear export factor, Exportin-5 (XPO5) that transports them to the cytoplasm in a RAN-GTP dependent manner (Okada et al., 2009) where they are further processed by Dicer and transactivation-responsive RNA-binding protein 2 (TARBP2) to yield a dsRNA duplex consisting of both the mature miRNA and its complementary strand (miRNA/miRNA*). The mature miRNA then joins with Argonaute protein (AGO) to assemble into the core

of the RNA-induced silencing complex (RISC), while the complementary strand (miRNA*) is degraded. The mature miRNA can then lead to mRNA degradation or repression of translation (Filipowicz et al., 2008).

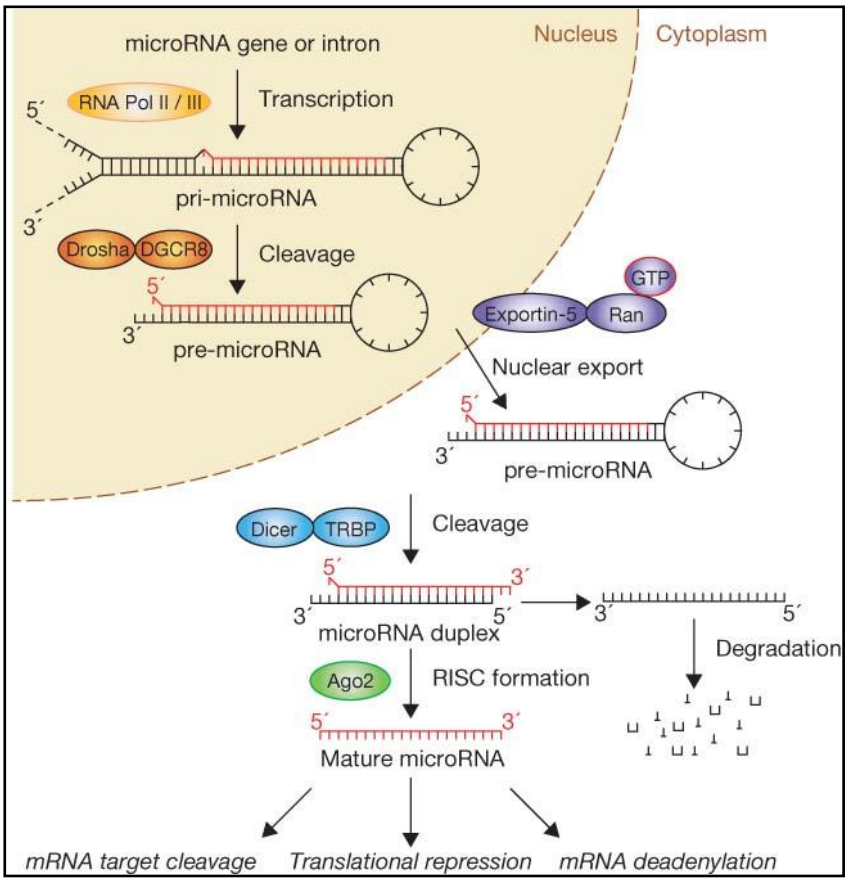

Figure 1.5 Biogenesis of miRNAs. Biogenesis of miRNAs can occur from miRNA genes in the canonical pathway or from the introns of protein-coding genes in the non-canonical pathway. The pre-miRNAs are cleaved and exported to the cytoplasm where they can have several consequences on their target genes. Mature miRNAs can cause cleavage of mRNA targets, translational repression and deadenylation (Winter et al., 2009).

1.7.4.3 Role of miRNAs in cancer

Under normal physiologic conditions, miRNAs are very stable and their biosynthesis and functional activities are tightly regulated (Mendell and Olson, 2012). This

regulatory control is often lost in malignant cells in response to various environmental stress signals like hypoxia or DNA damage, resulting in altered levels of miRNA expression (Hata and Lieberman, 2015; Orellana and Kasinki, 2015).

The first major evidence for the participation of miRNAs in cancer was made in 2002, with the identification of miR-15a/16-1 loci deletions in patients with B cell chronic lymphocytic leukemia (B-CLL) (Calin et al., 2002). Over the last few years, there has been a rapid increase in the identification of miRNAs and their putative targets in a number of cancer types (Orellana and Kasinki, 2015). Based on their functions, miRNAs can be oncogenic (oncomiRs), tumour suppressive (tumour suppressor miRs), or context-dependent (Zhang et al., 2007; Kasinki and Slack, 2011; Friedlander et al., 2014). OncomiRs target tumour suppressor genes and are usually found upregulated in cancers; for instance, *miR-21* can target tumour suppressor genes like *PTEN*, *PDCD4*, *TPM1*, *SPRY1/2* and *TP53BP2* (Leva et al., 2014). Conversely, tumour suppressor miRs target oncogenes and are generally downregulated in cancers; for instance, let-7 family of miRNAs that targets oncogenes such as *MYC* and *RAS* to suppress tumour growth, are frequently down regulated in cancers (Johnson et al., 2005; Kim et al., 2009). The context-dependent miRNAs can perform opposing roles in cancers depending on the cellular context, for example, miR-221 behaves like an oncogene in liver cancer, but in erythroblastic leukemia it exerts tumour suppressive role by targeting *KIT* oncogene (Felli et al., 2005; Pineau et al., 2010).

MiRNAs are potent mediators of several cellular processes such as differentiation, and apoptosis which are often deregulated in cancers (Hata and Lieberman, 2015).

They can modulate growth factor signalling networks through their interplay with specific growth factors. For example, overexpression of miR-7 induced cell cycle arrest and reduced invasiveness in GBM by regulation of EGFR expression and *Akt* pathway activity (Kefas et al., 2008). MiRNAs also play important roles in regulating glucose metabolism in many cancer types. MiR-195-5p has been shown to have sequence-specificity to target glucose transporter member 3 (GLUT3) in bladder cancer cells resulting in decreased transportation of glucose into the cells, inhibition of growth and promotion of apoptosis (Fei et al., 2012). The suppression of miR-143 was associated with increased levels of hexokinase 2 (HK2) in head and neck squamous cell carcinoma (Peschiaroli et al., 2013), colon cancer (Gregersen et al., 2012) and GBM (Zhao et al., 2013). The importance of miRNAs in cancer has been further highlighted by the observation that miRNAs are found in cancer exosomes and can induce tumour formation in normal cells by utilising their own mechanism to process mature oncogenic miRNAs from pre-miRNAs (Melo et al., 2014).

1.7.4.4 Deregulation of miRNAs during tumourigenesis

Aberrant expression of miRNAs in cancers is often associated with defective miRNA biogenesis machinery, which in turn could be attributed to genetic and epigenetic alterations. Loss of regulatory control can occur in virtually all steps involved in the biogenesis of miRNAs and has been linked with the widespread downregulation of miRNAs observed in most cancer types in comparison to their normal counterparts (Lu et al., 2005). Decreased production of pri-miRNA transcripts owing to mutations in the *miR-128b* gene in MLL-AF4 acute lymphoblastic leukemia (ALL) results in low levels of mature *miR-128b* and confers resistance to glucocorticoids (Kotani et

al., 2010). Mutations in XPO5 contribute to impaired export of pre-miRNA to the cytoplasm in tumours with microsatellite instability leading to uncontrolled levels of pre-miRNAs in the nucleus (Melo et al., 2010). In addition to impaired miRNA biogenesis, the expression levels of miRNAs in cancer cells are also influenced by the relative abundance of their mRNA targets. For instance, the increased expression of miR-155 in liposarcoma was associated with reduced expression of Dicer (Vincenzi et al, 2015).

1.8 Targeted therapy in paediatric HGG

Recently, significant progress has been made in the identification of novel perturbations affecting the critical components of regulatory networks in paediatric HGG including DIPG, and specific molecular subsets within these tumours have been delineated (Chamdine and Gajjar, 2014; Buczkowicz and Hawkins, 2015). Furthermore, mounting evidence have emphasised differences in the transformed phenotype of malignant glioma in children and adults (Jones et al., 2012). These findings have prompted clinical trials with novel small molecule inhibitors targeting specific aberrations in paediatric HGG. Table 1.1 summarises some of the major inhibitors that are currently under clinical investigation in paediatric HGG.

Genomic profiling of HGG in children have demonstrated simultaneous disruption of more than one signalling pathways; for instance, co-amplification of *IGFR,* along with other RTK kinases have been reported in paediatric HGG and DIPG (Puget et al., 2012). As a result, combinatorial strategies are adopted, often involving a selection of drugs directed against multiple aberrations, to increase the efficacy of the

treatment. For example, pre-clinical data have shown synergistic effect in the combined use of imatinib (PDGFR inhibitor) and NVP-AEW54 (IGF1R inhibitor) in paediatric HGG *in vitro* and *in vivo* (Bielen et al., 2011). Additionally, inhibitors directed against some of the common defects in paediatric HGG such as those affecting DNA repair or angiogenesis, have been combined with the existing treatment strategy (chemoradiation) to enhance the effects of chemotherapy and radiotherapy. The administration of veliparib (PARP-inhibitor) in conjunction with radiotherapy has shown improved response in paediatric HGG in the phase I trial.

Table 1.1 Targeted therapy in paediatric HGG

Target	*Inhibitor*	*Current status of investigation*	*Reference/Clinical trial*
EGFR	Erlotinib	No survival benefit in phase II trial	Qaddoumi t al., 2014
	Cetuximab	Currently in phase II trial	NCT01012609
	Nimotuzumab	5-year institutional study reported prolonged PFS and OS	Cabanas et al., 2013
	Gefitinib	Phase I trial in combination with radiation (halted due to intratumoural bleeding)	Geyer et al., 2010
PDGFR	Imatinib	Phase I trial halted due to intratumoural haemorrhage	Pollack et al., 2007
	Crenolanib	Currently in phase I trial	NCT01393912
PTEN/ Akt	MK-2206	Phase I trial	NCT01231919
BRAFv600e	Vemurafenib	Complete response in a GBM patient in phase I/II trial	Robinson et al., 2014
	Dabrafenib	Currently in phase I clinical trial	NCT01677741
PARP	Veliparib (ABT-888)	Phase I trial in recurrent CNS tumours	Su et al., 2014
		Phase I/II in combination with radiation and TMZ for newly diagnosed brainstem tumours is in progress	NCT00946335
HDAC	Valproic acid	Phase II trial with Bevacizumab	NCT00879437
	Vorinostat	Phase II trial in combination with TMZ and Bevacizumab	NCT01236560

PFS, Progression free survival; OS, overall survival (Vanan and Eisenstat, 2015).

1.9 Role of amino-acid metabolism in cancer

Aberrant cellular metabolism is a significant event in the growth and development of many cancers (Hanahan and Weinberg, 2011; Cantor and Sabatini, 2012; DeBerardinis and Tompson, 2012; Galluzi et al, 2013). Unlike normal cells, cancer cells need large inputs of energy to maintain their accelerated rates of proliferation and survival (Hirayama et al, 2009; vander Haiden et al., 2009; Kami et al, 2013). Accordingly, they undergo continuous metabolic reprogramming ensuring the most effective method of utilising cellular energy (Arif et al, 2014; Phan et al., 2014). Identification of such metabolic adaptations that are unique to tumour cells has been an area of high interest in the development of targeted therapeutics with improved tumour-specificity and minimal side effects. For instance, many cancers are auxotrophic for particular non-essential amino acids owing to abnormalities in amino acid biosynthetic pathways. This property can be advantageous to tumour cells as metabolic reactions involved in the synthesis of non-essential amino-acids are highly energy-consuming (Zhang and Yang, 2013).

The rationale for exploiting such auxotrophic tumours using specific enzymes to lower the amino-acid levels in the blood began with the use of L-asparaginase (an asparagine-degrading agent) for the treatment of paediatric acute lymphoblastic leukemia (ALL) (Broome, 1961; Pieters et al, 2011). In contrast to normal cells, ALL cells lack the enzyme asparagine synthetase (ASNS) and are incapable of producing asparagine. The resulting dependency of ALL cells on ectopic sources of asparagine for survival and proliferation can be selectively targeted using asparagine-depletion therapy. Currently, both native and pegylated forms of L-asparaginase are under

clinical investigation in phase I/II clinical trials in children with ALL, although there are few side effects associated with the drug (Parker et al, 2010; Messinger et al, 2012). Dissecting the molecular biology behind abnormal amino acid metabolism in tumours has therefore gained renewed interest in the identification of novel druggable biosynthetic pathways (Phillips et al, 2013).

1.9.1 Role of arginine in cancer

L-Arginine (L-2-amino-5-guanidino-valeric acid) is a multi-functional amino acid that plays diverse roles in both normal and tumour cells (Tapiero et al, 2002). The main sources of arginine within the body come from diet, protein-turn over and from endogenous synthesis via the intestinal-renal axis (Phillips et al, 2013). Arginine is utilised by cells to synthesise proteins via mTOR signalling pathway (Yao et al, 2008; Bauchart-Thevret et al, 2010). The first evidence of the role of arginine in tumour biology dates back to the early 1930s;xenograft models fed on arginine-rich diet showed enhanced tumour growth while those on arginine-free diet demonstrated reduction in tumour size (Gilroy, 1930). Since then, several investigations have been made to unravel the potential functions of arginine in cancer cells. Arginine can act as a precursor molecule for the synthesis of nitric oxide (NO), polyamines, proline, glutamate, agmatine, urea and creatinine, all of which are implicated in various aspects of carcinogenesis. Arginine-derived NO contributes to tumour initiation (by inhibiting DNA repair activities) (Roy et al, 2004), tumour angiogenesis (by upregulating vascular endothelial growth factor) (Cianchi et al, 2004), metastasis (by inhibiting the formation of tumour cell-platelet aggregates thereby evading host immune response) (Scott Lind, 2004) and induction of apoptosis or necrosis

depending on the types and amounts of NO (Xie and Huang, 2003). Arginine can generate polyamines that can modify hypusine-containing eukaryotic translation initiation factor 5A-2 (eIF5A-2) and thereby contribute to the higher rates of proliferation in tumour cells compared to normal cells (Paul et al, 2006). Being positively charged molecules, polyamines can interact with negatively charged DNA, RNA, phospholipids and proteins leading to modulation of various cellular processes including growth, proliferation and survival. Arginine can also lead to the production of proline, which is a key constituent of collagen and thus contributes to wound healing (Morris, 2006; Barbul, 2008). Proline can also act as a stress substrate, further indicating its putative role in tumourigenesis (Kaul et al., 2008). Arginine can also govern the production of the neurotransmitter glutamate, which is known for enhanced glutamate signalling in glioma cells (Morris, 2006; Yang et al., 2009).

1.9.2 Arginine biosynthesis pathway

Metabolism of arginine is highly dynamic and is modulated by various factors including age, cell type, stage of development, diet, state of health, arginine transporters across plasma and mitochondrial membranes, and the expression of enzymes involved in arginine recycling (Morris, 2007). In normal cells, de novo synthesis of arginine from its precursor citrulline is usually sufficient to meet the requirements for arginine. In contrast, the arginine demands of tumour cells are increased beyond the limits that could be attained by endogenous synthesis; hence it is classified as semi essential or conditionally essential amino acid (Morris, 2006).

The metabolic pathway of arginine biosynthesis, mediated by key enzymes can be summarised as follows: argininosuccinate synthetase (*ASS1*) converts L-citrulline

and aspartic acid into argininosuccinate, argininosuccinate lyase (*ASL*) then degrades argininosuccinate into L-arginine and fumaric acid followed by arginase that converts L-arginine to L-ornithine which is then converted back to L-citrulline by ornithine carbamyltransferase (OCT) (Haines et al., 2011). Tumours with aberrations in this metabolic pathway exhibit arginine auxotrophy and depend on ectopic sources of arginine. Therefore, arginine starvation using arginine-catabolising enzymes can be used to target such tumours. Studies report abnormalities in key components of arginine biosynthesis pathway in a variety of tumour types including renal cell carcinoma (RCC), hepatocellular carcinoma (HCC), melanoma, and some mesotheliomas making them auxotrophic for arginine (Cheng et al., 2007; Yoon et al., 2007; Bowles et al., 2008; Kim et al., 2009; Feun et al., 2012; Kelly et al, 2012; Allen et al., 2014). The sensitivity to such agents depends largely on the ability of these tumours to regenerate arginine from intermediate components such as ornithine, citrulline and argininosuccinate (Wheatley et al, 2005).

1.9.3 Dysregulation of *ASS1 and ASL*

Of the key urea cycle enzymes that regulate the levels of arginine in cells, *ASS1* can be considered the master switch controlling the rate-limiting step in arginine biosynthesis. Accumulating evidences show that *ASS1* is abundantly expressed in normal tissues as a house-keeping gene, but differentially expressed in many tumours (Bowles et al., 2008; Kim et al., 2009; Feun et al., 2012; Syed et al., 2013). While overexpression of *ASS1* is observed in some cancers such as gastric, colorectal and lung, downregulation is reported in numerous cancer types such as hepatocellular carcinoma, melanoma, mesothelioma and small cell lung. The mechanism of under

expression of *ASS1* in these tumours is attributed to hypermethylation in the CpG rich region of *ASS1* promoter (800-bp long) (Jinno et al., 1985).

ASL acts immediately downstream of ASS1 and plays a role in channelling arginine for the production of NO (Erez et al., 2012). However, the role of ASL in tumours is an area that remains underexplored. Studies on hepatocellular carcinoma reveal that upregulation of *ASL* contributes to aggressiveness of the tumour through signalling by NO and cyclinA2 (Huang et al., 2013). On the contrary, *ASL* is reported to be silenced by promoter hypermethylation in GBM and combined loss of *ASL* and *ASS1* conferred better sensitivity to arginine-depleting agents (Syed et al., 2013).

1.9.4 Targeting arginine-auxotrophic tumours with arginine-degrading enzymes

Arginine can be catabolised using a series of enzymes that include arginine deiminase (ADI), arginine decarboxylase (ADC), arginase, and nitric oxide synthases (NOS) (Morris, 2004). However ADI is the most commonly used arginine-depleting agent in arginine-auxotrophic tumours due to improved arginine-specificity, optimal pH and better stability *in vivo*. ADI is a microbial protein mainly derived from mycoplasma and demonstrates diverse anti-cancer activities depending on the types of ADI derived from different varieties of microbial strains (Hahn et al., 1974). The commonly used ADI produced from *M.arginini,* comprises of two subunits and has a molecular weight of 43 kDa (Sugimura et al, 1990). However, due to its high antigenicity and very short half-life (~5 hours) ADI is conjugated with polyethylene glycol (PEG) to form ADI-PEG20 (Polaris Pharmaceuticals, CA) which has a

molecular weight of 20 kDa and an increased half-life of 7 days (Holtsberg et al, 2002; Ni et al, 2008; Qiu et al., 2013).

1.9.4.1 ADI-PEG20

The anti-tumour activity of ADI-PEG20 has been investigated in several types of cancers and is an area of renewed interest. The mechanism of arginine-deprivation therapy in cancers is shown in Figure 1.6.

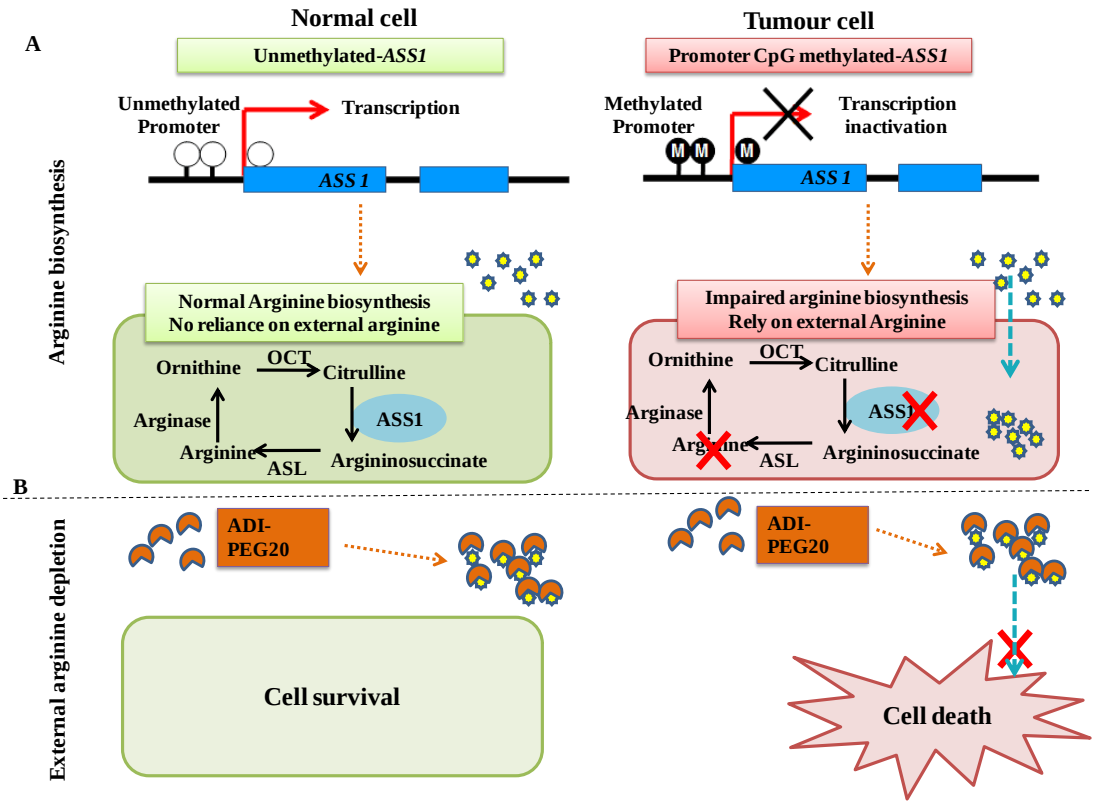

Figure 1.6 Mechanism of arginine deprivation therapy. A. In normal cells, ASS1 regulates cellular arginine renewal by *de novo* synthesis of arginine. Tumour cells with promoter CpG methylation have defective arginine biosynthesis machinery and rely on external sources of arginine. **B**. ADI-PEG20 depletes arginine in the periphery; normal cell survives, but tumour cell dies.

ADI-PEG20 has shown significant clinical response in small cell lung cancer, pancreatic cancer, prostate cancer, head and neck cancer, ovarian cancer, myxofibrosarcoma, malignant pleural mesothelioma, malignant melanoma (MM) and adult GBM (Izzo et al., 2004; Bowles et al., 2008; Kim et al., 2009; Nicholson et al., 2009; Ott et al., 2012; Kelly et al., 2012; Syed et al., 2013; Szlosarek et al., 2013). The exact mechanism of tumour suppression by the drug is not fully understood. Studies in breast cancer, prostate cancer and adult GBM suggest that the anti-tumour activity of ADI-PEG20 is mainly autophagy-dependent (Kim et al., 2009; Syed et al., 2013; Qiu et al., 2014). In gastric cancer cells, ADI-PEG20-induced apoptosis has been associated with the up-regulation of p-53 and p27Kip1 as well as the downregulation of cyclin D1, c-myc and Bcl-xL. In melanoma cells, it has been shown that nutrient deprivation by ADI-PEG20 leads to reduced ATP levels leading to activation of AMPK which eventually causes inhibition of mTOR signalling and decrease in cellular proliferation (Kimura et al, 2003).

1.10 Aims and objectives

The underlying molecular pathology of paediatric HGG including DIPG is not well understood resulting in poor clinical responses. Integrative genomic analysis has not been extensively employed in biological investigations in paediatric HGG. The aim of this study was to utilise high-resolution microarrays and integrative data analysis to facilitate the identification of potential therapeutic targets in paediatric HGG using well-characterised patient-derived short-term cell cultures. The focus of this study was to use genome-wide approaches;

- To compare mutation status, copy number, gene and, miRNA expression profiles between biopsy and cell culture in paired paediatric HGG biopsy samples in order to evaluate patient-derived paediatric HGG short-term cell cultures as reliable pre-clinical models.
- To investigate patterns of copy number changes and to identify non-random copy number alterations (CNAs) in paediatric HGG short-term cell cultures to extend the current understanding of the genomic changes in paediatric HGG.
- To identify differentially expressed miRNAs in paediatric HGG short-term cell cultures in comparison to NHA and to understand deregulated signaling pathways influenced by these miRNAs. Unique differentially expressed miRNAs and aberrant signaling pathways associated with paediatric HGG based on their tumour subtype and *H3F3A* mutation status were also identified.
- To understand the role of promoter CpG methylation in downregulation of genes in DIPG short-term cell cultures compared to non-DIPG short-term cell cultures.
- To identify and evaluate dysregulated candidate genes involved in druggable metabolic pathways, particularly genes involved in arginine biosynthesis and PI3K signalling.

CHAPTER 2

Materials and methods

2.1 Samples

2.1.1 Paediatric HGG biopsies and short-term cell cultures

Paediatric HGG biopsy samples were obtained from patients who underwent surgical debulking at Great Ormond Street Hospital (Great Ormond Street Hospital for Children, UK, REC 04/ Q0508/ 98) during 1980 to 2008. All samples were obtained with informed consent and were anonymised. Histological sections of the tumour tissues were examined by two neuropathologists and the samples were diagnosed according to the WHO classification system (Louis et al., 2007). The tumour tissue samples were processed in the laboratory at the Institute of Neurology (London, UK) to set up short-term cell cultures as described by Lewandowicz et al. (2000), and were stored in liquid nitrogen. For this study, all paediatric HGG short-term cell cultures were recovered from liquid nitrogen at low passage (below passage 10) and maintained in 4-(2-hydroxyethyl) piperazine-1-ethanesulfonic acid) (HEPES)-buffered Ham's F-10 media (Life Technologies Ltd, UK) supplemented with 10% foetal calf serum (FCS) (Life Technologies Ltd, UK). Paired fresh frozen biopsy material was also available for 3 samples. The details of paediatric HGG biopsies and short-term cell cultures used in this study are given in Table 1.1.

2.1.2 Cell lines

The adult GBM cell line, LN229 (**ATCC® Number:** CRL-2611™) was generously provided by Dr. Nelofer Syed (Imperial College London, UK) and was cultured in Dulbecco's modified Eagle medium (DMEM) (Life Technologies Ltd, UK) supplemented with 10% FCS and 2 mmol/L L-glutamine (Life Technologies Ltd,

UK). IN699, used as a cell culture model to investigate functional roles of candidate genes *in vitro*, was a cross-contamination of a rhabdomyosarcoma cell line TE-671.

Table 1.1 Pathological data of samples

Samples[1]	Age[2]	Sex[3]	Grade at diagnosis[4]	Location[5]	Sample Type[6]
IN178	13	M	GBM IV	L.Temporal	CC
IN179	13	M	GBM IV	Base of skull	CC
IN1163	0.2	M	GBM IV	R.Parietal	CC
IN1262	14	M	GBM IV	L.Parietal	CC
IN1419	8.5	F	GBM IV	Supratentorial	CC
IN1523	10	F	GBM IV	L.Parietal	CC
IN1566	6.4	F	GBM IV	Posterior Fossa	CC
IN1930	13	F	AA III	Temporal	CC
IN2087	3	M	GBM IV	Brainstem	CC
IN2102	8	M	AAIII	Brainstem	CC
IN2675	14	M	GBM IV	Brainstem	CC
IN3032	9.5	F	AA III	L.Thalamic	CC
IN3046	15.9	M	AA III	L.Frontal	CC
IN3180	9.8	M	AA III	Supratentorial	CC/B
IN3182	10.2	M	GBM IV	R.Parietal	CC/B
IN3183	6.6	M	GBM IV	R.Frontal	CC/B
IN3205	-	M	AA III	R.Temporal	CC

Samples[1]: IN-Institute of Neurology; Age in years[2]; Sex[3]: M-Male, F-Female; Grade at diagnosis[4]: GBM-Glioblastoma multiforme, AA- Anaplastic astrocytoma; Location[5]: L-Left, R-Right; Sample type[6]: CC-cell culture, B- Biopsy.

2.1.3 Control cells

As this study involved cultures of astrocytic origin, a culture of normal human foetal astrocytes (NHA) was used as a normal control (purchased from Cambrex Bio Sciences).

2.2 Routine cell culture methods

Routine cell culture procedures were carried out in a sterile class II Laminar flow cabinet (Telstar, UK) sterilised with 70% ethanol (Sigma-Aldrich, UK) and 1% Trigene (Sigma-Aldrich, UK) solution. A cryovial of cells removed from the liquid nitrogen storage tank was thawed at 37ºC. Cells were transferred to a universal containing 9 ml of media and centrifuged at 1000 rpm for 5 minutes. The supernatant was carefully removed and the cell pellet was re-suspended in 10 ml of fresh media in a 25 cm^2 flask. The cells were incubated at 37ºC in a non-CO_2 incubator and the media was replaced after 24-48 hours. Cells were regularly monitored for any changes in the growth media and cell density. They were usually fed every 3-4 days or when there was a change in the colour of media indicating drop in the pH of the growth medium. After the media was aspirated from the flasks, cells were washed with 1x HBSS and fresh media was added (10 ml of media was added into 25 cm^2 flasks and 20 ml into 75 cm^2 flasks). Cells were routinely passaged to expand their population by providing them with enough nutrients and space to grow and divide. Following aspiration of the media from the culture flask, cells were washed with 1x HBSS (1 ml for 25 cm^2 flask and 5 ml for 25 cm^2 flasks). 1x trypsin (Sigma-Aldrich, UK) (1 ml for 25 cm^2 flask and 2-3 ml for 25 cm^2 flask) was added to the flask, spread evenly to cover the entire surface and incubated at 37ºC for approximately 5

minutes. Cells were checked under the microscope to ensure they were detached and fresh media (3 ml for 25 cm^2 flask and 6 ml for 25 cm^2 flasks) was added to neutralize the trypsin. The contents of the flask were transferred into a sterile universal and centrifuged at 1000 rpm for 5 minutes. After removing the supernatant, the cell pellet was re-suspended in fresh media and transferred to flasks of required sizes (1x 25 cm^2 flask to 1 x 75 cm^2 flask, 1x 75 cm^2 flask to 3 x 75 cm^2 flasks). For freezing down cell pellets, cell pellets were re-suspended in a volume of FCS containing 10% DMSO such that the final cell density was 10^6 cells/ ml. 1 ml of the cell suspension was added to each labelled cryovial (Nalgene Cryoware™ Labware, Roskilde, Denmark) and stored at -80ºC for 24 hours. The vials were then transferred to liquid nitrogen storage tank (-196ºC). All short-term cultures were routinely tested for mycoplasma contamination. Approximately 100,000 cells were cytospun, fixed in ice-cold methanol (Sigma-Aldrich, UK), stained with Hoescht dye (Sigma-Aldrich, UK) and visualised under a fluorescent microscope for the presence of small, bright extranuclear dots.

2.3 Treatment of cells with 5-Aza-2'deoxycytidine (5-AZA)

The demethylating agents, 5-AZA (Sigma-Aldrich Ltd, Dorset, UK) was prepared in double distilled water and filter-sterilised. Cells were seeded in 75 cm^2 flasks at low densities, depending on their division times, such that they reached ~70% confluence at the end of the treatment and incubated overnight at 37ºC. The following day, cells were treated with 5 µM 5-AZA and the treatment was repeated on alternate days for three times to allow the cells to undergo at least 2-3 divisions and enhance the incorporation of the drug into DNA thereby causing efficient demethylation. The

control cells grown in parallel were cultured in media without the drug. Finally, cells were harvested by trypsinisation and centrifuged for 5 minutes at 1000 rpm to collect the pellet. Cells were washed by gentle resuspension in 1 ml phosphate buffered saline (PBS) (Life Technologies, UK) and spun down at low speed. The pellet was kept on ice and used for RNA extraction immediately.

2.4 Chemosensitivity assays

2.4.1 Sulforhodamine B (SRB) cell proliferation assay

The effects of experimental anti-cancer drugs on cellular proliferation were determined by the SRB colorimetric assay. Cells were seeded in triplicate in 96-well plates at a density of 2000 cells/well and incubated overnight at 37ºC. Twenty-four hours later, media was gently aspirated and fresh media (200µl/well) containing varying concentrations of the drug were added. Control cells were grown in media without the drug. The plates were then incubated at 37ºC for 1-9 days. Following incubation, the cells were fixed with 150 µL of 10% (wt/vol) ice-cold trichloroacetic acid (TCA) and incubated for 1 hour at 4ºC. The cells were washed 3-4 times in water, air-dried, and stained with 100 µL of 0.4% SRB (Sigma-Aldrich, UK) (dissolved in 1% (vol/vol) acetic acid) (Sigma-Aldrich Ltd, Dorset, UK) for 15-30 minutes at room temperature. The cells were then rinsed with water to remove the unbound SRB and allowed to air dry. The protein-bound SRB was solubilised in 10mM Tris base solution (100 µl/ well) for 10 minutes and the optical density (OD) values were read at 510 nm with a microplate reader. The results were analysed using MS excel and the IC_{50} value for each drug was calculated.

2.4.2 3-(4,5-dimethylthiazol-2-yl)-2,5-diphenyl-2H-tetrazoliumbromide (MTT) cytotoxicity assay

For MTT assay, cells were seeded in triplicate in 96-well plates at a density of 2000 cells/well and allowed to attach at 37ºC. Twenty four hours after seeding, media was removed from each well and the cells were cultured in media (200 µl) containing varying concentrations of the drug and incubated further at 37^{o}C for the required time. Following incubation, 50 µl of MTT solution (Sigma-Aldrich, UK) (5mg/mL prepared in sterile PBS) was added to the wells and the plates were wrapped in an aluminium foil and incubated for 3-4hrs at 37°C. At the end of the incubation period, media was removed and 80µl of 99.9% DMSO and 20µl glycine buffer were added and the absorbances were read at 540 nm. The percentage viability of cells was calculated and the IC_{50} values of the drug were determined.

2.5 Extraction and assessment of nucleic acids

2.5.1 Genomic DNA extraction

Genomic DNA was extracted from short-term cell cultures and frozen biopsies using DNeasy blood and tissue kit (Qiagen, Manchester, UK), following the manufacturer's instructions. For DNA extraction from cells, a suspension containing 2-3x 10^{6} cells was centrifuged for 5 minutes at 1000 rpm. After removing the supernatant, the pellet was re-suspended in 200 µL PBS, and 20 µl proteinase K was added to facilitate the degradation of proteins. For tissues, approximately 25 mg of tissue was chopped into very small pieces, 180 µl Buffer ATL was added and the sample was homogenised using a syringe and needle to enable efficient lysis. Twenty

µl proteinase K was added, vortexed to mix and incubated at 56ºC with occasional vortexing until the tissue was completely lysed. The homogenised cell/tissue lysate was treated with 4 µl RNase A (100mg/ml) (Qiagen, UK), vortexed to mix and incubated for 5 minutes at room temperature to obtain RNA-free genomic DNA. Two hundred µl of Buffer AL was then added, mixed thoroughly and incubated at 56ºC for 10 minutes. Following incubation, 200 µl of 96-100% ethanol was added, mixed well and the mixture was applied to a DNeasy mini spin column and centrifuged at 8000 rpm for 1 minute. The spin column with membrane-bound DNA was washed with 500 µl Buffer AW1 by centrifugation for 1 minute at 10000 rpm followed by a second wash for 3 minutes at 14000 rpm with 500 µl Buffer AW2 to prevent ethanol carry over to the elution step. Nuclease-free water (Life Technologies, UK) (20-30 µL) was added to the centre of the column, incubated for 1 minute at room temperature and centrifuged at 10000 rpm for 1 minute to elute the DNA.

2.5.2 RNA extraction

RNA was extracted from short-term cultures and frozen biopsies using RNeasy mini kit (Qiagen, Manchester, UK), according to the manufacturer's instructions. For RNA extraction from cell cultures, pellets with approximately 1-2x10^6 cells were disrupted by adding 350 µl Buffer RLT (containing β-mercaptoethanol at 10 µl per 1 ml Buffer RLT) and vortexed to mix. For tissues, 20-25 mg of tissue was cut into small pieces and homogenised in 600 µl Buffer RLT using a syringe and needle. The lysate was centrifuged for 3 minutes at 14000 rpm and the supernatant was carefully transferred to a new nuclease-free microcentrifuge tube. The cleared cell/tissue

lysate was mixed with 1 volume of 70% ethanol (350 µl for cells and 600 µl for tissues) in order to provide appropriate binding conditions for RNA. The sample (not exceeding 700 µl at a time) was applied to an RNeasy mini spin column placed in a 2 ml collection tube and centrifuged for 15 seconds at 10000 rpm. The spin column with membrane-bound RNA was washed with 700 µl Buffer RW1 and 500 µl Buffer RPE in two subsequent steps by centrifugation for 15 seconds at 10000 rpm. Following an additional wash with 500 µl Buffer RPE, the column was centrifuged for 2 minutes at 10000 rpm to prevent ethanol carry over during the RNA elution step. RNA was eluted in 20-30 µl nuclease-free water by centrifugation for 1 minute at 10000 rpm.

2.5.3 Nucleic acid assessment

The quantity and quality of nucleic acids were determined using a NanoDrop 2000 Spectrophotometer (Thermo Scientific, UK). The concentration of nucleic acids was given as ng/µl, based on a modified Beer-Lambert equation, $c = (A*\epsilon)/b$, where c is concentration in ng/µL, A is the absorbance in AU (260 nm), ϵ is the wavelength-dependent extinction coefficient in ng-cm/µL (50 ng-cm/µL for double stranded DNA and 40 ng-cm/µL for RNA) and b is the path length in cm. The quality of the sample was determined by the ratio of absorbance at 260 nm and 280 nm (260/280); a ratio of ~1.8 and ~2.0 were accepted for pure DNA and RNA respectively. The ratio of absorbance at 260 nm and 230 nm (260/230) was used as a second layer to assess the purity of the sample. DNA and RNA were considered highly pure if their 260/230 ratios were higher than their respective 260/280 ratios (generally in the range of 1.8-2.2).

2.6 Polymerase chain reaction (PCR)

2.6.1 Combined bisulfite restriction analysis (CoBRA) PCR

2.6.1.1 Bisulfite modification of genomic DNA

Genomic DNA from short-term cultures and fresh frozen biopsies, along with SAM modified positive controls were bisulfite treated using EZ DNA Methylation Gold kit (Zymo Research, USA) according to the manufacturer's instructions. 130 µL of the CT conversion reagent was added to 20 µL of DNA sample (containing 1µg DNA) and incubated for 10 minutes at 98ºC followed by 2.5 hours at 64ºC. Following incubation, the samples were kept on ice. 600 µL of M-Binding Buffer was mixed with each sample in a Zymo-spin IC column and centrifuged for 30 seconds at 14000 rpm. The column was washed with 100 µL of M-Wash Buffer by spinning for 30 seconds at maximum speed followed by incubation with 200 µL of M-Desulphonation Buffer for 15-20 minutes. After incubation, the column was spun at full speed for 30 seconds and washed twice with 200 µL of M-Wash Buffer. The DNA was eluted in 30 µL of M-Elution Buffer and stored at -20º for later use.

2.6.1.2 DNA methyltransferase modification of DNA

To generate fully methylated positive controls, 5 µg of genomic DNA was mixed with 5 µl NEB buffer, 2µl of DNMT (4 units), 2µl of SAM (New England Biolabs, UK) (32 mM) and PCR grade water to make a final volume of 50 µL and incubated for 2 hours at 37°C.

2.6.1.3 Primer design and TOUCH-UP gradient PCR

CoBRA primers were designed using MethPrimer software (http://www.urogene.org/methprimer/) using specified settings to maximise amplification efficiency. The CGIs of candidate genes were retrieved from UCSC Genome Browser (http://genome.ucsc.edu/cgi-bin/hgGateway) and primers were designed to span up to 300 bp on the CGI. Primers were ensured not to have recognition sequences (*CGCG)* of the restriction enzyme, BstUI (New England Biolabs, UK). The melting temperature was set to between 50 and 60ºC. The products were ensured to have a minimum of 4 CpGs. (The list of primer sequences are provided in Appendix II).

Bisulfite modified DNA (2 µL) was amplified using specific primers in a reaction volume of 40 µl containing 2mM dNTP (Sigma-Aldrich, UK), 2.5 mM MgCl2 (Qiagen, UK), 20µM of each primer (Sigma-Aldrich, UK) and 1 U HotStarTaq DNA polymerase (Qiagen, UK). Touch-UP gradient PCR method, previously developed in the lab (Rowther et al, 2012) was utilised for DNA amplification. HotStarTaq DNA polymerase required an initial activation step of 95°C for 15 min before the start of the cycling. In this method, 8 cycles consisting of 95ºC for 30 seconds, 48ºC for 30 seconds (+0.5ºC every cycle), 72ºC for 1 minute, was performed. The 8-cycle step was repeated five times (40 cycles) followed by final extension for 5 minutes. 10 µL of the PCR products were separated on ethidium bromide-stained (Sigma-Aldrich, UK), 2% agarose gel and visualised using the Gel Doc^{TM}EZ imager (Bio-Rad, UK) to confirm the amplification of the right product.

2.6.1.4 Restriction digestion and Gel electrophoresis

Following confirmation, another 10 µL of the products were digested by BstUI (CGCG) at 37°C for 2 hours at room temperature. The digested products along with equal volumes of corresponding undigested amplification products were electrophoresed on ethidium bromide-stained, 4% agarose gel. SAM modified DNA was used as positive control to assess methylation.

2.6.2 Methylation specific (MS-PCR)

2 µL of bisulphite modified DNA (protocol as described in) was added to a reaction mix consisiting of 2 µL 10xPCR Buffer, 0.4 µL dNTPs, 0.4 µL forward primer, 0.4 µL reverse primer, 0.8 µL MgCl2, 13.8 µL PCR grade water and 0.2 µL HotStarTaq DNA polymerase to make a final volume of 20 µL. For each sample, two sets of PCR reactions were performed with primers specific for methylated sequences and unmethylated sequences. Universal methylated primers and universal unmethylated primers were included as positive and negative controls, respectively. A no template control was used to ensure all reagents were free of contamination. The samples were placed on a thermal cycler; the cycling conditions included initial heat activation of 94ºC for 15 minutes, followed by 30 cycles of 94ºC for 1 minute, 56ºC for 1 minute and 72ºC for 1 minute, then a final extension of 72ºC for 10 minutes. The products were electrophoresed on ethidium bromide stained, 2% agarose gel and visualised using Gel Doc^{TM}EZ imager.

2.6.3 *Semi-quantitative RT- PCR*

2.6.3.1 RT-PCR primer design

RT primers were designed using *Primer 3* software (http://primer3.ut.ee/). Exon sequences of the desired genes were retrieved from Ensembl Genome Browser (http://www.ensembl.org/index.html) and a chunk of it was pasted in *Primer 3.* Primer sizes ranged from 18-25 bases with melting temperature 56-60ºC. (The list of primer sequences are given in Appendix II). To ensure that the product was amplified from cDNA and not from any DNA contaminant, primer pairs were selected in such a way that at least one of the primers encompassed an intron-exon junction. The maximum 3' complementarity was set to 0 to avoid primer-dimers.

2.6.3.2 Complementary DNA (cDNA) synthesis

Complementary DNA (cDNA) was synthesised from total RNA using Quantitect Reverse Transcription Kit (Qiagen, UK). 500 ng- 1µg of total RNA was mixed with 2 µL 7x gDNA Wipeout Buffer and a volume of nuclease-free water to make a final volume of 14 µL and incubated for 2 minutes at 42ºC to eliminate genomic DNA. The samples were then quickly placed on ice, transferred to tubes containing 6 µL of reverse-transcription master mix (1 µL Quantiscript Reverse Transcriptase, 4 µL 5x Quantiscript RT Buffer, 1 µL RT Primer Mix), mixed and incubated for 30 minutes at 42ºC followed by 3 minutes at 95ºC to inactivate Quantiscript Reverse Transcriptase. The reactions were placed on ice for immediate use or at -20ºC for long term storage.

2.6.3.3 PCR amplification and gel electrophoresis

For each RT-PCR reaction, 1µl prepared cDNA was used and a reaction mixture of 20µl was prepared with 2µl 10X PCR buffer (500 mM Tris-HCL), 2.5 mM MgCL2, 2.5 mM dNTP, 0.8 µM of each primer and 1U HotStarTaq DNA polymerase. PCR cycling conditions comprised of an initial activation step at 95ºC for 15 minutes followed by 94ºC denaturing for 30 seconds and annealing of 50-60 ºC for 1 minute for 40 cycles, and final extension at 72 ºC 10 minutes. The house keeping gene, β-actin was used as positive control. The PCR products were electrophoresed on ethidium bromide-stained, 2% agarose gels in 1x TBE buffer (Geneflow, UK) and visualised using Gel Doc^{TM}EZ imager connected to Syngene Gel Documentation and analysis software. A 100 bp DNA ladder (ThermoScientific, UK) was used to confirm the amplification of the product.

2.6.4 Quantitative PCR (Q-PCR)

The expression levels of candidate genes were quantitatively determined using Solaris qPCR Gene Expression assays (Thermo Scientific, UK) with FAM reporter (Ogrean et al., 2010). The assay includes a pre-designed primer-pair and a unique probe for each target under investigation. GAPDH was used as endogenous reference control. One µg of total RNA was reverse transcribed as described in 2.6.3.2. For each test sample, 2 µL of the cDNA was added to a reaction mix consisting of 10 µL 2X Solaris qPCR master mix, 1 µL 20X Solaris Primer/Probe set and 7 µL PCR grade water to make a final volume of 20 µL. A no-template control (NTC) was included to assess any reagent contamination. All reactions were performed in triplicate. The plate was sealed with an optically clear seal, gently tapped to remove

any air bubbles and run on ABI Prism 7900 HT Sequence Detection System (Applied Biosystems, UK). PCR cycling conditions consisted of initial enzyme activation at 95ºC for 15 minutes, followed by denaturation at 95 ºC for 1 minute and annealing at 60 ºC for 1 minute for 40 cycles, and final extension at 72 ºC 10 minutes. Data were exported to MS Excel 2007 for statistical analysis. The expression levels of target gene were normalised to GAPDH and the fold change (as a measure of relative expression) was calculated using comparative CT ($2^{-\Delta\Delta CT}$) method.

2.7 Direct DNA sequencing

For direct sequencing, 100 ng of DNA was amplified using gene-specific primers and HotStarTaq DNA polymerase. The amplification of the desired fragments were verified by gel electrophoresis (2% agarose gel for 1 hour at 120 V). The amplified products were purified from residual primers, unincorporated nucleotides, excess enzyme and salts using GenElute PCR Clean-Up Kit (Sigma-Aldrich, UK) according to the manufacturer's instructions. All centrifugation steps were done at 13000 rpm. Briefly, 500 µL of the Column Preparation Solution was added to a GenElute Miniprep Binding Column placed in a collection tube and centrifuged for 1 minute and the flow through was discarded. Ten µL of the amplification product, mixed with 50 µL of Binding Solution was applied to the spin column and spun down for 1 minute. The column was washed with 500 µL of diluted Wash Solution by centrifugation for 1 minute followed by 2 minutes without the wash solution to remove residual ethanol. A volume of 10-15 µL of nuclease-free water was applied to the centre of the column, incubated at room temperature for 1 minute and centrifuged for 1 minute to elute the DNA. The purified DNA was measured using

NanoDrop 2000 spectrophotometer and a sample volume at a concentration of 1ng/µl per 100 base pairs was used for the sequencing reaction conducted by Source BioScience LifeSciences (Cambridge, UK). The results were analysed using Sequence Scanner v 2.0 (Applied Biosystems Ltd, UK).

2.8 Microarray

2.8.1 CGH microarray

DNA samples were labelled using a genomic DNA ULS labelling kit and hybridised on Agilent 1x 244K CGH arrays (Agilent technologies Inc., USA) according to the recommended protocol for ULS labelling of cells v3.4.

2.8.1.1 Heat fragmentation and labelling

Genomic DNA was extracted from short-term cell cultures and fresh frozen biopsies as described in 2.5.1 with a modification in the final wash step; Buffer AW2 was replaced by freshly prepared 70% ethanol. Commercially available human genomic DNA was used as reference sample. The quantity and quality of both tumour and reference DNA (Promega, UK) were determined using a NanoDrop 2000 spectrophotometer. Good quality tumour and reference DNA samples (200-300 ng) were heat fragmented at 94ºC for 0, 5 and 10 minutes and run on 1% agarose gel to evaluate the integrity of the DNA prior to labelling as well as to determine the fragmentation time required to achieve the optimal DNA fragment size range (1000-3000 bp) for aCGH. Equal amounts (1.5 µg) of tumour DNA and sex-matched reference DNA were individually heat fragmented at 95ºC for 10 minutes followed by incubation on ice for 3 minutes. Tumour and reference DNA were mixed with

Cy3 and Cy5 labelling master mixes (1.5 µL of Cy3/Cy5 in 2 µL 10x Labelling solution) respectively. The mixture was incubated at 85ºC for 30 minutes followed by 4ºC for 3 minutes. The contents were then spun down for 1 minute at 8000 rpm. The labelled DNA was purified by removing the unincorporated ULS-dye in the sample using the Agilent-KREA pure purification column. Initially, the column material was resuspended by brief vortexing, the bottom closure snapped off and centrifuged for 1 minute at 14000 rpm. The column was centrifuged at the same speed for 1 minute with 300 µl of nuclease-free water followed by the labelled DNA (20 µl) and 1.5 µl of each sample was used to determine the concentration and degree of labelling, calculated by the formula: Degree of labelling = (340x pmol per µL dye/ ng per µL gDNAx1000) x100% Cy3 and Cy5 labelled samples were combined appropriately on the basis of the degrees of labelling of the dyes. The optimal Cy3 and Cy5 labelling ranged between 1.75% and 3.5%, and 0.75% and 2.5% respectively with Cy3 minus Cy5 ranging between 1% and 2%.

2.8.1.2 Hybridisation

Blocking agent (100x) (Agilent Technologies, UK) was prepared with nuclease-free distilled water, vortexed and incubated at room temperature for 60 minutes, and stored at -20ºC. Hybridisation master mix (353 µL) was prepared by adding 50 µl of Cot-1 DNA (1mg/mL), 5.2 µl of Agilent 100x Blocking agent, 37.8 µl of DNAse/RNase-free distilled water and 260 µl of 2x HI-RPM Hybridisation buffer (Agilent Technologies, UK). The reaction mix was added to the sample, mixed and quickly spun down in a centrifuge. The contents were incubated for 3 minutes at 95ºC followed by 30 minutes at 37ºC. Following incubation, 520 µL of Agilent-CGH

block was added to remove background noise on the array. A volume of 490 µL of the sample was then hybridised onto the microarray slide, which was assembled in a slide chamber. The chamber was placed in the rotator rack in a hybridisation oven (Agilent Technologies, UK) set at 65ºC and incubated for 40 hours with rotator speed of 20 rpm.

2.8.1.3 Microarray wash

The microarray slide chamber was carefully disassembled in a slide staining dish filled with Agilent Oligo aCGH/ChiP-on-Chip wash Buffer 1 at room temperature The array slide was washed with wash buffer 1 at room temperature for 5 minutes, followed by wash buffer 2 at 37°C for 1 minute, acetonitrile (Sigma-Aldrich, UK) at room temperature for 10 seconds and stabilisation and drying solution (Agilent Technologies, UK) at room temperature for 30 seconds. The slides were place in a slide holder and wrapped in an aluminium foil until ready to be scanned in order to prevent oxidising of the Cy5 dye.

2.8.1.4 Scanning and feature extraction

The slides were scanned on a Agilent DNA Microarray Scanner (model G2565B) (Agilent Technologies, UK) at 5 µM resolution and the resulting images were extracted using Agilent Feature Extraction Software. The software normalises the signal intensity of both dyes at each probe and computes their ratios expressed on a logarithmic scale. It also generates a set of Quality Control (QC) metrics including the Derivative Log Ratio Spread (DLRS), background signal (noise) and signal-to-noise ratio enabling the evaluation of data reliability.

2.8.1.5 Data analysis

Excellent and Good quality data as determined by the QC thresholds were analysed using Agilent CytoGenomics (v2.7, Agilent Technologies Ltd, UK) and Nexus copy number software (Biodiscovery Inc., USA) using various algorirthms as described below.

ADM-2 algorithm

DNA copy number analysis was performed using the ADM-2 algorithm in Agilent cytogenomics software (v3.0.1.1, Agilent Technologies, USA). This algorithm calculates a statistical score, which is a measure of the weighted average of the normalised log ratios from its expected value of zero computed using Derivative Log2 Ratio Standard Deviation algorithms. Aberrant intervals are then identified in samples with consistently low or high log ratios based on their statistical score. The following parameters were used for analysis: stringency threshold=6, minimum absolute average log ratio per region=0.25, maximum number of aberrant regions=100000, minimum number of consecutive probes per region=3, Diploid Peak Centralization-ON, and Combine Replicates (Intra Array) =ON. Genome positions were mapped to NCBI build 36.1 (hg18).

Segmentation analysis

For downstream statistical analysis, normalised raw data were dye swapped and processed using the recommended settings for Agilent FE files in Nexus Copy number (v8.0, Biodiscovery Inc., USA). The replicate probes within an array were combined using the mean values, probe log2 ratios were re-centered to the median,

and the sequential loess method was applied for systematic correction of wave artifact (Lepretre et al., 2010) with the smoothing parameter (default=0.2) in the recommended settings. Robust variance sample QC calculation was performed using the default value of 3, which removes 3% of extreme outliers in the data.

Rank segmentation algorithm

The Rank Segmentation algorithm is similar to the Circular Binary Segmentation (CBS) algorithm (Olshen et. al. 2004), but uses the probe's log-ratio rank order rather than the log-ratio value used in CBS to make copy number calls. For rank segmentation, the significance threshold for segmentation was set at 1.0E-5 and required a minimum number of 3 probes per segment. The maximum contiguous probe spacing (the space between two adjacent probes before making a segment) was set to 1000 kb. The log ratio thresholds for copy number gain and copy number loss were set at 0.2 and -0.23 respectively. High-copy gain and homologous loss were defined by log ratio thresholds of 1.14 and -1.1 respectively. Genome positions were mapped to NCBI build 36.1 (hg18).

FASST2 segmentation algorithm

The FASST2 Segmentation Algorithm is a Hidden Markov Model (HMM) based approach to make copy number calls. However, unlike other common HMM methods for copy number detection it does not restrict the estimation of the copy number state to each probe but uses multiple states to include the possibilities, such as mosaic events. These state values are then used to make copy number calls based on a log-ratio threshold. In this study, FASST2 segmentation algorithm was

performed with significance threshold for segmentation set to 1.0E-5 and requiring a minimum of 3 probes per segment. The maximum contiguous probe spacing was set to 1000 kb. The thresholds for copy number estimation were the same as used for rank segmentation algorithm.

2.8.2 Methylation microarray

2.8.2.1 Illumina Infinium HumaMethylation 450K BeadChip

The microarray-based DNA methylation analysis of DIPG derived short-term cultures was performed with Infinium Human Methylation 450 K BeadChip (Illumina Inc., CA, USA), which enables the quantitative probing of methylation at more than 485,000 CpG dinucleotides located across the genome (including CpG islands, shores, shelves, non-CpG sites and miRNA promoter regions). The beadchip covers 99% of Refseq genes with approximately 17 CpG sites per gene spanning across the promoter, 5'UTR, first exon, gene body and 3'UTR.

2.8.2.2 Labelling, hybridisation and data analysis

DNA was extracted from short-term cultures as described in 2.5.1, and the yield and purity was determined using NanoDrop 2000 spectrophotometer. The subsequent sample processing for methylation analysis using the Infinium HumanMethylation450 BeadChip Kit was conducted at Cambridge genomic services (University of Cambridge, UK) following the manufacturer's recommendations. Briefly, 500 ng of DNA was bisulfite treated to convert unmethylated cytosines to uracil, leaving methylated cytosines unaffected. The modified DNA was amplified, fragmented and hybridised to unique oligomer probes on the HM-450 Beadchip

(Illumina, catalog number: WG-314-1003). After hybridisation, the unhybridised DNA was washed off and the probes on the beadchip were extended using a labelled nucleotide. The BeadChip was fluorescently stained, scanned using HiScan SQ (Illumina) and the methylation signals were extracted with Illumina Genome Studio software. The data were background corrected and normalised and β values were computed using the software.

The normalised data were analysed using Partek genomics suite v 6.6 (Partek Inc., USA) to perform exploratory data analysis. Data were analysed using Microsoft Excel to identify differentially methylated genes on the basis of specified probe beta scores.

2.8.3 Gene expression microarray

2.8.3.1 Affymetric U133A plus microarray

The genome-wide analysis of gene expression profiles of the samples analysed in this study were carried out using Affymetrix U133A plus 2.0 arrays, which have 54675 mounted probes on each array slide representing about 20,000 genes. This represents about 6500 additional genes from the previous Affymetrix platform enabling better characterisation of samples based on their gene expression profiles.

2.8.3.2 Labelling, hybridisation and data analysis

Labelling and hybridisation procedures were carried out using aRNA amplification protocol (Life Technologies, UK) according to recommended protocols of Affymetrix. The first strand cDNA was synthesised by reverse transcription using

8µg of RNA, DEPC-treated water, T7-oligo (dT) primer and kept on ice. The reverse transcription master mix was added and incubated for 2 hours at 42ºC. This was followed by the second strand synthesis for which 80µl of second strand master mix was added and incubated for 2 hours at 16ºC. The cDNA was purified through a series of washes in the spin cartridges. The biotin labelled aRNA was then synthesised by mixing 20 µl of IVT master mix to each sample and incubated for 4-14 hours at 37ºC. A volume of 60µl of nuclease-free water was added to each sample. The aRNA wad then purified by passing the sample through a filter cartridge. The aRNA was then eluted in 100µl of nuclease-free water. The aRNA was then fragmented by mixing the sample with aRNA fragmentation mix and incubated at 94ºC for 35 minutes. The subsequent hybridisation and wash steps were conducted at Nottingham University. The normalised data were log transformed and analysed using Partek Genomics suite (v6.6, Partek Inc., USA).

2.8.4 MiRNA microarray

2.8.4.1 MiRNA extraction from frozen tissues/cell cultures

MiRNA was isolated from frozen tumour tissues or tumour-derived short-term cultures using mirVana miRNA isolation kit (Life Technologies, UK) in accordance with the manufacturer's protocol for isolation of total RNA. The procedure involves disruption of the sample in a lysis solution that stabilises RNA followed by organic extraction of the lysate with Acid: Phenol chloroform and purification of RNA using a glass-fiber filter, specifically formulated for miRNA retention.

For extraction of miRNA from tissues, approximately 30 mg of the tumour tissue was chopped into fine pieces in 300 µl Lysis/Binding Buffer (10 volumes of the Buffer was used per tissue mass) in a weigh boat kept on ice. The sample was transferred to a microcentrifuge tube, and homogenised using a syringe and needle. For miRNA isolation from cell cultures, cells were detached as described 2.2.3 and a suspension containing ~1-2 x 10^6 cells was centrifuged and the pellet was washed in 1 ml PBS by centrifugation at low speed. The supernatant was removed and 300 µl Lysis/Binding solution was added to the pellet, mixed by pipetting to obtain a homogenous lysate. To the homogenised lysate from either sample type, 1/10 volume (30 µl) of miRNA Homogenate Additive was added and mixed by inverting the tube several times and the mixture was left on ice for 10 minutes. Subsequently, a volume of Acid-Phenol: Chloroform equal to the initial lysate volume (300 µl) was added, vortexed for~ 1 minute and spun for 5 minutes at 10000 rpm at room temperature. Following centrifugation, the upper layer (aqueous phase) was carefully recovered in a fresh tube without disturbing the lower layer (organic phase) and 1.25 volumes of room temperature 100% ethanol was then added to the tube and mixed well. The mixture (700 µl at a time) was passed through a Filter Cartridge placed into a collection tube by spinning down the unit for ~15 seconds at 10000 rpm; the flow through containing contaminants was discarded. The filter-bound RNA was washed with 700 µl miRNA Wash Solution 1, followed by two additional wash steps with 500 µl Wash Solution 2/3 one after the other. The filter was transferred to a new collection tube and the RNA was eluted in 20-30 µl pre-heated nuclease-free water by centrifugation for ~30 seconds at 13000 rpm.

2.8.4.2 Labelling and hybridisation

High resolution miRNA expression profiles of paediatric HGG were generated utilising 3D-Gene® miRNA oligo chip (ver.16; Toray Industries, Japan), containing probes representing 1719 human miRNAs selected from the miRBase miRNA database, release 19. Total RNA was isolated from cell cultures and frozen biopsies as described in 2.5.2 and the quantity and quality of RNA determined using NanoDrop 2000 spectrophotometer as described in 2.5.3. The experimental procedures of the microarray were conducted by Cambridge Genomic Services (Department of Pathology, University of Cambridge, UK). Briefly, the integrity of the RNA was determined using Agilent 2100 bioanalyser (Agilent Technologies Ltd, UK) and the quality control reports showing the RNA Integrity Number (RIN) values for each sample were assessed. Good quality RNA samples (250 ng each) were then labelled with Hy5 using the miRCURY LNA Array miR labeling kit (Exiqon, Vedbaek, Denmark) according to the manufacturer's recommendations and subsequently hybridised on the 3D-Gene miRNA chip for 16 hours at 37ºC in a hybridisation oven with a rotator rack set at 250 rpm. Following hybridisation, the oligo chips underwent three stringent washes and the fluorescent signals were scanned with the 3D-Gene Scanner (Toray Industries).

2.8.4.3 Data analysis

The scanned images were processed using the 3D-Gene Extraction software (Toray Industries). The raw data were normalised and the relative expression levels of miRNA were calculated. The normalised data were analysed using Partek Genomics Suite v 6.6.

2.9 Protein detection methods

2.9.1 Protein extraction and quantification

Cells harvested by trypsinisation were washed with PBS and pelleted at 1500 rpm for 5 minutes. Cells were lysed in 100-200 µl (depending on the size of the pellet) of ice-cold RIPA buffer (Life Technologies, UK) containing protease and phosphatase 3 inhibitor cocktail (Roche, Germany) and incubated on ice for 5 minutes. The lysate was sonicated for 30-40 seconds for further cell disruption and proteins were extracted after centrifugation at 14000 rpm for 15-20 minutes at 4ºC. The concentrations of the extracted proteins were determined using a Bio-Rad protein Assay kit (Bio-Rad, UK), with Bovine Serum Albumin (BSA) (Sigma-Aldrich, UK) as the protein standard. The concentration of proteins in each sample was calculated based on the standard curve obtained by plotting absorbance versus protein concentrations of BSA.

2.9.2 Western blotting

Each protein sample (30-100 µg) was prepared in a final volume of 25 µL with loading buffer (4X), 100mM DTT (Sigma Aldrich, UK) and distilled water, and incubated on a heat block for 10 minutes at 96ºC. The proteins were resolved on 6% SDS-PAGE gels in 1x SDS-PAGE running buffer (Geneflow, UK) for 50-60 minutes at 200V. 10 µL of SeeBlue Plus2 Pre-stained Protein Standard (Life technologies, UK) was run on each gel to estimate the molecular weight of protein. Following electrophoresis, the proteins in the gel were transferred onto a polyvinylidene difluoride (PVDF) membrane (Amersham Hybond ™ - P (PVDF membrane), GE

Healthcare, UK) in transfer buffer in a semi-dry transfer unit. The membrane and gel were sandwiched between three layers of blotting papers pre-wet with transfer buffer. The transfer was done for 1.5 hours at 20 V and 200 mA. The membrane was blocked in 5 % non-fat milk for 2 hours at room temperature and probed with the primary antibody of interest by overnight incubation at 4ºC. The unbound antibody was removed by washing the membrane twice with 1xTBST (Geneflow, UK) for 10 minutes. The membrane was then incubated with the appropriate horseradish peroxide-conjugated secondary antibody solution for 1-2 hours at room temperature. Following incubation, the membrane was washed twice in 1xTBST for 10 minutes. The signals were detected using EZ-ECL chemiluminescent detection kit (Geneflow, UK) according to the manufacturer's instructions. The membrane was exposed to X-ray film (Kodak Medical X-ray film, Sigma-Aldrich, UK) in a dark room. The membrane was stripped by washing in 1X TBST for 20-30 minutes and re-probed with anti-mouse β-tubulin monoclonal antibody in order to confirm equal loading of protein.

2.10 Molecular cloning

2.10.1 Preparation of LB agar plates

LB (Luria-Bertani) agar medium was prepared by autoclaving 25 g LB broth (Sigma, UK) and 20 g agar (Sigma, UK) in 1 L of deionised water. Once the media was cooled to 50 ºC, 25 µg/ml kanamycin (Sigma-Aldrich, UK) was added and mixed well. About 15 ml media were poured into 10 cm^2 petri dishes and allowed to solidify at room temperature.

2.10.2 Transformation

To an aliquot of 50 µl DH5α competent cells (Life Technologies, UK), 500 ng of plasmid DNA was added and incubated on ice for 30 minutes. The mixture of DNA and cells were subjected to heat shock by incubation at 42ºC for exactly 30 seconds followed by immediate transfer to ice. A volume of 250 µL SOC recovery medium (Sigma Aldrich, UK), was added to the cells and incubated at 37 ºC for 1 hour with agitation. After incubation, 100 µL of the transformation mixture was spread evenly on an LB agar plate containing 25 µg/mL kanamycin and incubated overnight at 37 ºC.

2.10.3 Plasmid DNA mini-prep

A single bacterial colony from a freshly streaked selective plate was used to inoculate 5 ml of LB broth with 25 µg/mL kanamycin and incubated overnight at 37ºC with agitation. Plasmid DNA was purified from the overnight culture using Plasmid mini prep kit (Norgen biotek corporation, UK) following the manufacturer's instructions.

All centrifugation steps were carried out at room temperature at 14000 rpm. 1.5 mL overnight bacterial culture containing the desired plasmid was centrifuged for 30 seconds. The cell pellet was resuspended in 200 µl of RNAse containing Resuspension Solution AZ and incubated for 5 minutes followed by 250 µl of Lysis Buffer N added to the suspension and gently mixed to denature cellular proteins and genomic DNA. Buffer TN (350 µL) was then added, quickly mixed by inverting the tube several times and spun down for 10 minutes to clarify the lysate. The lysate was

transferred into a spin column placed in a collection tube and centrifuged for 1 minute; the flow through was discarded. The spin column was washed with 600 µL Wash Solution E by spinning down for 1 minute followed by an additional centrifugation for 2 minutes to dry the membrane. Finally, 50 µL of nuclease-free water was added to the centre of the column placed in a fresh collection tube, allowed to stand for 1 minute and centrifuged for 2 minutes to elute the DNA.

2.10.4 Restriction digestion

The purified DNA was quantified using NanoDrop 2000 spectrophotometer, digested with specific restriction enzymes for 2 hours at 37ºC and separated by electrophoresis on 1% agarose gel along with 10 µl of 1 kb DNA ladder to confirm the isolation of the extracted plasmid with the insert based on the molecular weight.

2.10.5 Creating a glycerol stock

To prepare glycerol stocks of bacteria for long term storage, 75 µL of sterile glycerol was added to 425 µL of overnight bacterial culture, mixed, snap frozen in liquid nitrogen and stored at -80ºC.

2.10.6 Plasmid DNA maxi-prep

A single bacterial colony was inoculated into 5 ml LB both and cultured for ~8 hours at 37ºC, shaking at ~300 rpm. The starter culture was diluted 1:500 into 500 ml LB broth and incubated at 37 ºC for 12-16 hours, shaking at ~300 rpm. Purification of plasmid DNA was done using Qiagen maxi prep kit (Qiagen, UK) according to the manufacturer's instructions.

Briefly, bacterial cells containing the plasmid of interest were centrifuged at 6000 rpm for 15 minutes at 4ºC. The pellet was thoroughly resuspended in 10 mL of RNase containing Buffer P1 by vortexing. Ten mL Buffer P2 was added to the lysate and mixed by inverting the tube several times; the mixture was incubated at room temperature for 5 minutes. Following incubation, 10 mL of pre-chilled buffer P3 was added and quickly mixed to incubate on ice for 20 minutes. The solution was centrifuged for 20000 g for 30 minutes at 4ºC. The supernatant containing plasmid was carefully removed and centrifuged again at 20000 g for 15 minutes at 4ºC to prevent suspended material from clogging the QIAGEN-tip. The supernatant was collected in a universal. 10 ml Buffer QBT was applied to a QIAGEN-tip 500 and allowed to drain by gravity flow. The supernatant from the previous step was allowed to pass through the equilibrated QIAGEN-tip and allowed to enter the resin by gravity flow. The QIAGEN-tip was then washed with 2x 30 mL Buffer QC and the DNA was eluted in 15 ml Buffer QF. DNA was precipitated with 10.5 mL room temperature isopropanol and was centrifuged at 15000 g for 30 minutes at 4ºC. The DNA pellet was washed with 5 ml of room temperature 70% ethanol and centrifuged at 15000 g for 10 minutes. The supernatant was carefully removed without disturbing the pellet, which was then air dried for 10-15 minutes and redissolved in 100-200 µl nuclease-free water. The concentration of the purified plasmid DNA was measured using NanoDrop 2000 spectrophotometer. Restriction digests of plasmid DNA were carried out using appropriate restriction enzymes in their optimal buffers and incubated at 37ºC for 2 hours. Agarose gel electrophoresis was performed to confirm the expected insert size.

2.10.7 Transfection

Cells were seeded at a density of 500,000 cells per well in 6-well plates and incubated overnight at 37ºC. The following day, a mixture of 10 µL lipofectamine 2000 transfection reagent (Life Technologies, UK) with 250 µL of OPTI-MEM reduced serum media (Life Technologies, UK) was prepared and incubated for 5 minutes at room temperature. After 5 minutes, the contents of the tube were combined with a mixture of 4 µg of plasmid DNA in 250 µL of OPTI-MEM reduced serum media and incubated for 20 minutes at room temperature. The procedure was repeated with equal concentration of the empty vector in parallel. Equal volumes of the transfection mixture were added to the cells drop-by-drop by simultaneously moving the plate back and forth. The plates were incubated at 37ºC for 24 hours.

2.10.8 siRNA-mediated gene knockdown

RNA interference (RNAi) method was used to transiently knock down genes in paediatric HGG short-term cultures using Silencer select pre-designed siRNAs (Ambion, USA). Cells were seeded in 6-well plates in 2 ml media at a density of 500,000 cells/well and incubated overnight at 37ºC. Following incubation, cells were transfected with siRNA oligos directed against the chosen gene. Cells were mock-transfected with negative siRNA oligos in parallel. Briefly, 20 pmol each of siRNA of interest and negative siRNA was separately diluted in 250 µL OPTI-MEM reduced serum media and mixed gently. To each mixture, 10 µL lipofectamine 2000 reagent (Invitrogen, UK) diluted in 250 µL OPTI-MEM reduced serum media after incubation for 5 minutes at room temperature, was added and incubated for 20 minutes at room temperature to allow the formation of siRNA: Lipofectamine 2000

complexes. Equal volumes (~500 µL) of each mixture were then added to cells by simultaneously moving the plate back and forth. The cells were incubated at 37ºC for 48 hours. Western blot analysis was carried out to confirm the knock down of genes.

2.11 Functional assays

2.11.1 In vitro colony formation assay

The roles of candidate genes on growth properties of tumour cells were determined by *in vitro* colony formation assays. Cells were transfected in triplicate with 4 µg of plasmid DNA and an equal molar amount of empty vector as described in 2.10.7. Forty-eight hours after transfection, cells were harvested by a brief treatment with trypsin/EDTA, centrifuged, resuspended in fresh media and seeded in a serial dilution in petri dishes. Cells were maintained in media containing 250µg/ ml G418 (Geneticin) (Life Technologies, UK) and monitored for formation of colonies. Twenty five days after initial seeding, colonies were washed in PBS and stained with 0.4% crystal violet in 50% methanol. The stained colonies were counted and images were captured.

2.11.2 Migration assay

The migratory potential of tumour cells upon overexpression of candidate genes was investigated with CytoSelect™ 24-Well Cell Migration and Invasion Assay (8 µm, Colorimetric Format) (Cell biolabs, UK) using the Cell migration portion of the kit, according to the manufacturer's instructions. Prior to setting up the assay, the plate was allowed to warm up at room temperature for 10 minutes. Cells were harvested by trypsinisation, centrifuged, resuspended in serum-free media, counted and placed

in the insert at a concentration of 0.5x 10^6 cells/ ml in 300 µl of media (150, 000 cells). In the lower well of the plate, 500 µl of serum containing media was added as a chemoattractant. After incubation at 37ºC for 24 hours, the media from the inserts were carefully aspirated and the non-migratory cells from the inside of the inserts were gently removed using a wet cotton-tipped swab without damaging the membrane. The inserts were then transferred to a clean well containing 400 µl of Cell Stain Solution and incubated for 10 minutes at room temperature to stain the migratory cells. The stained inserts were gently washed several times in water, air-dried, transferred to new wells with 200 µl of Extraction Solution and incubated for 10 minutes on a shaker. One hundred µl of this solution was then added to a 96-well plate and the optical density was read at 560nm using a plate reader (GloMax-Multi+ Microplate Multimode Reader, Promega, UK).

2.11.3 Invasion assay

Invasive abilities of tumour cells after transient knock down of genes were assessed with CytoSelect™ 24-Well Cell Migration and Invasion Assay (8 µm, Colorimetric Format) utilising the Cell Invasion portion of the kit, following the manufacturer's instructions.

The 24-well invasion chamber plate containing polycarbonate membrane inserts (8 µm pore size) was allowed to warm up at room temperature for 10 minutes. Three hundred µl of warm serum-free media was added to the insert to moisten the dried basement membrane layer, coated with matrix solution and incubated at room temperature for one hour. Meanwhile, cells were harvested and suspensions containing 0.5x 10^6 cells/ ml were prepared in serum free media. A volume of 500 µl

of serum containing media was added to the lower well of the plate as a chemoattractant. Following incubation, the rehydration media were gently aspirated without disturbing the basement membrane. Three hundred µl (150,000 cells) of the cell suspension was added to each insert and the plate was incubated at 37ºC for 48 hours. The media from the insert was gently removed and the non-invasive cells from the inside of the insert were gently swabbed using a wet cotton swab, without puncturing the membrane. The inserts were transferred to new wells with 400 µl of Cell Stain solution and incubated for 10 minutes at room temperature. The stained inserts were gently washed several times in water, air-dried and incubated with 200 µl of Extraction Solution in new wells for 10 minutes on a shaker. Optical density of 100 µl of the solution was then determined at 560 nm using a plate reader.

2.12 Statistical tests

2.12.1 Student's t-test

To determine the statistical significance of the difference between two groups by comparing their means, student's t-test was utilised, which was carried out in Graphpad prism software (http://www.graphpad.com/quickcalcs/contMenu/). The difference was considered to be significant if the p-value was less than 0.05.

2.12.2 Fisher's exact test

To assess the difference in the frequency of occurrence of an event between 2 groups, Fisher's exact test was used.

2.12.3 One-way analysis of variance (ANOVA)

To assess the significant differences between the means more than 2 unrelated groups, one-way ANOVA was performed using Partek Genomics suite (v6.6, Partek Inc., USA).

2.12.4 Principal component analysis (PCA)

To assess the level of similarity between 2 samples, PCA was utilised, performed using Partek Genomics suite (v6.6, Partek Inc., USA). For PCA, the dispersion matrix was calculated using correlation method that adjusts the data to be standardised to mean of 0 and standard deviation of 1. The distance between 2 samples indicate the level of similarity between them in high dimensional space. Samples that are close to each other are similar in a large number of the variables, while the samples that are far apart are different in a large of number of the variables.

CHAPTER 3

Evaluation of paediatric HGG-derived short-term cell cultures as *in vitro* models

3.1 Introduction

Despite continuous efforts to identify novel therapeutic targets in paediatric HGG, there has been very limited success in the development of effective chemotherapeutic agents that can significantly prolong the survival of children diagnosed with HGG (Hargrave et al., 2006; Chassot et al., 2012). One of the main obstacles in the validation of molecular targets *in vitro* and the translation of small molecule inhibitors of specific molecular targets from *in vitro* through *in vivo* models to the actual clinical setting in patients is the relative scarcity of well-characterised pre-clinical models.

Fresh frozen tumour biopsies and formalin fixed paraffin embedded tumour tissues have been utilised for molecular biology studies in paediatric HGG for many years. These studies have led to the identification of various candidate genes, which later developed as therapeutically relevant targets (Pollach et al., 2006; Andrae et al., 2008; Bax et al., 2009; Paugh et al., 2013). However, there are fewer investigations conducted in paediatric HGG in comparison to adult glioma mainly due to the lack of availability of tumour tissues. For tumours such as DIPG, surgical procedures are relatively rare owing to the critical location of these tumours in the brainstem (Warren et al., 2012; Fontebasso et al., 2014). Additional issues confined to the paediatric population include difficulties in procuring autopsy consents from parents of the affected children (Angelini et al., 2010).

For several years, established cell lines have been used to evaluate the efficacy of experimental therapeutics *in vitro* and to understand their mechanisms of action.

Although they have contributed to our existing understanding of tumour biology, they do not accurately represent the tumour in the patient as there is a tendency to acquire additional genetic alterations with increasing passage numbers (Gillet et al., 2011). Furthermore, it is difficult to recapitulate the genetic and epigenetic heterogeneity present between individual tumours as well as within the same tumour tissue (Lima et al., 2010; Sottoriva et al., 2013; McGranahan and Swanton, 2015). Studies have shown that primary cultures derived from tumour biopsies can retain a considerable proportion of the characteristic gene expression profiles of the biopsies (Ross and Perou, 2001; Bignotti et al., 2006). Moreover, a study by Yost et al. (2013) reported that GBM-derived cell cultures retained mutation and copy number changes detected in the tumour biopsy.

The aim of this study was to understand whether paediatric HGG short-term cell cultures are representative of the tumour *in vivo* by investigating the genomic profiles of paired biopsies and their derived cell cultures to determine if the characteristic aberrations of the tumour are maintained *in vitro.* In addition, the mutation status of HGG associated genes was ascertained in these paired paediatric HGG samples.

3.2 Results

3.2.1 Comparison of copy number changes in paediatric HGG biopsies and their derived short-term cultures

In order to assess whether copy number alterations (CNAs) in paediatric HGG biopsies are retained in their derived short-term cell cultures, genome-wide copy

number profiles were generated for 2 paediatric HGG biopsies/cell culture pairs (IN3182 and IN3183) using Agilent Human Genome 244K CGH microarrays.

Genomic DNA was isolated from the biopsies and derived short-term cell cultures of the 2 pairs and the purity and integrity of the isolated DNA were verified as described in 2.5.1 and 2.5.3 respectively. Each test sample was sex-matched with the reference normal DNA; the test and the reference DNA were then differentially labelled with Cy3 (green) and Cy5 (red) fluorescent dyes respectively and co-hybridized onto the microarray as described in 2.8. The arrays were scanned using an Agilent SureScan Microarray scanner (Agilent Technologies) and the data were extracted from the resulting Tagged Image File (TIF) images, followed by dye-normalisation and log2ratio calculation using Feature Extraction Software (v9.5, Agilent technologies). The QC report of each sample was carefully assessed to determine the level of background noise on the array. One of the most important QC metrics, which is an indicator of noise, is DLRS that calculates the probe-to-probe log ratio noise of an array. Agilent recommends DLRS value <0.2 for excellent, between 0.20 and 0.30 for good and >0.30 for poor quality arrays. All 4 samples in this analysis had DLRS values <0.20.

To assess the level of similarity between biopsies and their respective derived short-term cell cultures, PCA was performed with 2 paediatric HGG pairs (IN3182 B/CC and IN3183 B/CC) using Partek Genomics suite (v6.6, Partek Inc., USA) as described in 2.12.4. The results of PCA are shown in Figure 3.1 with each dot on the scatter plot representing a sample and X, Y and Z axes representing the first 3 principal components (PC1, PC2 and PC3) respectively. The distance between 2

samples indicate the level of similarity between them in high dimensional space. Samples that are close to each other are similar in a large number of the variables, while the samples that are far apart are different in a large of number of the variables.

PCA showed that the biopsies and their derived short-term cell cultures in both the pairs (IN3182 and IN3183) did not group together but neither did the 2 short-term cell cultures nor the 2 biopsies.

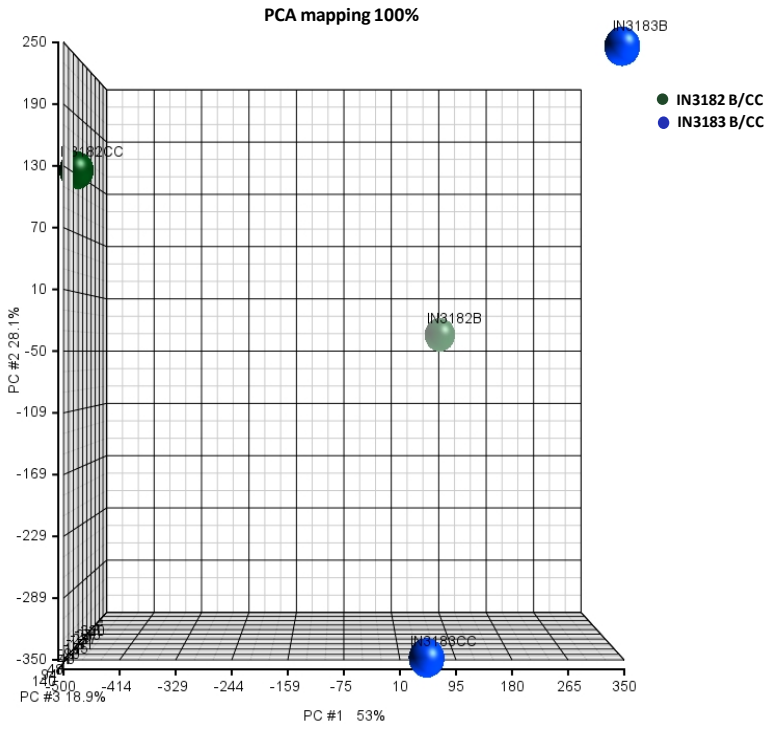

Figure 3.1 Three-dimensional PCA plot of paediatric HGG paired biopsies. PCA plot of IN3182 and IN3183 paired biopsies generated using the first three PCs, PC 1 (53%), PC 2 (28.1%) and PC 3 (18.9%). Each dot on the scatter plot represents a sample. Biopsy and derived short-term cell culture of the same B/CC pair are shown by the same colour. IN3182 pair is represented by green and IN3183 pair is represented by blue. B-biopsy; CC-cell culture.

CNAs in both pairs were identified using the ADM-2 algorithm in Agilent cytogenomics software (v3.0.1.1, Agilent Technologies, USA) as described in 2.8.1.5. The following parameters were used for analysis: stringency threshold=6, minimum absolute average log ratio per region=0.25, maximum number of aberrant regions=100000, minimum number of consecutive probes per region=3, Diploid Peak Centralization-ON, and Combine Replicates (Intra Array) =ON. Genome positions were mapped to NCBI build 36.1 (hg18).

In the IN3182 B/CC pair, there were 35 CNAs consisting of 9 gains, 22 losses and 4 deletions in the biopsy sample while there were 70 CNAs consisting of 51 gains, 8 losses and 11 deletions in its derived short-term cell culture. Approximately 43% (15/35) of the CNAs in the biopsy were maintained in the short-term cell culture. These consisted of 7 gains, 3 losses and 5 deletions and are listed in Table 3.1. The chromosome view illustrating representative CNAs shared by IN3182 B and CC such as gains at 10q21.1 and 20q12-q13.33 and losses at 6q14.1 and 13q21.1 and 20p13 are shown in Figure 3.2 A. There were CNAs involving large regions of chromosomes that were only present in the culture including gains of chromosomes 7 and 9, and loss of chromosome 22 and there were also large CNAs that were not retained in the cell culture such as loss of chromosome 19 (Figure 3.2 B).

Table 3.1 CNAs maintained in IN3182 paediatric HGG short-term cell culture

Chr	Cytoband	Start	Stop	CN event	Probes	Probe median	p-value	Gene Names
chr1	q21.1	147,307,637	147,499,105	Deletion	9	-1.140	1.15E-36	No genes in this region
chr1	q21.3	151,027,357	151,036,494	Deletion	3	-1.779	2.90E-21	*LCE1E, LCE1D*
chr2	p11.2	87,178,812	88,041,911	Gain	13	0.588	4.45E-21	*NCRNA00152, PLGLB2, PLGLB1, RGPD1, RGPD2*
chr6	q14.1	79,035,891	79,080,047	Deletion	3	-2.686	3.42E-23	No genes in this region
chr7	p14.1	38,259,147	38,336,023	Gain	13	1.287	6.50E-14	*TARP*
chr10	q21.1	56,122,417	56,135,443	Gain	3	1.939	1.69E-43	*PCDH15*
chr13	q21.1	56,658,479	56,673,242	Deletion	3	-3.357	3.31E-32	No genes in this region
chr14	q11.2	19,273,289	19,467,571	Gain	25	0.381	8.42E-19	*OR4Q3, OR4M1, OR4N2, OR4K2, OR4K5*
chr14	q11.2	21,662,700	22,052,858	Gain	48	0.491	1.75E-48	No genes in this region
chr14	q32.33	105,105,322	105,349,987	Loss	24	-0.376	2.11E-18	No genes in this region
chr15	q11.2	18,874,663	19,786,714	Loss	35	-0.376	4.01E-12	*GOLGA6L6, GOLGA8C, BCL8, LOC646214, CXADRP2, POTEB, NF1P1, LOC727924*
chr17	q12	31,461,588	31,486,599	Gain	4	1.141	2.78E-23	No genes in this region
chr17	q21.31	41,508,943	41,841,246	Loss	19	-0.317	9.58E-13	*KIAA1267, LRRC37A, ARL17B, NSFP1*
chr20	p13	1,516,966	1,539,201	Loss	3	-1.102	1.23E-12	*SIRPB1*
chr20	q12 - q13.33	38,605,932	62,379,118	Gain	2162	0.818	4.900e-324	*MAFB, TOP1, PRO0628, PLCG1, ZHX3, LPIN3, EMILIN3, CHD6, PTPRT, SRSF6, L3MBTL, SGK2, IFT52, MYBL2, GTSF1L, TOX2, JPH2, C20orf111, GDAP1L1, FITM2, R3HDML, HNF4A, TTPAL, SERINC3, PKIG, ADA, WISP2, KCNK15, RIMS4, YWHAB, PABPC1L, TOMM34, STK4, KCNS1, WFDC5, WFDC12, PI3, SEMG1, SEMG2, SLPI, MATN4, RBPJL, SDC4, SYS1, SYS1-DBNDD2, TP53TG5, DBNDD2, PIGT, WFDC2, SPINT3, WFDC6, SPINLW1, WFDC8, WFDC9, WFDC10A, WFDC11, WFDC10B, WFDC13, SPINT4, WFDC3, DNTTIP1, UBE2C, TNNC2, SNX21, ACOT8, ZSWIM3, ZSWIM1, C20orf165, NEURL2, CTSA, PLTP, PCIF1, ZNF335, MMP9, SLC12A5, NCOA5, CD40, CDH22, SLC35C2, ELMO2, LOC100240726, ZNF334, C20orf123, SLC13A3, TP53RK, SLC2A10, EYA2, ZMYND8, LOC100131496, NCOA3, SULF2, LOC284749, PREX1, ARFGEF2, CSE1L, STAU1, DDX27, ZNFX1, NCRNA00275, SNORD12C, MIR1259, SNORD12B, SNORD12, KCNB1, PTGIS, B4GALT5, SLC9A8, SPATA2, RNF114, SNAI1, UBE2V1, TMEM189-UBE2V1, TMEM189, CEBPB, PTPN1, MIR645, FAM65C, PARD6B, BCAS4, ADNP, DPM1, MOCS3, KCNG1, NFATC2, ATP9A, SALL4, ZFP64, TSHZ2, ZNF217, SUMO1P1, BCAS1, CYP24A1, PFDN4, DOK5, CBLN4, MC3R, C20orf108, AURKA, CSTF1, CASS4, C20orf43, GCNT7, C20orf106, C20orf107, TFAP2C, BMP7, SPO11, RAE1, MTRNR2L3, RBM38, CTCFL, PCK1, ZBP1, PMEPA1, C20orf85, PPP4R1L, RAB22A, VAPB, APCDD1L, STX16, NPEPL1, MIR296, MIR298, GNASAS, GNAS, TH1L, CTSZ, TUBB1, ATP5E, SLMO2, ZNF831, EDN3, PHACTR3, SYCP2, C20orf177, PPP1R3D, CDH26, C20orf197, MIR646, CDH4, MIR1257, TAF4, LSM14B, PSMA7, SS18L1, GTPBP5, HRH3, OSBPL2, ADRM1, LAMA5, RPS21, CABLES2, C20orf151, GATA5, C20orf200, C20orf166, MIR1-1, MIR133A2, SLCO4A1, LOC100127888, NTSR1, C20orf20, OGFR, COL9A3, TCFL5, DPH3B, DIDO1, C20orf11, SLC17A9, BHLHE23, LOC63930, NCRNA00029, LOC100144597, HAR1B, HAR1A, MIR124-3, YTHDF1, BIRC7, NKAIN4, FLJ16779, ARFGAP1, COL20A1, CHRNA4, KCNQ2, EEF1A2, PPDPF, PTK6, SRMS, C20orf195, PRIC285, GMEB2, STMN3, RTEL1, TNFRSF6B, ARFRP1, ZGPAT, LIME1, SLC2A4RG, ZBTB46, C20orf135, TPD52L2, DNAJC5, MIR941-1, MIR941-2, MIR941-3, UCKL1, MIR1914, MIR647, UCKL1AS, ZNF512B, SAMD10, PRPF6, NCRNA00176, SOX18, TCEA2, RGS19, OPRL1, C20orf201, NPBWR2, MYT1, PCMTD2*

CNAs were identified in IN3182 biopsy and its derived short-term cell culture using ADM-2 algorithm in Agilent Cytogenomics (Agilent technologies Inc., USA). CNAs maintained in IN3182 short-term cell culture are shown. Chr-chromosome; CN-copy number.

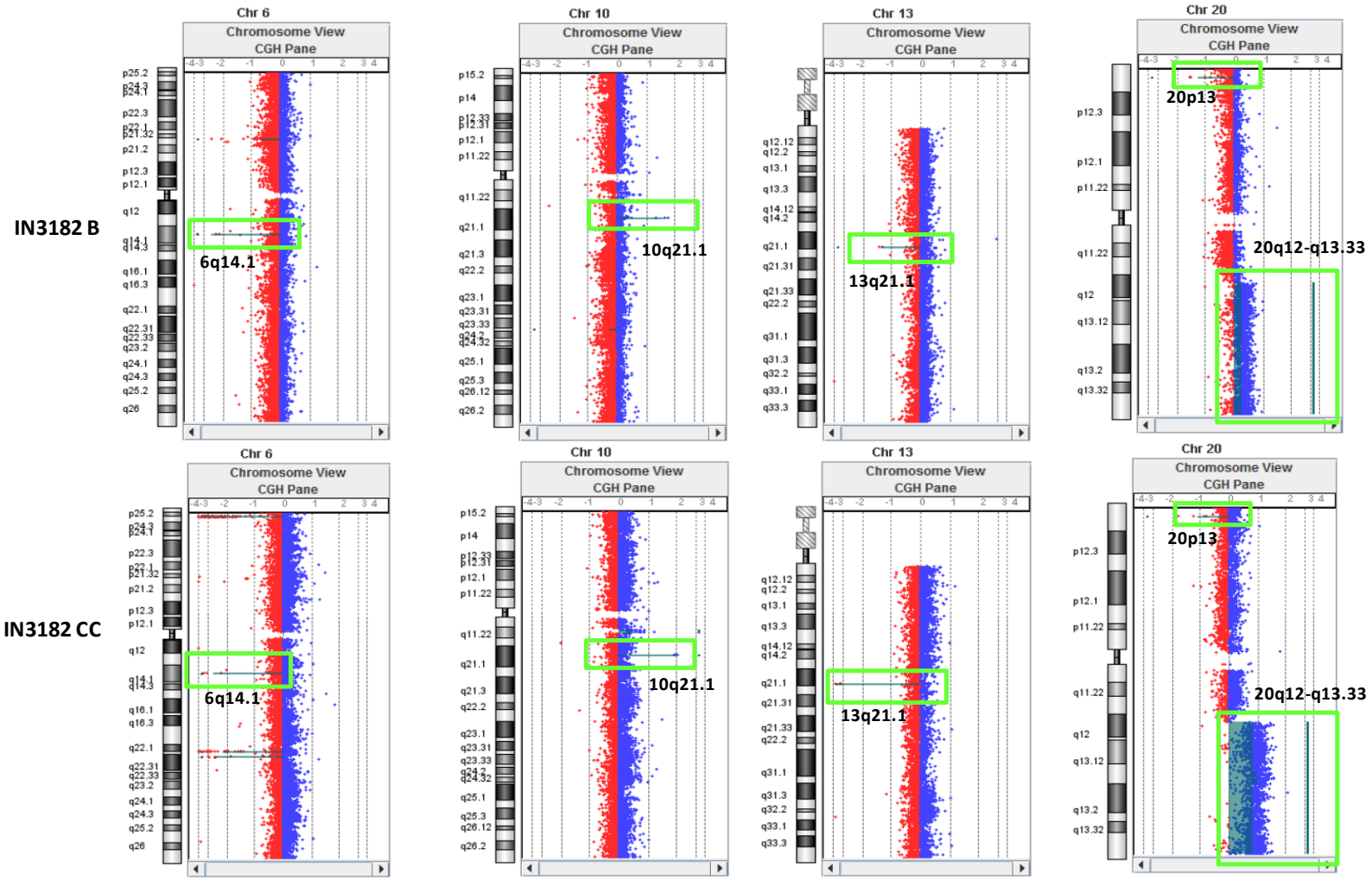

Figure 3.2 Comparison of copy number changes in IN3182 B and CC. A. Copy number changes maintained in IN3182 paediatric HGG short-term cell culture. Copy number analysis was performed in IN3182 B and CC using ADM-2 algorithm in Agilent cytogenomics (Agilent technologies Inc., USA). Each dot represents a single probe on the array. The log-ratio of each probe is plotted against chromosomal position shown on the ideogram on the left. Copy number gain (+1) and copy number loss (-1) shift the log-ratios to the right and left respectively, of the baseline (0). Red indicates copy loss and blue indicates copy gain; Chr- chromosome number; B-biopsy; CC-cell culture. **A. Copy number changes maintained in IN3182 paediatric HGG short-term cell culture.** Representative examples of CNAs maintained in IN3182 short-term cell culture such as -6q41, +10q21.1, -13q21.1, -20p13 and +20q12-q13.33 are shown.

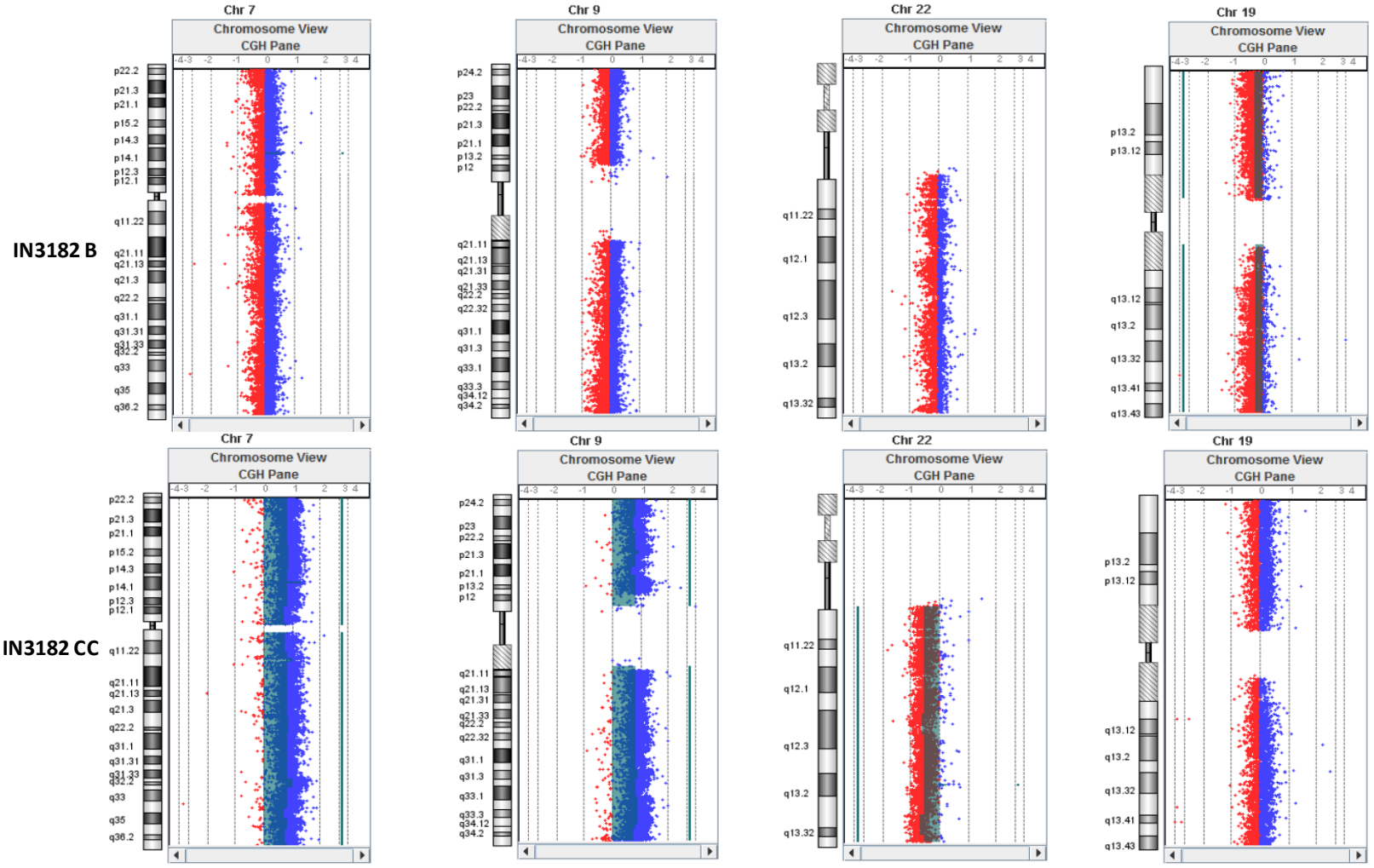

B. Copy number changes in IN3182 CC not representative of IN3182 B. Gains of chromosomes 7 and 9, and loss of 22q were not present in IN3182 B, but were detected in IN3182 CC. Loss of chromosome 19 in IN3182 B was not maintained in IN3182 CC.

In the IN3183 B/CC pair, there were 240 CNAs consisting of 5 high copy gains, 20 gains and 216 losses, while there were only 16 CNAs consisting of 9 gains, 6 losses and 1 deletion in its derived short-term cell culture. Only 6% (14/240) of the CNAs in the biopsy sample were maintained in the cell culture. However, only 2 CNAs were additionally acquired by the cell culture. The CNAs maintained in IN3183 short-term cell culture are listed in Table 3.2 and chromosome views of representative regions are shown in Figure 3.3 A. There were large CNAs in the biopsy that were not maintained in the cell culture such as losses of 9, 17, 19 and 22q (Figure 3.3 B).

Table 3.2 CNAs maintained in IN3183 paediatric HGG short-term cell culture

Chr	Cytoband	Start	Stop	CN event	Probes	Probe median	p-value	Gene Names
chr1	q21.3	150,839,754	150,848,568	Deletion	3	-1.074215	2.06E-13	*LCE3C*
chr1	q23.1	157,138,568	157,178,411	Loss	4	-0.826835	4.33E-13	*PYHIN1*
chr1	q44	246,822,838	246,862,088	Loss	7	-0.838577	4.18E-22	*OR2T10, OR2T11*
chr2	p11.2	89,377,632	90,982,989	Gain	18	0.517607	2.78E-24	No genes in this region
chr2	q13	110,234,644	110,340,992	Loss	15	-0.886895	6.18E-53	*NPHP1, NCRNA00116*
chr3	q11.2	98,483,619	98,517,809	Loss	5	-0.846896	5.10E-16	*EPHA6*
chr3	q26.1	164,038,917	164,101,835	Loss	6	-0.650289	1.26E-13	No genes in this region
chr6	p21.32	32,567,382	32,629,907	Gain	6	0.828468	1.16E-12	*HLA-DRB5, HLA-DRB6*
chr7	p14.1	38,259,147	38,336,023	Gain	13	0.502437	2.01E-16	*TARP*
chr8	p11.23 - p11.22	39,356,595	39,505,315	Gain	20	0.397046	9.43E-16	*ADAM5P, ADAM3A*
chr11	q11	55,118,214	55,195,049	Gain	12	0.449675	6.34E-13	*OR4C11, OR4P4, OR4S2, OR4C6*
chr12	p13.31	9,528,590	9,585,215	Gain	3	1.105748	2.25E-15	No genes in this region
chr14	q11.2	21,505,880	22,046,156	Gain	67	0.451051	8.51E-63	No genes in this region
chr20	p13	1,516,966	1,539,201	Loss	3	-0.985807	3.24E-12	*SIRPB1*

CNAs were identified in IN3183 biopsy and its derived short-term cell culture using ADM-2 algorithm in Agilent Cytogenomics (Agilent Technologies Inc., USA). CNAs maintained in IN3183 short-term cell culture are shown. Chr-chromosome; CN-copy number.

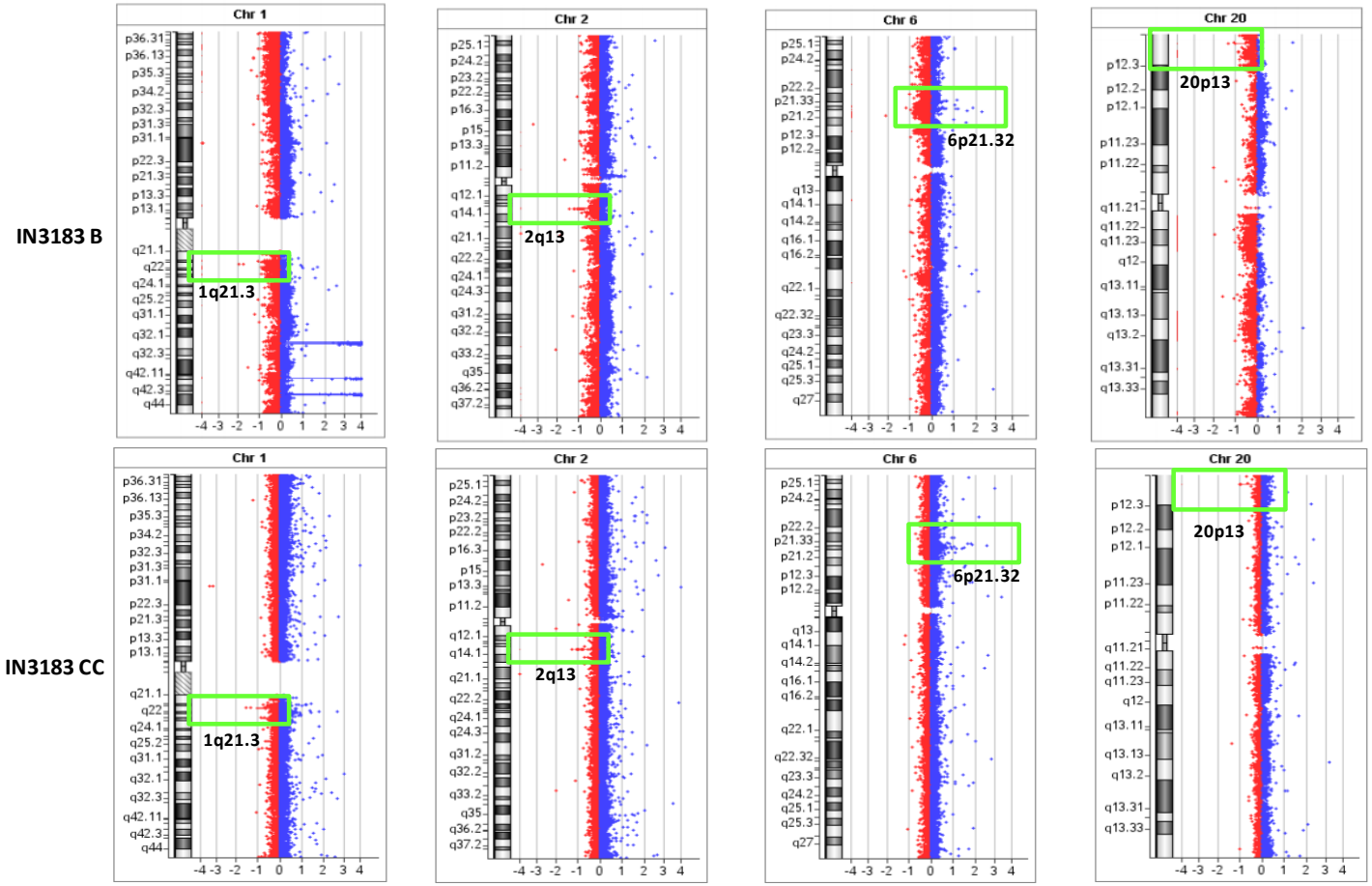

Figure 3.3 Comparison of copy number changes in IN3183 paired biopsy. A. CNAs maintained in IN3183 paediatric HGG short-term cell culture. Copy number analysis was performed in IN3183 B and CC using ADM-2 algorithm in Agilent cytogenomics (Agilent technologies Inc., USA). Each dot represents a single probe on the array. The log-ratio of each probe is plotted against chromosomal position shown on the ideogram on the left. Copy number gain (+1) and copy number loss (-1) shift the log-ratios to the right and left respectively, of the baseline (0). Red indicates copy loss and blue indicates copy gain; Chr- chromosome number; B-biopsy; CC-cell culture. **A**. Representative examples of CNAs maintained in IN3183 short-term cell culture such as -1q21.3, -2q13, +6p21.32 and -20p13 are shown.

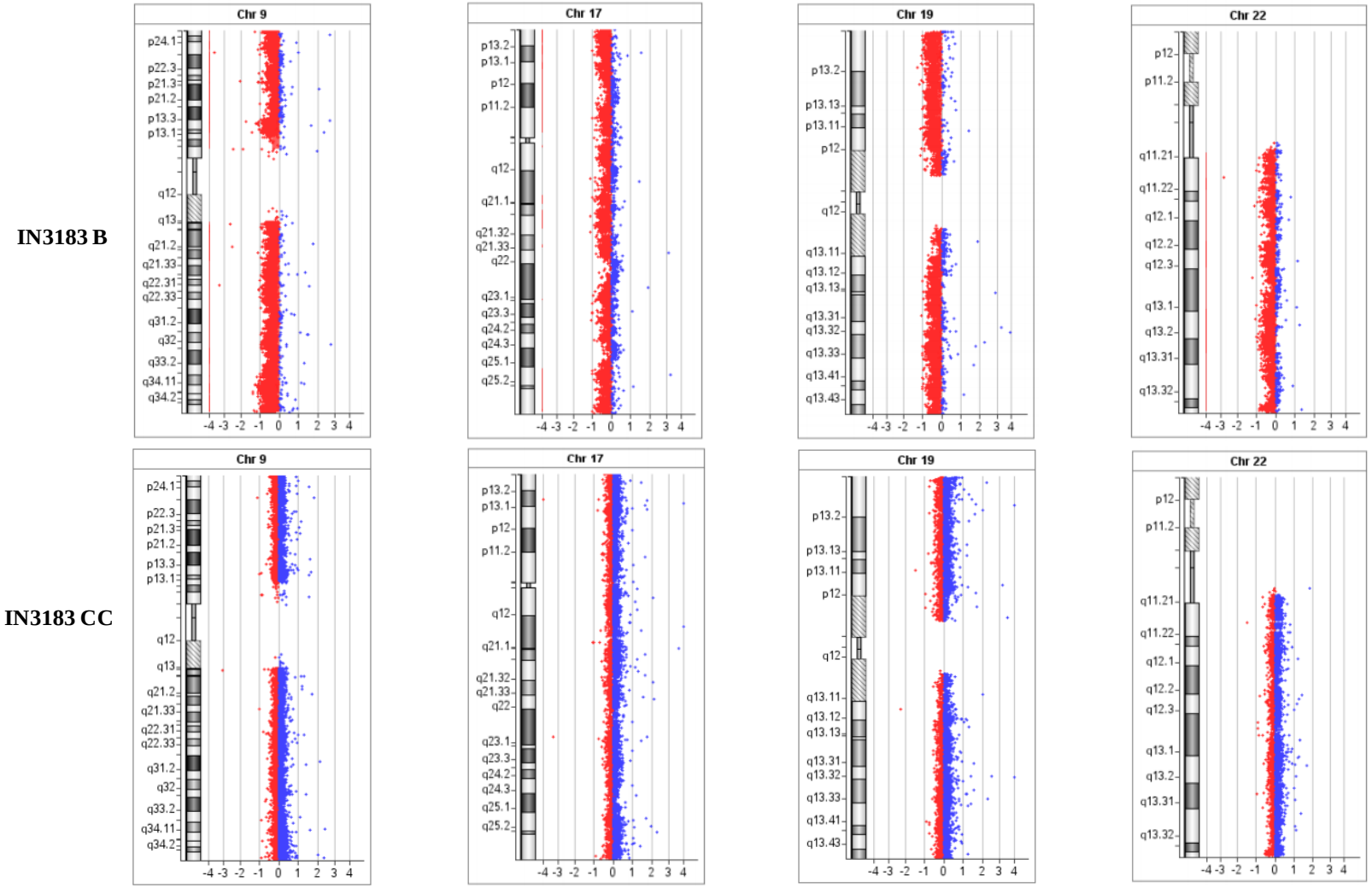

igure 3.3 B. Copy number changes in IN3183 CC not representative of IN3183 B. Losses of chromosomes 9, 17, 19 and 22q present in IN3183 B were not maintained in IN3183 short-term cell culture.

3.2.2 Comparison of gene expression profiles of tumour biopsies and their derived short-term cell cultures

To investigate whether paediatric HGG short-term cell cultures can represent the tumour *in vivo* at the mRNA level, 3 paediatric HGG short-term cell cultures and their parent biopsy samples (IN3180 B/CC, IN3182 B/CC and IN3183 B/CC) were profiled for gene expression changes using Affymetrix U133A plus 2 arrays as described in 2.8.3. The median log transformed data of 54675 mounted probes on each array from all 3 pairs were filtered to remove the control probes (n=61) prior to further statistical analysis using Partek Genomics suite (v6.6, Partek Inc., USA). PCA was performed using the remaining 54614 informative probes in all 3 paired samples to visually assess the level of similarity between the cell culture and biopsy sample in each pair, as described in 2.12.4. The results of PCA are illustrated as a 3-D scatter plot in Figure 3.4.

PCA revealed that the biopsies and derived short-term cell cultures of IN3180 and IN3183 pairs had different gene expression profiles and did not group together. Moreover, the gene expression profiles of IN3180 CC and IN3183 CC were relatively similar although their respective biopsies were different from each other, suggesting that artificial culture conditions may significantly alter gene expression profiles. Interestingly, the biopsy and the derived short-term cell culture in the third pair (IN3182 B/CC) had similar expression profiles and were clustered together.

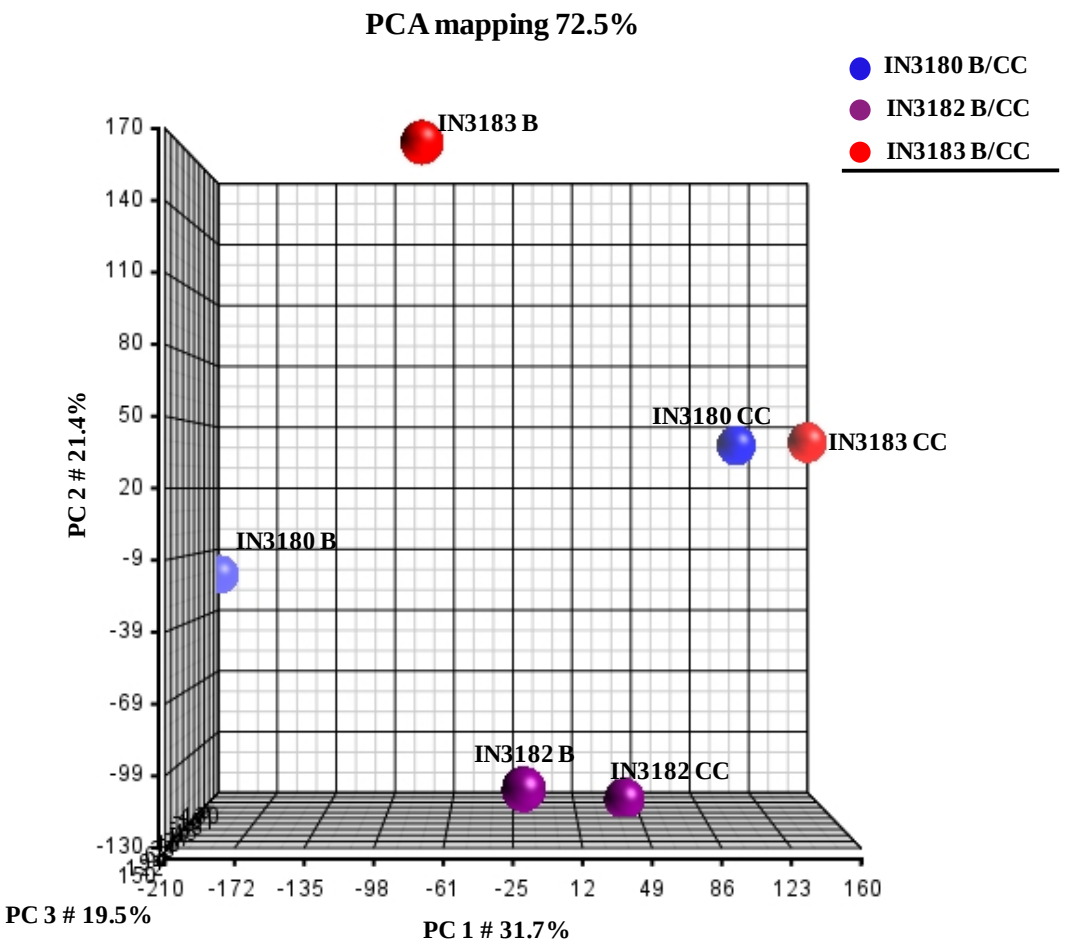

Figure 3.4 PCA plot of 3 paediatric HGG biopsies and their derived short-term cell cultures. PCA scatter plot of 3 paediatric HGG biopsies and their derived short-term cell cultures plotted using the first three PCs (PC1=31.7 %, PC2=21.4 % and PC3=19.5 %). Each dot on the PCA plot denotes a sample. Biopsy and derived short-term cell culture of individual pairs are represented using similar coloured dots. B-Biopsy, CC-cell culture.

Unsupervised hierarchical clustering of 54614 probes in 3 paediatric HGG paired biopsies was used to cluster samples according to the similarity of their expression profiles. The analysis was performed using the average linkage hierarchical clustering algorithm with Euclidean distance as similarity metric. The results are illustrated as a dendrogram in Figure 3.5, with samples having similar expression profiles clustered together. The dendrogram demonstrated that 2 biopsy samples

(IN3180 B and IN3183 B) were independent of any other sample, while the remaining samples were divided into 2 clusters. The shorter cluster had the 2 cell cultures of IN3180 and IN3183 paired samples clustered together, while the other cluster consisted of IN3182 B and CC.

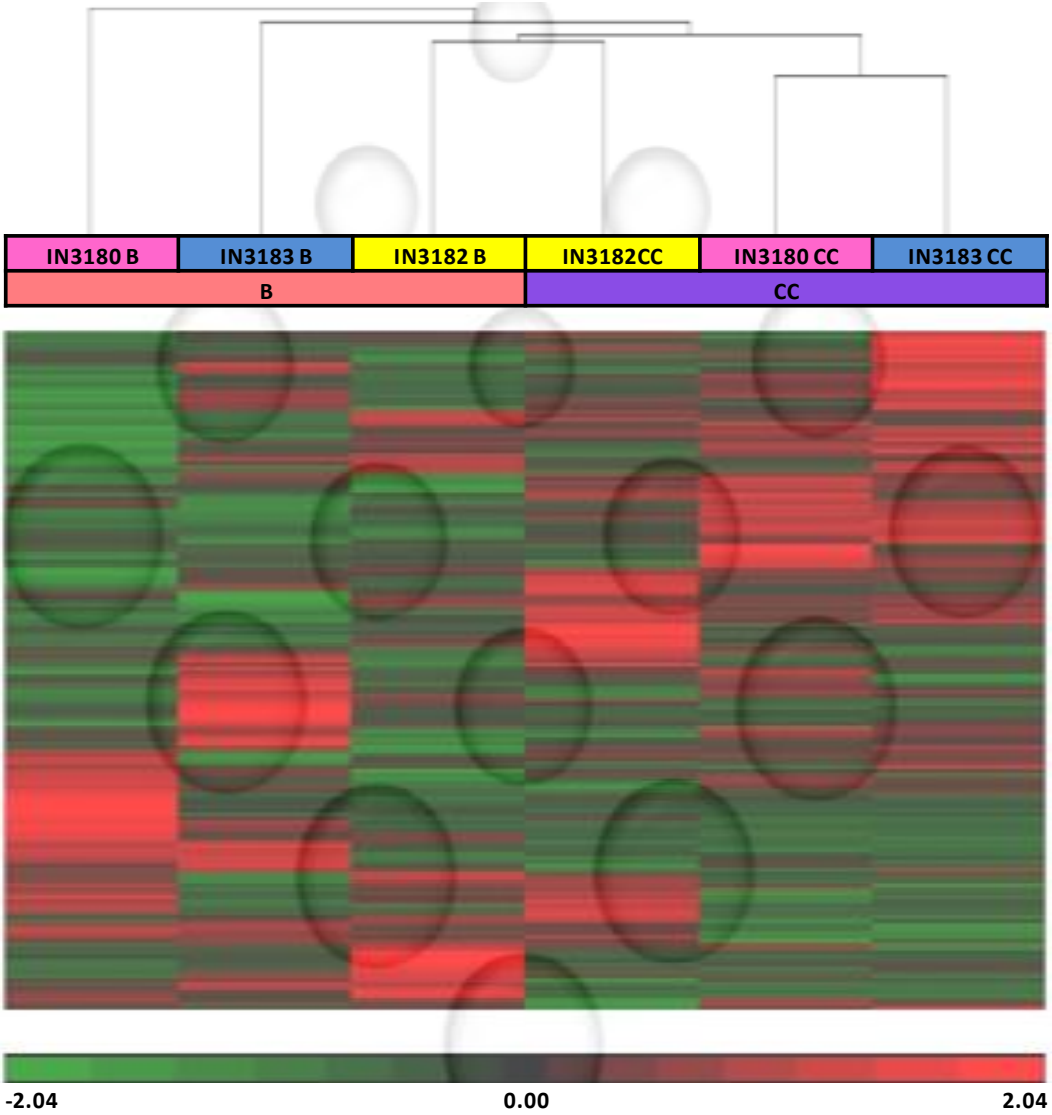

Figure 3.5 Unsupervised hierarchical clustering of paediatric HGG paired biopsies. Unsupervised hierarchical clustering analysis was performed using 54675 probes across 3 paediatric HGG paired biopsies using average linkage hierarchical clustering algorithm with Euclidean distance as similarity metric. Each row on the dendrogram represents the expression of a single probe and each column represents the expression levels for a single sample. Green and red colours indicate high and low expression respectively. B and CC in the IN3182 pair cluster together; B and CC in the IN3180 and IN3183 pairs do not cluster together. B-biopsy; CC-cell culture.

To determine the effect of cell culture-induced changes on cellular pathways, probes with >2-fold differential expression in the cell cultures compared to the biopsies in the 3 paediatric HGG paired samples were identified using one-way ANOVA test. A comparison of the number of differentially expressed probes in all 3 pairs is shown in Figure 3.6.

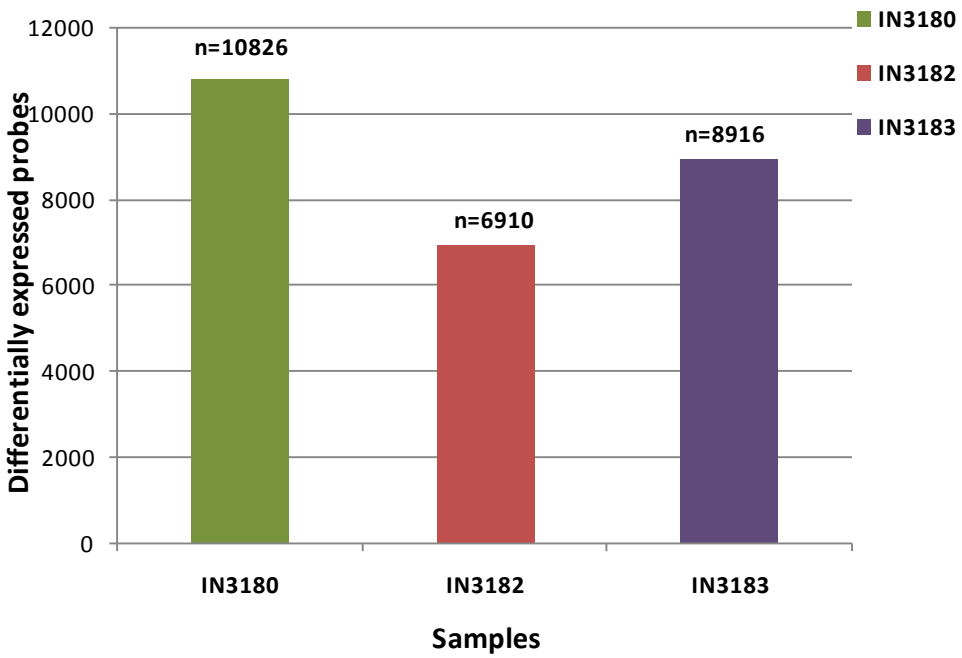

Figure 3.6 Comparison of differentially expressed probes in cell cultures compared to biopsies in paediatric HGG paired samples. Probes with 2-fold change in expression in paediatric HGG short-term cell cultures in comparison to their biopsies were identified in 3 paediatric HGG paired biopsies using one-way ANOVA test. The graph is plotted with paediatric HGG paired biopsies on x-axis and differentially expressed probes on y-axis. n represents the number of differential probes in cell culture compared to biopsy

For the IN3180 pair, there were 10826 differentially expressed probes, of which 4732 probes were upregulated and 6094 probes were downregulated in the cell culture. There were 8916 differentially expressed probes in IN3183 CC compared to

its biopsy consisting of 4116 upregulated and 4800 downregulated probes respectively. In comparison, IN3182 CC had only 6910 differentially expressed probes, of which 3431 were upregulated and 3479 were downregulated, confirming the relatively higher level of similarity between the cell culture and the biopsy in comparison to the other paired samples. The probes that were commonly upregulated in all the 3 pairs are displayed in a Venn diagram in Figure 3.7. Similarly, the probes that were commonly downregulated in all the 3 pairs are displayed in a Venn diagram in Figure 3.8. Overall, there were 1498 differentially expressed probes that were common to all 3 pairs. These comprised 677 upregulated and 821 downregulated probes.

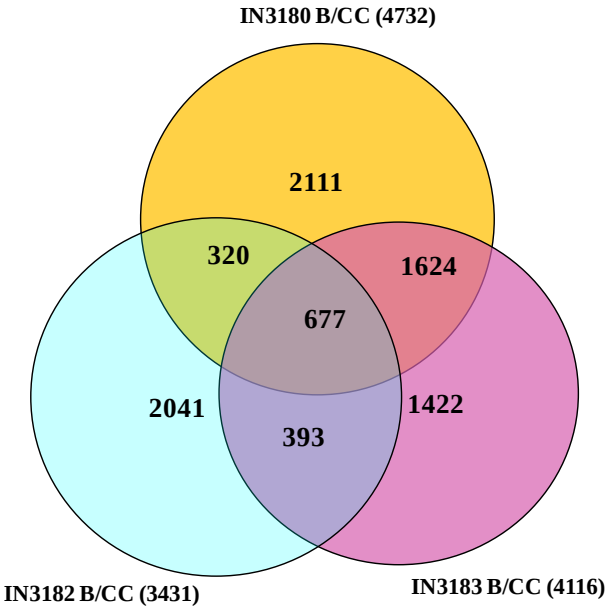

Figure 3.7 Venn diagram of commonly differentially upregulated expression probes in 3 paediatric HGG paired biopsies. Differentially upregulated (>2-fold) miRNAs in short-term cell culture compared to its parent biopsy were identified in 3 paediatric HGG paired biopsies (IN3180, IN3182 and IN3183) using one-way ANOVA test. The number of upregulated miRNAs in each pair is shown in parentheses.

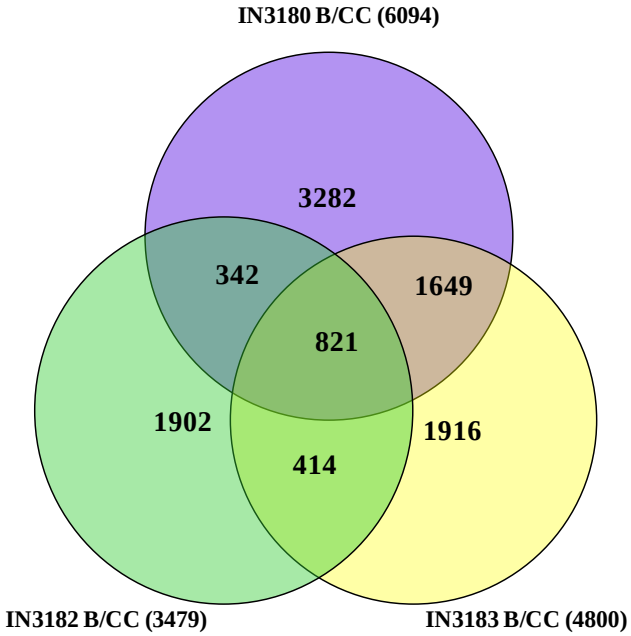

Figure 3.8 Venn diagram of commonly differentially downregulated expression probes in 3 paediatric HGG paired biopsies. Differentially upregulated (>2-fold) miRNAs in short-term cell culture compared to its parent biopsy were identified in 3 paediatric HGG paired biopsies (IN3180, IN3182 and IN3183) using one-way ANOVA test. The number of downregulated miRNAs in each pair is shown in parentheses.

To determine the effect of cell culture-induced changes on cellular pathways, Gene Ontology (GO) analysis was performed using the commonly differentially expressed probes in all 3 pairs and the enrichment scores for the most affected pathways were calculated. The key biological processes associated with these probes were cell proliferation (2.91), cellular process (0.90), pigmentation (0.78), growth (0.66), viral reproduction (0.25), and metabolic process (0.16) (Figure 3.9). Thus, it can be understood that the increase in the number of differentially expressed probes in cell cultures compared to the biopsies was induced by artificial culture conditions. However, the degree of differential expression of large number of probes was within 2-fold, indicating that paediatric HGG short-term cell cultures retain gene expression changes present in their parent biopsies.

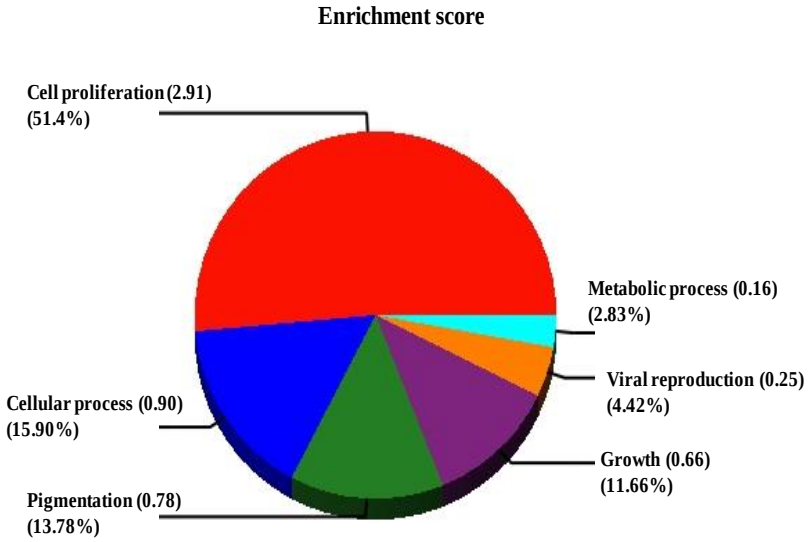

Figure 3.9 GO biological processes associated with commonly differentially expressed probes in 3 paediatric HGG paired biopsies. The commonly differentially expressed probes in 3 paediatric HGG short-term cell cultures (IN3180, IN3182 and IN3183) compared to their respective biopsies were used to perform GO analysis. The enrichment scores of the key biological processes are shown. The percentages in parentheses indicate the fraction of the total number of genes present in the GO biological process.

3.2.3 Comparison of miRNA expression profiles of tumour biopsies and their derived short-term cell cultures

To examine whether paediatric HGG short-term cell cultures retain the miRNA expression profiles of their parent biopsy samples, global miRNA expression profiles were generated for 3 paediatric HGG paired biopsies (IN3180 B/CC, IN3182 B/CC and IN3183 B/CC) using 3D-Toray miRNA Oligo chip as described in 2.8.4. The median-normalised data from all 3 paired biopsies provided by Toray Industries were filtered to remove unreliable probes that did not have any detected dye signal in biopsies and cell cultures for all 3 pairs. The remaining 807 informative probes were used for miRNA expression analyses using Partek Genomics Suite (version 6.6;

Partek Inc., USA). PCA was performed using the 3 paired samples to visually assess the level of similarity in the expression profiles between biopsies and their derived short-term cell cultures as described in 2.12.4. The results of PCA are illustrated as a 3-D scatter plot in Figure 3.10.PCA showed that the biopsy and the derived short-term cell culture in all 3 pairs (IN3180, IN3182 and IN3183) did not have similar expression profiles. However, the biopsy samples and the cell culture samples also did not form separate groups. Two paediatric HGG short-term cell cultures (IN3182 CC and IN3183 CC) had relatively similar miRNA expression profiles compared to the rest of the samples.

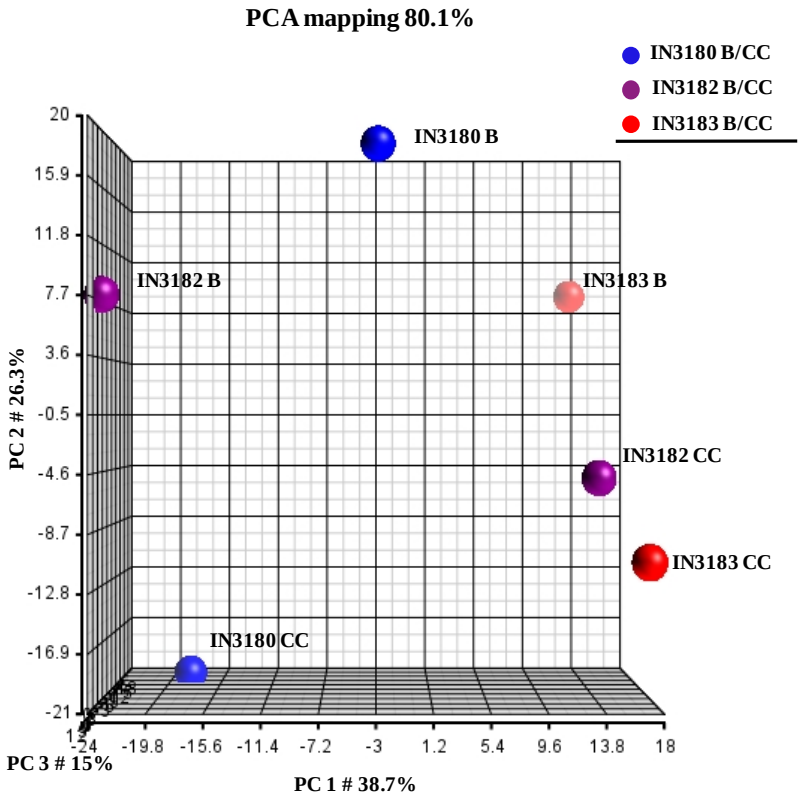

Figure 3.10 PCA plot of 3 paediatric HGG biopsies and their derived short-term cell cultures. PCA scatter plot of 3 paediatric HGG biopsies and their derived short-term cell cultures, plotted using the first three PCs (PC1=38.7 %, PC2=26.3 % and PC3=15 %). Each dot on the PCA plot denotes a sample. Biopsy and derived short-term cell culture of individual pairs are represented using similar coloured dots. B-Biopsy, CC-cell culture.

Unsupervised hierarchical clustering was performed using 807 reliable probes in all 3 paediatric HGG paired samples with the distance between 2 clusters calculated by the average linkage hierarchical clustering algorithm with Euclidean distance as a similarity metric. The results are illustrated as a dendrogram in Figure 3.11, with samples having similar expression profiles clustering together.

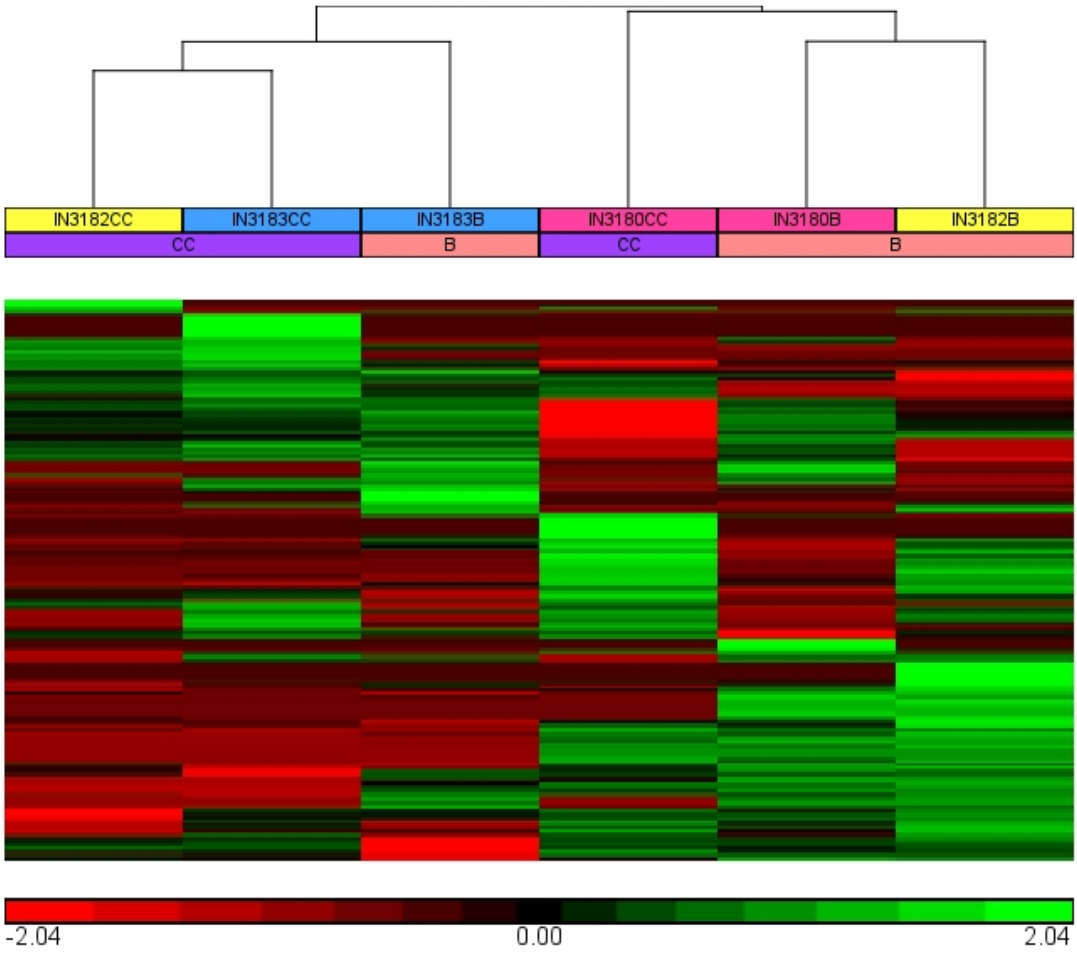

Figure 3.11 Unsupervised hierarchical clustering of paediatric HGG paired biopsies. Unsupervised hierarchical clustering analysis was performed using 807 probes across 3 paediatric HGG paired biopsies using average linkage hierarchical clustering algorithm with Euclidean distance as similarity metric. Each row on the dendrogram represents the expression of a single probe and each column represents the expression levels for a single sample. Green and red colours indicate high (2.04) and low (-2.04) expression respectively. B-biopsy; CC-cell culture.

The dendrogram showed that the 3 paediatric HGG paired biopsies formed 2 clusters, one containing IN3180 B, IN3180 CC and IN3182 B, with relatively similar expression profiles between the 2 biopsies (IN3180 B and IN3182 B), and the other containing IN3183 B and CC and IN3182 CC, with the 2 cell culture samples (IN3182 CC and IN3183 CC) having relatively similar expression profiles. The greatest difference in the miRNA expression profiles between the tumour biopsy and its derived short-term cell culture was observed in the IN3182 pair. The remaining pairs (IN3180 and IN3183) had comparatively similar expression profiles.

To further compare the miRNA expression profiles between the biopsies and their respective derived short-term cell cultures, the number of differentially expressed miRNAs in the cell culture sample compared to its parent biopsy sample was determined in each pair using one way ANOVA test. The miRNA probes with no detected signal intensities in both the biopsy and its derived short-term cell culture in each pair were excluded from the analysis. The miRNAs with 2-fold change in expression in the cell culture sample compared to its biopsy in IN3180, IN3182 and IN3183 pairs were determined. These miRNAs were then discounted from the total number of probes analysed in each paired biopsy to obtain the fraction of miRNAs that did not vary significantly in the cell culture sample compared to its biopsy. A comparison of the similarities and differences in the number of differentially expressed miRNAs in the cell culture sample compared to its parent biopsy across the 3 pairs (IN3180, IN3182 and IN3183) are shown in Figure 3.12. There were large numbers of miRNAs with 2-fold change in expression in the cell culture compared to its respective biopsy in all 3 paediatric HGG paired biopsies, demonstrating the influence of

cell culture conditions on miRNA expression profiles. The highest number of differentially expressed miRNAs was identified in the IN3182 pair (471miRNAs) followed by the IN3180 (438 miRNAs) and IN3183 (328 miRNAs) pairs respectively. However, a considerable fraction of miRNAs had less than 2-fold change in expression in the cell culture compared to the biopsy sample in each paediatric HGG paired biopsy, indicating that short-term cell cultures do retain some of the miRNA expression changes of the tumour *in vivo*. The IN3183 pair had the highest number of miRNAs (306) with less than 2-fold differential expression in the cell culture compared to its parent biopsy, followed by the IN3180 (250) and IN3182 (207) pairs respectively.

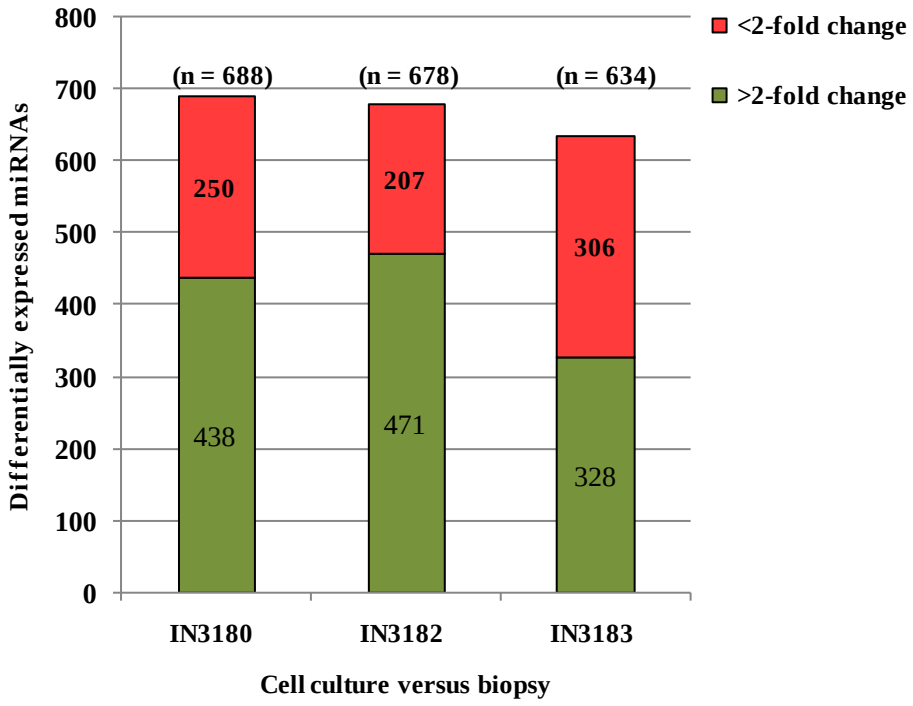

Figure 3.12 Comparison of differentially expressed miRNAs in paediatric HGG paired biopsies. MiRNAs with 2-fold differential expression in CC compared to biopsy in 3 paediatric HGG paired biopsies are shown. Green indicates miRNAs with more than 2-fold change in expression in CC compared to B. Red indicates miRNAs with less than 2-fold change in expression in CC compared to biopsy. 'n' indicates the total number of informative miRNAs used for the analysis in each pair (ie, miRNAs with detectable signal intensities in either B or CC). B-Biopsy, CC-Cell culture.

To investigate the effect of cell culture conditions on the miRNA expression profiles, the commonly differentially expressed miRNAs in all 3 paediatric HGG short-term cell cultures were identified. The upregulated miRNAs and the downregulated miRNAs in all 3 pairs were identified independently. There were 191 upregulated miRNAs in the IN3180 pair, 146 miRNAs in the IN3182 pair and 172 miRNAs in the IN3183 pair. There were 15 miRNAs that were commonly upregulated in all 3 cell culture samples (Figure 3.13).

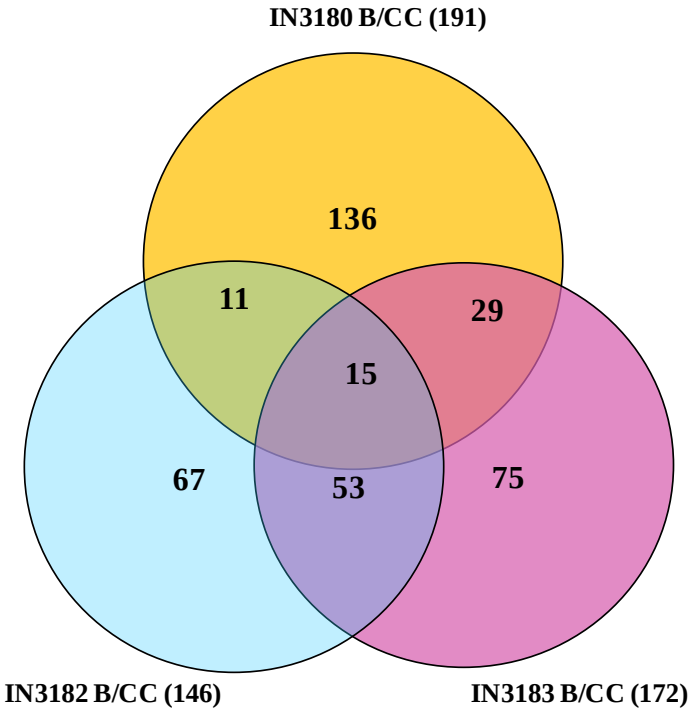

Figure 3.13 Venn diagram of commonly upregulated miRNAs in 3 paediatric HGG paired biopsies. Differentially upregulated (>2-fold) miRNAs in short-term cell culture compared to its parent biopsy were identified in 3 paediatric HGG paired biopsies (IN3180, IN3182 and IN3183) using one-way ANOVA test. The number of differentially upregulated miRNAs in each pair is shown in parentheses.

Similarly, there were 247, 325 and 156 downregulated miRNAs in the IN3180, IN3182 and IN3183 pairs respectively. There were 36 miRNAs that were commonly downregulated in all 3 pairs, as shown in Figure 3.14.

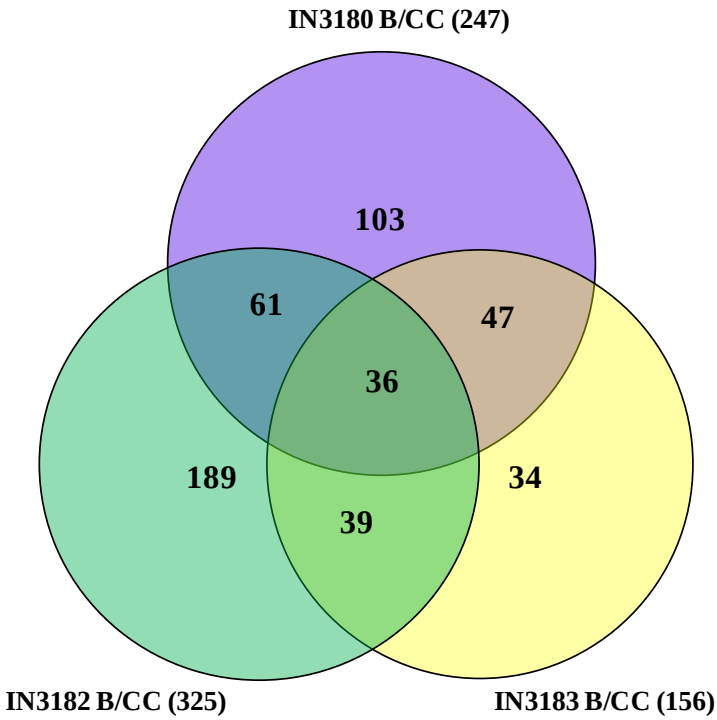

Figure 3.14 Venn diagram of commonly downregulated miRNAs in 3 paediatric HGG paired biopsies. Differentially upregulated (>2-fold) miRNAs in short-term cell culture compared to its parent biopsy were identified in 3 paediatric HGG paired biopsies (IN3180, IN3182 and IN3183) using one-way ANOVA test. The number of differentially downregulated miRNAs in each pair is shown in parentheses.

As illustrated in the Venn diagrams, there were 51 miRNAs that were commonly differentially expressed in cell cultures compared to biopsies in all pairs, of which 15 were upregulated and 36 were downregulated.

To understand the cellular pathways affected by miRNA expression changes induced by cell culture conditions, the commonly differentially expressed miRNAs were used

to perform KEGG pathway analyses using the pathways union module in DIANA-miRPath v3.0, (http://www.microrna.gr/miRPathv3). The putative mRNA targets of the deregulated miRNAs were identified using microT-CDS target prediction algorithm (minimum threshold of 0.80), which identifies miRNA targets both in 3'untranslated region (3'UTR) and in coding sequences (CDS) (Reczko et al, 2012). This resulted in 38 significantly enriched pathways ($p<0.05$). The 10 most significantly enriched pathways associated with the commonly differentially expressed miRNAs in the 3 paediatric HGG pairs are listed in Table 3.3. These included prostate cancer, ErbB signaling pathway, lysine degradation, pathways in cancer, adherens junction, TGF-beta signaling pathway, ubiquitin-mediated proteolysis, transcriptional misregulation in cancer, endometrial cancer and PI3K-Akt signaling pathway.

Table 3.3 KEGG pathways associated with commonly differentially expressed miRNAs in paediatric HGG paired biopsies

KEGG pathway	p-value	Genes	miRNAs
Prostate cancer	0	52	14
ErbB signaling pathway	0	46	15
Lysine degradation	1.11E-16	20	14
Pathways in cancer	5.55E-16	137	11
Adherens junction	5.55E-15	47	12
TGF-beta signaling pathway	2.02E-14	40	11
Ubiquitin mediated proteolysis	1.47E-13	61	9
Transcriptional misregulation in cancer	8.41E-13	76	11
Endometrial cancer	5.00E-12	30	13
PI3K-Akt signaling pathway	2.36E-11	129	11

Significantly enriched KEGG pathways associated with 51 commonly differentially expressed miRNAs in 3 paediatric HGG paired biopsies were identified using the 'pathways union' module (microT-threshold 0.8) in DIANA mirPath v3.0. The 10 most significantly enriched pathways (p-value<0.05 (FDR ON)) are shown. The table is ranked by enrichment p-value.

3.2.4 Mutation analysis of key genes in paediatric HGG short-term cell cultures

To investigate if paediatric HGG short-term cell cultures maintained gene mutations present in biopsies, mutation status of key genes *H3F3A, HIST1H3B, BRFAV600E* and *ACVR1* involved in paediatric HGG tumourigenesis were determined in 3 paediatric HGG biopsy/cell culture pairs and 14 additional paediatric HGG-derived short-term cell cultures (including 3 DIPG-derived short-term cell cultures) using direct sequencing as described in 2.7. The sequencing data were analysed using ABI Sequence Scanner v1.0. Heterozygous mutations in *H3F3A* involving an amino acid change from lysine to methionine (K27M) were detected in 2 out of 18 (11%) paediatric HGG short-term cultures, which included 1 DIPG (IN2675) (33%) and 1 non-DIPG (IN1566) (13%) short-term cell cultures. The sequencing chromatogram of a representative K27M mutant short-term cell culture is shown in Figure 3.15 A. *H3F3A* (K27M) mutations were not detected in any paediatric HGG biopsy/cell culture pairs included in this analysis. Also, none of the samples had mutations in *HIST1H3B* involving K27M substitutions. A mutation in *BRAF* leading to amino acid change from valine to glutamic acid (*BRAFV600E*) was identified in 1 (1/18, 6%) paediatric HGG short-term cell culture (IN179) (Figure 3.15 B). Mutations in *ACVR1,* which encodes activin A type I receptor *ALK2* have been identified predominantly in DIPGs (Taylor et al., 2014). In this study, none of the DIPG and non-DIPG short-term cell cultures had *ACVR1* mutations. None of the paired samples had mutation in any of the genes analysed. The summary of mutation analyses of all 4 genes in paediatric HGG paired biopsies and short-term cell cultures is provided in Table 3.4.

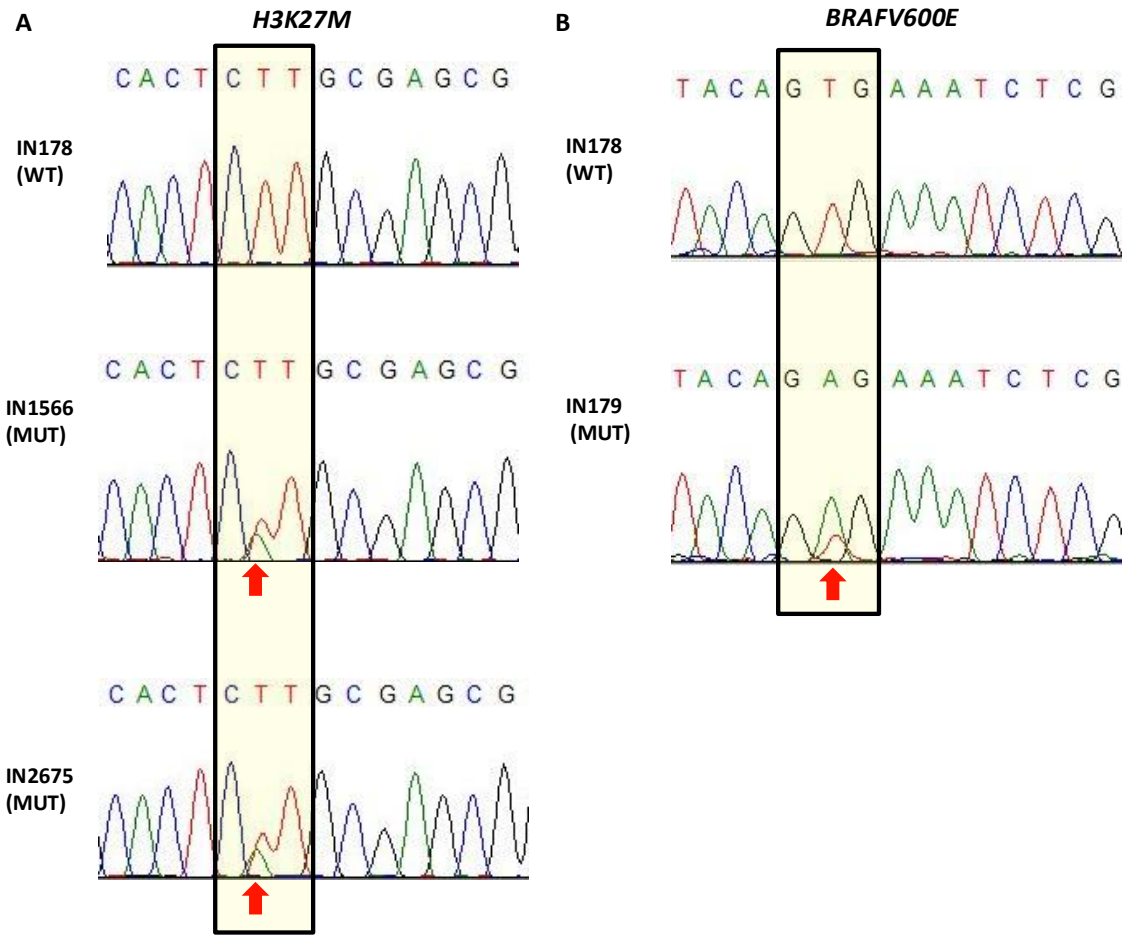

Figure 3.15 Mutations in *H3F3A* and *BRAF* in paediatric HGG short-term cell cultures. Sanger sequencing chromatogram of representative *H3F3A* or *BRAF* heterozygous mutations in paediatric HGG short-term cell cultures are shown. **A.** Mutation in *H3F3A* involving lysine to methionine (K27M) in IN1566 and IN2675. **B.** Mutation in *BRAF* involving valine to glutamine amino acid substitution (V600E) in IN179. Arrow denotes mutated nucleotide. IN178, IN179 and IN1566 are non-DIPG short-term cell cultures and IN2675 is a DIPG short-term cell culture. WT-wild type; MUT-mutant.

Table 3.4 Mutation status of *H3F3A, HIST1H3B, BRAF* and *ACVR1* in paediatric HGG short-term cell cultures

Samples	*H3F3A*	*HIST1H3B*	*BRAF*	*ACVR1*
Paediatric HGG short-term cell cultures				
IN178	WT	WT	WT	WT
IN179	WT	WT	**V600E**	WT
IN1163	WT	WT	WT	WT
IN1262	WT	WT	WT	WT
IN1419	WT	WT	WT	WT
IN1523	WT	WT	WT	WT
IN1566	**K27M**	WT	WT	WT
IN1930	WT	WT	WT	WT
IN2087	WT	WT	WT	WT
IN2102	WT	WT	WT	WT
IN2675	**K27M**	WT	WT	WT
IN3032	WT	WT	WT	WT
IN3046	WT	WT	WT	WT
IN3180	WT	WT	WT	WT
IN3182	WT	WT	WT	WT
IN3183	WT	WT	WT	WT
IN3205	WT	WT	WT	WT
Paediatric HGG biopsy samples				
IN3180	WT	WT	WT	WT
IN3182	WT	WT	WT	WT
IN3183	WT	WT	WT	WT

The mutation status of *H3F3A, HIST1H3B, BRAF* and *ACVR1* in 17 paediatric HGG short-term cell cultures and 3 biopsy samples is listed. DIPG are highlighted in red and non-DIPG is highlighted in blue.

3.3 Discussion

The feasibility of using primary tumour cultures for identification of novel candidate genes (tumour suppressors and/or oncogenes) and as experimental models for *in vitro* testing of therapies has often been debated. Genome-wide copy number, gene and miRNA expression analysis of paediatric HGG paired biopsies conducted in this study revealed variation between the tumour biopsies and their derived short-term

cell cultures. However, a considerable proportion of the genetic changes in the biopsies were maintained in their derived short-term cell cultures.

Paediatric HGG short-term cell cultures retain CNAs in culture

The comparative analysis of copy number profiles of the one of paired tumour samples, IN3182, demonstrated that although there were differences in the copy number profiles between cell culture and biopsy, the cell culture retained a considerable proportion of CNAs that were present in the tumour biopsy (~43%). Conversely, for the IN3183 paired sample, only ~6% of CNAs detected in the biopsy were also present in the culture. It is evident from the chromosome views of CNAs shown in Figures 3.2 A and B that the aCGH profile of IN3183 biopsy DNA sample had a characteristic 'wave' pattern of probe distribution. The data analysis of this sample resulted in over-segmentation indicating that many of these CNAs were not true copy number events. 'Waviness' in aCGH data is a common technical artefact that results mainly from the GC content of the probes and the samples or from other factors that are not very clear (Marioni et al., 2007; Sykulski et al., 2013). Although there are few algorithms that can correct the GC waves (van de Wiel et al., 2009; Leo et al., 2012), there is often the risk of large CNAs in samples to be smoothed away. As this analysis involved comparison of 2 samples, smoothing was not done so that the experimental bias can be kept minimal. The technical solutions to eliminate such wave patterns are not clear. Therefore, the experiment was repeated and a second profile was generated for this biopsy sample. Although the new aCGH profile had a DLRS value of 0.14 and fitted into the excellent QC range, the issue of waviness was not resolved (Appendix II). Overall, the large disproportion in the number of CNAs

in the IN3183 pair compared to IN3182 pair is likely to be an overrepresentation of the actual number of CNAs as segmentation algorithm often generates too many segments when such waviness is detected (van de Wiel et al., 2009; Przybytkowski, et al., 2011)

Other possible reasons for the observed variation in both paired samples could be attributed to the intratumour heterogeneity of the tumour biopsy sample, from which the short-term cell culture was established. Intratumour heterogeneity is a characteristic property of glioma and has been demonstrated at both cellular and molecular levels (Bonavia et al., 2011). In a study by Sottoriva et al., (2013), genome-wide assessment of CNAs in 38 tumour fragments from nine patients showed that all tumours exhibited variations in shared and unique copy number aberrations. In addition, it was observed that 2/4 fragments from a patient had no *PDGFRA* aberrations while the remaining 2 fragments displayed gain of the same region. The heterogeneous property of tumour cells may develop from expansion of clonal subpopulations of cells and incorporation of mutations during tumour progression (Greaves and Maley, 2012). The copy number profile of a tumour-derived short-term cell culture may therefore represent only a fraction of the various subpopulations present in the tumour tissue. It was also found that in one of the paired tumour biopsies (IN3182), there were additional CNAs in the cell culture compared to the biopsy such as gain of whole chromosome 7, which may have occurred due to artificial culture conditions. A similar finding was reported by Sareen and colleagues (2009) who observed chromosome 7 and 19 trisomy in human neural progenitor cell cultures. On the other hand, although IN3183 cell culture

retained only about 6% of CNAs present in its biopsy and also failed to maintain large regions of deletions, it was interesting to observe that there was minimal acquisition of additional CNAs in this culture (2 CNAs).

As both the biopsy DNA samples analysed in this study were extracted using the same protocol, it is less likely that the artefact may have got introduced during the DNA extraction step. Therefore, it can be speculated that source of this artefact may be the actual tumour tissue as biopsies are often a mixture of non-neoplastic cells, blood and lipid substances. A fresh preparation of DNA sample from a different area of the biopsy may have resulted in a smoother aCGH profile. However, due to concerns of scarcity of tumour samples, the experiment couldn't be repeated.

Paediatric HGG short-term cell cultures retain gene expression changes of tumour in vivo

The gene expression profiles of paediatric HGG paired tumour samples investigated here showed large number of differentially expressed genes between the biopsies and their derived short-term cell cultures in 2/3 pairs, indicating the possible influence of culture conditions on gene expression profiling. The differentially expressed genes were involved in cell proliferation, growth and metabolism, indicating the possible influence of the availability of oxygen and nutrients in the *in vitro* environment that enables cells to acquire additional gene expression changes under artificial culture conditions. Such changes could be attributed to tumour heterogeneity. In the study by Sottoriva et al. (2013), 51 tumour fragments from 10 patients were profiled for gene expression changes using microarrays and each sample was classified into proneural, classical, mesenchymal and neural subtypes according to an 840-gene signature

(Verhaak, 2010). It was found that tumour samples taken from the same patient could be stratified into at least two GBM subtypes in about 60% (6/10) of the patients. However, it was found that a considerable number of expression probes did not vary more than 2-fold in the derived cell-cultures in both the pairs compared to their biopsies indicating that paediatric HGG short-term cell cultures do retain expression changes of the tumour *in vivo.* A study by Potter et al. (2009) has shown that although differential gene expression was induced in short-term cell cultures derived from paediatric PA in comparison to their biopsies, a molecular signature of 608 genes could differentiate PA and adult GBM tumours irrespective of the sample source (cell culture or biopsy). As large number of differentially expressed genes did not differ more than 2-fold between the cell culture and the biopsy, these cultures can be used to evaluate the efficacy of drugs designed to act on specific molecular targets and may also indicate better likelihood of these responses to be translated to the tumour *in vivo.*

MiRNA expression changes in paediatric HGG short-term cell cultures are representative of tumour in vivo

The utility of tumour-derived short-term cell cultures for the investigation of miRNA expression changes in paediatric HGG have not been explored yet. The miRNA expression profiles of paediatric HGG paired biopsies analysed in this study showed large differences between the biopsies and their derived short-term cell cultures. One of the reasons for this could be the difference in the intrinsic stability of miRNAs in cell populations. Bail et al., (2010) reported that miRNAs possess distinct intrinsic stabilities, which determine the level of miRNAs in different cells. They

demonstrated that the processing of some miRNAs from primary and preliminary to mature stages continued to occur even after termination of transcription. The changes in miRNA expression in the tumour cell cultures relative to their biopsies could also be due to epigenetic changes like promoter hypermethylation in miRNA genes leading to transcriptional silencing. Abnormal methylation of genes under artificial culture conditions have been previously reported in various cancer cell lines (Varley et al., 2013). The increased downregulation of miRNAs can in turn induce gene expression changes further leading to alterations in expression levels of other miRNAs. This is supported by the observation that large numbers of differentially expressed (≥2-fold) miRNAs common to all 3 pairs were downregulated than upregulated (36 versus 15). The commonly differentially expressed miRNAs (2-fold change) in the cell cultures compared to their biopsies were involved in several cancer-related pathways demonstrating their role in providing the cells with increased growth potential in culture. However, paediatric HGG short-term cell cultures also maintained changes in miRNA-expression that were present in the tumour biopsies as illustrated by PCA and hierarchical clustering of the 3 paired biopsies. In addition, there was also a considerable number of miRNAs that had less than 2-fold differential expression in the cell-culture compared to the biopsy in each pairs.

Paediatric short-term cell cultures retain signature gene mutations of paediatric HGG

In the current study, the mutation status of 4 vital genes (*H3F3A, HIST1H3B, BRAFV600E* and *ACVR1*) involved in paediatric HGG tumourigenesis was evaluated

in 17 paediatric HGG short-term cell cultures and 3 biopsies. Of the 4 genes, mutations were detected in *H3F3A* and *BRAFV600E* in 11% (2/18) and 6% (1/18) paediatric HGG short-term cell cultures respectively. Recurrent somatic mutations in *H3F3A* encoding histone H3.3 are relatively more frequent in DIPGs than supratentorial HGGs (Wu et al., 2012). Although this study was constrained by very small sample numbers, the frequency of *H3F3A* mutation detected in this study was also higher in DIPG (33.3%, 1/3) compared to the non-DIPG short-term cell cultures (6.6%, 1/15). The overall low frequency of mutations detected in the cohort of paediatric HGG short-term cell cultures investigated in this study may be due to the artificial culture conditions that select only certain populations of cells in culture. However, the mutation burden in paediatric HGG is generally very low (Paugh et al., 2010). Therefore, extending this investigation in additional paired samples to find biopsies with mutations and then determine if they are retained in culture may provide better insights into whether paediatric HGG-derived short-term cell cultures maintain gene mutations.

Limitations

One of the main limitations of this investigation is the small sample number that was available. Inclusion of more paired tumour biopsies as well as several segments of the same tumour biopsy for comparison studies may provide better insights into the influence of tumour heterogeneity in introducing variation in genomic profiles of paediatric HGG short-term cell cultures. In addition, studies comparing tumour-derived short-term cell cultures over a number of passages may provide information to assess the effect of culture conditions on such variation over time.

3.3 Conclusions

Distinct genetic and epigenetic changes have been identified to drive paediatric HGG tumourigenesis depending on the tumour location, indicating the selective pressures of specific tumour environments (Jones and Baker, 2014). Hence, cell culture models that can closely resemble the actual tumour conditions should be essentially developed in order to identify and target the key tumour-associated genomic aberrations in paediatric HGG. Nevertheless, paediatric HGG short-term cell cultures with specific molecular defects may serve as preclinical models for *in vitro* testing of targeted therapeutics. For instance, IN179 short-term cell culture in this study could be used as an *in vitro* model for evaluating the efficacy and mode of action of *BRAFV600E* inhibitor such as PLX4720. Thus, well-characterised tumour-derived short-term cell cultures may be used as *in vitro* models for molecular studies with careful evaluation. This is particularly useful to extend the molecular studies on paediatric HGG, which remain largely understudied in comparison to other tumours.

CHAPTER 4

Genome-wide investigation of copy number changes in paediatric HGG short-term cell cultures

4.1 Introduction

Paediatric HGG are highly aggressive and extremely resistant to existing cancer therapeutic strategies such as surgery, chemo and radiotherapy. In comparison with adult glioma, HGG in children (including anaplastic astrocytoma and GBM) occur at much less frequency. However, paediatric HGG exhibit similar histological characteristics to those of adult HGG and patients of all ages have extremely poor prognosis (Puget et al., 2012). The median survival rate remains 12-15 months for patients with paediatric HGG and only 9-12 months for children with DIPG (Jones et al, 2012). Patients with DIPG exhibit particularly poor prognosis due to the highly infiltrative growth in the most critical part of the brain making surgical resection of these tumours virtually impossible (Vanan and Eisenstat, 2015). There is a compelling need for novel therapies or manipulation of existing treatment strategies to improve their clinical outcome.

Paediatric HGG is a highly complex and heterogeneous disease characterised by unique genetic abnormalities. Genome-wide profiling of DNA copy number changes in paediatric HGG using high-resolution microarrays have identified unique genetic differences between paediatric and adult HGGs. Some of the most frequent DNA copy number changes in adults such as gain of chromosome 7 (74%) and loss of 10q (80%) occur in only 12% and 27% of cases, respectively in the paediatric population (Paugh et al., 2010; Puget et al.; 2010, Qu et al., 2010; Jones et al., 2012). The copy number abnormalities that are more frequent in paediatric HGG compared to adult HGG include gain of 1q (20% versus 9% of cases), loss of 16q (18% versus 7% of cases) and loss of 4q (15% versus 2% of cases). Such studies have also reported that

paediatric HGG exhibit comparatively fewer DNA copy number changes than their adult counterparts (Paugh et al., 2010). An unbiased approach involving a comprehensive analysis of genetic aberrations in paediatric HGG is therefore critical to identify the distinct, non-random genetic changes in these tumours. The determination of such genetic changes can provide a better understanding of the disease and identify potential prognostic markers and therapeutic targets. One of the other major drawbacks for investigations in paediatric HGG is the availability of tumour samples. The utility of astrocytoma-derived short-term cell cultures in DNA copy number investigations using analogue CGH has been previously reported (Potter et al., 2009). The results presented in Chapter 3 have also demonstrated that paediatric HGG short-term cell cultures do retain a considerable proportion of genetic changes present in the tumour biopsies from which they were derived. The aim of this study was to conduct a comprehensive analysis of genome-wide DNA copy number changes in paediatric HGG short-term cell cultures using high-resolution microarrays in order to identify non-random genomic CNAs.

4.2 Results

4.2.1 QC evaluation of microarray data from pediatric HGG short-term cell cultures

Genomic DNA was isolated from 17 paediatric HGG short-term cell cultures (comprising 14 non-DIPG and 3 DIPG) and the purity and integrity of the isolated DNA were verified as described in 2.5.1 and 2.5.3 respectively. Each test sample was sex-matched with the reference normal DNA; the test and the reference DNA were then differentially labelled with Cy3 (green) and Cy5 (red) fluorescent dyes

respectively and co-hybridized onto Agilent Human Genome 244K CGH microarrays as described in 2.8.1. The details of the samples used in this study are given in Table 1.1. The arrays were scanned using an Agilent SureScan Microarray scanner (Agilent Technologies) and the data were extracted from the resulting Tagged Image File (TIF) images, followed by dye-normalisation and log2ratio calculation using Feature Extraction Software (v9.5, Agilent technologies).

The QC report of each sample was carefully assessed to determine the level of background noise on the array. Evaluation of data quality is important in microarray experiments as the presence of background noise may interfere with true copy number calls. One of the crucial QC metrics, which is an indicator of noise, is the DLRS value. The Agilent QC guidelines suggest a DLRS value<0.3 for good quality samples. Data were also analysed using Nexus copy number software (v 8.0, Biodiscovery Inc., USA). The robust variance QC value in Nexus, which is a measure of probe-probe variance, was obtained for each sample. Nexus suggests QC scores of 0.2 as the upper limit for good quality samples. For each sample, both DLRS value (obtained using Agilent Feature Extraction software) and the QC value (obtained using Nexus copy number software) were thoroughly examined. Based on the recommended values for each factor, the samples were segregated into 3 groups. The data quality of the samples with DLRS value<0.20 and QC value<0.2 were considered 'Excellent'; those with DLRS value between 0.20 and 0.30 and QC value<0.2 as 'Good'; and those with DLRS value >0.30 or QC value>0.2 as 'Poor'. The DLRS and the QC values for 17 paediatric HGG short-term cell cultures are given in Table 4.1.

With the exception of 3 paediatric HGG short-term cell cultures (IN178, IN3180 and IN2087 (DIPG)), the array data from all other members in the cohort were either excellent or good quality and were analysed using significance threshold for segmentation set at 1.0E-5.

Table 4.1 Summary of microarray data quality

Sample	Tumour type	DLRS value	QC value	Quality
IN178	non-DIPG	0.35	0.26	Poor
IN179	non-DIPG	0.28	0.15	Good
IN1163	non-DIPG	0.22	0.11	Good
IN1262	non-DIPG	0.13	0.03	Excellent
IN1419	non-DIPG	0.14	0.04	Excellent
IN1523	non-DIPG	0.17	0.05	Excellent
IN1566	non-DIPG	0.12	0.02	Excellent
IN1930	non-DIPG	0.15	0.04	Excellent
IN3032	non-DIPG	0.14	0.04	Excellent
IN3046	non-DIPG	0.12	0.02	Excellent
IN3180	non-DIPG	0.38	0.29	Poor
IN3182	non-DIPG	0.21	0.09	Good
IN3183	non-DIPG	0.16	0.05	Excellent
IN3205*	non-DIPG	0.15	0.05	Excellent
IN2087	DIPG	0.38	0.29	Poor
IN2102	DIPG	0.24	0.13	Good
IN2675	DIPG	0.17	0.06	Excellent

DLRS and QC values of microarray data from 17 paediatric HGG short-term cell cultures are shown. DLRS-Derivative Log-Ratio Spread; QC-Quality Control; Excellent-DLRS value<0.20 and QC value<0.2; Good- DLRS value between 0.20 and 0.30 and QC value<0.2; Poor-DLRS value>0.30 and QC value>0.2. *indicates sample analysed with high stringent analysis setting (significant threshold for segmentation set at 1.0E-6) despite excellent quality as determined by the recommended DLRS and QC values.

The stringency of analysis was increased (significance threshold for segmentation set at 1.0E-6) for samples with poor quality in order to minimise the detection of false positive copy number calls. Despite excellent quality determined by the DLRS and QC values, the distribution of probes was not uniform in the array data from IN3205. Hence, this sample was treated as a poor quality array and analysed with significance threshold for segmentation set at 1.0E-6. The probe distribution of a representative sample for each tumour is shown in Figure 4.1.

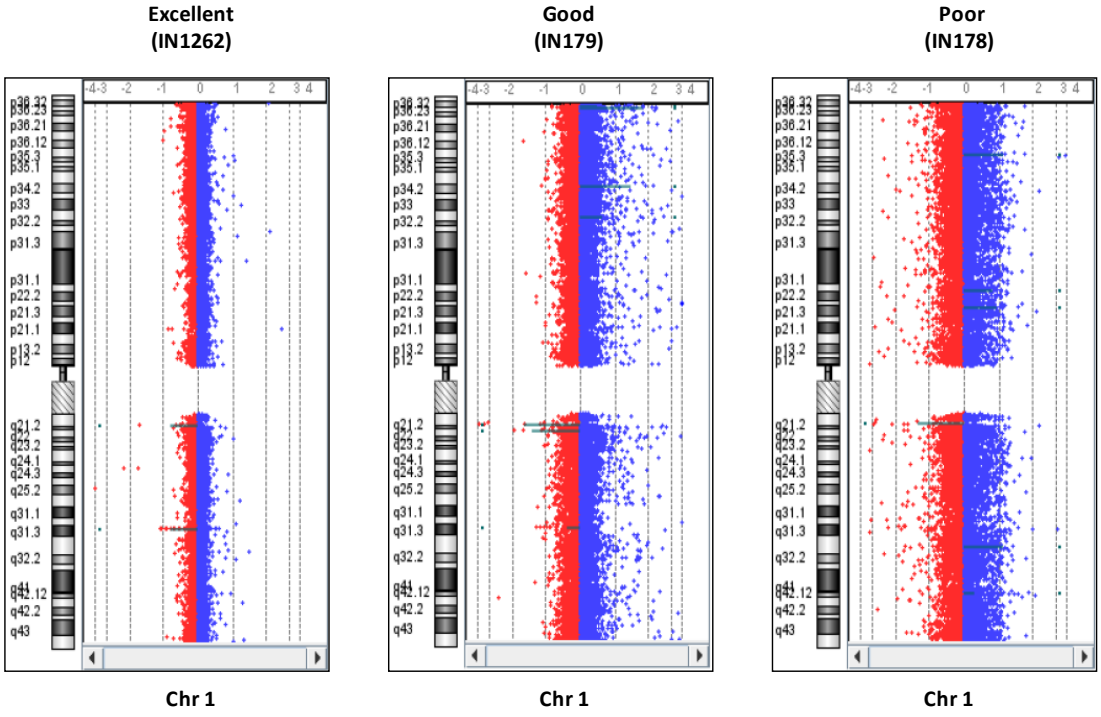

Figure 4.1 Evaluation of microarray data quality in paediatric HGG short-term cell cultures. This figure shows the chromosome view in Agilent Cytogenomics 3.0.1.1 software of chromosome 1 in samples with excellent, good and poor data quality. Sample names are given in parenthesis. The probes are distributed more uniformly in the excellent and good quality array data compared to the poor quality array data. Each dot represents a single probe on the array. The log-ratio of each probe is plotted against chromosomal position shown on the ideogram on the left. Copy number gain (+1) and copy number loss (-1) shift the log-ratios to the right and left respectively, of the baseline (0). Red indicates copy loss and blue indicates copy gain; Chr- chromosome number.

4.2.2 Evaluation of segmentation algorithms to determine CNAs in paediatric HGG short-term cell cultures

The choice of segmentation algorithm is another crucial factor in the determination of accurate copy number aberrations. The sample with the highest number of aberrations (IN1523) was analysed using ADM-2 (Agilent), Rank segmentation and FASST2 segmentation (Nexus), as described in 2.8.1.5, and the resultant genomic profiles were compared. In comparison to Rank segmentation algorithm, the FASST2 segmentation algorithm resulted in a much higher segmentation. This meant that higher number of CNAs was detected when the FASST2 algorithm was applied compared to ADM-2 and Rank segmentation algorithms. In addition, the genomic profile generated using Rank segmentation showed higher concordance with that obtained using ADM-2 algorithm. An example of the copy number calls on chromosomes 1, 5 and 10 in IN1523 short-term cell culture using Rank, FASST2 and ADM-2 algorithms are shown in Figure 4.2. Data analysis in this study was performed using Rank segmentation algorithm. Data were also analysed with ADM-2 algorithm and representative images of shared CNAs were used for appropriate illustrative purposes.

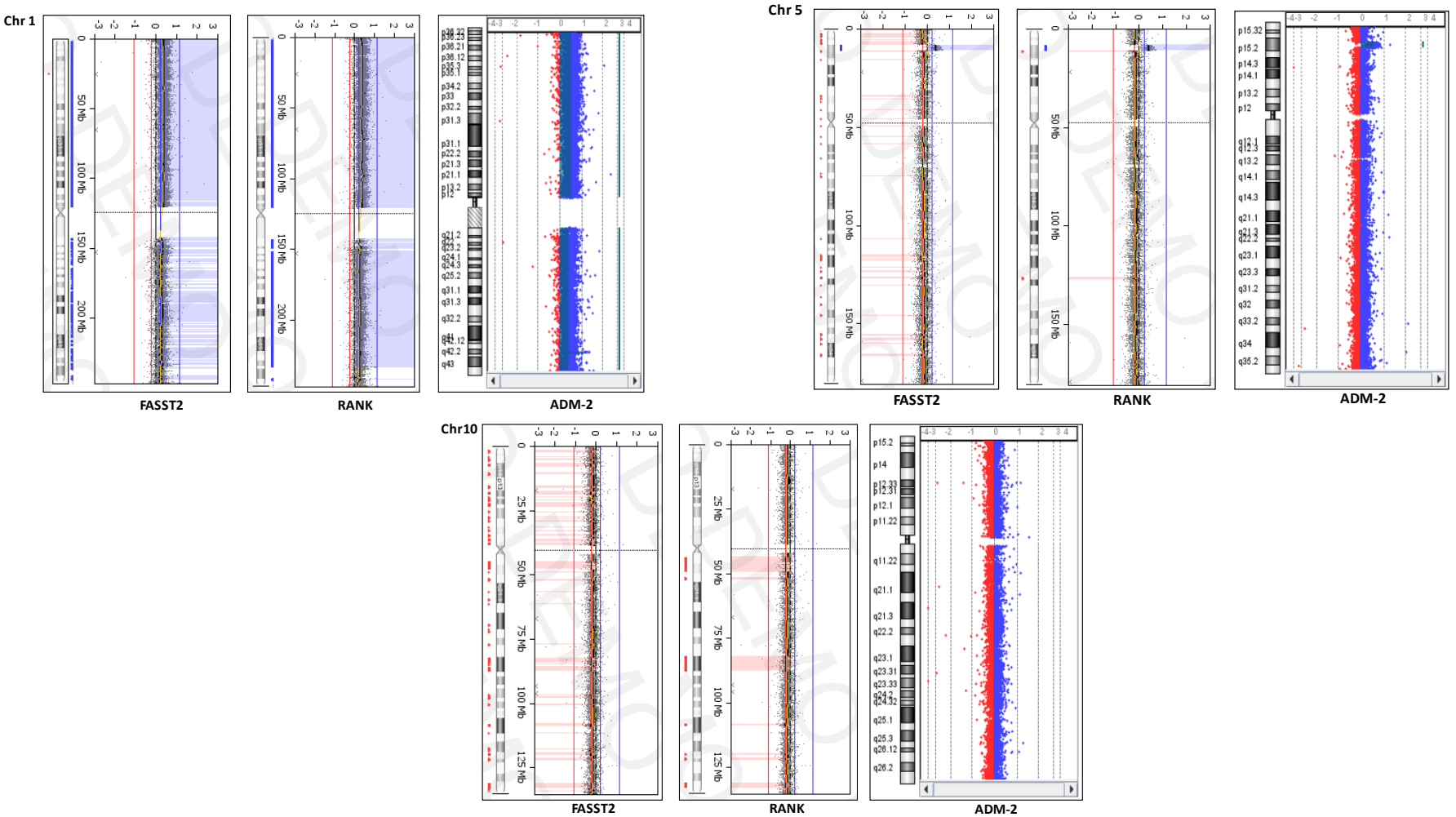

Figure 4.2 Illustration of copy number changes in IN1523 detected using Rank, FASST2 and ADM-2 algorithms. Copy number analysis was performed in IN1523 using FASST2 (Nexus copy number software), Rank (Nexus Copy number software) and ADM-2 (Agilent Cytogenomics software) algorithms **A)** There are more small interstitial gains seen on the q arm in FASST2 compared to Rank and ADM-2 algorithms. **B)** The gained region at 5p15.2 is retained by all the 3 algorithms, while more number of interstitial losses is detected by FASST2 compared to Rank and ADM-2 algorithms. **C)** Chromosome 10 shows no copy number changes by ADM-2, while higher number of interstitial losses is detected by FASST2 compared to Rank algorithm. In the chromosome view in Nexus copy number software, blue and red shaded region to the right and left respectively, of the baseline (0) indicates large region of copy number gain and loss; blue and red lines indicate focal copy number gain and loss respectively. In the chromosome view in Agilent Cytogenomics, each dot represents a probe on the array. Blue and red dots to the right and left, respectively of the central baseline (0) indicate copy number gain and loss. Large regions of gain are indicated by blue shaded blocks to the right of the baseline (0).

4.2.3 PCA of paediatric HGG short-term cell cultures

To examine similarities amongst paediatric HGG short-term cell cultures, PCA was performed using aCGH microarray data from 17 paediatric HGG short-term cell cultures as described in 2.12.4. The results are illustrated as a 3-D PCA plot in Figure 4.3. PCA showed that 12/17 paediatric HGG short-term cell cultures (IN178, IN1163, IN1262, IN1419, IN1566, IN1930, IN3032, IN3046, IN3183, IN3205, IN2102 (DIPG), and IN2675 (DIPG)) clustered together, while the remaining 5 samples did not cluster with the main group. Of these 5 samples, 2 grouped together (IN3180 and IN2087 (DIPG)), whilst the other 3 samples were all independent (IN179, IN1523, and IN3182).

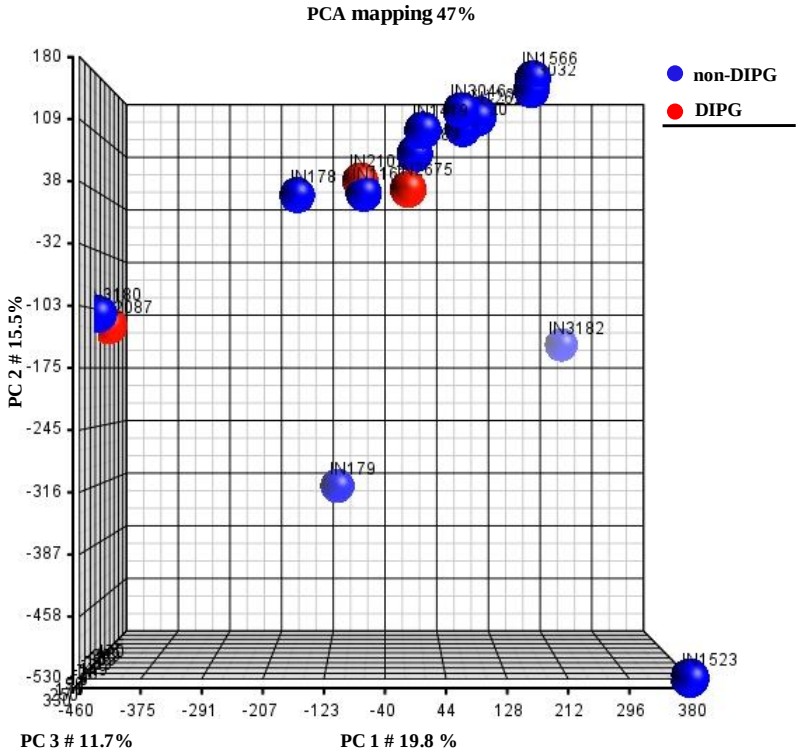

Figure 4.3 PCA of 17 paediatric HGG short-term cultures. The 3-D PCA plot of 17 paediatric HGG short-term cell cultures plotted with the first three principal components, PC1 (19.8%), PC2 (15.5%) and PC3 (11.7%) is shown. Each dot on the 3-D plot represents a sample; DIPG and non-DIPG short-term cell cultures are represented by red and blue-coloured dots respectively.

4.2.4 DNA copy number profiling in paediatric HGG short-term cell cultures

DNA copy number profiles were generated for 17 paediatric HGG short-term cell cultures using Rank segmentation algorithm in Nexus copy number software (v8.0, Biodiscovery Inc., USA) as described in section 2.8.1.5. For this analysis, the CNAs on Y-chromosome were as these are often unreliable (Hu et al., 2004). A summary of the overall DNA copy number changes in individual paediatric HGG short-term cell cultures is shown in Figure 4.4 and a quantitative summary of the CNAs identified in the dataset is given in Table 4.2. The majority of the paediatric HGG short-term cell cultures (11/17 cases, 64.71%) did not show large regions of copy number imbalances involving whole chromosome arms. These comprised IN178, IN1163, IN1262, IN1566, IN1930, IN2087, IN2102, IN3032, IN3046, IN3180, and IN3183. The number of CNAs per sample in this group ranged from 11-19 (median-16), which accounted to less than 1% of genomic changes in each sample. Three paediatric HGG short-term cell cultures (17.65%), IN1419, IN2675 and IN3205 showed large regions of genomic changes involving single chromosomes with the number of CNAs per sample in the group ranging from 21-48 (median-27), accounting for 3-6% of genomic changes in each sample. The remaining 3 paediatric HGG short-term cell cultures (IN179, IN1523 and IN3182) comprising 17.65% of the cohort) demonstrated CNAs across large regions on multiple chromosomes, with the number of CNAs per sample ranging from 54-85 (median-62), accounting for 17-59% of genomic changes.

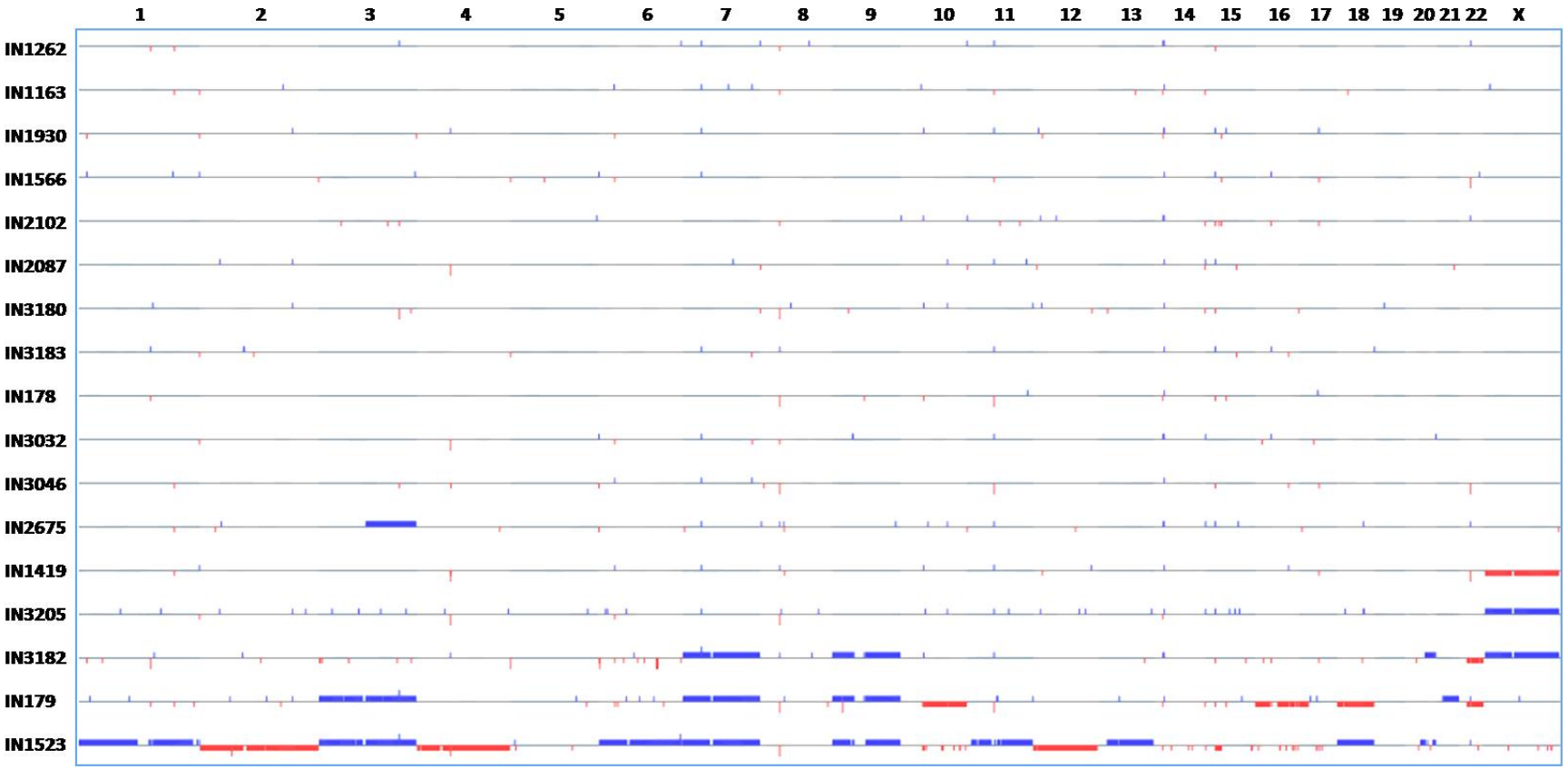

Figure 4.4 Genomic profiles of 17 paediatric HGG short-term cell cultures. aCGH profiles of 17 paediatric HGG short-term cell cultures were generated using Nexus copy number software v8.0. X-axis shows chromosomes and y-axis shows paediatric HGG short-term cell cultures ranked by the order of genomic changes. The paediatric HGG short-term cell culture with the highest proportion of genomic changes is shown at the bottom. The aberrations on all chromosomes excluding Y are displayed. Gains are represented in blue and losses are represented in red blocks above and below the threshold line (black) respectively, in each sample.

Table 4.2 Summary of DNA copy number analysis in paediatric HGG short-term cell cultures using Rank segmentation algorithm

Samples	% Genome Changed	Total CNAs	One copy gain	One copy loss	High copy gain	Homozygous copy loss
IN1262	0.14	14	10	4	0	0
IN1163	0.14	16	8	8	0	0
IN1930	0.21	18	11	7	0	0
IN1566	0.22	18	10	7	0	1
IN2102	0.22	21	9	12	0	0
IN2087	0.24	16	9	6	0	1
IN3180	0.25	19	9	8	0	2
IN3183	0.25	16	10	6	0	0
IN178	0.29	11	3	6	0	2
IN3032	0.32	16	9	6	0	1
IN3046	0.70	18	4	8	0	3
IN2675	3.57	27	17	10	0	0
IN1419	5.05	19	9	7	0	2
IN3205	5.81	48	37	3	0	2
IN3182	17.24	54	19	25	1	5
IN179	26.33	62	33	25	1	3
IN1523	58.42	85	32	44	2	3

DNA copy number analysis was performed in 17 paediatric HGG short-term cell cultures using Rank segmentation algorithm in Nexus copy number software with thresholds for copy number gain and copy number loss set at 0.2 and -0.23 respectively. High-copy gain and homologous loss were defined by log ratio thresholds of 1.14 and -1.1 respectively. The samples are ranked by the order of % genome changed. The sample with the highest % of genomic changes is shown at the bottom. Subgroup 1 (genomic changes <1%) is highlighted in red, subgroup 2 (genomic changes-3.57-5.81%) in blue and subgroup 3 (genomic changes 17.24-58.42%) in green respectively. CNA- copy number alteration.

Overall, a total of 460 segments of CNAs were identified, of which the frequency of single copy gains (n=239, 51.96%) was relatively higher than those of single copy losses (n=192, 41.74 %). Gains were also more frequent than losses in individual cases of paediatric HGG short-term cell cultures. Conversely, the frequency of high copy gains (n=4, 0.87%) was much lower in comparison to that of homozygous

losses (n=25, 5.43%). A cumulative summary of all the genomic changes in all samples is given in Figure 4.5.

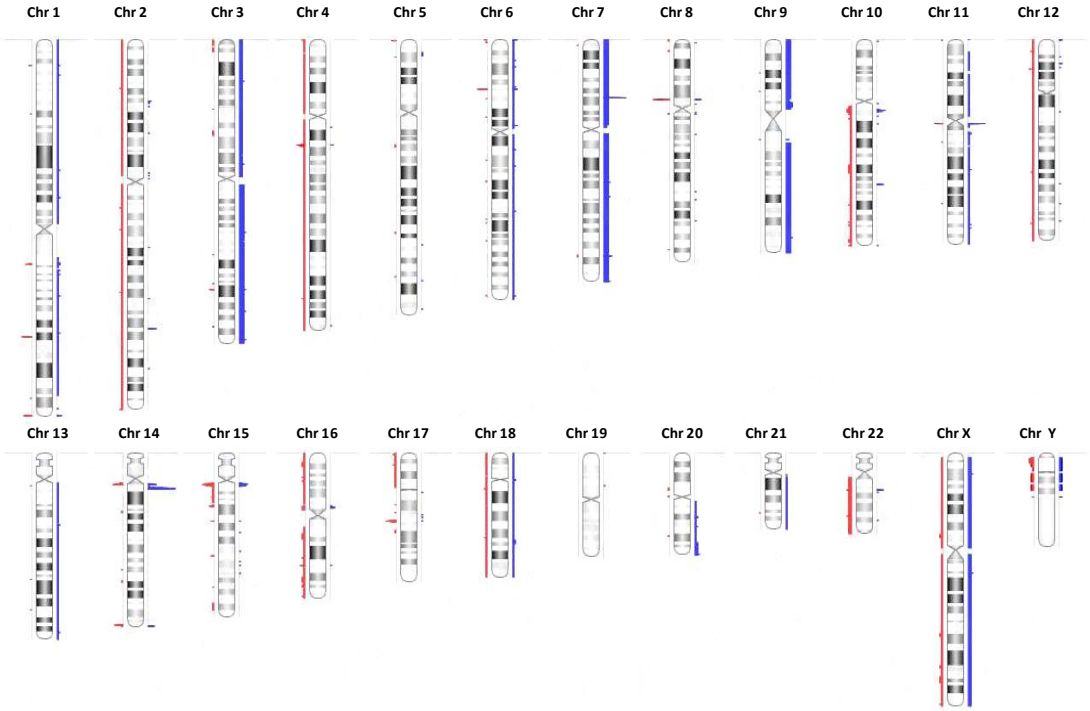

Figure 4.5 Summary of copy number aberrations on all chromosomes. DNA copy number analysis in 17 paediatric HGG short-term cell cultures using Rank segmentation algorithm in Nexus copy number software identified CNAs across all chromosomes, with the lowest number of CNAs on chromosomes 5 and 19. This figure shows a compact view of CNAs on all chromosomes. Red and blue shaded regions to the left and right of each ideogram respectively, indicates copy number loss and gain. Chr- Chromosome number.

4.2.5 Chromosome arm aberrations

The most frequent chromosome aberrations involving whole chromosomes were gains of chromosomes 7 and 9, which occurred concurrently in 3 cases (17.6%) comprising IN179, IN1523, and IN3182. The aCGH profiles of IN179, IN1523 and IN3182 paediatric HGG short-term cell cultures are shown in Figure 4.6, Figure 4.7 and Figure 4.8 respectively.

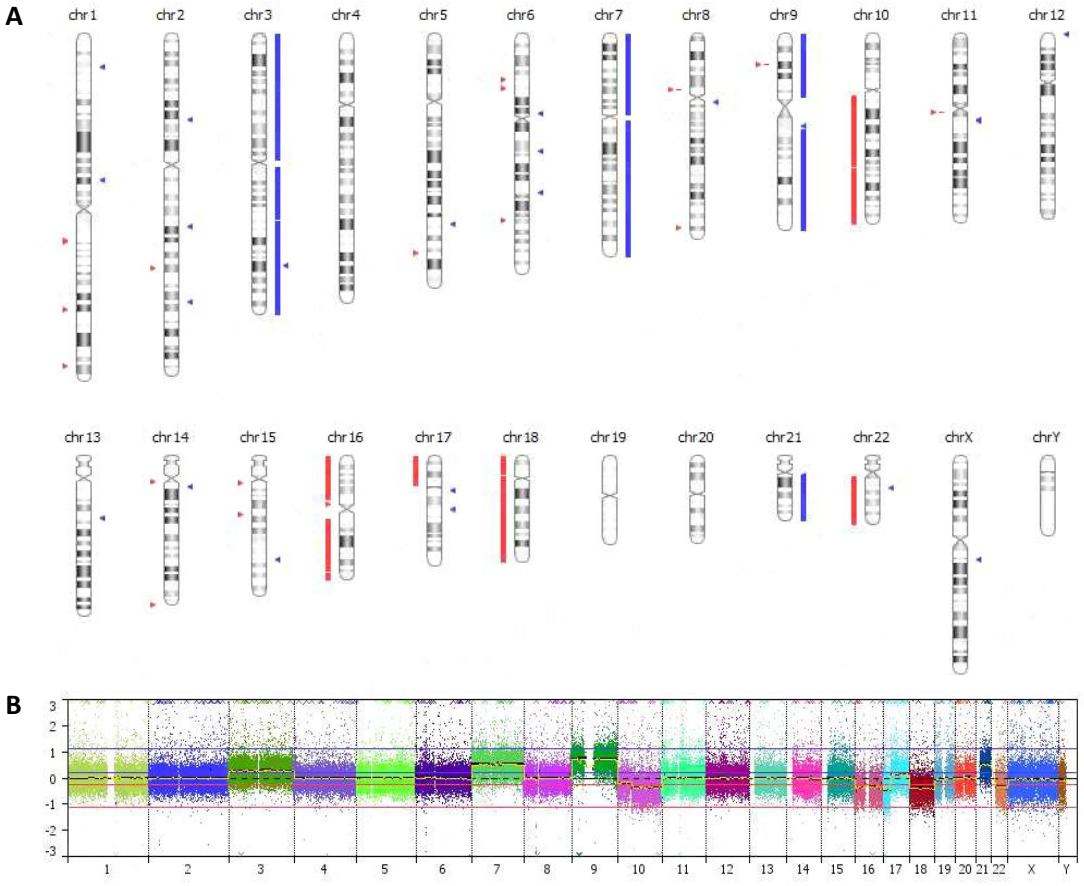

Figure 4.6 aCGH profile of IN179 paediatric HGG short-term cell culture. The ideogram (A) displays copy number gains represented by blue bar/arrow to the right and copy number losses by red bar/arrow to the left of each chromosome. High-copy gain is represented by double blue arrows to the right and homozygous loss is represented by double red arrows to the left of each chromosome. The probe distribution across the entire genome is also shown with chromosomes lined end to end (B). The thresholds for copy number gain and loss are indicated by blue and red horizontal lines, respectively in the copy number plots. The yellow line along the baseline (0) in the plot represents the moving average value.

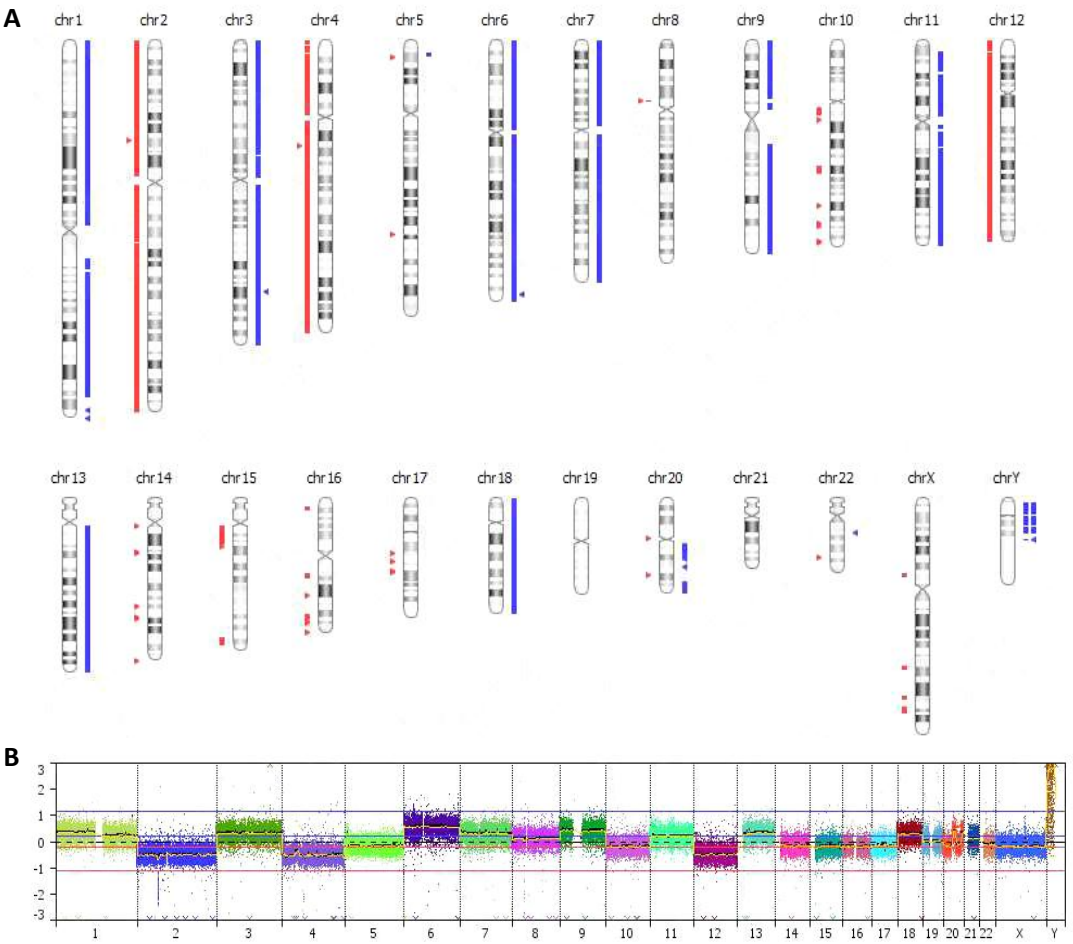

Figure 4.7 aCGH profile of IN1523 paediatric HGG short-term cell culture. The ideogram (A) displays copy number gains represented by blue bar/arrow to the right and copy number losses by red bar/arrow to the left of each chromosome. High-copy gain is represented by double blue arrows to the right and homozygous loss is represented by double red arrows to the left of each chromosome. The probe distribution across the entire genome is also shown with chromosomes lined end to end (B). The thresholds for copy number gain and loss are indicated by blue and red horizontal lines, respectively in the copy number plots. The yellow line along the baseline (0) in the plot represents the moving average value.

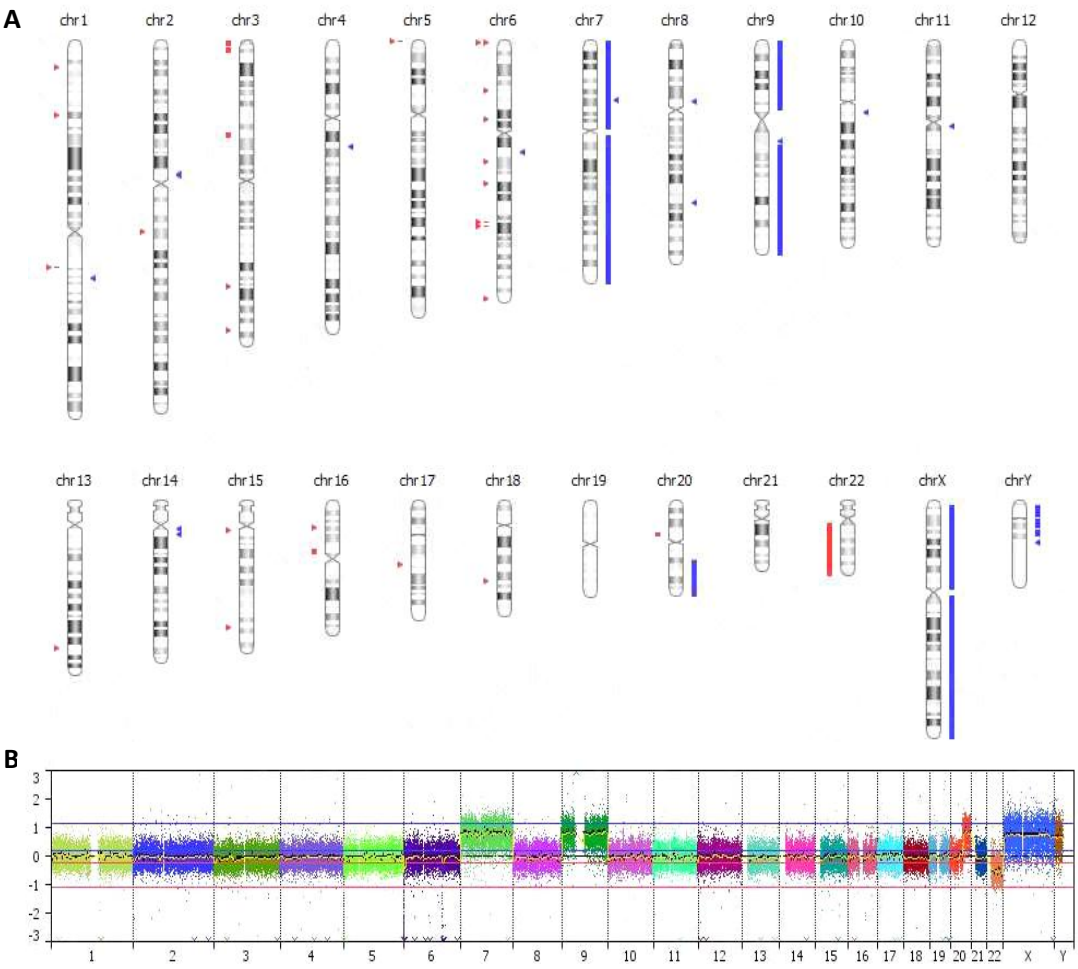

Figure 4.8 aCGH profile of IN3182 paediatric HGG short-term cell culture. The ideogram (A) displays copy number gains represented by blue bar/arrow to the right and copy number losses by red bar/arrow to the left of each chromosome. High-copy gain is represented by double blue arrows to the right and homozygous loss is represented by double red arrows to the left of each chromosome. The probe distribution across the entire genome is also shown with chromosomes lined end to end (B). The thresholds for copy number gain and loss are indicated by blue and red horizontal lines, respectively in the copy number plots. The yellow line along the baseline (0) in the plot represents the moving average value.

The list of chromosome arm aberrations and their frequencies of occurrence in 17 paediatric HGG short-term cell cultures is shown in Table 4.3. The most frequent chromosome arm aberration was gain of 3q, observed in 3 cases (17.6%) comprising IN179, IN1523 and IN2675 (DIPG). This was the only large CNA present in the DIPG short-term cell cultures. Gain of chromosome X and chromosome arms 3p and 20q, and loss of chromosome 16 and chromosome arms 10q, and 22q, were each seen in 2 cases (11.8%). Of these, gain of chromosome 3, loss of 10q, and loss of chromosome 16 occurred concurrently (IN179 and IN1523). Gain of chromosomes 1, 6, 11, and 18, and chromosome arms 13q and 21q, and loss of chromosomes 2, 4, and 12, and chromosome arm 15q, were each seen in a single case only (5.9%). Aneuploidies of chromosomes 5, 8, 10p, 14, 15, 17q, 19 and 20p were not detected in any samples.

Table 4.3 Summary of chromosome arm aberrations in paediatric HGG short-term cell cultures

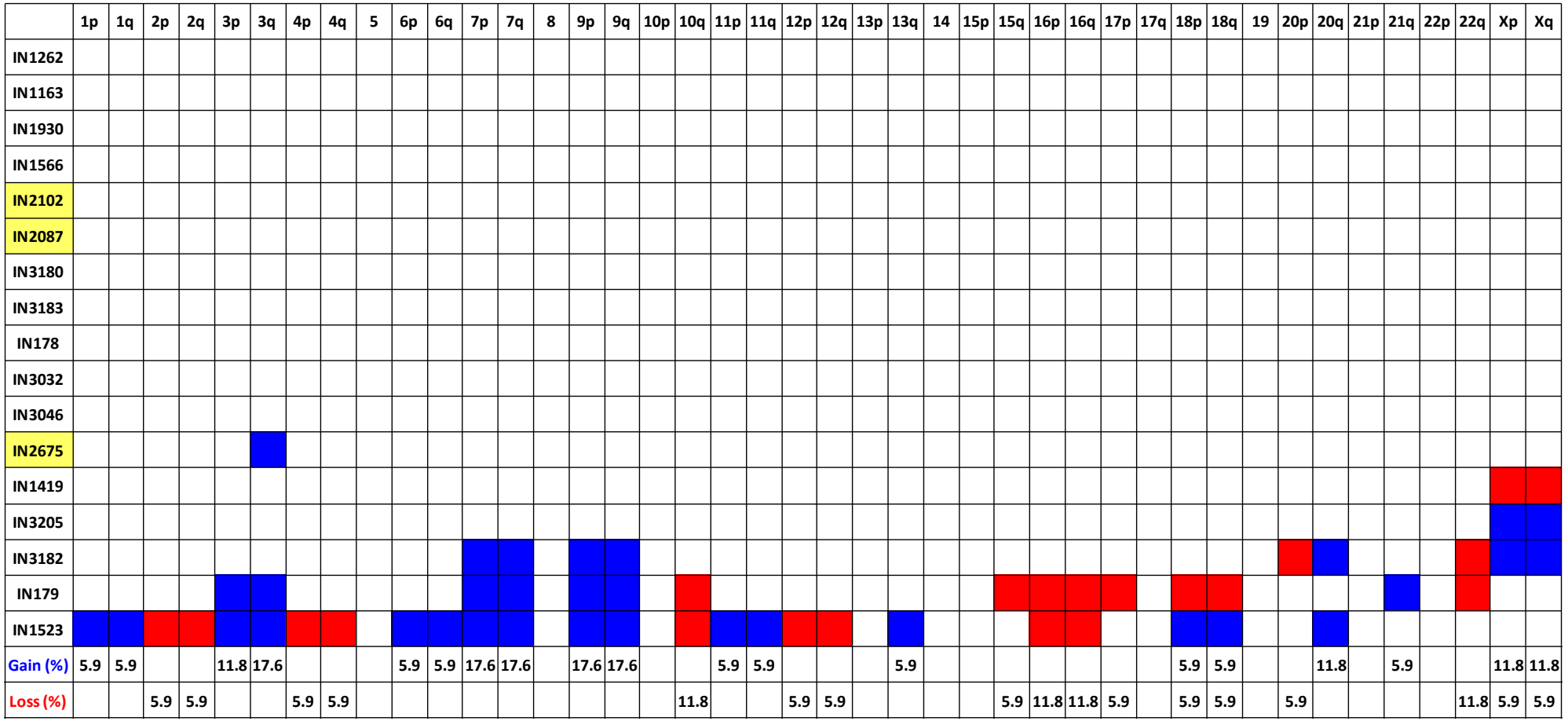

The table shows the aberration status of chromosome arms in 17 paediatric HGG short-term cell cultures. The chromosomes (excluding chromosome Y) are arranged in columns; samples are arranged in rows; copy number gain and copy number loss are represented by blue and red boxes respectively. The frequencies of gain and loss of chromosome arms is shown at the bottom. DIPG short-term cell cultures are highlighted in yellow.

4.2.6 Focal genomic CNAs in paediatric HGG short-term cell cultures

4.2.6.1 High copy gain

The high-copy gains identified in 17 paediatric HGG short-term cell cultures in this study are listed in Table 4.4. Three regions of high-copy gain were identified comprising 3q26.1, 6q27 and 7p14.1. The high copy-gain at 3q26.1 occurred in 2 paediatric HGG short-term cell cultures (IN179 and IN1523), but no genes have been mapped to this location. The high copy gain at 6q27 encompassing 2 long intergenic non-protein coding RNA genes *(LINC00473* and *LINC00602)* occurred in a single case (IN1523). The high-copy gain at 7p14.1 encompassing *TARP* (TCR gamma alternate reading frame protein) was also found in a single case (IN3182). Notably, the paediatric HGG short-term cell cultures with high-copy gains were all non-DIPG.

Table 4.4 High copy gains in paediatric HGG short-term cell cultures

Chromosome	Region	No. of samples	Samples with gain	Genes
3	q26.1	2 (non-DIPG)	IN179, IN1523	-
6	q27	1 (non-DIPG)	IN1523	*LINC00473, LINC00602*
7	p14.1	1 (non-DIPG)	IN3182	*TARP*

This table shows the regions of high-copy gains (determined by log2ratio threshold of 1.1) identified in paediatric HGG short-term cell cultures using Rank segmentation algorithm in Nexus copy number software. The CNAs are ranked by the order of chromosomal location.

4.2.6.2 Homozygous copy loss

The homozygous copy losses identified in 17 paediatric HGG short-term cell cultures are listed in Table 4.5. These CNAs were detected across chromosomes 1, 2, 3, 4, 5, 6, 8, 9, 11 and 22.

Table 4.5 Regions of homozygous loss in paediatric HGG short-term cultures

Chromosome	Region	No of samples	Samples with loss	Genes
1	q21.1	1	IN3182	*NBPF25P,LOC388692, FAM231D,FCGR1C*
2	p14	1	IN1523	*LOC400958, SLC1A4, CEP68, RAB1A, ACTR2, SPRED2*
3	q26.1	1	IN3180	No genes in region
4	q13.2	5	IN1419, IN1523, **IN2087,** IN3032, IN3205	*TMPRSS11E, UGT2B17, UGT2B15*
5	p15.33	1	IN3182	No genes in region
6	p25.3 - p25.2	1	IN3182	*GMDS,GMDS-AS1*
6	q22.2	1	IN3182	*ROS1, DCBLD1, GOPC*
6	q22.31	1	IN3182	*MIR3144*
8	p11.23 - p11.22	6	IN178, IN179, IN1523, IN3046, IN3180, IN3205	*ADAM5, ADAM3A*
9	p21.3	1	IN179	*CDKN2A, CDKN2B*
11	q11	3	IN178, IN179, IN3046	*OR4C11,OR4P4,OR4S2, OR4C6*
22	q11.23	3	IN1419, IN1566, IN3046	*GSTTP1,LOC391322, GSTT1-AS1,GSTT1, GSTTP2*

The table shows the regions of homozygous loss identified in paediatric HGG short-term cell cultures. The CNAs are ranked by the order of chromosomal location. DIPG short-term cell culture is highlighted in blue.

Of these, the most frequent loss involved 8p11.23-p11.22 encompassing *ADAM5* and *ADAM3A* and occurred in 6 cases (IN178, IN179, IN1523, IN3046, IN3180 and IN3205). Homozygous loss of 4q13.2 encompassing *TMPRSS1E*, *UGT2B17* and *UGT2B15* occurred in 5 cases (IN1419, IN1523, IN2087 (DIPG), IN3032 and IN3205). This was the only homozygous loss detected in a DIPG short-term cell culture.

One short-term cell culture (IN179) had homozygous loss of 9p21.3, encompassing *CDKN2A/CDKN2B* (Figure 4.9). Loss of *CDKN2A/CDKN2B* associated with oncogenic mutation in *BRAF* (*BRAFV600E*) has been previously identified as a distinct characteristic of a subset of paediatric HGG (Schiffman et al., 2012) and the *BRAFV600E* mutation was also present in IN179 (as previously shown in Figure 3.15).

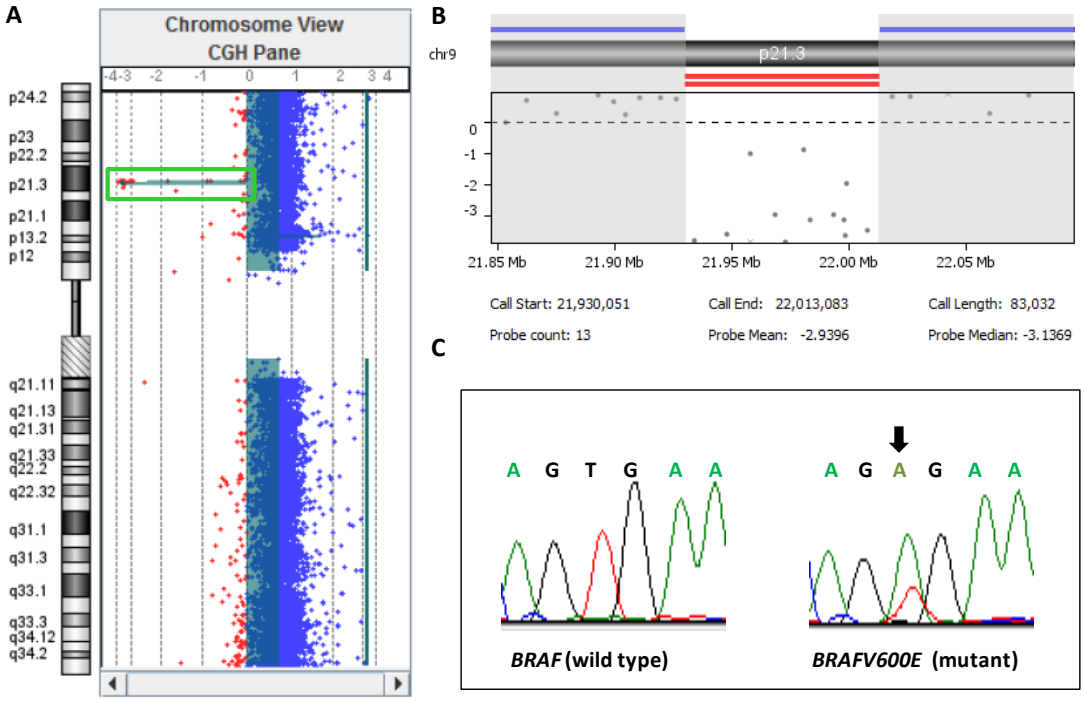

Figure 4.9 Concurrent loss of 9p21.3 and *BRAFV600E* mutation in IN179 paediatric HGG short-term cell culture. A) Chromosome view displaying loss of 9p21.3 in IN179 paediatric HGG short-term cell culture. Each dot represents a single probe on the array. The log2ratios of the probes are plotted against the chromosomal location. Copy number gain and copy number loss shifts the log2ratios to the right and left respectively, of the baseline (0). Gain is represented by blue and Loss is represented by red respectively **B)** Probe details of region of loss at 9p21.3 showing 13 probes in the region of loss with mean -2.9396 and median -3.1369. The chromosome position is shown on the x-axis and log2ratios are shown on the y-axis. The horizontal dotted line represents the baseline (0). **C)** *BRAFV600E* mutation causing amino acid substitution from valine to glutamic acid at position 600.

The other frequent regions of homozygous loss that have not been previously reported in paediatric HGG occurred at 11q11 (IN178, IN179 and IN3046) and 22q11.23 (IN1419, IN1566 and IN3046), each in 3 cases. Chromosome 11q11 contains 4 members of the olfactory family of genes such as *OR4C11, OR4P4, OR4S2* and *OR4C6.* Chromosome 22q11.23 encompasses *LOC391322, GSTT1-AS1, GSTT1, GSTTP1* and *GSTTP2*. There were 3 novel regions of homozygous loss on chromosome 6 (6p25.3-25.2, 6q22.2 and 6q22.31) all occurring in the same paediatric HGG short-term cell culture (IN3182). The miRNA gene, *MIR3144* maps to 6q22.31. The regions of homozygous loss at 1q21.1 (*LOC388692*) and 2p14 (*LOC400958*) occurred in single case only and involved lnc RNA genes.

4.2.6.3 Frequent and statistically significant CNAs

Recurrent and statistically significant CNAs in paediatric HGG short-term cell cultures were independently identified by 2 frequency significance tests; Significance Testing for Aberrant Copy number (STAC) (Diskin et al., 2006) and Genomic Identification of Significant Targets in Cancer (GISTIC) (Beroukhim et al., 2007). STAC identifies copy number events that are stacked on top of each other such that it would not occur randomly. A p-value is generated which indicates the level of significance of an event that occurs at a particular frequency, as defined by the aggregate % cut-off option. However, STAC may not identify statistically significant regions present in a lower frequency of cases. GISTIC identifies statistically high frequency of CNAs over background aberrations. A G-score, which indicates both the frequency of occurrence of a copy number event and the level of copy number

change in each of the sample in the data set, was generated. FDR multiple testing was applied to generate a q-bound value indicating the significance of the event.

The list of CNAs identified as significant ($p<0.05$) by STAC in a minimum of 4/17 (23.5%) paediatric HGG short-term cell cultures is given in Table 4.6. A total of 23 significantly altered regions were identified, which involved gains on chromosomes 2, 7, 10, 11, 14, 15 and 22, and losses on chromosomes 1, 4, 6, 11, 14, 15 and 17. The frequencies of these CNAs were compared between non-DIPG and DIPG short-term cell cultures and are given in Table 4.7.

Table 4.6 Frequent and statistically significant CNAs identified by STAC

Chr	Region Length (bp)	Cytoband Location	Event	Frequency (%)	P-Value	% of CNV Overlap	Gene count	Genes of interest
14	386482	q11.2	CN Gain	94.12	0	100	0	No genes in region
7	62512	p14.1	CN Gain	76.47	0	100	1	*TARP*
8	142664	p11.23 - p11.22	CN Loss	58.82	0	100	2	*ADAM5,ADAM3A*
11	69664	q11	CN Gain	58.82	0	100	4	*OR4C11,OR4P4,OR4S2,OR4C6*
15	629510	q11.2	CN Loss	41.18	0	100	16	*NBEAP1, LOC646214,CXADRP2, MIR3118-2, MIR3118-3, MIR3118-4, POTEB2, POTEB, POTEB3, NFIP2, MIR5701-1, MIR5701-2, MIR5701-3, LINC01193, LOC727924, LOC101927079*
1	24645	q31.3	CN Loss	35.29	0	100	1	*CFHR1*
6	103506	p21.32	CN Loss	35.29	0	100	3	*HLA-DRB5, HLA-DRB6, HLA-DRB1*
14	222794	q11.2	CN Loss	35.29	0	100	6	*OR4Q3, OR4M1,OR4N2,OR4K2,OR4K5,OR4K1*
17	211312	q21.31	CN Loss	35.29	0	100	4	*KANSL1, KANSL1-AS1, LRRC37A, ARL17B*
1	50830	q44	CN Loss	29.41	0	100	3	*OR2T10, OR2T11, OR2T35*
2	163679	q32.2	CN Gain	29.41	0	28	2	*COL5A2, MIR3129*
4	422840	q13.2	CN Loss	29.41	0	100	3	*TMPRSS11E, UGT2B17, UGT2B15*
10	123161	q11.22	CN Gain	29.41	0	100	4	*GPRIN2,NPY4R, CH17-360D5.1, LINC00842*
11	47731	q11	CN Loss	29.41	0	100	3	*OR4P4, OR4S2, OR4C6*
14	199613	q11.2	CN Gain	29.41	0	100	5	*OR4Q3, OR4M1, OR4N2, OR4K2, OR4K5*
14	176973	q32.33	CN Loss	29.41	0	100	5	*MIR8071-1, MIR8071-2, ELK2AP*
15	621648	q11.2	CN Gain	29.41	0	100	17	*HERC2P3, GOLGA6L6, GOLGA8CP, LOC646214,NBEAP1, CXADRP2, MIR3118-2, MIR3118-3, MIR3118-4, POTEB2, POTEB, POTEB3, NFIP2, MIR5701-1, MIR5701-2, MIR5701-3, LINC01193*
1	457712	q21.1	CN Loss	23.53	0	100	4	*NBPF25P,LOC388692,FAM231D,FCGR1C*
8	142024	p11.23	CN Gain	23.53	0	100	2	*ADAM5*
10	183002	q23.33	CN Gain	23.53	0	22	1	*MYOF*
14	21696	q32.33	CN Gain	23.53	0.009	100	0	No genes in region
15	516123	q11.2	CN Gain	23.53	0	100	12	*LOC727924,LOC101927079,OR4M2,OR4N4,OR4N3P, MIR1268A,REREP3,MIR4509-1, MIR4509-2, MIR4509-3, GOLGA8DP, GOLGA6L1*
22	53584	q11.23	CN Gain	23.53	0	100	5	*GSTTP1,LOC391322,GSTT1-AS1,GSTT1, GSTTP2*

CNAs identified as significant ($p<0.05$) by STAC algorithm in an aggregate of 23% (4/17 cases) of paediatric HGG short-term cell cultures are shown. The CNAs are ranked by the order of frequency of occurrence. The CNA with the least frequency of occurrence is at the bottom. Chr-Chromosome; bp-base pair; CN-copy number; CNV-copy number variation.

Table 4.7 Frequencies of significant CNAs identified by STAC algorithm in DIPG and non-DIPG short-term cell cultures

Chromosome	Cytoband	Length (bp)	IN178	IN179	IN1163	IN1262	IN1419	IN1523	IN1566	IN1930	IN3032	IN3046	IN3180	IN3182	IN3183	IN3205	IN2087	IN2102	IN2675	Overall frequency (%)	non-DIPG (%)	DIPG (%)
14	q11.2	386482																		94.12	13 (92.9)	3 (100)
7	p14.1	62512																		76.47	12(85.7)	1 (33.3)
8	p11.23 - p11.22	142664																		58.82	9 (64.3)	1 (33.3)
11	q11	69664																		58.82	8 (57.1)	2 (66.6)
15	q11.2	629510																		41.18	6 (42.9)	1 (33.3)
1	q31.3	24645																		35.29	5 (35.7)	1 (33.3)
6	p21.32	103506																		35.29	6 (42.9)	0
14	q11.2	222794																		35.29	6 (42.9)	0
17	q21.31	211312																		35.29	5 (35.7)	1 (33.3)
1	q44	50830																		29.41	5 (35.7)	0
2	q32.2	163679																		29.41	4 (28.6)	1 (33.3)
4	q13.2	422840																		29.41	4 (28.6)	1 (33.3)
10	q11.22	123161																		29.41	4 (28.6)	1 (33.3)
11	q11	47731																		29.41	5 (35.7)	0
14	q11.2	199613																		29.41	3 (21.4)	2 (66.6)
14	q32.33	176973																		29.41	3 (21.4)	2 (66.6)
15	q11.2	621648																		29.41	4 (28.6)	1 (33.3)
1	q21.1	457712																		23.53	4 (28.6)	0
8	p11.23	142024																		23.53	3 (21.4)	1 (33.3)
10	q23.33	183002																		23.53	2 (14.3)	2 (66.6)
14	q32.33	21696																		23.53	2 (14.3)	2 (66.6)
15	q11.2	516123																		23.53	4 (28.6)	0
22	q11.23	53584																		23.53	2 (14.3)	2 (66.6)

Frequent and significant CNAs (aggregate of 23.53% and $p<0.05$) in 17 paediatric HGG short-term cell cultures were identified by STAC algorithm in Nexus copy number software. The frequencies of occurrence of 23 significant CNAs in 14 non-DIPG and 3 DIPG short-term cell cultures are shown. DIPG are highlighted in yellow; red boxes indicate copy number loss and blue boxes indicate copy number gain; CNAs absent in DIPG short-term cell cultures are highlighted in pink; CNAs that are significantly different (differential threshold of 25% and $p<0.05$) from non-DIPG are highlighted in green; bp-base pair.

Significantly altered regions of copy number gain

The most frequent CNA in the cohort was gain at 14q11.2 (94.12%, 16/17 cases) covering 386,482 bp. With the exception of IN1523, gain of this region was observed in all paediatric HGG short-term cell cultures. However, there were no genes located in this region. Gain of 14q11.2 in a representative paediatric HGG short-term cell culture (IN1566) is shown in Figure 4.10.

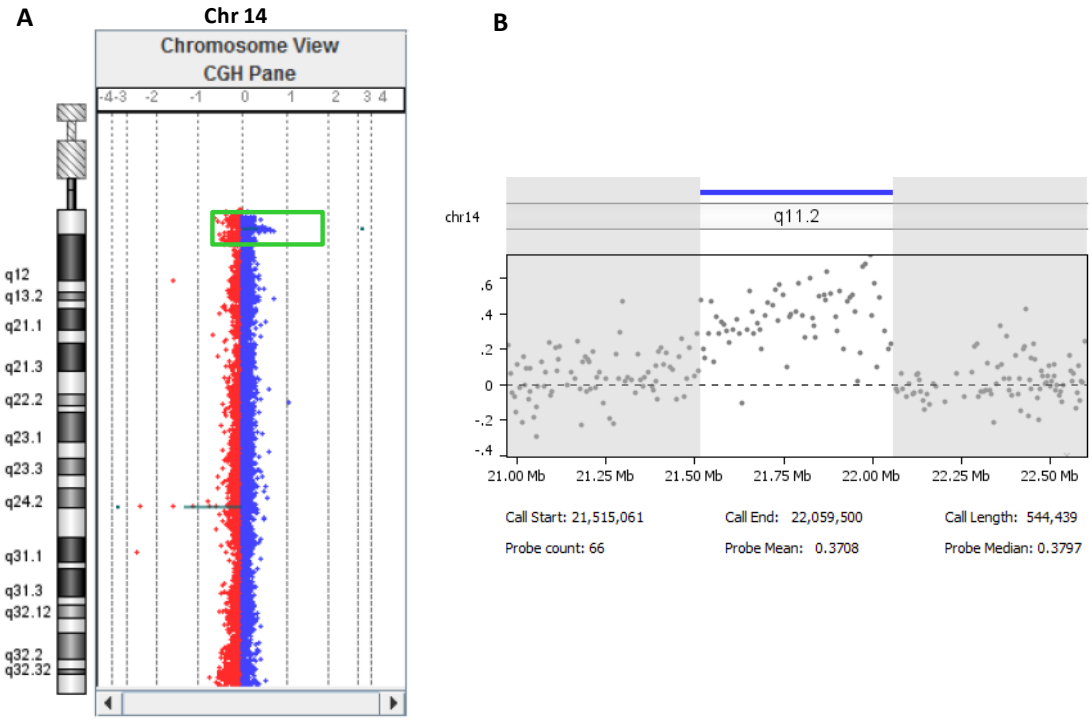

Figure 4.10 Gain of 14q11.2 in IN1566 paediatric HGG short-term cell culture. A) Chromosome view displaying the gained region at 14q11.2 in IN1566 paediatric HGG short-term cell culture. Each dot represents a single probe on the array. The log2ratios of the probes are plotted against the chromosomal location. Copy number gain and copy number loss shifts the log2ratios to the right and left respectively, of the baseline (0). Gain is represented by blue and Loss is represented by red respectively. **B)** Probe details of the gained region at 14q11.2 showing 66 probes in the gained region with mean 0.3708 and median 0.3797. The chromosome position is shown on the x-axis and log2ratios are shown on the y-axis. The horizontal dotted line represents the baseline (0).

Gain at 7p14.1 (62512 bp) encompassing *TARP* occurred in 76.47% (13/17) of cases comprising 12 non-DIPG (IN179, IN1163, IN1262, IN1419, IN1523, IN1566, IN1930, IN3032, IN3046, IN3182, IN3183 and IN3205) and 1 DIPG (IN2675) short-term cell cultures. Gain of 7p14.1 in a representative paediatric HGG short-term cell culture (IN3046) is shown in Figure 4.11.

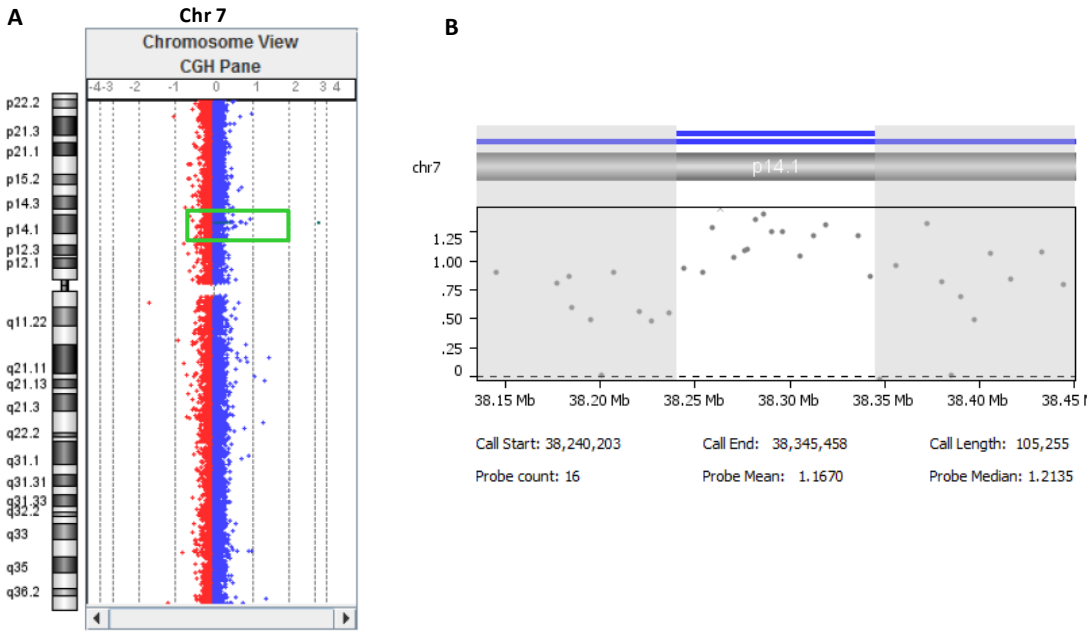

Figure 4.11 Gain of 7p14.1 in IN3046 paediatric HGG short-term cell culture. A) Chromosome view displaying the gained region at 7p14.1 in IN3046 paediatric HGG short-term cell culture. Each dot represents a single probe on the array. The log2ratios of the probes are plotted against the chromosomal location. Copy number gain and copy number loss shifts the log2ratios to the right and left respectively, of the baseline (0). Gain is represented by blue and loss is represented by red respectively **B)** Probe details of the gained region at 7p14.1 showing 16 probes in the gained region with mean 1.1670 and median 1.2135. Chromosome position is shown on the x-axis and log2ratios are shown on the y-axis. The horizontal dotted line represents the baseline (0).

Gain of 11q11 (69,664 bp) occurred in 58.82% (10/17) cases, which included 8 non-DIPG (IN1262, IN1419, IN1523, IN1930, IN3032, IN3182, IN3183 and IN3205)

and 2 DIPG (IN2087 and IN2675) short-term cell cultures. This region contains 4 genes, namely *OR4C11*, *OR4P4*, *OR4S2* and *OR4C6*, all members of the olfactory family genes.

Four regions of gain, 2q32.2 (163679 bp), 10q11.22 (123161 bp), 14q11.2 (199613 bp), and 15q11.2 (621648 bp) were present in 29.41% (5/17) of paediatric HGG short-term cell cultures. Gain of 2q32.2, encompassing *COL5A2* and a miRNA gene, *MIR3129* was present in 4 non-DIPG (IN179, IN1930, IN3180 and IN3205) and 1 DIPG (IN2087) short-term cell cultures. *COL5A2* encodes an alpha chain for one of the low abundance fibrillar collagens and is associated with axon guidance, extracellular matrix organization and ossification and may be involved in binding SMAD proteins. Gain of 10q11.22 was present in 4 non-DIPG (IN1419, IN1930, IN3180 and IN3182) and 1 DIPG (IN2102) short-term cell cultures. This region contains *GPRIN2, NPY4RCH17-360D5.1* and *LINC00842*. Gain of 14q11.2 (199613 bp) occurred in 3 non-DIPG (IN1262, IN3032 and IN3182) and 2 DIPG (IN2102 and IN2675) short-term cell cultures and encompasses 5 genes, namely *OR4Q3, OR4M1, OR4N2, OR4K2*, and *OR4K5*. Gain of 15q11.2 occurred in 4 non-DIPG (IN1566, IN1930, IN3183 and IN3205) and 1 DIPG (IN2675) short-term cell cultures, and contains 17 genes comprising *HERC2P3, GOLGA6L6, GOLGA8CP, LOC646214, NBEAP1, CXADRP2, POTEB2, POTEB, POTEB3, NFIP2,LINC01193* and 2 clusters of miRNA genes including *MIR3118-2, MIR3118-3, MIR3118-4, MIR5701-1, MIR5701-2* and *MIR5701-3*.The less frequent gains at 10q23.33 (142024 bp), 14q32.33 (21696 bp), 15q11.2 (516123 bp) and 22q11.23 (53584 bp) were present in 23% (4/17 cases) of paediatric HGG short-term cell cultures.

Significantly altered regions of copy number loss

The most frequent and statistically significant copy number loss occurred at 8p11.23-p11.22 encompassing *ADAM5* and *ADAM3A* (minimal region of loss covered *ADAM3A*). The chromosome view illustrating loss of *ADAM3A* in a representative paediatric HGG short-term cell culture (IN1523) is shown in Figure 4.12.

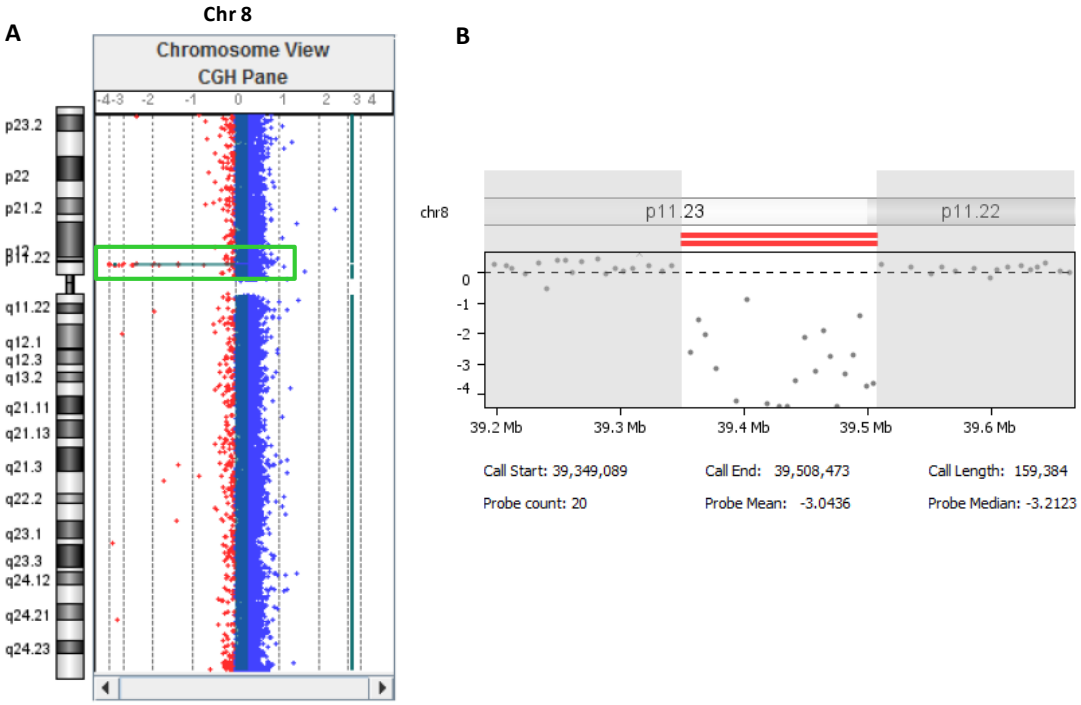

Figure 4.12 Loss of 8p11.23-p11.22 in IN1523 paediatric HGG short-term cell culture. A) Chromosome view displaying loss of 8p11.23-p11.22 in IN1523 paediatric HGG short-term cell culture. Each dot represents a single probe on the array. The log2ratios of the probes are plotted against the chromosomal location. Copy number gain and copy number loss shifts the log2ratios to the right and left respectively, of the baseline (0). Gain is represented by blue and loss is represented by red. **B)** Probe details of the gained region at 7p14.1 showing 16 probes in the gained region with mean 1.1670 and median 1.2135. Chromosome position is shown on the x-axis and log2ratios are shown on the y-axis. The horizontal dotted line represents the baseline (0).

Loss of this region covering 142, 664 bp, occurred in 58.82% (8/17) of samples, comprising 7 non-DIPG (IN179, IN1163, IN1262, IN1523, IN3046, IN3180,

IN3205) and 1 DIPG (IN2102) short-term cell culture (Table 4.7). Of these, homozygous loss of the locus was observed in 6/8 cases consisting of IN178, IN179, IN1523, IN3046, IN3180 and IN3205. This was also a region of gain in 4/17 cases, comprising IN1419, IN2675, IN3182 and IN3183.

The heat map showing loss of 8p11.23-p11.22 in paediatric HGG short-term cell cultures is shown in Figure 4.13.

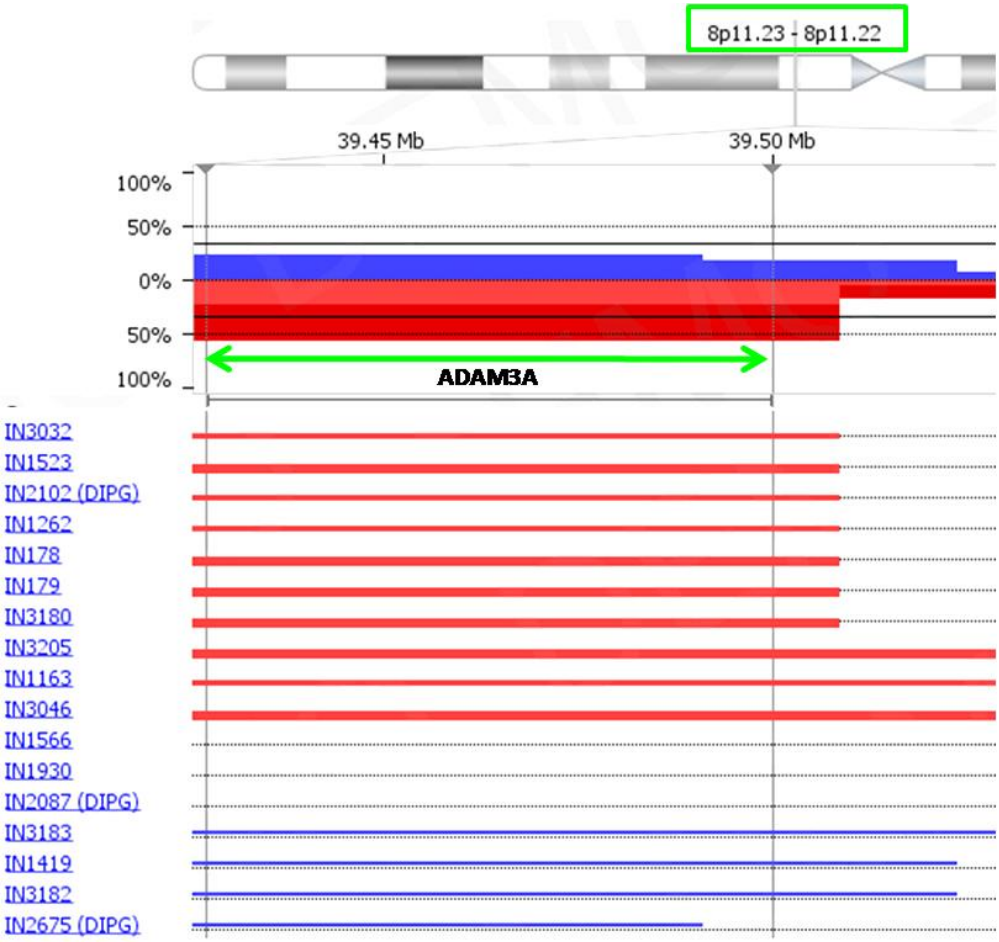

Figure 4.13 Heat map of CNA involving *ADAM3A* at 8p11.23-p11.22 in paediatric HGG short-term cell cultures. The heat map shows the minimal region of loss at 8p11.23-p11.22 encompassing *ADAM3A* in 10/17 cases, no change in copy number in 3/17 cases and copy number gain in 4/17 cases (complete-3, partial-1). X-axis shows chromosomal location; y-axis shows the overall frequency of CNA in 17 paediatric HGG short-term cell cultures; red thin line on the heatmap represents regions of loss, red thick line represents regions of homozygous loss, and blue thin line represents regions of gain.

The next most frequent region of loss was at 15q11.2 (629,510 bp) and occurred in 41.18% (7/17) paediatric HGG short-term cell cultures comprising 6 non-DIPG (IN178, IN179, IN1523, IN3046, IN3180 and IN3182) and 1 DIPG (IN2102) samples. There were 16 genes in this region, which included *NBEAP1, LOC646214, CXADRP2, MIR3118-2, MIR3118-3, MIR3118-4, POTEB2, POTEB, POTEB3, NFIP2, MIR5701-1, MIR5701-2, MIR5701-3, LINC01193, LOC727924,* and *LOC101927079.*

Loss of 1q31.3 (24645 bp), 6p21.32 (103506), 14q11.2 (222794 bp), and 17q21.31 (211312 bp) occurred in 35.29% (6/17) of paediatric HGG short-term cell cultures. The minimal region of loss at 1q31.3 was present in 5 non-DIPG (IN179, IN1163, IN1262, IN1419, IN3046) and 1 DIPG (IN2675) short-term cell cultures and encompassed a single gene *CFHR1.* Loss of 6p21.32 was exclusively present in non-DIPG short-term cell cultures (IN179, IN1566, IN1930, IN3032, IN3182 and IN3205) and encompassed the genes, *HLA-DRB1, HLA-DRB5,* and *HLA-DRB6.* Loss of 14q11.2 was also present exclusively in non-DIPG short-term cell cultures (IN178, IN179, IN1163, IN1523, IN1930 and IN3205) and encompassed 6 genes namely *OR4Q3, OR4M1, OR4N2, OR4K2, OR4K5,* and *OR4K1.* However, this was also a region of gain that occurred in 3 non-DIPG (IN1262, IN3032 and IN3182) and 2 DIPG (IN2102 and IN2675) short-term cell cultures. Loss of 17q21.31 containing *KANSL1, KANSL1-AS1, LRRC37A,* and *ARL17B,* occurred in 5 non-DIPG (IN1419, IN1523, IN1566, IN3046 and IN3182) and 1 DIPG (IN2102) short-term cell cultures.

Approximately 29.41% (5/17) paediatric HGG short-term cell cultures showed significant regions of losses at 1q44 (50830 bp), 4q13.2 (422840 bp), 11q11 (47731 bp) and 14q32.33 (176973 bp). Loss of 1q44 covering the genes *OR2T10, OR2T11,* and *OR2T35* was found in non-DIPG short-term cell cultures (IN1163, IN1930, IN3032, IN3205 and IN3183) only. Loss of 4q13.2 was found in 4 non-DIPG (IN1419, IN1523, IN3032 and IN3205) and 1 DIPG (IN2087) short-term cell cultures. The genes of interest in this region included *TMPRSS11E, UGT2B17,* and *UGT2B15.* Loss of 11q11 involving *OR4P4, OR4S2,* and *OR4C6* occurred in non-DIPG short-term cell cultures (IN178, IN179, IN1163, IN1566 and IN3046) only. Loss of 14q32.33, covering *MIR8071-1, MIR8071-2,* and *ELK2AP* was present in 3 non-DIPG (IN179, IN1163 and IN3180) and 2 DIPG (IN2087 and IN2102) short-term cell cultures.

Overall, the majority of the CNAs (17/23) that occurred in the non-DIPG short-term cell cultures were also present in at least 1 DIPG short-term cell culture. The CNAs identified as significant in the non-DIPG short-term cell cultures, but were not present in any DIPG short-term cell cultures involved gain of 15q11.2 and losses at 1q44, 1q21.1, 6p21.32, 11q11 and 14q11.2. There were 3 significantly altered regions involving gains at 10q23.33, 14q32.33 and 22q11.23, which occurred at a relatively higher frequency in DIPGs (66.6%) compared to the non-DIPGs (14.3%).

To maximise the identification of significantly altered regions that may be present in a smaller number of samples, significance testing was also performed using GISTIC algorithm in Nexus copy number software (v8.0, Biodiscovery Inc., USA). The list of highly statistically significant CNAs identified by GISTIC with a q-bound value

<0.25 (Beroukhim et al., 2007) and G-score cut-off value of 1.0 are listed in Table 4.8.

Twenty four CNAs were identified as statistically significant by GISTIC significance testing algorithm, including gains of Xp11.4 and Xq25. Of the remaining 22 CNAs, 13 were also identified by STAC. The CNA with the highest G-score and the lowest q-value was loss of 8p11.23-p11.22, which was also the most frequent and significant CNA in loss identified by STAC. Furthermore, the most significant gains such as 14q11.2 and 7p14.1 were also the most frequent and significant gains identified by STAC. The additional CNAs identified as significant by GISTIC were gains at 6p12.1, 3q24-q26.1, 7q34, 9p23, 9q34.11 and 16p11.2, and losses at 3q26.1, 5p15.33 and 22q11.23. Of note, these included copy number events on chromosomes that were shown to be unaltered by STAC analysis such as those involving chromosomes 3, 9 and 16. Among the identified CNAs, gains at 3q24-q26.1 and 16p11.2, and loss at 3q26.1 do not have genes mapping to these locations. The gain at 6p12.1 contains *DST*, which is associated with cell adhesion, cell cycle arrest, cell motility, cytoskeleton organization and extracellular matrix organization. The gains at 9p23 and 9q34.11 predominantly contain non-coding RNA genes.

Table 4.8 CNAs identified as significant by GISTIC algorithm in paediatric HGG short-term cell cultures.

Chr	Cytoband	Event	Q-Bound	G-Score	% of CNV Overlap	Genes
1	q21.1	CN Loss	0.06	3.996	100	*NBPF25P,LOC388692,FAM231D,FCGR1C*
2	q32.2	CN Gain	0.21	2.589	28	*COL5A2, MIR3129*
3 *	3q26.1	CN Loss	0.06	4.497	100	No genes in region
3 *	3q24-q26.1	CN Gain	0.21	3.319	100	No genes in region
4	q13.2	CN Loss	0.00	12.491	100	*TMPRSS11E, UGT2B17, UGT2B15*
5 *	5p15.33	CN Loss	0.15	3.523	100	No genes in region
6 *	p12.1	CN Gain	0.21	1.685	52	*DST*
7	p14.1	CN Gain	0.00	6.642	100	*TARP*
7 *	q34	CN Gain	0.21	3.665	100	*MTRNR2L6, PRSS1*
8	p11.23 - p11.22	CN Loss	0.00	16.960	100	*ADAM5, ADAM3A*
8	p11.23	CN Gain	0.21	2.001	100	*ADAM3A*
9 *	p23	CN Gain	0.21	2.421	42	*TYRP1, LURAP1L-AS1, LURAP1L*
9 *	q34.11	CN Gain	0.21	2.417	100	*SLC25A25-AS1,PTGES2, PTGES2-AS1, LCN2, C9orf16, CIZ1, DNM1, MIR199B, MIR3154, GOLGA2*
10	q11.22	CN Gain	0.21	2.332	100	*GPRIN2,NPY4R, CH17-360D5.1, LINC00842*
11	q11	CN Loss	0.00	8.546	100	*OR4P4, OR4S2, OR4C6*
11	q11	CN Gain	0.21	4.392	100	*OR4C11,OR4P4,OR4S2,OR4C6*
14	q11.2	CN Gain	0.00	7.269	100	No genes in region
14	q32.33	CN Gain	0.21	2.242	100	*MIR8071-1, MIR8071-2, ELK2AP*
15	q11.2	CN Gain	0.21	1.976	100	*HERC2P3, GOLGA6L6, GOLGA8CP, LOC646214,NBEAP1, CXADRP2, MIR3118-2, MIR3118-3, MIR3118-4, POTEB2, POTEB, POTEB3, NFIP2, MIR5701-1, MIR5701-2, MIR5701-3, LINC01193*
16 *	p11.2	CN Gain	0.21	1.577	100	No genes in region
22 *	q11.23	CN Loss	0.03	5.070	100	*GSTTP1,LOC391322,GSTT1-AS1,GSTT1, GSTTP2*
22	**q11.23**	**CN Gain**	**0.21**	**2.433**	**100**	***GSTTP1,LOC391322,GSTT1-AS1,GSTT1, GSTTP2***

The table shows the CNAs identified as significant by GISTIC (q-bound value <0.05 and G-score cut-off value 1.0.) in 17 paediatric HGG short-term cell cultures. * indicates CNAs that were not identified by STAC. Chr-Chromosome; CNV-copy number variation, CN-copy number.

4.2.7 Identification of association between CNAs

The 2 most frequent and significant CNAs identified in this study (gain of 7p14.1 and loss of 8p11.23-p11.22) were investigated to examine the association of their occurrence with other significant CNAs. In both the cases, the region that was completely covered by the aberration was included in the analysis (the region

involving *TARP* at 7p14.1 and the region involving *ADAM3A* at 8p11.23-p11.22). In each case, the Fisher's exact test was performed between two sample groups (samples with the copy number event versus samples without the copy number event) using the concordance tool in Nexus copy number software (v8.0, Biodiscovery Inc., USA). The CNAs with significant differences in occurrence ($p<0.05$) between the two sample groups at a differential threshold of 25% were identified (Table 4.9). The significant copy number events that co-occurred with loss of 8p11.23-p11.22 included loss at 14q11.1-q11.2 ($p=0.044$) covering 690,253 bp and 2 regions of loss at 15q11.2 covering 56,099 bp ($p=0.044$) and 353,868 bp ($p=0.044$) respectively (Table 4.9 and Figure 4.14). In all cases, the CNAs occurred at a frequency of 50% in samples with loss of 8p11.23-p11.22 versus 0% in samples without loss of the region. The region 14q11.1-q11.2 encompasses pseudogenes such as *DUXAP10, BMS1P17, BMS1P18* and *BMS1P22.* Of these, *DUXAP10* (double homeobox A pseudogene 10) is a homeobox gene that encodes DNA-binding proteins and may have potential involvement in early embryonic development. In addition, the region also covers *POTEG, POTEM, OR11H2*, non-coding RNA genes such as *POTEH-AS1, LINC01296* and 2 uncharacterised genes such as *LOC101929572* and *LOC100508046*. Of the two regions located in 15q11.2, no genes map to the first region. The genes found in the second region included *LOC727924, LOC101927079, OR4M2, OR4N4, OR4N3P, MIR1268A*, and *REREP3.*

Table 4.9 CNAs associated with loss of *ADAM3A* in paediatric HGG short-term cell cultures.

Chr	Cytoband Location	Event	Region Length (bp)	Frequency in samples with *ADAM3A loss* (%)	Frequency in samples without *ADAM3A loss* (%)	Frequency difference	Probe-level p-value	p-value	Genes
14	q11.1 - q11.2	CN Loss	690253	50	0	50	0.13	0.04	*LOC101929572, POTEH-AS1, POTEG, LINC01296, DUXAP10, BMS1P17, BMS1P18, BMS1P22, POTEM, LOC100508046, OR11H2*
15	q11.2	CN Loss	56099	50	0	50	0.05	0.04	No genes in region
15	q11.2	CN Loss	353868	50	0	50	0.00	0.04	*LOC727924, LOC101927079, OR4M2, OR4N4, OR4N3P, MIR1268A, REREP3*

CNAs that co-occurred in samples with *ADAM3A* loss in comparison to samples without the loss (minimum difference in threshold between the sample groups-25% and $p<0.05$) were identified. CN-copy number; bp- base pair.

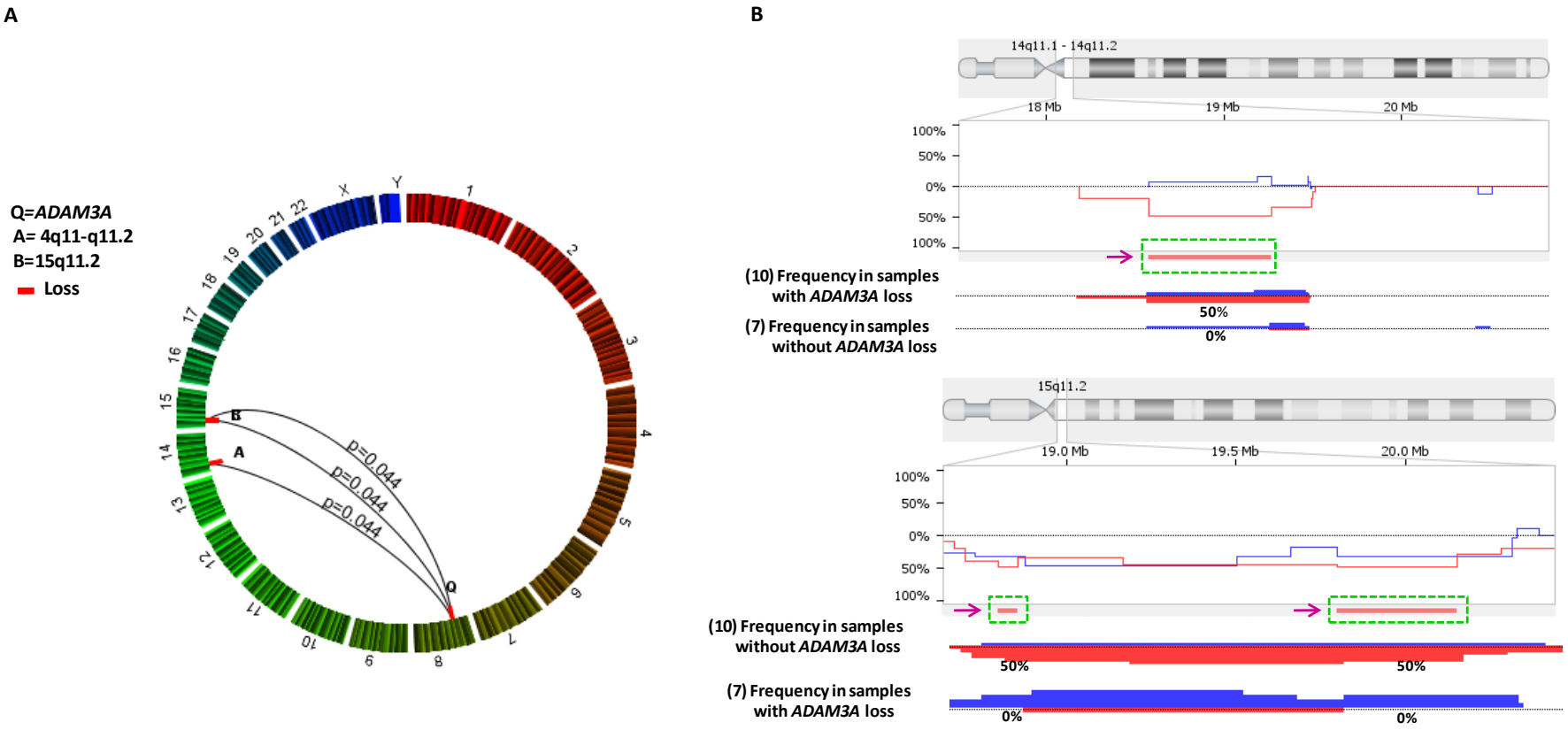

Figure 4.14 CNAs associated with loss of *ADAM3A* in paediatric HGG short-term cell cultures. A. The circular plot illustrates the association of loss of *ADAM3A* (Q) with loss of 14q11-q11.2 (A) and loss of 15q11.2 (B). Black lines indicate higher frequency of occurrence of the concordant copy number events in samples with *ADAM3A* loss compared to samples without *ADAM3A* loss. Red rectangular box indicates copy number loss. **B**. Chromosome view showing the relative frequencies of significantly associated alterations in samples with *ADAM3A* loss compared to samples without loss. X-axis shows the regions on chromosomes; y-axis shows the percentage frequencies of the concordant copy number events. The number of samples in each group is given in parenthesis. Loss of 14q11.1-q11.2 was seen in 50% of samples with *ADAM3A* loss. Loss of 15q11.2 (regions 1 and 2) was seen in 50% of samples with *ADAM3A* loss.

The significant CNAs that co-occurred with gain of *TARP* included 2 regions of loss at 11q11 covering 6731 bp and 15073 bp respectively. Loss at 11q11 covering 21,804 bp, after the 2 adjacent regions were combined occurred at a frequency of 63.48% in samples with gain of *TARP* versus 0% in samples without gain of *TARP* (Table 4.10 and Figure 4.15), with a frequency difference of 58.33%.

Table 4.10 CNAs associated with gain of *TARP* in paediatric HGG short-term cell cultures

Chr	Cytoband Location	CN Event	Region Length (bp)	Frequency in samples with *TARP gain* (%)	Frequency in samples without *TARP gain* (%)	Frequency difference	Probe-level p-value	p-value	Genes
11	q11	Gain	6731	75	0	75	0.11	0.01	No genes in region
11	q11	Gain	15073	58.33	0	58.33	0.21	0.04	No genes in region
Regions combined									
11	q11	Gain	21804	63.48	0	58.33	0.05	0.04	No genes in region

CNAs that co-occurred in samples with gain of *TARP* in comparison to samples without the gain (difference in threshold between the sample groups 25% and $p<0.05$) were identified. CN- Copy number; bp- base pair.

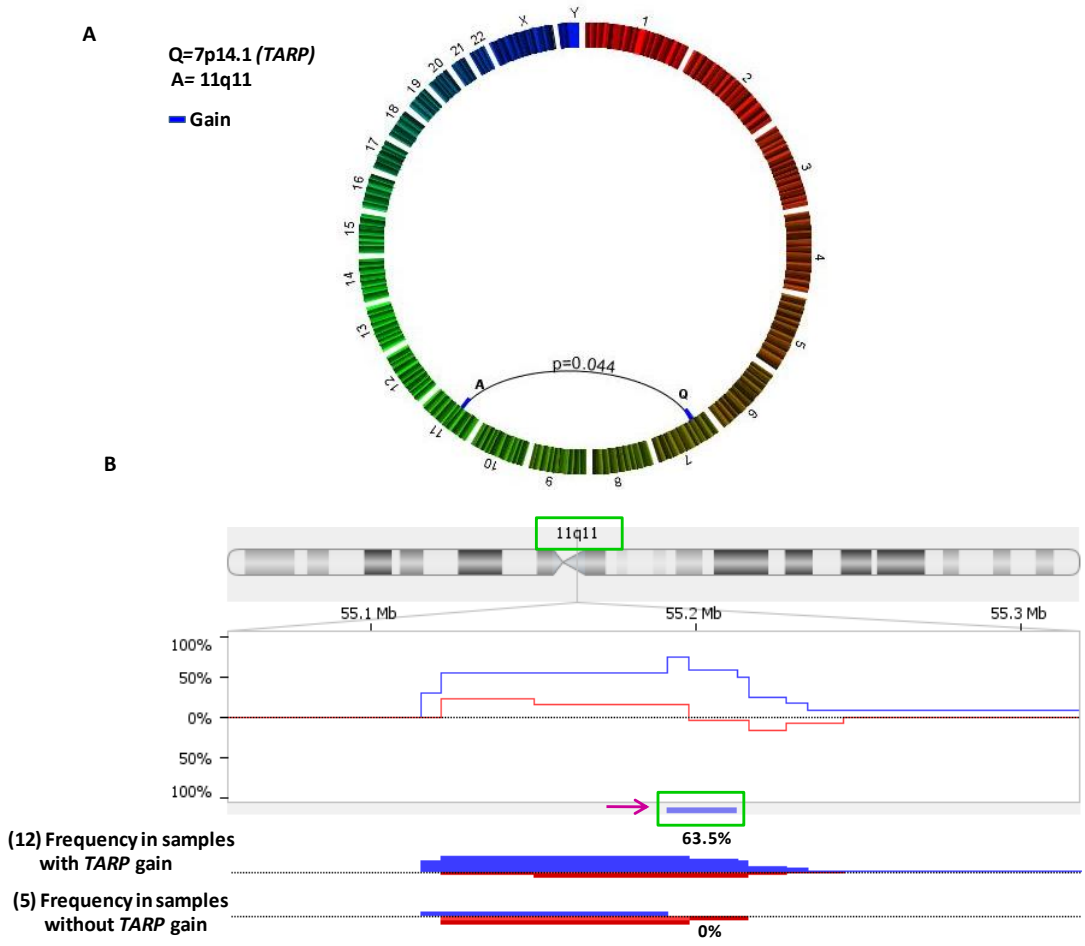

Figure 4.15 CNAs associated with gain of *TARP* in paediatric HGG short-term cell cultures. A) The circular plot shows the association between gain of *TARP* (Q) and gain of 11q11 (A) in paediatric HGG short-term cell cultures. The black line indicates higher frequency of the concordant copy number event in samples with gain of *TARP* as opposed to samples without gain of *TARP*. Blue box indicates copy number gain. **B)**. Chromosome view showing the relative frequency of alteration of the concordant event in samples with gain of *TARP* versus sample without gain of *TARP*. X-axis shows the region of CNA on the chromosome and y-axis shows the percentage frequency of the concordant CNA between the two groups. Blue line indicates the frequency of the event in samples with gain of *TARP* and red line indicates the frequency of the event in samples without gain of *TARP*. The blue line (shown by the arrow) indicates the region of concordant CNA. The number of samples with or without gain of *TARP* is given in parenthesis. Blue colour indicates copy number gain and red colour indicates copy number loss.

4.2.8 Hierarchical clustering identifies subgroups within paediatric HGG short-term cell cultures

To identify subgroups of paediatric HGG short-term cell cultures based on copy number aberration profiles, hierarchical clustering analysis was performed on 17 paediatric HGG short-term cell cultures using complete linkage hierarchical clustering algorithm in Nexus copy number software (v8.0, Biodiscovery Inc., USA). Euclidean distance metric was used to calculate the distances between clusters. For this analysis, the CNAs on sex chromosomes were excluded. Tumour subtype (DIPG or non-DIPG) was assigned to individual paediatric HGG short-term cell cultures to examine the influence of this factor on clustering. The resultant dendrogram is shown in Figure 4.16. The dendrogram revealed that IN1523 had a distinct genomic profile and did not cluster with any other paediatric HGG short-term cell culture. It was possible to identify 3 main clusters within the remaining members of the cohort. Cluster 1 (n=3) included IN1262, IN3046 and IN3180; cluster 2 (n=7) included IN178, IN179, IN1163, IN1566, IN2102, IN3032, and IN3205; and cluster 3 (n=6) included IN1419, IN1930, IN2087 (DIPG), IN2675 (DIPG), IN3182 and IN3183. The tumour subtype did not affect the clustering as DIPG and non-DIPG short-term cell cultures did not form separate clusters.

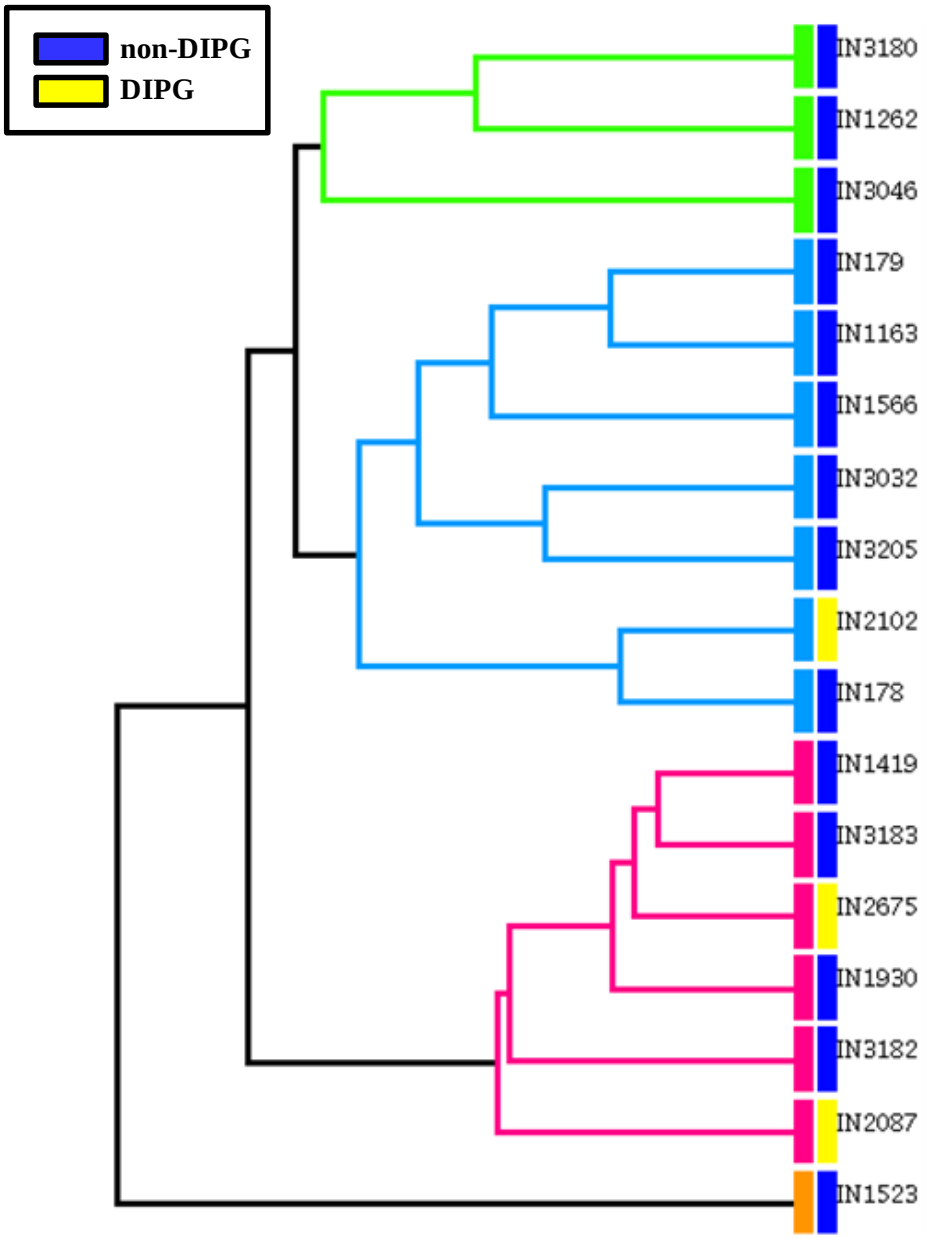

Figure 4.16 Hierarchical clustering an alysis. Hierarchical clustering analysis of 17 paediatric HGG short-term cell cultures was performed using complete linkage hierarchical clustering algorithm, excluding CNAs on the sex chromosomes. The dendrogram of 17 paediatric HGG short-term cell cultures branches into 3 major clusters represented by green, blue and pink respectively. IN1523 was independent. DIPG and non-DIPG short-term cell cultures are represented by yellow and blue blocks respectively.

Identification of CNAs by clusters

Both STAC and GISTIC significance testing algorithms were applied independently to identify significant CNAs within each cluster. STAC identified CNAs were defined by p-value<0.05 and occurring in a minimum of 50% of samples in each cluster. GISTIC significant CNAs in each cluster were defined by q-bound values <0.25 and G-score cut-off values <1.0. A combined list of CNAs identified by both algorithms and their distribution in clusters 1, 2 and 3 are shown in Figure 4.16.

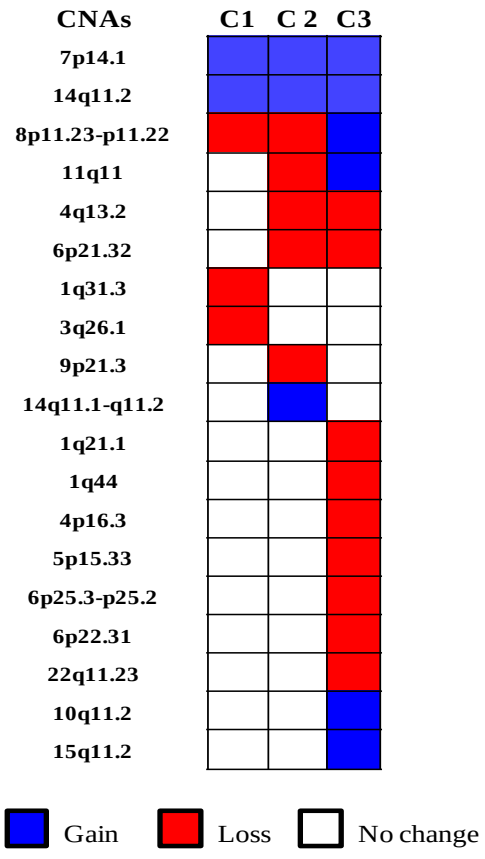

Figure 4.17 CNAs identified in clusters 1, 2 and 3. The CNAs identified as significant by STAC (aggregate- 50%, p<0.05) and GISTIC (q<0.25, G –score cut-off-1) in clusters 1, 2 and 3. Red indicates copy number loss; blue indicates copy number gain. C-Cluster.

With the exception of gained regions at 7p14.1 and at 14q11.2, CNAs identified as significant showed different patterns in the clusters. Loss of 8p11.23-p11.22 was seen in clusters 1 and 2, while gain of this region was found in cluster 3. The region involving 11q11 demonstrated copy loss in cluster 2, copy gain in cluster 3 and no change in copy number in cluster 1. Clusters 2 and 3 showed 2 distinct CNAs such as loss of 4q13.2 and loss of 6p21.32 that were not seen in cluster 1. Loss of 1q31.3 and loss of 3q26.1 were identified as significant and distinct in cluster 1, while loss of 9p21.3 and gain of 14q11.1-q11.2 were identified in cluster 2. The unique CNAs identified as significant in cluster 3 included losses involving 1q21.1, 1q44, 4p16.3, 5p15.33, 6p25.3-p25.2, 6p22.31, and 22q11.23, and gains involving 10q11.2 and 15q11.2.

4.2.9 CNAs in glioma-associated genes in paediatric HGG short-term cell cultures

The aberrations of well-known glioma-associated genes were examined in paediatric HGG short-term cell cultures (Table 4.12). For this analysis, only genes that were completely included in the CNA and identified as significant by both STAC and GISTIC were included. Probe median was computed in each case. Copy number gains of genes *CDK6*, *EGFR*, and *MET* were found in 17.65% of paediatric HGG short-term cell cultures including IN178, IN1523 and IN3182. Gain of *PIK3CA* was also seen in 17.65% of cases, which included 2 non-DIPG (IN179, IN1523) and 1 DIPG (IN2675) short-term cell cultures. Gain in other glioma- associated oncogenes such as *FGFR1*, *MYC*, *MYCN*, and *PDGFRA* were absent in the cohort. Loss of *CDKN2A* was present in 1 case (IN179) as previously shown in Figure 4.9. Losses

involving *PTEN* and *TP53* were absent in the paediatric HGG short-term cell cultures analysed here.

Table 4.11 Summary of frequencies of CNAs in known glioma-associated genes in paediatric HGG short-term cell cultures

Genes	CN Gain (%)	CN Loss (%)	Samples with CN event	Chromosome location
CDK6	17.65	0	IN179 , IN1523, IN3182	7q21.2
CDKN2A	0	0.0588	IN179	9p21.3
EGFR	17.65	0	IN179 , IN1523, IN3182	7p11.2
FGFR1	0	0	-	8p12
MET	17.65	0	IN179 , IN1523, IN3182	7q31.2
MYC	0	0	-	8q24.21
MYCN	0	0	-	2p24.3
PDGFRA	0	0	-	4q12
PIK3CA	17.65	0	IN179, IN1523, **IN2675**	3q26.32
PTEN	0	0	-	10q23.31
TP53	0	0	-	17p13.1

DIPG short-term cell culture is highlighted in blue. CN-copy number

4.3 Discussion

This study has characterised genome-wide DNA copy number changes in 17 paediatric HGG short-term cell cultures (comprising 14 non-DIPG and 3 DIPG short-term cell cultures) using high-resolution aCGH technology. The findings of this study not only validated some of the genetic changes previously reported in paediatric HGG but also revealed novel CNAs not previously described in these tumours.

Distinct subgroups within paediatric HGG

Genomic changes in the paediatric HGG short-term cell cultures in this study varied from a minimum of 0.14% to a maximum of 58.42% involving both broad and focal CNAs on different chromosomes, indicating genetic instability. The majority of the paediatric HGG short-term cell cultures (~65%) including 2/3 DIPG short-term cell cultures did not have large regions of DNA copy number imbalances involving whole chromosome arms. Such balanced genomic profiles have been previously reported in paediatric HGG (Bax et al., 2010; Barrow et al., 2011) as well as in other paediatric brain tumours such as ependymoma (Johnson et al., 2010), CNS PNETs (Li et al., 2009) and cribriform neuroepithelial tumours (CRINET) of the CNS (Gessi et al., 2015), indicating possible similarities in the developmental origins of these tumours. Moreover, these types of genomic profiles are not common in adult HGG, suggesting that the relatively normal profiles observed in this study may reflect the characteristic difference in paediatric HGG from their adult counterparts. Instead, samples in this study had very small, yet significant CNAs, some of which were not previously detected by conventional cytogenetic studies.

Subgroups of paediatric HGG with genetic changes resembling those found in adult HGG have been previously reported and were associated with worst prognosis (Paugh et al., 2010; Puget et al., 2010). Similar to these findings, large regions of chromosome aberrations were restricted to a small subgroup of paediatric HGG short-term cell cultures (IN179, IN1523 and IN3182). Two major genetic changes that reflected the characteristic chromosomal abnormalities seen in adult HGG were gain of 7 (Hun et al., 1999; Koschny et al., 2002; Lopez-Gines et al., 2005; Crespo et

al., 2011) and loss of 10q (Lopez-Gines et al., 2005). Chromosome 7 harbours important genes that are associated with gliomagenesis. Interestingly, the gain of chromosome 7 in this subgroup included the focal and significant ($q<0.25$) gain of *EGFR* (7p11.2). However, it should be noted that trisomy 7 can also be acquired by cells maintained under artificial culture conditions (Briand et al., 1996; Sareen et al., 2009). For instance, human neural progenitor cells (hNPCs) isolated from foetal brain tissue were found to have additional copies of chromosomes 7 and 19 as well as increased expression of *EGFR*, after 9-15 weeks in culture (Sareen et al., 2009). A comparison of CNAs in biopsy and its derived short-term cell culture in 2 B/CC pairs previously described in 3.2.1 revealed that trisomy 7 was absent in the biopsy, but present in the derived short-term cell culture for one of the pairs (IN3182 B/CC), while it was not present in either the biopsy or the derived culture for the other pair (IN3183 B/CC). Further studies in more B/CC pairs may provide a better understanding of the relevance of trisomy 7 in paediatric HGG. Loss of 10q is the most frequent large chromosome abnormality seen in adult GBM, which includes the loss of *PTEN* (10q23) (Mohapatra et al., 1998; Paugh et al., 2010; Qu et al., 2010). It also distinguishes adult from paediatric HGG, with frequencies of ~80% in adult HGG compared with ~27% in paediatric HGG (Paugh et al., 2010, Qu et al., 2010; Barrow et al., 2011, Jones et al., 2012). In this study, either complete or partial loss of 10q was seen in 2/3 members of this subgroup, which were not associated with loss of *PTEN*. *PTEN* is an important tumour suppressor gene that functions as a major negative regulator of PI3K/Akt signaling by catalysing PIP3 to PIP2 (Maher et al., 2001; Cully et al., 2006). This suggests that alternative mechanisms of activation of PI3K/Akt pathway may be active in these tumours.

Overall, 3 subgroups were identified within the paediatric HGG short-term cell cultures based on their genomic profiles: the subgroup without large scale chromosomal imbalances, and 2 other subgroups with large chromosomal imbalances involving either single or multiple chromosomes. Interestingly, the study by Bax et al., (2010) has identified similar genomic subtypes within paediatric HGG, which had prognostic potential. In that study, the tumours had either stable, aneuploid, highly rearranged or amplifier genomic profiles. The subtype with stable genomes had better prognosis, while those with amplifier genomes had poor prognosis. Therefore, specific patterns of genomic profiles may have roles as prognostic indicators in paediatric HGG.

Similarities of CNAs between paediatric and adult HGG

The most predominant chromosome arm aberrations previously reported in paediatric HGG include gains of 1q and losses of 4q and 16q (Bax et al., 2010; Barrow et al., 2011; Paugh et al., 2010). Gain of 1q and loss of 4q were seen in 5.9% and loss of 16q in 11.8% of paediatric HGG short-term cell cultures, respectively. The low frequencies of occurrence of these CNAs may be due to the low sample number (n=17) in this study. The highest frequencies of chromosome arm aberrations in this cohort were gains involving 3q, 7p, 7q, 9p and 9q each seen in 17.6% of paediatric HGG. Although gain of chromosome 7 (Paugh et al., 2010; Barrow et al., 2011) and 9q (Paugh et al., 2010) have been previously described in paediatric HGG, frequent gains of 3q and 9q have not been reported. Chromosome 7 and 9 gains occurred concurrently, the relevance of which has not been investigated in these tumours. Of particular interest was the gain of chromosome 3q as this was also present in 1 DIPG

short-term cell culture (IN2675). Moreover, chromosome 3q harbours several important genes involved in DNA damage response and repair (*ATR, MBD4, PSMD2, SENP2, TP63* and *ZMAT3*), BMP signaling (*SLC33A1* and *FSTL1*), bone morphogenesis (*OSTN, BBX* and *IFT8*), and cell cycle arrest (*SKIL*) (GO enrichment analysis, Nexus copy number software (v8.0, Biodiscovery Inc., USA)). Importantly, it also contains genes involved in PI3K/Akt pathway (*PIK3CA, PIK3CB* and *PIK3R4*), suggesting a potential role for this pathway in paediatric HGG including DIPG. Gain of 3q in all cases was concordant with focal gain of *PIK3CA* and *PIK3CB.* In a study by Warren et al., (2012), the gained region on 3q encoding *PAK2* (p21 protein (Cdc42/Rac)-activated kinase 2), an apoptosis-related gene, was found in both the low-grade and high-grade regions of a DIPG sample from the same patient. It has also been associated with tumour progression in glioma (Vranova et al., 2007), tumour aggressiveness in epithelial cancers (Chaluvally-Raghavan et al., 2014), invasiveness in cervical carcinoma (Rao et al., 2004) and poor prognosis in early stage cervical squamous cell carcinoma (Huang et al., 2007). Gain of 3q may therefore be an alternative mechanism of activation of PI3K pathway in these tumours which do not typically harbour *PTEN* loss.

Frequent CNAs in paediatric HGG

Genes with oncogenic roles in cancers are often found in gained/amplified genomic regions, while those with tumour suppressors may be found in regions of loss/deletion. Considering these, genomic CNAs recurring in a minimum of 4/17 paediatric HGG short-term cell cultures were evaluated to identify candidate genes that may function either as drivers or as passengers through their cooperative

interaction with other genes and contribute to tumourigenesis or progression. In addition, significance tests were performed to eliminate CNAs that may have occurred due to chance phenomena. The unbiased approach in this study has led to the identification of gains at 14q11.2 and 7p14.1 as the most frequent (94% and 76.4% respectively) CNAs in the paediatric HGG short-term cell cultures, with high-copy gain of 7p14.1 observed in one of them (IN3182). Both these CNAs have not been previously identified in paediatric HGG. The gain at 7p14.1 encompassed *TARP*, which encodes a protein expressed in prostate cancer cells as well as in adenocarcinoma of prostate and breast cancers (Wolfgang et al., 2000). Interestingly, CNVs at 7p14.1and 14q11.2 have been reported to be associated with Dupuytren's disease, a fibroproliferative disorder characterised by deformities in the fingers (Shih et al., 2012). A similar connection in genetic aberrations between paediatric HGG and an inherited disorder has been reported in DIPG patients with *ACVR1* mutations, which were also found in patients with Fibrodysplasia ossificans progressiva (FOP), a disorder that causes ossification of soft tissues leading to muscular deformities. It is therefore likely that developmental processes may have a role in tumourigenesis of paediatric HGG. In this study, gain of a region at 11q11 appeared to have significantly co-occurred with gain of 7p14.1 at a frequency of approximately 63.5% in paediatric HGG with gain of 7p14.1. The co-occurrence of 7p14.1 and 11q11 may be an indicator of poor prognosis in paediatric HGG, but this requires detailed investigation.

Paediatric HGG including DIPG are characterised by diffuse infiltration into the surrounding normal brain structures making them less vulnerable to therapeutic

intervention (Demuth and Berens, 2004; Buczkowicz and Hawkins, 2015). The invasive phenotype of these tumour cells is the net result of their interactions with the tumour microenvironment, primarily composed of stromal cells and the extracellular matrix (ECM) (Payne and Huang, 2013). Collagens form the major components of ECM and play vital roles in modulating cell invasion, growth and survival of glioma. Recently, Cockle et al. (2015) demonstrated efficacy of anti-migratory agents in paediatric HGG and DIPG cells using 2D and 3D assays. In this study, approximately 30% of paediatric HGG short-term cell cultures including 1 DIPG (IN2087) had gain of chromosome 2q32, which contains *COL5A2*, an important collagen encoding gene. *COL5A2* encodes an alpha chain for one of the low abundance fibrillar collagens. Genetic aberrations in this gene have not been previously identified in paediatric HGG. Novel mutations in this gene have been identified in Ehlers-Danlos syndrome, a rare inherited connective tissue disorder characterised by joint hypermobility (Ritelli et al., 2013). Chromosome 2q32 also contains *MIR3129,* a novel miRNA gene the role of which has not been investigated.

Potential role of CNAs in non-coding RNA genes in paediatric HGG

The significance of non-coding elements of the human genome such as non-coding RNA genes and pseudogenes as markers of cellular identity and prognosis in various types of cancers are being increasingly understood (Chan et al., 2013; Han et al., 2014; Rutnam et al., 2014; Guo et al., 2015). Bioinformatic analysis in adult glioma has identified a specific six-pseudogene signature consisting of *TDH, LPAL2, CLCA3P*, *SP3P*, *PTTG3P* and *ANXA2P3* that revealed prognostic significance, independent of patient age and gender (Gao et al., 2015). *TDH* was identified to have

a protective role, while the other 5 genes were considered high risk and were associated with reduced overall survival. In this study, several pseudogenes were identified predominantly in the regions of copy number loss. The most frequent loss at 8p11.23-p11.22 found in 58.82% of paediatric HGG short-term cell cultures contains 2 pseudogenes *ADAM5* and *ADAM3A.* This was also the most frequent region of homozygous loss detected in the paediatric HGG short-term cell cultures (35.3%). Interestingly, the minimal region of deletion at 8p11.23 encompassing *ADAM3A* was also a region of gain in a small subgroup that consisted of 4 paediatric HGG short-term cell cultures (IN1419, IN2675 (DIPG), IN3182 and IN3183), suggesting that *ADAM3A* may be a target of frequent genetic disruption in paediatric HGG.

The members of the *ADAM* family of genes encode catalytically active or inactive membrane-bound metalloproteases, which participate in various cellular processes such as adhesion, cell-cell and cell-matrix interactions (Wolfsberg et al., 1995; Brocker et al., 2009). Predominantly expressed in testicular cells, *ADAM3A* belongs to the catalytically inactive subgroup that lacks protease activity. The basic function of this gene is associated with integrin-dependent binding and fusion of gamete plasma membrane during fertilisation (Yuan et al., 1997; McLaughlin et al., 2001). Recent studies indicate that dysregulation of *ADAM3A* may be associated with cancer. For instance, homozygous loss of *ADAM3A* has been previously reported in paediatric HGG (Barrow et al., 2011), as well as in other cancers such as laryngeal basaloid squamous cell carcinoma (Ecsedi et al., 2012), lung cancer (Liu et al., 2012), malignant mesothelioma (Klorin et al., 2013) and NK/T-cell lymphoma (Sun

et al., 2014). The loss of *ADAM3A* in NK/T-cell lymphoma was associated with significantly poor survival (*P*=0.024). Frequent amplification and overexpression of *ADAM3A* was reported in conjunctival squamous cell carcinoma (Asnaghi et al., 2014) and gain was reported in CNS CRINETs (Gessi et al., 2015), a rare type of paediatric brain tumour. It was interesting to note that the majority of these studies were published after 2011 and involved the use of high-resolution microarrays, emphasising the strength of these arrays in detecting aberrations that were previously unidentified in cancers. The loss of *ADAM3A* in this study was significantly concordant ($p<0.05$) with losses at 14q11.1-q11.2 and 15q11.2. Both 14q11.1-q11.2 and 15q11.2 contain several non-coding RNA genes and pseudogenes, suggesting a possible role for other pseudogenes in *ADAM3A* regulation. Of interest, 14q11.1-q11.2 included a homeobox gene, *DUXAP10* with potential involvement in early embryonic development. The region covered by 15q11.2 contains a miRNA gene, *MIR1268A* which has not been previously reported in cancer. Given the role of pseudogenes and their interactions with non-coding RNA genes as well as protein coding genes in cancer (Xiao-Jie et al., 2014), *ADAM3A* may be a potential candidate gene in paediatric HGG and further investigations are required to validate this finding. The loss at 1q21.1 contains 2 pseudogenes *NBPF25P,* a member of the neuroblastoma breakpoint family gene and *FCGR1C.* A CNV at 1q21.1, which included *NBPFX* has been identified as susceptibility locus in the childhood cancer neuroblastoma (Diskin et al., 2009), and a CNV at this locus, which included *NBPF23* has been reported in paediatric GBM (Giunti et al., 2014). Therefore, this raises the question whether a potential likelihood of inherited predisposition to cancer exists in a subset of paediatric HGG, and if so, whether pseudogenes play any

role in this process, but this requires further investigation. Pseuodegenes were also found in regions of copy number gain as at 15q11.2, which included *HERC2P3, GOLGA8CP, NBEAP1* and *CXADRP2.* This region also had 2 clusters of miRNAs, *MIR5701* and *MIR3118.* Interestingly, the role of pseudogenes in regulating the effects of miRNAs on their mRNA targets by competing with miRNAs has been reported in cancers. For instance, deletion of *PTENP1* (the pseudogene of *PTEN*) in melanoma has been observed to cause enhanced miRNA-mediated inhibition of PTEN and tumour progression (Poliseno et al., 2011). The CNA in gain at 9q34.11 had protein coding genes including a sense-antisense gene pair (*PTGES2* and *PTGES2-AS1*), also present along with miRNA genes such as *MIR199B* and *MIR3154.* Recently, prognostic significance for sense-antisense gene pairs has been reported in cancers (Balbin et al., 2015). These suggest a putative cross-communication between coding and non-coding genes in paediatric HGG. Genomic studies have shown that DIPG and non-DIPG HGG may share certain genomic CNAs despite their origins in different locations in the brain (Barrow et al., 2011). Homozygous loss at 4q13 has been previously reported in paediatric HGG (Barrow et al., 2011, Giunti et al., 2014) including DIPG. However, no studies have established its role in these tumours. In this study, homozygous loss of 4q13.2 was found in approximately 30% of paediatric HGG, including 1 DIPG. This was the only homozygous loss detected in the DIPG short-term cell cultures (IN2087). This region contains *TMPRSS11E,* a type II transmembrane serine protease, involved in the degradation of ECM (Hooper et al., 2001). The genes found in this region encode members of the UDP-glucuronosyltransferases (UGT) family of enzymes (UGT2B15 and UGT2B17), that catalyze the transfer of glucuronic acid from uridine 5'-

diphosphoglucuronic acid to a variety of substrates with functional groups of oxygen, nitrogen, sulphur or carbon, making them water-soluble and less-toxic for easy elimination from the body (Tukey and Strassburg, 2000). In prostate cancer cells, UGT2B15 and UGT2B17 participate in the degradation of dihydrotestosterone (DHT) and the failure of these enzymes to completely degrade DHT may be associated with cancer susceptibility (Park et al., 2007). Loss of 4q13.2 may therefore play a role in causing increased susceptibility to carcinogens in paediatric HGG. Several recent investigations have led to the identification of the prominent role of epigenetic mechanisms in paediatric HGG, particularly DIPG. Copy number loss of 17q21.31 detected in approximately 35% of paediatric HGG short-term cell cultures including 1 DIPG (IN2102) in this study, contains genes that encode chromatin modifiers, notably *KANSL1*. This gene encodes a nuclear protein participating in histone acetylation. In addition, genome-wide association studies (GWAS) have revealed association of 17q21.31 locus with susceptibility to ovarian cancer (Couch et al., 2013), suggesting this as an important site of genetic disruption that may likely increase the risk of cancer development.

Concurrent loss of 9p21.3 and BRAFV600E mutation in a subset of paediatric HGG

Deletion at 9p21.3 encompassing *CDKN2A/CDKN2B* has been reported in paediatric and adult HGG (McLendon et al., 2008; Paugh et al., 2010). The co-occurrence of homozygous loss of 9p21.3 and oncogenic *BRAFV600E* point mutation has been identified as a characteristic genetic signature associated with a subset of paediatric HGG (Schiffman et al, 2010; Huillard et al., 2012). In this study, loss of 9p21.3 and

BRAFV600E mutation was concordant in a single case (IN179), further validating the existence of this tumour subset within paediatric HGG. Interestingly, this was not a DIPG-derived short-term cell culture, further supporting the previous reports of extremely low frequency of *CDKN2A/CDKN2B* deletion in DIPG (2/119 cases, 2%) relative to paediatric HGG ($p<0.0001$). From a clinical perspective, patients with these characteristic genetic changes may benefit from a combined treatment strategy that targets both the aberrations. *CDKN2A* is a well-known tumour suppressor gene that stabilises p53 through its interaction with the E3 ubiquitin-protein ligase MDM2, resulting in degradation of p53 and is a frequent target of mutation or deletion in several types of tumours. *CDKN2B* lies adjacent to *CDKN2A*, which encodes a protein that forms a complex with CDK4 or CDK6 inhibiting activation of the CDK kinases.

Comparison between DIPG and non-DIPG

Differences in copy number changes that differentiate DIPG from both non-DIPG as well as adult HGG have been reported, indicating that these tumours may form unique subgroups within paediatric HGG (Bax et al., 2010; Paugh et al., 2010; Paugh et al., 2011). In the current study, there was no significant difference at the copy number level that distinguished DIPG from their non-DIPG counterparts, but this may be due to the relatively low numbers of DIPG short-term cell cultures available for this study. However, there were 2 genomic CNAs (gains at 10q23.33 and 22q11.23) that were relatively more frequent (66.6%) in the DIPG compared to the non-DIPG (14.3%) short-term cell cultures, although the differences in their frequencies of occurrence between the 2 tumour subgroups were not quite

statistically significant (p=0.06). Interestingly, both these CNAs encompassed genes that have not been previously linked to DIPG tumour biology. Chromosome 10q23.33 contains *MYOF*, which encodes a member of the ferlin family of membrane proteins involved in plasma membrane fusion events, repair and endocytosis (Cipta and Patel, 2009). Initially identified as a muscle specific protein (Davis et al., 2000), increased expression of *MYOF* at mRNA or protein levels has been reported in breast cancer (Labhart et al., 2005), pancreas ductal carcinoma (lacobuzio-Donahue et al., 2003) and oropharyngeal squamous cell carcinoma (OSCC) (Kumar et al., 2016) cells. In OSCC, *MYOF* has been identified to be associated with poor clinical outcome. Excessive production of MYOF in breast cancer cell lines have shown to cause increased invasion and secretion of MMPs, while silencing of the gene reverses the process possibly by degradation of EGFR signaling pathway (Li et al., 2012; Turtoi et al., 2013). Another major reason for the extremely poor clinical response in DIPG patients is the inherent drug-resistance of these tumours. For instance, DIPG patients have failed to show clinical response in trials involving radiotherapy and concomitant TMZ (Buczkowicz and Hawkins, 2015), despite the lack of expression of MGMT that repairs TMZ alkylated O6-guanine nucleotides and contribute to resistance (Zarghooni et al., 2010). The gain at 22q11.23 contains members of the glutathione-S-transferase family of genes such as *GSTT1, GSTTP1* and *GSTTP2,* which encode detoxification enzymes that catalyze the conjugation of glutathione with xenobiotic compounds thereby protecting the cells from a variety of toxic substances such as carcinogens and chemotherapeutic agents (Frova, 2006). This may have a role in predicting drug response in DIPG as increased expression of these enzymes may lead to accelerated detoxification of

drugs resulting in poor clinical response. Copy number gain of *GSTT1* has been reported as a predictive marker for poor response to imatinib in gastrointestinal stromal tumours (Lee et al., 2013).

Notably, gain of 22q11.23 was found in 2 DIPG (IN2102 and IN2675), and 2/3 non-DIPG short-term cell cultures that carried large genomic rearrangements (IN179 and IN1523), while this was also a region of deletion in 3 paediatric HGG short-term cell cultures (IN1419, IN1566 and IN3046) with relatively less number of CNAs (average, 18 CNAs per sample). Deletion of 22q11.23 has been found in ovarian, cervical and endometrial carcinoma cells (Ueda et al., 2003; Howells et al., 2001) and also reported to cause predisposition in cells to p53 mutation in breast cancer (Gudmundsdottir et al., 2001). Therefore, paediatric HGG with loss of 22q11.23 may be more susceptible to environmental and genotoxic stress leading to the development and progression of tumours.

Key focal CNAs and genomic clusters

The hierarchical clustering analysis stratified the paediatric HGG short-term cell cultures into three major clusters, while one of them (IN1523) that had highly rearranged genomic profile was independent. There were 4 regions, the copy number statuses of which differentiated the three clusters and consisted of 8p11.23-p11.22, 11q11, 4q13.2 and 6p21.32. It is likely that these aberrations have prognostic roles in paediatric HGG. However, these subgroups were not similar to the subgroups that were described earlier based on the proportion of genomic changes.

Limitations

High-resolution DNA microarray is indeed a powerful molecular biology technology that aids the precise detection of genomic DNA copy number changes. However, accurate detection of CNAs depends largely on good microarray data quality and optimised segment analysis. Extraction of good quality microarray data from samples can be challenging as background noise may be introduced at any stage between sample processing to the final wash step, which may affect the DLRS ratios and lead to false copy number calls. To avoid this, the analysis criteria that were used to assess the data quality as well as for the segmentation analysis were kept at the higher end of stringency. At the same time, as the majority of the paediatric HGG short-term cell cultures in this study had very small focal CNAs, care was also taken to identify as precisely as possible, the most significant events in these tumours using 2 significance testing algorithms, STAC and GISTIC. However, it is likely that these processes may have resulted in the loss of some data. In addition, segmentation algorithms vary from software to software influencing the outcome of analysis to some extent. In this study, the 3 segmentation algorithms tested using the cell culture with the highest number of CNAs revealed that the different algorithms retained the major chromosome changes, while some of the smaller changes were not concordant among them. This is crucial especially for analysis of tumours like paediatric HGG that do not have many copy number changes. It would also be interesting to compare the level of concordance in the detected segments using additional cultures in the cohort.

3.3 Conclusions

The utilisation of high-resolution DNA microarrays has enabled the identification of several small interstitial CNAs which were not previously detected by conventional cytogenetic studies that were of comparatively low-resolution. The detection in this study of previously reported genomic changes in paediatric HGG strengthens the utility of paediatric HGG derived-short-term cell cultures for genome-wide copy number studies. The novel CNAs detected in this study contribute to the current understanding of tumour biology in paediatric HGG including DIPG. These CNAs, which included coding and non-coding genetic elements, reveal the genetic complexity in paediatric HGG. Further investigations in an extended cohort of samples may provide valuable insights into their roles in the development and progression of these devastating tumours, which may lead to the identification of effective prognostic and therapeutic targets.

CHAPTER 5

Genome-wide miRNA expression profiling in paediatric HGG short-term cell cultures

5.1 Introduction

MiRNAs are a family of small non-coding RNAs of ~18-25 nucleotides in length that are key post-transcriptional regulators of gene expression, mediating various aspects of the tumourigenic process including migration, invasion, proliferation, apoptosis evasion, angiogenesis, and metabolism (Farazi et al., 2013). They interact with protein-coding genes based on complementary base-pairing between sequences in their seed regions (nucleotides 2-8) and 3'UTRs of their target mRNAs leading to translation inhibition or mRNA degradation. Widespread dysregulation of miRNAs has been reported in almost all types of cancers (Birks et al., 2011; Kotani et al., 2010; Farazi et al., 2013).

Microarray-based high-throughput analyses have provided valuable insights into the significance of miRNAs as diagnostic, prognostic and therapeutic biomarkers in cancers (Yanaihara et al., 2006; Greither et al., 2009; Valladares-Ayerbes et al., 2011). It has been increasingly recognised that miRNAs can not only distinguish tumours from their normal counterparts, but also differentiate tumour subtypes as well as different stages of tumour progression (Calin et al., 2004; Lu et al., 2005). In adult glioma, several studies have identified significant involvement of miRNAs in almost all aspects of gliomagenesis. For instance, mir-7 exerts tumour suppressive roles in glioma by inhibition of EGFR pathway as well as by independent suppression of Akt (Kefas et al., 2008). MiR-10b is identified as an oncomiR in malignant glioma cells that can target *CDKN1A* and *CDKN2A* (Gabriely et al., 2011). Besides individual miRNAs, characteristic miRNA expression signatures with potential therapeutic significance have also been identified in adult glioma. A

comprehensive analysis of miRNA expression profiles of 261 glioma from the TCGA data has identified a set of 121 miRNAs that stratified these tumours into five different subclasses (Kim et al., 2011).

Among the very few studies conducted in paediatric HGG, genome-wide miRNA expression analysis in a panel of 24 paediatric CNS tumours including 4 paediatric HGGs has identified dysregulation of miR-129, miR-142-5p and miR-25. Hierarchical clustering of these tumour subtypes revealed distinct patterns of miRNA expression among the tumour sub groups, particularly paediatric GBMs (Birks et al., 2011). Recently, Jha et al. (2014) reported differential expression of miRNAs such as miR-10b, miR-891a, miR-182, (upregulated), miR-138, miR-7 and miR-129 (downregulated) in supratentorial paediatric HGG compared to normal brain. They also identified unique miRNAs regulating PDGFR and SMAD 2/3 pathways in paediatric HGG compared to adult HGG.

Studies have shown that paediatric HGG are distinct tumour entities characterised by unique molecular changes compared to their adult counterparts (Jones et al., 2014). Mutations in *H3F3A* involving lysine to methionine amino acid substitution (K27M) have been identified as characteristic driver mutations in paediatric HGG, particularly DIPG. A study by Jha et al. (2014) has reported miRNAs associated with *H3F3A* mutation that can potentially target genes involved in the regulation of apoptosis, cell cycle, and proliferation such as *CDK6, FOXO1, FOXG1* and *MEIS2.* It is probable that distinct patterns of miRNA expression may exist in these tumours that could be exploited for the development of diagnostic, prognostic or therapeutic biomarkers. Work in Chapter 3 has identified *H3F3A* (K27M) mutation involving

lysine to methionine amino acid substitution at position 27, in 2 out of 17 paediatric HGG short-term cell cultures.

Recently, homozygous loss of *ADAM3A*, a pseudogene was observed in paediatric HGG glioma including DIPG, (Barrow et al., 2011) but further studies investigating the consequence of this genetic aberration in paediatric HGG have not been reported. The work in Chapter 4 detected copy number loss of *ADAM3A* in a subgroup of paediatric HGG short-term cell cultures (10/17 cases).

The aims of this chapter were to investigate the differential expression of miRNAs in paediatric HGG short-term cell cultures compared to NHA and to identify deregulated gene targets of these miRNAs using integrative analyses of miRNA and mRNA expression profiles in the same samples. The miRNA expression patterns associated with tumour subtypes (DIPG or non-DIPG), *H3F3A* mutation, and copy number loss of *ADAM3A* in paediatric HGG short-term cell cultures were also investigated.

5.2 Results

5.2.1 Differential expression of miRNAs between paediatric HGG short-term cell cultures and normal human astrocytes (NHA)

Using Toray's 3D-Gene Human miRNA Oligo chips (Toray industries, Tokyo, Japan), the expression patterns of 1719 miRNAs were investigated in 17 paediatric HGG short-term cell cultures (comprising 14 non-DIPG and 3 DIPG) and a control population of Normal Human Astrocytes (NHA), as described in 2.8.4. Data analysis

was performed using Partek Genomics Suite (version 6.6; Partek Inc., USA). The data obtained from processed microarray images were normalised with log2 median and filtered to remove unreliable probes prior to downstream statistical analysis. These consisted of control probes as well as miRNAs without detectable expression in any of the samples (n=866). PCA was performed with the remaining 853 informative miRNA probe sets across 17 paediatric HGG short-term cell cultures and NHA as described in 2.12.4. Tumour subtype (non-DIPG or DIPG) and *H3F3A* (K27M) mutation status (mutant or wild type) were assigned to each paediatric HGG short-term cell culture. The results are illustrated as a 3-D scatter plot in Figure 5.1. PCA showed that the paediatric HGG short-term cell cultures and NHA clustered separately.

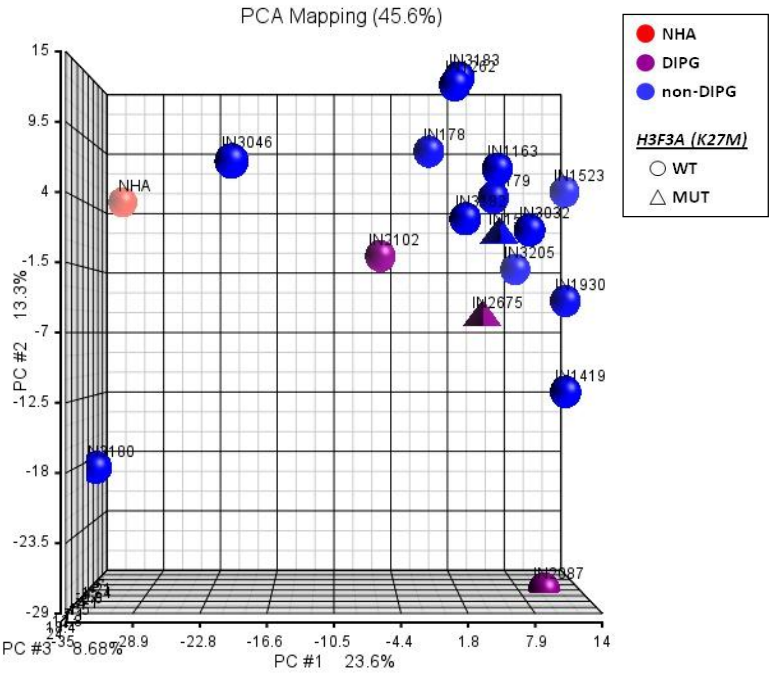

Figure 5.1 PCA plot of 17 paediatric HGG short-term cell cultures and NHA. PCA scatter plot of 17 paediatric HGG short-term cell cultures and NHA, plotted using the first three PCs (PC1=23.6%, PC2=13.3% and PC3=8.68%). Each dot on the PCA plot denotes a sample. NHA, non-DIPG and DIPG short-term cultures are represented by red, blue and dark purple, respectively. Tetrahedron indicates *H3F3A* (K27M) mutation.

Of the 17 paediatric HGG short-term cell cultures, 14 clustered together, which included the 2 *H3F3A*-mutant (K27) samples (IN1566 and IN2675 (DIPG)), while the remaining 3 samples (IN3046, IN3180 and IN2087 (DIPG) did not cluster with the main group and were independent of each other. Unsupervised hierarchical clustering was performed using the average linkage hierarchical clustering algorithm with Euclidean distance as similarity metric. Figure 5.2 shows the resultant dendrogram illustrating samples with similar expression profiles clustered together. With the exception of a single case (IN3180), paediatric HGG short-term cell cultures clustered distinctly from NHA. There were sub clusters within the large group, but these did not differentiate the tumour subtypes. However, the 2 *H3F3A*-mutant paediatric HGG short-term cell cultures clustered together within the large group.

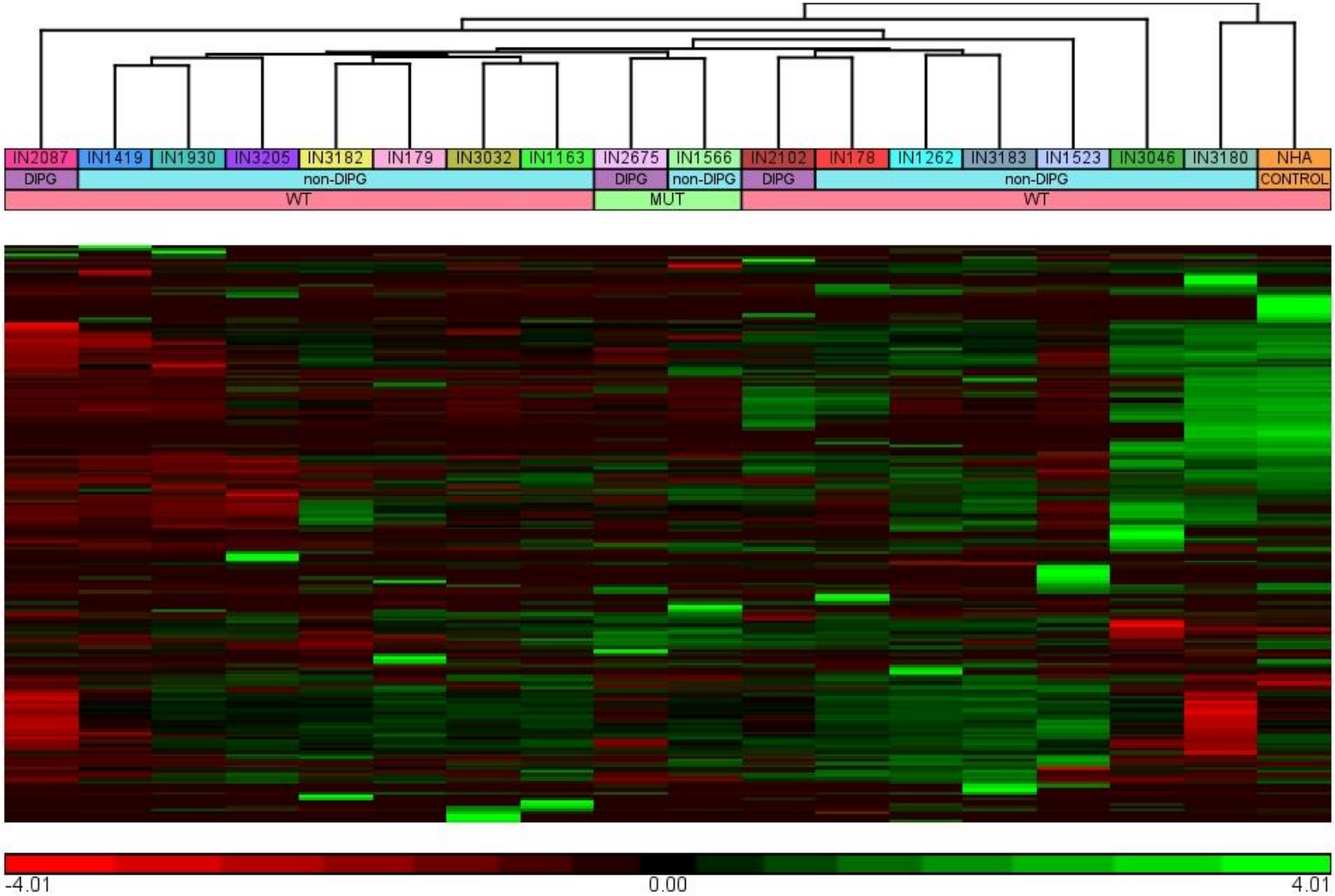

Figure 5.2 U**nsupervised hierarchical clustering of 893 miRNAs in 17 paediatric HGG short-term cell cultures and NHA.** Unsupervised hierarchical clustering of samples performed using average linkage algorithm in Partek Genomics suite v6.6. The dendrogram shows samples with similar expression profiles clustered together. On the heat map, the rows represent miRNAs and the columns represent samples. Green and red colours represent high and low levels of miRNA expression respectively. WT- *H3F3A* (K27) wild type, MUT- *H3F3A* (K27M) mutant.

5.2.2 Differentially expressed miRNAs in paediatric HGG short-term cell cultures compared to NHA

To determine differentially expressed miRNAs between paediatric HGG short-term cell cultures and NHA, one-way ANOVA test was performed with 893 reliable miRNAs, using Partek Genomics Suite (version 6.6; Partek Inc., USA). Of 893 analysed miRNAs, 162 were significantly differentially expressed ($p<0.05$) with a minimum of 2-fold change in expression in the paediatric HGG short-term cell cultures compared to NHA. These comprised 152 (93.83%) downregulated and 10 (6.17%) upregulated miRNAs. The upregulated miRNAs are listed in Table 5.1 and dot-plots of these miRNAs are shown in Figure 5.3.

Table 5.1 Upregulated miRNAs in paediatric HGG short-term cell cultures compared to NHA.

miRNA	FC (pHGG vs. NHA)	p-value	Accession
hsa-miR-142-3p	337.09	0.005	MIMAT0000434
hsa-miR-144	151.50	0.015	MIMAT0000436
hsa-miR-138	32.17	0.013	MIMAT0000430
hsa-miR-496	24.33	0.000	MIMAT0002818
hsa-miR-98	18.31	0.030	MIMAT0000096
hsa-miR-3174	14.86	0.000	MIMAT0015051
hsa-miR-4258	12.61	0.002	MIMAT0016879
hsa-miR-563	10.17	0.003	MIMAT0003227
hsa-miR-3142	2.47	0.035	MIMAT0015011
hsa-miR-544	2.11	0.025	MIMAT0003164

Significantly upregulated miRNAs (2-fold change, unadjusted p-value<0.05) were identified by one-way ANOVA test in paediatric HGG short-term cell cultures versus NHA. FC- fold change.

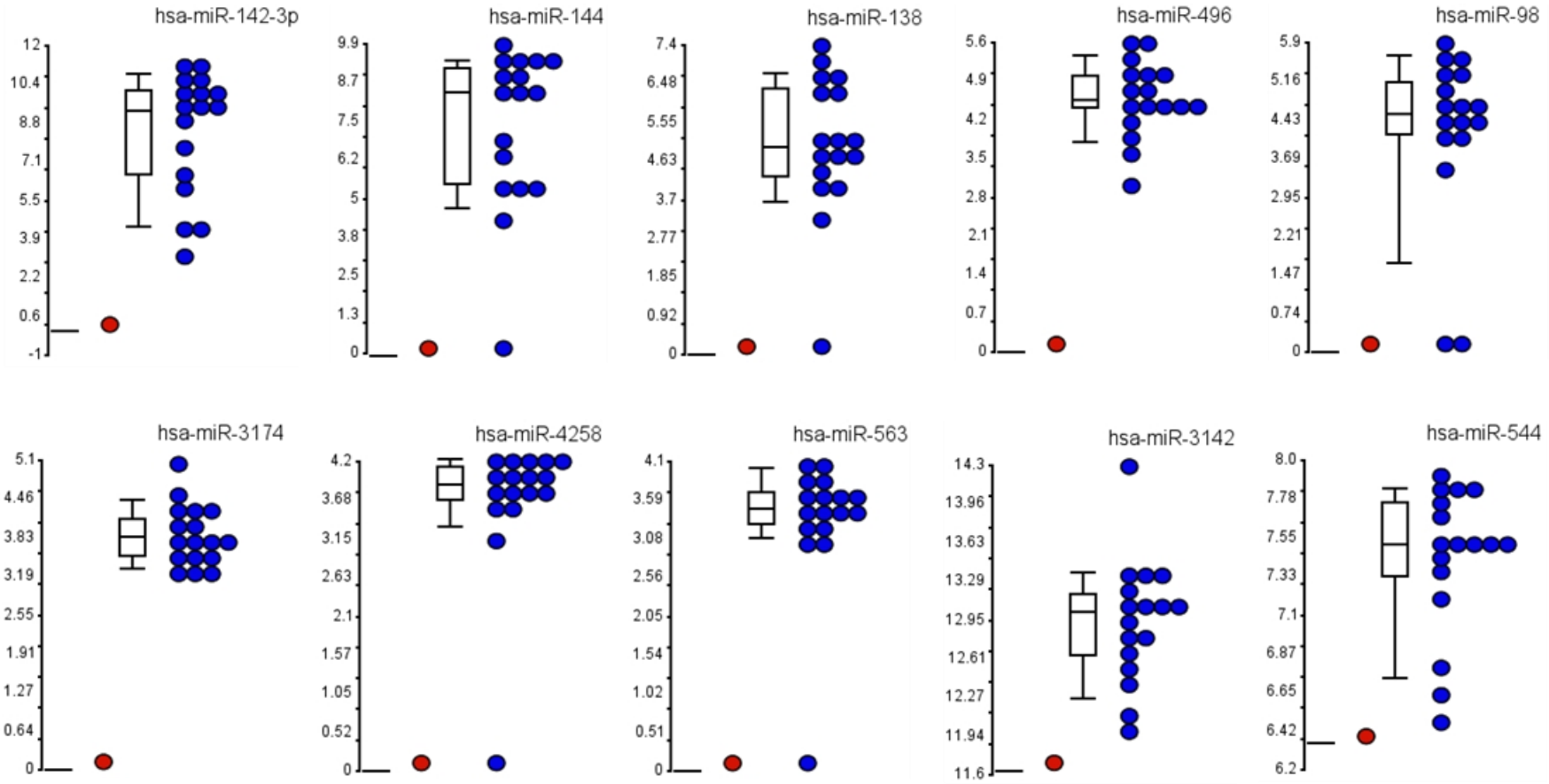

Figure 5.3 Dot-plots of upregulated miRNAs in paediatric HGG short-term cell cultures compared to NHA. Each dot represents a sample. Red represents NHA and blue represents paediatric HGG short-term cell cultures.

MiR-142-3p showed the largest upregulation with a 337.09-fold change in expression in the paediatric HGG short-term cell cultures compared to NHA. This was followed by miR-144 with a 151.50 fold change in expression. Six miRNAs comprising miR-138, miR-496, miR-98, miR-3174, miR-4258 and miR-563 showed a minimum of 10-fold change in expression, while 2 miRNAs, miR-3142 and miR-544 had relatively low level of upregulation with fold changes in expression just over 2-fold.

Of the 152 downregulated miRNAs, miR-3621 showed the largest downregulation (~45 fold), which was followed by miR-759 and miR-1237 with minimum of 40-fold change in expression in paediatric HGG short-term cell cultures compared to NHA. In total, there were 16 miRNAs with minimum of 20 fold-change in expression, which were investigated further (Table 5.2). The other downregulated miRNAs were miR-520a-3p, miR-136, miR-4769-3p, miR-921, miR-191, miR-613, miR-4306, miR-4505, miR-4778-5p, miR-1286, miR-4505, miR-4690-3p and miR-200 c. The dot-plots of the 10 most downregulated miRNAs are shown in Figure 5.4.

Table 5.2 Downregulated miRNAs in paediatric HGG short-term cell cultures compared to NHA

miRNA	FC (pHGG vs. NHA)	p-value	Accession
hsa-miR-3621	-44.94	0.009	MIMAT0018002
hsa-miR-759	-42.02	0.040	MIMAT0010497
hsa-miR-1237	-41.86	0.007	MIMAT0005592
hsa-miR-520a-3p	-38.40	0.017	MIMAT0002834
hsa-miR-136	-36.91	0.018	MIMAT0000448
hsa-miR-4769-3p	-27.47	0.021	MIMAT0019923
hsa-miR-921	-27.35	0.006	MIMAT0004971
hsa-miR-191	-24.37	0.034	MIMAT0000440
hsa-miR-613	-23.40	0.031	MIMAT0003281
hsa-miR-4306	-22.94	0.005	MIMAT0016858
hsa-miR-4505	-22.70	0.000	MIMAT0019041
hsa-miR-4778-5p	-22.10	0.043	MIMAT0019936
hsa-miR-1286	-22.09	0.021	MIMAT0005877
hsa-miR-4506	-21.86	0.000	MIMAT0019042
hsa-miR-4690-3p	-20.88	0.007	MIMAT0019780
hsa-miR-200c	-20.61	0.033	MIMAT0000617

Significantly downregulated miRNAs (2-fold change and unadjusted p-value <0.05) identified by one-way ANOVA in paediatric HGG short-term cell cultures versus NHA are shown. FC-fold change.

To understand the biological impact of the differentially expressed miRNAs, KEGG pathway analyses were performed using DIANA-miRPath v3.0, (http://www.microrna.gr/miRPathv3). The putative mRNA targets of the deregulated miRNAs were identified using microT-CDS target prediction algorithm (minimum threshold of 0.70), which identifies miRNA targets both in 3'untranslated region (3'UTR) and in coding sequences (CDS) (Reczko et al, 2012), increasing the sensitivity of target prediction.

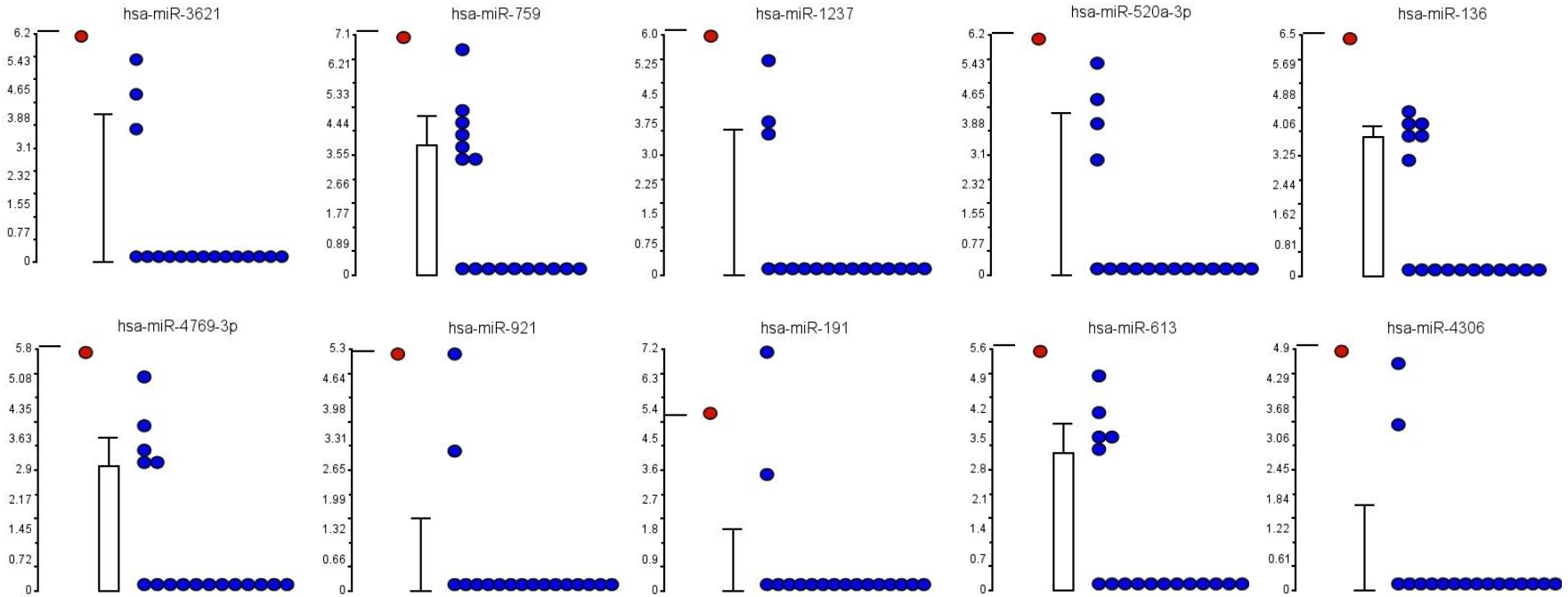

Figure 5.4 Dot plots of the 10 most downregulated miRNAs in paediatric HGG short-term cell cultures compared to NHA (FC<20). Each dot represents a sample. NHA is represented by red and paediatric HGG short-term cell cultures are represented by blue dots respectively.

Using the 'genes union' module in DIANA-miRPath v3.0 (http://www.microrna.gr/miRPathv3), a union set of miRNA targets were generated. The enrichment analysis was performed using Fisher's exact test (hypergeometric distribution) and Benjamini-Hochberg adjustment was used for multiple test correction. This identifies pathways that are significantly enriched with all genes targeted by at least 1 miRNA in the list. The significantly enriched ($p<0.05$) KEGG pathways associated with the upregulated miRNAs that were identified using 'genes union module' is given in Table 5.3. In total, there were 42 KEGG pathways, of which the 10 most significantly enriched were mucin type O-glycan biosynthesis, TGF beta signaling pathway, thyroid hormone signaling pathway, Hippo signaling pathway Glioma, Signaling pathways regulating pluripotency of stem cells, FoxO signaling pathway, Proteoglycans in cancer, Pathways in cancer and Pancreatic cancer. Besides these, there were other significantly enriched cancer-related pathways such as MAPK signaling pathway, Wnt signaling pathway, Ras signaling pathway, ErbB signaling pathway, PI3K/Akt pathway and mTOR signaling pathway and Rap1 signaling pathway.

Table 5.3 KEGG pathways associated with upregulated miRNAs

	KEGG pathway	p-value	Genes	miRNAs
1	Mucin type O-Glycan biosynthesis	0	19	8
2	TGF-beta signaling pathway	0	40	9
3	Thyroid hormone signaling pathway	0	53	9
4	Hippo signaling pathway	0	63	10
5	Glioma	0	33	7
6	Signaling pathways regulating pluripotency of stem cells	0	64	10
7	FoxO signaling pathway	0	63	8
8	Proteoglycans in cancer	0	85	10
9	Pathways in cancer	0.001	152	10
10	Pancreatic cancer	0.002	33	8
11	Chronic myeloid leukemia	0.002	35	8
12	MAPK signaling pathway	0.002	103	10
13	Wnt signaling pathway	0.002	64	10
14	Melanoma	0.002	35	7
15	Focal adhesion	0.004	86	9
16	Prolactin signaling pathway	0.005	32	8
17	AMPK signaling pathway	0.005	54	9
18	Axon guidance	0.006	52	9
19	Ras signaling pathway	0.008	90	10
20	ErbB signaling pathway	0.008	41	8
21	cAMP signaling pathway	0.008	81	9
22	PI3K-Akt signaling pathway	0.008	129	10
23	Lysine degradation	0.017	20	8
24	mTOR signaling pathway	0.018	29	8
25	Colorectal cancer	0.020	27	8
26	Prostate cancer	0.021	41	9
27	Endocytosis	0.021	77	9
28	Adrenergic signaling in cardiomyocytes	0.021	59	9
29	Adherens junction	0.023	30	9
30	Platelet activation	0.026	52	9
31	Ether lipid metabolism	0.029	21	7
32	Neurotrophin signaling pathway	0.030	51	8
33	Small cell lung cancer	0.034	37	8
34	cGMP-PKG signaling pathway	0.034	66	9
35	Acute myeloid leukemia	0.036	26	7
36	Insulin signaling pathway	0.036	57	9
37	Thyroid hormone synthesis	0.038	24	8
38	Rap1 signaling pathway	0.042	76	10
39	Endometrial cancer	0.045	23	8
40	Long-term potentiation	0.045	30	9
41	Transcriptional misregulation in cancer	0.045	67	9
42	Choline metabolism in cancer	0.047	42	9

Significantly enriched KEGG pathways associated with upregulated miRNAs were identified using the 'genes union' module (microT-threshold 0.7) in DIANA mirPath. Pathways with enrichment p-value<0.05 (FDR ON) are shown. The table is ranked by enrichment p-value.

Furthermore, the most commonly targeted pathways associated with the upregulated miRNAs were identified using the 'pathways union module' in DIANA-miRPath v3.0 (http://www.microrna.gr/miRPathv3). This identified 8 significantly enriched pathways (p-value <0.05, FDR-ON) as shown in Table 5.4. The heat map showing the clusters of miRNAs associated with the enriched pathways is shown in Figure 5.5. Two major clusters of miRNAs were observed, one comprising miR-142-3p, miR-3142, miR-496, miR-3174, and miR-4258, and the other comprising miR-138-5p, miR-144-3p, miR-544a, miR-563 and miR-98-5p.

Table 5.4 Commonly targeted KEGG pathways associated with upregulated miRNAs

KEGG pathway	p-value	Genes	miRNAs
ECM-receptor interaction	0	16	2
Mucin type O-Glycan biosynthesis	0	17	5
Lysine degradation	0.001	15	3
Hippo signaling pathway	0.007	22	2
Adherens junction	0.011	17	1
Thyroid hormone signaling pathway	0.020	16	2
TGF-beta signaling pathway	0.021	24	3
Proteoglycans in cancer	0.022	36	1

Commonly targeted pathways by upregulated miRNAs were identified using the 'pathways union' module (microT-threshold 0.7) in DIANA mirPath. Pathways with enrichment p-value<0.05 (FDR ON) are shown. The table is ranked by enrichment p-value.

As shown in Table 5.4, the most significant pathway was ECM-receptor interaction. Notably, the most number of miRNAs were associated with mucin type O-Glycan biosynthesis. The upregulated miRNAs and their putative gene targets affecting various components of mucin type O-Glycan biosynthesis are illustrated in Figure 5.6.

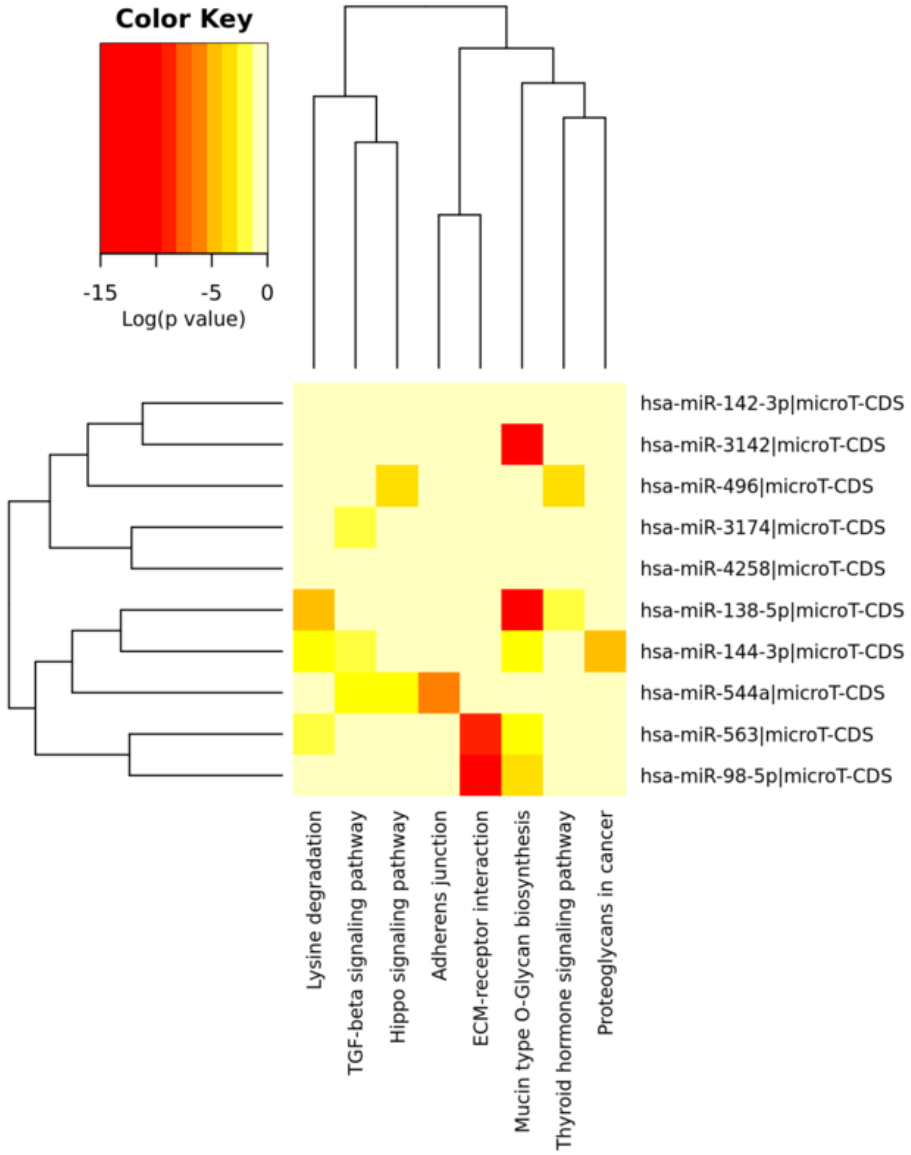

Figure 5.5 Heat map of pathways associated with upregulated miRNAs. Commonly targeted pathways by upregulated miRNAs (microT-CDS>0.70, p<0.05, FDR ON) identified by 'pathways union' module in DIANA mirPath v3.0. On the heat map, each row represents a miRNA and each column represents a pathway.

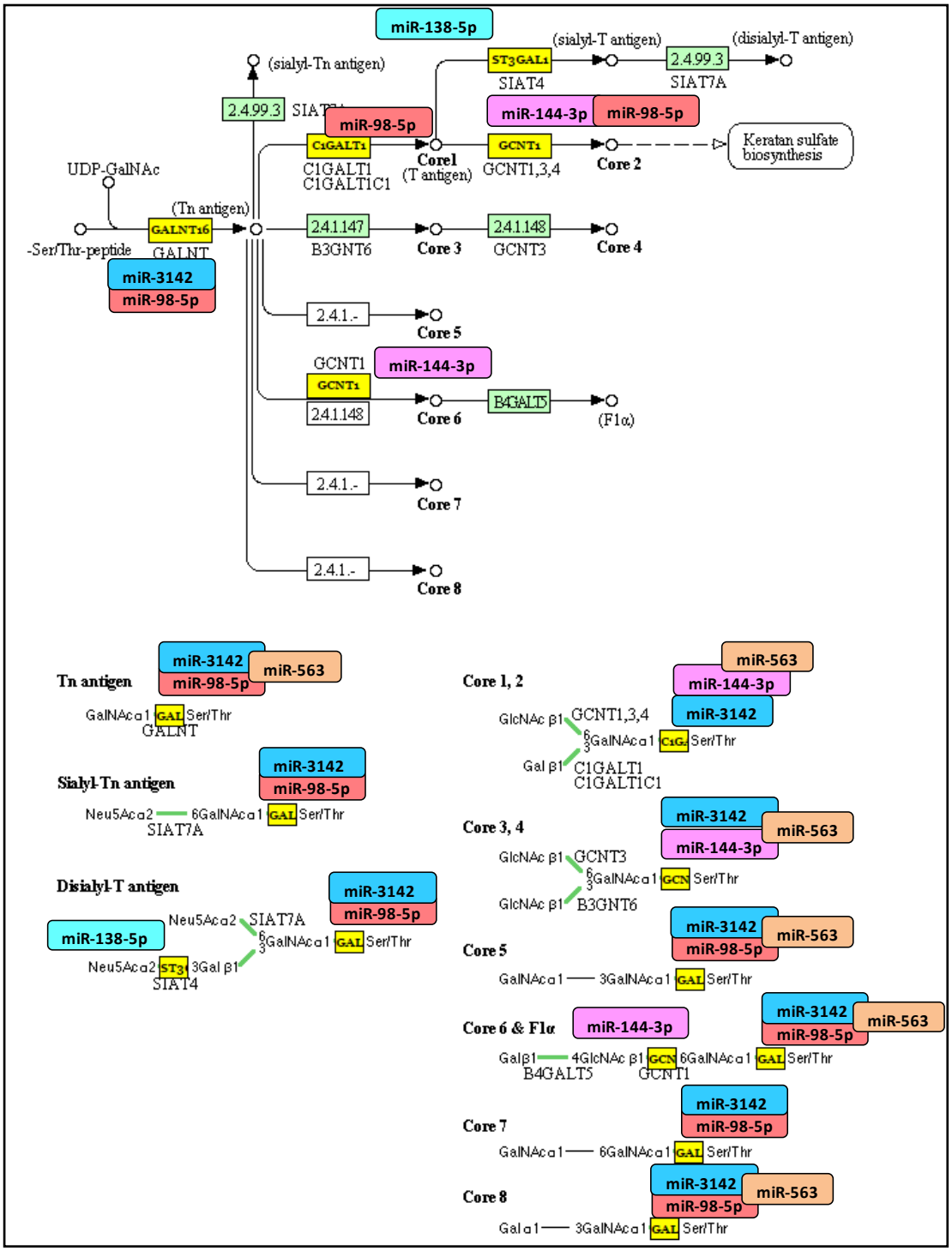

Figure 5.6 Upregulated miRNAs associated with Mucin type O-glycan biosynthesis pathway. Upregulated miRNAs and their gene targets (highlighted in yellow) are shown.

The significantly enriched ($p<0.05$, FDR ON) KEGG pathways associated with the 16 most downregulated miRNAs (FC<20) using 'genes union' module is shown in Table 5.5. There were 52 pathways associated with the downregulated miRNAs, most of which were associated with tumourigenic processes. Among the most significant pathways, those which are cancer-related included mucin type O-glycan biosynthesis, axon guidance, endocytosis, hippo signalling pathway ErbB signalling pathway, proteoglycans in cancer, TGF beta signalling pathway, ECM-receptor interaction, and glioma.

Table 5.5 KEGG pathways associated with downregulated miRNAs

KEGG pathway	p-value	Genes	miRNAs
Mucin type O-Glycan biosynthesis	0	18	11
Axon guidance	0	80	15
Endocytosis	0	128	16
Glycosphingolipid biosynthesis - lacto and neolacto series	0	17	11
Hippo signaling pathway	0	89	15
ErbB signaling pathway	0	59	16
Proteoglycans in cancer	0	116	14
TGF-beta signaling pathway	0	50	15
Circadian entrainment	0	63	14
Endocrine and other factor-regulated calcium reabsorption	0	32	14
Glioma	0	42	14
GABAergic synapse	0	53	14
Adherens junction	0	50	14
Morphine addiction	0	54	14
Retrograde endocannabinoid signaling	0	65	15
Lysine degradation	0	28	13
Phosphatidylinositol signaling system	0.001	50	15
Thyroid hormone signaling pathway	0.001	72	15
Pathways in cancer	0.001	217	15
Adrenergic signaling in cardiomyocytes	0.002	90	14
Colorectal cancer	0.002	42	13
Neurotrophin signaling pathway	0.002	75	15
Glutamatergic synapse	0.004	69	14
Bacterial invasion of epithelial cells	0.004	50	14
Glycosphingolipid biosynthesis - ganglio series	0.005	11	10
Renal cell carcinoma	0.006	43	15
Circadian rhythm	0.008	23	11
Melanoma	0.009	45	14
MAPK signaling pathway	0.009	141	15
Nicotine addiction	0.010	24	14
Calcium signaling pathway	0.010	102	15
Ras signaling pathway	0.010	132	15
cGMP-PKG signaling pathway	0.013	94	14
Rap1 signaling pathway	0.013	116	15
Type II diabetes mellitus	0.015	31	12
Chronic myeloid leukemia	0.017	42	14
Pancreatic cancer	0.017	42	14
Arrhythmogenic right ventricular cardiomyopathy (ARVC)	0.019	45	14
p53 signaling pathway	0.019	44	15
Glycosphingolipid biosynthesis - globo series	0.022	10	10
Wnt signaling pathway	0.022	78	14
Focal adhesion	0.024	114	16
Gap junction	0.028	50	15
Cholinergic synapse	0.029	63	14
RNA degradation	0.029	49	15
Amino sugar and nucleotide sugar metabolism	0.030	29	11
Aldosterone-regulated sodium reabsorption	0.035	26	13
Sphingolipid signaling pathway	0.043	64	13
mTOR signaling pathway	0.048	37	14
Thyroid hormone synthesis	0.048	39	13
Inflammatory mediator regulation of TRP channels	0.049	57	14
Vasopressin-regulated water reabsorption	0.050	27	14

Significantly enriched KEGG pathways associated with downregulated miRNAs were identified using the 'genes union' module (microT-threshold 0.7) in DIANA mirPath. Pathways with enrichment p-value<0.05 (FDR ON) are shown. The table is ranked by enrichment p-value.

KEGG pathway enrichment was also performed using the downregulated miRNAs using the 'pathways union' module with microT-threshold 0.07 and p-value<0.05 (FDR ON). The results are shown in Table 5.6. The most significant cancer-related pathway was ECM-receptor interaction and the most number of miRNAs involved in a cancer-related pathway was in Lysine degradation. The miRNAs associated with Glioma were miR-520a-3p, miR-613 and miR-4778-5p. Mir-520a-3p had 13 gene targets including *BRAF, EGFR, CDK6, PIK3CA, PTEN* and the experimentally validated target, *CCND1*. Mir-613 had 9 targets including *IGF1, PDGFA, EGFR* and *MAPK1*. Mir-4778-5p had 12 targets including *PIK3R1, PIK3CA, CDK6, BRAF* and *MTOR*.

Table 5.6 Commonly targeted KEGG pathways associated with downregulated miRNAs

KEGG pathway	p-value	Genes	miRNAs
Morphine addiction	0	44	7
ECM-receptor interaction	0	25	3
Fatty acid degradation	0	4	3
Proteoglycans in cancer	0	67	4
Axon guidance	0	62	5
Glycosphingolipid biosynthesis - lacto and neolacto series	0	11	4
Lysine degradation	0	21	6
Steroid hormone biosynthesis	0	8	1
ErbB signaling pathway	0	39	4
Fatty acid metabolism	0	5	3
Circadian entrainment	0	49	5
Other types of O-glycan biosynthesis	0.004	7	2
TGF-beta signaling pathway	0.020	28	3
Glioma	0.037	23	3

KEGG pathways targeted by downregulated miRNAs were identified using the 'pathways union' module (microT-threshold 0.7) in DIANA mirPath. Pathways with enrichment p-value<0.05 (FDR ON) are shown. The table is ranked by enrichment p-value.

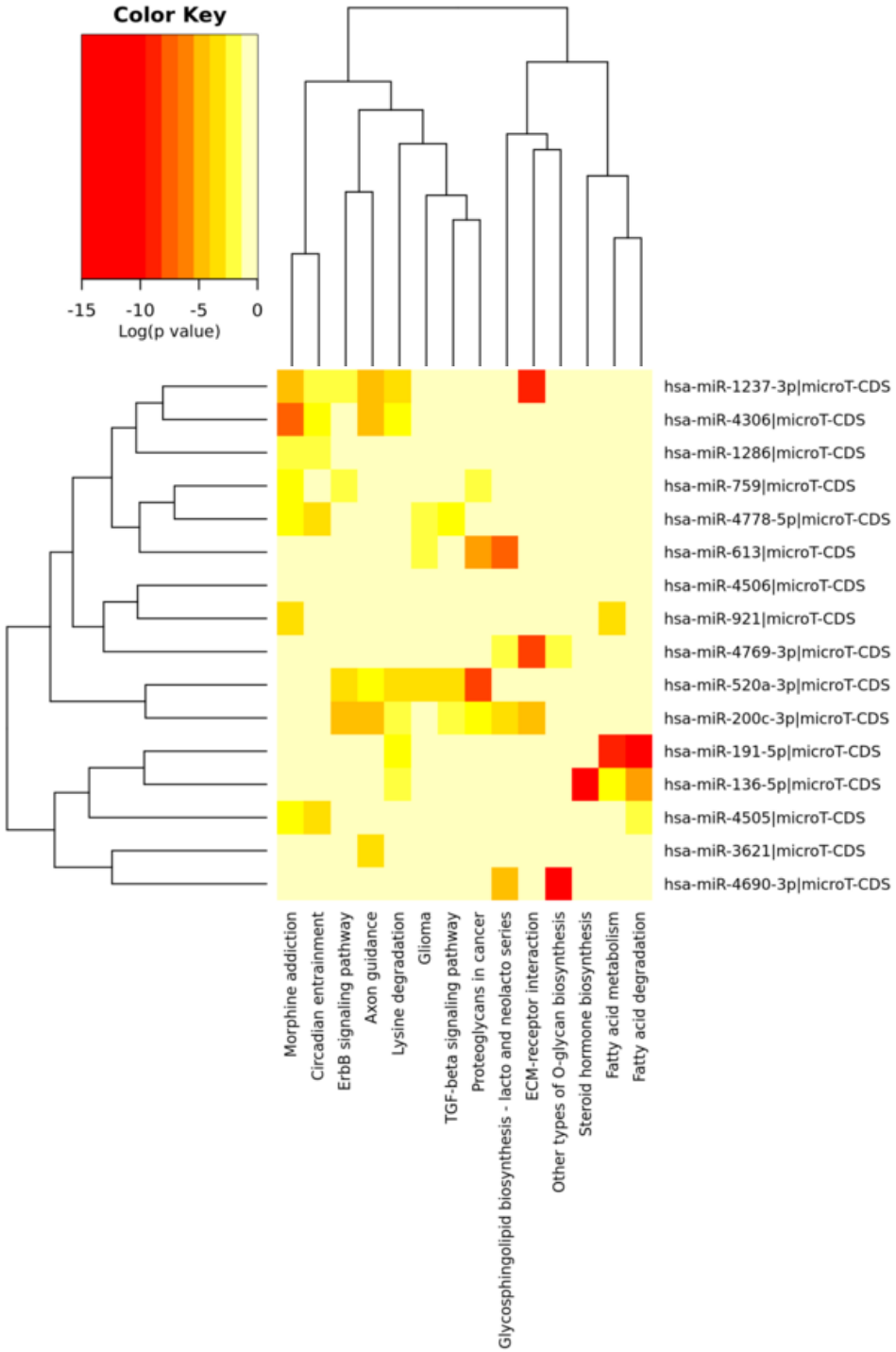

Figure 5.7 Heat map of pathways associated with downregulated miRNAs. KEGG pathways targeted by downregulated miRNAs (microT-CDS>0.70, p<0.05, FDR ON) were identified by 'pathways union' module in DIANA mirPath v3.0. On the heat map, each row represents a miRNA and each column represents a pathway.

5.2.3 Integrated miRNA and mRNA expression analysis to identify mRNA targets of deregulated miRNAs in paediatric HGG short-term cell cultures

To identify the most reliable mRNA targets of the deregulated miRNAs, miRNA expression data were integrated with the mRNA expression data from the same dataset using Partek Genomics suite (v 6.6, Partek Inc., USA). The mRNA expression profiles of paediatric HGG short-term cell cultures analysed in this study were previously generated in the laboratory by Dr. Nicola Potter using Affymetrix Gene Chip HG_U133A (unpublished data). Normalised mRNA expression data were available for 13/17 paediatric HGG short-term cultures and NHA, which were profiled for miRNA expression.

Data were log2 transformed and one-way ANOVA test was used to identify genes that were significantly differentially expressed between paediatric HGG short-term cell cultures and NHA. This identified 853 probes (759 downregulated and 94 upregulated), which showed significant ($p<0.05$) and 2-fold change in expression in paediatric HGG short-term cell cultures compared to NHA. The spreadsheet containing differentially expressed mRNAs was then integrated with the spreadsheet containing differentially expressed miRNAs (n=162) using the 'correlate microRNA and mRNA data' integration tool in Partek Genomics suite (v6.6, Partek Inc., USA). This approach identifies putative mRNA targets of differentially expressed miRNAs from TargetScan 7.0 database and computes a Pearson correlation coefficient and p-value for each miRNA and its predicted gene target. Positive correlation indicates that high expression level of the miRNA is associated with high expression of its predicted mRNA, while negative correlation indicates that high expression of the

miRNA is associated with low level of its predicted gene target. The integrated analysis identified 192 miRNA-mRNA interaction pairs that consisted of 170 positive and 22 negative associations. The statistically significant miRNA-mRNA pairs were defined by $p<0.05$ and Pearson correlation coefficient threshold of 0.50 (medium strong correlation). This resulted in 81 miRNA-mRNA interaction pairs, of which 78 were positive and only 3 were negative. The positive associations included 5 mRNAs that were each represented by 2 probes. Discounting the repeated probes, 73 unique miRNA-mRNA positive associations remained.

As expected, each miRNA had multiple mRNA targets. MiR-520a-3p had the highest number of targets (21 targets), followed by miR-613, miR-4306, miR-378f, miR-502-3p, miR-369-3p, and miR-4676-3p with 19, 13, 9, 8, 7 and 4 gene targets respectively. Conversely, there were 12 genes targeted by multiple miRNAs. *ZFHX4* was targeted by the highest number of miRNAs (4 miRNAs), followed by *AAK1, CADM4, IGF1, INHBA, NDST1, PRIM2, RAI14, RUNX1, SLC23A2*, *TRHDE* and *TRIM2* each targeted by 2 miRNAs.

Table 5.7 Summary of miRNA-mRNA associations in paediatric HGG short-term cell cultures

Count	miRNA	Gene Symbol	Pearson correlation coefficient	p-value
1	**hsa-miR-520a-3p**	***NBEAL2***	**0.871**	**0.0001**
2	**hsa-miR-520a-3p**	***AAK1***	**0.817**	**0.0004**
3	**hsa-miR-4306**	***GTPBP1***	**0.799**	**0.0006**
4	**hsa-miR-4306**	***NLRP1***	**0.794**	**0.0007**
5	**hsa-miR-520a-3p**	***ZFHX4***	**0.793**	**0.0007**
6	**hsa-miR-520a-3p**	***EIF5***	**0.779**	**0.0010**
7	**hsa-miR-378f**	***KSR1***	**0.760**	**0.0016**
8	**hsa-miR-613**	***ZFHX4***	**0.758**	**0.0017**
9	**hsa-miR-378f**	***PRIM2***	**0.755**	**0.0018**
10	**hsa-miR-520a-3p**	***MINK1***	**0.748**	**0.0021**
11	**hsa-miR-378f**	***ALPK3***	**0.746**	**0.0022**
12	**hsa-miR-4676-3p**	***IGF1***	**0.742**	**0.0024**
13	**hsa-miR-613**	***SLC23A2***	**0.739**	**0.0025**
14	**hsa-miR-520a-3p**	***PDLIM5***	**0.736**	**0.0027**
15	**hsa-miR-4306**	***TMC5***	**0.735**	**0.0027**
16	**hsa-miR-502-3p**	***ZFHX4***	**0.726**	**0.0033**
17	**hsa-miR-502-3p**	***LUZP1***	**0.720**	**0.0037**
18	**hsa-miR-369-3p**	***ZFHX4***	**0.718**	**0.0038**
19	**hsa-miR-520a-3p**	***MINK1***	**0.714**	**0.0041**
20	**hsa-miR-613**	***SIM2***	**0.704**	**0.0049**
21	**hsa-miR-4306**	***PRIM2***	**0.703**	**0.0051**
21	hsa-miR-520a-3p	*POU6F1*	0.698	0.0055
22	hsa-miR-520a-3p	*FBXO11*	0.697	0.0056
23	hsa-miR-520a-3p	*RAI14*	0.682	0.0072
24	hsa-miR-520a-3p	*ESR1*	0.672	0.0084
25	hsa-miR-613	*RRBP1*	0.666	0.0093
26	hsa-miR-4306	*NDST1*	0.658	0.0105
27	hsa-miR-520a-3p	*ST3GAL5*	0.657	0.0106
28	hsa-miR-4306	*SIX3*	0.655	0.0110
29	hsa-miR-378f	*AAK1*	0.649	0.0119
30	hsa-miR-520a-3p	*CNN1*	0.649	0.0120
31	hsa-miR-520a-3p	*TRHDE*	0.648	0.0122
33	hsa-miR-502-3p	*OGT*	0.647	0.0123
34	hsa-miR-613	*KCTD13*	0.645	0.0128
35	hsa-miR-613	*FNBP1L*	0.642	0.0132
36	hsa-miR-613	*ROR1*	0.642	0.0133
37	hsa-miR-4306	*EIF5A*	0.638	0.0140
38	hsa-miR-502-3p	*SEMA4G*	0.636	0.0145
39	hsa-miR-369-3p	*ACTC1*	0.634	0.0149
40	hsa-miR-520a-3p	*TRIM2*	0.632	0.0154
41	hsa-miR-378f	*IGF1*	0.622	0.0176
42	hsa-miR-502-3p	*OGT*	0.621	0.0177
43	hsa-miR-502-3p	*FBN2*	0.618	0.0184
44	hsa-miR-613	*NDST1*	0.616	0.0190
45	hsa-miR-613	*RUNX1*	0.609	0.0209
46	hsa-miR-378f	*CADM4*	0.605	0.0219
47	hsa-miR-520a-3p	*RUNX1*	0.604	0.0221
48	hsa-miR-4676-3p	*INHBA*	0.604	0.0223

contd.

49	hsa-miR-4676-3p	*IGF2BP2*	0.602	0.0229
50	hsa-miR-613	*WDR6*	0.601	0.0232
51	hsa-miR-520a-3p	*INHBA*	0.600	0.0234
52	hsa-miR-520a-3p	*FRMD4A*	0.598	0.0237
53	hsa-miR-4306	*NR1D1 THRA*	0.597	0.0241
54	hsa-miR-4306	*NR1D1 THRA*	0.597	0.0241
55	hsa-miR-613	*NEDD4L*	0.593	0.0254
56	hsa-miR-369-3p	*FOXO1*	0.593	0.0255
57	hsa-miR-378f	*ZNF335*	0.586	0.0275
58	hsa-miR-378f	*SKP2*	0.586	0.0277
59	hsa-miR-613	*DLG1*	0.583	0.0287
60	hsa-miR-613	*TRHDE*	0.575	0.0313
61	hsa-miR-520a-3p	*TM4SF1*	0.574	0.0318
62	hsa-miR-613	*TRIM2*	0.566	0.0347
63	hsa-miR-502-3p	*PTBP2*	0.565	0.0352
64	hsa-miR-613	*PARVA*	0.565	0.0353
65	hsa-miR-502-3p	*RAI14*	0.561	0.0369
66	hsa-miR-4306	*LIF*	0.560	0.0374
67	hsa-miR-520a-3p	*METAP1*	0.558	0.0383
68	hsa-miR-520a-3p	*FGF16*	0.553	0.0403
69	hsa-miR-613	*GPR125*	0.549	0.0420
70	hsa-miR-4306	*TCF12*	0.547	0.0431
71	hsa-miR-369-3p	*ECE1*	0.543	0.0448
72	hsa-miR-369-3p	*ZDHHC17*	0.540	0.0464
73	hsa-miR-378f	*SLC38A1*	0.539	0.0465
74	hsa-miR-369-3p	*ZDHHC17*	0.538	0.0473
75	hsa-miR-4306	*CADM4*	0.537	0.0477
76	hsa-miR-613	*FUBP1*	0.535	0.0485
77	hsa-miR-4676-3p	*SLC23A2*	0.535	0.0487
78	hsa-miR-613	*ROR1*	0.533	0.0499
1	hsa-miR-4306	*CYB561*	-0.554	0.0400
2	hsa-miR-613	*MR1*	-0.687	0.0067
3	**hsa-miR-369-3p**	***TMX4***	**-0.765**	**0.0014**

Pearson correlation coefficients of differentially expressed miRNAs and their predicted mRNA targets were calculated using Partek Genomics suite v6.6. The significant ($p<0.05$, R-0.50) miRNA-mRNA associations are shown with the table ranked by P-values. Negative associations are highlighted yellow. The strong positive ($R>0.70$) and strong negative ($R<0.70$) miRNA-mRNA pairs are shown in bold. MiRNA with single gene target is coloured green; genes targeted by multiple miRNAs are coloured blue (*ZFHX4*) or red (*PRIM2*).

The strongest positive correlation was observed between miR-520a-3p and *NBEAL2*, followed by miR-520a-3p and *AAK1* with Pearson correlation coefficients of 0.871 and 0.817 respectively (Figure 5.8 A and B). The strongest negative correlation was observed between miR-369-3p and *TMX4* (Figure 5.8 C).

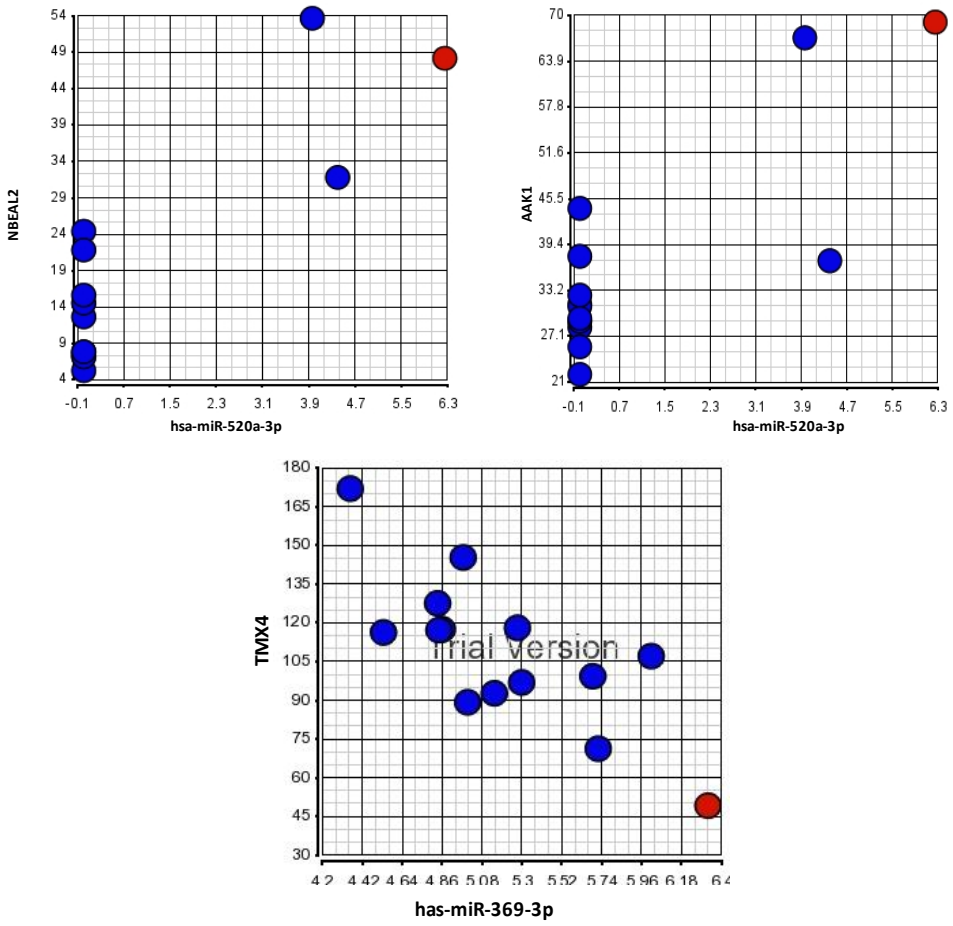

Figure 5.8 Scatter plot of miRNA-mRNA interaction pairs in paediatric HGG short-term cell cultures. Each dot represents a sample. NHA is represented by red and paediatric HGG short-term cell cultures are represented by blue coloured dots respectively.

To further identify the most genuine miRNA-mRNA matches, the results were filtered based on Pearson correlation coefficient cut-off value 0.70 (strong positive, r>0.70 and strong negative, r<0.70). This identified 22 miRNA-mRNA associations, of which 21 were positive and 1 was negative. These are shown in bold in Table 5.7. Among the positive associations, *MINK1* was represented by 2 probes (therefore, the number of unique positive associations=20). Interestingly, miR-520a-3p that had the highest number of targets also made the highest number of strong positive associations (6 associations, r>0.70). These gene targets comprised *AAK1, ZFHX4, EIF5, MINK1, NBEAL2,* and *PDLIM5.* With the exception of miR-4676-3p, all other

miRNAs had multiple mRNA targets. In addition, all 4 miRNAs that targeted *ZFHX4* involved strong positive associations (r>0.70). *PRIM2* was targeted by 2 miRNAs comprising hsa-miR-378f and hsa-miR-4306. As TargetScan cannot identify mRNA targets in the coding sequences, the gene targets of the identified miRNAs were compared with those predicted by microT-CDS. Table 5.8 shows microT-CDS scores of the miRNA-mRNA interaction pairs that were predicted by TargetScan.

Table 5.8 Comparison of gene targets of deregulated miRNAs in miRNA-mRNA interaction pairs predicted by TargetScan and microT-CDS (threshold 0.60) algorithm

miRNA	Target count	Targets	microT-CDS score	Experimentally supported	Additional targets
hsa-miR-520a-3p	6	*AAK1*	0.912	Yes	*ZFHX4* (0.854), *LUZP1* (0.716), *IGF1* (0.624)
		EIF5	0.633		
		MINK1	0.880		
		NBEAL2	0.634		
		PDLIM5	0.633		
hsa-miR-4306	4	*GTPBP1*	-		*KSR1* (0.895), *SLC23A2* (0.792), *ALPK3* (0.747), *IGF1* (0.726), *MINK1* (0.696), *LUZP1* (0.678)
		NLRP1	-		
		TMC5	-		
		PRIM2	-		
hsa-miR-613	3	*SIM2*	-		*IGF1* (0.986), *MINK1* (0.704), *AAK1* (0.626), *SLC23A2* (0.678)
		SLC23A2	-		
		ZFHX4	0.616		
hsa-miR-378f	3	*ALPK3*	0.689		*IGF1* (0.667)
		KSR1	0.642		
		PRIM2			
hsa-miR-502-3p	2	*LUZP1*	0.629		Nil
		ZFHX4	0.882	Yes	
hsa-miR-369-3p	2	*TMX4*	0.687		*IGF1* (0.832), *PDLIM5* (0.765),*AAK1*, *SIM2* (0.709)
		ZFHX4	0.612	Yes	
hsa-miR-4676-3p	1	*IGF1*	0.768		*EIF5* (0.783), *ZFHX4* (0.745), *SLC23A2* (0.687)

The most significant miRNA-mRNA interaction pairs (Pearson correlation coefficient threshold 0.6) as predicted by TargetScan miRNA target prediction algorithm in Partek Genomics suite (v6.6, Partek Inc., USA) were analysed for targets predicted by micro T-CDS algorithm (threshold 6) in DIANA miRPath, v3.0 and Tarbase, v7.0 (experimentally supported).

With the exception of the predicted gene targets of miR-4306, the majority of the target predictions by TargetScan were concordant with those predicted using microT-CDS. There were additional associations predicted by microT-CDS, some of them with high prediction scores as in case of hsa-miR-613- *IGF1* (microT-CDS=0.986) and miR-4306-*KSR1* (microT-CDS=0.895).

To investigate the biological significance of the deregulated miRNA-mRNA interactions in paediatric HGG short-term cell cultures, GO and KEGG pathway analyses were performed using DIANA-miRPath v3.0 (http://www.microrna.gr/miRPathv3). This analysis was performed using all 81 significant miRNA-mRNA associations. The enrichment p-value was calculated using Fisher's exact test (hypergeometric distribution) and corrected by Benjamini-Hochberg adjustment. The GO biological processes associated with the miRNA-mRNA interaction pairs are shown in Table 5.9. Fourteen significant GO biological processes ($p<0.05$) were associated with the dysregulated miRNAs and mRNAs. Regulation of neural precursor cell proliferation was the most significantly enriched biological process. Other notable biological processes included actin-mediated cell contraction, cellular protein-modification process, cellular nitrogen compound metabolic process, cell-cell signaling, glycolate metabolic process, phosphatidylinositol-mediated signaling and cytoskeleton organisation. The most number of miRNAs (7 miRNAs) were associated with cell-cell signaling and biological process.

Table 5.9 Significant GO biological processes associated with miRNA-mRNA interaction pairs

	GO Category	p-value	Genes	miRNAs
1	regulation of neural precursor cell proliferation	0.003	3	4
2	actin-mediated cell contraction	0.011	2	3
3	cellular protein modification process	0.012	13	6
4	lung lobe morphogenesis	0.028	2	4
5	water homeostasis	0.028	2	5
6	prostate epithelial cord arborization involved in prostate glandular acinus morphogenesis	0.028	2	6
7	cellular nitrogen compound metabolic process	0.028	18	6
8	lung vasculature development	0.029	2	4
9	biosynthetic process	0.035	16	6
10	cell-cell signaling	0.035	6	7
11	glycolate metabolic process	0.039	1	4
12	phosphatidylinositol-mediated signaling	0.039	3	5
13	biological_process	0.039	45	7
14	cytoskeleton organization	0.042	6	6

Significantly enriched GO biological processes associated with miRNA-mRNA pairs were identified using the 'categories union' module (microT-threshold 0.7) in DIANA mirPath. Pathways with enrichment p-value<0.05 (FDR ON) are shown. The table is ranked by enrichment p-value.

The significantly enriched KEGG pathways associated with the miRNA-mRNA interaction pairs consisted of important cancer-related pathways such as transcriptional misregulation in cancer, FoxO signalling pathway, pathways in cancer and estrogen signalling pathway (Table 5.10).

Table 5.10 Significant KEGG pathways associated with miRNA-mRNA interaction pairs

KEGG pathway	p-value	Genes	miRNAs
Transcriptional misregulation in cancer	0	*RUNX1, IGF1, FOXO1*	hsa-miR-369-3p, hsa-miR-520a-3p, hsa-miR-4306, hsa-miR-4676-3p, hsa-miR-613,
FoxO signaling pathway	0.003	*SKP2, IGF1, FOXO1*	hsa-miR-369-3p, hsa-miR-378f, hsa-miR-4306, hsa-miR-4676-3p, hsa-miR-613
Pathways in cancer	0.013	*RUNX1, SKP2, IGF1, FGF16, FOXO1*	hsa-miR-369-3p, hsa-miR-378f, hsa-miR-520a-3p, hsa-miR-4306, hsa-miR-613, hsa-miR-4676-3p
Estrogen signaling pathway	0.027	*ESR1*	hsa-miR-520a-3p, hsa-miR-502-3p

Significantly enriched KEGG pathways associated with the miRNA-mRNA pairs were identified using the 'genes union' module (microT-threshold 0.7) in DIANA mirPath. Pathways with enrichment p-value<0.05 (FDR ON) are shown. The table is ranked by enrichment p-value.

5.2.4 Comparison of miRNA expression profiles between non-DIPG and DIPG short-term cell cultures relative to NHA

To compare the miRNA expression profiles between non-DIPG (n=14) and DIPG (n=3) short-term cell cultures, one-way ANOVA test was performed in each tumour group relative to NHA. There were 153 miRNAs that were significantly differentially expressed (2-fold change, $p<0.05$) in non-DIPG (10 upregulated and 143 downregulated), where as 145 miRNAs were significantly differentially expressed in DIPG (8 upregulated and 137 downregulated) as compared to NHA. These differentially expressed miRNAs were then compared between the 2 groups. The Venn diagram in Figure 5.9 shows the independent comparison of

downregulated miRNAs and upregulated miRNAs between DIPG and non-DIPG short-term cell cultures as compared to NHA.

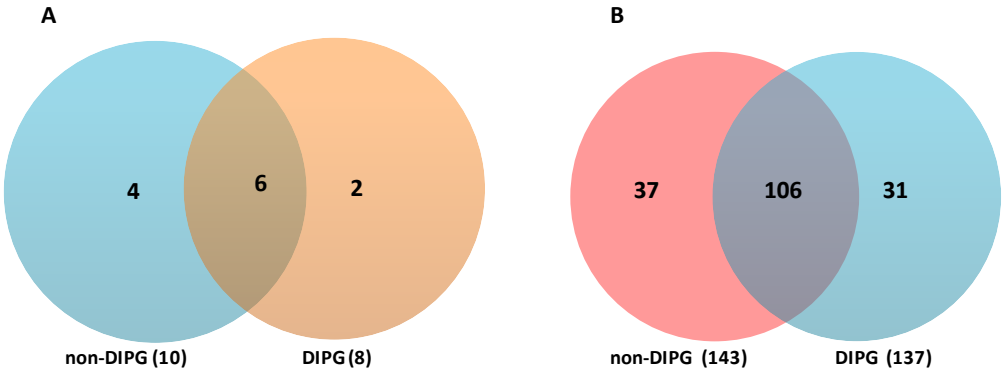

Figure 5.9 Venn diagram of deregulated miRNAs in non-DIPG versus DIPG short-term cell cultures. A. Venn diagram of upregulated miRNAs in non-DIPG and DIPG short-term cell cultures. There are 6 miRNAs common to non-DIPG and DIPG subgroups, while 4 miRNAs are unique to non-DIPG and 2 miRNAs are unique to DIPG subgroups. **B.** Venn diagram of downregulated miRNAs in non-DIPG and DIPG short-term cell cultures. There are 106 miRNAs common to non-DIPG and DIPG subgroups, while 37 miRNAs are unique to non-DIPG and 31 miRNAs are unique to DIPG subgroups. The numbers in parenthesis show the total number of differentially expressed (upregulated/downregulated) miRNAs in comparison to NHA.

On comparison, there were 112 differentially expressed miRNAs (6 upregulated and 106 downregulated) that were common to both non-DIPG and DIPG subgroups, 41 miRNAs (4 upregulated and 37 downregulated) were unique to the non-DIPG subgroup, and a total of 33 miRNAs (2 upregulated and 31 downregulated) were unique to the DIPG subgroup. The unique differentially expressed miRNAs in non-DIPG and DIPG subgroups of paediatric HGG short-term cell cultures are shown in Table 5.11.

To investigate the role of dysregulated miRNAs in each subgroup of paediatric HGG short-term cell cultures, KEGG pathway analyses were performed using DIANA-miRPath v3.0 (http://www.microrna.gr/miRPathv3). The enrichment p-value was

calculated using Fisher's exact test (hypergeometric distribution) and corrected by Benjamini-Hochberg adjustment. The microT-CDS threshold for gene target prediction was set to 0.70. The significantly enriched pathways associated with non-DIPG-specific differentially expressed miRNAs are shown in Table 5.12 and those associated with DIPG-specific differentially expressed miRNAs are shown in Table 5.13. Among the 10 most significantly enriched pathways associated with each subgroup, 4 pathways were common to both subgroups, comprising proteoglycans in cancer, Mucin type O-glycan biosynthesis, Glioma and ErbB signaling pathway. Notably, 2 important cancer-related pathways were identified in DIPG. These were Estrogen signalling pathway and signalling pathways regulating pluripotency of stem cells.

Table 5.11 Differentially expressed miRNAs unique to tumour subgroups within paediatric HGG short-term cell cultures

A

	Upregulated	
	miRNAs	**Accession**
1	hsa-miR-138	MIMAT0000430
2	hsa-miR-144	MIMAT0000436
3	hsa-miR-3142	MIMAT0015011
4	hsa-miR-98	MIMAT0000096
	Downregulated	
	miRNAs	**Accession**
1	hsa-miR-16-2*	MIMAT0004518
2	hsa-miR-191	MIMAT0000440
3	hsa-miR-1915*	MIMAT0007891
4	hsa-miR-200c	MIMAT0000617
5	hsa-miR-3074-3p	MIMAT0015027
6	hsa-miR-3121-5p	MIMAT0019199
7	hsa-miR-34a*	MIMAT0004557
8	hsa-miR-3659	MIMAT0018080
9	hsa-miR-3671	MIMAT0018094
10	hsa-miR-3917	MIMAT0018191
11	hsa-miR-3923	MIMAT0018198
12	hsa-miR-421	MIMAT0003339
13	hsa-miR-425	MIMAT0003393
14	hsa-miR-432*	MIMAT0002815
15	hsa-miR-4324	MIMAT0016876
16	hsa-miR-4454	MIMAT0018976
17	hsa-miR-4467	MIMAT0018994
18	hsa-miR-4478	MIMAT0019006
19	hsa-miR-4493	MIMAT0019028
20	hsa-miR-4498	MIMAT0019033
21	hsa-miR-4503	MIMAT0019039
22	hsa-miR-4535	MIMAT0019075
23	hsa-miR-4638-5p	MIMAT0019695
24	hsa-miR-4757-3p	MIMAT0019902
25	hsa-miR-4769-3p	MIMAT0019923
26	hsa-miR-4778-5p	MIMAT0019936
27	hsa-miR-4783-5p	MIMAT0019946
28	hsa-miR-4787-5p	MIMAT0019956
29	hsa-miR-4802-3p	MIMAT0019982
30	hsa-miR-4803	MIMAT0019983
31	hsa-miR-502-3p	MIMAT0004775
32	hsa-miR-504	MIMAT0002875
33	hsa-miR-520a-3p	MIMAT0002834
34	hsa-miR-521	MIMAT0002854
35	hsa-miR-613	MIMAT0003281
36	hsa-miR-759	MIMAT0010497
37	hsa-miR-769-3p	MIMAT0003887

B

	Upregulated	
	miRNAs	**Accession**
1	hsa-miR-181a-2*	MIMAT0004558
2	hsa-miR-3144-3p	MIMAT0015015
	Downrregulated	
	miRNAs	**Accession**
1	hsa-miR-1225-3p	MIMAT0005573
2	hsa-miR-1231	MIMAT0005586
3	hsa-miR-1233	MIMAT0005588
4	hsa-miR-1234	MIMAT0005589
5	hsa-miR-125b	MIMAT0000423
6	hsa-miR-1272	MIMAT0005925
7	hsa-miR-1827	MIMAT0006767
8	hsa-miR-2277-5p	MIMAT0017352
9	hsa-miR-296-3p	MIMAT0004679
10	hsa-miR-3136-3p	MIMAT0019203
11	hsa-miR-3155b	MIMAT0019012
12	hsa-miR-3159	MIMAT0015033
13	hsa-miR-3185	MIMAT0015065
14	hsa-miR-3607-3p	MIMAT0017985
15	hsa-miR-3647-3p	MIMAT0018067
16	hsa-miR-371-3p	MIMAT0000723
17	hsa-miR-3960	MIMAT0019337
18	hsa-miR-4291	MIMAT0016922
19	hsa-miR-4508	MIMAT0019045
20	hsa-miR-4529-3p	MIMAT0019068
21	hsa-miR-4639-3p	MIMAT0019698
22	hsa-miR-4640-3p	MIMAT0019700
23	hsa-miR-4692	MIMAT0019783
24	hsa-miR-4704-5p	MIMAT0019803
25	hsa-miR-4742-5p	MIMAT0019872
26	hsa-miR-4747-5p	MIMAT0019882
27	hsa-miR-4774-5p	MIMAT0019929
28	hsa-miR-4793-5p	MIMAT0019965
29	hsa-miR-501-5p	MIMAT0002872
30	hsa-miR-549	MIMAT0003333
31	hsa-miR-616	MIMAT0004805

A. Differentially expressed miRNAs unique to non-DIPG paediatric subgroup. **B.** Differentially expressed miRNAs unique to DIPG subgroup.

Table 5.12 KEGG pathways associated with differentially expressed miRNAs unique to non-DIPG short-term cell cultures

	KEGG pathway	p-value	Genes	miRNAs
1	Proteoglycans in cancer	0	149	33
2	Mucin type O-Glycan biosynthesis	0	23	26
3	Pancreatic cancer	0	58	32
4	Choline metabolism in cancer	0	84	33
5	Glioma	0	53	32
6	ErbB signaling pathway	0	72	35
7	Thyroid hormone signaling pathway	0	93	33
8	Colorectal cancer	0	53	33
9	Adherens junction	0	61	34
10	Endocytosis	0	153	37
11	mTOR signaling pathway	0	52	32
12	Renal cell carcinoma	0	56	32
13	GABAergic synapse	0	65	31
14	Phosphatidylinositol signaling system	0	61	33
15	Melanoma	0	59	32
16	Ras signaling pathway	0	163	34
17	MAPK signaling pathway	0	183	37
18	Hippo signaling pathway	0	110	37
19	Endometrial cancer	0	44	30
20	Pathways in cancer	0	276	38
21	Lysine degradation	0.001	37	32
22	Axon guidance	0.001	91	36
23	Prostate cancer	0.001	69	30
24	ABC transporters	0.001	38	24
25	Platelet activation	0.001	94	34
26	FoxO signaling pathway	0.001	100	33
27	Non-small cell lung cancer	0.002	44	32
28	Gap junction	0.002	65	35
29	HIF-1 signaling pathway	0.002	80	31
30	Bacterial invasion of epithelial cells	0.002	59	31
31	Glutamatergic synapse	0.002	83	34
32	Endocrine and other factor-regulated calcium reabsorption	0.002	34	31
33	Chronic myeloid leukemia	0.002	55	32
34	Insulin signaling pathway	0.003	103	33
35	Neurotrophin signaling pathway	0.004	89	36
36	Circadian rhythm	0.004	26	25
37	Focal adhesion	0.006	145	36
38	Rap1 signaling pathway	0.006	146	34
39	Signaling pathways regulating pluripotency of stem cells	0.006	99	34
40	Fc gamma R-mediated phagocytosis	0.007	68	32
41	AMPK signaling pathway	0.007	88	34
42	Nicotine addiction	0.008	30	32
43	Sphingolipid signaling pathway	0.008	81	34
44	TGF-beta signaling pathway	0.008	59	34
45	Acute myeloid leukemia	0.008	45	30
46	PI3K-Akt signaling pathway	0.008	228	36
47	Morphine addiction	0.009	66	32

Significantly enriched KEGG pathways associated with differentially expressed miRNAs unique to non-DIPG subgroup of paediatric HGG were identified using the 'genes union' module (microT-threshold 0.7) in DIANA mirPath. Pathways with enrichment p-value<0.05 (FDR ON) are shown. The table is ranked by enrichment p-value.

Table 5.13 KEGG pathways associated with differentially expressed miRNAs unique to DIPG short-term cell cultures

	KEGG pathway	p-value	Genes	miRNAs
1	Mucin type O-Glycan biosynthesis	0	22	16
2	Pathways in cancer	0	255	30
3	ErbB signaling pathway	0	68	26
4	Estrogen signaling pathway	0	68	27
5	Signaling pathways regulating pluripotency of stem cells	0	99	27
6	Cocaine addiction	0	37	27
7	Renal cell carcinoma	0	53	25
8	Glioma	0	48	25
9	Proteoglycans in cancer	0	128	28
10	Glutamatergic synapse	0	77	29
11	Endocrine and other factor-regulated calcium reabsorption	0	36	26
12	Adrenergic signaling in cardiomyocytes	0	97	29
13	Axon guidance	0	84	28
14	Prostate cancer	0	64	28
15	Ubiquitin mediated proteolysis	0	96	26
16	Dopaminergic synapse	0	87	29
17	Thyroid hormone signaling pathway	0	80	28
18	Amphetamine addiction	0	46	27
19	Ras signaling pathway	0	141	31
20	Prion diseases	0.001	17	17
21	Endometrial cancer	0.001	39	27
22	Melanoma	0.001	51	25
23	Glycosaminoglycan biosynthesis - chondroitin sulfate / dermatan sulfate	0.001	14	13
24	Chronic myeloid leukemia	0.001	51	25
25	Colorectal cancer	0.001	44	26
26	Endocytosis	0.001	135	30
27	Non-small cell lung cancer	0.001	40	24
28	Cholinergic synapse	0.001	78	26
29	Prolactin signaling pathway	0.002	47	28
30	Hepatitis B	0.003	92	29
31	Wnt signaling pathway	0.003	89	28
32	Choline metabolism in cancer	0.004	68	26
33	Neurotrophin signaling pathway	0.004	80	30
34	Melanogenesis	0.004	67	28
35	TGF-beta signaling pathway	0.004	50	26
36	cGMP-PKG signaling pathway	0.004	104	29
37	Thyroid hormone synthesis	0.005	46	26
38	Gap junction	0.005	58	27
39	cAMP signaling pathway	0.005	125	30
40	Long-term potentiation	0.006	47	29
41	Adherens junction	0.008	50	26
42	GnRH signaling pathway	0.008	61	26
43	Rap1 signaling pathway	0.009	129	29
44	Pancreatic cancer	0.009	45	22
45	Sphingolipid signaling pathway	0.009	72	26
46	Phosphatidylinositol signaling system	0.009	54	25
47	FoxO signaling pathway	0.009	84	27

Significantly enriched KEGG pathways associated with differentially expressed miRNAs unique to DIPG subgroup of paediatric HGG were identified using the 'genes union' module (microT-threshold 0.7) in DIANA mirPath. Pathways with enrichment p-value<0.05 (FDR ON) are shown. The table is ranked by enrichment p-value.

5.2.5 Differential expression of miRNAs between *H3F3A*-mutant and wild type paediatric HGG short-term cell cultures

To determine the association between miRNA expression and *H3F3A* mutation (K27M) in paediatric HGG short-term cell cultures, the miRNA expression profiles were generated for *H3F3A*-mutant and wild-type subgroups of paediatric HGG short-term cell cultures as compared to NHA. A one-way ANOVA test was performed to identify significantly differentially expressed miRNAs (FC-2, $p<0.05$) in each subgroup versus NHA using Partek Genomics suite v6.6 (Partek Inc., USA). There were 164 miRNAs (22 upregulated and 142 downregulated) that were significantly differentially expressed in *H3F3A*-mutant subgroup and 151 miRNAs (12 upregulated and 139 downregulated) that were significantly differentially expressed in the *H3F3A*-wild type subgroup as compared to NHA. Both common and unique miRNAs in these 2 subgroups are displayed as a Venn diagram as shown in Figure 5.10.

There were 124 miRNAs common (5 upregulated and 119 downregulated) between the 2 subgroups. There were 39 miRNAs (17 upregulated and 22 downregulated) unique to *H3F3A*-mutant subgroup and 27 miRNAs (7 upregulated and 20 downregulated) unique to the wild type subgroup. KEGG pathway analysis was performed using the unique miRNAs identified in each subgroups using DIANA-miRPath v3.0 (http://www.microrna.gr/miRPathv3). Using the 'pathways union' module in DIANA mirPath, a union set of significantly enriched pathways were generated. The gene targets of miRNAs were predicted using microT-CDS algorithm (threshold-0.7). The enrichment analysis was performed using Fisher's exact test

(hypergeometric distribution); Benjamini-Hochberg adjustment was used for multiple test correction. The significantly enriched ($p<0.05$) KEGG pathways associated with the *H3F3A*-mutant subgroup and the wild-type subgroup are given in Table 5.15 and Table 5.16 respectively.

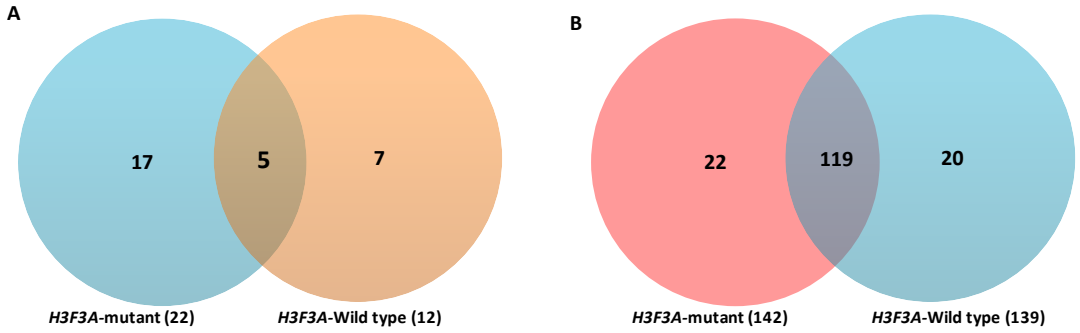

Figure 5.10 Venn diagram showing common and unique miRNAs in *H3F3A* (K27M)-mutant and wild type paediatric HGG short-term cell cultures. A. The upregulated miRNAs (2-fold change, $p<0.05$) in *H3F3A* (K27M) mutant and upregulated miRNAs in wild type subgroups relative to NHA are compared. The *H3F3A*-mutant subgroup had 17 unique miRNAs; the *H3F3A*-wild type subgroup had 7 unique miRNAs, while 5 miRNAs were common to both the subgroups. The numbers in parenthesis show the total number of differentially upregulated miRNAs identified in each subgroup. **B.** The downregulated miRNAs (2-fold change, $p<0.05$) in *H3F3A* (K27M) mutant and downregulated miRNAs in wild type subgroups relative to NHA are compared. The *H3F3A*-mutant subgroup had 22 unique miRNAs; *H3F3A*-wild type subgroup had 20 unique miRNAs, while 119 miRNAs were common to both the subgroups. The numbers in parenthesis show the total number of differentially upregulated miRNAs identified in each subgroup.

Table 5.14 Differentially expressed miRNAs unique to *H3F3A* (27M)-mutant and wild type subgroups

A

Upregulated	
miRNAs	Accession
hsa-miR-100*	MIMAT0004512
hsa-miR-1539	MIMAT0007401
hsa-miR-30d*	MIMAT0004551
hsa-miR-3126-3p	MIMAT0015377
hsa-miR-3591-5p	MIMAT0019876
hsa-miR-4656	MIMAT0019723
hsa-miR-4677-5p	MIMAT0019760
hsa-miR-4699-5p	MIMAT0019794
hsa-miR-4713-5p	MIMAT0019820
hsa-miR-4776-5p	MIMAT0019932
hsa-miR-518f*	MIMAT0002841
hsa-miR-520g	MIMAT0002858
hsa-miR-548g	MIMAT0005912
hsa-miR-575	MIMAT0003240
hsa-miR-181a-2*	MIMAT0004558
hsa-miR-3622a-3p	MIMAT0018004
hsa-miR-486-5p	MIMAT0002177
Downregulated	
miRNAs	Accession
hsa-miR-1236	MIMAT0005591
hsa-miR-1272	MIMAT0005925
hsa-miR-212	MIMAT0000269
hsa-miR-3065-3p	MIMAT0015378
hsa-miR-324-5p	MIMAT0000761
hsa-miR-3616-3p	MIMAT0017996
hsa-miR-3687	MIMAT0018115
hsa-miR-369-3p	MIMAT0000721
hsa-miR-380*	MIMAT0000734
hsa-miR-3937	MIMAT0018352
hsa-miR-4278	MIMAT0016910
hsa-miR-4291	MIMAT0016922
hsa-miR-4326	MIMAT0016888
hsa-miR-4440	MIMAT0018958
hsa-miR-4640-3p	MIMAT0019700
hsa-miR-4692	MIMAT0019783
hsa-miR-4704-5p	MIMAT0019803
hsa-miR-4774-5p	MIMAT0019929
hsa-miR-4778-5p	MIMAT0019936
hsa-miR-4787-5p	MIMAT0019956
hsa-miR-502-3p	MIMAT0004775
hsa-miR-549	MIMAT0003333
hsa-miR-616	MIMAT0004805

B

Upregulated	
miRNAs	Accession
hsa-miR-138	MIMAT0000430
hsa-miR-142-3p	MIMAT0000434
hsa-miR-144	MIMAT0000436
hsa-miR-183*	MIMAT0004560
hsa-miR-199a-5p	MIMAT0000231
hsa-miR-4258	MIMAT0016879
hsa-miR-98	MIMAT0000096
Downregulated	
miRNAs	Accession
hsa-miR-1266	MIMAT0005920
hsa-miR-136	MIMAT0000448
hsa-miR-16-2*	MIMAT0004518
hsa-miR-191	MIMAT0000440
hsa-miR-1915*	MIMAT0007891
hsa-miR-200c	MIMAT0000617
hsa-miR-3074-3p	MIMAT0015027
hsa-miR-3121-5p	MIMAT0019199
hsa-miR-3185	MIMAT0015065
hsa-miR-3917	MIMAT0018191
hsa-miR-425	MIMAT0003393
hsa-miR-4516	MIMAT0019053
hsa-miR-4535	MIMAT0019075
hsa-miR-4638-5p	MIMAT0019695
hsa-miR-4674	MIMAT0019756
hsa-miR-4703-3p	MIMAT0019802
hsa-miR-4749-3p	MIMAT0019886
hsa-miR-4795-5p	MIMAT0019968
hsa-miR-4803	MIMAT0019983
hsa-miR-759	MIMAT0010497

A) Differentially upregulated miRNAs unique to *H3F3A* (K27M)-mutant subgroup **B)** Differentially upregulated miRNAs unique to *H3F3A* (K27M)-wild type subgroup.

Table 5.15 KEGG pathways associated with differentially expressed miRNAs unique to *H3F3A*-mutant paediatric HGG short-term cell cultures

KEGG pathway	p-value	Genes	miRNAs
Prion diseases	0	2	3
Mucin type O-Glycan biosynthesis	0	14	9
ECM-receptor interaction	0	33	9
TGF-beta signaling pathway	0	49	9
Biosynthesis of unsaturated fatty acids	0	5	5
Lysine degradation	0	15	6
Signaling pathways regulating pluripotency of stem cells	0	61	5
Proteoglycans in cancer	0.005	115	6
Estrogen signaling pathway	0.017	49	7
Hippo signaling pathway	0.019	69	6

Commonly targeted pathways by *H3F3A*-mutant paediatric HGG identified using the 'pathways union' module (microT-threshold 0.7) in DIANA mirPath. Pathways with enrichment p-value<0.05 (FDR ON) are shown. The table is ranked by enrichment p-value. Pathways that are unique to *H3F3A*-mutant in comparison to *H3F3A*-wild type are highlighted in blue.

Table 5.16 KEGG pathways associated with differentially expressed miRNAs unique to *H3F3A*-wild type paediatric HGG short-term cell cultures

KEGG pathway	p-value	Genes	miRNAs
ECM-receptor interaction	0	26	4
Lysine degradation	0	25	8
Fatty acid degradation	0	5	4
Mucin type O-Glycan biosynthesis	0	14	3
Steroid hormone biosynthesis	0	10	2
Proteoglycans in cancer	0.001	84	5
Morphine addiction	0.001	24	5
Fatty acid metabolism	0.002	8	4
Thyroid hormone signaling pathway	0.004	35	4
Hippo signaling pathway	0.016	50	3
Phosphatidylinositol signaling system	0.016	33	5

Commonly targeted pathways by *H3F3A*-wild type paediatric HGG identified using the 'pathways union' module (microT-threshold 0.7) in DIANA mirPath. Pathways with enrichment p-value<0.05 (FDR ON) are shown. The table is ranked by enrichment p-value. Pathways that are unique to *H3F3A*-wild type in comparison to *H3F3A*-mutant are highlighted in blue.

The miRNAs associated with ‘signaling pathways regulating pluripotency of stem cells’ were miR-212-3p, miR-369-3p, miR-4704-5p, miR-520g-3p and miR-548g-3p. The miRNAs associated with prion diseases were miR-1272, miR-30d-3p and miR-520g-3p, and those associated with TGF-beta signaling pathway were miR-1236-3p, miR-212-3p, miR-369-3p, miR-4326, miR-4704-5p, miR-4778-5p, miR-520g-3p, miR-548g-3p and miR-486-5p.

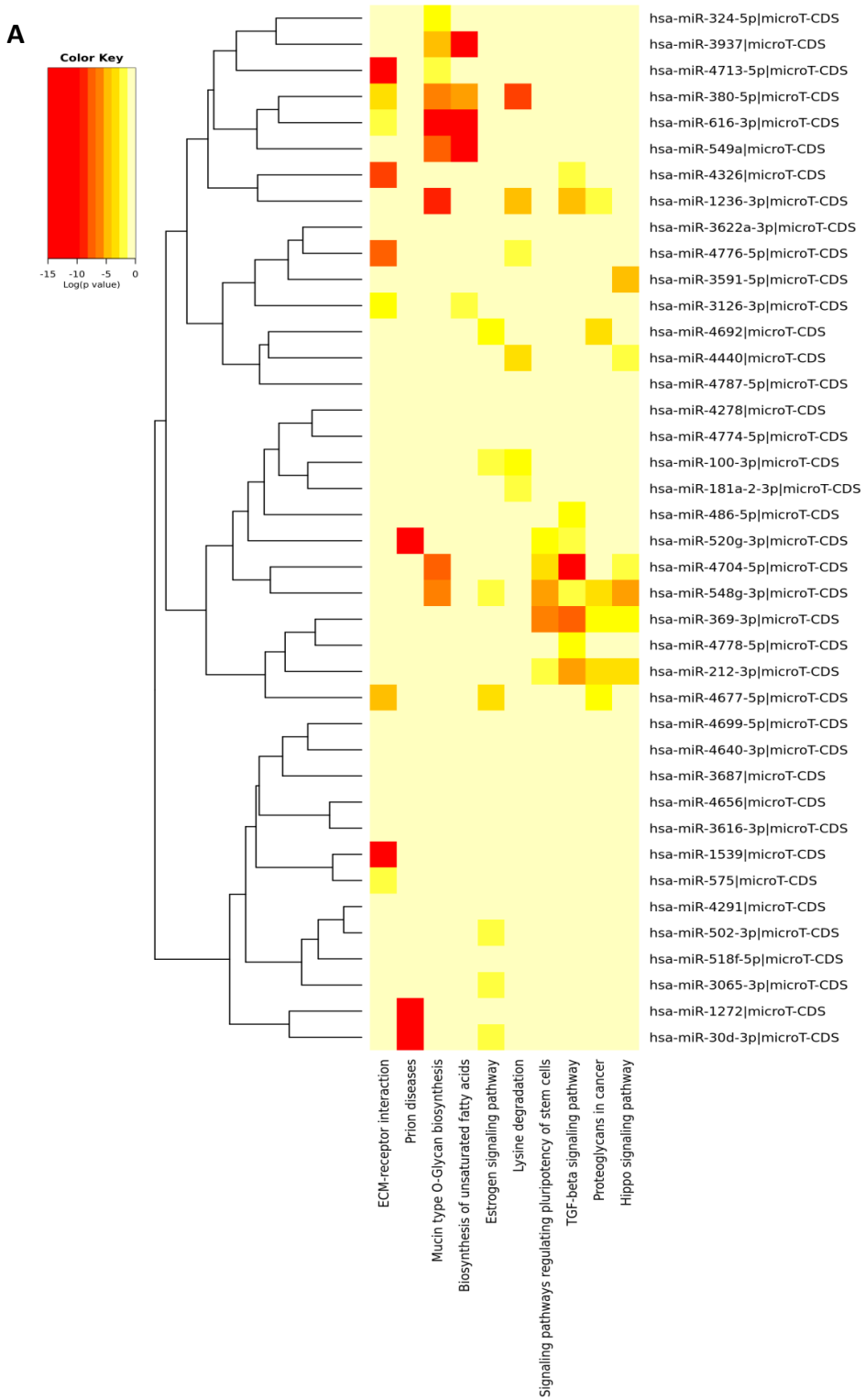

Figure 5.11 Heat map of miRNAs versus pathways. Commonly targeted pathways by differentially expressed miRNAs (microT-CDS>0.70, p<0.05, FDR ON) identified by 'pathways union' module in DIANA mirPath v3.0**. A. Pathways associated with *H3F3A*-mutant paediatric HGG short-term cell cultures.**

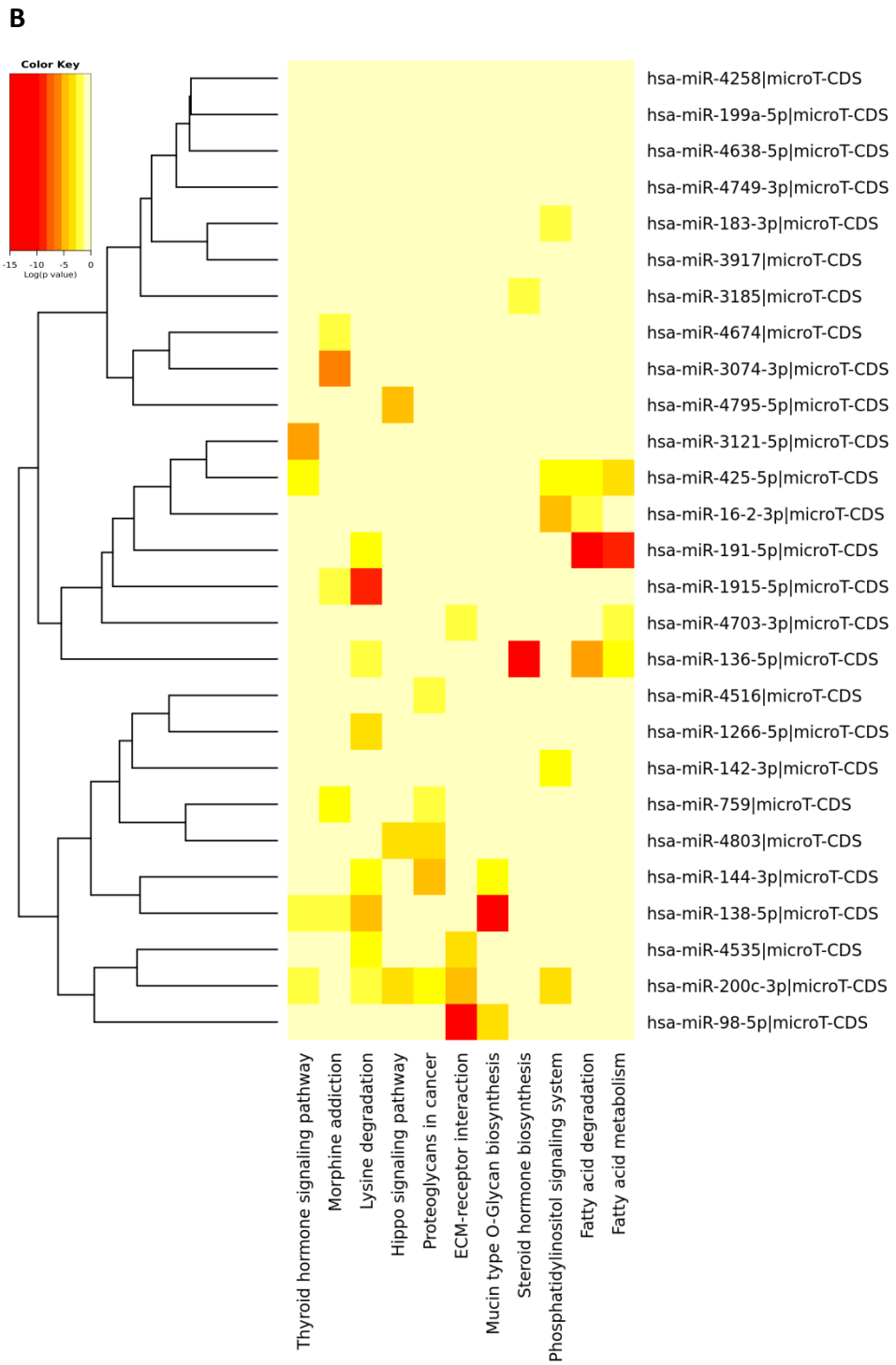

Figure 5.11 Heat map of miRNAs versus pathways. Commonly targeted pathways by differentially expressed miRNAs (microT-CDS>0.70, p<0.05, FDR ON) identified by 'pathways union' module in DIANA mirPath v3.0. On the heat map, each row represents a miRNA and each column represents a pathway. **B. Pathways associated with *H3F3A*-wild-type paediatric HGG short-term cell cultures.**

5.2.6 Association between copy number loss of *ADAM3A* and miRNA expression profiles in paediatric HGG short-term cell cultures.

To determine the association of miRNA expression with copy number loss of *ADAM3A* in paediatric HGG short-term cell cultures, the miRNA expression profiles were compared between the subgroup of paediatric HGG short-term cell cultures with copy number loss of *ADAM3A* (n=10) and the subgroup without the copy number loss (n=7) as compared to NHA. Of the 7 members in the subgroup without *ADAM3A* loss, 4 members had gain of *ADAM3A.* Therefore, in order to identify specific changes associated with *ADAM3A*-loss, the subgroup with gain of *ADAM3A* gene was considered as separate subgroup. One-way ANOVA test was performed to identify differentially expressed and significant (FC-2, $p<0.05$) miRNAs in each group (samples with loss/gain/no change) as compared to NHA.

There were 128 miRNAs (119 downregulated and 9 upregulated) that were differentially expressed in the subgroup of paediatric HGG with *ADAM3A* loss; 180 miRNAs (171 downregulated and 9 upregulated) in the subgroup with *ADAM3A* gain and 216 miRNAs (208 downregulated and 8 upregulated) in the subgroup with intact *ADAM3A.* The unique miRNAs in each subgroup are represented as a Venn diagram in Figure 5.12. There were 112 differentially expressed miRNAs common among all subgroups, of which 5 were upregulated and 107 were downregulated. There were 3 miRNAs (1 upregulated and 2 downregulated) unique to the subgroup with *ADAM3A* loss, 10 miRNAs (10 downregulated) unique to the subgroup with *ADAM3A* gain and 47 miRNAs (2 upregulated and 45 downregulated) unique to the subgroup with intact *ADAM3A.* The uniquely differentially expressed miRNAs associated with

ADAM3A loss were miR-3142 (upregulated), and miR-3140-3p and miR-4503 (downregulated).

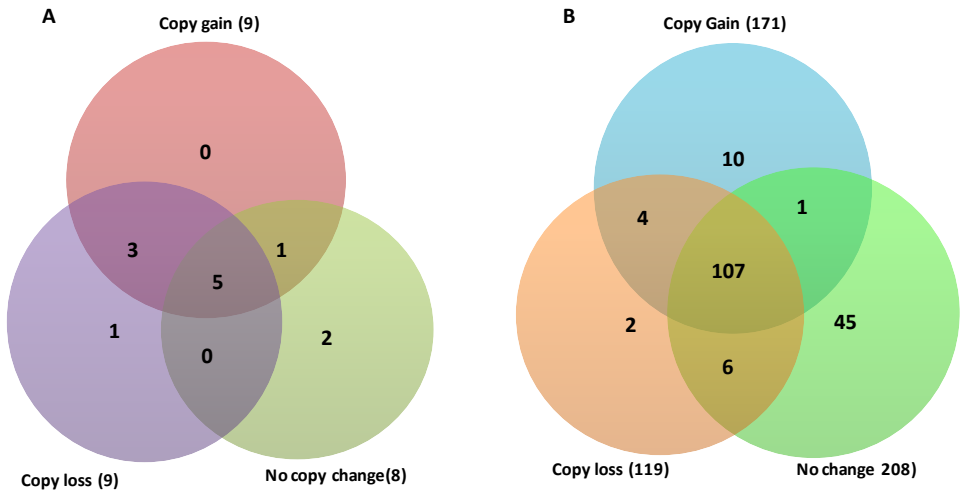

Figure 5.12 Venn diagram of differentially expressed miRNAs between samples with loss, gain and no change in copy number of *ADAM3A*. A. Upregulated miRNAs. There are 5 miRNAs common to all subgroups; 1 miRNA unique to *ADAM3A* loss. **B.** Downregulated miRNAs. There are 107 miRNAs common to all subgroups; 2 miRNAs unique to *ADAM3A* loss. The numbers in parentheses indicate the differentially expressed miRNAs as compared to NHA.

The KEGG pathways associated with the unique miRNAs associated with *ADAM3A* loss in paediatric HGG short-term cell cultures were identified by DIANA-miRPath v3.0 (http://www.microrna.gr/miRPathv3). The gene targets of deregulated miRNAs were predicted using microT-CDS algorithm (threshold 0.70). The p-value for enrichment was calculated using Fisher's exact test. The results are shown in Table 5.17.

Table 5.17 KEGG pathways associated with miRNAs unique to paediatric HGG short-term cell cultures with *ADAM3A* loss

KEGG pathway	p-value	Gene count	Genes
Mucin type O-Glycan biosynthesis	0	8	*GALNT7, GALNT4, GALNT3*
Ras signaling pathway	0	56	*AKT3, EGFR, FGF12, KRAS, PAK2, PDGFC, VEGFC*
ErbB signaling pathway	0	27	*BRAF, GSK3B,EGFR, ERBB3, PAK6, AKT3*
Pathways in cancer	0	83	*BRAF, FGF12, EGFR, SMAD2, WNT2B, RAF1, CDK6*
Glioma	0	19	*AKT3, BRAF, EGFR, RB1, MDM2, RAF1, PPIK3R5*
Focal adhesion	0	51	*EGFR, PAK6, RELN, VEGFC, COL4A4, BCL2, ROCK2*
Proteoglycans in cancer	0.001	45	*BRAF, PIK3R5, SMAD2, CAV2, ERBB3, COL21A1*
Prostate cancer	0.001	24	*BRAF, GSK3B, CTNNB1, PDGFC, RB1*
Thyroid hormone signaling pathway	0.002	26	*FOXO1, MDM2, GSK3B, PRKCA*
Endometrial cancer	0.002	16	*BRAF, GSK3B, AKT3, EGFR, KRAS, PIK3R1*
Prolactin signaling pathway	0.002	18	*CCND1, PIK3R1, KRAS, MAPK14, RELA, GSK3B*
Signaling pathways regulating pluripotency of stem cells	0.004	33	*SMAD2, SMAD3, SMAD5, INHBA, BMPR2, PAX6, SMARCAD1*
Axon guidance	0.004	27	*SEMA61, ROCK2, NFATC2, SEMA5A*
Renal cell carcinoma	0.006	20	*BRAF, TGFB2, KRAS, PAK6*
Endocytosis	0.009	38	*CAV2, TGFB2, SMAd2, SMURF2*
Neurotrophin signaling pathway	0.009	29	*BRAF, BCL2, PLCG2, IRS1, AKT3*

Significantly enriched KEGG pathways associated with differentially expressed miRNAs unique to subgroup of paediatric HGG with *ADAM3A* loss, were identified using the 'genes union' module (microT-threshold 0.7) in DIANA mirPath. Pathways with enrichment p-value<0.05 (FDR ON) are shown. The table is ranked by enrichment p-value.

5.3 Discussion

This chapter has focussed on the genome wide investigation of differential miRNA expression in 17 paediatric HGG short-term cell cultures compared to NHA, with the aim of understanding the involvement of miRNAs in the development and progression of paediatric HGG. The expression patterns of miRNAs associated with *H3F3A* (K27M) mutation and copy number loss of *ADAM3A*, 2 of the distinct

genetic aberrations encountered in paediatric HGG were examined. The miRNA expression profiles in DIPG and non-DIPG short-term cell cultures were also compared with respect to NHA. Furthermore, mRNA targets of dysregulated miRNAs were identified using integrated analyses of miRNA and mRNA expression profiles in the paediatric HGG short-term cell cultures versus NHA. The findings of this study highlight the link between miRNAs and paediatric HGG pathogenesis.

Global expression analysis in this study revealed distinct miRNA expression profiles for paediatric HGG short-term cell cultures compared to their normal counterparts. This is encouraging as identification of candidate miRNAs could lead to the development of biomarkers for early diagnosis of this disease. Large-scale variation in miRNA expression was observed amongst the paediatric HGG short-term cell cultures as identified by PCA and hierarchical clustering, which may reflect the characteristic heterogeneity of glioma. Each paediatric HGG short-term cell culture used in this study was established from a distinct population of cells from individual tumour biopsies and the miRNA expression profile of each paediatric HGG short-term cell culture reflects the average expression levels of miRNAs in these population of cells. Regional intra-tumour heterogeneity comprised of core necrotic cells surrounded by cells that are highly proliferative and vascular is a well-documented characteristic of GBM. Lages et al., (2011) reported that a set of miRNAs consisting of miR-15b, miR-16, miR-17, miR-20a, miR-210, let-7a, let-7b, let-7d and let-7f showed increased expression in the core cells that are characterised by hypoxic conditions.

MiRNA down regulation is predominant in paediatric HGG compared to normal cells

In this study, the expression of 853 miRNAs was examined in 17 paediatric HGG short-term cell cultures in comparison to NHA. There were 162 significantly differentially expressed miRNAs (FC-2, $p<0.05$) with strikingly higher number of downregulated than upregulated miRNAs (152 versus 10 miRNAs). Such relative abundance of downregulated miRNAs has been observed in other cancers (Lu et al., 2005). One of the reasons for this enhanced downregulation could be attributed to the influence of genetic aberrations on miRNA expression. It has been identified that about 52.5% of miRNA genes are located in regions of chromosomal instability such as common fragile sites that are regions of deletion (Calin et al., 2004), which may have an impact on the transcription of miRNA genes. Epigenetic mechanisms such as hypermethylation in miRNA gene promoters may also cause reduced expression of miRNAs. Promoter-hypermethylation-induced downregulation of miRNAs has been reported in several cancers (Chen et al., 2012; Lopez-Serra and Esteller, 2012; Menigatti et al., 2013; Vrba et al., 2013). Moreover, defective miRNA biogenesis could cause decreased miRNA expression. For instance, hemizygous deletion of the gene encoding DICER1 has been reported in 27% of various tumours and the reductions in DICER1 is linked to defective miRNA processing (Kumar et al., 2009).

MiRNAs not previously reported in paediatric HGG

The dysregulated miRNAs identified in this study included known miRNAs with putative oncogenic and/or tumour suppressive roles as well as miRNAs that were not previously reported in cancers. The 3 most significantly upregulated miRNAs were

miR-142-3p, miR-144, miR-138. None of these miRNAs have been previously reported in paediatric HGG, although increased expression of miR-142-5p has been identified in paediatric brain tumours such as atypical teratoid/rhabdoid tumour, ependymoma, adult GBM, medulloblastoma, and pilocytic astrocytoma compared to normal cells (Birks et al., 2011). Interestingly, deregulation of these miRNAs has been identified in adult glioma, suggesting similarities in miRNA deregulation between paediatric and adult HGG. For instance, increased expression of miR-142-3p, the miRNA with the highest upregulation observed in this study (FC-337.09), has been reported in GBM cell lines (Chaudhry et al., 2010). The functional significance of mir-142-3p has also been observed in other cancer types. Taichi et al. (2014) reported a role for miR-142-3p in regulating the tumourigenicity of breast cancer stem cells possibly through the involvement of the canonical WNT signaling pathway. It has been identified as crucial in maintaining the balance between proliferation and differentiation of mesenchymal cells during lung development (Carraro et al., 2014).

MiR-144 has shown oncogenic roles in adult glioma and other cancers (Lin et al., 2014; Cai et al., 2015; Zhang et al., 2012), while tumour suppressive roles in uveal melanoma (Sun et al., 2015), suggesting context-dependent roles for this miRNA. The study by Lin et al., (2014) has identified *EZH2* as the gene target of miR-144 in glioma. Overexpression of *EZH2* has been identified in both adult and paediatric HGG (Purkait et al., 2015). MiR-138 has a pro-survival role in tumour-initiating glioma stem cells (GSC) and is associated with tumour recurrence, highlighting its role as a prognostic marker in malignant glioma (Chan et al., 2012). It has been

shown that miR-138 can enhance the oncogenic activity of MYC by targeting MXD1 that competes with MYC in forming a stable complex with MAX. As MYC is a frequently altered target in paediatric glioma (Wu et al., 2014), this prompts speculation of a potential role for this miRNA in paediatric HGG. MiR-138 has also been shown to promote TMZ resistance in gliomas by binding to BIM, a BCL2 interacting mediator (Stojcheva et al., 2016). This may contribute to TMZ resistance in paediatric HGG. The 2 most significantly downregulated miRNAs included miR-3621 and miR-759. These miRNAs have not been reported in paediatric HGG and their role in other cancers has also not yet been investigated. However, based on the functional significance of their predicted targets, it can be speculated that these miRNAs may regulate important gene regulatory networks in paediatric HGG pathogenesis. For instance, mutations in H3.3-ATRX-DAXX chromatin remodelling pathway have been identified almost exclusively in paediatric HGG and in some cases have shown strong associations with *TP53* mutations (Schwartzentruber et al., 2012). MiR-3621 can target *CHD3* (chromodomain helicase DNA binding protein 3) (microT-CDS prediction score-0.771), a key component of the Mi-2/NuRD histone deacteylase complex involved in chromatin remodelling by deacetylating histones and miR-759 has been identified to target *TP53* (Tay et al., 2014), suggesting a possible link for these miRNAs to tumourigenic events in paediatric HGG.

Role of miRNAs in paediatric HGG in modulating cancer-related pathways

The KEGG pathway analysis of differentially expressed miRNAs in paediatric HGG short-term cell cultures (upregulated and downregulated) revealed alterations in 2 important glycan-related pathways comprising Mucin type O-glycan biosynthesis

and Proteoglycans in cancer, indicating the potential significance of aberrant glycan biosynthesis in paediatric HGG. Glycans and membrane-bound glyco-conjugates constitute a large spectrum of biomolecules mediating a variety of fundamental cellular processes associated with cancer development and progression such as cell-cell and cell-ECM interactions (Pinho et al., 2009; Zhao et al., 2008), inflammation, immune surveillance (Rabinovich and Toscano 2009), signal transduction (Dennis et al, 2009) and cellular metabolism (Gomes et al., 2013). Mucin-type O-glycosylation, the most common form of protein O-glycosylation constitutes glycans attached via O-linked N-acetylgalactosamine (GalNAc) to amino acid residues such as serine and threonine. Aberrant O-linked glycosylation is associated with many tumour types including tumours of brain, breast, ovary and pancreatic cells (Song et al., 2010; Hofmann et al., 2015; Pinho and Reis, 2015). Characteristic patterns of glycosylation exist in different cancers and identification of such tumour-specific changes in glycosylation has shown encouraging results in the development of diagnostic biomarkers in some cancers. For instance, α-fetoprotein L3 and α-fetoprotein P4+P5 can act as early diagnostic biomarkers and differentiate HCC from liver cirrhosis (Sato et al., 1993; Song et al., 2010). Given the complexity of the human glycome and proteoglycome it is highly challenging to characterise the glcosylation patterns in tumours. However, development of high-throughput glycan microarrays (Rillahan and Paulson, 2011) may hold promise for the identification of specific glycosylation signatures associated with paediatric HGG that could be exploited for the development of early diagnostic/prognostic biomarkers and may also help to understand their contribution to the heterogeneity of these tumours.

Integrative analysis to identify gene targets of miRNAs

One of the approaches to interpret the effect of miRNA dysregulation in cancers is to identify the role of its mRNA targets. However, miRNA target identification is highly challenging as each miRNA can target hundreds of mRNAs while a single mRNA can also be targeted by several miRNAs (Krek et al., 2005; Lee et al., 2005). To add to the complexity, multiple miRNAs can also cooperatively target a number of mRNAs and miRNAs also exhibit tissue-specific expression signatures (Calin et al., 2004; Krek et al., 2005; Lu et al., 2005). Although databases such as TargetScan and microT-CDS enable putative identification of miRNA targets based on sequence complementarity in 3'UTR and/or CDS regions, the false positive rates for such speculative matches is very high (Friedman et al., 2009). Integrative miRNA-mRNA expression analysis helps to identify more accurate miRNA-mRNA interaction pairs. The integrative analysis in this study identified 22 miRNA-mRNA interaction pairs, which predominantly included miRNAs with multiple gene targets. Six gene targets were identified for miR-520a-3p comprising *AAK1, EIF5, MINK1, NBEAL2*, *PDLIM5* and *ZFHX4*. Little is known about the role of these targets in paediatric HGG. *PDLIM5* (PDZ and LIM domain containing 5) is a member of the PDZ-LIM family of genes that are involved in signal transduction between the nucleus and the cytoskeleton and contributes to organ development. It has been identified as a novel AMPK (AMP-activated protein kinase) substrate and participates in inhibition of cell migration that occurs via suppression of the Rac1-Arp2/3 signaling pathway (Yan et al., 2015). Among the multiple mRNAs that were targeted by single miRNAs, *ZFHX4* (zinc finger

homeobox 4) had the highest number of targeting miRNAs comprising miR-520a-3p, miR-613, miR-502-3p and miR-369-3p. *ZFHX4* has been identified to interact with the chromatin remodelling complex NuRD and has been shown to regulate the tumour initiating cells (TICs) in GBM (Chudnovsky et al., 2014).

Comparison of miRNA expression profiles between DIPG and non-DIPG short-term cell cultures

Comparison of the miRNA expression profiles between DIPG and non-DIPG paediatric HGG short-term cell cultures revealed that the majority of the differentially expressed miRNAs were common to both the groups, but this could be due to the relatively smaller number of DIPG samples analysed here compared to non-DIPG. There were 33 miRNAs (8 upregulated and 137 downregulated) that were uniquely deregulated in the DIPG short-term cell cultures. The detection of specific miRNAs that were deregulated in the DIPG subgroup in this study further supports that these tumours indeed harbour unique molecular events. Most of these miRNAs have not yet been investigated in DIPG. Interestingly, some of the downregulated miRNAs have been previously reported in other cancer types. Of note, miR-125b is one of the widely investigated miRNAs and has demonstrated contradicting roles in different cancers, suggesting a context-dependent role for this miRNA. For instance, upregulation and oncogenic potential of miR-125b has been shown in adult glioma, pancreatic and colorectal cancers, while downregulation of this miRNA has been identified in breast cancer, head and neck cancers, melanoma, hepatocellular carcinoma and osteosarcoma (Xia et al., 2009; Liu et al., 2011; Gong et al., 2013; Kappelmann et al., 2013; Nakanishi et al., 2014). Among the most uniquely enriched

pathways in DIPG, estrogen signaling pathway and signalling pathways regulating pluripotency of stem cells were the most affected. Some GBM cells express estrogen receptors (ERs) and specific modulation of ER activity has shown apoptosis inhibition activity *in vitro* and *in vivo* in ER-negative GBM cells (Hui et al., 2004). Combined histone deacetylase and estrogen receptor inhibition has shown apoptotic activity in breast cancer through HDAC-mediated Akt1 downregulation in an estrogen-dependent mechanism (Thomas et al., 2013). With HDAC1 inhibitors holding promise for clinical trials in DIPG, it would be interesting to investigate the contribution of estrogen receptors in the progression of these tumours as it may provide opportunities for combination therapy and improved clinical response. The existence of a tumour sub-population of cells with self-renewing capacities termed as 'cancer stem cells' or 'cancer initiating cells' has been demonstrated in DIPG (Monje et al., 2011; Puget et al., 2012; Caretti et al., 2014). The contribution of these cells to treatment resistance and tumour recurrence has been extensively investigated in adult GBM as well as in several other cancers. Validation of the identified miRNAs and identification their deregulated gene targets in DIPG can therefore help us understand more about the clinical heterogeneity and resistance mechanisms in these tumours that can accelerate the development of efficient therapeutic targets.

MiRNAs associated with H3F3A (K27M) mutation

The *H3F3A* (K27M) mutation is an important driver event in paediatric HGG, particularly DIPG and has raised great interest owing to its connection with chromatin remodelling and regulation of other epigenetic mechanisms. Recently, Jha et al. (2014) has reported a unique set of 97 miRNAs (62 upregulated and 35

downregulated) in *H3F3A*-mutant paediatric GBM compared to the wild type. In the current study, the unique profiles of *H3F3A*-mutant subgroup was evident from the unsupervised hierarchical clustering analysis in which the 2 mutant paediatric HGG short-term cell cultures clustered together irrespective of their tumour type or the presence/absence of other genetic aberration (*ADAM3A* loss) (See Figure 5.12). A total of 39 miRNAs (17 upregulated and 22 downregulated) were uniquely differentially expressed in the *H3F3A*-mutant subgroup. This clearly indicates that *H3F3A* (K27M) mutation influences the miRNA expression in paediatric HGG. Pathway analysis of these miRNAs using their predicted gene targets revealed KEGG pathways such as Prion diseases, TGF-beta signaling, biosynthesis of unsaturated fatty acids, signaling pathways regulating pluripotency of stem cells and estrogen signaling pathway to be uniquely deregulated in the mutant subgroup. Dysregulation of these pathways are associated with highly aggressive tumours. For instance, TGF-beta signaling pathway regulates a number of crucial cellular processes such as growth, embryogenesis, differentiation, wound healing, and apoptosis (Bottner et al., 2000). Increased activation of this pathway confers poor prognosis in GBM patients (Bruna et al, 2007). It can also induce the self-renewal capacity of glioma-initiating cells (GICs) (Peneulas et al., 2009). Prion proteins contribute to invasiveness and doxorubicin-resistance in colon cancer (Chieng and Say, 2015) and lower expression of estrogen receptor Erβ has been associated with poor clinical outcome (Batistatou et al., 2006). All these point toward a highly aggressive phenotype for the mutant subtype and a potential role for miRNAs in establishing this phenotype in paediatric HGG. Integrative analysis of miRNA and mRNA expression profiles of the mutant and wild type subgroups may provide better

insights into how *H3F3A* mutation regulates the miRNA expression and how it affects downstream cellular processes in paediatric HGG.

MiRNAs associated with ADAM3A loss in paediatric HGG short-term cell cultures

An important finding in this study was the identification of miRNAs associated with loss of the pseudogene, *ADAM3A.* Over the last few years, there has been increasing interest in understanding the role of pseudogenes and their interaction with the coding and non-coding part of the genome. Studies have demonstrated in multiple cancers that processed transcripts of some pseudogenes share miRNA responsive elements (MREs) with their parent genes competing for the same miRNAs and thereby regulating the transcription of the parent genes (Chen et al., 2015; Yu et al., 2014). Interestingly, an extensive genome-wide integrative mRNA-miRNA analysis in adult GBM has revealed over 248,000 miRNA-mRNA interactions, of which the transcripts of approximately 7000 genes act as competing endogenous RNAs and 148 genes act through alternative mechanisms (Sumazin et al., 2011). This provides clues to the strikingly complex network of cellular events regulated by non-coding elements in glioma. In the current study, 3 miRNAs were uniquely expressed in paediatric HGG short-term cell cultures with loss of *ADAM3A* and the predicted mRNA targets of all of them have potential links to cancer-related pathways, indicating a putative role for *ADAM3A* in tumourigenesis. The miRNAs associated with *ADAM3A* loss were miR-3142 (upregulated), and miR-3140-3p and miR-4503 (downregulated); the roles of these miRNAs have not been investigated yet. However, as each miRNA can regulate hundreds of targets, it can be speculated that the deregulated expression of these miRNAs may have significant consequence on

the miRNA-mRNA equilibrium in various cellular pathways. As described in Chapter 4, dysregulation of *ADAM3A* has been observed in paediatric HGG and a few other cancer types, but not in adult HGG, suggesting this as a distinguishing property of these tumours. Therefore, the potential involvement of *ADAM3A*-associated miRNAs in crucial cancer-related pathways highlights the importance of future investigation of this finding in paediatric HGG. This may also provide insights into the selective pressure that may exist in these tumours for driving the genetic loss of *ADAM3A.*

Limitations

There are several limitations to this study. Although the 3D microarray Oligo chip used in this study is highly sensitive and can monitor the expression of 1719 miRNAs, nearly half of these miRNAs did not show any expression in any of the samples. A similar issue was reported by Koo and colleagues who used the 3D microarray chip with 2019 mounted probes and observed missing valued data for a significant proportion of these miRNAs (Koo et al., 2015). However, the number of miRNAs with missing values was not mentioned. It is not clear if this observed loss of data is a technical fault. A limitation of the integrative analysis in this study was that the miRNA and mRNA expression profiling of paediatric HGG short-term cultures was not conducted at the same time. Also, not all samples that were profiled for miRNA expression were analysed for mRNA expression. Simultaneous investigation of miRNA and mRNA expression analysis of the same samples is ideal for identification of accurate miRNA-mRNA interaction pairs. However, such ideal scenario is difficult to achieve in microarray experiments

using paediatric HGG samples due to the difficulty in procuring these rare samples. Considering this, only those miRNA-mRNA pairs with strong correlation (R=0.70) were chosen as highly statistically significant in order to avoid reporting false positives.

5.3 Conclusions

To conclude, although the data provided here remain descriptive, evidence suggests crucial roles for the identified miRNA targets in cellular processes associated with tumourigenesis emphasising the importance of future functional studies to examine the roles of these tarets in paediatric HGG. These may lead to the translation of miRNAs into useful biomarkers and therapeutic targets for paediatric HGG.

CHAPTER 6

Genome-wide methylation profiling in DIPG short-term cultures using illumina infinium HumanMethylation 450K methylation array

6.1 Introduction

Genetic studies in paediatric HGG including DIPGs have primarily focussed on copy number events and mutations in genes that contribute to the molecular pathogenesis of these tumours (Barrow et al., 2010; Paugh et al., 2010; Jones et al., 2012; Diaz and Baker, 2014). However, compared to adult HGG, such genetic changes are found at low frequencies in childhood HGG. In addition, a proportion of these tumours do not show any major chromosomal aberrations (Bax et al., 2010; Buczkowicz et al., 2014). Nevertheless, these studies have unveiled valuable information on similarities and disparities in genetic alterations between distinct subgroups within paediatric HGG, especially between DIPGs and supratentorial HGG (Wu et al., 2012; Jones and Baker, 2014; Wu et al., 2014). It is apparent that the development of paediatric HGG is not only determined by changes at the DNA level, but also by variations in the levels of expression of a range of genes regulated by epigenetic mechanisms. The discovery of histone mutations, as well as the identification of miRNA dysregulation in paediatric HGG provides further evidence of the influence of epigenetic abnormalities on gliomagenesis in the paediatric population (Jha et al., 2014; Schwartzentruber et al., 2012; Wu et al., 2012).

Aberrant DNA methylation in promoter CpG islands and associated gene silencing has been the most widely explored epigenetic alteration in cancers (Jones, 2002). Promoter hypermethylation-induced gene silencing of multiple tumour suppressor genes has been identified in almost all cancers (Jones and Laird, 1999; Jones and Baylin, 2007; Esteller, 2008; Morris et al., 2008; Baylin and Herman, 2000; Pellacani et al., 2014; Du et al., 2016; He et al., 2016). In adult astrocytoma, DNA

hypermethylation has been reported in genes such as *MGMT, HIC-1, ABL, PTEN, THBS1, TIMP3, CDKN2A,* and *CDKN2B*, among numerous others (Esteller et al., 2000; Reifenberger et al., 2012; Lee et al, 2015). Promoter methylation of *MGMT* represents an important diagnostic and prognostic biomarker to predicting clinical response to alkylating agent therapy in adult GBM patients (Esteller et al., 2000; Stupp et al., 2005; Weller et al., 2010). In contrast to methylation studies in adult GBM, there are very few comprehensive DNA methylation studies conducted in paediatric HGG so far. Jha et al. (2014) conducted methylation profiling of 21 paediatric GBM tumours using the Infinium HumanMethylation 27 BeadChip and reported hypermethylation of some of the known cancer-related genes such as *RASSF1, TTC12* and *CCDC8* in these tumours. They also identified distinct differences in methylation profiles between adult and paediatric GBM. There are only 2 reported studies that carried out genome-wide methylation profiling in DIPG (Buczkowicz et al., 2014; Saratsis et al., 2014). In the study by Buczkowicz et al., 2014, 3 distinct subgroups within these tumours were identified, which included a subgroup with a hypermethylated profile.

Investigation of DIPG-specific DNA hypermethylation events may aid the identification of candidate genes that can provide better insights into the pathogenesis of these tumours and may also lead to the identification of biomarkers of therapeutic/prognostic/diagnostic significance. The aim of this study was to identify candidate genes that were downregulated in DIPG short-term cell cultures due to promoter hypermethylation, using Illumina Infinium Human Methylation 450K BeadChip array. The downregulation of the identified genes was validated in

DIPG and non-DIPG short-term cell cultures and the frequencies of downregulation of these genes in both the tumour subgroups were compared. In addition, tumour suppressive roles of candidate genes were evaluated in cell culture models.

6.2 Results

6.2.1 Genome-wide methylation profiling in paediatric DIPG short-term cell cultures using Illumina Infinium HumanMethylation 450 K microarray

To identify candidate genes dysregulated in DIPG short-term cell cultures due to promoter CpG hypermethylation, global methylation profiles were generated for 3 DIPG short-term cultures (IN2087, IN2102 and IN2675) and a normal human astrocytes control sample (NHA) using Illumina Infinium HumanMethylation 450K BeadChip microarray as described in 2.8.2. The normalised data from these samples provided by Cambridge Genome Services, UK, were analysed using a comprehensive screening strategy. The Methylation 450 K data for 14 non-DIPG short-term cell cultures used in this analysis were generated from the same BeadChip by a colleague as part of ongoing research in the laboratory.

The Infinium microarray interrogates 485,577 probes covering about 99% of Refseq genes with several sites in the transcription start site (TSS200 and TSS1500), 5'UTR, first exon, gene body and 3'UTR. To ensure only promoter-associated genes were included in the analysis, the probes spanning 5' regions (5'UTR) of the genes and up to 1500 base pairs upstream of their transcription start sites (TSS200 and TSS1500) (n=132665) were used for this analysis. This excluded probes with CpGs on the X chromosome to avoid gender-related bias. As the focus of this study was to identify

methylation of protein-coding genes, the probes representing miRNA genes located in 5'UTR, TSS200 and TSS1500 (n=1100) were also excluded from this analysis. Bioinformatic analysis of these miRNA-associated probes in DIPG short-term cell cultures were carried out separately, the results of which are presented in 6.2.5.

The promoter-associated probes were filtered based on their beta values to identify those probes that were frequently hypermethylated in DIPG short-term cell cultures in comparison to NHA. A beta value is a quantitative measure of methylation that ranges from 0- 'no methylation' to 1- 'complete methylation'. This value corresponds to the ratio of the methylated probe intensity over the sum of methylated and unmethylated probe intensities. Previous methylation 450 K data analyses of cancer samples using beta value method have used beta values above 0.75 (methylated) in tumour and below 0.25 (unmethylated) in its respective normal sample to consider probes as differentially methylated (Milani et al., 2010; Lokk et al., 2012; Lu et al., 2014). In this study, 2 levels of stringency were applied to identify methylated probes in DIPG short-term cell cultures – one with probe beta values of $\geq$0.75 in tumour and $\leq$0.25 in normal control, the other with probe beta values of $\geq$0.85 in tumour and $\leq$0.15 in normal control (more stringent). Based on these, 2 approaches were followed in this study to identify differentially methylated genes in DIPG short-term cell cultures compared to NHA. The genes identified in each approach were subjected to further filters to identify biologically significant candidates. A schematic of the screening strategy for identification of candidate genes is given in Figure 6.1.

As a first approach, a relaxed filter was applied to identify frequently methylated genes in DIPG in comparison to NHA. A methylated probe in this approach was defined by beta value ≥0.75 in 2 of 3 DIPG short-term cell cultures and beta value ≤ 0.25 in NHA, which identified 1054 probes representing 998 genes. To prioritise genes to those in which promoter hypermethylation likely induces transcription inactivation, an additional filter was applied. The gene expression profiles of the same samples were previously generated in the lab using Affymetrix U133A array (unpublished data). The normalised and filtered data consisting of 22,215 informative probes from these samples were available as .txt files with present (expressed), absent (not expressed) or marginal (marginally expressed) calls for each probe on the array. To identify frequently downregulated genes in DIPG short-term cell cultures in comparison to NHA, probes with absent calls in 2 of 3 DIPG short-term cell cultures, and present calls in NHA were identified, which resulted in 928 probes representing 805 genes. These genes were then compared with the differentially methylated genes, which identified 43 common genes that were both frequently methylated and downregulated in DIPG short-term cell cultures. Of these, 8 genes did not have CpG Island in its promoter region as predicted by the human genome browser (www.genome.ucsc.edu) and were excluded, resulting in 35 genes.

A broad literature review was carried out on the shortlisted genes to prioritise candidate genes for further validation. Genes with known associations with cancers or with functional significance in cellular processes deregulated in cancers such as cell cycle, apoptosis, proliferation, invasion, migration, or angiogenesis were prioritised.

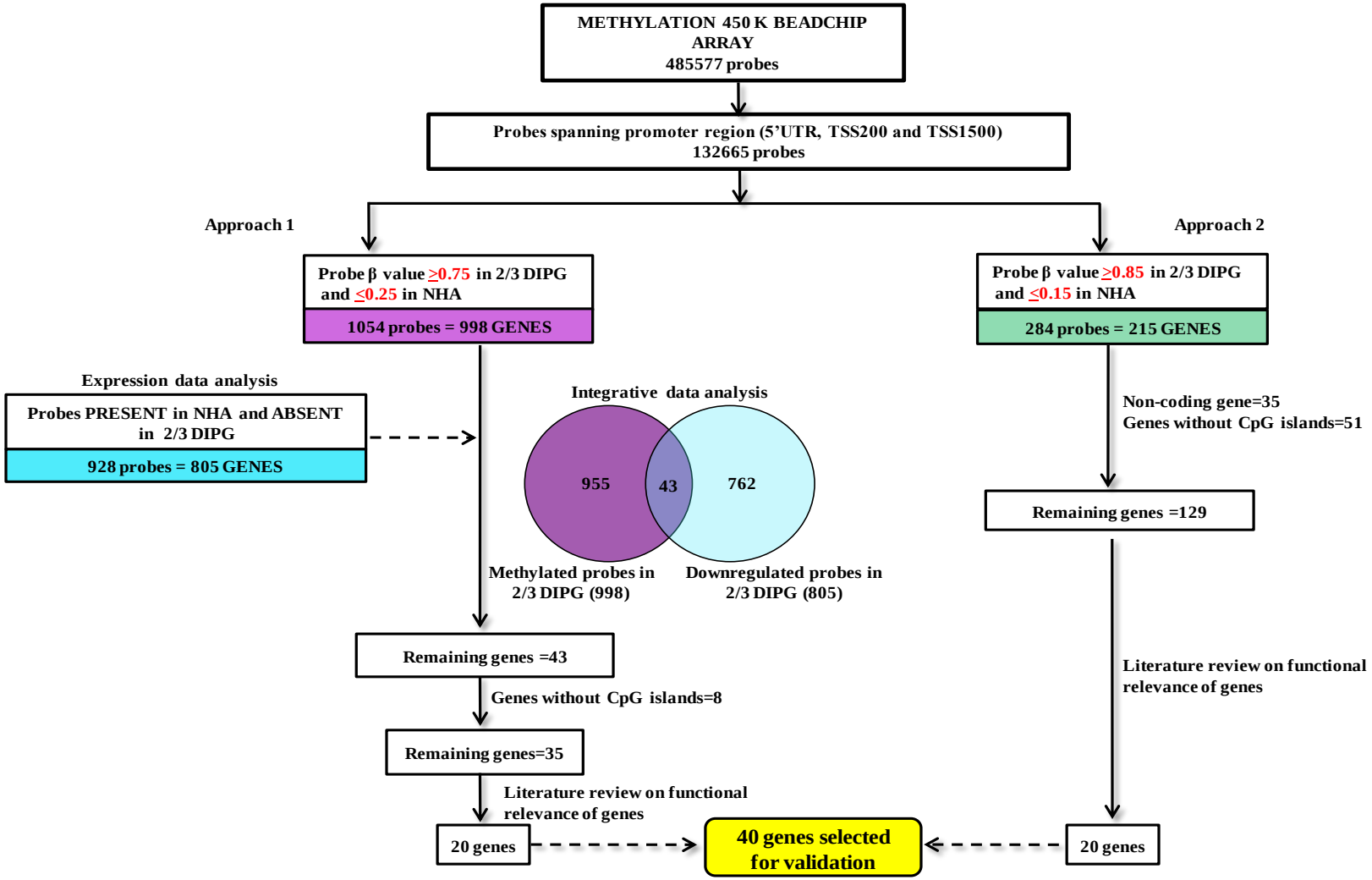

Figure 6.1 Schematic of the screening strategy used in the identification of candidate genes differentially methylated in DIPG. Methylation 450 K data from 3 DIPG short-term cell cultures and NHA were analysed using 2 approaches. Forty genes were shortlisted for validation in the laboratory.

As the gene expression data used in this study were run on an older platform of Affymetrix microarray (U133A), there were several probes on the array with missing annotations. For instance, of the 928 probes with absent calls in 2 of 3 DIPG short-term cell cultures, 87 probes did not have annotations. Also, taking into account that the gene expression and methylation microarray analysis were done at 2 different time points, a second approach was followed to identify candidate genes based on methylation data only. For this approach, a high stringent filter (β-value>=0.85 in 2/3 DIPG β-value<=0.15 in NHA) was applied to identify differentially methylated probes in 2/3 DIPG short-term cell cultures. Of 215 methylated genes identified by this approach, non-coding genes (n=35) and genes without CpG islands in their promoter regions (n=51) as predicted by the human genome browser (www.genome.ucsc.edu) were eliminated, resulting in 129 unique genes. Literature review was carried out on these genes, as described in the first approach and 20 genes were shortlisted.

A total of 40 genes identified by both approaches were validated in the laboratory. The gene descriptions and functions of 40 genes are given in Table 6.1.

Table 6.1 Genes hypermethylated in DIPG short-term cultures compared to NHA

Gene symbol	NCBI Accession	Gene description	Function
A2BP1	**NM_145891.2**	RNA binding protein, fox-1 homolog (C. elegans)	Regulates alternative splicing required for neuronal functions (Fogel et al., 2012)
ADAMTS18	**NM_199355.2**	ADAM metallopeptidase with thrombospondin type 1 motif 18	Degradation of matrix proteoglycans (Porter et al., 2005)
APBB2	**NM_004307.1**	Amyloid beta (A4) precursor protein-binding, family B, member 2	Modulation of amyloid precursor protein (APP) processing (Penna et al., 2013)
BMP3	**NM_001201.2**	Bone morphogenetic protein 3	Regulation of bone formation (Amedee et al., 1994)
CABLES1	**NM_138375.2**	Cdk5 and Abl enzyme substrate 1	Inhibitor of CDKs (Shi et al., 2015)
CASZ1	**NM_001079843.2**	Castor zinc finger 1	Regulates transcription by NuRD complex recruitement (Liu et al., 2015)
CAV1	**NM_001753.4**	Caveolin 1, caveolae protein, 22kD	Required for caveolae formation (Fernández-Rojo et al., 2012)
COL14A1	**NM_021110.2**	Collagen, type XIV, alpha 1	Regulation of fibrillogenesis (Young et al., 2002)
CXCL14	**NM_004887.4**	chemokine (C-X-C motif) ligand 14	Inhibitor of CXCL12-CXCR4 pathway (Tanegashima et al., 2013)
DAB1	**NM_021080.3**	Dab, reelin signal transducer, homolog 1 (Drosophila)	Cortical neuronal migration (Chai et al., 2009)
DAB2IP	**NM_032552.3**	DAB2 interacting protein	Regulates neuronal migration and maturation (Lee et al., 2012)
DLK1	**NM_003836.6**	delta-like 1 homolog (Drosophila)	Inhibitor of Notch signalling (Falix et al., 2012)
EYA4	**NM_004100.4**	EYA Transcriptional Coactivator And Phosphatase 4	Regulator of innate immune response (Okabe et al., 2009)
FGFR2	**NM_000141.4**	Fibroblast growth factor receptor 2	Bone and skeletal development (Wilkie et al., 2002)
FHIT	**NM_002012.2**	Fragile histidine triad	Prevents double strand DNA breaks (Waters et al., 2015)
GRM8	**NM_000845.2**	Glutamate receptor, metabotropic 8	Potential driver cancer gene in endometrial cancer (Liang et al., 2012)
KRT8	**NM_001256282.1**	Keratin 8	Regulates TNF and fas-mediated cell death (Oshima et al., 2002)
MGMT	**NM_002412.4**	O-6-methylguanine-DNA methyltransferase	DNA damage repair (Pegg et al., 1990)
MICAL2	**NM_014632.3**	Microtubule associated monoxygenase, calponin and LIM domain containing 2	Regulation of actin stress fibers (Giridharan et al., 2012)
MYH10	**NM_001256012.1**	Myosin, heavy chain 10, non-muscle	Regulates primary cilia biogenesis (Rao et al., 2014)
PARP4	**NM_006437.3**	Poly(ADP-ribose) polymerase family member 4	Role in telomerase activity (Liu et al., 2004)

Table 6.1 contd.

PDE4B	**NM_002600.3**	Phosphodiesterase 4B, cAMP-specific	Regulation of cyclic nucleotides (Millar et al., 2005)
PDE4D	**NM_001104631.1**	Phosphodiesterase 4D, cAMP-specific	Regulates cAMP signalling (Mika et al., 2015)
PDPN	**NM_006474.4**	Podoplanin	Metastasis (martin Villar et al., 2006), Actin remodelling (Wicki et al., 2006)
PKNOX2	**NM_022062.2**	PBX/knotted 1 homeobox 2	Homeobox containing gene, transcription regulator (Imoto et al., 2001)
PLCH2	**NM_014638.3**	Phospholipase C, eta 2	Calcium mobilisation in cells (Suh et al., 2008)
PLXNB1	**NM_002673.5**	Plexin B1	Semaphorin 4D receptor, induces growth cone collapse (Oinuma et al., 2010)
PRKG2	**NM_006259.2**	protein kinase, cGMP-dependent, type II	Development of growth plate (Koltes et al., 2015)
PRR5L	**NM_001160167.1**	Proline rich 5 like	mTOR-associated protein, regulates apoptosis (Thedieck et al., 2007)
PTPRE	**NM_006504.5**	protein tyrosine phosphatase, receptor type, E	Regulation of insulin signalling (Moller et al., 1995)
RANBP17	**NM_022897.4**	RAN binding protein 17	Member of importin beta family (Kutay et al., 2000)
RFX3	**NM_002919.3**	regulatory factor X, 3 (influences HLA class II expression)	Regulation of ciliogenesis (Bonnafe et al., 2004)
RHBDF2	**NM_024599.5**	rhomboid 5 homolog 2 (Drosophila)	Regulation of EGF ligand secretion (Adrain and Freeman, 2012)
SBNO2	**NM_014963.2**	strawberry notch homolog 2 (Drosophila)	Regulation of inflammatory gene expression (Kasmi et al., 2007)
SEMA6A	**NM_001300780.1**	Sema domain, transmembrane domain (TM), and cytoplasmic domain	Regulator of VEGF signalling (Segarra et al., 2012)
SETBP1	**NM_015559.2**	SET binding protein 1	Binds SET oncoprotein (Minakuchi et al., 2001)
SH3BP4	**NM_014521.2**	SH3-domain binding protein 4	Negative regulator of Rag GTPases (Kim et al., 2013)
SIPA1L3	**NM_015073.2**	Signal-induced proliferation-associated 1 like 3	Component of tight junction (Matsuda et al., 2008)
TRIM2	**NM_015271.4**	Tripartite motif containing 2	Regulates neuronal polarization (Khazaei et al., 2011)

Methylation 450K data from 3 DIPG short-term cell cultures and NHA were analysed using 2 different approaches. Forty genes were identified; gene descriptions and functions of these genes are provided.

6.2.2 Comparison of differential expression of genes in DIPG and non-DIPG short-term cultures by RT-PCR analyses

To confirm downregulation of 40 candidate genes, their expression levels were determined in the 3 DIPG short-term cell cultures and NHA using RT-PCR analysis as described in 2.6.3. The expression levels of these genes were also determined in 14 non-DIPG short-term cultures and the frequencies of downregulation of 40 genes were compared between DIPG and non-DIPG short-term cultures with respect to their expression levels in NHA. The summary of downregulation status of 40 genes in DIPG and non-DIPG short-term cultures is shown in Table 4.1.

It was observed that 50% (20/40) of analysed genes demonstrated satisfactory correlation with the microarray results in DIPG short-term cell cultures i.e. these genes were expressed in NHA and downregulated and/or silenced in at least 1 DIPG short-term cell culture. These genes were stratified into 2 groups according to their expression patterns in DIPG short-term cell cultures and the frequencies of downregulation in DIPG were compared to those in the non-DIPG short-term cell cultures (Table 6.2 and Figure 6.2). The first group consisted of 12 genes (60%), which were frequently downregulated in DIPG short-term cultures (2/3 cases). Of these, 10 genes were also downregulated in at least 64% in the non-DIPG short-term cell cultures and comprised *ADAMTS18* (100%), *RFX3* (100%), *PRKG2* (93%), *PTPRE* (93%), *RHBDF2* (93%), *DAB1* (64%), *EYA4* (79%), *DLK1* (93%), *CXCL14* (86%) and *SBNO2* (79%). In contrast, 2 genes, *SH3BP4* and *FGFR2* were downregulated in only 29% and 7% respectively in the non-DIPG short-term cell

cultures. The RT-PCR gel images of 7 genes that were downregulated in all 3 DIPG short-term cell cultures in comparison to NHA are given in Figure 6.3.

The second group consisting of 8 genes (40%) were infrequently downregulated (1/3 cases) in the DIPG short-term cultures. Of these, 5/8 genes were also infrequently downregulated in the non-DIPG short-term cell cultures with the frequencies of downregulation of the genes not exceeding 29%. In contrast, 3 genes demonstrated higher frequencies of downregulation in the non-DIPG short-term cultures, which included *APBB2* (93%), *MYH10* (50%) and *RANBP17* (43%).

Table 6.2 Expression status of 40 candidate genes in DIPG and non-DIPG short-term cultures

	C	DIPG			NON-DIPG													% downregulation	
GENES	NHA	IN2675	IN2102	IN2087	IN178	IN179	IN1163	IN1419	IN1930	IN1523	IN1566	IN3180	IN3182	IN3183	IN3032	IN3046	IN3205	IN1262	DIPG (n=3)	non-DIPG (n=14)
Genes frequently downregulated in DIPG																				
ADAMTS18																			100	100
RFX3																			100	100
PRKG2																			100	93
PTPRE																			100	93
RHBDF2																			100	93
DAB1																			100	64
EYA4																			100	79
DLK1																			67	93
CXCL14																			67	86
SBNO2																			67	79
SH3BP4																			67	29
FGFR2																			67	7
Genes infrequently downregulated in DIPG																				
APBB2																			33	93
MYH10																			33	50
RANBP17																			33	43
COL14A1																			33	29
CASZ1																			33	29
GULP1																			33	21
PARP4																			33	21
PLXNB1																			33	7
Genes expressed in DIPG																				
PRR5L																			0	36
PKNOX2																			0	14
CAV1																			0	7
SIPA1L3																			0	7
DAB2IP																			0	0
TRIM2																			0	0
Genes lacking expression in NHA																				
A2BP1																			100	100
PDE4D																			100	100
SEMA6A																			100	93
KRT8																			100	86
FHIT																			100	79
SETBP1																			100	64
PLCH2																			67	71
PDE4B																			33	64
GRM8																			0	71
PDPN																			0	21
CABLES1																			0	14
BMP3																			0	14
MGMT																			0	14
MICAL2																			0	0

RT-PCR analysis was performed to determine the expression levels of 40 candidate genes in NHA, 3 DIPG and 14 non-DIPG short-term cell cultures. Frequencies of downregulation of these genes in DIPG and non-DIPG tumour subgroups are shown. Green indicates expression; pink indicates downregulation and red indicates silencing of genes.

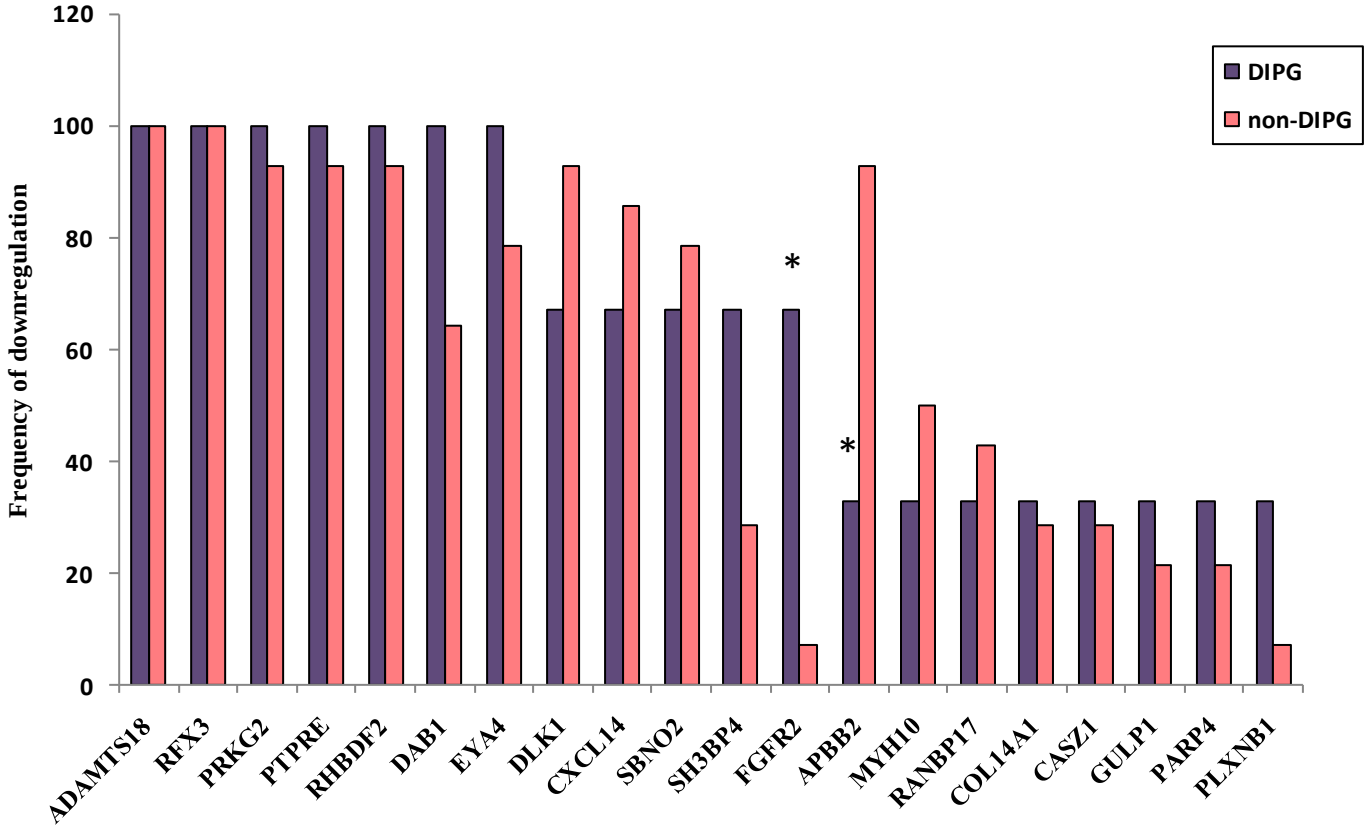

Figure 6.2 Frequency of downregulation of 20 genes in DIPG and non-DIPG short-term cultures. The frequencies of downregulation of 20 genes that were frequently or infrequently downregulated in DIPG short-term cell cultures (n=3) were compared with their frequencies of downregulation in non-DIPG short-term cell cultures (n=14). The differences in the frequencies of downregulation of *FGFR2* and *APBB2* between DIPG and non-DIPG short-term cell cultures are approaching statistical significance (p=0.063) (indicated by *).

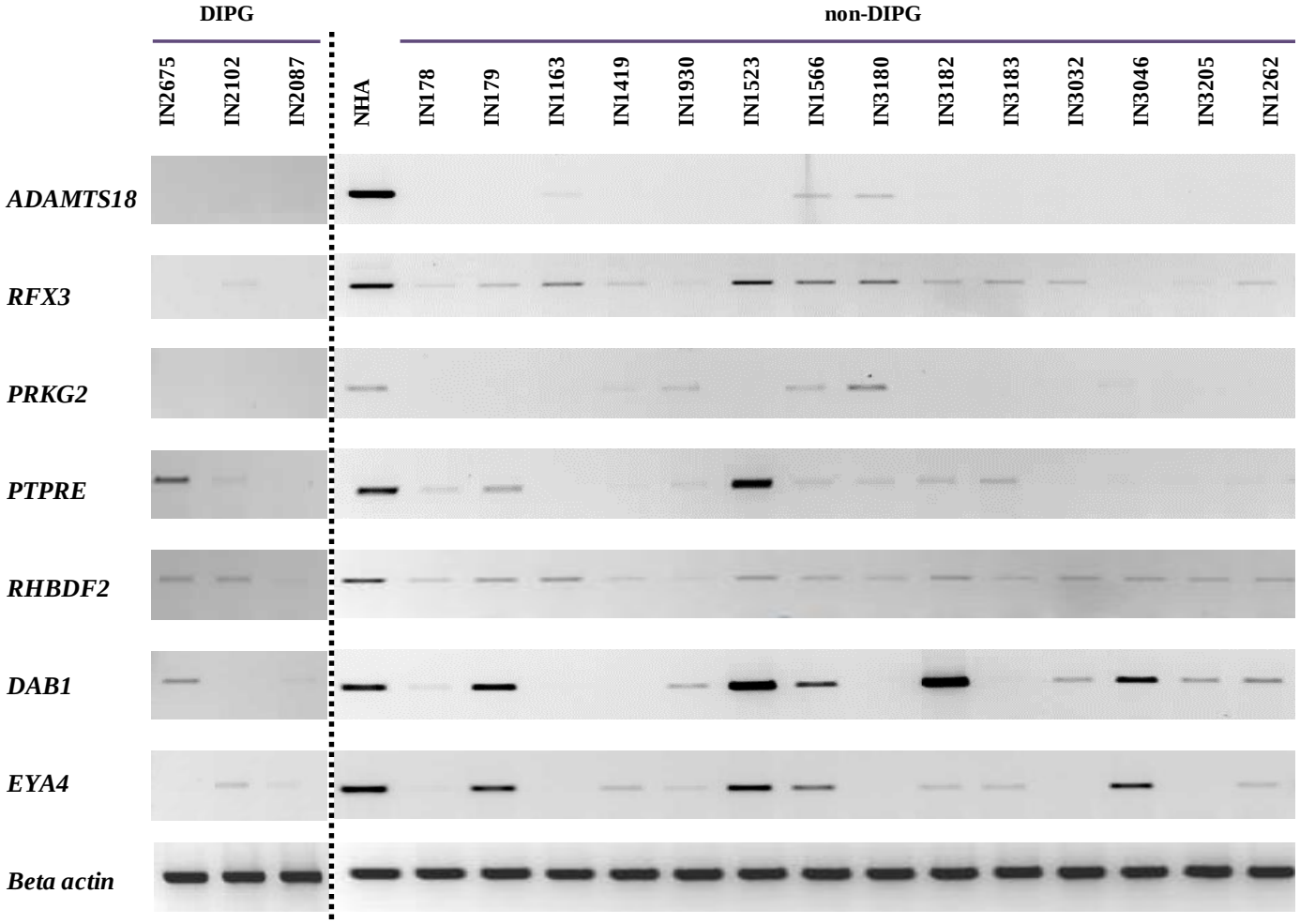

Figure 6.3 RT-PCR analyses of 7 genes frequently downregulated in DIPG short-term cultures. RT-PCR analyses demonstrate the expression statuses of the most commonly downregulated genes in DIPG short-term cultures which are also frequently downregulated in the non-DIPG short-term cultures in comparison to NHA. Beta actin was used as the endogenous control.

The remaining 20 genes (50%) did not demonstrate correlation with downregulation and/or methylation observed in the microarray analysis. Of these, 6 genes (*PRR5L, PKNOX2, CAV1, SIPA1L3, DAB2IP* and *TRIM2*) did not show downregulation in any of the DIPG short-term cell cultures. These genes were therefore not assessed further. The remaining 14 genes (*A2BP1, PDE4D, SEMA6A, KRT8, FHIT, SETBP1, PLCH2, PDE4B, GRM8, PDPN, CABLES1, BMP3, MGMT* and *MICAL2*) had no detectable mRNA expression in NHA. Seven (50%) of these were frequently downregulated (2/3 cases) in the DIPG short-term cultures, and in the non-DIPG short-term cell cultures. These included *A2BP1* (100% vs 93%), *PDE4D* (100% vs 93%), *SEMA6A* (100% vs 87%), *KRT8* (100% vs 87%), *FHIT* (100% vs 73%), *SETBP1* (100% vs 60%) and *PLCH2* (67% vs 73%). The remaining 7 genes were infrequently downregulated in the DIPG short-term cell cultures, of which 6 genes were not downregulated in any of the samples. Also, the majority of the genes (5/7 cases) which were not downregulated in the DIPG short-term cultures were also not downregulated in most of the non-DIPG short-term cultures. These included *PDPN* (0% vs 27%), *CABLES1* (0% vs 20%), *BMP3* (0% vs 13%), *MGMT* (0% vs 13%), and *MICAL2* (0% vs 0%). Two genes, *PDE4B* (33% vs 67%) and *GRM8* (0% vs 67%) had relatively higher frequencies of downregulation in the non-DIPG short-term cell cultures.

Overall, there were no major differences between the DIPG and the non-DIPG short-term cell cultures based on the downregulation of the identified genes in these tumours. On a global scale, these tumour subgroups did not show unique methylation profiles, which were evident from the PCA scatter plot, as shown in Figure 6.4. The

normalised Methylation 450 K data from NHA, 3 DIPG and 14 non-DIPG short-term cell cultures were used to perform PCA using Partek Genomics Suite (v6.6, Partek Inc., USA) as described in 2.12.4.

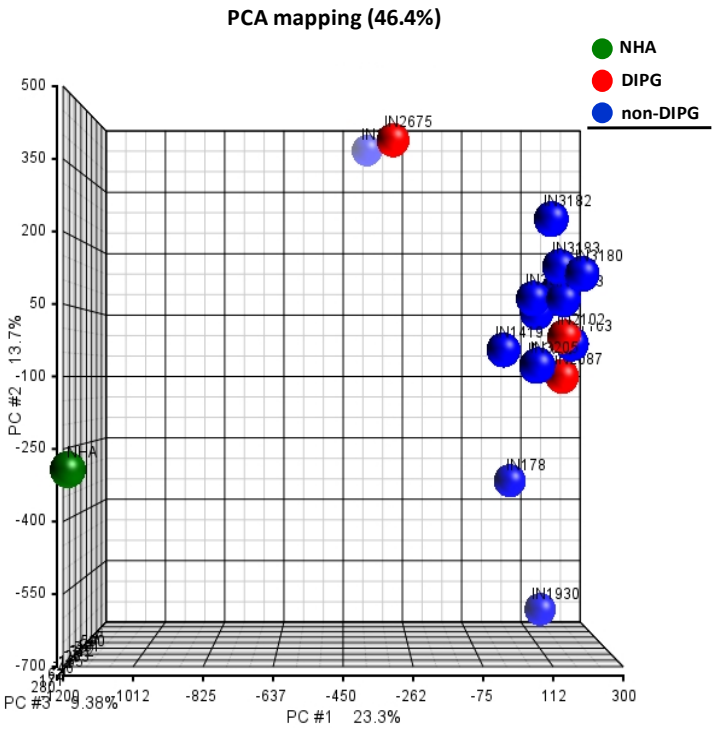

Figure 6.4 Principal component analyses of NHA, DIPG and non-DIPG short-term cultures. PCA plot of NHA, 3 DIPG and 14 non-DIPG short-term cell cultures generated using the first three PCs, PC 1 (23.3%), PC 2 (13.7%) and PC 3 (9.38%). Each point on the scatter plot represents a sample. NHA is represented by green, and DIPG and non-DIPG short-term cell cultures are represented by red and blue colours respectively.

PCA confirmed that the normal and the tumour samples had distinct methylation profiles and clustered separately. It was evident that the DIPG and the non-DIPG short-term cultures did not form separate clusters. Two of 3 DIPG short-term cell cultures clustered closely together, indicating similarities in their methylation profiles while the third sample (IN2675) was independent. Interestingly, IN2675 was

H3F3A (K27M)-mutant, while the other 2 were *H3F3A* wild type, as shown in 3.15. However, the non-DIPG *H3F3A* (K27M)-mutant short-term cell culture (IN1566) did not group with the mutant-DIPG short-term cell culture.

6.2.3 Validation of methylation status of downregulated genes in DIPG short-term cultures

To confirm the role of methylation in downregulation of the identified genes, 10 paediatric HGG short-term cell cultures (1 DIPG and 9 non-DIPG) were treated with the global demethylating agent, 5-AZA to reactivate the downregulated genes, as described in 2.3, and changes in gene expression were measured by RT-PCR analyses as described in 2.6.3. Seven genes (*ADAMTS18, RFX3, PRKG2, PTPRE, RHBDF2, DAB1* and *EYA4*) that were expressed in NHA and downregulated in all 3 DIPG short-term cell cultures were prioritised for this validation analysis. The re-expression of 7 genes in paediatric HGG short-term cell cultures following demethylation with 5-AZA as determined by RT-PCR analysis is shown in Figure 6.5. With the exception of *PRKG2,* all other genes were re-expressed in the DIPG short-term cell culture (IN2102) following 5-AZA treatment. The frequencies of re-expression of these genes in paediatric HGG short-term cell cultures following treatment with 5-AZA are given in Table 6.3. *RHBDF2* had the highest frequency of re-expression after treatment with 5-AZA (90%) followed by *DAB1* (78%), *PTPRE* (60%), *ADAMTS18* (50%), *EYA4* (50%), *PRKG2* (50%) and *RFX3* (36%) respectively.

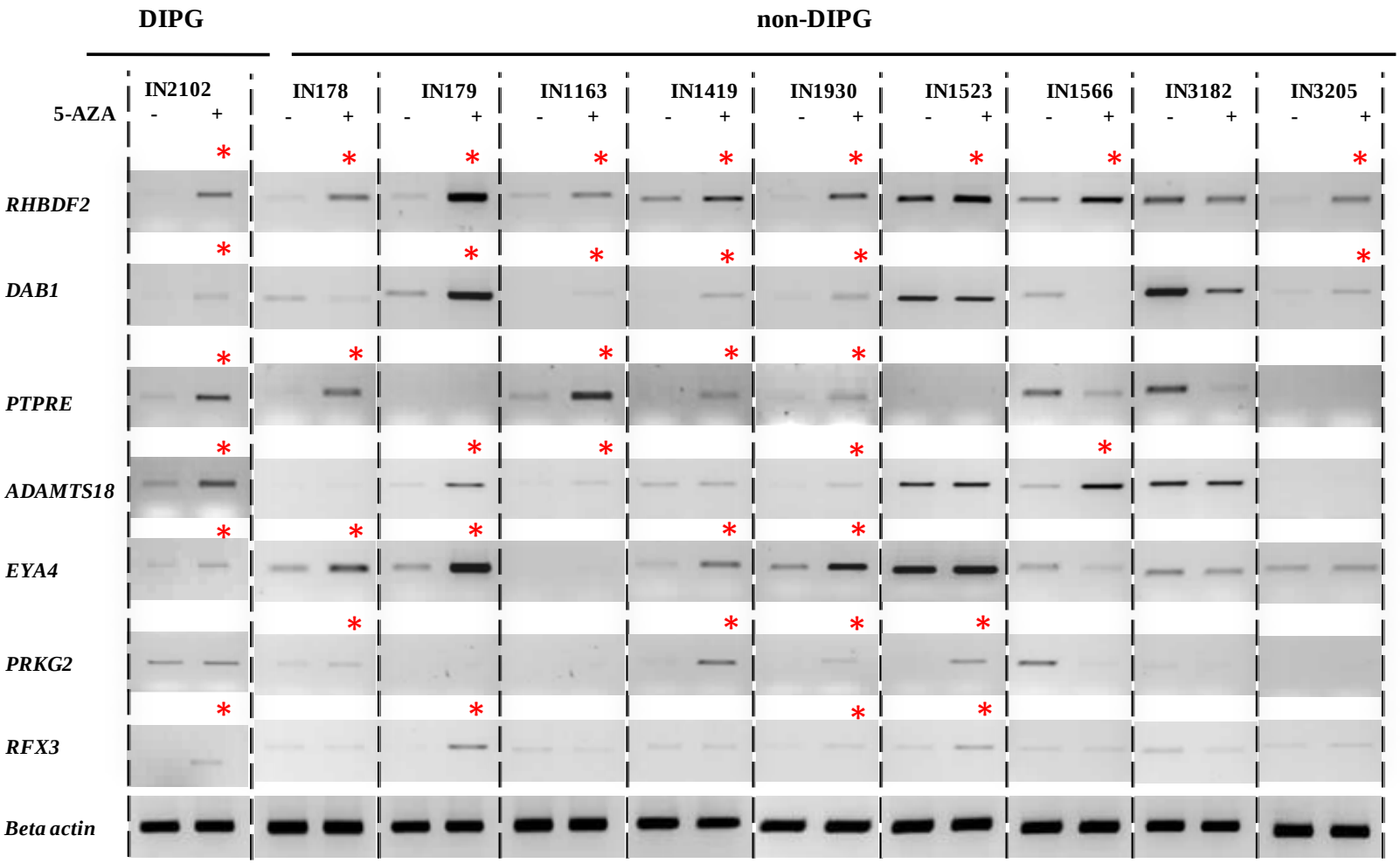

Figure 6.5 Re-expression of candidate genes in DIPG and non-DIPG short-term cultures following demethylation with 5-AZA. One DIPG and 9 non-DIPG short-term cell cultures were treated with 5-AZA and gene expression following treatment was determined using RT-PCR analyses. Re-expression of 7 genes (*RHDBF2, DAB1, PTPRE, ADAMTS18, EYA4, PRKG2* and *RFX3*) after treatment with 5-AZA are shown. Red stars indicate re-expression. Beta actin was used as endogenous control.

Table 6.3 Frequencies of re-expression of candidate genes in paediatric HGG short-term cell cultures following demethylation

Genes	No. of cases of gene re-expression after demethylation	Frequency of re-expression (%)
RHBDF2	**9**	**90 (n=10)**
DAB1	**7**	**78 (n=9)**
PTPRE	**6**	**60 (n=10)**
ADAMTS18	**5**	**50 (n=10)**
EYA4	**5**	**50 (n=10)**
PRKG2	**5**	**50 (n=10)**
RFX3	**4**	**36 (n=11)**

Ten paediatric HGG short-term cell cultures (1 DIPG and 9 non-DIPG) were treated with the demethylating agent, 5-AZA; untreated cells were used as control. RT-PCR analyses were performed to determine expression levels of 7 candidate genes in treated and untreated samples. Frequencies of re-expression of genes in 5-AZA treated paediatric HGG short-term cell cultures are shown. 'n' indicates cell cultures with low basal level expression of genes.

It was also noted that some of these genes were downregulated following treatment with 5-AZA. The most evident cases were downregulation of *DAB1* in IN3182, *PRKG2* in IN1566 and *ADAMTS18* in IN1566 and IN3182 respectively. This is a common event as 5-AZA is a global demethylating agent and demethylates the genome indiscriminately leading to dysregulation of several networks of genes.

To evaluate the functional role of candidate genes, genes were further prioritised based on their frequencies of re-expression in paediatric HGG short-term cell cultures following treatment with 5-AZA. Three genes (*RHBDF2, DAB1* and *PTPRE*), demonstrated re-expression in more than 50% paediatric HGG short-term cell cultures treated with 5-AZA. Of these, *DAB1* and *PTPRE* have been identified to have roles in the druggable PI3K pathway and the functional significance of these

was investigated further. *DAB1* encodes the intracellular adaptor protein of reelin signaling pathway. *PTPRE* has been identified as a physiological inhibitor of ERK.

6.2.4 Functional analyses of *DAB1* and *PTPRE* in paediatric HGG *in vitro*

The putative functional roles of 2 genes (*DAB1* and *PTPRE*) were further investigated. The tumour suppressor activities of these genes were assessed by colony formation and wound healing assays. A non-expressing cell culture (IN699) was used as an *in vitro* experimental model to study the effects of re-expressing these genes on *in vitro* growth and migratory characteristics. Wild-type *DAB1* or *PTPRE* expression plasmids (PCMV6/*DAB1* or PCMV6/*PTPRE*) were each transiently transfected into IN699. An empty vector (PCMV6) was transfected into the same cells and used as control as described in 2.10.7. The overexpression of *DAB1* and *PTPRE* in IN699 was verified by western blot analyses, 48 hours after transfection, as shown in (Figure 6.6).

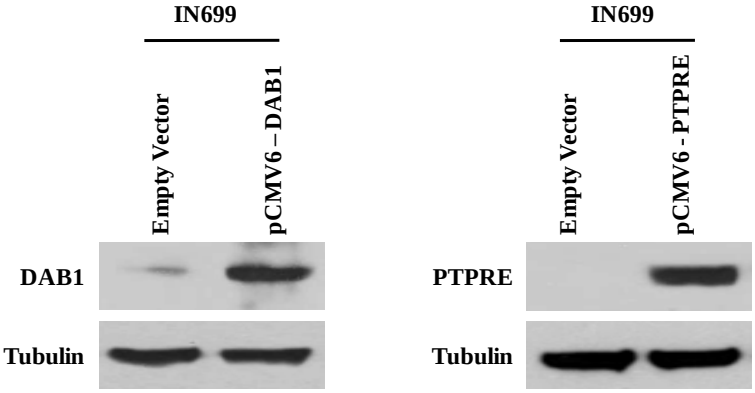

Figure 6.6 Overexpression of DAB1 and PTPRE in IN699 cells as determined by western blot analysis. Western blot analysis was performed with empty vector and *DAB1* expression plasmid after transfection. Tubulin was used as the loading control.

6.2.4.1 Ectopic overexpression of DAB1 and PTPRE reduces colony formation ability *in vitro*

To assess the effect of re-expressing *DAB1* or *PTPRE* on *in vitro* growth characteristics, wild-type *DAB1* or *PTPRE* expression plasmids (PCMV6/*DAB1* or PCMV6/*PTPRE*) were each transiently transfected into IN699. An empty vector (PCMV6) transfected into the same cells was used as control (as described in 2.10.7). Forty-eight hours after transfection, diluted cell suspensions (containing 25,000 cells) were plated in triplicates and were maintained in media containing geneticin (250µg/ml). After 25 days, colonies were stained with crystal violet and were counted. As shown in Figure 6.7, the number of IN699 colonies expressing *DAB1* was reduced by 55% (p=0.028) in comparison to the control cells transfected with the empty vector. Re-expression of *PTPRE* in IN699 cells also demonstrated a statistically significant reduction in colony formation ability to 35% of that observed in control cells (p=0.003). As evident from Figure 6.7, the colonies formed by *DAB1* or *PTPRE*- transfected cells were smaller in sizes compared to those formed by their respective control cells.

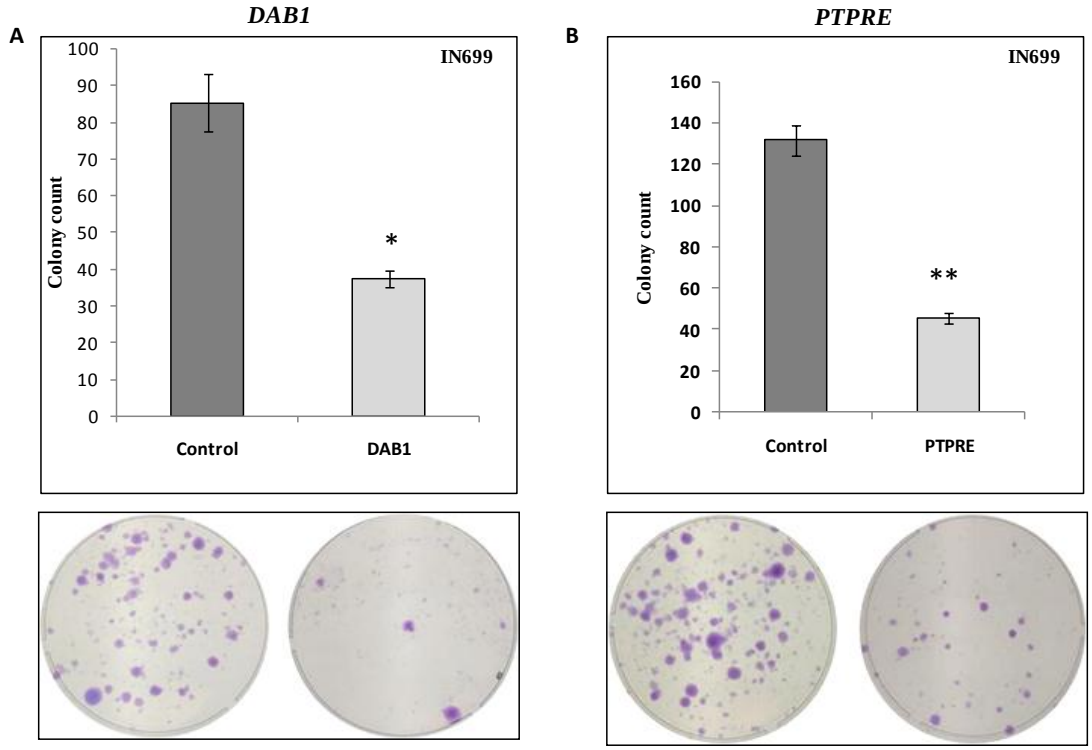

Figure 6.7 Ectopic overexpression of *DAB1* and *PTPRE* decreases colony formation capacity in IN699. **A.** Equal amounts of wild type PCMV6/*DAB1* or PCMV6/*PTPRE* plasmids or EV were transfected into IN699 cells. Twenty five days later, the colonies were stained and counted. **A.** IN699 cells transfected with *DAB1* showed statistically significant reduction (p=0.028) in the number of colonies compared to the control cells. **B**. IN699 cells transfected with *PTPRE* showed statistically significant reduction (35.36%, p=0.003) in the number of colonies compared to the control cells. Graphs represent the average number of colonies; error bars represent standard deviation. * indicates p<0.05, ** indicates p<0.005. Representative images of the plates showing reduced number of colonies following re-expression of genes are given below each graph.

6.2.4.2 Transient overexpression of *DAB1* reduces migratory potential of cells *in vitro*

The role of *DAB1* in migratory potential of cells was assessed using transwell assays. For this assay, IN699 cells were transiently transfected with wild type *DAB1* expression plasmids (PCMV6/*DAB1*) and the same cells transfected with empty vector were used as control as described in section 2.10.7. The transfected cells were

seeded in transwells and allowed to migrate across the polycarbonate membrane inserts. Forty-eight hours later, the migrated cells were stained and quantified in a colorimetric assay.

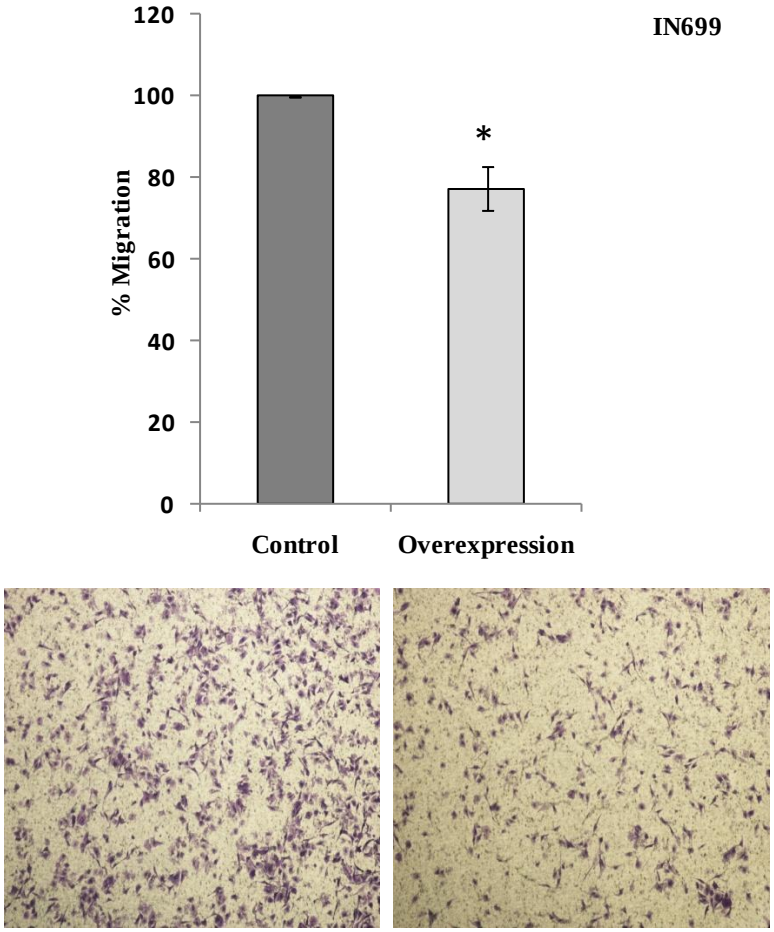

Figure 6.8 Transient overexpression of *DAB1* reduces migratory ability of cells *in vitro* A. IN699 cells were transfected with wild type *DAB1* expression plasmid or EV. The transfected cells were seeded in transwells and allowed to migrate. Twenty four hours later, the migrated cells were stained and quantitatively assessed by colorimetric method. Cells transfected with *DAB1* show statistically significant reduction in the migratory capacity than the control cells (p=0.006). The experiment was set up in triplicate; error bars represent standard error. Images of migratory cells in control versus *DAB1*-transfected cells captured at 4x magnification are shown below the graph.

DAB1-overexpressing cells exhibited statistically significant reduction (24%, p=0.006) in migration compared to the control cells. Images of stained cells in both control and *DAB1*-transfected cells were captured at 4x magnification (Figure 6.8).

6.2.4.3 Reduced expression of *DAB1* promotes migratory ability of paediatric HGG short-term cell culture

The role of *DAB1* in the migratory potential of cells was further assessed in a paediatric HGG short-term cell culture (IN1523) that expressed endogenous levels of *DAB1*. *DAB1* was knocked down in IN1523 culture using RNAi methodology and the migratory potential of these cells was assessed in a transwell assay as described in 2.10.8. The knock-down of DAB1 in IN1523 after transfection was confirmed by western blot analysis as shown in Figure 6.9. IN1523 cells transfected with non targeting siRNA oligos were used as control.

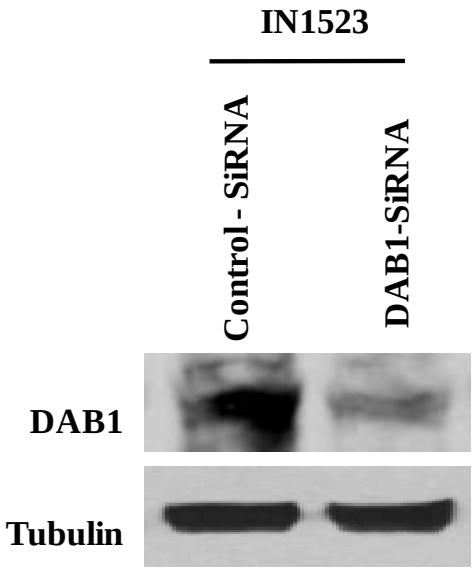

Figure 6.9 Western blot analysis confirms knockdown of *DAB1* in IN1523 paediatric HGG short-term cell culture. IN1523 transfected with *DAB1* siRNA or negative siRNA were used to perform western blot analysis.

In a cell migration assay, si*DAB1*IN1523 cells or siNT control IN1523 cells were seeded in transwells and incubated for 24 hours before staining of migrated cells. si*DAB1* cells were significantly more migratory compared to the siNT control cells

(p=0.0005), as shown in Figure 6.11. Following incubation and staining of migrated cells, *DAB1*-knocked down cells were more migratory compared to the control cells. Colorimetric quantification of migrated cells revealed statistically significant increase (p=0.0005) in the optical density, (indicative of more cells) compared to the control cells.

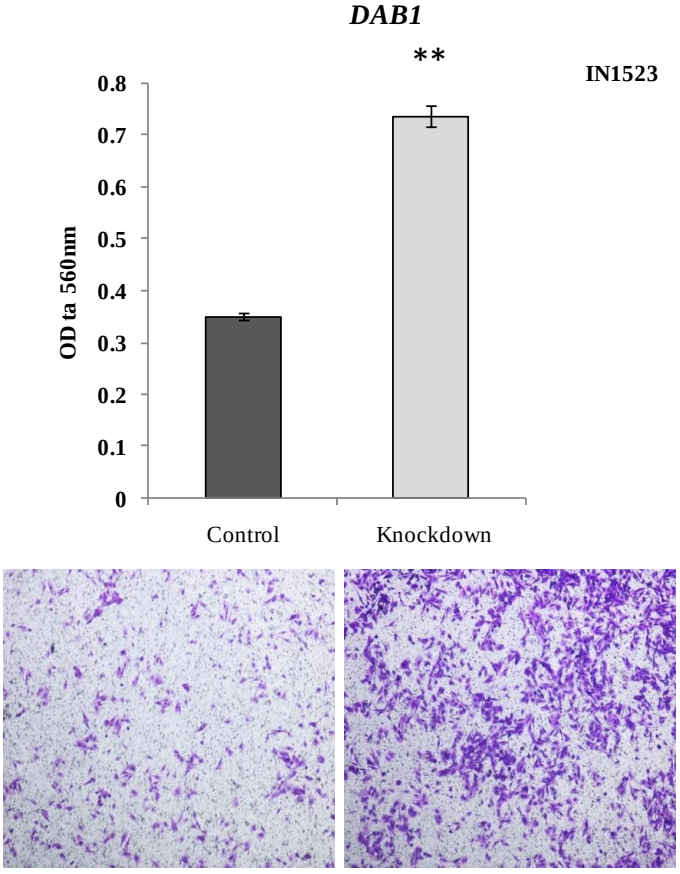

Figure 6.10 Reduced expression of *DAB1* increases migratory ability of paediatric HGG short-term culture. A. The migratory capacity of IN1523 cells were evaluated in transwell assays. Upon *DAB1* knockdown, IN1523 cells displayed increased migratory capacity in comparison to control cells transfected with non-targeting siRNA oligos The experiment was done in triplicate; error bars represent standard error. Images of increased number of migratory cells in *DAB1*-transfected cells compared to control are shown below the graph.

6.2.5 Analysis of methylation 450K data to identify hypermethylated promoters of genes associated with *H3F3A* (K27M)-mutant DIPG short-term cell cultures

H3F3A (K27M) mutation is an important genetic event that drives tumourigenesis in paediatric HGG, particularly DIPG (Schwartzentruber et al., 2012; Wu et al., 2012; Castell et al., 2015). Distinct miRNA expression changes were associated with this mutation in paediatric HGG short-term cell culture, as described in Chapter 5. To investigate promoter hypermethylation-induced changes associated with *H3F3A* (K27M) mutation in DIPG short-term cell cultures, genes with promoter CpG hypermethylation in *H3F3A* (K27M)-mutant compared to wild-type DIPG short-term cell cultures were identified.

To identify genes regulated by promoter hypermethylation, those probes located in the 5'UTR regions and up to 1500 bases upstream of the TSS (TSS200 and TSS1500) were utilised (n=132665), as described earlier in 6.2.1. Those probes with beta value $\geq$0.85 (highly methylated) in the *H3F3A* (K27M)-mutant DIPG short-term cell culture, IN2675 and $\leq$0.15 (unmethylated) in NHA and the wild-type cultures (IN2087 and IN2102) were identified, resulting in 37 probes representing 23 genes. A comprehensive literature review was carried out on these genes using PubMed, GeneCards (www.genecards.org) and OMIM (www.ncbi.nlm.nih.gov/omim) to investigate the role of these genes in cancers. Most of these genes were participants in regulating apoptosis, cell proliferation, invasion and migration in a variety of cancers. The promoter hypermethylated genes associated with *H3F3A* (K27M) mutation in the DIPG short-term cell cultures and their potential significance in

cancers are provided in Table. Notably, there were 2 homeobox genes (*HOXD3* and *SATB2*), associated with early development, genes regulating stem cell fate (*KCNB1*, *ENTPD2* and *PIWIL1*) and a single gene encoding the histone variant H2A.2 (*HIST2H2AA4*).

Table 6.4 Promoter hypermethylated genes in *H3F3A* (K27M) DIPG short-term cell culture

Probe ID	Probe location	Gene name	Gene description	Gene function/association with cancer	Chr
cg26808747 cg05237641 cg14621053 cg13488201	TSS1500 TSS200 TSS200 TSS200	*ADAM12*	ADAM Metallopeptidase Domain 12	Cell adhesion and fusion, ECM remodelling, cell signaling (Nyren-Erickson et al., 2013)	10
cg12191938	5'UTR	*AGAP11*	nkyrin Repeat And GTPase Domain Arf GTPase Activating Protein 11	Arf GTPase activator activity, potential role in cell migration and invasion (Campa et al., 2008)	10
cg07925085	TSS1500	*CCDC114*	Coiled-Coil Domain Containing 114	Required for ciliary movement (Knowles et al., 2013)	19
cg12944530	5'UTR	*CFLAR*	CASP8 And FADD-Like Apoptosis Regulator	Regulates apoptosis (Irmler et al., 1997), and Wnt signaling (Katayama et al., 2010)	2
cg13247581	TSS200	*ENTPD2*	Ectonucleoside Triphosphate Diphosphohydrolase 2	Regulates proliferation of neural progenitor cells (Gampe et al., 2015)	9
cg05298677 cg13133961	TSS200 TSS200	*ETV7*	Ets Variant 7	Transcription factor associated with regulation of cell proliferation (Bisio et al., 2014)	6
cg21461470	TSS1500	*HIST2H2AA4*	Histone Cluster 2, H2aa4	Downregulated in epithelial ovarian cancer (Morone et al., 2012)	1
cg14666564	5'UTR	*HOXD3*	Homeobox D3	Cell proliferation and differentiation (Yunhong et al., 2012)	2
cg00976453 cg10951120	TSS1500 TSS200	*KCNB1*	Potassium Channel, Voltage Gated Shab Related Subfamily B, Member 1	Associated with proneural subtype of GBM (Brennon et al., 2009)	20
cg02033258 cg09877947 cg11843238	TSS200 TSS200 TSS200	*PDLIM4*	PDZ And LIM Domain 4	Inhibits growth in prostate cancer (Krishna Vanaja et al., 2011), tumour suppressor in RCC (Morris et al., 2010;)	5
cg17575602	TSS1500	*PGCP*	Carboxypeptidase Q	Biomarker for Hepatitis C-virus associated HCC (Smith et al., 2003)	8

cg13900773	5'UTR	*PIWIL1*	Piwi-Like RNA-Mediated Gene Silencing 1	Required for stem cell self-renewal and division (Cox et al., 1998), regulates EMT (Chen et al, 2015), negatively regulates cell invasion in ovarian cancer (Ly Lim et al., 2014)	12
cg19942237	TSS1500	*PRR15*	Proline Rich 15	Role in early development (Purcell et al., 2009)	7
cg07075840	TSS200				
cg01206378 cg20701556 cg26537280	TSS1500 TSS1500 TSS1500	*RWDD3*	RWD Domain Containing 3	Regulates tumour suppressive function of VHL (Gerez et al., 2015)	1
cg07855083	5'UTR	*SATB2*	SATB Homeobox 2	Inhibits cell proliferation and migration in gastric cancer (Wu et al., 2015), Inactivates MEK5/ERK5 signaling in colorectal cancer (Mansour et al, 2015)	2
cg01934626	TSS200	*SCGB3A1*	Secretoglobin, Family 3A, Member 1	Tumour suppressive role in breast (Krop et al., 2001), ovarian (Wu et al., 2007), and esophageal squamous cancer (Guo et al., 2008)	5
cg24486037 cg26065909	TSS200 TSS200	*SELENBP1*	Selenium Binding Protein 1	Tumour suppressor in prostate cancer (Ansong et al., 2016)	1
cg05302542 cg25326998	TSS1500 TSS1500	*SLC25A19*	Solute Carrier Family 25 (Mitochondrial Thiamine Pyrophosphate Carrier), Member 19	Role in thiamine homeostasis (Kim et al., 2015)	17
cg07769015	TSS200	*SLC45A4*	Solute Carrier Family 45, Member 4	Sucrose transport (Bartölke et al., 2014)	8
cg04096619	TSS1500	*SNORD123*	Small Nucleolar RNA, C/D Box 123	CpG hypermathylation in colorectal cancer (Ferreira et al., 2012)	5
cg01332054	5'UTR	*STRA6*	Stimulated By Retinoic Acid 6	Role in p53-induced apoptosis in response to DNA damage (Carrera et al., 2013)	15
cg08162803 cg11731626	TSS200 TSS200	*TCIRG1*	T-Cell, Immune Regulator 1, ATPase, H+ Transporting, Lysosomal V0 Subunit A3	Mutations in *TCIRG1* is associated with osteopetrosis in children (Simanovsky et al., 2016)	11
cg06377106	5'UTR	*VWA5B1*	Von Willebrand Factor A Domain Containing 5B1	Homeostasis	1

Methylation 450 K data from *H3F3A* (K27M) –mutant and wild type DIPG short-term cell cultures were analysed based on the probe beta values (β value $\geq$0.85 in *H3F3A* (K27M) mutant and β value $\leq$ 0.15 in NHA and *H3F3A* wild type).

6.2.6 Analysis of methylation 450K data to identify miRNAs deregulated by promoter CpG hypermethylation in DIPG short-term cell cultures

Deregulation of miRNAs in paediatric HGG including DIPG, at genetic and transcriptomic levels have been described in Chapters 4 and 5, respectively. Recently, there has been great interest in the identification of promoter hypermethylation-induced downregulation of miRNAs in various types of cancers (Chen et al., 2012; Lopez-Serra and Esteller, 2012; Menigatti et al., 2013; Yongsheng et al., 2015).

To identify miRNAs regulated by promoter hypermethylation in DIPG short-term cultures, the Methylation 450K data from the 3 DIPG short-term cell cultures (IN087, IN2102 and IN2675) and NHA were utilised. As described in 6.2.1, there were 1100 probes representing miRNA genes that were in the 5'UTR region and up to 1500 bases upstream of the TSS (TSS200 and TSS1500). To identify frequently methylated miRNAs in DIPG short-term cell cultures, those probes with beta value $\geq$0.75 (methylated) in 2 of 3 DIPG short-term cell cultures, and beta value $\leq$0.25 (unmethylation) in NHA were identified. This resulted in 21 probes corresponding to 15 miRNAs. A comprehensive literature review was conducted to determine the potential significance of these miRNAs in tumourigenic events. These miRNAs and their potential associations with cancers are listed in Table 6.5. Most of these miRNAs either had associations with cellular processes linked to cancer or were reported as deregulated in cancers and not yet functionally evaluated.

Table 6.5 MiRNAs regulated by promoter hypermethylation in DIPG short-term cell cultures

Methylated Probe ID	Location	miRNA	Association with cancers	Chr
cg22144942	TSS200	MIR1179	Promotes cell invasion in esophageal squamous cell carcinoma (Jiang et al., 2015)	15
cg17033471	TSS200	MIR1257	Downregulated in liposarcoma (Hisaoka et al., 2012)	20
cg03599197	TSS1500	MIR187	Regulates ovarian cancer progression by targeting *DAB2* (Chao et al., 2012)	18
cg10420310 cg07665535 cg06273075 cg04018325 cg09918657	TSS1500 TSS200 TSS200 TSS200 TSS1500	MIR193B	Promotes cell proliferation by targeting Smad3 in adult glioma, (Zhong et al., 2014)	16
cg11869773	TSS1500	MIR299	Regulates proliferation, apoptosis, migration and invasion in prostate cancer cells (Formosa et al., 2014)	14
cg14148088	TSS200	MIR494	Inhibits growth in epithelial ovarian cancer by targeting c-Myc (Yuang et al., 2016), associated with poor prognosis in pancreatic cancer (Ma et al., 2015), Inhibits cell proliferation by repressing *HOXA10* in oral cancer (Libório-Kimura et al., 2015)	14
cg24091975	TSS200	MIR515-1	Regulates proliferation in breast cancer cells by targeting *SK1* (Pinho et al., 2013)	19
cg24787924	TSS1500	MIR518E	Induces cell cycle arrest in HCC by targeting *CCND3* (Wang et al., 2012)	19
cg22166633	TSS1500	MIR520E	Suppresses growth of hepatoma cells by targeting NIK/p-ERK1/2/NF-κB signaling pathway (Zhang et al., 2012)	19
cg16204151	TSS1500	MIR523	Regulates metastasis in malignant melanoma (Mueller et al., 2009)	19
cg01716465	TSS1500	MIR548H3	Methylated in HCC (Shen et al., 2015)	9
cg16530970	TSS200	MIR549	Deregulated in colorectal cancer (Cummins et al., 2006)	15
cg06606539	TSS1500	MIR572	Regulates cell proliferation in ovarian cancer cells (Zhang et al., 2015; Wu et al., 2016)	4
cg04726985 cg25837979	TSS1500 TSS1500	MIR708	Suppresses tumour invasion and migration in HCC (Li et al., 2015), regulates the NF-κB pathway by targeting IKKβ in leukemia (Baer et al., 2015)	11
cg18604419 cg09337069	TSS1500 TSS1500	MIR889	Regulates cell proliferation in squamous cell carcinoma by targeting *DAB2IP* (Xu et al., 2015)	14

Methylation 450K data from DIPG short-term cell cultures (n=3) and NHA were analysed based on β-values of probes (β-value >=0.75 in 2/3 DIPG, and <=0.25 in NHA). Twenty one probes representing 15 miRNAs, and their potential significance in cancers is shown. Chr-chromosome.

6.3 Discussion

DIPG represent extremely severe brainstem lesions of childhood and are currently the leading cause of death from brain tumours in children (Buczkowicz and Hawkins, 2015). Previous genetic studies have identified molecular targets for DIPG, but as yet, none of these have been successfully translated into effective therapies (Bailey et al., 2013). The identification of recurrent histone mutations in H3.3 and H3.1 histone variants in DIPG, and the recent large-scale genomic profiling in these tumours indicate that they may have distinct genetic and epigenetic characteristics and may require tailored therapeutic strategies (Buczkowicz et al., 2014; Schwartzentruber et al., 2012; Wu et al., 2012). This Chapter has focussed on the identification of candidate genes dysregulated due to promoter hypermethylation in 3 DIPG short-term cell cultures compared to NHA using Illumina Infinium HumanMethylation 450 K BeadChip array.

Promoter hypermethylation in DIPG short-term cell cultures

The key role of promoter methylation in the inactivation of tumour suppressor genes has been widely explored in almost all cancers. Genome-wide evaluation of methylation profiles in normal and tumour samples is a valuable tool for the identification of tumour-specific changes that are either driver events in cancers or markers of disease progression. The clear separation of the 3 DIPG short-term cell cultures (IN2675, IN2102 and IN2087) from NHA, as summarised by the PCA plot in Figure 6.1 implies that these tumours can be distinguished from their respective normal tissues based on their methylation profiles. The comprehensive analyses of

methylation 450 K data from the 3 DIPG short-term cell cultures and NHA further revealed large number of differentially methylated probes in these tumours. There were 284 methylated probes with minimum β-value of 0.85 and 1054 methylated probes with minimum β-value of 0.75 that were differentially methylated in 2 of 3 DIPG short-term cell cultures compared to NHA. The screening strategy employed in this analysis initially identified 40 candidate genes, and further validation confirmed downregulation of 20 of these genes in DIPG short-term cell cultures compared to NHA. Twelve genes were frequently differentially methylated (2/3 cases) in DIPG and comprised *ADAMTS18, RFX3, PRKG2, PTPRE, RHBDF2, DAB1, EYA4, DLK1, CXCL14, SBNO2, SH3BP4* and *FGFR2.*

DIPG and non-DIPG did not differ significantly in their methylation profiles

Comparison of the frequencies of downregulation of 20 candidate genes in DIPG and non-DIPG short-term cell cultures did not reveal significant differences between the two tumour subgroups in the majority of the cases. The lack of differences in the global methylation profiles of DIPG and non-DIPG short-term cell cultures was further demonstrated in the PCA scatter plot, as the 2 tumour groups did not cluster separately (Figure 6.4), but this may be due to the small number of DIPGs available for this study. However, 2 genes (*FGFR2* and *APBB2*) demonstrated differences in their frequencies of downregulation between the 2 groups. While *FGFR2* was relatively more frequently downregulated in the DIPG (67% versus 7%, p=0.063), *APBB2* was more frequently downregulated in the non-DIPG (93% versus 33%, p=0.063) short-term cell cultures.

FGFR2 plays crucial roles in cellular signaling as the encoded protein can interact with fibroblast growth factors affecting mitogenesis and differentiation. Dysregulation of *FGFR2* has been linked to several developmental disorders highlighting its importance in organ development (Larbuisson et al., 2013; Zhigang et al., 2013). It has been reported to play a role in skeletal development, proliferation, differentiation and apoptosis in human calvaria osteoblasts, indicating its connection with BMP signaling (Marie et al., 2002). This is interesting as a subset of DIPGs have been associated with deregulations in BMP signaling (Song et al., 2010). *APBB2/Fe65* encodes a neuronal adaptor protein that functions both within the nucleus regulating transcription and at the cell surface regulating cell migration and motility (Standen et al., 2003). The transcriptional activity of this gene can regulate genes involved in DNA damage signaling pathways (Ryu et al., 2015). It is therefore likely that DIPG and non-DIPG may differ in their level of susceptibility to DNA damage and subsequently, different DNA damage signaling pathways may operate between them. *SH3BP4* is involved in the internalisation of specific protein receptors, and in the negative regulation of the mTOR pathway leading to regulation of cell growth, differentiation and autophagy (GeneCards (www.genecards.org)). Aberrant expression of *SH3BP4* in DIPG may indicate a potential role of mTOR pathway in these tumours. The protein encoded by *RANBP17* is a relatively new member of the importin β-like family of nuclear transport receptors sharing about 67% amino acid similarity with importin β proteins (Lee et al., 2010). Members of the importin β superfamily are involved in the transport of substrates such as proteins and large RNAs from cytoplasm to nucleus across nuclear pore complexes (Kutay et al., 2000). Recently, *RANBP17* mutations have been identified in a patient with

urothelial carcinoma (Wagle et al., 2014). Chromosomal aberration in this gene has been reported in osteosarcomas (Both et al., 2014). *MYH10* belongs to the myosin family of genes that encode actin-dependent motor proteins and are involved in a range of functions including regulation of cytokinesis, cell motility and cell polarity (Catherine et al., 2010; GeneCards (www.genecards.org)). It has a role in the PI3K regulation of trophoblast cell differentiation, in which it is negatively regulated by this pathway (Lindsey et al., 2010).

Candidate tumour suppressor genes frequently methylated in DIPG short-term cell cultures

One of the important aspects of this study was the experimental validation of candidate genes identified by the microarray analysis. Seven of 40 genes (*ADAMTS18, DAB1, EYA4, PRKG2, PTPRE, RFX3* and *RHBDF2*) were downregulated in all DIPG short-term cell cultures (3/3 cases). These genes were further validated to confirm the role of promoter methylation in the downregulation of these genes. Treatment of cells with demethylating agent (5-AZA) to reactivate downregulated genes is an indirect, yet useful strategy to evaluate promoter methylation of genes. Re-expression of genes post demethylation were evaluated in 1 DIPG and an additional cohort of 10 non-DIPG short-term cell cultures. The remaining paediatric HGG short-term cell cultures had comparatively slower growth rate and were couldn't be treated for sufficient time periods that ensured demethylation. The majority of these genes were re-expressed in a minimum of 4 paediatric HGG short-term cell cultures following demethylation, confirming the role of DNA methylation in the downregulation of these genes in these tumours.

Interestingly, there were also several cases with gene downregulation but no re-expression following demethylation. It is therefore possible that additional mechanisms such as deletions, mutations, histone modifications or non-coding RNAs may operate as alternative mechanisms in inducing downregulation of these genes in DIPG short-term cell cultures. The requirement of coordinated activities of DNA methylation and histone modifications for the establishment of gene silencing has been studied in many cancers (Zhang et al., 2005; Cedar and Bergman, 2009; Rose et al., 2014). It was also observed that some of the tumour cultures which expressed basal levels of gene expression that were included in the experiment as positive controls, exhibited downregulation after treatment. This may be due to the global demethylating effect of 5-AZA which could cause gene body DNA demethylation, resulting in gene silencing (Yang et al., 2014). Gene body methylation and the associated downregulation of gene expression have been previously reported (Maunakea et al., 2010; Varley et al., 2013; Yang et al., 2014).

Each of 7 genes has been reported to have associations with other cancers and also with altered cellular processes linked to cancer and may contribute to DIPG pathogenesis. None of these genes have previously been reported to be methylated in DIPG, although some genes were previously reported to be dysregulated by other mechanisms. The tumour suppressive roles of 2 genes (*DAB1* and *PTPRE*) were further investigated.

The ADAMTS family of disintegrin-like and secreted metalloproteinases with thrombospondin motifs consist of 19 members, which participate in diverse functions such as collagen processing, degradation of matrix proteoglycans, inhibition of

angiogenesis and regulation of homeostasis (Porter et al., 2005). *ADAMTS18* is a relatively new member of this group, which is expressed abundantly in almost all normal human tissues including brain. Mutation in this gene is reported to cause a developmental disorder, called Knobloch syndrome characterised by occipital skull defect and vision problems (Aldahmesh et al., 2011). It is frequently mutated in RCC and colorectal cancers, downregulated in breast cancers and hypermethylated in RCC, pancreatic, gastric and colorectal cancers (Porter et al., 2004; Jin et al., 2007; Xu et al., 2015). A potential role for this gene in paediatric HGG may be postulated as 16q has been identified as a critical region of loss in paediatric HGG including DIPG and non-DIPG at a frequency much higher than in adult HGG (18% versus 7%) (Bax et al., 2010; Qu et al., 2010; Jones et al., 2012).

EYA4 encodes a member of the eyes absent homolog family of proteins that possess separate domains for tyrosine phosphatase and threonine phosphatase activities and can also act as transcription factors (Tadjuidje et al., 2013). These activities enable these proteins to participate in diverse functions including DNA damage repair, innate immunity and development of organs such as eye, inner ear and kidney. It has been shown to promote dephosphorylation of *H2AX,* thereby promoting repair and survival in response to DNA damage (Cook et al., 2009). Mutations in this gene have been identified to cause deafness (Wayne et al., 2001; Huang et al., 2015). Recently, De Carvalho and colleagues (2012) attempted to identify methylation in driver genes involved in tumourigenesis. They found that *EYA4* methylation was cancer-specific and that it did not cluster with genes influenced by culture-induced methylation. Increased methylation of the gene was present in viable cancer cells than early

apoptotic cells indicating a beneficial role for methylation of this gene in cancer cell survival. *EYA4* has been identified as a prognostic marker in hepatocellular carcinoma (Hou et al., 2014). Methylation of this gene has been widely studied in colorectal cancer (Oster et al., 2011; Kim et al., 2015) which has led to the development of its role as biomarker in stools. It is also found to be methylated in Barret's oesophagus and oesophageal adenocarcinoma, (Zou et al., 2005) and breast carcinoma (Conway et al., 2014).

PRKG2, which encodes cyclic guanosine monophosphate (cGMP)-dependent protein kinase II is a serine/threonine kinase involved in the phosphorylation of genes essential for the proper development of growth plate (Koltes et al., 2015). It has been identified to control differentiation and proliferation of chondrocytes in mice cells. The enzyme is abundantly expressed in brain and its decreased activity in glioma cells has shown correlation with increased levels of Akt phosphorylation (Swartling et al., 2009). Ectopic expression of *PRKG2* in glioma cells was found to inhibit *SOX9* production resulting in decreased Akt levels and reduced proliferation. It is possible that the altered expression of *PRKG2* observed in paediatric HGG short-term cultures in this study may therefore have links to alterations in the PI3K/Akt pathway in these tumours. The inhibitory effects of *PRKG2* on cell proliferation have also been demonstrated in colon (Wang et al., 2012), gastric (Chen et al., 2010) and breast cancer cells (Ting et al., 2012). In breast cancer cells, the reduced proliferation was achieved through inhibition of EGF and its downstream pathway components including MAPK/ERK. Hence, downregulation of *PRKG2* in paediatric HGG may likely contribute to dysregulation of *EGFR*. In addition, *PRKG2* has also

demonstrated both anti-proliferative and anti-apoptotic effects in prostate cancer cells (Cook et al., 2004). A recent study revealed that the downstream targets of *PRKG2* are associated with p53 pathway (Koltes et al., 2015).

RFX3 encodes regulatory factor X-3, 1 of 5 TFs belonging to the regulatory factor X family of genes involved in the control of expression of genes essential for ciliogenesis (Choksi et al., 2014). Primary cilia projecting from the plasma membrane on the cell surface are capable of acting as sensory structures in cell signalling. Many cancers such as pancreatic cancer, renal cell carcinoma, melanoma and ovarian cancers display very low frequencies of primary cilia. Primary cilia play vital roles in regulating proliferation of neural cells (Han et al., 2008), migration (Higginbotham et al., 2012), and survival (Yoshimura et al., 2011) in childhood and adult CNS. They are also associated with signalling pathways such Hedgehog (Hh) signalling (Hassounah et al., 2012). Interestingly, Hh pathway has been implicated in many cancers and has been reported to be active in a subgroup of DIPG tumour cells (Michelle et al., 2010). In a DIPG cell culture model, it was observed that the self-renewal ability of the tumour cells in neurospheres was positively regulated by the level of activation of Hh signalling. The Hh inhibitors targeting Smoothened (Smo) require proper functioning of clilia. Therefore, downregulation of *RFX3* may contribute to dysregulated ciliogenesis and tumours with decreased *RFX3* may not be ideal candidates for Hh inhibitors targeting Smo. Ina et al., (2014) reported that dysregulated formation of primary cilia was associated with pre-invasive breast cancer lesions indicating this as an early event in cancers. Moreover, genes required for formation and function of primary cilia were found to be disrupted in these

cancers. Therefore, further functional studies to elucidate the role of altered ciliogenesis in paediatric HGG may provide better insights into the biology of these tumours.

RHBDF2 encodes one of two inactive homologues of rhomboid proteases iRhom 2 that lacks the proteolytic residues of its active counterpart but possess additional domains acquired during its evolutionary process (Zettl et al., 2011; Adrain and Freeman, 2012). The inactive rhomboid (iRhom) family of proteins have been discovered recently and are thought to have crucial regulatory roles as they are preserved during evolution under continuous selective pressure. iRhoms have been identified to inhibit EGFR signalling by regulating the release of EGF ligands mediated by the endoplasmic reticulum-associated protein degradation (ERAD) pathway. Deletion and loss of expression of *RHBDF2* have been identified in both benign and malignant types of epithelial ovarian cancer cells (Paulina et al., 2012). Mutations in this gene have been linked with tylosis esophageal cancer and contribute to dysregulated EGFR signalling, increased migration and proliferation of tumours cells in comparison to their normal tissues (Blaydon et al., 2012).

DAB1 and PTPRE demonstrate tumour suppressive activities in vitro

The regulatory potential of *DAB1* and *PTPRE* on growth characteristics of cells investigated in this study suggests potential tumour suppressive roles for these genes in DIPG short-term cell cultures. The role of *DAB1* on regulating growth has previously been demonstrated in breast cancer cell lines (McAvoy et al., 2008). The re-expression of *DAB1* in a breast cancer cell line resulted in decreased growth. The role of *PTPRE* has not been previously explored in cancers. In this study, re-

expression of *DAB1* or *PTPRE* in a cell culture model with no expression of these genes showed reduction in colony forming ability of cells, indicating a potential role for these genes in regulating growth characteristics of cells.

DAB1 encodes the intracellular adaptor protein of reelin, a large ECM-associated glycoprotein secreted by the Cajal-Retzius cells in the CNS that is critical for normal brain development. Reelin binds to the 2 lipoprotein receptors (VLDLR and ApoER2) on cell surface activating the src family of kinases (SFKs) (D' Arcangelo et al., 1999). Upon clustering of these ligands, *DAB1* binds to the intracellular domain of these receptors followed by its phosphorylation by SFKs (Howell et al., 1999; Kuo et al., 2005). Phosphorylated *DAB1* further activates multiple downstream signaling pathways such as Crk/Rap1 signaling regulating cell adhesion and PI3K/Akt and mTOR signaling, which contributes to formation of spine (Beffert et al., 2002; Niu et al., 2004; Feng and Cooper, 2009; Franco et al., 2011). Reduced expression of *DAB1* in GBM cell lines and xenograft models and endometrial cancers has been previously reported (McAvoy et al., 2008). Teixeira et al. (2014) demonstrated that downregulation of *DAB1* caused altered structural layering in the neocortex and hippocampus while inactivation of *DAB1* in adult brain did not show additional abnormalities in layering. This may suggest a specific role for *DAB1* in the developmental phase. In addition, *DAB1* can also affect F-actin stabilisation through its interaction with LIMK1 and n-cofilin as shown in Figure 6.12 (Assadi et al., 2003).

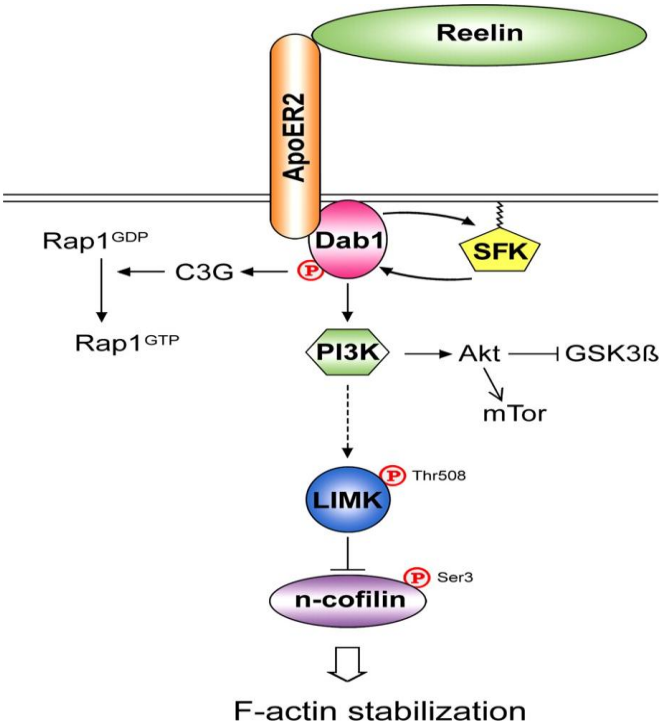

Figure 6.11 Role of *DAB1* in reelin pathway. *DAB1* encodes the intracellular adaptor in reelin signaling pathway. *DAB1* plays a major role in the transduction of extracellular signals from reelin and participates in F-actin-stabilization (Assadi et al., 2003)

DAB1 is a common fragile site (CFS) gene that has been reported to be inactivated in multiple cancer types, suggesting its role as a tumour suppressor (McAvoy et al., 2007; McAvoy et al., 2008; Smith et al., 2006). Other major tumour suppressors that are also CFS genes include *FHIT* and, *VWOX*. Methylation of *DAB1* been reported in a subtype of HCC that was associated with *PIK3CA* mutations, Akt hyperactivation and poor prognosis (Calvisi et al., 2007). In this study, overexpression of *DAB1* in a cell culture lacking *DAB1* expression has shown significant reduction in growth as well as migratory potential of cells *in vitro*, further supporting its role as a potential tumour suppressor. In addition, knockdown of *DAB1* in a paediatric HGG-derived short-term cell culture showed significant increase in cell migration. These suggest a

putative role for *DAB1* in paediatric HGG in the regulation of tumour cell migration. Taken together, it is likely that promoter hypermethylation of *DAB1* may be an early event in paediatric HGG tumourigenesis and warrants further investigation.

PTPRE is a member of the family of protein tyrosine phosphatases (PTPs) that play crucial roles in mediating signal transduction and cell adhesion in the developing nervous system (Ostman et al., 2006). Putative regulatory roles for *PTPRE* in Ras-related signal transduction pathways, and in the inhibition of MAPK cascade through the ERK 1 and 2 pathways have been demonstrated in animal models (Wabakken et al., 2002; Toledano-Katchalski et al., 2003). Although promoter hypermethylation of *PTPRE* has not previously been reported in other cancers, other mechanisms of disruption of this gene have been identified in few cancers. For instance, inactivation of *PTPRE* by homozygous deletion (10q26.2) has been identified in adult GBM has been identified (Nord et al., 2009). More importantly, intragenic deletion of this gene has been reported in paediatric HGG (Carvalho et al., 2014).

PTPRE was found to be associated with decreased expression and repressive histone mark, H3K27Me3 in malignant pheochromocytoma (Sandgren et al., 2010). It has been identified as a negative regulator of insulin signaling in primary liver cells (Nakagawa et al., 2005), and as an essential factor for the maintenance of proper structure and function of osteoclasts *in vitro* and *in vivo* (Chiusaroli et al., 2004).. Considering its significance in tumour-related processes in other cancers, dysregulation of *PTPRE* may be a key biomarker in DIPG.

H3F3A (K27M) *mutation differentiates methylation profiles in DIPG short-term cell cultures*

Of the 3 DIPG short-term cell cultures investigated in this study, the methylation profile of the *H3F3A* (H3K27M)-mutant sample (IN2675) was different from the others, as was evident from the PCA scatter plot (Figure 6.4). Interestingly, the mutant sample also did not share similarities in the global methylation profile with the majority of the non-DIPG short-term cell cultures, which also included the *H3F3A* (H3K27M)-mutant non-DIPG short-term cell culture (IN1566). This may indicate that *H3F3A* (K27M) may influence the methylation profiles of tumours depending on their different microenvironment in the brain. This was further supported by the fact that the remaining 2 DIPG short-term cell cultures grouped together with the majority of the non-DIPG short-term cell cultures. Thus, DIPG may share similarities in their methylation profiles with non-DIPG short-term cell cultures, but may also have unique subgroups within them that may be different from their non-brainstem counterparts. The presence of 3 distinct genomic subgroups within DIPG has recently been identified in a large-scale microarray-based integrative analysis involving copy number, gene expression and methylation profiles of 44 DIPG tumours. These consisted of a MYCN-amplified subgroup, a silent subgroup with stable genomes and a H3-K27M-mutant subgroup (Buczkowicz et al., 2014). The H3-K27M mutant subgroup had unstable genomes, and decreased levels of H3K27me3 histone marks. Interestingly, the *H3F3A*-mutant DIPG short-term cell culture (IN2675) had a relatively unstable genome compared to the other DIPGs, as described in Table 4.2. In IN2675, 3.57% of the genome was gained or

lost compared to 0.24% and 0.22% of alterations in IN2087 and IN2102, respectively. The identification of such different methylation profiles within such a small cohort of DIPG may indicate the genomic complexity of these tumours. A total of 37 probes representing 23 genes were identified to be hypermethylated (β value of methylated probe≥0.85) in the *H3F3A* (K27M)-mutant DIPG short-term cell culture, while these genes were hypomethylated (β value of methylated probe≤0.15) in the wild-type DIPG short-term cell cultures. The majority of these genes serve as biomarkers of tumour aggressiveness in other cancers, indicating that further investigation of these genes may lead to the development of potential biomarkers for a subset of DIPG with *H3F3A* mutation. Genes regulating stem-cell self renewal such as *ENTPD2* and *PIWIL1* were also hypermethylated in this subgroup. This may indicate that these tumours may harbour cancer stem-cell-like population of cells which may be one of the reasons for their highly aggressive and chemoresistant phenotypes. This is interesting as dysregulated miRNAs identified to be associated with *H3F3A* (K27M)-mutant paediatric HGG short-term cell cultures, described in Chapter 5 also suggested the potential role of pathways related to stem cell renewal in this tumour subgroup Table 5.15. This is therefore an area that is worth further investigation.

Promoter methylation of miRNA genes in DIPG short-term cell cultures

This study also identified promoter-hypermethylation in miRNA genes in DIPG short-term cell cultures. Twenty one probes representing 15 miRNA genes were identified to be frequently hypermethylated in DIPG short-term cell cultures compared to NHA (β value≥0.75 in 2/3 DIPG, and β value≤0.25 in NHA). However,

these represent interesting targets for future investigation owing to their potential tumour-related roles in other cancers. In addition, this also highlights the possibility of alternative mechanisms of miRNA dysregulation in DIPG pathogenesis.Of particular interest was *MIR193B* that has been identified to have tumour suppressing roles in many cancers. Downregulation of mir-193b has been identified in non small cell lung cancer in comparison to matching normal tissues and its ectopic overexpression in these cancers resulted in reduced migration, invasion and proliferation (Xu et al., 2010; Hu et al., 2012). *CCND1*, a key regulator of cell cycle and DNA damage control has been identified as an important target of mir-193b (Chen et al., 2010). A recent study by Kaukoniemi et al. (2015) has reported hypermethylation of mir-193b in prostate cancer and also demonstrated its ability to target *CCND1* in these tumour cells. Other important targets of mir-193b include *SMAD* and *KIT* (Gao et al., 2011). *CCND1* and *KIT* are frequent targets of amplification in paediatric HGG including DIPG and the importance of Smad signalling in these tumours has been implicated recently (Barrow et al., 2011; Bax et al., 2010; Wu et al., 2014). Taken together, hypermethylation of *MIR193B* may have roles in paediatric HGG pathogenesis. Some of the other miRNAs with putative functional significance in DIPG were *MIR1179* and *MIR549*. *MIR1179* has shown metastasis promoting roles in colorectal cancers and pro-invasive properties in eosaphageal squamous cell carcinoma (Jiang et al., 2015). One of the prime predicted targets of *MIR1179* using miRDB is anoctamin 3 (*ANO3*), a member of the family of anoctamins that are highly expressed in many cancers contributing to proliferative, migratory and metastatic abilities (Wanitchakool et al., 2014). Although not completely clear, a link between *ANO1* upregulation and *HDAC* has been reported in

head and neck squamous cell carcinoma where a dose-dependent decrease in proliferation of cells was observed upon treatment with HDAC inhibitors. Considering the important roles of HDAC in DIPG, downregulation of *MIR1179* may have novel implications in DIPG tumourigenesis. The role of *MIR549* in cancers has not extensively been investigated studied so far. It is located within *KIAA1199,* which has been recently identified as a regulator of *EGFR* stability and has demonstrated to promote cell survival in keratinocytes (Shostak et al., 2014). Another study in colorectal cancers has reported upregulation of mir-549 (Hamfjord et al., 2012). An attempt to predict the potential targets of *MIR549* using miRDB and TargetScan revealed that frequently upregulated genes in cancers such as *HIF1A* and *HMGB1*. A recent study by Li et al. (2015) reported that *HMGB1* mediates epithelial-mesenchymal transition via increased expression of *TGF-B1* and phosphorylation of Smad 2/3 signalling. Dysregulation of Smad signalling has been reported in paediatric HGG, particularly DIPGs (Wu et al., 2014).

Experimental validation of candidate genes is critical

This study emphasises the importance of experimental validation of candidate genes identified from microarray data analysis. The initial analysis of the Methylation 450 K data and Affymetrix U133a plus data in this study identified 40 candidate genes. Of these, only 20 genes showed satisfactory correlation with the microarray data, while the remaining 20 genes (50%) did not show correlation with the analysed data. Fourteen of 20 genes were not expressed in the control sample (NHA). Of the 14 genes that did not show expression in NHA, 7 genes were frequently downregulated in the DIPG short-term cell cultures and included genes with potential associations

with paediatric HGG, as well as with other cancers. A notable member among these genes was *A2BP1,* which was deleted in paediatric GBM, deleted (10%, 430 TCGA GBM tumour samples) and downregulated in adult GBM, deleted in other nervous system tumours such as medulloblastoma and neuroblastoma, as well as in other cancers such as colon cancer cancer and sarcoma indicating a tumour suppressive role for this gene (Beroukhim et al., 2010; Jian et al., 2013; Novara et al., 2014). There were also known tumour suppressors like *FHIT* and genes with potential tumour suppressive roles like *KRT8* in this subgroup (Jayachandran et al., 2007; Mizuuchi et al., 2009). The role of promoter hypermethylation induced downregulation has been reported for *FHIT,* and it has also been demonstrated to induce apoptosis via inactivation of PI3K/Akt pathway (Semba et al., 2006; Kelley and Berberich, 2011; Huang et al., 2014; He et al., 2015). It is not clear why these genes did not show expression in NHA. The availability of only 1 normal sample was therefore a limitation in this analysis. The suitability and availability of normal control samples for paediatric HGG studies remains a contentious issue.

Six of 20 genes were expressed in NHA, but failed to show downregulation in any of the DIPG short-term cell cultures. This could be due to several reasons. One of the possibilities is the interference of background noise from the microarray leading to technical artefacts. These could affect the signal intensities of probes leading to false positives. The other reason could be attributed to the location of the methylated probes around the promoter region. In this analysis, probes located up to 1500 base pairs from TSS were analysed. The proximity of a methylated probe to the core promoter region where transcription factors bind may influence the degree of

transcription. It would be interesting to evaluate the location of the methylated probes in these genes that failed to demonstrate correlation with the microarray data. Furthermore, discrepancies may also arise as cell culture conditions can influence gene methylation. Cells in culture tend to acquire more changes in methylation, which can influence the expression of transcription factors leading to global changes in gene expression. The various analyses to validate the genes identified in this analysis therefore raise confidence in their suitability for further investigations in DIPG.

6.3 Conclusions

To conclude, this study highlights the importance of promoter hypermethylation in the dysregulation of coding and non-coding genes in the development and progression of paediatric HGG. The candidate genes identified in this study are found to have significant associations with tumourigenesis and may be developed as potential biomarkers in the treatment of DIPG and/or non-DIPG tumours in future. Importantly, the tumour suppressive potential of *DAB1* and *PTPRE* demonstrated in this study highlights aberrations in novel pathways in DIPG. Further investigations of these genes may lead to their development into useful biomarkers of tumourigenesis in DIPG. However, it has to be taken into account that culture conditions may cause changes in methylation, and therefore additional validation in more samples are indispensable to confirm the genuine associations of these genes with the tumour. Furthermore, although microarrays provide rich sources of information, this study emphasises the importance of experimental validation of genes identified by microarray analysis, in order to limit false positives.

CHAPTER 7

Preliminary investigation of targeted therapeutics in paediatric HGG short-term cell cultures

7.1 Introduction

Children with high grade glioma commonly develop serious late effects associated with endocrine dysfunction and neurocognitive delay as a result of conventional radio- and chemotherapy (Merchant et al., 2010; Sands et al., 2012). The sensitivity of the brain and its developmental stage in children are some of the major issues which need to be considered in the generation of novel treatment agents for HGG in this age group.

One of the peculiarities of tumour cells is their requirement for particular amino acids to accommodate the demands of increased proliferation (Hanahan and Weinberg, 2011), which has laid the foundation for the development of anti-cancer agents that can deplete specific amino acids in the circulation (Delage et al., 2010; Agrawal et al., 2011; Covini et al., 2012; Phillips et al., 2013). The preference of tumour cells for glutamine has long been established and recent metabolomic profiling in some tumours has provided evidence of the critical roles of glycine and serine in the rapid proliferation of tumour cells (DeBerardinis et al., 2007; Possemato et al., 2011; Jain et al., 2012; Zhang et al., 2014; Boroughs and DeBerardinis, 2015). Recent discoveries of arginine-dependency in tumours have raised the therapeutic possibilities of using arginine-degrading enzymes for such tumours (Delage et al, 2012; Feun et al., 2015).

Arginine is involved in various cellular activities, notably growth and proliferation, and tumour cells exhibit higher demands for arginine than normal cells (Caso et al., 2004; Morris, 2007; Morris, 2009). In a healthy individual, cells can synthesise

arginine *de novo* from its precursor citrulline via the arginine biosynthesis machinery as well as obtaining it from external sources. Cellular arginine renewal is controlled by two primary enzymes, argininosuccinate synthetase (ASS1) and argininosuccinate lyase (ASL) encoded by *ASS1* and *ASL* respectively. The coordinated activities of these enzymes regulate the conversion of citrulline to arginine through argininosuccinate (Morris, 2004; Haines et al., 2011). Tumours with deregulated *ASS1* and/or *ASL* fail to synthesise arginine *de novo*, which forces them to rely on external arginine sources. Therefore, starving such tumours of arginine using agents that can deplete arginine from the circulation can selectively eradicate tumour cells (Qiu et al, 2015).

Deficiency of ASS1, the enzyme that catalyses the rate-limiting step in the arginine pathway, has been reported in a number of cancers including melanoma, HCC, RCC, small cell lung, prostate, pancreatic and bladder cancers (Cheng et al., 2007; Yoon et al., 2007; Bowles et al., 2008; Kim et al., 2009; Feun et al., 2012; Kelly et al, 2011; Allen et al., 2013). Decreased expression of *ASS1* expression was correlated with advanced tumour stage and poor survival in nasopharyngeal carcinoma and myxofibrosarcoma (Huang et al., 2013; Lan et al., 2013). In ovarian and bladder cancers, ASS1-deficiency was associated with reduced overall survival rates (Nicholson et al., 2009; Allen et al, 2013). *ASL* has also shown tumour suppressive roles in some cancers (Syed et al., 2013).

Of particular interest, deregulation of *ASS1* and *ASL* by promoter methylation was recently reported in adult GBM primary cultures, which also demonstrated anti-proliferative responses to ADI-PEG20 (Syed et al., 2013). Interestingly, the anti-

tumour activity of ADI-PEG20 in GBM cells was due to the induction of autophagic cell death, circumventing the apoptotic route to which these cells are intrinsically resistant. Autophagy acts as an initial pro-survival mechanism during conditions of nutrient stress, but can mediate caspase-independent cell death when pushed beyond a particular threshold (Fulda and Kogel, 2015). In addition, a study by Pavlyk et al. (2014) reported that arginine deprivation in GBM cell lines reduced migration and invasion *in vitro.*

ADI-PEG20 is a polyethylene glycol-conjugated formulation of a microbial-derived arginine hydrolysing enzyme and possesses reduced immunogenicity and extended half life in serum than native ADI (Feun and Savaraj, 2006; Feun et al., 2008). The clinical performance of ADI-PEG20 has been evaluated in adults with melanoma (Ascierto et al., 2005, Ott et al., 2012), HCC (Izzo et al., 2004), and malignant pleural mesothelioma (Szlosarek et al., 2013). In phase I/II clinical trials conducted in these patients, the use of very low doses of the drug has shown improved overall survival with minimal side effect, and a phase III trial for HCC is in progress (clinical trial identifier NCT01287585).

The PI3K/Akt/mTOR signaling pathway, which plays an integral role in cancer cell growth and survival, is one of the most frequently altered signaling networks in human tumours (Samuels et al., 2004; Cancer Genome Atlas Research Network 2008). The PI3Ks are a group of intracellular lipid kinases that phosphorylate the 3-OH group of phosphatidylinositides (PtdIns) in response to extracellular cues such as growth factors and hormones. This triggers a series of events leading to the regulation of cell growth, survival and metabolism (Cantley, 2002; Engelman et al.,

2006; Vanhaesebroeck et al., 2012; Thorpe et al., 2014). Among the three classes of PI3Ks (I-III), class I PI3Ks are the most frequently deregulated in cancer and are divided into two subgroups-class 1A and 1B. Class 1A, activated by growth factor RTKs are heterodimers composed of regulatory (p85) and catalytic (p110) subunits. The genes *PIK3R1*, *PIK3R2* and *PIK3R3* encode p85α, p85β and p55γ isoforms of the p85 subunit respectively. The p110α, p110β and p110δ isoforms of p110 catalytic subunit of class 1A are encoded by *PIK3CA*, *PIK3CB* and *PIK3CD* respectively. Class IB PI3Ks, activated by GPCRs are heterodimers consisting of a single catalytic subunit p110γ (*PIK3CG*) and two regulatory subunits p101 and p87 encoded by *PIK3R5* and *PIK3R6* respectively (Engelman et al., 2006). Upon ligand-receptor binding, the activated PI3Ks catalyse the phosphorylation of PIP2 to PIP3, which recruits Akt, a serine/threonine kinase that is the immediate effector of the PI3K pathway to the plasma membrane (Franke et al., 1997; Klippel et al., 1997). Phosphorylated Akt activates mTOR leading to stimulation of protein synthesis and cell growth. The PI3K pathway is further regulated by the intricate feedback loop of PTEN (Maehama et al., 1998) as well as the crosstalk between components of the PI3K pathway and other signaling networks (Lee et al., 2008).

Hyperactivation of the PI3K pathway has been widely investigated in adult HGGs and occurs commonly through gain of function mutations in *PIK3CA* (Samuels et al., 2004) or loss of the tumour suppressor, *PTEN*. In contrast, very few studies have investigated the role of PI3K activation in paediatric HGG. It has been reported that the frequency of *PIK3CA* mutations in paediatric HGG occur at relatively lower rates compared to those in adults (Jones et al., 2012). In a study by Mueller et al. (2012),

aberrant activation of PI3K/Akt/mTOR pathway was identified in 80% (12/15) of paediatric HGG and the evaluation of *PTEN* alterations revealed correlation of lack of PTEN protein expression and promoter methylation in 50% (5/10) cases. It is therefore likely that constitutive PI3K activation exist in paediatric HGG, possibly initiated through alternative mechanisms. A number of small molecule inhibitors that can target PI3K and/or its network components have been developed, some of which are being evaluated in clinical trials. PI-103, a dual inhibitor of class1 isoform of PI3K and mTOR (molecular weight of 348.36), has shown significant anti-proliferative effect in xenograft models of glioma (Fan et al., 2006; Fan et al., 2007).

In this study, the expression of *ASS1* and/or *ASL* in paediatric HGG has been investigated and the response of these tumours to ADI-PEG20 treatment *in vitro* has been assessed. The growth inhibitory effect of PI-103 in paediatric HGG short-term cell cultures has also been evaluated.

7.2. Results

7.2.1 Evaluation of arginine biosynthesis pathway as a therapeutic target in paediatric HGG short-term cell cultures

7.2.1.1 Promoter methylation of *ASS1/ASL* in paediatric HGG short-term cell cultures

To investigate if *ASS1/ASL* was deregulated by promoter hypermethylation in paediatric HGG short-term cell-cultures, the Illumina Infinium HumanMethylation 450 K data generated from NHA and 17 paediatric HGG short-term cell cultures (consisting of 3 DIPG and 14 non-DIPG) were screened for differentially methylated

probes representing *ASS/ASL*. Data were also available for 5 paediatric HGG biopsy samples, which included 3 paired biopsies and their derivative cell cultures. To ensure only promoter-associated probes were screened, the probes located in 5'UTR and up to 1500 bases upstream of TSS (n=132,665) were identified, as described in 6.2.1. Of these, 7 probes represented *ASS1* and 3 probes represented *ASL*. To identify the differentially methylated probes in paediatric HGG compared to NHA, these probes were evaluated based on their beta values (ranging from 0 to 1, indicative of percentage of methylation). To ensure that *ASS1/ASL* methylation in paediatric HGG short-term cell cultures was not disregarded because of stringent probe beta value thresholds for methylation, a relaxed criterion was initially defined to identify differentially methylated probes. Those probes that had beta value$\geq$0.50 in paediatric HGG short-term cell cultures and beta value<0.5 in NHA were considered differentially methylated, which identified a single probe representing *ASS1* (cg22791453) and a single probe representing *ASL* (cg22723802), respectively. The probe beta values of *ASS1* and *ASL* in NHA, 17 paediatric HGG short-term cell cultures and 5 biopsy samples are given in Figure 7.1. Methylation of the probes representing *ASS1* and *ASL* were detected in 17/17 (100%) and 15/17 (~88%) paediatric HGG short-term cell cultures, respectively. Methylation of the *ASS1* probe was not detected in any of the paediatric HGG biopsy samples in the cohort. However, *ASL* methylation was detected in 4/5 paediatric HGG biopsy samples, which included the 3 paired samples. Of these pairs, methylation was present in biopsy and its derived short-term cell culture in 2 cases (IN3182 and IN3183).

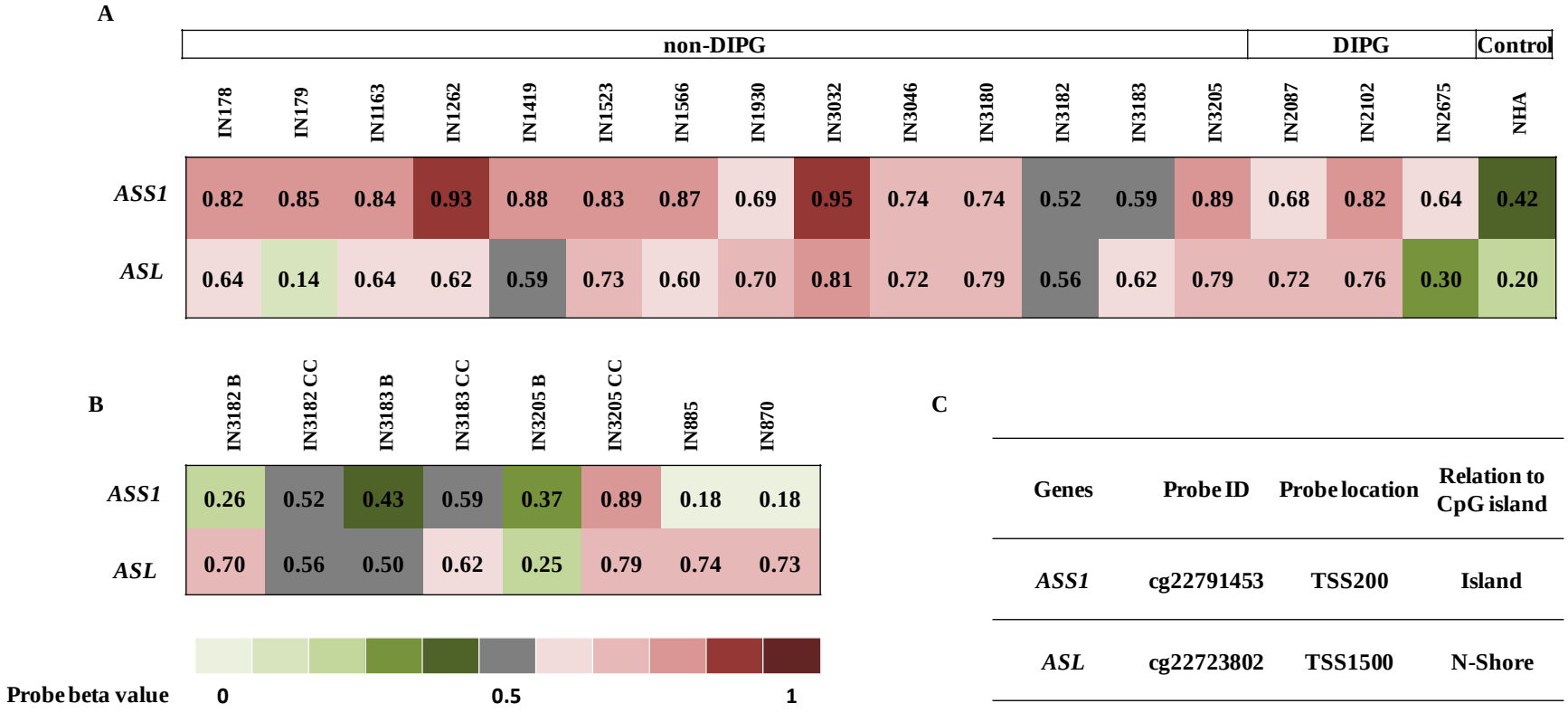

Figure 7.1 Probe beta values of *ASS1/ASL* in NHA, 17 paediatric HGG short-term cell cultures and 5 biopsies. The Illumina Infinium HumanMethylation 450 K data from NHA, 17 paediatric HGG short-term cell-cultures and 5 biopsy samples were analysed to identify promoter-associated and differentially methylated probes (probe β value≥0.50 in tumour and <0.50 in NHA) corresponding to *ASS1/ASL*. **A**. Probe beta values of *ASS/ASL* in NHA and paediatric HGG short-term cell cultures. **B**. Probe beta values of *ASS1/ASL* in 5 paediatric HGG biopsies including 3 paired biopsies (IN3182 B/CC, IN3183 B/CC and IN3205 B/CC). **C.** Location of *ASS1/ASL* methylated probe in the promoter region. Colour codes of probe beta values range from 0 (unmethylated) to 1 (complete methylation). N_shore indicates north shore, the region upstream (up to 2 kb) from the CpG Island; B-Biopsy; CC cell culture.

7.2.1.2 Validation of promoter methylation of *ASS1/ASL* in paediatric HGG short-term cell cultures

To validate methylation of *ASS1*/*ASL* in paediatric HGG short-term cell cultures, DNA was extracted from 17 paediatric HGG short-term cell cultures and CpG methylation in the promoter region was determined using combined bisulfite restriction analysis (CoBRA), as described in 2.2.8.3. DNA available for 2 paired biopsies was also included for validation. For *ASS1* methylation analysis, the location of the methylated probe (cg22791453), as described in the UCSC genome browser (www.genome.ucsc.edu) was identified (Figure 7.2) and methylation of CpGs within and/or around the promoter region containing the probe was determined. The details of the probe CpGs of *ASS1* are shown in Figure 7.2.

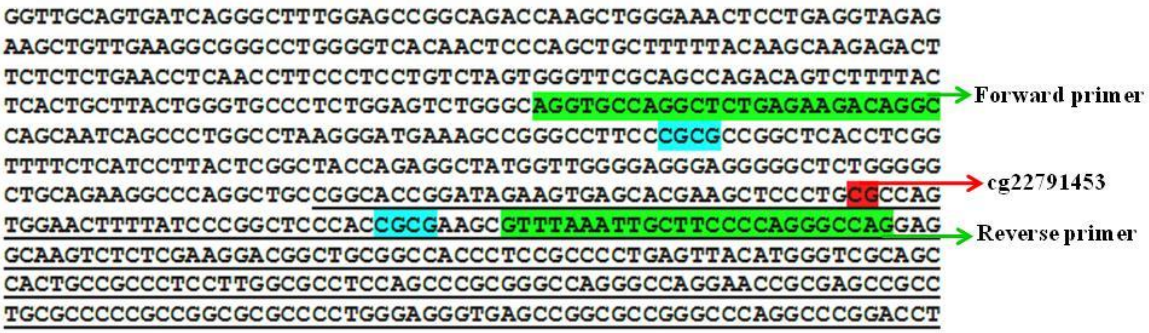

Figure.7.2 Methylated probe CpG in *ASS1* promoter CpG Island. The *ASS1* methylated probe (cg22791453) located on the CpG Island was retrieved from the UCSC genome browser. Methylated CpG is highlighted in red. BstUI recognition sites are highlighted in aqua. Forward and reverse CoBRA primers are highlighted in green.

The PCR amplified products were digested with the restriction enzyme, BstUI (recognition sequence-*CGCG*). The methylation status of *ASS1* in 17 paediatric HGG short-term cell cultures including 2 paired biopsies, as determined by CoBRA is shown in Figure 7.3 A. *ASS1* was methylated in 8/17 (~24%) paediatric HGG short-

term cell cultures consisting of 6 non-DIPG (IN1163, IN1262, IN1419, IN3032, IN3180 and IN3183) and 2 DIPG (IN2087 and IN2102) samples. With the exception of IN3182, all the remaining samples (9/17) consisting of 7 non-DIPG (IN178, IN179, IN1523, IN1566, IN1930, IN3046 and IN3205) and 1 DIPG (IN2675) short-term cell cultures had partial methylation of *ASS1*. The lack of *ASS1* methylation observed in IN3182 CC was also observed in its respective biopsy. *ASS1* was methylated in IN3183 CC, but only partially methylated in its respective biopsy.

For methylation analysis of *ASL,* primers were designed to amplify regions within its promoter region and the amplified products were digested with BstUI. The results of methylation analysis of *ASL* in paediatric HGG as determined by CoBRA is shown in Figure 7.3 B. In contrast to *ASS1*, *ASL* was not methylated in any of the samples analysed.

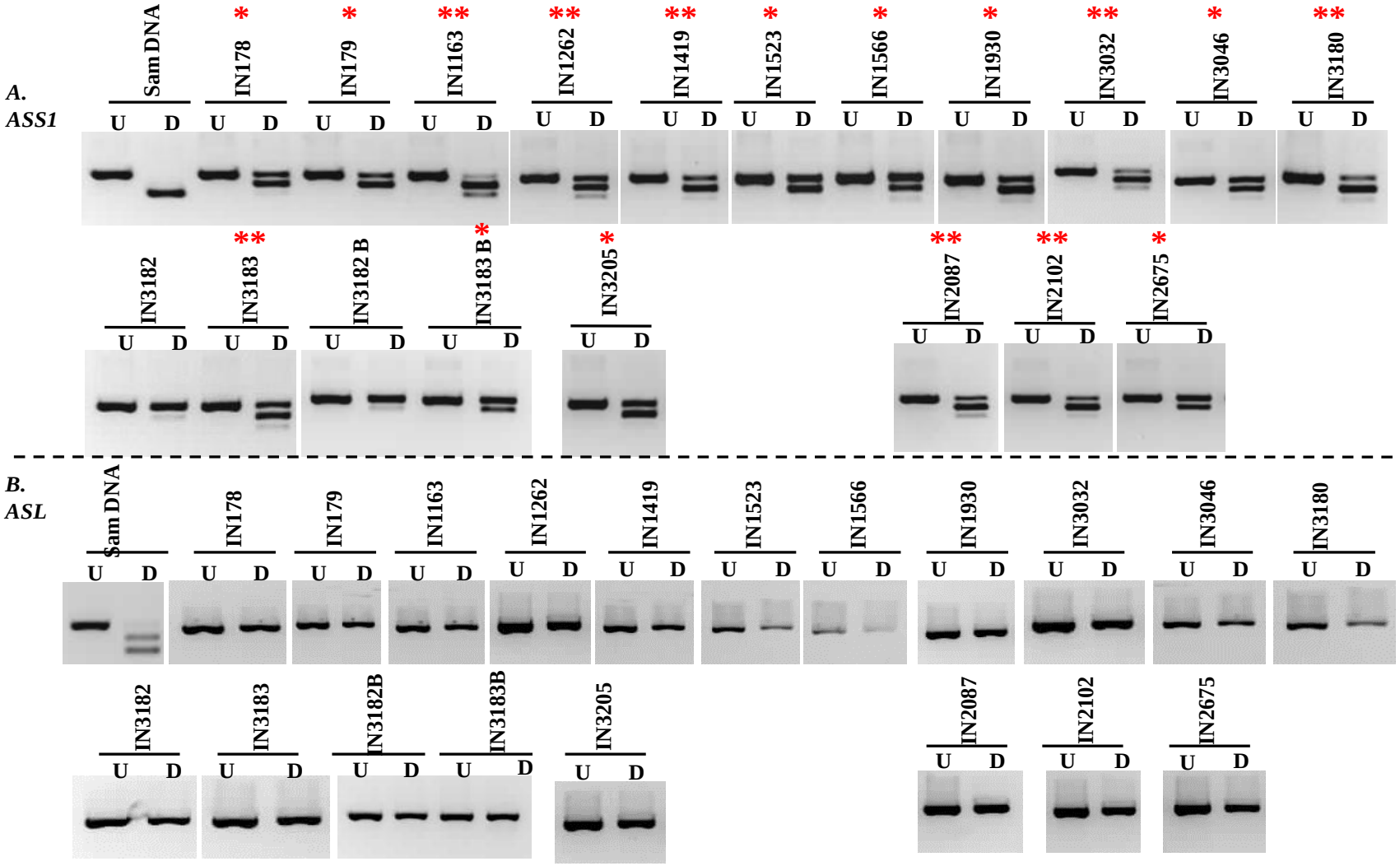

Figure 7.3 Methylation status of *ASS1* and *ASL* in paediatric HGG as determined by CoBRA. CoBRA was used to determine the methylation status of *ASS1* and *ASL* in 17 paediatric HGG short-term cell cultures. Methylation in a sample is indicated by digested (D) PCR products compared to undigested (U). ** indicates partial methylation. **B**. *ASL* was not methylated in paediatric HGG short-term cell cultures or paired biopsies.

To further investigate *ASS1/ASL* CpG methylation in paediatric HGG short-term cell cultures, methylation in additional CpG sites in the promoter regions of these genes were analysed. Previously, Syed et al. (2013) has shown *ASS1* promoter CpG methylation in 2 regions (regions 1 and 2 in Figure 7.4 A), and *ASL* promoter CpG methylation in 2 regions (regions 1 and 2 in Figure 7.5A), respectively, which correlated with silencing of these genes in adult GBM primary cultures. To investigate if *ASS1/ASL* CpGs in these regions were methylated in paediatric HGG short-term cell cultures, DNA was extracted from 17 paediatric HGG short-term cell cultures and 2 paired biopsies and the methylation status of these regions was determined by MSP, as described in 2.2.8.3. The methylation status of *ASS1* CpG sites in regions 1 and 2 is shown in Figure 7.4 B, and that of *ASL* CpG sites in regions 1 and 2 in these samples is shown in Figure 7.5 B.

ASS1 methylation in region 1 was detected in 7/17 (~41%) paediatric HGG short-term cell cultures consisting of 5 non-DIPG (IN1163, IN1262, IN1419, IN3032 and IN3205) and 2 DIPG (IN2087 and IN2675) cases. Methylation of *ASS1* in this region was not detected in either the biopsy or the cell culture of the 2 paediatric HGG paired samples (IN3182 B/CC and IN3183 B/CC) analysed. Methylation of *ASS1* in region 2 was detected in 8/17 (~47%) paediatric HGG short-term cell cultures consisting of 6 non-DIPG (IN179, IN1163, IN1262, IN3032, IN3182 and IN3205) and 2 DIPG (IN2087 and IN2675) samples. The methylation detected in IN3182 CC was also detected in its respective biopsy, but at comparatively lower levels than observed in the cell culture. For the IN3183 pair, partial methylation of *ASS1* was

detected in IN3183 biopsy, which was comparable to the amounts of methylation in its derived short-term cell culture.

In contrast, *ASL* CpG methylation in regions 1 and 2 was not detected in any of the paediatric HGG samples including the 2 paired biopsies (Figure 7.5).

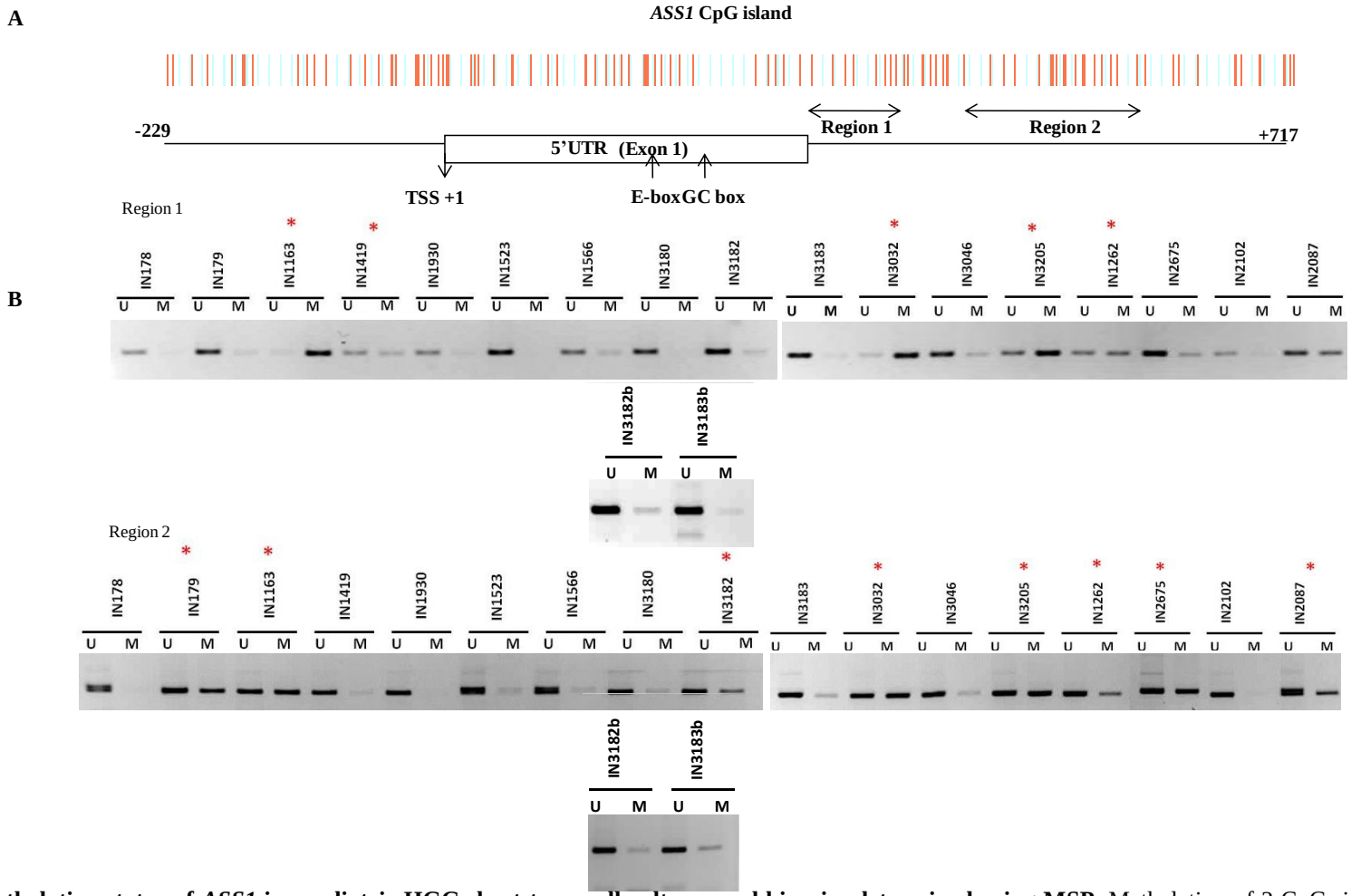

Figure 7.4 Methylation status of *ASS1* in paediatric HGG short-term cell cultures and biopsies determined using MSP. Methylation of 2 CpG rich sites in *ASS1* promoter was determined in paediatric HGG short-term cell cultures using MSP. **A**. *ASS1* promoter CpG site used for methylation analysis by MSP (Syed et al., 2013). **B.** Methylation (*) was detected in IN1163, I1419, IN3032, IN3205 and IN1262 in region 1, and in IN179, IN1163, IN3182, IN3032, IN3205, IN1262, IN2675 and IN2087 in region 2, respectively.

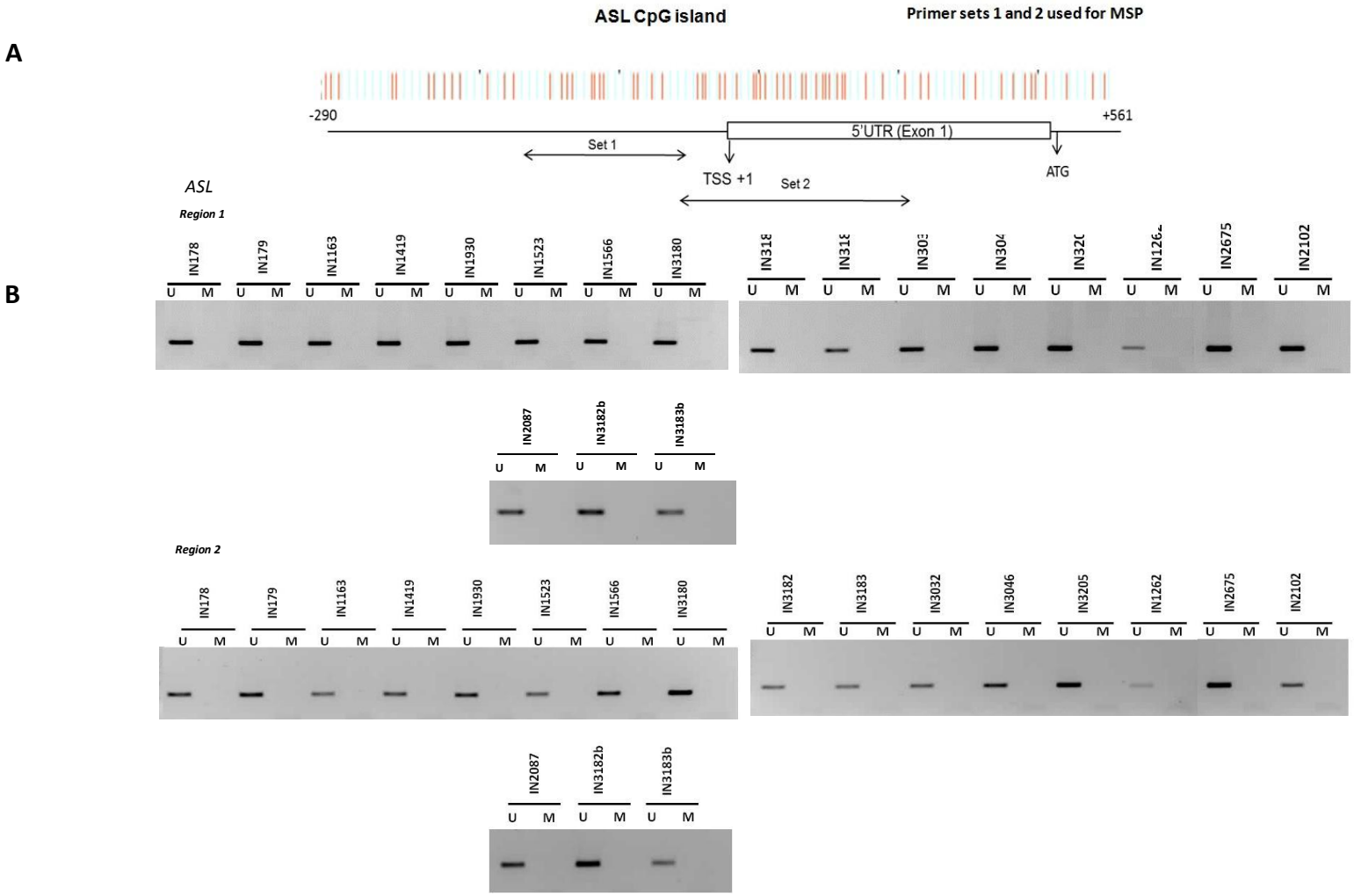

Figure 7.5 Methylation status of *ASL* in paediatric HGG short-term cell cultures and biopsies determined using MSP. Methylation of *ASL* in paediatric HGG short-term cell cultures was determined using MSP. Methylation was not detected in any of the samples analysed. **A**. *ASL* promoter CpG site used for methylation analysis by MSP (Syed et al., 2013). **B.** Methylation of *ASL* in regions 1 and 2 was absent in paediatric HGG short-term cell cultures.

In addition to the investigation of *ASS1/ASL* methylation in specific CpG sites in their promoter regions by CoBRA and MSP, promoter methylation of these genes in paediatric HGG short-term cell cultures were evaluated based on upregulation in their expression following treatment with the demethylating agent 5-AZA. Nine paediatric HGG short-term cell cultures (8 non-DIPG and 1 DIPG) were treated with 5μM 5-AZA and changes in expression of *ASS1/ASL* following demethylation were determined by quantitative PCR (Q-PCR), as described in 2.2.9.4. The results of Q-PCR analysis of *ASS1/ASL* expression in 9 paediatric HGG short-term cell cultures following demethylation with 5-AZA are shown in Figure 7.7. *ASS1* was upregulated in 4/9 (IN1419, IN2102, IN3182 and IN3205) cultures and *ASL* was upregulated in 4/9 (IN1163, IN1930, IN3182 and IN3205) cultures. Interestingly, *ASS1* and *ASL* were both upregulated in 2 cases (IN3182 and IN3205).

It was also observed that expression of *ASS1* was reduced following demethylation in 3/9 paediatric HGG short-term cell cultures (IN178, IN179 and IN1163) and expression of *ASL* was also reduced following demethylation in 3/9 cultures (IN179, IN1523 and IN2102). This is not surprising as these genes are involved in complex networks of regulation and 5-AZA treatment indiscriminately demethylates the whole genome.

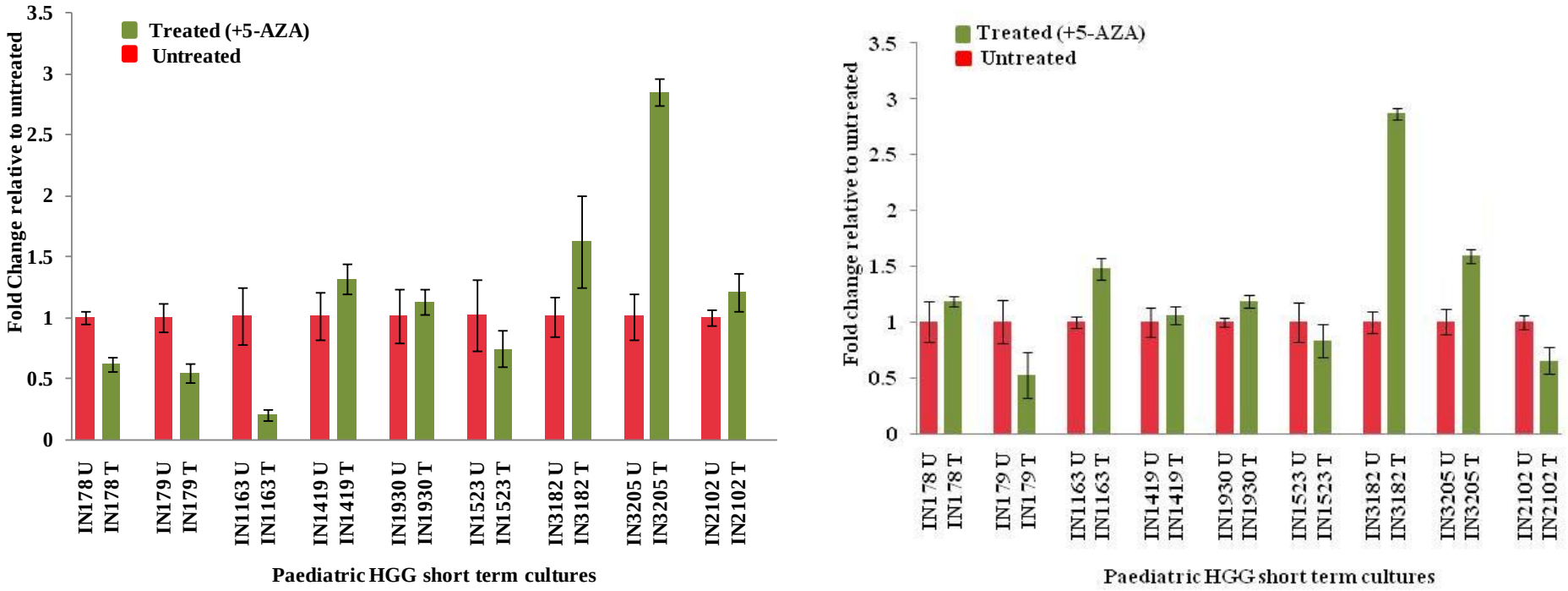

Figure 7.6 Upregulation of *ASS1* in paediatric HGG short-term cell cultures following demethylation. Paediatric HGG short-term cell cultures were treated with the demethylating agent (5-AZA) and changes in *ASS1/ASL* expression following treatment were measured using Q-PCR. **A**. Increase in expression of *ASS1*following treatment was detected in IN1419, IN2102, IN3182 and IN3205. **B.** Increase in expression of *ASL* following treatment was detected in IN1163, IN1930, IN3182 and IN3205.

7.2.1.3 Downregulation of *ASS1/ASL* in paediatric HGG short-term cell cultures

To determine the basal levels of expression of *ASS1/ASL* in paediatric HGG short-term cell cultures, RNA was extracted from NHA and 17 paediatric HGG short-term cell cultures and all 3 biopsies and *ASS1/ASL* mRNA expression levels in these samples were determined using Q-PCR, as described in 2.2.9.4. *ASS1/ASL* expression in these samples was normalised to the expression levels of an endogenous control (*GAPDH*). The expression of *ASS1* and *ASL* in paediatric HGG short-term cell cultures in comparison to NHA as determined by Q-PCR analysis are shown in Figures 7.9 and 7.10 respectively.

Of the 4 *ASS1*-methylated paediatric HGG short-term cell cultures as determined by the upregulation of *ASS1* expression following demethylation with 5-AZA (IN1419, IN2102, IN3182 and IN3205), very low expression was observed in 1 culture (IN3205) in comparison to the expression of *ASS1* in NHA demonstrating correlation of promoter hypermethylation with reduced transcription. However, the other 3 paediatric HGG short-term cell cultures had higher expression of *ASS1* compared to the expression level in NHA, but this might be because NHA in this analysis demonstrated very little basal *ASS1* mRNA levels. In addition to IN3205, low expression of *ASS1* was found in 2 paediatric HGG short-term cell cultures, both of which were DIPG (IN2087 and IN2675). Among the 3 paired biopsies, *ASS1* was downregulated in all 3 biopsies, with relatively higher expression in their respective cell cultures. However, it was interesting to note that the increase in expression of *ASS1* in 2/3 pairs (IN3182 and IN3183) was <2-fold. For the IN3180 pair, *ASS1* expression in the cell culture was relatively higher compared to its parent biopsy.

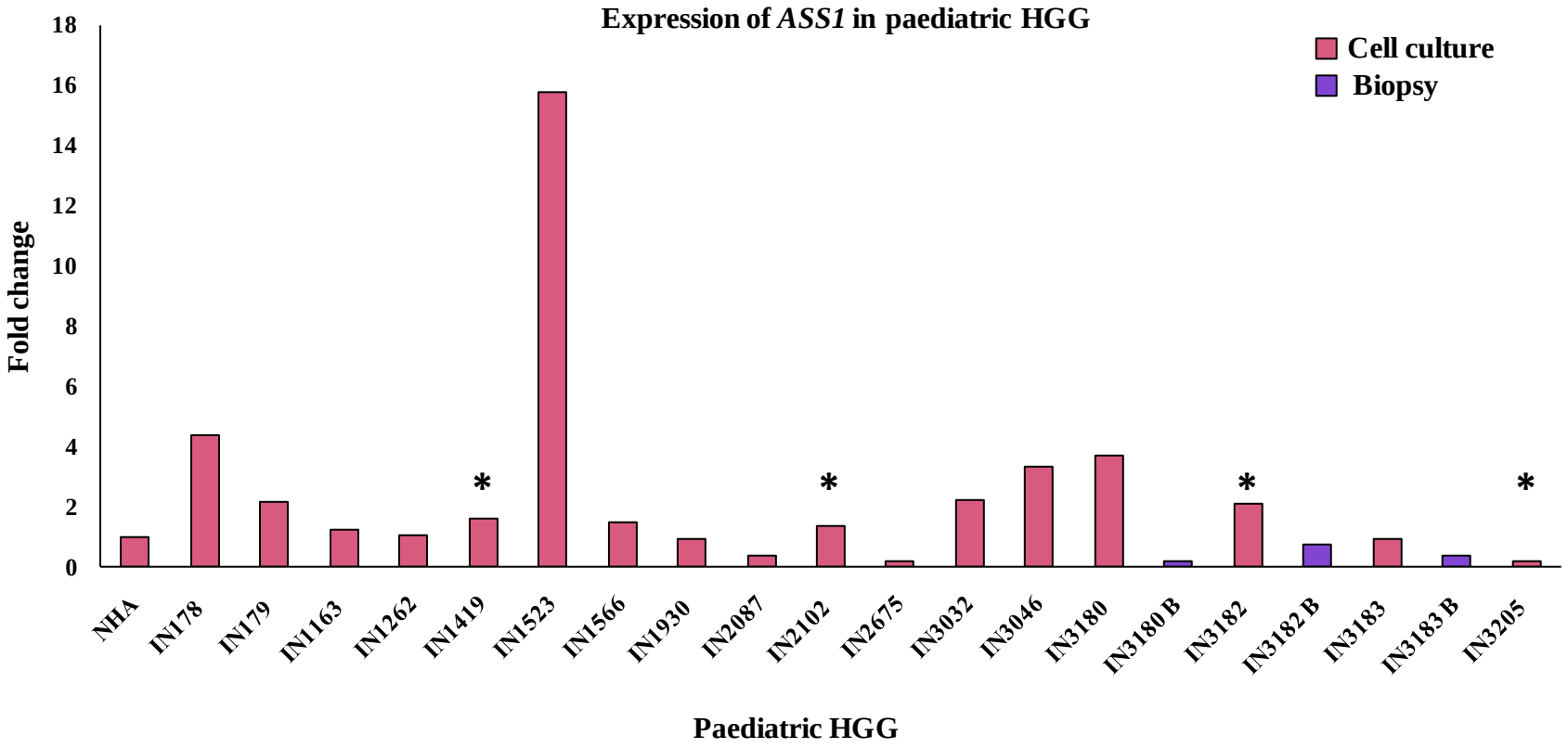

Figure 7.8 Reduced expression of *ASS1* in paediatric HGG. Expression of *ASS1* in NHA, 17 paediatric HGG short-term cell cultures and 3 biopsy samples was determined using q-PCR. *GAPDH* was used as an endogenous control. The fold change in expression of *ASS1* is shown with respect to NHA. (*) indicates paediatric HGG short-term cell cultures that demonstrated upregulation of *ASS1* following treatment with 5-AZA. IN3205 had very low levels of *ASS1* mRNA.

Expression of *ASL* was lower than NHA in 11/17 (~57%) paediatric HGG short-term cell cultures comprising 9 non-DIPG (IN178, IN1163, IN1419, IN1930, IN3032, IN3180, IN3182, IN3183 and IN3205) and 2 DIPG (IN2102 and IN2675) samples. Notably, *ASL* expression was much lower in all 3 paired biopsies in comparison to NHA. There were 4 paediatric HGG short-term cell cultures with comparatively higher levels of *ASL* expression comprising 3 non-DIPG (IN1262, IN1566 and IN3046) and 1 DIPG (IN2087) short-term cell culture respectively.

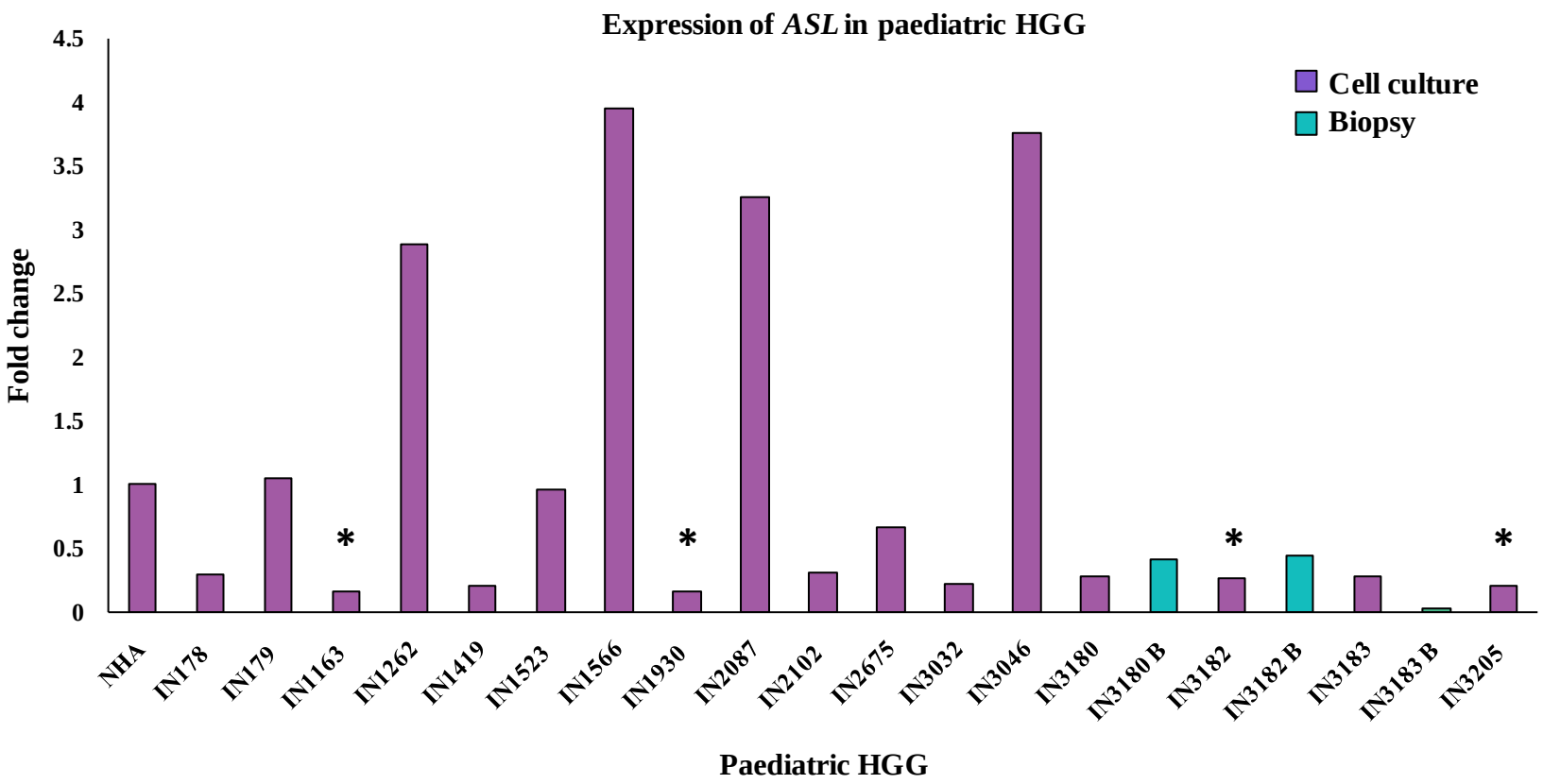

Figure 7.9 Reduced expression of *ASL* in paediatric HGG. Expression of *ASL* in NHA, 17 paediatric HGG short-term cell cultures and 3 biopsy samples was determined using q-PCR. *GAPDH* was used as an endogenous control. The fold change in expression for each sample with respect to NHA is shown. (*) indicates paediatric HGG short-term cell cultures which demonstrated upregulation of *ASL* following treatment with 5-AZA. All *ASL*- methylated paediatric HGG short-term cell cultures (IN1163, IN1930, IN3182 and IN3205) had very low levels of mRNA.

To investigate if downregulation of *ASS1* in paediatric HGG short-term cell cultures caused decreased protein expression, the expression of ASS1 protein was determined using western blot analysis as described 2.2.11.2. Only 2 of the 4 cultures with methylated *ASS1* as determined by Q-PCR analysis following demethylation with 5-AZA (IN1419 and IN3182), were included in this analysis as it was not possible to extract good quality protein from the others. Seven additional cultures (IN178, IN179, IN1163, IN1930, IN1523, IN1566 and IN3032) were included in the western blot analysis and the results are shown in Figure 7.10. ASS1 protein expression was detected in both the *ASS1*-methylated paediatric HGG short-term cell cultures. This was surprising as both these cultures had shown upregulation of *ASS1* following demethylation with 5-AZA.

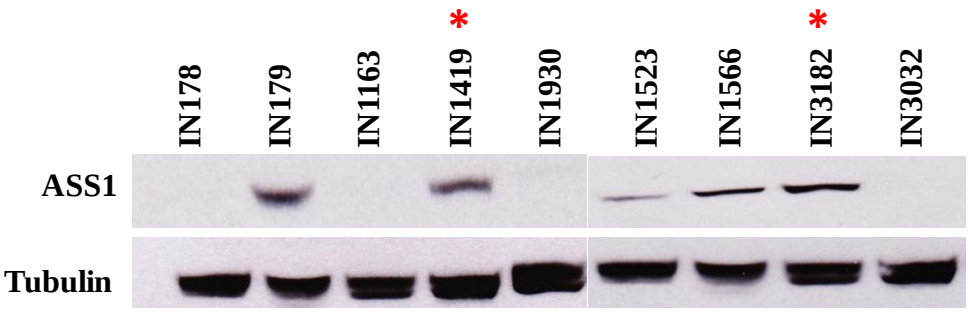

Figure 7.10 Loss of ASS1 protein in paediatric HGG short-term cell cultures. Using western blot analysis, ASS1 protein expression was determined in 9 paediatric HGG short-term cell cultures. Proteins were extracted from cells; 50µg of the extracted protein was used for protein detection; tubulin was used as loading control. (*) indicates *ASS1*-methylaed paediatric HGG short-term cell cultures as determined by Q-PCR analysis following treatment of cells with 5-AZA.

However, similar findings were reported by Syed et al. (2013) in adult GBM primary cultures. They showed that CpG methylation in *ASS1/ASL* inhibits the adaptive transcriptional upregulation of these genes and it is this factor that determines the

sensitivity of cells to ADI-PEG20 rather than the absolute expression levels of these genes.

Among the other paediatric HGG short-term cell cultures assessed for ASS1 protein expression, 5 paediatric HGG short-term cell cultures (IN178, IN1163, IN1930, IN1523 and IN3032) had little or no expression of ASS1, while the remaining paediatric HGG short-term cell cultures (IN179 and IN1566) had relatively higher amounts of ASS1 protein. On comparison of ASS1 protein expression with *ASS1* mRNA in these cultures, it was observed that paediatric HGG short-term cell cultures with relatively similar amounts of mRNA expression had large differences in the rate of translation. For instance, IN179 and IN3032 had comparatively similar mRNA expression with respect to NHA, but the protein product was detected in only IN179. Also, IN1523, which showed highest expression of *ASS1* mRNA had very little protein product compared to other paediatric HGG short-term cell cultures with much less *ASS1* mRNA (IN1566). The disparities in mRNA expression and the translation rate of *ASS1* clearly indicate the complexity of *ASS1* regulation in paediatric HGG short-term cell cultures.

7.2.1.5 Methylation of *ASS1/ASL* predicts sensitivity of paediatric HGG short-term cell cultures to ADI-PEG20

To investigate if *ASS1/ASL*-deficient paediatric HGG short-term cell cultures respond to arginine deprivation therapy using ADI-PEG20, the viability of cells treated with ADI-PEG20 was measured over a period of up to 9 days following initial treatment using SRB cytotoxicity assay, as described in 2.2.3. Initially, the effect of ADI-PEG20 was investigated in 1 of 2 paediatric HGG short-term cell cultures that

demonstrated upregulation of both *ASS1* and *ASL* following treatment with 5-AZA (IN3205). The *ASS1*-methylated adult GBM cell line, LN229 was used as a positive control. Cells were treated with increasing concentrations of ADI-PEG20 (range 0-1 µg/mL) in the presence of citrulline (1 mM) (Sigma-Aldrich Ltd, Dorset, UK), a key precursor of arginine, and cell viability was determined on 1, 3 and 5 days after treatment. Following 5 days of treatment, IN3205 showed comparatively less sensitivity to ADI-PEG20 than LN299. However, the number of IN3205 cells treated with 1µg/mL of ADI-PEG20 was significantly less ($p=0.002$) compared to the untreated control cells. Interestingly, this sensitivity to ADI-PEG20 was comparable to that of LN229 treated with the same concentration of the drug ($p=0.006$). The difference in sensitivity between the 2 *ASS1*-methylated cultures may be due to the difference in their cell type. LN229 is a cell line, while IN3205 is a short-term cell culture. Also, there could be differences in ADI-PEG20 sensitivity between adult and paediatric tumours. However, having observed an encouraging response in the sensitivity to ADI-PEG20 in IN3205, this investigation was extended in additional paediatric HGG short-term cell cultures.

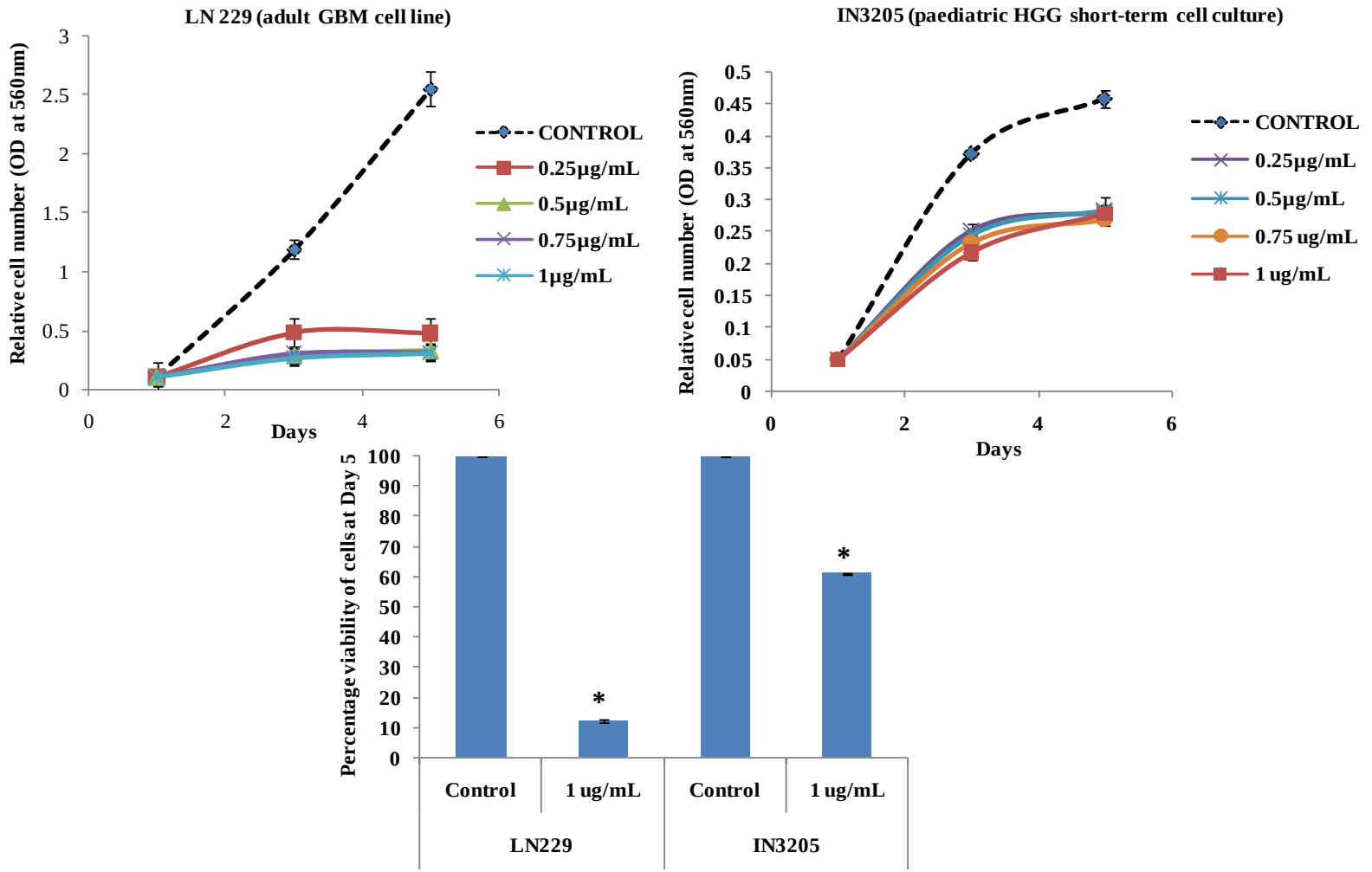

Figure 7.11 Effect of ADI-PEG20 on cell proliferation in paediatric HGG short-term cell culture. IN3205 (*ASS1* and *ASL* methylated) cells were treated with ADI-PEG20 in varying concentrations (0-1µg/mL) and the reduction in cell number was determined in a SRB cytotoxic assay following treatment for 1, 3 and 5 days. LN229, an *ASS1*-methylated adult GBM cell line was used as positive control. The bar chart shows the percentage viability of IN3205 and LN229 cells 5 days following treatment. IN3205 (p=0.002) and LN229 (p=0.006) demonstrated statistically significant reduction in cell number compared to the untreated control cells.

Syed et al. (2013) has demonstrated that methylation of *ASS1*, but not *ASL* is the decisive factor that predicts sensitivity of adult GBM cells to ADI-PEG20 and that co-methylation of *ASS1* and *ASL* results in hypersensitivity to the drug (Syed et al., 2013). To investigate this in paediatric HGG short-term cell cultures, 3 cell cultures with varying *ASS1/ASL* methylation status (IN178-*ASS1*-unmethylated, *ASL*-methylated; IN1419-*ASS1*-methylated, *ASL*-unmethylated and IN3182-*ASS1*-methylated, *ASL*-methylated) were assessed for their sensitivity to ADI-PEG20 using SRB assay as described above. The *ASS1* and *ASL*-unmethylated paediatric HGG short-term cell culture, IN179 was used as a negative control. The antiproliferative effect of ADI-PEG20 in 4 paediatric HGG short-term cell cultures including the negative control is shown in Figure 7.12.

The paediatric HGG short-term cell culture with co-methylation of *ASS1* and *ASL* (IN3182) or methylation of *ASS1*, but not *ASL* (IN1419) demonstrated similar dose response curves for ADI-PEG20. By contrast, the paediatric HGG short-term cell culture with unmethylated *ASS1*, but methylated *ASL* (IN178) showed little/no sensitivity to ADI-PEG20, demonstrating similar response to that of the negative control (IN179). These results showed that *ASS1* is the key determinant of ADI-PEG20 in paediatric HGG short-term cell cultures and were in agreement with the findings of Syed et al. (2013) in adult GBM primary cultures. However, unlike adult GBM cell cultures, co-methylation of *ASS1* and *ASL* did not result in increased sensitivity to ADI-PEG20 compared to methylation in only *ASS1* or *ASL*.

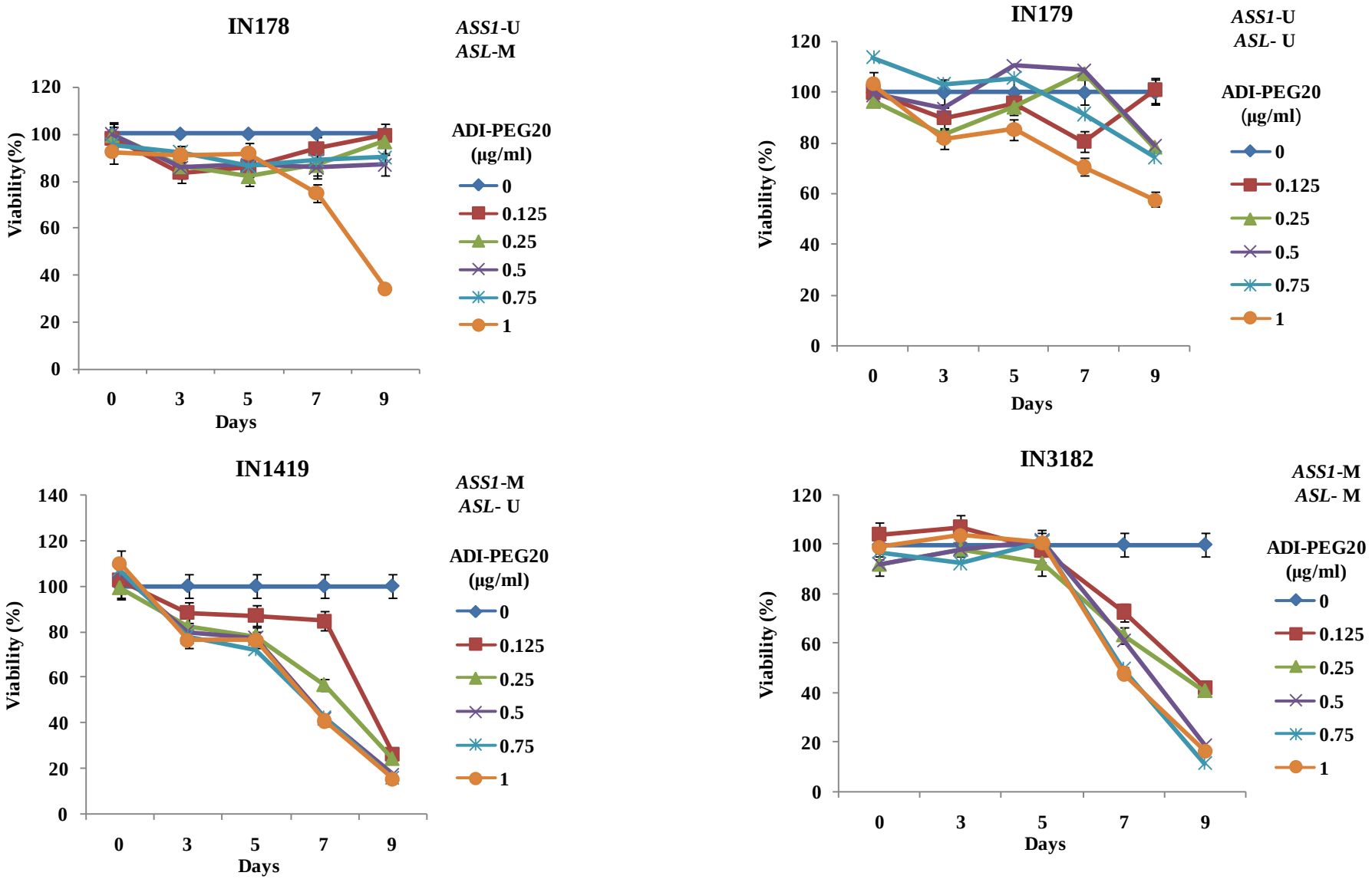

Figure 7.12 Antiproliferative effect of ADI-PEG20 in paediatric HGG short-term cell cultures. Cells were treated with ADI-PEG20 (0-1 µg/mL) and reduction in cell number treatment were determined at 3, 5, 7 and 9 days following treatment using a SRB cytotoxicity assay. Methylation status of *ASS1* and *ASL* in each samples are shown M indicates methylated and U indicates unmethylated.

7.2.2 Targeting PI3K/Akt pathway in paediatric HGG short-term cell cultures

7.2.2.1 Aberrations in the PI3K pathway network in paediatric HGG short-term cell cultures

The majority of the investigations to identify PI3K pathway alterations in cancers have focused on alterations in the core components of the pathway such as *PIK3CA, PIK3R1, AKT, PTEN* and mTOR. However, alterations in these targets occur at relatively lower frequencies in paediatric HGG. In this study, alterations in genes that may indirectly contribute to aberrant activation of the PI3K pathway in paediatric HGG were identified. Genetic and/or epigenetic changes that contribute to aberrant activation of PI3K pathway were identified from genome-wide copy number changes and genetic mutations (described in Chapter 4), gene and miRNA expression (described in Chapters 5 and 6) and methylation changes (described in Chapter 7) identified in paediatric HGG short-term cell cultures. A summary of these genes is given in Figure 7.13.

Copy number gain of *PIK3CA*, one of the core components of the PI3K subunit was altered in 17.65% paediatric HGG short-term cell cultures (Table 4.12). BRAFV600E mutation was detected in 1 paediatric HGG short-term cell culture (IN179). There were 3 miRNAs that were upregulated in these cultures consisting of miR142-3p, miR-16-2-3p, miR-138 and miR-183. *PIK3CA* and the 2 major downstream signaling components, *AKT1* and *AKT2* were upregulated in these tumours. Interestingly, there were several genes that were hypermethylated and/or downregulated in these short-term cell cultures that have potential roles in the aberrant activation of PI3K pathway. These comprised *MYH10, PTPRE, ITGB2,*

KRT8, DAB1, FHIT, PIK3R5 and *PRKG2. PIK3R5* encodes the regulatory subunit of PI3K, which has not previously been investigated. Two miRNAs, associated with PI3K pathway were downregulated in these cultures.

PIK3R5 encodes the core component of PI3K complex and has not previously been investigated. Promoter hypermethylation of *PIK3R5* in paediatric HGG short-term cell cultures was validated by CoBRA, as described in 2.2.8.3. Methylation was detected in 13/17 (76.5%) paediatric HGG short-term cell cultures (Figure 7.14 A). To assess if promoter hypermethylation of *PIK3R5* induced downregulation in paediatric HGG short-term cell cultures, the expression of this gene was determined in 10 paediatric HGG short-term cell cultures following demethylation with 5µM 5-AZA. *PIK3R5* was re-expressed in 6/10 (60%) paediatric HGG short-term cell cultures treated with 5-AZA compared to the untreated control cells (7.14 B). Furthermore, RT-PCR analysis was carried out to determine the differential expression of *PIK3R5* in paediatric HGG short-term cell cultures in comparison to NHA. *PIK3R5* was absent in 12/17 (71%) paediatric HGG short-term cell cultures consisting of 9 non-DIPG (IN178, IN179, IN1163, IN1419, IN1523, IN1566, IN3046, IN3182 and IN3183) and all 3 DIPG (IN2087, IN2102 and IN2675) (Figure 7.14 C). The only paediatric HGG short-term cell culture with relatively higher expression of *PIK3R5* was IN3205, but this difference is more likely due to the low expression observed in NHA as upregulation of this gene was observed in IN3205 following demethylation with 5-AZA (Figure 7.14 B).

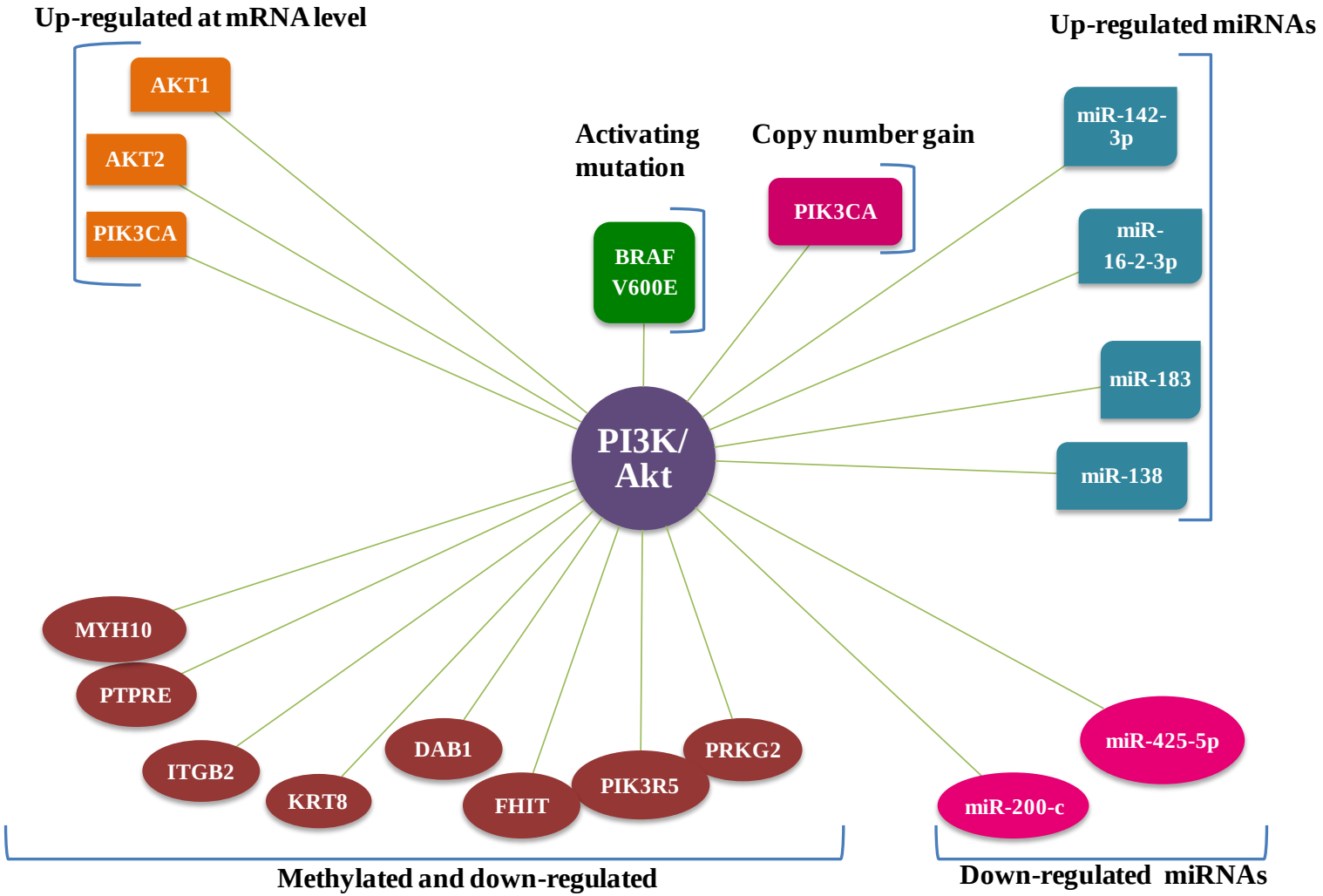

Figure 7.13 Genes contributing to aberrant PI3K signaling in paediatric HGG short-term cell cultures. Using microarray technology, genomic CNAs, promoter DNA methylation, mRNA and micro RNA expression in 17 paediatric GBM short-term cell cultures, including 3 diffuse intrinsic pontine glioma (DIPGs) were assessed. Dysregulated genes that may contribute to aberrant PI3K signaling were identified. A summary of the most relevant genes is shown.

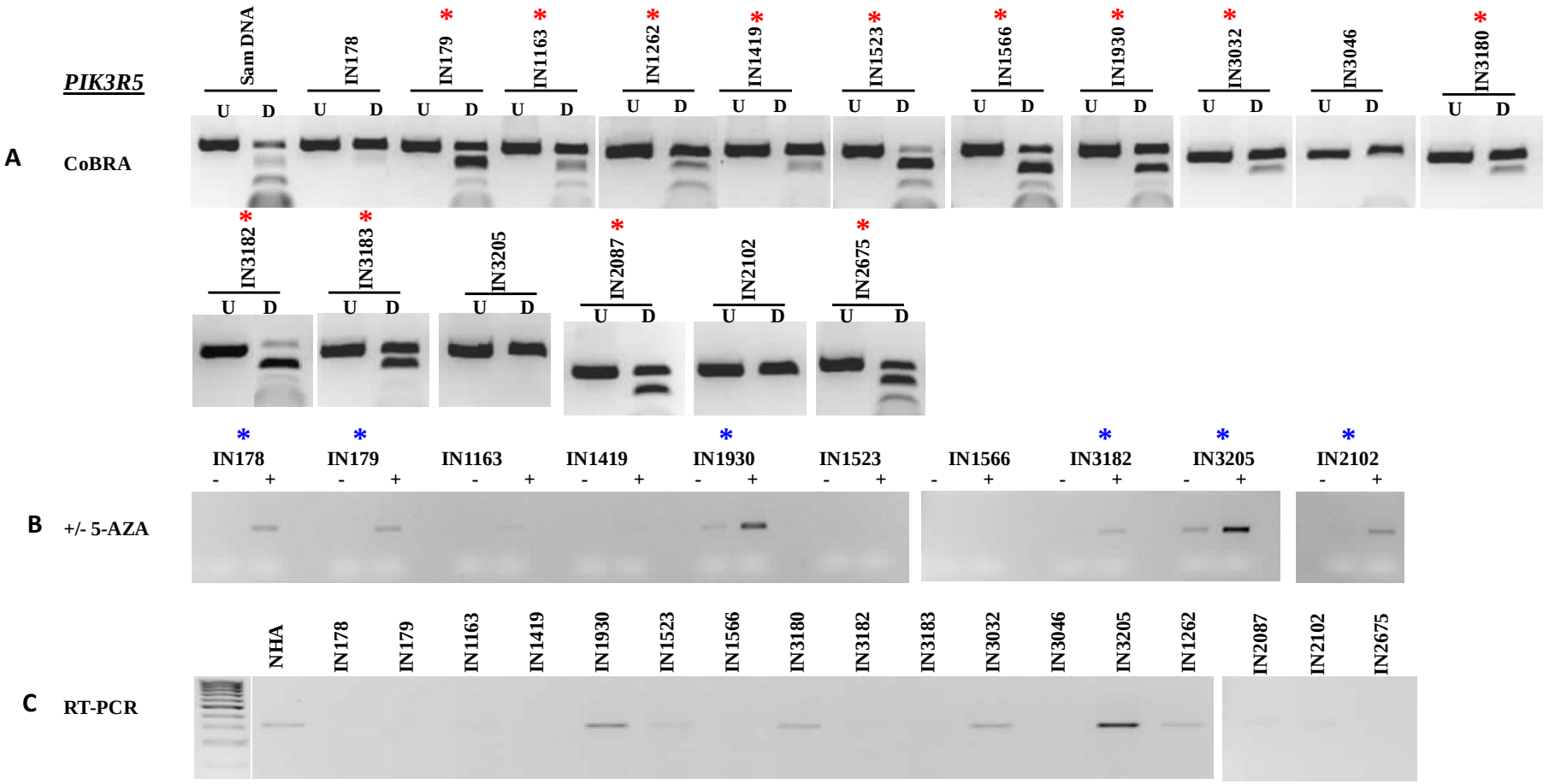

Figure 7.14 Promoter hypermethylation-induced down regulation of *PIK3R5* in paediatric HGG short-term cell cultures. Dysregulation of *PIK3R5* was assessed in 17 paediatric HGG short-term cell cultures. **A.** CoBRA PCR was used to determine methylation status of *PIK3R5* (Sam DNA- Fully methylated DNA used as positive control; U-undigested, D-digested; (*) indicates methylation). **B.** Cells were treated with 5μM 5-AZA and the mRNA expression of *PIK3R5* following treatment was determined in untreated (-) and treated (+) cells using RT-PCR analysis (*indicates re-expression after treatment). **C.** Endogenous expression of *PIK3R5* in paediatric HGG short-term cell cultures as determined by RT-PCR analysis. With the exception of IN3205, *PIK3R5* was downregulated in the majority of the paediatric HGG short-term cell cultures in comparison to a normal control (NHA).

7.2.2.2 Investigation of the effect of PI-103 on cell viability in paediatric HGG short-term cell cultures

To investigate the growth inhibitory effect of PI-103 in paediatric HGG short-term cell cultures, 3 paediatric HGG short-term cell cultures that had genetic aberrations associated with aberrant PI3K signaling (IN3182, IN179 and IN1523) were treated with a PI3K-inhibitor, PI-103 (Selleckchem, USA) and the reduction in cell viability after 72 hours was assessed using MTT cytotoxicity assay, as described in 2.4.2. IN3182 had gain of *EGFR,* and IN179 and IN1523 had gain of *PIK3CA* (Table 4.12). The antiproliferative effect of PI-103 was also assessed in NHA. The results are shown in Figure 7.15.

Following treatment with PI-103, all 3 paediatric HGG short-term cell cultures demonstrated dose-dependent effects on cell proliferation. The reduction in cell number following 72 hours of treatment with PI-103 was much higher in IN1523 (IC50-105.7nm) compared to IN3182 (IC50-582.9nm) and IN179 (IC50-634.6nm). Interestingly, PI-103 showed very little effect on NHA (IC50-6684.9 nm). The main difference between IN1523 and the other cultures was that IN1523 had higher number of CNAs (Table 4.4) and it also had a unique genetic profile and clustered independently of all other samples analysed in this study (Figure 4.16).

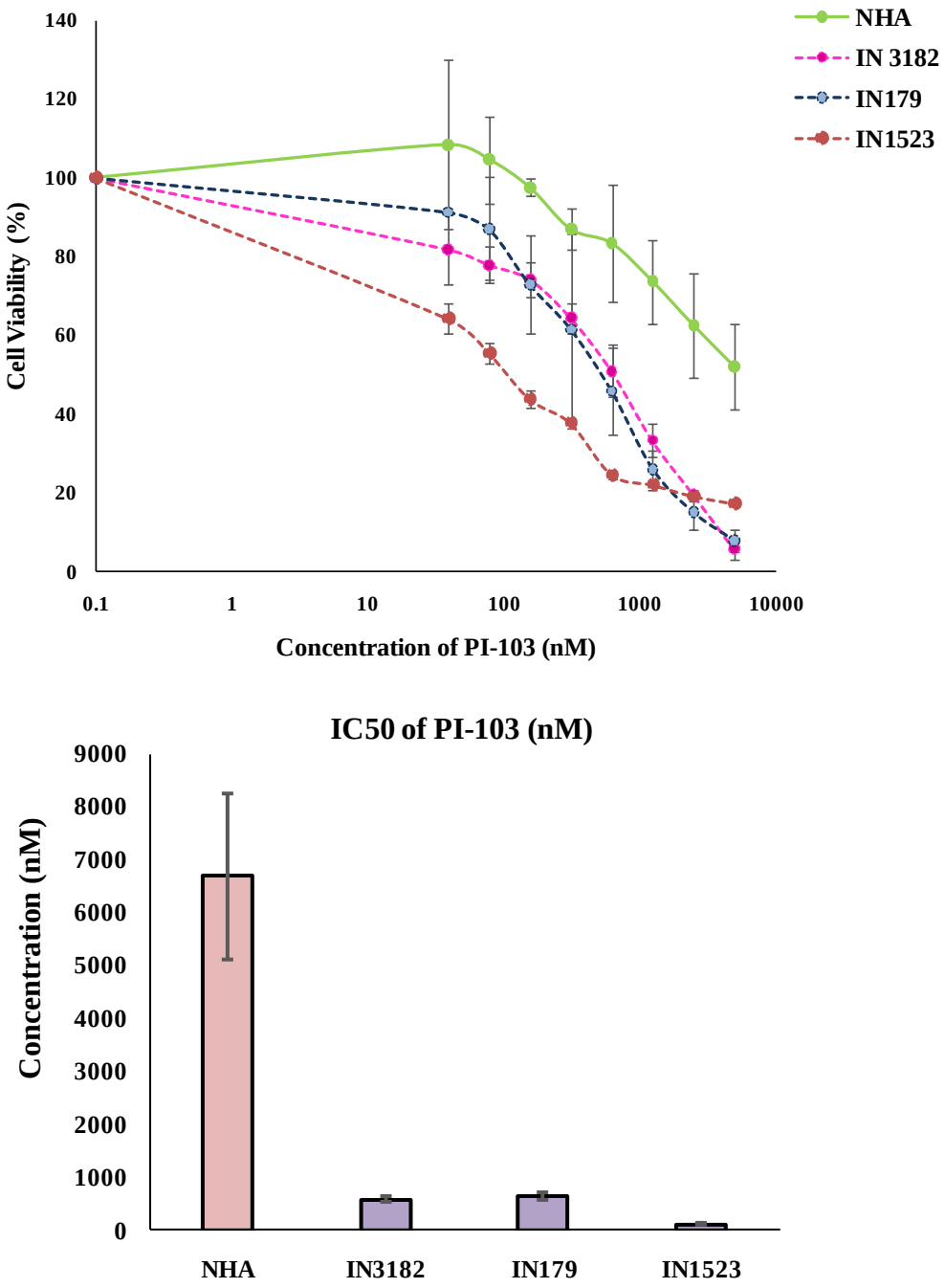

Figure 7.15 PI-103 reduced cell proliferation in paediatric HGG short-term cell cultures *in vitro.* MTT cytotoxicity assay was performed using PI-103 (0-10000nm) in NHA and 3 paediatric HGG short-term cell cultures. **A.** PI-103 reduced cell viability in paediatric HGG short-term cell cultures and demonstrated much reduced anti-proliferative effect on NHA. **B**. IC50 of PI-103 in NHA, IN3182, IN179 and IN1523 are shown. Error bars indicate standard deviation.

7.3 Discussion

HGG in children are extremely aggressive with no effective treatment that can significantly prolong the survival rates in the affected population (Fangusaro, 2012; Gerges et al., 2013). As such, the requirement to identify novel therapeutic strategies that are less damaging to the developing brain is critical. This Chapter has focussed on the investigation of deregulations in 2 important cellular pathways in paediatric HGG short-term cell cultures; the arginine biosynthesis pathway and the PI3K/Akt pathway. The data presented here show that these pathways are disrupted in a proportion of paediatric HGG short-term cell cultures including DIPG. The potential clinical utility of specific small molecule inhibitors that can target these pathways were investigated in paediatric HGG short-term cell cultures *in vitro*.

Dysregulation of arginine biosynthesis pathway in paediatric HGG short-term cell cultures

Promoter hypermethylation of ASS1/ASL in paediatric HGG short-term cell cultures

Tumour cells with deficient ASS1 and/or ASL, the 2 key elements of the arginine biosynthesis pathway have shown increased dependency on external arginine resources making them sensitive to cell death induced by arginine deprivation (Scott et al., 2000; Seyfried et al., 2013). Although deregulation of *ASS1/ASL* has been identified in a number of tumour types, its incidence in paediatric HGG has not been widely investigated (Huang et al., 2013; Syed et al., 2013; Lan et al., 2014). This study reports that *ASS1* and/or *ASL* are deregulated in a subset of paediatric HGG short-term cell cultures, and promoter hypermethylation plays a major role in their downregulation in a proportion of these tumours.

The Illumina Infinium HumanMethylation 450 K microarray analysis conducted on NHA, 17 paediatric HGG short-term cell cultures and 5 biopsy samples revealed that *ASS1* and *ASL* were frequently methylated in these tumours compared to NHA with relatively higher frequency of methylation of *ASS1* over *ASL*. Three independent techniques (CoBRA, MSP and Q-PCR analysis following global demethylation by 5-AZA) were used to validate promoter methylation of *ASS1/ASL* in paediatric HGG short-term cell cultures. Using CoBRA and MSP, *ASS1* methylation was identified in paediatric HGG short-term cell cultures in specific CpG rich regions in its promoter CpG Island. However, as these two techniques were designed to determine methylation in different CpG sites, there was little concordance between these techniques in most cases. Nevertheless, both the techniques uniformly detected methylation of *ASS1* in a minimum of 3/17 (~18%) paediatric HGG short-term cell cultures (IN1163, IN1262 and IN3032), which provided the first experimental evidence for *ASS1* methylation in these paediatric HGG short-term cell cultures. Independently, *ASS1* methylation was detected by CoBRA in ~24% and by MSP in 41-47% (regions 1 and 2) of paediatric HGG short-term cell cultures, respectively. The role of promoter hypermethylation as a crucial epigenetic mechanism regulating the expression of tumour suppressor genes is widely established (Estellar, 2007). Methylation of *ASS1* in the promoter CpG sites in paediatric HGG short-term cell cultures indicates a potential tumour suppressive role for this gene in these tumours. In comparison to *ASS1*, *ASL* methylation in paediatric HGG short-term cell cultures could not be detected by the PCR-based methods used in this study, but this may be mainly due to the limited number of CpG sites that could be analysed for methylation using these techniques.

Interestingly, promoter methylation of *ASS1* in paediatric HGG short-term cell cultures was demonstrated by its upregulation in cells following global demethylation with 5-AZA. Upregulation of *ASS1* was detected in 4/9 (~44%) paediatric HGG short-term cell cultures (IN1419, IN2102, IN3182 and IN3205), and that of *ASL* was identified in 4/9 (~44%) paediatric HGG short-term cell cultures (IN1163, IN1930, IN3182 and IN3205), with co-methylation of *ASS1* and *ASL* in 2 cases (IN3182 and IN3205). One of the commonalities of IN3182 and IN3205 cultures was their highly unstable genetic profiles relative to the majority of the other samples analysed here (as described in Chapter 4, Table 4.14). IN3182 and IN3205 had CNAs in 17.24% and 5.81% of their genomes respectively, whilst the majority of the paediatric HGG short-term cell cultures had relatively normal karyotypes (<1% genome changed). This indicates a potential association of *ASS1* methylation with tumour aggressiveness. The incidence of co-methylation of *ASS1* and *ASL* has not been reported in many cancers, but has been identified in adult GBM (Syed et al., 2013). The overlap of this epigenetic event in paediatric HGG short-term cell cultures may therefore reflect the unique microenvironment persisting in the brain in comparison to any other organ in the body that may cause larger selective pressure to disrupting the arginine biosynthetic pathway in tumours originating from brain. However, the investigation of the therapeutic intervention of arginine biosynthetic pathway in cancers is in its early stage. Therefore, further investigations of these specific epigenetic mechanisms in brain tumours may provide better insights into the possibility of such unique selection pressure in these tumours.

Paediatric HGG short-term cell cultures demonstrate sensitivity to AD1-PEG20

Promoter hypermethylation of *ASS1* in cancers such as lymphoma, melanoma and adult GBM has been identified as a biomarker for predicting sensitivity to cell death induced by arginine depleting agents like ADI-PEG20 (Delage et al., 2012; Feun et al., Syed et al., 2013). The sensitivity of paediatric HGG short-term cell cultures to ADI-PEG20 observed in this study identifies a similar role for *ASS1* methylation in these tumours. ADI-PEG20 readily induced a decrease in cell viability in *ASS1*-methylated paediatric HGG short-term cell cultures (IN1419, IN3182 and IN3205) compared to the unmethylated cell culture (IN179) at very low concentrations of the drug (up to 1µg/mL). In addition, the paediatric HGG short-term cell culture with methylation of only *ASL* and not *ASS1* (IN178) demonstrated less sensitivity to ADI-PEG20 in comparison to the cell culture with methylation of only *ASS1* but not *ASL* (IN1419) or methylation of both *ASS1* and *ASL* (IN3182), which supports the previous findings on the predictive role of *ASS1* methylation on ADI-PEG20 sensitivity in adult GBM primary cultures (Syed et al., 2013). However, unlike in adult GBM cultures, there was no increase in the sensitivity to ADI-PEG20 in paediatric HGG short-term cell cultures that had co-occurrence of *ASS1* and *ASL* methylation compared to the cell culture with only *ASS1* methylation, although this may be due to the small number of samples available for this study. In this analysis, there were only 2 paediatric HGG short-term cell cultures with methylation in both *ASS1* and *ASL*, of which only 1 (IN3182) could be included in the comparison study of ADI-PEG20 sensitivity using samples with varying *ASS1/ASL* methylation status. The other paediatric HGG short-term cell culture (IN3205) had a very low growth rate and was difficult to utilise for drug testing over a period of 9 days (Figure 7.11).

However, there is also a possibility that the co-disruption of *ASS1* and *ASL* and the consequent failure in arginine renewal may modulate different downstream cellular processes in paediatric HGG compared to those in an adult setting, or may affect similar processes but in different ways. For instance, ADI-PEG20 has demonstrated induction of an initial autophagic response in adult GBM cells and showed enhanced antiproliferative activity upon blockade of such response using an autophagy inhibitor, chloroquine (Syed at al., 2013). Increased autophagic responses to nutrient starvation have been demonstrated in paediatric brain tumours such as medulloblastoma and teratoid/ rhabdoid tumour cell lines (Levy and Thornburn, 2012). However, the differences in responses to specific nutrient depletion between adult and paediatric brain tumours are not very clear.

One of the main hurdles in the development of efficient chemotherapeutics for treatment of brain tumours is the failure of these agents to cross the BBB. As ADI-PEG20 works by depleting arginine from peripheral blood, crossing of the BBB is not a requirement for its anti-tumour activity (Syed et al., 2013). In addition, as ADI-PEG20 acts in a tumour-specific manner, it should cause little/no damage to the normal brain. This is extremely important in paediatric HGG patients as chemotherapeutic agents can cause irreversible damage to the developing brain leaving the survivors of this age group with poor quality of life due to serious late effects on cognition and in some cases, making them vulnerable to secondary malignancies (Karremann et al., 2015). Taken together, the sensitivity to ADI-PEG20 demonstrated in paediatric HGG short-term cell cultures in this preliminary investigation holds promise for the therapeutic intervention of arginine biosynthesis pathway in the management of these tumours.

Complexity of ASS1 regulation in paediatric HGG may be cell type dependent

In comparison to *ASL*, *ASS1* displayed a high degree of complexity in its regulation in the paediatric HGG short-term cell cultures analysed here. In all 3 cases of *ASL* promoter methylation identified in this study, *ASL* mRNA was downregulated supporting the role of promoter methylation in *ASL* regulation. However, such straightforward correlation was absent for *ASS1*. Although *ASS1* was upregulated in paediatric HGG short-term cell cultures following demethylation with 5-AZA, methylation of *ASS1* did not always induce its transcriptional down regulation in these cells. One of the reasons for this lack of correlation between promoter methylation and relatively high expressions of *ASS1* in these paediatric HGG short-term cell cultures could be due to the low basal levels of *ASS1* detected in the control NHA that was available for this study, making the absolute expression levels of this gene in the tumour cells appear much higher. Further investigations using additional normal controls such as normal brain may provide better understanding of the level of *ASS1* expression in such samples. The other reason for *ASS1* methylation not always resulting in its down regulation could be attributed to the requirement of additional mechanisms of gene regulation such as histone modifications that may be essential for the establishment of *ASS1* silencing in these tumours.

In addition, the expression of *ASS1* was found to decrease in some cells following demethylation with 5-AZA. This is not unexpected to occur as 5-AZA is a global demethylating agent of CpGs across the whole genome that may relieve the repression of some transcription factors leading to changes in gene expression (Maunakea et al., 2010). For instance, transcription factors such as c-Myc/Myn, have recognition sites containing CpG sites that are inhibited by methylation (Allis et al.,

2007). De-repression of such TFs may have significant consequences in the expression levels of genes regulated by them. Thus, the downregulation of *ASS1* post-demethylation in paediatric HGG short-term cell cultures provide clues about additional metabolic players in the regulation of *ASS1* that may be valuable indicators of therapeutic resistance to metabolism-based treatment strategies in paediatric HGG.

Moreover, *ASS1* demonstrated differences between its mRNA expression levels and translation rates that varied between cell cultures, indicating inter-tumour heterogeneity in the regulation of this gene. For instance, IN1523 demonstrated the highest *ASS1* mRNA expression but had very low levels of ASS1 protein, and cultures with similar mRNA expression (IN179 and IN3032) demonstrated large differences in their levels of protein expression. These imply that different mechanisms of post translational events such as regulation by non-coding RNAs could operate in different tumours that may affect the rate of translation of *ASS1*. Furthermore, although promoter methylation is widely recognised in inducing gene silencing, 2/3 *ASS1*-methylated paediatric HGG short-term cell cultures (IN1419 and IN3182) demonstrated a considerable amount of ASS1 protein expression. Interestingly, a similar finding was also reported by Syed et al. (2013) in adult GBM cell lines in which methylation of *ASS1/ASL* rather than their absolute expression levels was the key predictor of sensitivity to arginine deprivation therapy. These authors demonstrated that treatment with ADI-PEG20 caused adaptive increase of *ASS1/ASL* mRNA in unmethylated GBM cell line, but not in the methylated GBM cell line. However, upregulation of these genes in the methylated GBM cell line was induced upon demethylation with 5-AZA. It has been reported that modifications in gene promoters not always result in gene repression as transactivators can compete

with methyl binding proteins to maintain an open chromatin state (Curradi et al., 2002). This genomic complexity of *ASS1* may explain some of the discrepancies observed between different levels of *ASS1* regulation in the paediatric HGG short-term cell cultures analysed here.

The exact impact of ASS1/ASL loss in cancers is not clear. However, methylation-induced down regulation of *ASS1* in many cancers including osteosarcoma, ovarian and pancreatic cancers is reported to be associated with poor clinical outcome (Nicholson et al., 2009; Kobayashi et al., 2010; Allen et al., 2014). In paediatric HGG, aberrations in this pathway may have crucial impact on the development of brain as arginine is an important amino acid required for normal brain development and developmental disorders in children may have an impact on predisposing them to cancer.

Limitations of the analysis

Promoter CpG methylation of *ASS1* and/or *ASL* as determined by CoBRA and MSP reported in this study did not demonstrate satisfactory correlation between methylation and mRNA/protein expression of these genes. This could be due to the limitations of such PCR-based techniques that can only examine methylation in specific lengths of DNA. More efficient techniques such as pyrosequencing may provide better in-depth analysis of *ASS1/ASL* CpG methylation in these tumours. In addition, although demethylation by 5-AZA and the presence of mRNA expression post-treatment is a good indicator of promoter methylation the use of 5-AZA alone does not always result in reactivation of hypermethylated genes. The role of the cross-talk between DNA methylation and histone modifications in gene silencing has been increasingly understood, which involves the recruitment of histone deacetylases

to methylated DNA and MeCP2 (Jones et al., 1998). Therefore, treatment with 5-AZA alone may not restore hypermethylated genes in sufficient amounts to be detected by PCR. This could be one of the reasons why re-expression of *ASS1* was not detected following treatment with 5-AZA in at least some cases of low basal expression. Treatment of cells with 5-AZA and HDAC inhibitors may be useful for future investigations.

Dysregulations in the PI3K pathway in paediatric HGG short-term cell cultures

Genetic and/or epigenetic changes contribute to aberrant activation of PI3K pathway in paediatric HGG short-term cell cultures

The PI3K pathway is regulated by a complex network of genes that operate in a coordinated fashion in normal cells to maintain their growth, survival and proliferation (Liu et al., 2009). The high frequency of PI3K pathway aberrations in cancers has elicited great interest in targeting this pathway using small molecule inhibitors that can specifically inhibit various isoform of PI3K. The majority of the investigations on PI3K pathway alterations in cancers have focused on alterations in the core components of the pathway such as *PIK3CA, PIK3CB, PIK3R1, AKT, PTEN* and *mTOR.* However, alterations in these targets occur at relatively lower frequencies in paediatric HGG (Jones et al., 2012). The data from this analysis reveal that genetic and/or epigenetic alterations in paediatric HGG short-term cell cultures contribute to aberrant signaling by PI3K and offer therapeutic opportunity to target such tumours using specific small molecule inhibitors like PI-103. The major genetic changes that contribute to dysregulated PI3K pathway signaling in a subset of the paediatric HGG short-term cell cultures analysed here included gain of *PIK3CA,* activating mutations in *BRAF* and overexpression of *AKT1, AKT2* and *PIK3CA.*

Interestingly, there were genes with known associations with aberrant PI3K signalling that were hypermethylated and/or downregulated in paediatric HGG short-term cell cultures, indicating the role of epigenetic mechanisms in regulating PI3K pathway. One of the frequently hypermethylated gene identified in this study was *PIK3R5*, a gene that encodes the 101 kDa regulatory subunit of the PI3K enzyme complex. Promoter hypermethylation-induced down regulation of *PIK3R5* was identified in 60% of the paediatric HGG short-term cell cultures investigated here. Deregulation of *PIK3R5* by promoter hypermethylation in paediatric HGG has not previously been reported. However, cancer-specific genetic and epigenetic changes in this gene have been previously identified. For instance, novel activating mutations in *PIK3R5* have been reported in metastatic melanoma and a high frequency of differential hypermethylation has been reported in primary oral squamous cell carcinoma (Khor et al., 2014). It has also been identified to be downregulated in gastric cancers, while overexpression of this gene has been demonstrated to induce sarcomagenesis (Martin et al., 2011; Shull et al., 2012; Khor et al., 2014). It is likely that down regulation of *PIK3R5* may be a potential biomarker that would be useful as a prognostic indicator in paediatric HGG.

Other frequently dysregulated genes included *DAB1* and *PTPRE*, the anti-growth effects of which have been demonstrated in paediatric HGG short-term cell cultures *in vitro* (6.2.4.1). *DAB1* has important roles in neuronal migration and in mediating extracellular signals from reelin through PI3K/Akt pathway (Beffert et al., 2002; Franco et al., 2011; Niu et al., 2004). Recently, *PTPRE* has been identified as a regulator of autophagy and this perhaps relates its functional activity to PI3K pathway activation in these tumours (Puustinen et al., 2014).

The incidence of *FHIT* aberrations in cancers has been widely studied, and its two-way functionality as tumour suppressor or oncogene in different cancers has been reported. The down regulation of this gene by promoter hypermethylation in paediatric HGG short-term cell cultures indicates that is likely to have tumour suppressive roles in paediatric HGG; this requires additional validation of this finding in an extended cohort of samples. *FHIT* has been identified as an inhibitor of proliferation and facilitator of apoptosis in cholangiocarcinoma cells through the inhibition of PI3K/Akt pathway, while *FHIT* itself is repressed by PI3K and AKT through the PI3K/Akt/FOXO pathway (Kelly and Berberich, 2011; Huang et al., 2014).

PRKG2, which encodes a cyclic guanosine monophosphate (cGMP)-dependent protein kinase that belongs to the family of serine/threonine protein kinases has been demonstrated as an inhibitor of cell proliferation in adult glioma cells through suppression of Akt phosphorylation (Swartling et al., 2009). It has also been identified as an inhibitor of *EGFR* activation in breast and gastric cancer cells (Lan et al., 2012; Jiang et al., 2014).

MYH10 belongs to the myosin family of genes that encode actin-dependent motor proteins called myosins involved in a variety of functions such cell division and motility (Catherine et al., 2010). It is negatively regulated by PI3K pathway (Lindsey et al., 2010).

One of the important miRNAs identified in this study was miR-142-3p, recently identified as a regulator of cancer stem cell-like characteristics (Chai et al., 2014). MiR-142-3p regulates stem-cell like properties in HCC by directly targeting CD133 and hyperactivation of PI3K pathway is critical for cancer stem cell renewal

(Dubrovska et al., 2009). Identification of the mRNA targets of this miRNA in paediatric HGG short-term cell cultures may lead to better insights into its role as a modulator of the PI3K pathway in stem cell-like phenotypes in these tumours. Further investigations into the role of these genes in PI3K pathway activation in paediatric HGG may lead to the development of predictive biomarkers for therapeutic intervention of this pathway in the clinical management of these tumours.

Targeted therapy in paediatric HGG short-term cell cultures using PI-103

PI-103, a dual inhibitor of PI3K and mTOR signaling pathway has shown promising results in preclinical studies conducted *in vitro* as well as *in vivo* preclinical models in cancers including adult glioma (Fan et al., 2008; Zou et al., 2009). However, its therapeutic efficacy in paediatric HGG has not been previously demonstrated. The preliminary drug testing assays in this study have shown that paediatric HGG short-term cell cultures are sensitive to PI-103, at very low concentrations (range of IC50-100-700nM). In addition, the normal astrocytoma cells (NHA) were much less sensitive to PI-103, suggesting the tumour-specific hyperactivation of this pathway, thus providing hopes for therapeutic targeting of this pathway in paediatric HGG. However, considering the essential role of this pathway in the regulation of growth and survival in normal cells in the body and its position in cellular metabolism as a master regulator of various intricate signalling networks essential for normal development, the successful manipulation of this pathway in cancer cells is an open challenge, particularly in paediatric brain tumours due to concerns of damage to the developing brain. Combination therapy involving low concentrations of small molecule inhibitors of PI3K with inhibitors targeting other aberrant pathways in paediatric HGG may be the key for a better exploitation of this pathway as a

therapeutic strategy in these tumours. The therapeutic efficacy of combination therapy with PI-103 and stem cell-delivered secretable tumour necrosis factor apoptosis-inducing ligand (S-TRAIL) has been demonstrated *in vitro* as well as in intracranial glioma mouse models, offering the scope for the potential extension of such investigations in the paediatric population (Bagci-onder et al., 2010). The occurrence of epigenetic dysregulation of genes contributing to aberrant PI3K signaling in paediatric HGG short-term cell cultures in this study together with the increasing understanding of the role of chromatin and histone modifications in the development of these tumours offers opportunities for the investigation of combination strategies targeting such events in these tumours. The combined use of BEZ235, a PI3K inhibitor and panobinostat, a histone deacetylase inhibitor has shown significant anti-tumour response in other cancers such as prostate cancer in comparison to the independent use of each treatment by attenuating the DNA damage repair protein ATM (Ellis et al., 2013).

7.3 Conclusions

One of the important aspects of this study was the use of well-characterised paediatric HGG short-term cell culture models, which were demonstrated to maintain a considerable proportion of genomic changes, originally present in their parent biopsies (see 3.2.1, 3.2.2, 3.2.3 and 3.2.4). This raises confidence in the observed sensitivity of paediatric HGG short-term cell cultures to the anti-cancer agents tested in this study. These therapeutic opportunities generated by genetic and/or epigenetic changes in paediatric HGG short-term cell cultures may provide better approaches to effective management of these tumours.

CHAPTER 8

Final discussion and conclusions

8.1 Discussion

Paediatric HGG are a group of heterogeneous tumours that represent 8-12% of CNS tumours in children (Bondy et al., 2008). The current treatment strategies for these tumours largely involve focal radiotherapy and chemotherapy, but unfortunately, they fail to respond to such treatments and continue to remain fatal tumours of childhood. Even in patients who survive, the complications of serious late effects on cognition and endocrine dysfunction have undesirable impacts on the quality of life (Reimers et al., 2003; Mulhern et al., 2004; Sanders et al., 2007). As such, there is a compelling need for the development of effective therapeutics for the management of these tumours in children.

One of the major obstacles in the development of effective chemotherapeutics for the treatment of paediatric HGG is the lack of understanding of the molecular biology of underlying pathogenesis. Very few investigations have been carried out in paediatric HGG in comparison to adult HGG (Bax et al., 2010; Jones et al., 2012). One of the main hindrances in conducting paediatric HGG studies is the difficulty in obtaining tumour samples as well as the lack of availability of well-characterised, representative pre-clinical models. Furthermore, the approaches followed by the majority of previous studies in paediatric HGG was largely based on evaluating the similarities and differences in selected candidate genes between adult and paediatric HGG. It is only recently that genome-wide analyses of these tumours have begun to reveal unique genomic changes associated with paediatric HGG. This study, to an extent, has addressed these two issues encountered in paediatric HGG studies in order to improve the prospects of future investigations.

Analysis of paired biopsy and culture samples in this study revealed that the patient-derived paediatric HGG short-term cell cultures maintained a considerable proportion of genomic changes present in the original tumour biopsies and may be used as pre-clinical models for paediatric HGG molecular biology studies. Although there were relatively more genomic changes in the cell cultures compared to the biopsies in each pair that reflected the influence of artificial culture conditions, these patient-derived cell cultures retained some of the characteristic signatures of paediatric HGG making them appropriate *in vitro* models for evaluation of targeted therapeutics. This was further supported by the identification of paediatric HGG-associated mutations in these cell cultures. For instance, *H3F3A* (K27M) mutation was detected in 2/17 (~12%) cases (1/14 non-DIPG and 1/3 DIPG) and *BRAFV600E* mutation in 1/17 (1 non-DIPG) (~6%) case, respectively. Although this study was constrained by small sample size, these frequencies were comparable to the reported frequencies in paediatric HGG (Wu et al., 2012). Moreover, *H3F3A* (K27M) are relatively more frequent in DIPGs than supratentorial HGGs, and *BRAFV600E* has been restricted to non-DIPG; these are in agreement with the data presented here. The potential utility of patient-derived cell cultures has been demonstrated in other cancers including adult GBM (Bignotti et al., 2006; Potter et al., 2009; Yost et al., 2013). In the study by Yost et al. (2013), adult GBM-derived cultures retained mutations in classic GBM genes such as *PTEN* and *TP53.*

The evidence for cross talk between genetic and epigenetic mechanisms in paediatric HGG was laid with the identification of histone mutations in these tumours (Schwartzentruber et al., 2012; Wu et al., 2012). Taking these into account, high-resolution microarray technology was used to conduct genome-wide profiling of copy number, gene and miRNA expression, and methylation changes in 17

paediatric HGG short-term cell cultures including 3 DIPG. This also incorporated integrated approaches for data analysis and algorithms for identification of small, yet non-random changes. This study has identified genomic changes in paediatric HGG distinct from those arising in HGG in adults with distinct subsets within them, with a few notable similarities with adult HGG. Unlike in adult HGG, about 65% (11/17) of paediatric HGG short-term cell cultures in this study had balanced genomic profiles with no large scale chromosomal rearrangements, but had unique genomic changes associated with this subset, with one of them harbouring *H3F3A* (K27M) mutation. Similar subgroups of paediatric HGG with such balanced profiles have previously been reported in paediatric HGG (Bax et al., 2010; Barrow et al., 2011). A subset (17.65%) of paediatric HGG shared similarities with adults with copy number events such as gain of chromosome 7 and loss of 10q.

The unbiased approach in this study identified gains at 14q11.2 and 7p14.1 as the most frequent (94% and 76.4% respectively) CNAs in the paediatric HGG short-term cell cultures. Both these focal CNAs were present in the biopsy and cell culture of the 2 paired biopsy samples analysed here raising the confidence in the validity of this finding. These 2 regions have not been previously reported in paediatric glioma. CNVs at 7p14.1and 14q11.2 have been reported to be associated with Dupuytren's disease, a fibroproliferative disorder characterised by deformities in the fingers and may suggest a potential link between developmental errors in children and their susceptibility to HGG development (Shih et al., 2012).There was also gain of 2q32 present in 30% of paediatric HGG short-term cell cultures that was linked with a connective tissue disorder, Ehler-Danlos syndrome (Ritelli et al., 2013). Similar observations connecting paediatric HGG and developmental disorders have been reported in DIPG patients with *ACVR1* mutations, which were also found in patients

with Fibrodysplasia ossificans progressiva (FOP), a disorder that causes ossification of soft tissues leading to muscular deformities (Taylor et al., 2014). It is therefore likely that developmental process may have a role in tumourigenesis of paediatric HGG.

Some of the previously known genetic aberrations associated with paediatric HGG were identified in this study. Notable genetic changes included homozygous loss of 8p11.23-p11.22 encompassing *ADAM3A* (~35%) and cooperative loss of *CDKN2A* and *BRAFV600E* (~6%) (Schiffman et al., 2010; Barrow et al., 2013). Loss of *ADAM3A* was the most frequent event of copy number loss identified in the paediatric HGG short-term cell cultures in this study. Loss of *ADAM3A* in a subset of paediatric HGG short-term cell cultures was concordant with losses of regions containing novel non-coding RNA genes (*MIR1268A*) and pseudogenes associated with embryonic development (*DUXAP10*) and ribosome biogenesis (*BMS1P18*). In addition, 3 miRNAs (miR-3142, miR-3140-3p and miR-4503) were uniquely differentially expressed in paediatric HGG short-term cell cultures with *ADAM3A* loss and their predicted targets were associated with important cancer-related pathways including Ras and ErbB signaling and stem cell renewal. Considering the significance of miRNA and pseudogene signatures as prognostic biomarkers in tumours, along with the existing evidence of deletion of *ADAM3A* in other aggressive cancers, this study not only strengthens the potential role that *ADAM3A* may have as a prognostic/therapeutic biomarker in paediatric HGG, but also highlights the importance of further investigations on the non-coding elements of the genome in paediatric HGG.

Paediatric HGG short-term cell cultures in this study could be distinguished from normal controls based on their miRNA and methylation signatures, emphasising the role of epigenetic mechanisms in these tumours. Unique patterns of miRNA expression were associated with these tumours, with specific miRNA signatures that could distinguish between tumour types (DIPG or non-DIPG) as well as between *H3F3A* (K27M)-mutant and wild type cultures. Similar studies in adult HGG have identified miRNA-signatures that could predict response to therapy (Hayes et al., 2015; Tumilson et al., 2014). The miRNAs identified in this study were informative of the aberrant signalling pathways in these subgroups. Some of the pathways such as mucin type-o-glycan biosynthesis and ECM-receptor interactions have not been previously reported in paediatric HGG short-term cell cultures. Integration of miRNAs with their dysregulated mRNA targets in these cultures revealed aberrations in phosphoinositide signaling pathway. The evidence for this pathway dysregulation in paediatric HGG was also observed from genes dysregulated due to promoter methylation, indicating the interconnections between various epigenetic mechanisms. Preliminary investigations of a PI3K inhibitor, PI-103 showed antiproliferative responses in a subset of paediatric HGG short-term cell cultures. This warrants further validation of this therapeutic agent in a larger cohort of samples.

This study also identified and validated 7 candidate genes comprising *ADAMTS18, RFX3, PRKG2, PTPRE, RHBDF2, DAB1* and *EYA4* that were frequently downregulated in paediatric HGG short-term cell cultures. Of these, *PTPRE* was demonstrated to have anti-growth, and *DAB1* was demonstrated to have anti-growth and anti-migratory properties *in vitro.* An important finding of this study is the identification of promoter CpG methylation of *ASS1* and *ASL,* the 2 key components

of the arginine metabolic pathway in a subset of paediatric HGG short-term cell cultures. Paediatric HGG short-term cell cultures with methylated *ASS1* and/or *ASL* demonstrated sensitivity to the arginine deprivation agent, ADI-PEG20, with *ASS1* being the predominant determinant of sensitivity to the drug. This was in agreement with the findings of Syed et al. (2013) in adult GBM primary cultures. However, unlike in adults, the sensitivity of paediatric HGG short-term cell cultures with co-methylated *ASS1* and *ASL* was not higher than either *ASS1* or *ASL* only methylated cultures, but this could be an artefact due to the small number of samples available for this study. ADI-PEG20 has the advantage of overcoming some of the common problems associated with chemotherapy failure in glioma. For instance, as it exerts its anti-tumour activity by depleting arginine from peripheral blood, crossing of BBB is not required (Syed et al., 2013). In addition, as this therapeutic strategy targets only tumour cells, this should cause very little damage to normal brain structures.

This study has revealed evidence for the potential interplay of genetic and epigenetic changes in paediatric HGG. For instance, loss of 17q21.31 detected in approximately 35% of paediatric HGG short-term cell cultures including 1 DIPG (IN2102), contains genes encoding chromatin modifiers such as *KANSL1* that encodes a nuclear protein involved in histone acetylation. A potential association of this locus with susceptibility to ovarian cancer has been previously reported (Couch et al., 2013). In addition, the unique miRNAs and promoter methylated genes associated with *H3F3A* (K27M)-mutant paediatric HGG short-term cell cultures and the identification of frequent copy number changes in miRNA genes and pseudogenes in this study further supports the importance of both genetic and epigenetic dysregulation in paediatric HGG. Thus, integrated data analysis approaches may be the key for better understanding of these tumours.

8.2 Conclusions

Through genome-wide studies on well-characterised paediatric HGG short-term cell cultures, this study has identified genetic and/or epigenetic dysregulations in several candidate genes involved in important cellular processes and druggable metabolic pathways associated with cancer. Some of these, such as methylation of genes involved in arginine biosynthesis pathway (*ASS1* and *ASL*) are exciting findings as this provides opportunity for selectively targeting HGG patients with such aberrations using a non-toxic drug, ADI-PEG20. The therapeutic response displayed by a subset of paediatric HGG short-term cell cultures to ADI-PEG20 in preliminary investigations in this study holds promise for further validation. The identification of candidate genes deregulated due to methylation involved in ECM-interactions (*ADAMTS18*), reelin/PI3K signaling (*DAB1*), DNA damage repair (*EYA4*), PI3K signaling (*PRKG2),* RTK signaling (*PTPRE),* ciliagenesis (*RFX3*) and EGFR signaling (*RHBDF2*) highlights the roles of promoter methylation in regulating important tumourigeneic events in paediatric HGG. The anti-growth and anti-migratory properties of *DAB1* and *PTPRE* demonstrated *in vitro* strengthens their role in paediatric HGG. Further validation of these and the other candidates may lead to the identification of potential biomarkers in paediatric HGG. Some of the other changes such as gains at 14q11.2 and 7p14.1, and gain at 2q32 associated with developmental disorders may provide novel insights into the development of HGG in children. This study also emphasises the potential role of cooperative genetic and epigenetic changes in these tumours.

APPENDIX

Appendix I: aCGH profiles of paediatric HGG short-term cell cultures

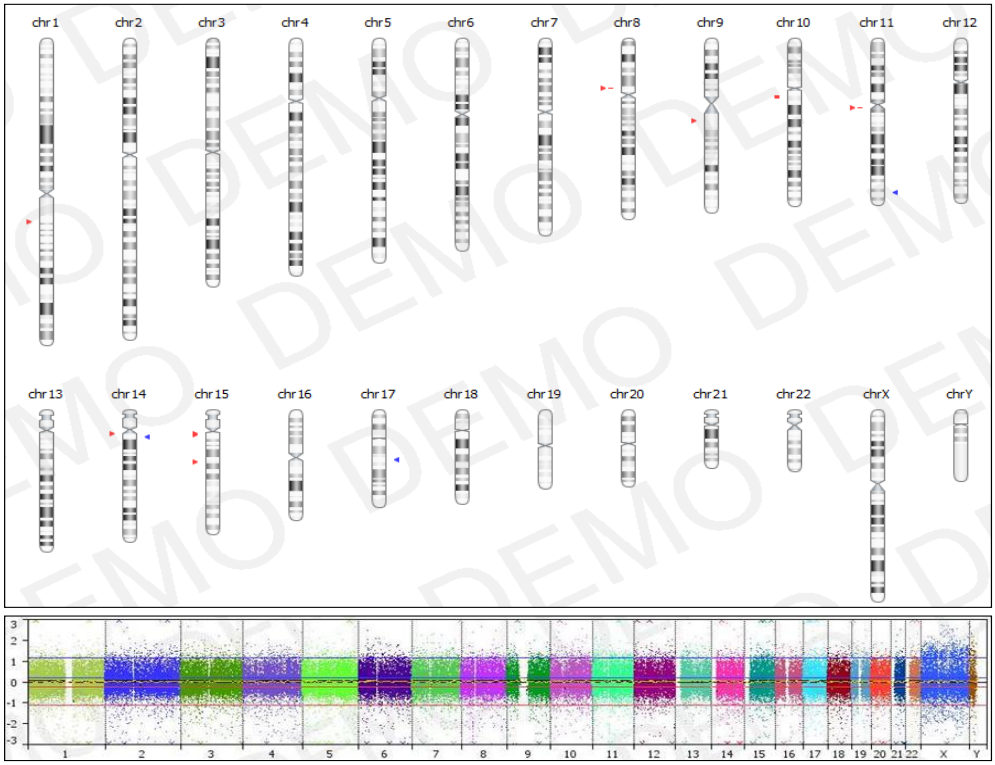

Figure A1 . aCGH profile of IN178 paediatric HGG short-term cell culture (non-DIPG)

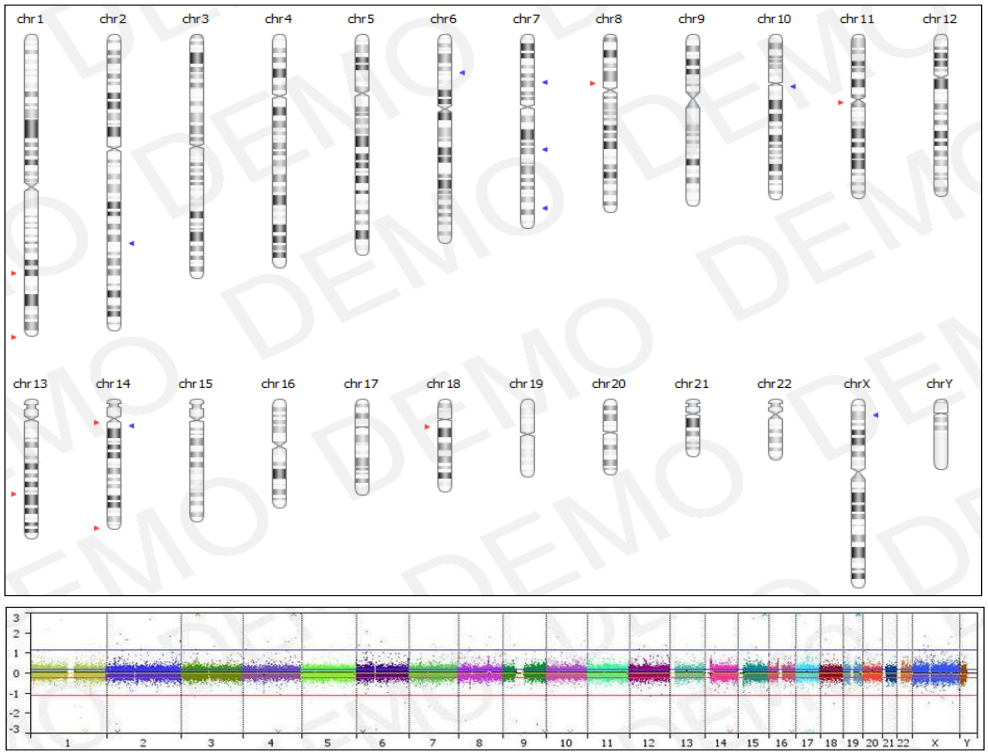

Figure A2. aCGH profile of IN1163 paediatric HGG short-term cell culture (non-DIPG)

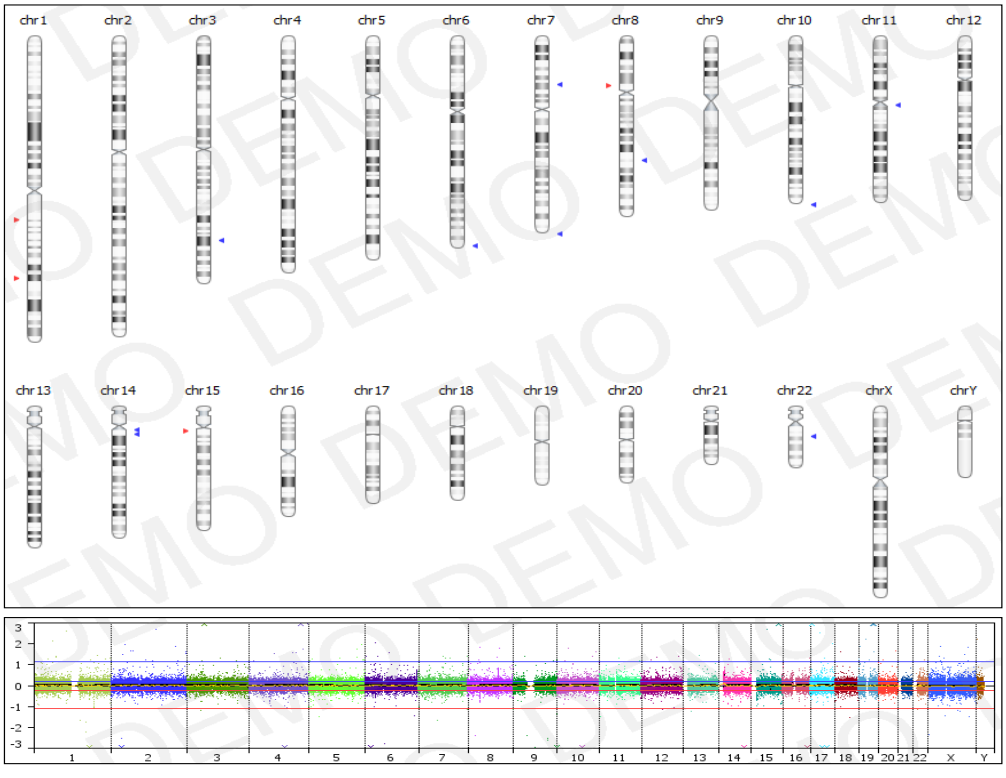

Figure A3. aCGH profile of IN1262 paediatric HGG short-term cell culture (non-DIPG)

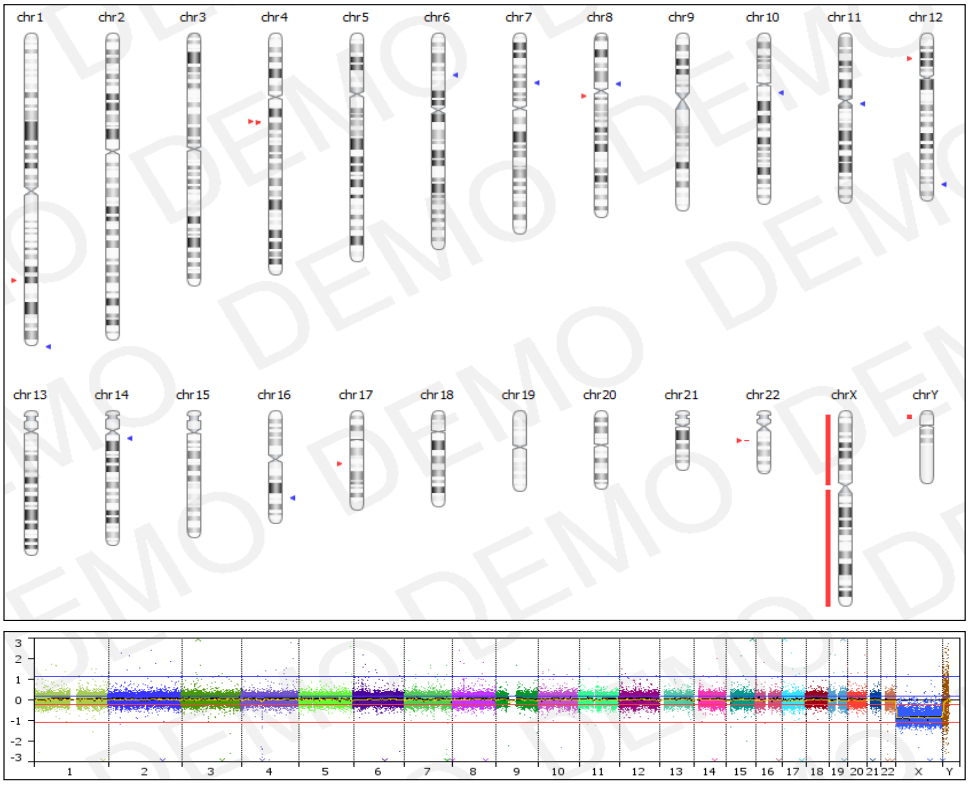

Figure A4. aCGH profile of IN1419 paediatric HGG short-term cell culture (non-DIPG)

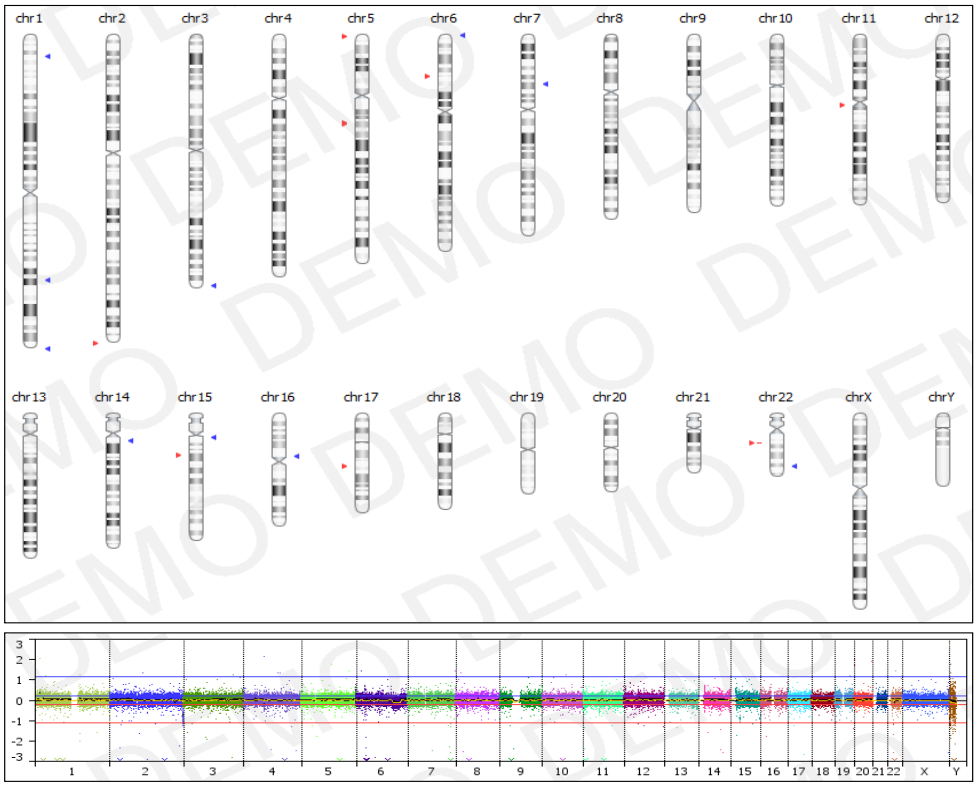

Figure A5. aCGH profile of IN1566 paediatric HGG short-term cell culture (non-DIPG)

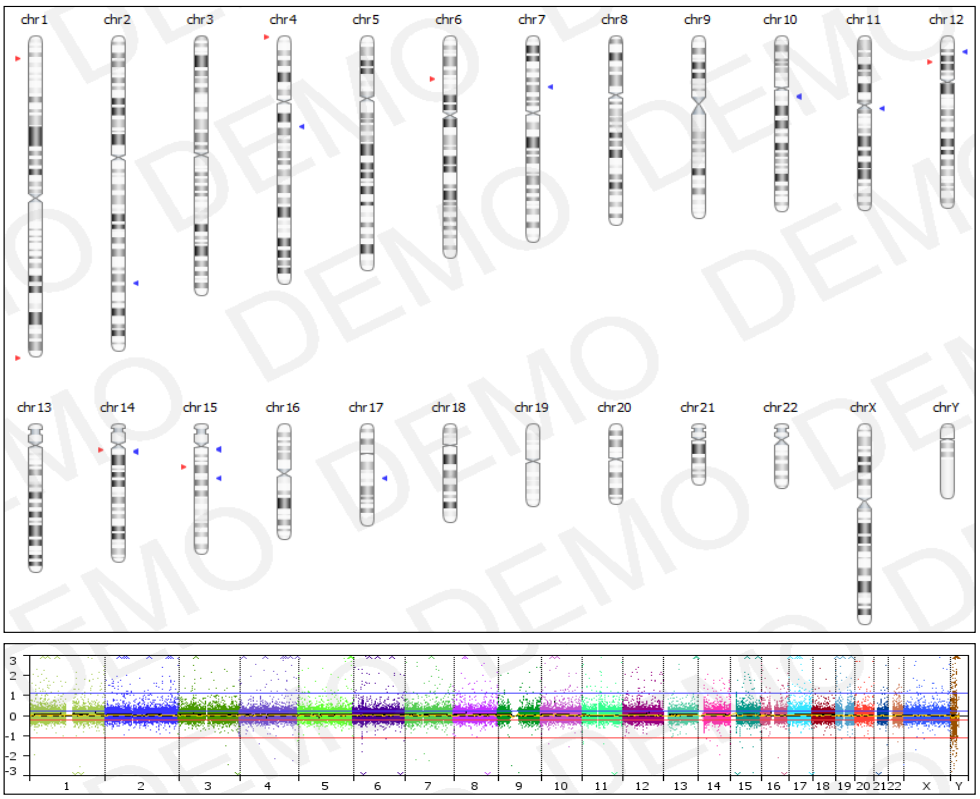

Figure A6. aCGH profile of IN1930 paediatric HGG short-term cell culture (non-DIPG)

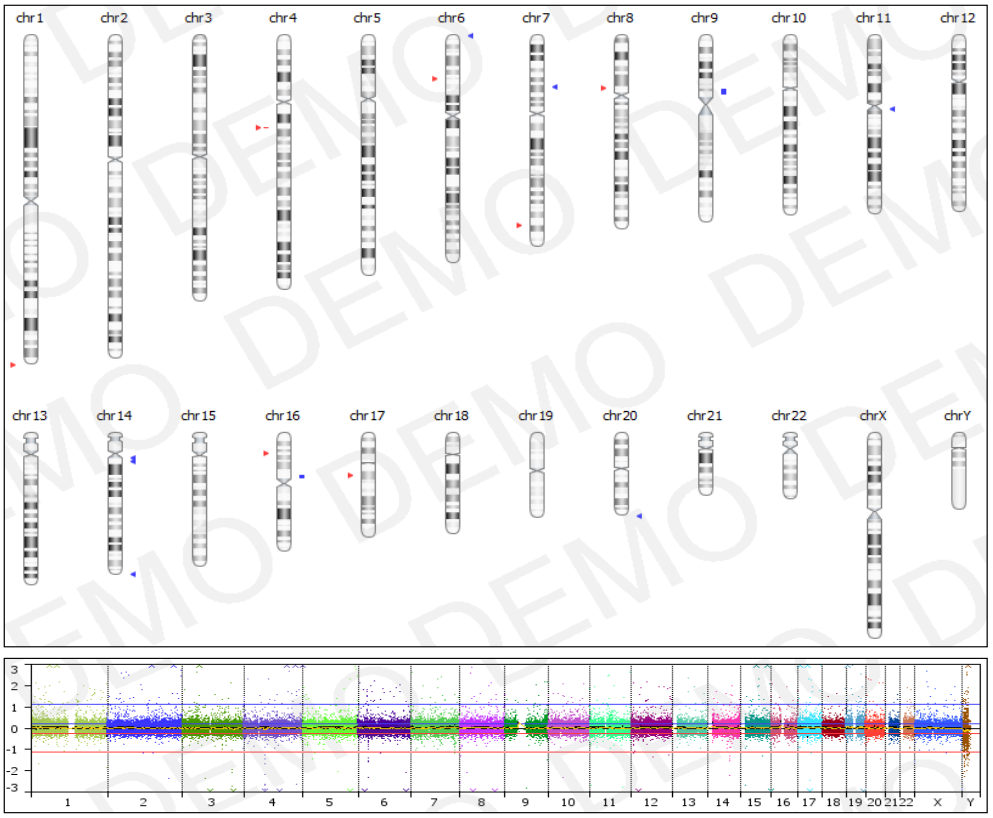

Figure A7. aCGH profile of IN3032 paediatric HGG short-term cell culture (non-DIPG)

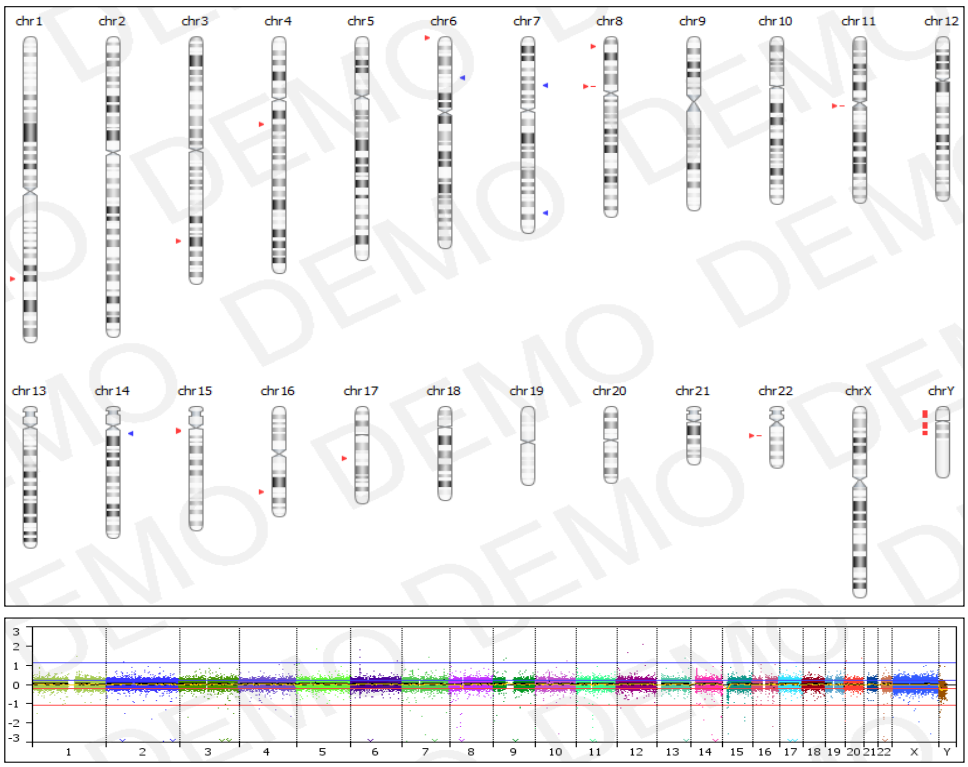

Figure A8. aCGH profile of IN3046 paediatric HGG short-term cell culture (non-DIPG)

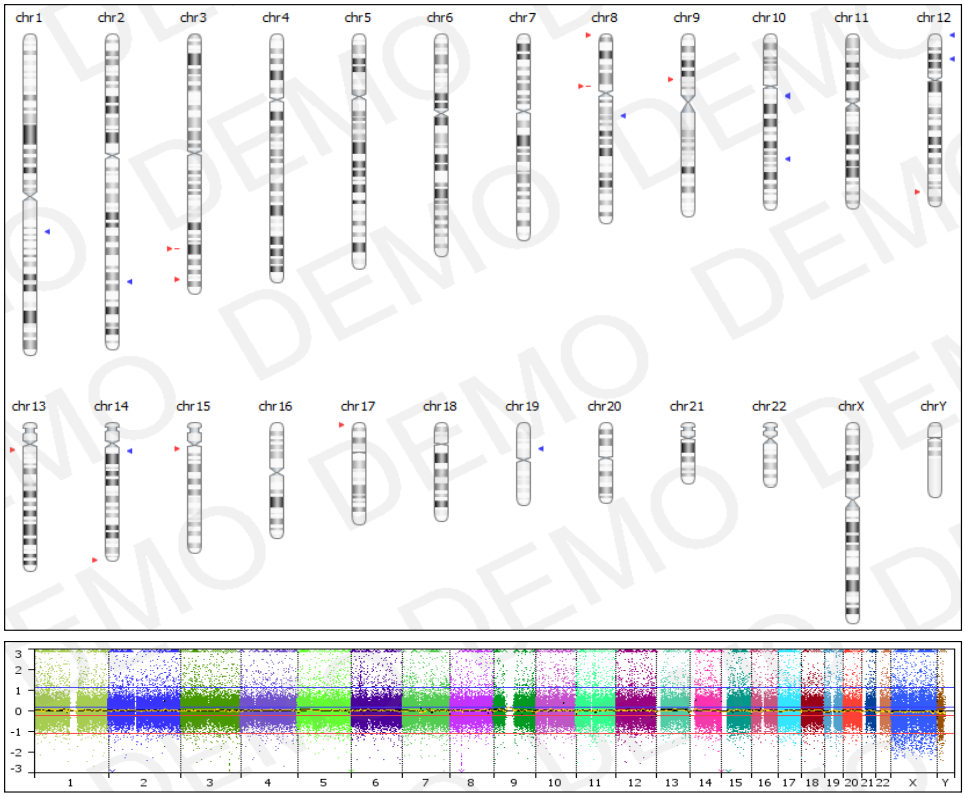

Figure A9. aCGH profile of IN3180 paediatric HGG short-term cell culture (non-DIPG)

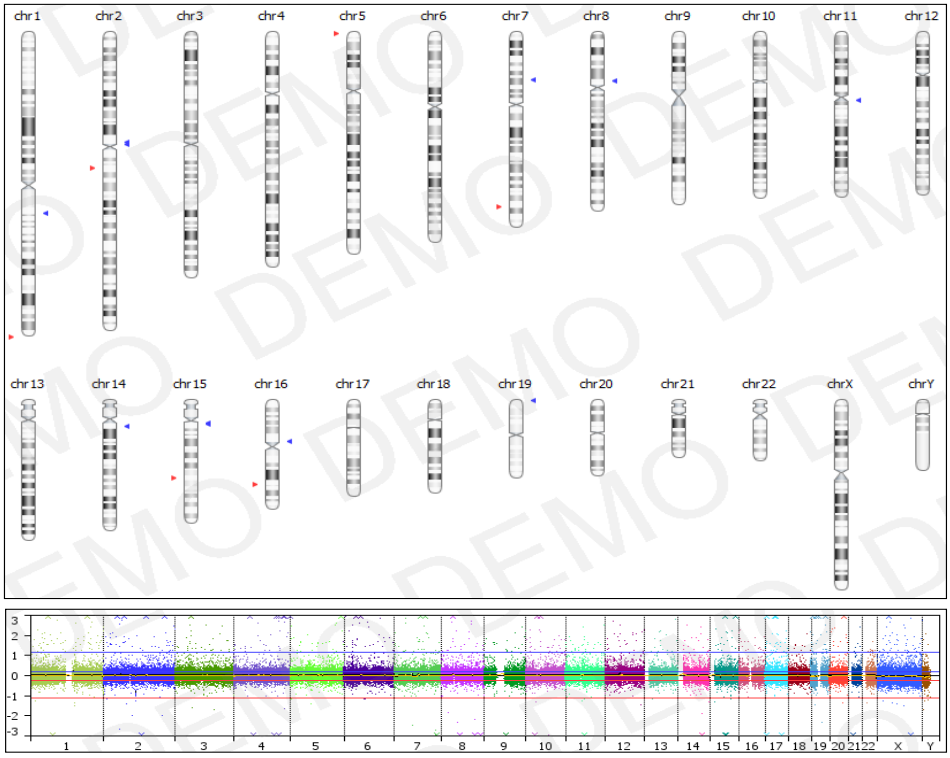

Figure A10. aCGH profile of IN3183 paediatric HGG short-term cell culture (non-DIPG)

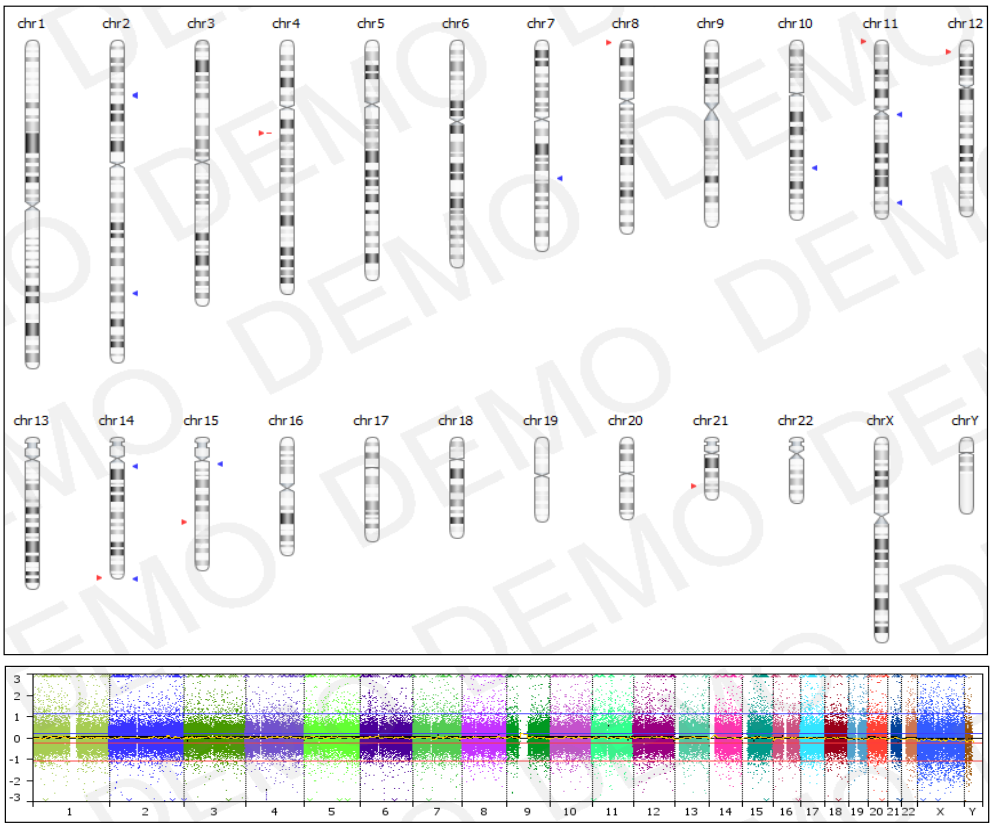

Figure A11. aCGH profile of IN2087 paediatric HGG short-term cell culture (DIPG)

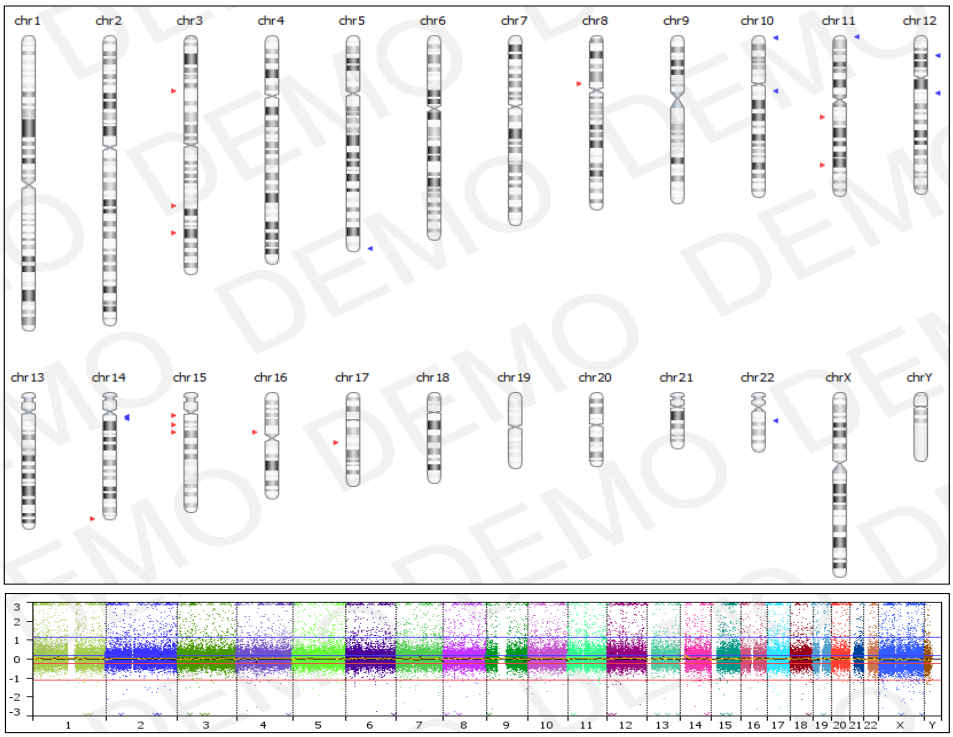

Figure A12. aCGH profile of IN2102 paediatric HGG short-term cell culture (DIPG)

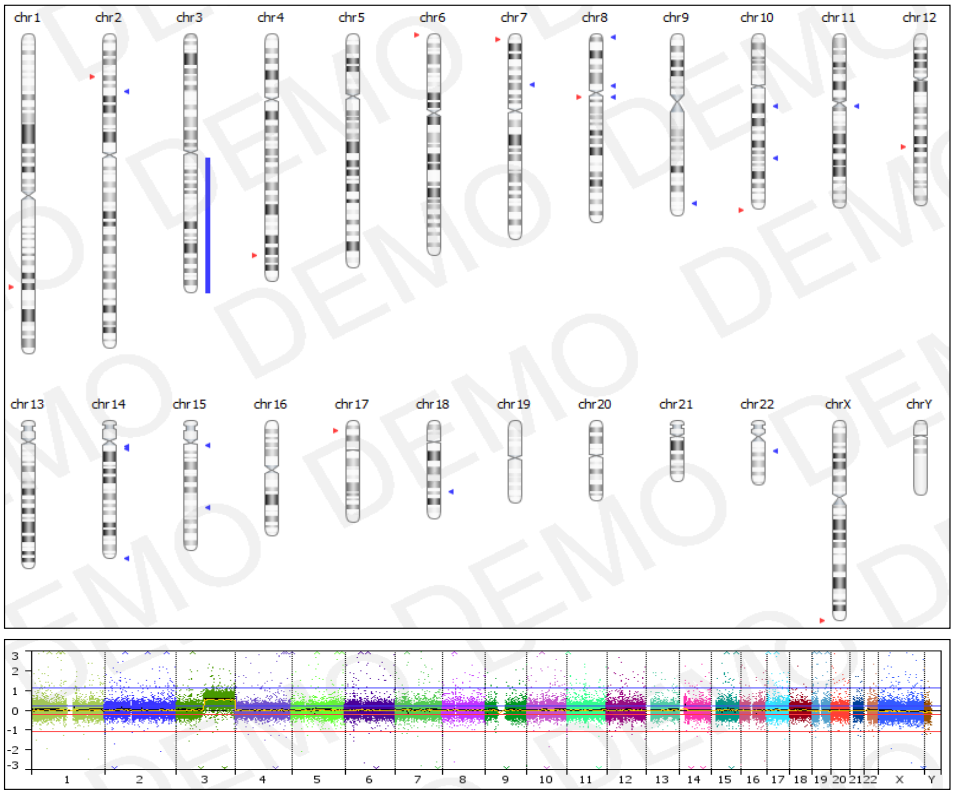

Figure A13. aCGH profile of IN2675 paediatric HGG short-term cell culture (DIPG)

Appendix II Primer sequences

RT PRIMERS

ADAMTS18	F	AGACACTGCAATAACCCCAAG
	R	TCACAAACCCCGTCAATACA
APBB2	F	TTCTGTAACGCCATCTCCA
	R	TTTCCCCTCTCCCCAAATCC
BMP3	F	ATGAGGTGTGGGAGGAGAGA
	R	AGACTTTGGCATGGGGAAC
CABLES1	F	ATCTTCCTTGGAGACCCTGG
	R	ACAGTCTTCCCATCAGCACC
CASZ1	F	CGTCTCCACTGTCAAGAACG
	R	GCATGCAGTGATAGTGGGTG
CAV1	F	TCTACAAGCCCAACAACAAGG
	R	AGGAAAGAGAGAATGGCGAAG
COL14A1	F	AAGTATGTAAGGCGGCCAAG
	R	CCACGATAACCTTTGGGATG
CXCL14	F	GTGGACGGGTCCAAATGCAA
	R	CCAGGCGTTGTACCACTTGA
DAB1	F	AAGGTCAGGATCGCAGTGAA
	R	AAAGGCCCGGTGATCTGTAA
DAB2IP	F	CAGGACAAGCTGCGAATCTC
	R	GCTTCTCCTGGGCATCAATG
DLK1	F	TGGCCTCTATGAATGCTCCT
	R	ACCTGTGAACTCGGGCTTG
EYA4	F	TCCCCACAGCTGTATCCTTC
	R	AACTGAGGCAGCCACTCTGT
FGFR2	F	GATGGTGCGGAAGATTTTGT
	R	CCAGGTGGTACGTGTGATTG
GRM8	F	CCCTGATCTCCTTTCCAACA
	R	CAATGCAAACACCACCAATC

GULP1	F	GACAGCGAAAAGTGTGCTGA
	R	GGGTCAAAAGGTTCTGCTCC
KRT8	F	GTAGGGGTTGGGTGGTTATG
	R	ATGGTAGAGGCAGGAGTGGA
MYH10	F	AAGAGCAAGGTTCCCACTCC
	R	ATCCAATTTTCCAGCCCTCT
PARP4	F	AATGCCCAAAGAAGTGAACC
	R	GGTAAAAGCAACCCTCGACA
PDE4D	F	CCCGGCCTGAAGAAATCCAG
	R	CAGACTGGCCAAGACCTGAG
PKNOX2	F	CCCTCCATCAACCTTCACTC
	R	GGCAAGACTCCTCGTTTGTT
PLXNB1	F	GTTCCTGTGGCTTCCTGTG
	R	GAAAACCTCCCTCGTCTCCT
PRKG2	F	TGATGAACCCACCTCCAAA
	R	GCAAATCCAAAGTCAACCAA
PRR5L	F	ACCTTCCCCGATTCCAAG
	R	GCAGATTTTCACCTTCACACA
RHBDF2	F	GGAGACTTTGGCCACTTTTG
	R	GGAGCAGAGTGTTGCTTCT
RANBP17	F	TGCAATTCTGTGGTTCTTGG
	R	ACCATCAGAAGGCGAGTGAG
RFX3	F	CGACTTCCGAAAGCAAAGCT
	R	CATCCCATGGTCACAGTTACACA
SBNO2	F	GAGCGAGAAGCCCAGATAGA
	R	GGACGAGGAGAAGATGGAGA
SEMA6A	F	ACATTGCTGCTAGGGACCAT
	R	TCATCCCCGAATGGTTCCAA
SETBP1	F	TCCAAAAAGAAGCTCCTCACA
	R	CCTGCACTGCCTTTCTTACC
SH3BP4	F	TCCCTTCTCTCCTGGACAGA
	R	CAGTGTGGTGAAGTTGGTGG
SIPA1L3	F	TCAACCTCATCTCCCTGACC
	R	AGCCACTGGTCATCACCTTC
TRIM2	F	GGGAGATCCTGGACAACAAG
	R	CCTTTGGTACCCACTCGAAA

CoBRA primers		
PIK3R5	F	GGGAGTTTTAGGTAGAGTTGGAG
	R	AAACAAAAAACTAAAAACACAAC
ASS1	F	TAGTTTTGGTTTAAGGGATGAAAGT
	R	CCTAACCCTAAAAAAACAATTTAAAC
ASL	F	GGCCGCTTAGCCTCCAGCTCAGC
	R	GTCAGTCCGGTCTTGTCTTCCAGAC
MSP primers		
ASS1 Region 1	F	TTTTCGTTGTTTATTTTTTAGTCGA
	R	CGAAACGAACGTCTTCTACG
	F	TTTTTGTTGTTTATTTTTTAGTTGA
	R	CCCAAAACAAACATCTTCTACAC
ASS1 Region 2	F	GTAGGAGGGAAGGGGTTTTC
	R	GCAAAAAACAAATAACCCGAA
	F	GTAGGAGGGAAGGGGTTTTT
	R	ACAAAAAACAAATAACCCAAA
ASL Region 1	F	ATGGAGGTAACGTTTATTTCGTC
	R	ACTAACCAAAACTTTTCTAACCGAA
	F	GGATGGAGGTAATGTTTATTTTGTT
	R	CCACTAACCAAAACTTTTCTAACCA
ASL Region 2	F	AGTGTTTAGAATTCGGAGTTAGTTC
	R	ATATTAAACGATTCCTCGTCGTC
	F	TGTTTAGAATTTGGAGTTAGTTTGG
	R	CATATTAAACAATTCCTCATCATC
Sequencing primers		
BRAF	F	GCTTGCTCTGATAGGAAAATGAG
	R	GTAACTCAGCAGCATCTCAGG
ACVR1	F	GATGCAACTCACCTAACCATTG
	R	GATGACATTTACTGTGTAGGTCGC

REFERENCES

Abella, J. and Park, M. (2009) Breakdown of endocytosis in the oncogenic activation of receptor tyrosine kinases. *AJP: Endocrinology and Metabolism*, 296(5), pp. E973-E984.

Adamski, J., Tabori, U. and Bouffet, E. (2014) Advances in the Management of Paediatric High-Grade Glioma. *Current Oncology Reports*, 16(12).

Agrawal, V., Alpini, S., Stone, E., Frenkel, E. and Frankel, A. (2011) Targeting methionine auxotrophy in cancer: discovery & exploration. *Expert Opinion on Biological Therapy*, 12(1), pp. 53-61.

Agrelo, R., Cheng, W., Setien, F., Ropero, S., Espada, J., Fraga, M., Herranz, M., Paz, M., Sanchez-Cespedes, M., Artiga, M., Guerrero, D., Castells, A., von Kobbe, C., Bohr, V. and Esteller, M. (2006) Epigenetic inactivation of the premature aging Werner syndrome gene in human cancer.*Proceedings of the National Academy of Sciences*, 103(23), pp. 8822-8827.

Ahmad, K. and Henikoff, S. (2002) The Histone Variant H3.3 Marks Active Chromatin by Replication-Independent Nucleosome Assembly. *Molecular Cell*, 9(6), pp. 1191-1200.

Alejandro Fernández-Rojo, M., Restall, C., Ferguson, C., Martel, N., Martin, S., Bosch, M., Kassan, A., Leong, G., Martin, S., McGee, S., Muscat, G., Anderson, R., Enrich, C., Pol, A. and Parton, R. (2012) Caveolin-1 orchestrates the balance between glucose and lipid-dependent energy metabolism: Implications for liver regeneration. *Hepatology*, 55(5), pp. 1574-1584.

Alessandrini, F., Sharma, V., Bisio, A., Zaccara, S., Inga, A. and Ciribilli, Y. (2015) Abstract 419: Cooperative interactions between p53 and NFκB enhance cell plasticity. *Cancer Research*, 75(15 Supplement), pp. 419-419.

Alizadeh, A., Eisen, M., Davis, R., Ma, C., Lossos, I., Rosenwald, A., Boldrick, J., Sabet, H., Tran, T., Yu, X., Powell, J., Yang, L., Marti, G., Moore, T., Hudson, J., Lu, L., Lewis, D., Tibshirani, R., Sherlock, G., Chan, W., Greiner, T., Weisenburger, D., Armitage, J., Warnke, R., Levy, R., Wilson, W., Grever, M., Byrd, J., Botstein, D., Brown, P. and Staudt, L. (2000) Distinct types of diffuse large B-cell lymphoma identified by gene expression profiling. *Nature*, 403(6769), pp. 503-511.

Allen, M., Luong, P., Hudson, C., Leyton, J., Delage, B., Ghazaly, E., Cutts, R., Yuan, M., Syed, N., Lo Nigro, C., Lattanzio, L., Chmielewska-Kassassir, M., Tomlinson, I., Roylance, R., Whitaker, H., Warren, A., Neal, D., Frezza, C., Beltran, L., Jones, L., Chelala, C., Wu, B., Bomalaski, J., Jackson, R., Lu, Y., Crook, T., Lemoine, N., Mather, S., Foster, J., Sosabowski, J., Avril, N., Li, C. and Szlosarek, P. (2013) Prognostic and Therapeutic Impact of Argininosuccinate Synthetase 1 Control in Bladder Cancer as Monitored Longitudinally by PET Imaging. *Cancer Research*, 74(3), pp. 896-907.

Amatschek, S., Koenig, U., Auer, H., Steinlein, P., Pacher, M., Gruenfelder, A., Dekan, G., Vogl, S., Kubista, E., Heider, K., Stratowa, C., Schreiber, M. and Sommergruber, W. (2004) Tissue-Wide Expression Profiling Using cDNA Subtraction and Microarrays to Identify Tumor-Specific Genes.*Cancer Research*, 64(3), pp. 844-856.

Andersen, J., Elson, A., Lammers, R., Rømer, J., Clausen, J., Møller, K. And Møller, N. (2001) Comparative study of protein tyrosine phosphatase-ε isoforms: membrane localization confers specificity in cellular signalling. *Biochem. J.*, 354(3), pp. 581-590.

Angelini, P., Hawkins, C., Laperriere, N., Bouffet, E. and Bartels, U. (2010) Post mortem examinations in diffuse intrinsic pontine glioma: challenges and chances. *J Neurooncol*, 101(1), pp. 75-81.

Ascierto, P. (2005) Pegylated Arginine Deiminase Treatment of Patients With Metastatic Melanoma: Results From Phase I and II Studies. *Journal of Clinical Oncology*, 23(30), pp. 7660-7668.

Asnaghi, L., Alkatan, H., Mahale, A., Othman, M., Alwadani, S., Al-Hussain, H., Jastaneiah, S., Yu, W., Maktabi, A., Edward, D. and Eberhart, C. (2014) Identification of Multiple DNA Copy Number Alterations Including Frequent 8p11.22 Amplification in Conjunctival Squamous Cell Carcinoma. *Investigative Ophthalmology & Visual Science*, 55(12), pp. 8604-8613.

Assadi, A., Zhang, G., Beffert, U., McNeil, R., Renfro, A., Niu, S., Quattrocchi, C., Antalffy, B., Sheldon, M., Armstrong, D., Wynshaw-Boris, A., Herz, J., D'Arcangelo, G. and Clark, G. (2003) Interaction of reelin signaling and Lis1 in brain development. *Nature Genetics*, 35(3), pp. 270-276.

Attisano, L. (1993) Identification of human activin and TGFβ type I receptors that form heteromeric kinase complexes with type II receptors. *Cell*, 75(4), pp. 671-680.

Auger, K., Serunian, L., Soltoff, S., Libby, P. and Cantley, L. (1989) PDGF-dependent tyrosine phosphorylation stimulates production of novel polyphosphoinositides in intact cells. *Cell*, 57(1), pp. 167-175.

Baer, C., Oakes, C., Ruppert, A., Claus, R., Kim-Wanner, S., Mertens, D., Zenz, T., Stilgenbauer, S., Byrd, J. and Plass, C. (2015) Epigenetic silencing of miR-708 enhances NF-κB signaling in chronic lymphocytic leukemia. *International Journal of Cancer*, 137(6), pp. 1352-1361.

Bagci-Onder, T., Wakimoto, H., Anderegg, M., Cameron, C. and Shah, K. (2010) A Dual PI3K/mTOR Inhibitor, PI-103, Cooperates with Stem Cell-Delivered TRAIL in Experimental Glioma Models.*Cancer Research*, 71(1), pp. 154-163.

Bail, S., Swerdel, M., Liu, H., Jiao, X., Goff, L., Hart, R. and Kiledjian, M. (2010) Differential regulation of microRNA stability. *RNA*, 16(5), pp. 1032-1039.

Bailey, S., Howman, A., Wheatley, K., Wherton, D., Boota, N., Pizer, B., Fisher, D., Kearns, P., Picton, S., Saran, F., Gibson, M., Glaser, A., Connolly, D. and Hargrave, D. (2013) Diffuse intrinsic pontine glioma treated with prolonged temozolomide and radiotherapy – Results of a United Kingdom phase II trial (CNS 2007 04). *European Journal of Cancer*, 49(18), pp. 3856-3862.

Balbin, O., Malik, R., Dhanasekaran, S., Prensner, J., Cao, X., Wu, Y., Robinson, D., Wang, R., Chen, G., Beer, D., Nesvizhskii, A. and Chinnaiyan, A. (2015) The landscape of antisense gene expression in human cancers. *Genome Research*, 25(7), pp. 1068-1079.

Bannister, A. and Kouzarides, T. (2011) Regulation of chromatin by histone modifications. *Cell Res*, 21(3), pp. 381-395.

Barbul, A. (2008) Proline precursors to sustain mammalian collagen synthesis. *The Journal of nutrition*, *138*(10), pp.2021S-2024S.

Barrow, J., Adamowicz-Brice, M., Cartmill, M., MacArthur, D., Lowe, J., Robson, K., Brundler, M., Walker, D., Coyle, B. and Grundy, R. (2010) Homozygous loss of ADAM3A revealed by genome-wide analysis of pediatric high-grade glioma and diffuse intrinsic pontine gliomas. *Neuro-Oncology*, 13(2), pp. 212-222.

Bartölke, R., Heinisch, J., Wieczorek, H. and Vitavska, O. (2014) Proton-associated sucrose transport of mammalian solute carrier family 45: an analysis in Saccharomyces cerevisiae. *Biochem. J.*, 464(2), pp. 193-201.

Bashtrykov, P., Ragozin, S. and Jeltsch, A. (2012) Mechanistic details of the DNA recognition by the Dnmt1 DNA methyltransferase. *FEBS Letters*, 586(13), pp. 1821-1823.

Bauchart-Thevret, C., Cui, L., Wu, G. and Burrin, D. (2010) Arginine-induced stimulation of protein synthesis and survival in IPEC-J2 cells is mediated by mTOR but not nitric oxide. *AJP: Endocrinology and Metabolism*, 299(6), pp. E899-E909.

Bax, D., Mackay, A., Little, S., Carvalho, D., Viana-Pereira, M., Tamber, N., Grigoriadis, A., Ashworth, A., Reis, R., Ellison, D., Al-Sarraj, S., Hargrave, D. and Jones, C. (2010) A Distinct Spectrum of Copy Number Aberrations in Pediatric High-Grade Gliomas. *Clinical Cancer Research*, 16(13), pp. 3368-3377.

Baylin, S. and Herman, J. (2000) DNA hypermethylation in tumorigenesis: epigenetics joins genetics.*Trends in Genetics*, 16(4), pp. 168-174.

Baylin, S. and Jones, P. (2011) A decade of exploring the cancer epigenome — biological and translational implications. *Nature Reviews Cancer*, 11(10), pp. 726-734.

Beffert, U. (2002) Reelin-mediated Signaling Locally Regulates Protein Kinase B/Akt and Glycogen Synthase Kinase 3beta. *Journal of Biological Chemistry*, 277(51), pp. 49958-49964.

Bender, S., Tang, Y., Lindroth, A., Hovestadt, V., Jones, D., Kool, M., Zapatka, M., Northcott, P., Sturm, D., Wang, W., Radlwimmer, B., Højfeldt, J., Truffaux, N., Castel, D., Schubert, S., Ryzhova, M., Şeker-Cin, H., Gronych, J., Johann, P., Stark, S., Meyer, J., Milde, T., Schuhmann, M., Ebinger, M., Monoranu, C., Ponnuswami, A., Chen, S., Jones, C., Witt, O., Collins, V., von Deimling, A., Jabado, N., Puget, S., Grill, J., Helin, K., Korshunov, A., Lichter, P., Monje, M., Plass, C., Cho, Y. and Pfister, S. (2013) Reduced H3K27me3 and DNA Hypomethylation Are Major Drivers of Gene Expression in K27M Mutant Pediatric High-Grade Gliomas. *Cancer Cell*, 24(5), pp. 660-672.

Berdasco, M. and Esteller, M. (2010) Aberrant Epigenetic Landscape in Cancer: How Cellular Identity Goes Awry. *Developmental Cell*, 19(5), pp. 698-711.

Bernstein, B., Meissner, A. and Lander, E. (2007) The Mammalian Epigenome. *Cell*, 128(4), pp. 669-681.

Bernstein, B., Mikkelsen, T., Xie, X., Kamal, M., Huebert, D., Cuff, J., Fry, B., Meissner, A., Wernig, M., Plath, K., Jaenisch, R., Wagschal, A., Feil, R., Schreiber, S. and Lander, E. (2006) A Bivalent Chromatin Structure Marks Key Developmental Genes in Embryonic Stem Cells. *Cell*, 125(2), pp. 315-326.

Beroukhim, R., Getz, G., Nghiemphu, L., Barretina, J., Hsueh, T., Linhart, D., Vivanco, I., Lee, J., Huang, J., Alexander, S., Du, J., Kau, T., Thomas, R., Shah, K., Soto, H., Perner, S., Prensner, J., Debiasi, R., Demichelis, F., Hatton, C., Rubin, M., Garraway, L., Nelson, S., Liau, L., Mischel, P., Cloughesy, T., Meyerson, M., Golub, T., Lander, E., Mellinghoff, I. and Sellers, W. (2007) Assessing the significance of chromosomal aberrations in cancer: Methodology and application to glioma. *Proceedings of the National Academy of Sciences*, 104(50), pp. 20007-20012.

Bielen, A., Perryman, L., Box, G., Valenti, M., de Haven Brandon, A., Martins, V., Jury, A., Popov, S., Gowan, S., Jeay, S., Raynaud, F., Hofmann, F., Hargrave, D., Eccles, S. and Jones, C. (2011) Enhanced Efficacy of IGF1R Inhibition in

Pediatric Glioblastoma by Combinatorial Targeting of PDGFR /. *Molecular Cancer Therapeutics*, 10(8), pp. 1407-1418.

Bignotti, E., Tassi, R., Calza, S., Ravaggi, A., Romani, C., Rossi, E., Falchetti, M., Odicino, F., Pecorelli, S. and Santin, A. (2006) Differential gene expression profiles between tumor biopsies and short-term primary cultures of ovarian serous carcinomas: Identification of novel molecular biomarkers for early diagnosis and therapy. *Gynecologic Oncology*, 103(2), pp. 405-416.

Bird, A. (2002) DNA methylation patterns and epigenetic memory. *Genes & Development*, 16(1), pp. 6-21.

Birks, D., Barton, V., Donson, A., Handler, M., Vibhakar, R. and Foreman, N. (2011) Survey of MicroRNA expression in pediatric brain tumors. *Pediatr. Blood Cancer*, 56(2), pp. 211-216.

Bonavia, R., Inda, M., Cavenee, W. and Furnari, F. (2011) Heterogeneity Maintenance in Glioblastoma: A Social Network. *Cancer Research*, 71(12), pp. 4055-4060.

Bondy, M., Scheurer, M., Malmer, B., Barnholtz-Sloan, J., Davis, F., Il'yasova, D., Kruchko, C., McCarthy, B., Rajaraman, P., Schwartzbaum, J., Sadetzki, S., Schlehofer, B., Tihan, T., Wiemels, J., Wrensch, M. and Buffler, P. (2008) Brain tumor epidemiology: Consensus from the Brain Tumor Epidemiology Consortium. *Cancer*, 113(S7), pp. 1953-1968.

Boroughs, L. and DeBerardinis, R. (2015) Metabolic pathways promoting cancer cell survival and growth. *Nature Cell Biology*, 17(4), pp. 351-359.

Both, J., Krijgsman, O., Bras, J., Schaap, G., Baas, F., Ylstra, B. and Hulsebos, T. (2014) Focal Chromosomal Copy Number Aberrations Identify CMTM8 and GPR177 as New Candidate Driver Genes in Osteosarcoma. *PLoS ONE*, 9(12), p. e115835.

Böttner, M., Krieglstein, K. and Unsicker, K. (2000) The Transforming Growth Factor-bs: Structure, Signaling, and Roles in Nervous System Development and Functions. *Journal of Neurochemistry*, 75(6), pp. 2227-2240.

Bowles, T., Kim, R., Galante, J., Parsons, C., Virudachalam, S., Kung, H. and Bold, R. (2008) Pancreatic cancer cell lines deficient in argininosuccinate synthetase are sensitive to arginine deprivation by arginine deiminase. *International Journal of Cancer*, 123(8), pp. 1950-1955.

Brennan, C., Momota, H., Hambardzumyan, D., Ozawa, T., Tandon, A., Pedraza, A. and Holland, E. (2009) Glioblastoma Subclasses Can Be Defined by Activity among Signal Transduction Pathways and Associated Genomic Alterations. *PLoS ONE*, 4(11), p. e7752.

Brennan, C.W., Verhaak, R.G., McKenna, A., Campos, B., Noushmehr, H., Salama, S.R., Zheng, S., Chakravarty, D., Sanborn, J.Z., Berman, S.H. and Beroukhim, R., (2013) The somatic genomic landscape of glioblastoma. *Cell*,*155*(2), pp.462-477.

Brocker, C., Vasiliou, V. and Nebert, D. (2009) Evolutionary divergence and functions of the ADAM and ADAMTS gene families. *Human Genomics*, 4(1), p. 43.

Broderick, D. (2004) Mutations of PIK3CA in Anaplastic Oligodendrogliomas, High-Grade Astrocytomas, and Medulloblastomas. *Cancer Research*, 64(15), pp. 5048-5050.

Broniscer, A. (2004) Supratentorial High-Grade Astrocytoma and Diffuse Brainstem Glioma: Two Challenges for the Pediatric Oncologist. *The Oncologist*, 9(2), pp. 197-206.

Broniscer, A., Baker, S., Wetmore, C., Pai Panandiker, A., Huang, J., Davidoff, A., Onar-Thomas, A., Panetta, J., Chin, T., Merchant, T., Baker, J., Kaste, S., Gajjar, A. and Stewart, C. (2013) Phase I Trial, Pharmacokinetics, and Pharmacodynamics of Vandetanib and Dasatinib in Children with Newly Diagnosed Diffuse Intrinsic Pontine Glioma. *Clinical Cancer Research*, 19(11), pp. 3050-3058.

Broome, J. (1961) Evidence that the L-Asparaginase Activity of Guinea Pig Serum is responsible for its Antilymphoma Effects. *Nature*, 191(4793), pp. 1114-1115.

Bruna, A., Darken, R., Rojo, F., Ocaña, A., Peñuelas, S., Arias, A., Paris, R., Tortosa, A., Mora, J., Baselga, J. and Seoane, J. (2007) High TGFβ-Smad Activity Confers Poor Prognosis in Glioma Patients and Promotes Cell Proliferation Depending on the Methylation of the PDGF-B Gene.*Cancer Cell*, 11(2), pp. 147-160.

Bucci, M., Maity, A., Janss, A., Belasco, J., Fisher, M., Tochner, Z., Rorke, L., Sutton, L., Phillips, P. and Shu, H. (2004) Near complete surgical resection predicts a favorable outcome in pediatric patients with nonbrainstem, malignant gliomas. *Cancer*, 101(4), pp. 817-824.

Buczkowicz, P. and Hawkins, C. (2015) Pathology, Molecular Genetics, and Epigenetics of Diffuse Intrinsic Pontine Glioma. *Front. Oncol.*, 5.

Cadieux, B., Ching, T., VandenBerg, S. and Costello, J. (2006) Genome-wide Hypomethylation in Human Glioblastomas Associated with Specific Copy Number Alteration, Methylenetetrahydrofolate Reductase Allele Status, and Increased Proliferation. *Cancer Research*, 66(17), pp. 8469-8476.

Calin, G., Dumitru, C., Shimizu, M., Bichi, R., Zupo, S., Noch, E., Aldler, H., Rattan, S., Keating, M., Rai, K., Rassenti, L., Kipps, T., Negrini, M., Bullrich, F. and Croce, C. (2002) Nonlinear partial differential equations and applications: Frequent deletions and down-regulation of micro- RNA genes miR15 and miR16 at 13q14 in chronic lymphocytic leukemia. *Proceedings of the National Academy of Sciences*, 99(24), pp. 15524-15529.

Calin, G., Sevignani, C., Dumitru, C., Hyslop, T., Noch, E., Yendamuri, S., Shimizu, M., Rattan, S., Bullrich, F., Negrini, M. and Croce, C. (2004) Human microRNA genes are frequently located at fragile sites and genomic regions involved in cancers. *Proceedings of the National Academy of Sciences*, 101(9), pp. 2999-3004.

Calvisi, D., Ladu, S., Gorden, A., Farina, M., Lee, J., Conner, E., Schroeder, I., Factor, V. and Thorgeirsson, S. (2007) Mechanistic and prognostic significance of aberrant methylation in the molecular pathogenesis of human hepatocellular carcinoma. *Journal of Clinical Investigation*, 117(9), pp. 2713-2722.

Campa, F. and Randazzo, P. (2008) Arf GTPase-activating proteins and their potential role in cell migration and invasion. *Cell Adhesion & Migration*, 2(4), pp. 258-262.

Cantley, L. (2002) The Phosphoinositide 3-Kinase Pathway. *Science*, 296(5573), pp. 1655-1657.

Cantor, J. and Sabatini, D. (2012) Cancer Cell Metabolism: One Hallmark, Many Faces. *Cancer Discovery*, 2(10), pp. 881-898.

Caretti, V., Sewing, A., Lagerweij, T., Schellen, P., Bugiani, M., Jansen, M., van Vuurden, D., Navis, A., Horsman, I., Vandertop, W., Noske, D., Wesseling, P., Kaspers, G., Nazarian, J., Vogel, H., Hulleman, E., Monje, M. and Wurdinger, T. (2014) Human pontine glioma cells can induce murine tumors. *Acta Neuropathologica*, 127(6), pp. 897-909.

Carracedo, A. and Pandolfi, P. (2008) The PTENâ€“PI3K pathway: of feedbacks and cross-talks. *Oncogene*, 27(41), pp. 5527-5541.
Carraro, G., Shrestha, A., Rostkovius, J., Contreras, A., Chao, C., El Agha, E., MacKenzie, B., Dilai, S., Guidolin, D., Taketo, M., Gunther, A., Kumar, M., Seeger, W., De Langhe, S., Barreto, G. and Bellusci, S. (2014) miR-142-3p balances proliferation and differentiation of mesenchymal cells during lung development. *Development*, 141(6), pp. 1272-1281.
Carrera, S., Cuadrado-Castano, S., Samuel, J., Jones, G., Villar, E., Lee, S. and Macip, S. (2013) Stra6, a retinoic acid-responsive gene, participates in p53-induced apoptosis after DNA damage. *Cell Death Differ*, 20(7), pp. 910-919.
Carvalho, D., Mackay, A., Bjerke, L., Grundy, R., Lopes, C., Reis, R. and Jones, C. (2014) The prognostic role of intragenic copy number breakpoints and identification of novel fusion genes in paediatric high grade glioma. *Acta Neuropathologica Communications*, 2(1), p. 23.
Caso, G., Mcnurlan, M., Mcmillan, N., Eremin, O. And Garlick, P. (2004) Tumour cell growth in culture: dependence on arginine. *Clin. Sci.*, 107(4), pp. 371-379.
Chai, X., Forster, E., Zhao, S., Bock, H. and Frotscher, M. (2009) Reelin Stabilizes the Actin Cytoskeleton of Neuronal Processes by Inducing n-Cofilin Phosphorylation at Serine3. *Journal of Neuroscience*, 29(1), pp. 288-299.
Chaluvally-Raghavan, P., Zhang, F., Pradeep, S., Hamilton, M., Zhao, X., Rupaimoole, R., Moss, T., Lu, Y., Yu, S., Pecot, C., Aure, M., Peuget, S., Rodriguez-Aguayo, C., Han, H., Zhang, D., Venkatanarayan, A., Krohn, M., Kristensen, V., Gagea, M., Ram, P., Liu, W., Lopez-Berestein, G., Lorenzi, P., Børresen-Dale, A., Chin, K., Gray, J., Dusetti, N., McGuire, S., Flores, E., Sood, A. and Mills, G. (2014) Copy Number Gain of hsa-miR-569 at 3q26.2 Leads to Loss of TP53INP1 and Aggressiveness of Epithelial Cancers. *Cancer Cell*, 26(6), pp. 863-879.
Chamdine, O. and Gajjar, A. (2014) Molecular characteristics of pediatric high-grade gliomas. *CNS Oncology*, 3(6), pp. 433-443.
Chan, J. (2005) MicroRNA-21 Is an Antiapoptotic Factor in Human Glioblastoma Cells. *Cancer Research*, 65(14), pp. 6029-6033.
Chan, K., Jiang, P., Zheng, Y., Liao, G., Sun, H., Wong, J., Siu, S., Chan, W., Chan, S., Chan, A., Lai, P., Chiu, R. and Lo, Y. (2013) Cancer Genome Scanning in Plasma: Detection of Tumor-Associated Copy Number Aberrations, Single-Nucleotide Variants, and Tumoral Heterogeneity by Massively Parallel Sequencing. *Clinical Chemistry*, 59(1), pp. 211-224.
Chan, X., Nama, S., Gopal, F., Rizk, P., Ramasamy, S., Sundaram, G., Ow, G., Vladimirovna, I., Tanavde, V., Haybaeck, J., Kuznetsov, V. and Sampath, P. (2012) Targeting Glioma Stem Cells by Functional Inhibition of a Prosurvival OncomiR-138 in Malignant Gliomas. *Cell Reports*, 2(3), pp. 591-602.
Chao, A., Lin, C., Lee, Y., Tsai, C., Wei, P., Hsueh, S., Wu, T., Tsai, C., Wang, C., Chao, A., Wang, T. and Lai, C. (2011) Regulation of ovarian cancer progression by microRNA-187 through targeting Disabled homolog-2. *Oncogene*, 31(6), pp. 764-775.
Chassot, A., Canale, S., Varlet, P., Puget, S., Roujeau, T., Negretti, L., Dhermain, F., Rialland, X., Raquin, M., Grill, J. and Dufour, C. (2011) Radiotherapy with concurrent and adjuvant temozolomide in children with newly diagnosed diffuse intrinsic pontine glioma. *J Neurooncol*, 106(2), pp. 399-407.

Chaudhry, M., Sachdeva, H. and Omaruddin, R. (2010) Radiation-Induced Micro-RNA Modulation in Glioblastoma Cells Differing in DNA-Repair Pathways. *DNA and Cell Biology*, 29(9), pp. 553-561.

Chen, J., Feilotter, H., Paré, G., Zhang, X., Pemberton, J., Garady, C., Lai, D., Yang, X. and Tron, V. (2010) MicroRNA-193b Represses Cell Proliferation and Regulates Cyclin D1 in Melanoma. *The American Journal of Pathology*, 176(5), pp. 2520-2529.

Chen, J., Zhang, X., Lentz, C., Abi-Daoud, M., Paré, G., Yang, X., Feilotter, H. and Tron, V. (2011) miR-193b Regulates Mcl-1 in Melanoma. *The American Journal of Pathology*, 179(5), pp. 2162-2168.

Chen, T., Ueda, Y., Dodge, J., Wang, Z. and Li, E. (2003) Establishment and Maintenance of Genomic Methylation Patterns in Mouse Embryonic Stem Cells by Dnmt3a and Dnmt3b. *Molecular and Cellular Biology*, 23(16), pp. 5594-5605.

Chen, Y., Cairns, R., Papandreou, I., Koong, A. and Denko, N. (2009) Oxygen Consumption Can Regulate the Growth of Tumors, a New Perspective on the Warburg Effect. *PLoS ONE*, 4(9), p. e7033.

Chen, Y., Hakin-Smith, V., Tio, M., Xinarianos, G., Gellinek, D., Carroll, T., McDowell, D., MacFarlane, M., Boet, R., Baguley, B., Braithwaite, A., Reddel, R. and Royds, J. (2006) Association of Mutant TP53 with Alternative Lengthening of Telomeres and Favorable Prognosis in Glioma. *Cancer Research*, 66(13), pp. 6473-6476.

Chen, Y., Sprung, R., Tang, Y., Ball, H., Sangras, B., Kim, S., Falck, J., Peng, J., Gu, W. and Zhao, Y. (2007) Lysine Propionylation and Butyrylation Are Novel Post-translational Modifications in Histones. *Molecular & Cellular Proteomics*, 6(5), pp. 812-819.

Chen, Z., Jin, Y., Yu, D., Wang, A., Mahjabeen, I., Wang, C., Liu, X. and Zhou, X. (2012) Down-regulation of the microRNA-99 family members in head and neck squamous cell carcinoma. *Oral Oncology*, 48(8), pp. 686-691.

Cheng, P., Lam, T., Lam, W., Tsui, S., Cheng, A., Lo, W. and Leung, Y. (2007) Pegylated Recombinant Human Arginase (rhArg-peg5,000mw) Inhibits the In vitro and In vivo Proliferation of Human Hepatocellular Carcinoma through Arginine Depletion. *Cancer Research*, 67(1), pp. 309-317.

Chieng, C. and Say, Y. (2015) Cellular prion protein contributes to LS 174T colon cancer cell carcinogenesis by increasing invasiveness and resistance against doxorubicin-induced apoptosis.*Tumor Biol.*, 36(10), pp. 8107-8120.

Chiusaroli, R. (2003) Tyrosine Phosphatase Epsilon Is a Positive Regulator of Osteoclast Function *in vitro* and In Vivo. *Molecular Biology of the Cell*, 15(1), pp. 234-244.

Christophorou, M., Castelo-Branco, G., Halley-Stott, R., Oliveira, C., Loos, R., Radzisheuskaya, A., Mowen, K., Bertone, P., Silva, J., Zernicka-Goetz, M., Nielsen, M., Gurdon, J. and Kouzarides, T. (2014) Citrullination regulates pluripotency and histone H1 binding to chromatin. *Nature*, 507(7490), pp. 104-108.

Chuang, L. (1997) Human DNA-(Cytosine-5) Methyltransferase-PCNA Complex as a Target for p21WAF1. *Science*, 277(5334), pp. 1996-2000.

Chudnovsky, Y., Kim, D., Zheng, S., Whyte, W., Bansal, M., Bray, M., Gopal, S., Theisen, M., Bilodeau, S., Thiru, P., Muffat, J., Yilmaz, O., Mitalipova, M., Woolard, K., Lee, J., Nishimura, R., Sakata, N., Fine, H., Carpenter, A., Silver, S., Verhaak, R., Califano, A., Young, R., Ligon, K., Mellinghoff, I., Root, D., Sabatini, D., Hahn, W. and Chheda, M. (2014) ZFHX4 Interacts with the NuRD

Core Member CHD4 and Regulates the Glioblastoma Tumor-Initiating Cell State. *Cell Reports*, 6(2), pp. 313-324.
Cianchi, F., Cortesini, C., Fantappie, O., Messerini, L., Sardi, I., Lasagna, N., Perna, F., Fabbroni, V., Di Felice, A., Perigli, G., Mazzanti, R. and Mazini, E. (2004) Cyclooxygenase-2 Activation Mediates the Proangiogenic Effect of Nitric Oxide in Colorectal Cancer. *Clinical Cancer Research*, 10(8), pp. 2694-2704.
Cipta, S. and Patel, H. (2009) Molecular bandages: inside-out, outside-in repair of cellular membranes. Focus on "Myoferlin is critical for endocytosis in endothelial cells". *AJP: Cell Physiology*, 297(3), pp. C481-C483.
Citro, S., Miccolo, C., Meloni, L. and Chiocca, S. (2015) PI3K/mTOR mediate mitogen-dependent HDAC1 phosphorylation in breast cancer: a novel regulation of estrogen receptor expression.*Journal of Molecular Cell Biology*, 7(2), pp. 132-142.
Cockle, J., Picton, S., Levesley, J., Ilett, E., Carcaboso, A., Short, S., Steel, L., Melcher, A., Lawler, S. and Brüning-Richardson, A. (2015) Cell migration in paediatric glioma; characterisation and potential therapeutic targeting. *Br J Cancer*, 112(4), pp. 693-703.
Cohen, K., Heideman, R., Zhou, T., Holmes, E., Lavey, R., Bouffet, E. and Pollack, I. (2011) Temozolomide in the treatment of children with newly diagnosed diffuse intrinsic pontine gliomas: a report from the Children's Oncology Group. *Neuro-Oncology*, 13(4), pp. 410-416.
Collins, V. (2014) Pathology of Gliomas and Developments in Molecular Testing. *Clinical Oncology*, 26(7), pp. 377-384.
Collins, V., Jones, D. and Giannini, C. (2015) Pilocytic astrocytoma: pathology, molecular mechanisms and markers. *Acta Neuropathologica*, 129(6), pp. 775-
Costa, F., Bischof, J., Vanin, E., Lulla, R., Wang, M., Sredni, S., Rajaram, V., de Fátima Bonaldo, M., Wang, D., Goldman, S., Tomita, T. and Soares, M. (2011) Identification of MicroRNAs as Potential Prognostic Markers in Ependymoma. *PLoS ONE*, 6(10), p. e25114.
Covini, D., Tardito, S., Bussolati, O., R. Chiarelli, L., V. Pasquetto, M., Digilio, R., Valentini, G. and Scotti, C. (2012) Expanding Targets for a Metabolic Therapy of Cancer: L-Asparaginase. *Recent Patents on Anti-Cancer Drug Discovery*, 7(1), pp. 4-13.
Cox, D., Chao, A., Baker, J., Chang, L., Qiao, D. and Lin, H. (1998) A novel class of evolutionarily conserved genes defined by piwi are essential for stem cell self-renewal. *Genes & Development*, 12(23), pp. 3715-3727.
Crespo, I., Vital, A., Nieto, A., Rebelo, O., Tão, H., Lopes, M., Oliveira, C., French, P., Orfao, A. and Tabernero, M. (2011) Detailed Characterization of Alterations of Chromosomes 7, 9, and 10 in Glioblastomas as Assessed by Single-Nucleotide Polymorphism Arrays. *The Journal of Molecular Diagnostics*, 13(6), pp. 634-647.
Cully, M., You, H., Levine, A. and Mak, T. (2006) Beyond PTEN mutations: the PI3K pathway as an integrator of multiple inputs during tumorigenesis. *Nature Reviews Cancer*, 6(3), pp. 184-192.
Curradi, M., Izzo, A., Badaracco, G. and Landsberger, N. (2002) Molecular Mechanisms of Gene Silencing Mediated by DNA Methylation. *Molecular and Cellular Biology*, 22(9), pp. 3157-3173.
Cutter, A. and Hayes, J. (2015) A brief review of nucleosome structure. *FEBS Letters*, 589(20PartA), pp. 2914-2922.

Dahiya, S., Emnett, R., Haydon, D., Leonard, J., Phillips, J., Perry, A. and Gutmann, D. (2013) BRAF-V600E mutation in pediatric and adult glioblastoma. *Neuro-Oncology*, 16(2), pp. 318-319.

D'Arcangelo, G., Homayouni, R., Keshvara, L., Rice, D., Sheldon, M. and Curran, T. (1999) Reelin Is a Ligand for Lipoprotein Receptors. *Neuron*, 24(2), pp. 471-479.

Davis, D., Delmonte, A., Ly, C. and McNally, E. (2000) Myoferlin, a candidate gene and potential modifier of muscular dystrophy. *Human Molecular Genetics*, 9(2), pp. 217-226.

De Carvalho, D., You, J. and Jones, P. (2010) DNA methylation and cellular reprogramming. *Trends in Cell Biology*, 20(10), pp. 609-617.

DeBerardinis, R. and Thompson, C. (2012) Cellular Metabolism and Disease: What Do Metabolic Outliers Teach Us?. *Cell*, 148(6), pp. 1132-1144.

DeBerardinis, R., Mancuso, A., Daikhin, E., Nissim, I., Yudkoff, M., Wehrli, S. and Thompson, C. (2007) Beyond aerobic glycolysis: Transformed cells can engage in glutamine metabolism that exceeds the requirement for protein and nucleotide synthesis. *Proceedings of the National Academy of Sciences*, 104(49), pp. 19345-19350.

Delage, B., Fennell, D., Nicholson, L., McNeish, I., Lemoine, N., Crook, T. and Szlosarek, P. (2010) Arginine deprivation and argininosuccinate synthetase expression in the treatment of cancer.*International Journal of Cancer*, p. NA-NA.

Delage, B., Luong, P., Maharaj, L., O'Riain, C., Syed, N., Crook, T., Hatzimichael, E., Papoudou-Bai, A., Mitchell, T., Whittaker, S., Cerio, R., Gribben, J., Lemoine, N., Bomalaski, J., Li, C., Joel, S., Fitzgibbon, J., Chen, L. and Szlosarek, P. (2012) Promoter methylation of argininosuccinate synthetase-1 sensitises lymphomas to arginine deiminase treatment, autophagy and caspase-dependent apoptosis. *Cell Death Dis*, 3(7), p. e342.

Demuth, T. and Berens, M. (2004) Molecular Mechanisms of Glioma Cell Migration and Invasion. *J Neurooncol*, 70(2), pp. 217-228.

Dennis, J., Lau, K., Demetriou, M. and Nabi, I. (2009) Adaptive Regulation at the Cell Surface byN-Glycosylation. *Traffic*, 10(11), pp. 1569-1578.

Dillon, B., Prieto, V., Curley, S., Ensor, C., Holtsberg, F., Bomalaski, J. and Clark, M. (2004) Incidence and distribution of argininosuccinate synthetase deficiency in human cancers. *Cancer*, 100(4), pp. 826-833.

Diskin, S. (2006) STAC: A method for testing the significance of DNA copy number aberrations across multiple array-CGH experiments. *Genome Research*, 16(9), pp. 1149-1158.

Diskin, S., Hou, C., Glessner, J., Attiyeh, E., Laudenslager, M., Bosse, K., Cole, K., Mossé, Y., Wood, A., Lynch, J., Pecor, K., Diamond, M., Winter, C., Wang, K., Kim, C., Geiger, E., McGrady, P., Blakemore, A., London, W., Shaikh, T., Bradfield, J., Grant, S., Li, H., Devoto, M., Rappaport, E., Hakonarson, H. and Maris, J. (2009) Copy number variation at 1q21.1 associated with neuroblastoma. *Nature*, 459(7249), pp. 987-991.

Downing, J., Wilson, R., Zhang, J., Mardis, E., Pui, C., Ding, L., Ley, T. and Evans, W. (2012) The Pediatric Cancer Genome Project. *Nature Genetics*, 44(6), pp. 619-622.

Dubrovska, A., Kim, S., Salamone, R., Walker, J., Maira, S., Garcia-Echeverria, C., Schultz, P. and Reddy, V. (2009) The role of PTEN/Akt/PI3K signaling in the maintenance and viability of prostate cancer stem-like cell populations. *Proceedings of the National Academy of Sciences*, 106(1), pp. 268-273.

Edmunds, J., Mahadevan, L. and Clayton, A. (2008) Dynamic histone H3 methylation during gene induction: HYPB/Setd2 mediates all H3K36 trimethylation. *EMBO J*, 27(2), pp. 406-420.

Ehrlich, M. (2009) DNA hypomethylation in cancer cells. *Epigenomics*, 1(2), pp. 239-259.

Ehrlich, M., Gama-Sosa, M., Huang, L., Midgett, R., Kuo, K., McCune, R. and Gehrke, C. (1982) Amount and distribution of 5-methylcytosine in human DNA from different types of tissues or cells. *Nucl Acids Res*, 10(8), pp. 2709-2721.

Ellis, L., Ku, S., Ramakrishnan, S., Lasorsa, E., Azabdaftari, G., Godoy, A. and Pili, R. (2013) Combinatorial antitumor effect of HDAC and the PI3K-Akt-mTOR pathway inhibition in a Pten defecient model of prostate cancer. *Oncotarget*, 4(12), pp. 2225-2236.

Engelman, J., Luo, J. and Cantley, L. (2006) The evolution of phosphatidylinositol 3-kinases as regulators of growth and metabolism. *Nat Rev Genet*, 7(8), pp. 606-619.

Esteller, M. (2002) CpG island hypermethylation and tumor suppressor genes: a booming present, a brighter future. *Oncogene*, 21(35), pp. 5427-5440.

Esteller, M., Toyota, M., Sanchez-Cespedes, M., Capella, G., Peinado, M.A., Watkins, D.N., Issa, J.P.J., Sidransky, D., Baylin, S.B. and Herman, J.G. (2000) Inactivation of the DNA repair gene O6-methylguanine-DNA methyltransferase by promoter hypermethylation is associated with G to A mutations in K-ras in colorectal tumorigenesis. *Cancer research*, *60*(9), pp.2368-2371.

Fan, Q., Cheng, C., Nicolaides, T., Hackett, C., Knight, Z., Shokat, K. and Weiss, W. (2007) A Dual Phosphoinositide-3-Kinase /mTOR Inhibitor Cooperates with Blockade of Epidermal Growth Factor Receptor in PTEN-Mutant Glioma. *Cancer Research*, 67(17), pp. 7960-7965.

Fan, Q., Knight, Z., Goldenberg, D., Yu, W., Mostov, K., Stokoe, D., Shokat, K. and Weiss, W. (2006) A dual PI3 kinase/mTOR inhibitor reveals emergent efficacy in glioma. *Cancer Cell*, 9(5), pp. 341-349.

Fangusaro, J. (2012) Pediatric High Grade Glioma: a Review and Update on Tumor Clinical Characteristics and Biology. *Front. Oncol.*, 2.

Faria, C., MiguÃ©ns, J., Antunes, J., Salgado, D., Nunes, S., Barroso, C., Martins, M., Nunes, V. and Roque, L. (2010) Pediatric brain tumors: genetics and clinical outcome. *Journal of Neurosurgery: Pediatrics*, 5(3), pp. 263-270.

Faury, D., Nantel, A., Dunn, S., Guiot, M., Haque, T., Hauser, P., Garami, M., Bognar, L., Hanzely, Z., Liberski, P., Lopez-Aguilar, E., Valera, E., Tone, L., Carret, A., Del Maestro, R., Gleave, M., Montes, J., Pietsch, T., Albrecht, S. and Jabado, N. (2007) Molecular Profiling Identifies Prognostic Subgroups of Pediatric Glioblastoma and Shows Increased YB-1 Expression in Tumors.*Journal of Clinical Oncology*, 25(10), pp. 1196-1208.

Fei, X., Qi, M., Wu, B., Song, Y., Wang, Y. and Li, T. (2012) MicroRNA-195-5p suppresses glucose uptake and proliferation of human bladder cancer T24 cells by regulating GLUT3 expression.*FEBS Letters*, 586(4), pp. 392-397.

Feinberg, A. and Tycko, B. (2004) The history of cancer epigenetics. *Nature Reviews Cancer*, 4(2), pp. 143-153.

Felli, N., Fontana, L., Pelosi, E., Botta, R., Bonci, D., Facchiano, F., Liuzzi, F., Lulli, V., Morsilli, O., Santoro, S., Valtieri, M., Calin, G., Liu, C., Sorrentino, A., Croce, C. and Peschle, C. (2005) MicroRNAs 221 and 222 inhibit normal erythropoiesis and erythroleukemic cell growth via kit receptor down-

modulation. *Proceedings of the National Academy of Sciences*, 102(50), pp. 18081-18086.

Feng, L. and Cooper, J. (2009) Dual Functions of Dab1 during Brain Development. *Molecular and Cellular Biology*, 29(2), pp. 324-332.

Ferlay, J., Soerjomataram, I., Dikshit, R., Eser, S., Mathers, C., Rebelo, M., Parkin, D., Forman, D. and Bray, F. (2014) Cancer incidence and mortality worldwide: Sources, methods and major patterns in GLOBOCAN 2012. *International Journal of Cancer*, 136(5), pp. E359-E386.

Ferreira, H., Heyn, H., Moutinho, C. and Esteller, M. (2012) CpG island hypermethylation-associated silencing of small nucleolar RNAs in human cancer. *RNA Biology*, 9(6), pp. 881-890.

Feun, L. and Savaraj, N. (2006) Pegylated arginine deiminase: a novel anticancer enzyme agent. *Expert Opinion on Investigational Drugs*, 15(7), pp. 815-822.

Feun, L., Kuo, M. and Savaraj, N. (2015) Arginine deprivation in cancer therapy. *Current Opinion in Clinical Nutrition and Metabolic Care*, 18(1), pp. 78-82.

Feun, L., Marini, A., Walker, G., Elgart, G., Moffat, F., Rodgers, S., Wu, C., You, M., Wangpaichitr, M., Kuo, M., Sisson, W., Jungbluth, A., Bomalaski, J. and Savaraj, N. (2012) Negative argininosuccinate synthetase expression in melanoma tumours may predict clinical benefit from arginine-depleting therapy with pegylated arginine deiminase. *Br J Cancer*, 106(9), pp. 1481-1485.

Filipowicz, W., Bhattacharyya, S. and Sonenberg, N. (2008) Mechanisms of post-transcriptional regulation by microRNAs: are the answers in sight?. *Nat Rev Genet*, 2008(2), pp. 102-114.

Fisher, P., Tihan, T., Goldthwaite, P., Wharam, M., Carson, B., Weingart, J., Repka, M., Cohen, K. and Burger, P. (2008) Outcome analysis of childhood low-grade astrocytomas. *Pediatr. Blood Cancer*, 51(2), pp. 245-250.

Fogel, B., Wexler, E., Wahnich, A., Friedrich, T., Vijayendran, C., Gao, F., Parikshak, N., Konopka, G. and Geschwind, D. (2012) RBFOX1 regulates both splicing and transcriptional networks in human neuronal development. *Human Molecular Genetics*, 21(19), pp. 4171-4186.

Fontebasso, A., Papillon-Cavanagh, S., Schwartzentruber, J., Nikbakht, H., Gerges, N., Fiset, P., Bechet, D., Faury, D., De Jay, N., Ramkissoon, L., Corcoran, A., Jones, D., Sturm, D., Johann, P., Tomita, T., Goldman, S., Nagib, M., Bendel, A., Goumnerova, L., Bowers, D., Leonard, J., Rubin, J., Alden, T., Browd, S., Geyer, J., Leary, S., Jallo, G., Cohen, K., Gupta, N., Prados, M., Carret, A., Ellezam, B., Crevier, L., Klekner, A., Bognar, L., Hauser, P., Garami, M., Myseros, J., Dong, Z., Siegel, P., Malkin, H., Ligon, A., Albrecht, S., Pfister, S., Ligon, K., Majewski, J., Jabado, N. and Kieran, M. (2014) Recurrent somatic mutations in ACVR1 in pediatric midline high-grade astrocytoma. *Nature Genetics*, 46(5), pp. 462-466.

Fontebasso, A., Papillon-Cavanagh, S., Schwartzentruber, J., Nikbakht, H., Gerges, N., Fiset, P., Bechet, D., Faury, D., De Jay, N., Ramkissoon, L., Corcoran, A., Jones, D., Sturm, D., Johann, P., Tomita, T., Goldman, S., Nagib, M., Bendel, A., Goumnerova, L., Bowers, D., Leonard, J., Rubin, J., Alden, T., Browd, S., Geyer, J., Leary, S., Jallo, G., Cohen, K., Gupta, N., Prados, M., Carret, A., Ellezam, B., Crevier, L., Klekner, A., Bognar, L., Hauser, P., Garami, M., Myseros, J., Dong, Z., Siegel, P., Malkin, H., Ligon, A., Albrecht, S., Pfister, S., Ligon, K., Majewski, J., Jabado, N. and Kieran, M. (2014) Recurrent somatic mutations in

ACVR1 in pediatric midline high-grade astrocytoma. *Nature Genetics*, 46(5), pp. 462-466.

Formosa, A., Markert, E., Lena, A., Italiano, D., Finazzi-Agro', E., Levine, A., Bernardini, S., Garabadgiu, A., Melino, G. and Candi, E. (2013) MicroRNAs, miR-154, miR-299-5p, miR-376a, miR-376c, miR-377, miR-381, miR-487b, miR-485-3p, miR-495 and miR-654-3p, mapped to the 14q32.31 locus, regulate proliferation, apoptosis, migration and invasion in metastatic prostate cancer cells. *Oncogene*, 33(44), pp. 5173-5182.

Fouladi, M., Hunt, D., Pollack, I., Dueckers, G., Burger, P., Becker, L., Yates, A., Gilles, F., Davis, R., Boyett, J. and Finlay, J. (2003) Outcome of children with centrally reviewed low-grade gliomas treated with chemotherapy with or without radiotherapy on Children's Cancer Group high-grade glioma study CCG-945. *Cancer*, 98(6), pp. 1243-1252.

Franco, S., Martinez-Garay, I., Gil-Sanz, C., Harkins-Perry, S. and Müller, U. (2011) Reelin Regulates Cadherin Function via Dab1/Rap1 to Control Neuronal Migration and Lamination in the Neocortex. *Neuron*, 69(3), pp. 482-497.

Franke, T. (1997) Direct Regulation of the Akt Proto-Oncogene Product by Phosphatidylinositol-3,4-bisphosphate. *Science*, 275(5300), pp. 665-668.

Friedländer, M., Lizano, E., Houben, A., Bezdan, D., Báñez-Coronel, M., Kudla, G., Mateu-Huertas, E., Kagerbauer, B., González, J., Chen, K., LeProust, E., Martí, E. and Estivill, X. (2014) Evidence for the biogenesis of more than 1,000 novel human microRNAs. *Genome Biol*, 15(4), p. R57.

Friedman, R., Farh, K., Burge, C. and Bartel, D. (2009) Most mammalian mRNAs are conserved targets of microRNAs. *Genome Research*, 19(1), pp. 92-105.

Frova, C. (2006) Glutathione transferases in the genomics era: New insights and perspectives.*Biomolecular Engineering*, 23(4), pp. 149-169.

Fujiki, R., Hashiba, W., Sekine, H., Yokoyama, A., Chikanishi, T., Ito, S., Imai, Y., Kim, J., He, H., Igarashi, K., Kanno, J., Ohtake, F., Kitagawa, H., Roeder, R., Brown, M. and Kato, S. (2011) GlcNAcylation of histone H2B facilitates its monoubiquitination. *Nature*.

Fujimoto, A., Totoki, Y., Abe, T., Boroevich, K., Hosoda, F., Nguyen, H., Aoki, M., Hosono, N., Kubo, M., Miya, F., Arai, Y., Takahashi, H., Shirakihara, T., Nagasaki, M., Shibuya, T., Nakano, K., Watanabe-Makino, K., Tanaka, H., Nakamura, H., Kusuda, J., Ojima, H., Shimada, K., Okusaka, T., Ueno, M., Shigekawa, Y., Kawakami, Y., Arihiro, K., Ohdan, H., Gotoh, K., Ishikawa, O., Ariizumi, S., Yamamoto, M., Yamada, T., Chayama, K., Kosuge, T., Yamaue, H., Kamatani, N., Miyano, S., Nakagama, H., Nakamura, Y., Tsunoda, T., Shibata, T. and Nakagawa, H. (2012) Whole-genome sequencing of liver cancers identifies etiological influences on mutation patterns and recurrent mutations in chromatin regulators. *Nature Genetics*, 44(7), pp. 760-764.

Fulda, S. and KÃ¶gel, D. (2015) Cell death by autophagy: emerging molecular mechanisms and implications for cancer therapy. *Oncogene*, 34(40), pp. 5105-5113.

Gabriely, G., Yi, M., Narayan, R., Niers, J., Wurdinger, T., Imitola, J., Ligon, K., Kesari, S., Esau, C., Stephens, R., Tannous, B. and Krichevsky, A. (2011) Human Glioma Growth Is Controlled by MicroRNA-10b. *Cancer Research*, 71(10), pp. 3563-3572.

Gallia, G., Rand, V., Siu, I., Eberhart, C., James, C., Marie, S., Oba-Shinjo, S., Carlotti, C., Caballero, O., Simpson, A., Brock, M., Massion, P., Carson, B. and

Riggins, G. (2006) PIK3CA Gene Mutations in Pediatric and Adult Glioblastoma Multiforme. *Molecular Cancer Research*, 4(10), pp. 709-714.

Galluzzi, L., Kepp, O., Vander Heiden, M.G. and Kroemer, G. (2013) Metabolic targets for cancer therapy. *Nature reviews Drug discovery*, *12*(11), pp.829-846.

Gampe, K., Stefani, J., Hammer, K., Brendel, P., Pötzsch, A., Enikolopov, G., Enjyoji, K., Acker-Palmer, A., Robson, S. and Zimmermann, H. (2014) NTPDase2 and Purinergic Signaling Control Progenitor Cell Proliferation in Neurogenic Niches of the Adult Mouse Brain. *STEM CELLS*, 33(1), pp. 253-264.

Gao, X., Lin, J., Gao, L., Li, Y., Wang, L. and Yu, L. (2011) MicroRNA-193b regulates c-Kit proto-oncogene and represses cell proliferation in acute myeloid leukemia. *Leukemia Research*, 35(9), pp. 1226-1232.

Gerez, J., Tedesco, L., Bonfiglio, J., Fuertes, M., Barontini, M., Silberstein, S., Wu, Y., Renner, U., Páez-Pereda, M., Holsboer, F., Stalla, G. and Arzt, E. (2014) RSUME inhibits VHL and regulates its tumor suppressor function. *Oncogene*, 34(37), pp. 4855-4866.

Gerges, N., Fontebasso, A., Albrecht, S., Faury, D. and Jabado, N. (2013) Pediatric high-grade astrocytomas: a distinct neuro-oncological paradigm. *Genome Medicine*, 5(7), p. 66.

Gessi, M., Japp, A., Dreschmann, V., zur Mühlen, A., Goschzik, T., Dörner, E. and Pietsch, T. (2015) High-Resolution Genomic Analysis of Cribriform Neuroepithelial Tumors of the Central Nervous System. *J Neuropathol Exp Neurol*, 74(10), pp. 970-974.

Gillet, J., Calcagno, A., Varma, S., Marino, M., Green, L., Vora, M., Patel, C., Orina, J., Eliseeva, T., Singal, V., Padmanabhan, R., Davidson, B., Ganapathi, R., Sood, A., Rueda, B., Ambudkar, S. and Gottesman, M. (2011) Redefining the relevance of established cancer cell lines to the study of mechanisms of clinical anti-cancer drug resistance. *Proceedings of the National Academy of Sciences*, 108(46), pp. 18708-18713.

Gilroy, E. (1930) The influence of arginine upon the growth rate of a transplantable tumour in the mouse. *Biochem. J.*, 24(3), pp. 589-595.

Giunti, L., Pantaleo, M., Sardi, L., Provenzano, A., Magi, A., Cardellicchio, S., Castiglione, F., Tattini, L., Novara, F., Buccoliero, A., de Martino, M., Genitori, L., Zuffardi, O. and Giglio, S. (2014) Genome-wide copy number analysis in pediatric glioblastoma multiforme. *Am J Cancer Res*, 4(3), pp. 293-303.

Goldberg, A., Allis, C. and Bernstein, E. (2007) Epigenetics: A Landscape Takes Shape. *Cell*, 128(4), pp. 635-638.

Gomes, C., Osório, H., Pinto, M., Campos, D., Oliveira, M. and Reis, C. (2013) Expression of ST3GAL4 Leads to SLex Expression and Induces c-Met Activation and an Invasive Phenotype in Gastric Carcinoma Cells. *PLoS ONE*, 8(6), p. e66737.

Gong, J., Zhang, J., Li, B., Zeng, C., You, K., Chen, M., Yuan, Y. and Zhuang, S. (2012) MicroRNA-125b promotes apoptosis by regulating the expression of Mcl-1, Bcl-w and IL-6R. *Oncogene*, 32(25), pp. 3071-3079.

Grasso, C., Tang, Y., Truffaux, N., Berlow, N., Liu, L., Debily, M., Quist, M., Davis, L., Huang, E., Woo, P., Ponnuswami, A., Chen, S., Johung, T., Sun, W., Kogiso, M., Du, Y., Qi, L., Huang, Y., Hütt-Cabezas, M., Warren, K., Le Dret, L., Meltzer, P., Mao, H., Quezado, M., van Vuurden, D., Abraham, J., Fouladi, M., Svalina, M., Wang, N., Hawkins, C., Nazarian, J., Alonso, M., Raabe, E., Hulleman, E., Spellman, P., Li, X., Keller, C., Pal, R., Grill, J. and Monje, M.

(2015) Functionally defined therapeutic targets in diffuse intrinsic pontine glioma. *Nature Medicine*, 21(6), pp. 555-559.

Grasso, C., Wu, Y., Robinson, D., Cao, X., Dhanasekaran, S., Khan, A., Quist, M., Jing, X., Lonigro, R., Brenner, J., Asangani, I., Ateeq, B., Chun, S., Siddiqui, J., Sam, L., Anstett, M., Mehra, R., Prensner, J., Palanisamy, N., Ryslik, G., Vandin, F., Raphael, B., Kunju, L., Rhodes, D., Pienta, K., Chinnaiyan, A. and Tomlins, S. (2012) The mutational landscape of lethal castration-resistant prostate cancer. *Nature*, 487(7406), pp. 239-243.

Greaves, M. and Maley, C. (2012) Clonal evolution in cancer. *Nature*, 481(7381), pp. 306-313.

Gregersen, L., Jacobsen, A., Frankel, L., Wen, J., Krogh, A. and Lund, A. (2012) MicroRNA-143 down-regulates Hexokinase 2 in colon cancer cells. *BMC Cancer*, 12(1), p. 232.

Greither, T., Grochola, L., Udelnow, A., Lautenschläger, C., Würl, P. and Taubert, H. (2009) Elevated expression of microRNAs 155, 203, 210 and 222 in pancreatic tumors is associated with poorer survival. *International Journal of Cancer*, 126(1), pp. 73-80.

Grill, J., Puget, S., Andreiuolo, F., Philippe, C., MacConaill, L. and Kieran, M. (2011) Critical oncogenic mutations in newly diagnosed pediatric diffuse intrinsic pontine glioma. *Pediatr. Blood Cancer*, 58(4), pp. 489-491.

Guay, C., Joly, Ã., Pepin, Ã., Barbeau, A., Hentsch, L., Pineda, M., Madiraju, S., Brunengraber, H. and Prentki, M. (2013) A Role for Cytosolic Isocitrate Dehydrogenase as a Negative Regulator of Glucose Signaling for Insulin Secretion in Pancreatic ÃŸ-Cells. *PLoS ONE*, 8(10), p. e77097.

Gui, Y., Guo, G., Huang, Y., Hu, X., Tang, A., Gao, S., Wu, R., Chen, C., Li, X., Zhou, L., He, M., Li, Z., Sun, X., Jia, W., Chen, J., Yang, S., Zhou, F., Zhao, X., Wan, S., Ye, R., Liang, C., Liu, Z., Huang, P., Liu, C., Jiang, H., Wang, Y., Zheng, H., Sun, L., Liu, X., Jiang, Z., Feng, D., Chen, J., Wu, S., Zou, J., Zhang, Z., Yang, R., Zhao, J., Xu, C., Yin, W., Guan, Z., Ye, J., Zhang, H., Li, J., Kristiansen, K., Nickerson, M., Theodorescu, D., Li, Y., Zhang, X., Li, S., Wang, J., Yang, H., Wang, J. and Cai, Z. (2011) Frequent mutations of chromatin remodeling genes in transitional cell carcinoma of the bladder. *Nature Genetics*, 43(9), pp. 875-878.

Guo, X., Gao, L., Wang, Y., Chiu, D., Wang, T. and Deng, Y. (2015) Advances in long noncoding RNAs: identification, structure prediction and function annotation. *Briefings in Functional Genomics*.

Guo, Z., Maki, M., Ding, R., Yang, Y., zhang, B. and Xiong, L. (2014) Genome-wide survey of tissue-specific microRNA and transcription factor regulatory networks in 12 tissues. *Sci. Rep.*, 4.

Hackenberg, M., Barturen, G., Carpena, P., Luque-Escamilla, P., Previti, C. and Oliver, J. (2010) Prediction of CpG-island function: CpG clustering vs. sliding-window methods. *BMC Genomics*, 11(1), p. 327.

Hahn, R.G. and Kenny, G.E. (1974) Differences in arginine requirement for growth among arginine-utilizing Mycoplasma species. *Journal of bacteriology*,*117*(2), pp.611-618.

Haines, R.J., Pendleton, L.C. and Eichler, D.C. (2011) Argininosuccinate synthase: at the center of arginine metabolism. *International journal of biochemistry and molecular biology*, *2*(1), p.8.

Han, Y., Yang, Y., Yuan, H., Zhang, T., Sui, H., Wei, X., Liu, L., Huang, P., Zhang, W. and Bai, Y. (2014) UCA1, a long non-coding RNA up-regulated in colorectal

cancer influences cell proliferation, apoptosis and cell cycle distribution. *Pathology*, 46(5), pp. 396-401.
Hanahan, D. and Weinberg, R. (2011) Hallmarks of Cancer: The Next Generation. *Cell*, 144(5), pp. 646-674.
Handa, V. and Jeltsch, A. (2005) Profound Flanking Sequence Preference of Dnmt3a and Dnmt3b Mammalian DNA Methyltransferases Shape the Human Epigenome. *Journal of Molecular Biology*, 348(5), pp. 1103-1112.
Hargrave, D., Bartels, U. and Bouffet, E. (2006) Diffuse brainstem glioma in children: critical review of clinical trials. *The Lancet Oncology*, 7(3), pp. 241-248.
Hata, A. and Lieberman, J. (2015) Dysregulation of microRNA biogenesis and gene silencing in cancer.*Science Signaling*, 8(368), pp. re3-re3.
Hayes, J., Thygesen, H., Tumilson, C., Droop, A., Boissinot, M., Hughes, T., Westhead, D., Alder, J., Shaw, L., Short, S. and Lawler, S. (2015) Prediction of clinical outcome in glioblastoma using a biologically relevant nine-microRNA signature. *Molecular Oncology*, 9(3), pp. 704-714.
Hedenfalk, I., Duggan, D., Chen, Y., Radmacher, M., Bittner, M., Simon, R., Meltzer, P., Gusterson, B., Esteller, M., Raffeld, M. and Yakhini, Z. (2001) Gene-expression profiles in hereditary breast cancer. *New England Journal of Medicine*, *344*(8), pp.539-548.
Herman, J. and Baylin, S. (2003) Gene Silencing in Cancer in Association with Promoter Hypermethylation. *New England Journal of Medicine*, 349(21), pp. 2042-2054.
Herman, J., Latif, F., Weng, Y., Lerman, M., Zbar, B., Liu, S., Samid, D., Duan, D., Gnarra, J. and Linehan, W. (1994) Silencing of the VHL tumor-suppressor gene by DNA methylation in renal carcinoma. *Proceedings of the National Academy of Sciences*, 91(21), pp. 9700-9704.
Herman, J., Umar, A., Polyak, K., Graff, J., Ahuja, N., Issa, J., Markowitz, S., Willson, J., Hamilton, S., Kinzler, K., Kane, M., Kolodner, R., Vogelstein, B., Kunkel, T. and Baylin, S. (1998) Incidence and functional consequences of hMLH1 promoter hypermethylation in colorectal carcinoma.*Proceedings of the National Academy of Sciences*, 95(12), pp. 6870-6875.
Hervouet, E., Vallette, F. and Cartron, P. (2009) Dnmt3/transcription factor interactions as crucial players in targeted DNA methylation. *Epigenetics*, 4(7), pp. 487-499.
Hirayama, A., Kami, K., Sugimoto, M., Sugawara, M., Toki, N., Onozuka, H., Kinoshita, T., Saito, N., Ochiai, A., Tomita, M., Esumi, H. and Soga, T. (2009) Quantitative Metabolome Profiling of Colon and Stomach Cancer Microenvironment by Capillary Electrophoresis Time-of-Flight Mass Spectrometry. *Cancer Research*, 69(11), pp. 4918-4925.
Hisaoka, M., Matsuyama, A. and Nakamoto, M. (2012) Aberrant Calreticulin Expression Is Involved in the Dedifferentiation of Dedifferentiated Liposarcoma. *The American Journal of Pathology*, 180(5), pp. 2076-2083.
Hofmann, B., Schlüter, L., Lange, P., Mercanoglu, B., Ewald, F., Fölster, A., Picksak, A., Harder, S., El Gammal, A., Grupp, K., Güngör, C., Drenckhan, A., Schlüter, H., Wagener, C., Izbicki, J., Jücker, M., Bockhorn, M. and Wolters-Eisfeld, G. (2015) COSMC knockdown mediated aberrant O-glycosylation promotes oncogenic properties in pancreatic cancer. *Molecular Cancer*, 14(1).
Holtsberg, F., Ensor, C., Steiner, M., Bomalaski, J. and Clark, M. (2002) Poly(ethylene glycol) (PEG) conjugated arginine deiminase: effects of PEG

formulations on its pharmacological properties.*Journal of Controlled Release*, 80(1-3), pp. 259-271.

Howell, B., Herrick, T. and Cooper, J. (1999) Reelin-induced tryosine phosphorylation of Disabled 1 during neuronal positioning. *Genes & Development*, 13(6), pp. 643-648.

Howells, R., Holland, T., Dhar, K., Redman, C., Hand, P., Hoban, P., Jones, P., Fryer, A. and Strange, R. (2001) Glutathione S-transferase GSTM1 and GSTT1 genotypes in ovarian cancer: association with p53 expression and survival. *Int J Gynecol Cancer*, 11(2), pp. 107-112.

Hu, H., Li, S., Liu, J. and Ni, B. (2012) MicroRNA-193b modulates proliferation, migration, and invasion of non-small cell lung cancer cells. *Acta Biochimica et Biophysica Sinica*, 44(5), pp. 424-430.

Huang, H., Wu, W., Wang, Y., Wang, J., Fang, F., Tsai, J., Li, S., Hung, H., Yu, S., Lan, J., Shiue, Y., Hsing, C., Chen, L. and Li, C. (2013) ASS1 as a Novel Tumor Suppressor Gene in Myxofibrosarcomas: Aberrant Loss via Epigenetic DNA Methylation Confers Aggressive Phenotypes, Negative Prognostic Impact, and Therapeutic Relevance. *Clinical Cancer Research*, 19(11), pp. 2861-2872.

Huang, K., Lee, W., Huang, S., Lin, Y., Kang, C., Liou, C. and Tzeng, C. (2007) Chromosomal Gain of 3q and Loss of 11q Often Associated with Nodal Metastasis in Early Stage Cervical Squamous Cell Carcinoma. *Journal of the Formosan Medical Association*, 106(11), pp. 894-902.

Huang, Q., Liu, Z., Xie, F., Liu, C., Shao, F., Zhu, C. and Hu, S. (2014) Fragile Histidine Triad (FHIT) Suppresses Proliferation and Promotes Apoptosis in Cholangiocarcinoma Cells by Blocking PI3K-Akt Pathway. *The Scientific World Journal*, 2014, pp. 1-7.

Huillard, E., Hashizume, R., Phillips, J., Griveau, A., Ihrie, R., Aoki, Y., Nicolaides, T., Perry, A., Waldman, T., McMahon, M., Weiss, W., Petritsch, C., James, C. and Rowitch, D. (2012) Cooperative interactions of BRAFV600E kinase and CDKN2A locus deficiency in pediatric malignant astrocytoma as a basis for rational therapy. *Proceedings of the National Academy of Sciences*, 109(22), pp. 8710-8715.

Iacobuzio-Donahue, C., Maitra, A., Olsen, M., Lowe, A., Van Heek, N., Rosty, C., Walter, K., Sato, N., Parker, A., Ashfaq, R., Jaffee, E., Ryu, B., Jones, J., Eshleman, J., Yeo, C., Cameron, J., Kern, S., Hruban, R., Brown, P. and Goggins, M. (2003) Exploration of Global Gene Expression Patterns in Pancreatic Adenocarcinoma Using cDNA Microarrays. *The American Journal of Pathology*, 162(4), pp. 1151-1162.

Irmler, M., Thome, M., Hanhe, M., Schneider, P., Hofmann, K., Steiner, V., Bodmer, J., Schröter, M., Burns, K., Mattmann, C., Rimoldi, D., French, L. and Tschopp, J. (1997) Inhibition of death receptor signals by cellular FLIP. *Nature*, 388, pp. 190-195.

Isobe, T., Hisamori, S., Hogan, D., Zabala, M., Hendrickson, D., Dalerba, P., Cai, S., Scheeren, F., Kuo, A., Sikandar, S., Lam, J., Qian, D., Dirbas, F., Somlo, G., Lao, K., Brown, P., Clarke, M. and Shimono, Y. (2014) miR-142 regulates the tumorigenicity of human breast cancer stem cells through the canonical WNT signaling pathway. *eLife*, 3.

Ito, S., D'Alessio, A., Taranova, O., Hong, K., Sowers, L. and Zhang, Y. (2010) Role of Tet proteins in 5mC to 5hmC conversion, ES-cell self-renewal and inner cell mass specification. *Nature*, 466(7310), pp. 1129-1133.

Izzo, F. (2004) Pegylated Arginine Deiminase Treatment of Patients With Unresectable Hepatocellular Carcinoma: Results From Phase I/II Studies. *Journal of Clinical Oncology*, 22(10), pp. 1815-1822.

Jain, M., Nilsson, R., Sharma, S., Madhusudhan, N., Kitami, T., Souza, A., Kafri, R., Kirschner, M., Clish, C. and Mootha, V. (2012) Metabolite Profiling Identifies a Key Role for Glycine in Rapid Cancer Cell Proliferation. *Science*, 336(6084), pp. 1040-1044.

Jakacki, R.I., Zeltzer, P.M., Boyett, J.M., Albright, A.L., Allen, J.C., Geyer, J.R., Rorke, L.B., Stanley, P., Stevens, K.R. and Wisoff, J. (1995) Survival and prognostic factors following radiation and/or chemotherapy for primitive neuroectodermal tumors of the pineal region in infants and children: a report of the Childrens Cancer Group. *Journal of clinical oncology*, *13*(6), pp.1377-1383.

Jalali, R., Rishi, A., Goda, J., Sridhar, E., Gurav, M., Sharma, P., Moiyadi, A., Shetty, P. and Gupta, T. (2015) Clinical outcome and molecular characterization of pediatric glioblastoma treated with postoperative radiotherapy with concurrent and adjuvant temozolomide: a single institutional study of 66 children. *Neuro-Oncology Practice*, p. npv024.

Jansen, M., van Vuurden, D., Vandertop, W. and Kaspers, G. (2012) Diffuse intrinsic pontine gliomas: A systematic update on clinical trials and biology. *Cancer Treatment Reviews*, 38(1), pp. 27-35.

Jeltsch, A. and Jurkowska, R. (2014) New concepts in DNA methylation. *Trends in Biochemical Sciences*, 39(7), pp. 310-318.

Jenuwein, T. (2001) Translating the Histone Code. *Science*, 293(5532), pp. 1074-1080.

Jha, P., Agrawal, R., Pathak, P., Kumar, A., Purkait, S., Mallik, S., Suri, V., Chand Sharma, M., Gupta, D., Suri, A., Sharma, B., Julka, P., Kulshreshtha, R. and Sarkar, C. (2015) Genome-wide small noncoding RNA profiling of pediatric high-grade gliomas reveals deregulation of several miRNAs, identifies downregulation of snoRNA cluster HBII-52 and delineates H3F3A and TP53 mutant-specific miRNAs and snoRNAs. *International Journal of Cancer*, 137(10), pp. 2343-2353.

Jia, D., Jurkowska, R., Zhang, X., Jeltsch, A. and Cheng, X. (2007) Structure of Dnmt3a bound to Dnmt3L suggests a model for de novo DNA methylation. *Nature*, 449(7159), pp. 248-251.

Johnson, S., Grosshans, H., Shingara, J., Byrom, M., Jarvis, R., Cheng, A., Labourier, E., Reinert, K., Brown, D. and Slack, F. (2005) RAS Is Regulated by the let-7 MicroRNA Family. *Cell*, 120(5), pp. 635-647.

Jones, C. and Baker, S. (2014) Unique genetic and epigenetic mechanisms driving paediatric diffuse high-grade glioma. *Nature Reviews Cancer*.

Jones, C., Perryman, L. and Hargrave, D. (2012) Paediatric and adult malignant glioma: close relatives or distant cousins?. *Nature Reviews Clinical Oncology*, 9(7), pp. 400-413.

Jones, D., Mulholland, S., Pearson, D., Malley, D., Openshaw, S., Lambert, S., Liu, L., Bäcklund, L., Ichimura, K. and Collins, V. (2011) Adult grade II diffuse astrocytomas are genetically distinct from and more aggressive than their paediatric counterparts. *Acta Neuropathologica*, 121(6), pp. 753-761.

Jones, P. (2002) DNA methylation and cancer. *Oncogene*, 21(35), pp. 5358-5360.

Jones, P. and Laird, P. (1999) Cancer epigenetics comes of age. *Nat Genet*, 21(2), pp. 163-7.

Jones, P.A. and Baylin, S.B. (2007) The epigenomics of cancer. *Cell*, *128*(4), pp.683-692.

Jones, P.L., Veenstra, G.C.J., Wade, P.A., Vermaak, D., Kass, S.U., Landsberger, N., Strouboulis, J. and Wolffe, A.P. (1998). Methylated DNA and MeCP2 recruit histone deacetylase to repress transcription. *Nature genetics*,*19*(2), pp.187-191.

Jurkowska, R., Jurkowski, T. and Jeltsch, A. (2010) Structure and Function of Mammalian DNA Methyltransferases. *ChemBioChem*, 12(2), pp. 206-222.

Kami, K., Fujimori, T., Sato, H., Sato, M., Yamamoto, H., Ohashi, Y., Sugiyama, N., Ishihama, Y., Onozuka, H., Ochiai, A., Esumi, H., Soga, T. and Tomita, M. (2012) Metabolomic profiling of lung and prostate tumor tissues by capillary electrophoresis time-of-flight mass spectrometry.*Metabolomics*, 9(2), pp. 444-453.

Kappelmann, M., Kuphal, S., Meister, G., Vardimon, L. and Bosserhoff, A. (2013) MicroRNA miR-125b controls melanoma progression by direct regulation of c-Jun protein expression. *Oncogene*, 32(24), pp. 2984-2991.

Karremann, M., Hoffmann, M., Benesch, M., Kwiecien, R., von Bueren, A. and Kramm, C. (2015) Secondary Solid Malignancies After High-Grade Glioma Treatment in Pediatric Patients. *Pediatric Hematology and Oncology*, 32(7), pp. 467-473.

Karremann, M., Rausche, U., Roth, D., Kühn, A., Pietsch, T., Gielen, G., Warmuth-Metz, M., Kortmann, R., Straeter, R., Gnekow, A., Wolff, J. and Kramm, C. (2013) Cerebellar location may predict an unfavourable prognosis in paediatric high-grade glioma. *Br J Cancer*, 109(4), pp. 844-851.

Kasinski, A. and Slack, F. (2011) MicroRNAs en route to the clinic: progress in validating and targeting microRNAs for cancer therapy. *Nature Reviews Cancer*, 11(12), pp. 849-864.

Katayama, R., Ishioka, T., Takada, S., Takada, R., Fujita, N., Tsuruo, T. and Naito, M. (2009) Modulation of Wnt signaling by the nuclear localization of cellular FLIP-L. *Journal of Cell Science*, 123(1), pp. 23-28.

Kawagoe, H. (2004) TEL2, an ETS Factor Expressed in Human Leukemia, Regulates Monocytic Differentiation of U937 Cells and Blocks the Inhibitory Effect of TEL1 on Ras-Induced Cellular Transformation. *Cancer Research*, 64(17), pp. 6091-6100.

Kefas, B., Godlewski, J., Comeau, L., Li, Y., Abounader, R., Hawkinson, M., Lee, J., Fine, H., Chiocca, E., Lawler, S. and Purow, B. (2008) microRNA-7 Inhibits the Epidermal Growth Factor Receptor and the Akt Pathway and Is Down-regulated in Glioblastoma. *Cancer Research*, 68(10), pp. 3566-3572.

Kelley, K. and Berberich, S.J. (2011) FHIT gene expression is repressed by mitogenic signaling through the PI3K/AKT/FOXO pathway. *American journal of cancer research*, *1*(1), p.62.

Kelly, M., Jungbluth, A., Wu, B., Bomalaski, J., Old, L. and Ritter, G. (2011) Arginine deiminase PEG20 inhibits growth of small cell lung cancers lacking expression of argininosuccinate synthetase. *Br J Cancer*, 106(2), pp. 324-332.

Kelly, M., Jungbluth, A., Wu, B., Bomalaski, J., Old, L. and Ritter, G. (2011) Arginine deiminase PEG20 inhibits growth of small cell lung cancers lacking expression of argininosuccinate synthetase. *Br J Cancer*, 106(2), pp. 324-332.

Khazaei, M., Bunk, E., Hillje, A., Jahn, H., Riegler, E., Knoblich, J., Young, P. and Schwamborn, J. (2010) The E3-ubiquitin ligase TRIM2 regulates neuronal polarization. *Journal of Neurochemistry*, 117(1), pp. 29-37.

Khor, G.H., Froemming, G.R., Zain, R.B., Abraham, M.T. and Thong, K.L. (2014) Screening of differential promoter hypermethylated genes in primary oral squamous cell carcinoma. *Asian Pac J Cancer Prev*, *15*(20), pp.8957-8961.

Khuong-Quang, D., Buczkowicz, P., Rakopoulos, P., Liu, X., Fontebasso, A., Bouffet, E., Bartels, U., Albrecht, S., Schwartzentruber, J., Letourneau, L., Bourgey, M., Bourque, G., Montpetit, A., Bourret, G., Lepage, P., Fleming, A., Lichter, P., Kool, M., von Deimling, A., Sturm, D., Korshunov, A., Faury, D., Jones, D., Majewski, J., Pfister, S., Jabado, N. and Hawkins, C. (2012) K27M mutation in histone H3.3 defines clinically and biologically distinct subgroups of pediatric diffuse intrinsic pontine gliomas. *Acta Neuropathologica*, 124(3), pp. 439-447.

Kim, R., Coates, J., Bowles, T., McNerney, G., Sutcliffe, J., Jung, J., Gandour-Edwards, R., Chuang, F., Bold, R. and Kung, H. (2009) Arginine Deiminase as a Novel Therapy for Prostate Cancer Induces Autophagy and Caspase-Independent Apoptosis. *Cancer Research*, 69(2), pp. 700-708.

Kim, R., Coates, J., Bowles, T., McNerney, G., Sutcliffe, J., Jung, J., Gandour-Edwards, R., Chuang, F., Bold, R. and Kung, H. (2009) Arginine Deiminase as a Novel Therapy for Prostate Cancer Induces Autophagy and Caspase-Independent Apoptosis. *Cancer Research*, 69(2), pp. 700-708.

Kim, S., Rhee, J., Yoo, H., Lee, H., Lee, E., Lee, J., Yu, J., Son, B., Gong, G., Kim, S., Singh, S., Ahn, S. and Chang, S. (2015) Bioinformatic and metabolomic analysis reveals miR-155 regulates thiamine level in breast cancer. *Cancer Letters*, 357(2), pp. 488-497.

Kim, S., Tae, C., Hong, S., Min, B., Chang, D., Rhee, P., Kim, J., Kim, H., Kim, D. and Kim, Y. (2015) EYA4 Acts as a New Tumor Suppressor Gene in Colorectal Cancer. *Mol. Carcinog.*, 54(12), pp. 1748-1757.

Kim, T., Huang, W., Park, R., Park, P. and Johnson, M. (2011) A Developmental Taxonomy of Glioblastoma Defined and Maintained by MicroRNAs. *Cancer Research*, 71(9), pp. 3387-3399.

Kimura, N., Tokunaga, C., Dalal, S., Richardson, C., Yoshino, K., Hara, K., Kemp, B., Witters, L., Mimura, O. and Yonezawa, K. (2003) A possible linkage between AMP-activated protein kinase (AMPK) and mammalian target of rapamycin (mTOR) signalling pathway. *Genes to Cells*, 8(1), pp. 65-79.

Kleihues, P. and Sobin, L.H. (2000) World Health Organization classification of tumors. *Cancer*, *88*(12), pp.2887-2887.

Klippel, A., Kavanaugh, W., Pot, D. and Williams, L. (1997) A specific product of phosphatidylinositol 3-kinase directly activates the protein kinase Akt through its pleckstrin homology domain.*Molecular and Cellular Biology*, 17(1), pp. 338-344.

Klorin, G., Rozenblum, E., Glebov, O., Walker, R., Park, Y., Meltzer, P., Kirsch, I., Kaye, F. and Roschke, A. (2013) Integrated high-resolution array CGH and SKY analysis of homozygous deletions and other genomic alterations present in malignant mesothelioma cell lines. *Cancer Genetics*, 206(5), pp. 191-205.

Knowles, M., Leigh, M., Ostrowski, L., Huang, L., Carson, J., Hazucha, M., Yin, W., Berg, J., Davis, S., Dell, S., Ferkol, T., Rosenfeld, M., Sagel, S., Milla, C., Olivier, K., Turner, E., Lewis, A., Bamshad, M., Nickerson, D., Shendure, J. and Zariwala, M. (2013) Exome Sequencing Identifies Mutations in CCDC114 as a Cause of Primary Ciliary Dyskinesia. *The American Journal of Human Genetics*, 92(1), pp. 99-106.

Kobayashi, E., Masuda, M., Nakayama, R., Ichikawa, H., Satow, R., Shitashige, M., Honda, K., Yamaguchi, U., Shoji, A., Tochigi, N., Morioka, H., Toyama, Y.,

Hirohashi, S., Kawai, A. and Yamada, T. (2010) Reduced Argininosuccinate Synthetase Is a Predictive Biomarker for the Development of Pulmonary Metastasis in Patients with Osteosarcoma. *Molecular Cancer Therapeutics*, 9(3), pp. 535-544.

Kohli, R. and Zhang, Y. (2013) TET enzymes, TDG and the dynamics of DNA demethylation. *Nature*, 502(7472), pp. 472-479.

Koltes, J., Kumar, D., Kataria, R., Cooper, V. and Reecy, J. (2015) Transcriptional profiling of PRKG2-null growth plate identifies putative down-stream targets of PRKG2. *BMC Research Notes*, 8(1).

Koo, C., Kobiyama, K., Shen, Y., LeBert, N., Ahmad, S., Khatoo, M., Aoshi, T., Gasser, S. and Ishii, K. (2015) RNA Polymerase III Regulates Cytosolic RNA:DNA Hybrids and Intracellular MicroRNA Expression. *Journal of Biological Chemistry*, 290(12), pp. 7463-7473.

Koschny, R., Koschny, T., Froster, U., Krupp, W. and Zuber, M. (2002) Comparative genomic hybridization in glioma. *Cancer Genetics and Cytogenetics*, 135(2), pp. 147-159.

Kotani, A., Ha, D., Schotte, D., Armstrong, S. and Lodish, H. (2010) A novel mutation in the miR-128b gene reduces miRNA processing and leads to glucocorticoid resistance of MLL-AF4 Acute Lymphocytic Leukemia cells. *Cell Cycle*, 9(6), pp. 1037-1042.

Kouzarides, T. (2007) Chromatin Modifications and Their Function. *Cell*, 128(4), pp. 693-705.

Krause, D.S. and Van Etten, R.A. (2005) Tyrosine kinases as targets for cancer therapy. *New England Journal of Medicine*, *353*(2), pp.172-187.

Krek, A., Grün, D., Poy, M., Wolf, R., Rosenberg, L., Epstein, E., MacMenamin, P., da Piedade, I., Gunsalus, K., Stoffel, M. and Rajewsky, N. (2005) Combinatorial microRNA target predictions.*Nature Genetics*, 37(5), pp. 495-500.

Krop, I., Sgroi, D., Porter, D., Lunetta, K., LeVangie, R., Seth, P., Kaelin, C., Rhei, E., Bosenberg, M., Schnitt, S., Marks, J., Pagon, Z., Belina, D., Razumovic, J. and Polyak, K. (2001) HIN-1, a putative cytokine highly expressed in normal but not cancerous mammary epithelial cells. *Proceedings of the National Academy of Sciences*, 98(17), pp. 9796-9801.

Kumar, B., Brown, N., Swanson, B., Schmitt, A., Old, M., Ozer, E., Agrawal, A., Schuller, D., Teknos, T. and Kumar, P. (2016) High expression of myoferlin is associated with poor outcome in oropharyngeal squamous cell carcinoma patients and is inversely associated with HPV-status.*Oncotarget*.

Kumar, M., Pester, R., Chen, C., Lane, K., Chin, C., Lu, J., Kirsch, D., Golub, T. and Jacks, T. (2009) Dicer1 functions as a haploinsufficient tumor suppressor. *Genes & Development*, 23(23), pp. 2700-2704.

Kuo, G., Arnaud, L., Kronstad O'Brien, P. and Cooper, J. (2005) Absence of Fyn and Src Causes a Reeler-Like Phenotype. *Journal of Neuroscience*, 25(37), pp. 8578-8586.

Kutay, U., Hartmann, E., Treichel, N., Calado, A., Carmo-Fonseca, M., Prehn, S., Kraft, R., Gorlich, D. and Bischoff, F. (2000) Identification of Two Novel RanGTP-binding Proteins Belonging to the Importin beta Superfamily. *Journal of Biological Chemistry*, 275(51), pp. 40163-40168.

Labhart, P., Karmakar, S., Salicru, E., Egan, B., Alexiadis, V., O'Malley, B. and Smith, C. (2005) Identification of target genes in breast cancer cells directly regulated by the SRC-3/AIB1 coactivator. *Proceedings of the National Academy of Sciences*, 102(5), pp. 1339-1344.

Lages, E., Guttin, A., El Atifi, M., Ramus, C., Ipas, H., Dupré, I., Rolland, D., Salon, C., Godfraind, C., deFraipont, F., Dhobb, M., Pelletier, L., Wion, D., Gay, E., Berger, F. and Issartel, J. (2011) MicroRNA and Target Protein Patterns Reveal Physiopathological Features of Glioma Subtypes.*PLoS ONE*, 6(5), p. e20600.

Lamb, J. and Wheatley, D. (2000) Single Amino Acid (Arginine) Deprivation Induces G1 Arrest Associated with Inhibition of Cdk4 Expression in Cultured Human Diploid Fibroblasts.*Experimental Cell Research*, 255(2), pp. 238-249.

Lan, J., Tai, H., Lee, S., Chen, T., Huang, H. and Li, C. (2013) Deficiency in expression and epigenetic DNA Methylation of ASS1 gene in nasopharyngeal carcinoma: negative prognostic impact and therapeutic relevance. *Tumor Biol.*, 35(1), pp. 161-169.

Lane, D. (1992) p53, guardian of the genome. *Nature*, 358(6381), pp. 15-16.

Larbuisson, A., Dalcq, J., Martial, J. and Muller, M. (2013) Fgf receptors Fgfr1a and Fgfr2 control the function of pharyngeal endoderm in late cranial cartilage development. *Differentiation*, 86(4-5), pp. 192-206.

Lee, E., Kang, G., Kang, S., Jang, K., Lee, J., Park, J., Park, C., Sohn, T., Kim, S. and Kim, K. (2013) GSTT1 Copy Number Gain and ZNF Overexpression Are Predictors of Poor Response to Imatinib in Gastrointestinal Stromal Tumors. *PLoS ONE*, 8(10), p. e77219.

Lee, I., Ajay, S., Yook, J., Kim, H., Hong, S., Kim, N., Dhanasekaran, S., Chinnaiyan, A. and Athey, B. (2009) New class of microRNA targets containing simultaneous 5'-UTR and 3'-UTR interaction sites. *Genome Research*, 19(7), pp. 1175-1183.

Lee, J., Smith, E. and Shilatifard, A. (2010) The Language of Histone Crosstalk. *Cell*, 142(5), pp. 682-685.

Lee, J., Zhou, S. and Smas, C. (2010) Identification of RANBP16 and RANBP17 as novel interaction partners for the bHLH transcription factor E12. *Journal of Cellular Biochemistry*, 111(1), pp. 195-206.

Lee, T., Yao, G., Nevins, J. and You, L. (2008) Sensing and Integration of Erk and PI3K Signals by Myc. *PLoS Computational Biology*, 4(2), p. e1000013.

Lee, Y., Kim, M., Han, J., Yeom, K.H., Lee, S., Baek, S.H. and Kim, V.N. (2004) MicroRNA genes are transcribed by RNA polymerase II. *The EMBO journal*, *23*(20), pp.4051-4060.

Leivonen, S., Rokka, A., Östling, P., Kohonen, P., Corthals, G., Kallioniemi, O. and Perälä, M. (2011) Identification of miR-193b Targets in Breast Cancer Cells and Systems Biological Analysis of Their Functional Impact. *Mol Cell Proteomics*, 10(7), pp. M110.005322.

Leo, A., Walker, A., Lebo, M., Hendrickson, B., Scholl, T. and Akmaev, V. (2012) A GC-Wave Correction Algorithm that Improves the Analytical Performance of aCGH. *The Journal of Molecular Diagnostics*, 14(6), pp. 550-559.

Lepretre, F., Villenet, C., Quief, S., Nibourel, O., Jacquemin, C., Troussard, X., Jardin, F., Gibson, F., Kerckaert, J., Roumier, C. and Figeac, M. (2010) Waved aCGH: to smooth or not to smooth. *Nucleic Acids Research*, 38(7), pp. e94-e94.

Levy, J. and Thorburn, A. (2011) Modulation of pediatric brain tumor autophagy and chemosensitivity. *J Neurooncol*, 106(2), pp. 281-290.

Lewandowicz, G., Harding, B., Harkness, W., Hayward, R., Thomas, D. and Darling, J. (2000) Chemosensitivity in childhood brain tumours in vitro. *European Journal of Cancer*, 36(15), pp. 1955-1964.

Lewis, B., Shih, I., Jones-Rhoades, M., Bartel, D. and Burge, C. (2003) Prediction of Mammalian MicroRNA Targets. *Cell*, 115(7), pp. 787-798.

Lewis, P., Elsaesser, S., Noh, K., Stadler, S. and Allis, C. (2010) Daxx is an H3.3-specific histone chaperone and cooperates with ATRX in replication-independent chromatin assembly at telomeres.*Proceedings of the National Academy of Sciences*, 107(32), pp. 14075-14080.

Li, E., Beard, C. and Jaenisch, R. (1993) Role for DNA methylation in genomic imprinting. *Nature*, *366*(6453), pp.362-365.

Li, G., Yang, F., Xu, H., Yue, Z., Fang, X. and Liu, J. (2015) MicroRNA-708 is downregulated in hepatocellular carcinoma and suppresses tumor invasion and migration. *Biomedicine & Pharmacotherapy*, 73, pp. 154-159.

Li, M., Lee, K., Lu, Y., Clarke, I., Shih, D., Eberhart, C., Collins, V., Van Meter, T., Picard, D., Zhou, L., Boutros, P., Modena, P., Liang, M., Scherer, S., Bouffet, E., Rutka, J., Pomeroy, S., Lau, C., Taylor, M., Gajjar, A., Dirks, P., Hawkins, C. and Huang, A. (2009) Frequent Amplification of a chr19q13.41 MicroRNA Polycistron in Aggressive Primitive Neuroectodermal Brain Tumors.*Cancer Cell*, 16(6), pp. 533-546.

Li, R., Ackerman, W., Mihai, C., Volakis, L., Ghadiali, S. and Kniss, D. (2012) Myoferlin Depletion in Breast Cancer Cells Promotes Mesenchymal to Epithelial Shape Change and Stalls Invasion. *PLoS ONE*, 7(6), p. e39766.

Liang, G., Chan, M., Tomigahara, Y., Tsai, Y., Gonzales, F., Li, E., Laird, P. and Jones, P. (2002) Cooperativity between DNA Methyltransferases in the Maintenance Methylation of Repetitive Elements. *Molecular and Cellular Biology*, 22(2), pp. 480-491.

Libório-Kimura, T., Jung, H. and Chan, E. (2015) miR-494 represses HOXA10 expression and inhibits cell proliferation in oral cancer. *Oral Oncology*, 51(2), pp. 151-157.

Lima, S., Hernandez-Vargas, H. and Herceg, Z. (2010) Epigenetic signatures in cancer: Implications for the control of cancer in the clinic. *Current Opinion in Molecular Therapeutics*, 12(3), pp. 316-24.

Lin, L., Zheng, Y., Tu, Y., Wang, Z., Liu, H., Lu, X., Xu, L. and Yuan, J. (2014) MicroRNA-144 suppresses tumorigenesis and tumor progression of astrocytoma by targeting EZH2. *Human Pathology*, 46(7), pp. 971-980.

Ling, H., Vincent, K., Pichler, M., Fodde, R., Berindan-Neagoe, I., Slack, F. and Calin, G. (2015) Junk DNA and the long non-coding RNA twist in cancer genetics. *Oncogene*, 34(39), pp. 5003-5011.

Lino, M., Merlo, A. and Boulay, J. (2010) Notch signaling in glioblastoma: a developmental drug target?. *BMC Medicine*, 8(1), p. 72.

Liu, J., Lee, W., Jiang, Z., Chen, Z., Jhunjhunwala, S., Haverty, P., Gnad, F., Guan, Y., Gilbert, H., Stinson, J., Klijn, C., Guillory, J., Bhatt, D., Vartanian, S., Walter, K., Chan, J., Holcomb, T., Dijkgraaf, P., Johnson, S., Koeman, J., Minna, J., Gazdar, A., Stern, H., Hoeflich, K., Wu, T., Settleman, J., de Sauvage, F., Gentleman, R., Neve, R., Stokoe, D., Modrusan, Z., Seshagiri, S., Shames, D. and Zhang, Z. (2012) Genome and transcriptome sequencing of lung cancers reveal diverse mutational and splicing events. *Genome Research*, 22(12), pp. 2315-2327.

Liu, L., Li, H., Li, J., Zhong, H., Zhang, H., Chen, J. and Xiao, T. (2011) miR-125b suppresses the proliferation and migration of osteosarcoma cells through down-regulation of STAT3. *Biochemical and Biophysical Research Communications*, 416(1-2), pp. 31-38.

Liu, P., Cheng, H., Roberts, T. and Zhao, J. (2009) Targeting the phosphoinositide 3-kinase pathway in cancer. *Nature Reviews Drug Discovery*, 8(8), pp. 627-644.

Liu, Y., Snow, B., Kickhoefer, V., Erdmann, N., Zhou, W., Wakeham, A., Gomez, M., Rome, L. and Harrington, L. (2004) Vault Poly(ADP-Ribose) Polymerase Is Associated with Mammalian Telomerase and Is Dispensable for Telomerase Function and Vault Structure In Vivo. *Molecular and Cellular Biology*, 24(12), pp. 5314-5323.

Liu, Z., Lam, N. and Thiele, C. (2015) Zinc finger transcription factor CASZ1 interacts with histones, DNA repair proteins and recruits NuRD complex to regulate gene transcription. *Oncotarget*, 6(29), pp. 27628-27640.

Lopez-Serra, P. and Esteller, M. (2012) DNA methylation-associated silencing of tumor-suppressor microRNAs in cancer. *Oncogene*, 31(13), pp. 1609-1622.

Louis, D.N., Ohgaki, H., Wiestler, O.D., Cavenee, W.K., Burger, P.C., Jouvet, A., Scheithauer, B.W., Kleihues, P. (2007) The 2007 WHO classification of tumours of the central nervous system. *Acta neuropathologica*, **114**(2), 97–109.

Lu, J., Getz, G., Miska, E., Alvarez-Saavedra, E., Lamb, J., Peck, D., Sweet-Cordero, A., Ebert, B., Mak, R., Ferrando, A., Downing, J., Jacks, T., Horvitz, H. and Golub, T. (2005) MicroRNA expression profiles classify human cancers. *Nature*, 435(7043), pp. 834-838.

Ma, L., Teruya-Feldstein, J. and Weinberg, R. (2008) Tumour invasion and metastasis initiated by microRNA-10b in breast cancer. *Nature*, 455(7210), pp. 256-256.

Ma, Y., Li, G., Hu, J., Liu, X. and Shi, B. (2015) Correlation of miR-494 expression with tumor progression and patient survival in pancreatic cancer. *Genetics and Molecular Research*, 14(4), pp. 18153-18159.

MacDonald, T., Aguilera, D. and Kramm, C. (2011) Treatment of high-grade glioma in children and adolescents. *Neuro-Oncology*, 13(10), pp. 1049-1058.

Maehama, T. and Dixon, J. (1998) The Tumor Suppressor, PTEN/MMAC1, Dephosphorylates the Lipid Second Messenger, Phosphatidylinositol 3,4,5-Trisphosphate. *Journal of Biological Chemistry*, 273(22), pp. 13375-13378.

Maher, E., Brennan, C., Wen, P., Durso, L., Ligon, K., Richardson, A., Khatry, D., Feng, B., Sinha, R., Louis, D., Quackenbush, J., Black, P., Chin, L. and DePinho, R. (2006) Marked Genomic Differences Characterize Primary and Secondary Glioblastoma Subtypes and Identify Two Distinct Molecular and Clinical Secondary Glioblastoma Entities. *Cancer Research*, 66(23), pp. 11502-11513.

Marioni, J., Thorne, N., Valsesia, A., Fitzgerald, T., Redon, R., Fiegler, H., Andrews, T., Stranger, B., Lynch, A., Dermitzakis, E., Carter, N., Tavaré, S. and Hurles, M. (2007) Breaking the waves: improved detection of copy number variation from microarray-based comparative genomic hybridization. *Genome Biol*, 8(10), p. R228.

Matsuda, M., Kobayashi, Y., Masuda, S., Adachi, M., Watanabe, T., Yamashita, J., Nishi, E., Tsukita, S. and Furuse, M. (2008) Identification of adherens junction-associated GTPase activating proteins by the fluorescence localization-based expression cloning. *Experimental Cell Research*, 314(5), pp. 939-949.

Maunakea, A., Nagarajan, R., Bilenky, M., Ballinger, T., D'Souza, C., Fouse, S., Johnson, B., Hong, C., Nielsen, C., Zhao, Y., Turecki, G., Delaney, A., Varhol, R., Thiessen, N., Shchors, K., Heine, V., Rowitch, D., Xing, X., Fiore, C., Schillebeeckx, M., Jones, S., Haussler, D., Marra, M., Hirst, M., Wang, T. and Costello, J. (2010) Conserved role of intragenic DNA methylation in regulating alternative promoters. *Nature*, 466(7303), pp. 253-257.

McAvoy, S., Zhu, Y., Perez, D., James, C. and Smith, D. (2007) Disabled-1 is a large common fragile site gene, inactivated in multiple cancers. *Genes Chromosom. Cancer*, 47(2), pp. 165-174.

McGranahan, N. and Swanton, C. (2015) Biological and Therapeutic Impact of Intratumor Heterogeneity in Cancer Evolution. *Cancer Cell*, 27(1), pp. 15-26.

McLaughlin, E., Frayne, J., Bloomerg, G. and Hall, L. (2001) Do fertilin beta and cyritestin play a major role in mammalian sperm-oolemma interactions? A critical re-evaluation of the use of peptide mimics in identifying specific oocyte recognition proteins. *Molecular Human Reproduction*, 7(4), pp. 313-317.

McLendon, R., Friedman, A., Bigner, D., Van Meir, E., Brat, D., M. Mastrogianakis, G., Olson, J., Mikkelsen, T., Lehman, N., Aldape, K., Alfred Yung, W., Bogler, O., VandenBerg, S., Berger, M., Prados, M., Muzny, D., Morgan, M., Scherer, S., Sabo, A., Nazareth, L., Lewis, L., Hall, O., Zhu, Y., Ren, Y., Alvi, O., Yao, J., Hawes, A., Jhangiani, S., Fowler, G., San Lucas, A., Kovar, C., Cree, A., Dinh, H., Santibanez, J., Joshi, V., Gonzalez-Garay, M., Miller, C., Milosavljevic, A., Donehower, L., Wheeler, D., Gibbs, R., Cibulskis, K., Sougnez, C., Fennell, T., Mahan, S., Wilkinson, J., Ziaugra, L., Onofrio, R., Bloom, T., Nicol, R., Ardlie, K., Baldwin, J., Gabriel, S., Lander, E., Ding, L., Fulton, R., McLellan, M., Wallis, J., Larson, D., Shi, X., Abbott, R., Fulton, L., Chen, K., Koboldt, D., Wendl, M., Meyer, R., Tang, Y., Lin, L., Osborne, J., Dunford-Shore, B., Miner, T., Delehaunty, K., Markovic, C., Swift, G., Courtney, W., Pohl, C., Abbott, S., Hawkins, A., Leong, S., Haipek, C., Schmidt, H., Wiechert, M., Vickery, T., Scott, S., Dooling, D., Chinwalla, A., Weinstock, G., Mardis, E., Wilson, R., Getz, G., Winckler, W., Verhaak, R., Lawrence, M., O'Kelly, M., Robinson, J., Alexe, G., Beroukhim, R., Carter, S., Chiang, D., Gould, J., Gupta, S., Korn, J., Mermel, C., Mesirov, J., Monti, S., Nguyen, H., Parkin, M., Reich, M., Stransky, N., Weir, B., Garraway, L., Golub, T., Meyerson, M., Chin, L., Protopopov, A., Zhang, J., Perna, I., Aronson, S., Sathiamoorthy, N., Ren, G., Yao, J., Wiedemeyer, W., Kim, H., Won Kong, S., Xiao, Y., Kohane, I., Seidman, J., Park, P., Kucherlapati, R., Laird, P., Cope, L., Herman, J., Weisenberger, D., Pan, F., Van Den Berg, D., Van Neste, L., Mi Yi, J., Schuebel, K., Baylin, S., Absher, D., Li, J., Southwick, A., Brady, S., Aggarwal, A., Chung, T., Sherlock, G., Brooks, J., Myers, R., Spellman, P., Purdom, E., Jakkula, L., Lapuk, A., Marr, H., Dorton, S., Gi Choi, Y., Han, J., Ray, A., Wang, V., Durinck, S., Robinson, M., Wang, N., Vranizan, K., Peng, V., Van Name, E., Fontenay, G., Ngai, J., Conboy, J., Parvin, B., Feiler, H., Speed, T., Gray, J., Brennan, C., Socci, N., Olshen, A., Taylor, B., Lash, A., Schultz, N., Reva, B., Antipin, Y., Stukalov, A., Gross, B., Cerami, E., Qing Wang, W., Qin, L., Seshan, V., Villafania, L., Cavatore, M., Borsu, L., Viale, A., Gerald, W., Sander, C., Ladanyi, M., Perou, C., Neil Hayes, D., Topal, M., Hoadley, K., Qi, Y., Balu, S., Shi, Y., Wu, J., Penny, R., Bittner, M., Shelton, T., Lenkiewicz, E., Morris, S., Beasley, D., Sanders, S., Kahn, A., Sfeir, R., Chen, J., Nassau, D., Feng, L., Hickey, E., Zhang, J., Weinstein, J., Barker, A., Gerhard, D., Vockley, J., Compton, C., Vaught, J., Fielding, P., Ferguson, M., Schaefer, C., Madhavan, S., Buetow, K., Collins, F., Good, P., Guyer, M., Ozenberger, B., Peterson, J. and Thomson, E. (2008) Comprehensive genomic characterization defines human glioblastoma genes and core pathways. *Nature*, 455(7216), pp. 1061-1068.

Melean, G., Sestini, R., Ammannati, F. and Papi, L. (2004) Genetic insights into familial tumors of the nervous system. *American Journal of Medical Genetics*, 129C(1), pp. 74-84.

Melo, S., Moutinho, C., Ropero, S., Calin, G., Rossi, S., Spizzo, R., Fernandez, A., Davalos, V., Villanueva, A., Montoya, G., Yamamoto, H., Schwartz, S. and Esteller, M. (2010) A Genetic Defect in Exportin-5 Traps Precursor MicroRNAs in the Nucleus of Cancer Cells. *Cancer Cell*, 18(4), pp. 303-315.

Melo, S., Sugimoto, H., O'Connell, J., Kato, N., Villanueva, A., Vidal, A., Qiu, L., Vitkin, E., Perelman, L., Melo, C., Lucci, A., Ivan, C., Calin, G. and Kalluri, R. (2014) Cancer Exosomes Perform Cell-Independent MicroRNA Biogenesis and Promote Tumorigenesis. *Cancer Cell*, 26(5), pp. 707-721.

Mendell, J. and Olson, E. (2012) MicroRNAs in Stress Signaling and Human Disease. *Cell*, 148(6), pp. 1172-1187.

Menigatti, M., Staiano, T., Manser, C., Bauerfeind, P., Komljenovic, A., Robinson, M., Jiricny, J., Buffoli, F. and Marra, G. (2013) Epigenetic silencing of monoallelically methylated miRNA loci in precancerous colorectal lesions. *Oncogenesis*, 2(7), p. e56.

Merchant, T., Pollack, I. and Loeffler, J. (2010) Brain Tumors Across the Age Spectrum: Biology, Therapy, and Late Effects. *Seminars in Radiation Oncology*, 20(1), pp. 58-66.

Messinger, Y., Gaynon, P., Sposto, R., van der Giessen, J., Eckroth, E., Malvar, J. and Bostrom, B. (2012) Bortezomib with chemotherapy is highly active in advanced B-precursor acute lymphoblastic leukemia: Therapeutic Advances in Childhood Leukemia & Lymphoma (TACL) Study. *Blood*, 120(2), pp. 285-290.

Mika, D., Richter, W. and Conti, M. (2015) A CaMKII/PDE4D negative feedback regulates cAMP signaling. *Proceedings of the National Academy of Sciences*, 112(7), pp. 2023-2028.

Mikkelsen, T., Ku, M., Jaffe, D., Issac, B., Lieberman, E., Giannoukos, G., Alvarez, P., Brockman, W., Kim, T., Koche, R., Lee, W., Mendenhall, E., O'Donovan, A., Presser, A., Russ, C., Xie, X., Meissner, A., Wernig, M., Jaenisch, R., Nusbaum, C., Lander, E. and Bernstein, B. (2007) Genome-wide maps of chromatin state in pluripotent and lineage-committed cells. *Nature*, 448(7153), pp. 553-560.

Minakuchi, M., Kakazu, N., Gorrin-Rivas, M., Abe, T., Copeland, T., Ueda, K. and Adachi, Y. (2001) Identification and characterization of SEB, a novel protein that binds to the acute undifferentiated leukemia-associated protein SET. *European Journal of Biochemistry*, 268(5), pp. 1340-1351.

Mohapatra, G., Bollen, A., Kim, D., Lamborn, K., Moore, D., Prados, M. and Feuerstein, B. (1998) Genetic analysis of glioblastoma multiforme provides evidence for subgroups within the grade.*Genes Chromosom. Cancer*, 21(3), pp. 195-206.

Moller, N., Moller, K., Lammers, R., Kharitonenkov, A., Hoppe, E., Wiberg, F., Sures, I. and Ullrich, A. (1995) Selective Down-regulation of the Insulin Receptor Signal by Protein-tyrosine Phosphatases a and e. *Journal of Biological Chemistry*, 270(39), pp. 23126-23131.

Momparler, R., Côté, S., Momparler, L. and Idaghdour, Y. (2014) Epigenetic therapy of acute myeloid leukemia using 5-aza-2'-deoxycytidine (decitabine) in combination with inhibitors of histone methylation and deacetylation. *Clin Epigenetics*, 6(1), p. 19.

Monje, M., Mitra, S., Freret, M., Raveh, T., Kim, J., Masek, M., Attema, J., Li, G., Haddix, T., Edwards, M., Fisher, P., Weissman, I., Rowitch, D., Vogel, H., Wong, A. and Beachy, P. (2011) Hedgehog-responsive candidate cell of origin for diffuse intrinsic pontine glioma. *Proceedings of the National Academy of Sciences*, 108(11), pp. 4453-4458.

Morris Jr, S. (2009) Recent advances in arginine metabolism: roles and regulation of the arginases. *British Journal of Pharmacology*, 157(6), pp. 922-930.

Morris Jr., S. (2016) Arginine Metabolism: Boundaries of Our Knowledge. *The Journal of Nutrition*, 137(6), pp. 1602S-1609S.

Morris, M., Gentle, D., Abdulrahman, M., Clarke, N., Brown, M., Kishida, T., Yao, M., Teh, B., Latif, F. and Maher, E. (2008) Functional epigenomics approach to identify methylated candidate tumour suppressor genes in renal cell carcinoma. *Br J Cancer*, 98(2), pp. 496-501.

Morris, M., Ricketts, C., Gentle, D., McRonald, F., Carli, N., Khalili, H., Brown, M., Kishida, T., Yao, M., Banks, R., Clarke, N., Latif, F. and Maher, E. (2011) Genome-wide methylation analysis identifies epigenetically inactivated candidate tumour suppressor genes in renal cell carcinoma.*Oncogene*, 30(12), pp. 1390-1401.

Morris, S.M. (2004) Enzymes of arginine metabolism. *The Journal of nutrition*, *134*(10), pp.2743S-2747S.

Mueller, D., Rehli, M. and Bosserhoff, A. (2009) miRNA Expression Profiling in Melanocytes and Melanoma Cell Lines Reveals miRNAs Associated with Formation and Progression of Malignant Melanoma. *Journal of Investigative Dermatology*, 129(7), pp. 1740-1751.

Mueller, S., Phillips, J., Onar-Thomas, A., Romero, E., Zheng, S., Wiencke, J., McBride, S., Cowdrey, C., Prados, M., Weiss, W., Berger, M., Gupta, N. and Haas-Kogan, D. (2012) PTEN promoter methylation and activation of the PI3K/Akt/mTOR pathway in pediatric gliomas and influence on clinical outcome. *Neuro-Oncology*, 14(9), pp. 1146-1152.

Mulhern, R., White, H., Glass, J., Kun, L., Leigh, L., Thompson, S. And Reddick, W. (2004) Attentional functioning and white matter integrity among survivors of malignant brain tumors of childhood. *Journal of the International Neuropsychological Society*, 10(02).

Nakagawa, Y., Aoki, N., Aoyama, K., Shimizu, H., Shimano, H., Yamada, N. and Miyazaki, H. (2005) Receptor-Type Protein Tyrosine Phosphatase ε (PTPεM) is a Negative Regulator of Insulin Signaling in Primary Hepatocytes and Liver. *Zoological Science*, 22(2), pp. 169-175.

Nakanishi, H., Taccioli, C., Palatini, J., Fernandez-Cymering, C., Cui, R., Kim, T., Volinia, S. and Croce, C. (2014) Loss of miR-125b-1 contributes to head and neck cancer development by dysregulating TACSTD2 and MAPK pathway. *Oncogene*, 33(6), pp. 702-712.

Neglia, J., Robison, L., Stovall, M., Liu, Y., Packer, R., Hammond, S., Yasui, Y., Kasper, C., Mertens, A., Donaldson, S., Meadows, A. and Inskip, P. (2006) New Primary Neoplasms of the Central Nervous System in Survivors of Childhood Cancer: a Report From the Childhood Cancer Survivor Study. *JNCI Journal of the National Cancer Institute*, 98(21), pp. 1528-1537.

Neri, F., Krepelova, A., Incarnato, D., Maldotti, M., Parlato, C., Galvagni, F., Matarese, F., Stunnenberg, H. and Oliviero, S. (2013) Dnmt3L Antagonizes DNA Methylation at Bivalent Promoters and Favors DNA Methylation at Gene Bodies in ESCs. *Cell*, 155(1), pp. 121-134.

Ni, Y., Schwaneberg, U. and Sun, Z. (2008) Arginine deiminase, a potential anti-tumor drug. *Cancer Letters*, 261(1), pp. 1-11.

Nicholson, L., Smith, P., Hiller, L., Szlosarek, P., Kimberley, C., Sehouli, J., Koensgen, D., Mustea, A., Schmid, P. and Crook, T. (2009) Epigenetic silencing of argininosuccinate synthetase confers resistance to platinum-induced cell death

but collateral sensitivity to arginine auxotrophy in ovarian cancer. *International Journal of Cancer*, 125(6), pp. 1454-1463.
Nigro, J. (2005) Integrated Array-Comparative Genomic Hybridization and Expression Array Profiles Identify Clinically Relevant Molecular Subtypes of Glioblastoma. *Cancer Research*, 65(5), pp. 1678-1686.
Niu, S., Renfro, A., Quattrocchi, C., Sheldon, M. and D'Arcangelo, G. (2004) Reelin Promotes Hippocampal Dendrite Development through the VLDLR/ApoER2-Dab1 Pathway. *Neuron*, 41(1), pp. 71-84.
Nord, H., Hartmann, C., Andersson, R., Menzel, U., Pfeifer, S., Piotrowski, A., Bogdan, A., Kloc, W., Sandgren, J., Olofsson, T., Hesselager, G., Blomquist, E., Komorowski, J., von Deimling, A., Bruder, C., Dumanski, J. and de Stahl, T. (2009) Characterization of novel and complex genomic aberrations in glioblastoma using a 32K BAC array. *Neuro-Oncology*, 11(6), pp. 803-818.
Nyren-Erickson, E., Jones, J., Srivastava, D. and Mallik, S. (2013) A disintegrin and metalloproteinase-12 (ADAM12): Function, roles in disease progression, and clinical implications. *Biochimica et Biophysica Acta (BBA) - General Subjects*, 1830(10), pp. 4445-4455.
Ogrean, C., Jackson, B. and Covino, J. (2010) Quantitative Real-Time PCR using the Thermo Scientific Solaris qPCR Assay. *Journal of Visualized Experiments*, (40).
Oinuma, I., Ito, Y., Katoh, H. and Negishi, M. (2010) Semaphorin 4D/Plexin-B1 Stimulates PTEN Activity through R-Ras GTPase-activating Protein Activity, Inducing Growth Cone Collapse in Hippocampal Neurons. *Journal of Biological Chemistry*, 285(36), pp. 28200-28209.
Okabe, Y., Sano, T. and Nagata, S. (2009) Regulation of the innate immune response by threonine-phosphatase of Eyes absent. *Nature*.
Okada, C., Yamashita, E., Lee, S., Shibata, S., Katahira, J., Nakagawa, A., Yoneda, Y. and Tsukihara, T. (2009) A High-Resolution Structure of the Pre-microRNA Nuclear Export Machinery. *Science*, 326(5957), pp. 1275-1279.
Okano, M., Bell, D., Haber, D. and Li, E. (1999) DNA Methyltransferases Dnmt3a and Dnmt3b Are Essential for De Novo Methylation and Mammalian Development. *Cell*, 99(3), pp. 247-257.
Okano, M., Xie, S. and Li, E. (1998) Cloning and characterization of a family of novel mammalian DNA (cytosine-5) methyltransferases. *Nature genetics*,*19*(3), pp.219-220.
Olshen, A., Venkatraman, E., Lucito, R. and Wigler, M. (2004) Circular binary segmentation for the analysis of array-based DNA copy number data. *Biostatistics*, 5(4), pp. 557-572.
Orellana, E. and Kasinski, A. (2015) MicroRNAs in Cancer: A Historical Perspective on the Path from Discovery to Therapy. *Cancers*, 7(3), pp. 1388-1405.
Oshima, R. (2002) Apoptosis and keratin intermediate filaments. *Cell Death Differ*, 9(5), pp. 486-492.
Øster, B., Thorsen, K., Lamy, P., Wojdacz, T., Hansen, L., Birkenkamp-Demtröder, K., Sørensen, K., Laurberg, S., Ørntoft, T. and Andersen, C. (2011) Identification and validation of highly frequent CpG island hypermethylation in colorectal adenomas and carcinomas. *International Journal of Cancer*, 129(12), pp. 2855-2866.
Östman, A., Hellberg, C. and Böhmer, F. (2006) Protein-tyrosine phosphatases and cancer. *Nature Reviews Cancer*, 6(4), pp. 307-320.

Ostrom, Q., Gittleman, H., Farah, P., Ondracek, A., Chen, Y., Wolinsky, Y., Stroup, N., Kruchko, C. and Barnholtz-Sloan, J. (2013) CBTRUS Statistical Report: Primary Brain and Central Nervous System Tumors Diagnosed in the United States in 2006-2010. *Neuro-Oncology*, 15(suppl 2), pp. ii1-ii56.

Ott, P., Carvajal, R., Pandit-Taskar, N., Jungbluth, A., Hoffman, E., Wu, B., Bomalaski, J., Venhaus, R., Pan, L., Old, L., Pavlick, A. and Wolchok, J. (2012) Phase I/II study of pegylated arginine deiminase (ADI-PEG 20) in patients with advanced melanoma. *Invest New Drugs*, 31(2), pp. 425-434.

Park, I., Kang, S., Shin, Y., Chae, K., Park, M., Kim, M., Wheatley, D. and Min, B. (2003) Arginine deiminase: a potential inhibitor of angiogenesis and tumour growth. *Br J Cancer*, 89(5), pp. 907-914.

Park, J., Tanner, J., Sellers, T., Huang, Y., Stevens, C., Dossett, N., Shankar, R., Zachariah, B., Heysek, R. and Pow-Sang, J. (2007) Association Between Polymorphisms in HSD3B1 and UGT2B17 and Prostate Cancer Risk. *Urology*, 70(2), pp. 374-379.

Parsons, D., Jones, S., Zhang, X., Lin, J., Leary, R., Angenendt, P., Mankoo, P., Carter, H., Siu, I., Gallia, G., Olivi, A., McLendon, R., Rasheed, B., Keir, S., Nikolskaya, T., Nikolsky, Y., Busam, D., Tekleab, H., Diaz, L., Hartigan, J., Smith, D., Strausberg, R., Marie, S., Shinjo, S., Yan, H., Riggins, G., Bigner, D., Karchin, R., Papadopoulos, N., Parmigiani, G., Vogelstein, B., Velculescu, V. and Kinzler, K. (2008) An Integrated Genomic Analysis of Human Glioblastoma Multiforme.*Science*, 321(5897), pp. 1807-1812.

Pastor, W., Aravind, L. and Rao, A. (2013) TETonic shift: biological roles of TET proteins in DNA demethylation and transcription. *Nature Reviews Molecular Cell Biology*, 14(6), pp. 341-356.

Paugh, B., Broniscer, A., Qu, C., Miller, C., Zhang, J., Tatevossian, R., Olson, J., Geyer, J., Chi, S., da Silva, N., Onar-Thomas, A., Baker, J., Gajjar, A., Ellison, D. and Baker, S. (2011) Genome-Wide Analyses Identify Recurrent Amplifications of Receptor Tyrosine Kinases and Cell-Cycle Regulatory Genes in Diffuse Intrinsic Pontine Glioma. *Journal of Clinical Oncology*, 29(30), pp. 3999-4006.

Paugh, B., Qu, C., Jones, C., Liu, Z., Adamowicz-Brice, M., Zhang, J., Bax, D., Coyle, B., Barrow, J., Hargrave, D., Lowe, J., Gajjar, A., Zhao, W., Broniscer, A., Ellison, D., Grundy, R. and Baker, S. (2010) Integrated Molecular Genetic Profiling of Pediatric High-Grade Gliomas Reveals Key Differences With the Adult Disease. *Journal of Clinical Oncology*, 28(18), pp. 3061-3068.

Paugh, B., Zhu, X., Qu, C., Endersby, R., Diaz, A., Zhang, J., Bax, D., Carvalho, D., Reis, R., Onar-Thomas, A., Broniscer, A., Wetmore, C., Zhang, J., Jones, C., Ellison, D. and Baker, S. (2013) Novel Oncogenic PDGFRA Mutations in Pediatric High-Grade Gliomas. *Cancer Research*, 73(20), pp. 6219-6229.

Pavlyk, I., Rzhepetskyy, Y., Jagielski, A., Drozak, J., Wasik, A., Pereverzieva, G., Olchowik, M., Kunz-Schugart, L., Stasyk, O. and Redowicz, M. (2014) Arginine deprivation affects glioblastoma cell adhesion, invasiveness and actin cytoskeleton organization by impairment of Î²-actin arginylation. *Amino Acids*, 47(1), pp. 199-212.

Pellacani, D., Kestoras, D., Droop, A., Frame, F., Berry, P., Lawrence, M., Stower, M., Simms, M., Mann, V., Collins, A., Risbridger, G. and Maitland, N. (2014) DNA hypermethylation in prostate cancer is a consequence of aberrant epithelial differentiation and hyperproliferation. *Cell Death Differ*, 21(5), pp. 761-773.

Penman, C., Faulkner, C., Lowis, S. and Kurian, K. (2015) Current Understanding of BRAF Alterations in Diagnosis, Prognosis, and Therapeutic Targeting in Pediatric Low-Grade Gliomas. *Front. Oncol.*, 5.

Penna, I., Vassallo, I., Nizzari, M., Russo, D., Costa, D., Menichini, P., Poggi, A., Russo, C., Dieci, G., Florio, T., Cancedda, R. and Pagano, A. (2013) A novel snRNA-like transcript affects amyloidogenesis and cell cycle progression through perturbation of Fe65L1 (APBB2) alternative splicing. *Biochimica et Biophysica Acta (BBA) - Molecular Cell Research*, 1833(6), pp. 1511-1526.

Peñuelas, S., Anido, J., Prieto-Sánchez, R., Folch, G., Barba, I., Cuartas, I., García-Dorado, D., Poca, M., Sahuquillo, J., Baselga, J. and Seoane, J. (2009) TGF-β Increases Glioma-Initiating Cell Self-Renewal through the Induction of LIF in Human Glioblastoma. *Cancer Cell*, 15(4), pp. 315-327.

Peschiaroli, A., Giacobbe, A., Formosa, A., Markert, E., Bongiorno-Borbone, L., Levine, A., Candi, E., D'Alessandro, A., Zolla, L., Finazzi Agrò, A. and Melino, G. (2012) miR-143 regulates hexokinase 2 expression in cancer cells. *Oncogene*, 32(6), pp. 797-802.

Phan, L.M., Yeung, S.C.J. and Lee, M.H. (2014) Cancer metabolic reprogramming: importance, main features, and potentials for precise targeted anti-cancer therapies. *Cancer biology & medicine*, *11*(1), pp.1-19.

Phillips, M., Sheaff, M. and Szlosarek, P. (2013) Targeting Arginine-Dependent Cancers with Arginine-Degrading Enzymes: Opportunities and Challenges. *Cancer Res Treat*, 45(4), pp. 251-262.

Pieters, R., Hunger, S., Boos, J., Rizzari, C., Silverman, L., Baruchel, A., Goekbuget, N., Schrappe, M. and Pui, C. (2010) L-asparaginase treatment in acute lymphoblastic leukemia: a focus on Erwinia asparaginase. *Cancer*, 117(2), pp. 238-249.

Pineau, P., Volinia, S., McJunkin, K., Marchio, A., Battiston, C., Terris, B., Mazzaferro, V., Lowe, S., Croce, C. and Dejean, A. (2010) miR-221 overexpression contributes to liver tumorigenesis.*Proceedings of the National Academy of Sciences*, 107(1), pp. 264-269.

Pinho, F., Frampton, A., Nunes, J., Krell, J., Alshaker, H., Jacob, J., Pellegrino, L., Roca-Alonso, L., de Giorgio, A., Harding, V., Waxman, J., Stebbing, J., Pchejetski, D. and Castellano, L. (2013) Downregulation of microRNA-515-5p by the Estrogen Receptor Modulates Sphingosine Kinase 1 and Breast Cancer Cell Proliferation. *Cancer Research*, 73(19), pp. 5936-5948.

Pinho, S., Reis, C., Paredes, J., Magalhaes, A., Ferreira, A., Figueiredo, J., Xiaogang, W., Carneiro, F., Gartner, F. and Seruca, R. (2009) The role of N-acetylglucosaminyltransferase III and V in the post-transcriptional modifications of E-cadherin. *Human Molecular Genetics*, 18(14), pp. 2599-2608.

Poliseno, L., Haimovic, A., Christos, P., Vega y Saenz de Miera, E., Shapiro, R., Pavlick, A., Berman, R., Darvishian, F. and Osman, I. (2011) Deletion of PTENP1 Pseudogene in Human Melanoma.*Journal of Investigative Dermatology*, 131(12), pp. 2497-2500.

Poliseno, L., Marranci, A. and Pandolfi, P. (2015) Pseudogenes in Human Cancer. *Front. Med.*, 2.

Poliseno, L., Salmena, L., Zhang, J., Carver, B., Haveman, W. and Pandolfi, P. (2010) A coding-independent function of gene and pseudogene mRNAs regulates tumour biology. *Nature*, 465(7301), pp. 1033-1038.

Pollack, I. (2003) The influence of central review on outcome associations in childhood malignant gliomas: Results from the CCG-945 experience. *Neuro-Oncology*, 5(3), pp. 197-207.

Pollack, I., Finkelstein, S., Woods, J., Burnham, J., Holmes, E., Hamilton, R., Yates, A., Boyett, J., Finlay, J. and Sposto, R. (2002) Expression of p53 and Prognosis in Children with Malignant Gliomas. *New England Journal of Medicine*, 346(6), pp. 420-427.

Pollack, I., Hamilton, R., Burger, P., Brat, D., Rosenblum, M., Murdoch, G., Nikiforova, M., Holmes, E., Zhou, T., Cohen, K. and Jakacki, R. (2010) Akt activation is a common event in pediatric malignant gliomas and a potential adverse prognostic marker: a report from the Children's Oncology Group. *J Neurooncol*, 99(2), pp. 155-163.

Pollack, I., Hamilton, R., James, C., Finkelstein, S., Burnham, J., Yates, A., Holmes, E., Zhou, T. and Finlay, J. (2006) Rarity of PTEN deletions and EGFR amplification in malignant gliomas of childhood: results from the Children's Cancer Group 945 cohort. *Journal of Neurosurgery: Pediatrics*, 105(5), pp. 418-424.

Possemato, R., Marks, K., Shaul, Y., Pacold, M., Kim, D., Birsoy, K., Sethumadhavan, S., Woo, H., Jang, H., Jha, A., Chen, W., Barrett, F., Stransky, N., Tsun, Z., Cowley, G., Barretina, J., Kalaany, N., Hsu, P., Ottina, K., Chan, A., Yuan, B., Garraway, L., Root, D., Mino-Kenudson, M., Brachtel, E., Driggers, E. and Sabatini, D. (2011) Functional genomics reveal that the serine synthesis pathway is essential in breast cancer. *Nature*, 476(7360), pp. 346-350.

Potter, N., Phipps, K., Harkness, W., Hayward, R., Thompson, D., Jacques, T., Harding, B., Thomas, D., Rees, J., Darling, J. and Warr, T. (2009) Astrocytoma derived short-term cell cultures retain molecular signatures characteristic of the tumour in situ. *Experimental Cell Research*, 315(16), pp. 2835-2846.

Potter, N., Phipps, K., Harkness, W., Hayward, R., Thompson, D., Jacques, T., Harding, B., Thomas, D., Rees, J., Darling, J. and Warr, T. (2009) Astrocytoma derived short-term cell cultures retain molecular signatures characteristic of the tumour in situ. *Experimental Cell Research*, 315(16), pp. 2835-2846.

Przybytkowski, E., Ferrario, C. and Basik, M. (2011) The use of ultra-dense array CGH analysis for the discovery of micro-copy number alterations and gene fusions in the cancer genome. *BMC Med Genomics*, 4(1), p. 16.

Puente, X., Pinyol, M., Quesada, V., Conde, L., Ordóñez, G., Villamor, N., Escaramis, G., Jares, P., Beà, S., González-Díaz, M., Bassaganyas, L., Baumann, T., Juan, M., López-Guerra, M., Colomer, D., Tubío, J., López, C., Navarro, A., Tornador, C., Aymerich, M., Rozman, M., Hernández, J., Puente, D., Freije, J., Velasco, G., Gutiérrez-Fernández, A., Costa, D., Carrió, A., Guijarro, S., Enjuanes, A., Hernández, L., Yagüe, J., Nicolás, P., Romeo-Casabona, C., Himmelbauer, H., Castillo, E., Dohm, J., de Sanjosé, S., Piris, M., de Alava, E., Miguel, J., Royo, R., Gelpí, J., Torrents, D., Orozco, M., Pisano, D., Valencia, A., Guigó, R., Bayés, M., Heath, S., Gut, M., Klatt, P., Marshall, J., Raine, K., Stebbings, L., Futreal, P., Stratton, M., Campbell, P., Gut, I., López-Guillermo, A., Estivill, X., Montserrat, E., López-Otín, C. and Campo, E. (2011) Whole-genome sequencing identifies recurrent mutations in chronic lymphocytic leukaemia. *Nature*, 475(7354), pp. 101-105.

Puget, S., Philippe, C., Bax, D., Job, B., Varlet, P., Junier, M., Andreiuolo, F., Carvalho, D., Reis, R., Guerrini-Rousseau, L., Roujeau, T., Dessen, P., Richon, C., Lazar, V., Le Teuff, G., Sainte-Rose, C., Geoerger, B., Vassal, G., Jones, C.

and Grill, J. (2012) Mesenchymal Transition and PDGFRA Amplification/Mutation Are Key Distinct Oncogenic Events in Pediatric Diffuse Intrinsic Pontine Gliomas. *PLoS ONE*, 7(2), p. e30313.

Purcell, S., Cantlon, J., Wright, C., Henkes, L., Seidel, G. and Anthony, R. (2009) The Involvement of Proline-Rich 15 in Early Conceptus Development in Sheep. *Biology of Reproduction*, 81(6), pp. 1112-1121.

Purkait, S., Sharma, V., Jha, P., Sharma, M., Suri, V., Suri, A., Sharma, B. and Sarkar, C. (2015) EZH2 expression in gliomas: Correlation with CDKN2A gene deletion/ p16 loss and MIB-1 proliferation index. *Neuropathology*, 35(5), pp. 421-431.

Puustinen, P., Rytter, A., Mortensen, M., Kohonen, P., Moreira, J. and Jäättelä, M. (2014) CIP2A oncoprotein controls cell growth and autophagy through mTORC1 activation. *J Cell Biol*, 204(5), pp. 713-727.

Qaddoumi, I., Sultan, I. and Gajjar, A. (2009) Outcome and prognostic features in pediatric gliomas.*Cancer*, 115(24), pp. 5761-5770.

Qiu, F., Chen, Y., Liu, X., Chu, C., Shen, L., Xu, J., Gaur, S., Forman, H., Zhang, H., Zheng, S., Yen, Y., Huang, J., Kung, H. and Ann, D. (2014) Arginine Starvation Impairs Mitochondrial Respiratory Function in ASS1-Deficient Breast Cancer Cells. *Science Signaling*, 7(319), pp. ra31-ra31.

Qiu, F., Huang, J. and Sui, M. (2015) Targeting arginine metabolism pathway to treat arginine-dependent cancers. *Cancer Letters*, 364(1), pp. 1-7.

Quackenbush, J. (2006) Microarray Analysis and Tumor Classification. *New England Journal of Medicine*, 354(23), pp. 2463-2472.

Rabinovich, G. and Toscano, M. (2009) Turning 'sweet' on immunity: galectin–glycan interactions in immune tolerance and inflammation. *Nat Rev Immunol*, 9(5), pp. 338-352.

Rao, Y., Hao, R., Wang, B. and Yao, T. (2014) A Mec17-Myosin II Effector Axis Coordinates Microtubule Acetylation and Actin Dynamics to Control Primary Cilium Biogenesis. *PLoS ONE*, 9(12), p. e114087.

Reczko, M., Maragkakis, M., Alexiou, P., Grosse, I. and Hatzigeorgiou, A. (2012) Functional microRNA targets in protein coding sequences. *Bioinformatics*, 28(6), pp. 771-776.

Reddy, E., Reynolds, R., Santos, E. and Barbacid, M. (1982) A point mutation is responsible for the acquisition of transforming properties by the T24 human bladder carcinoma oncogene. *Nature*, 300(5888), pp. 149-152.

Reimers, T., Ehrenfels, S., Mortensen, E., Schmiegelow, M., SÃ¸nderkaer, S., Carstensen, H., Schmiegelow, K. and MÃ¼ller, J. (2002) Cognitive deficits in long-term survivors of childhood brain tumors: Identification of predictive factors. *Med. Pediatr. Oncol.*, 40(1), pp. 26-34.

Renouf, S., Fairand, A. and Husson, A. (1998) Developmental Control of Argininosuccinate Lyase Gene by Methylation. *Biology of the Neonate*, 73(3), pp. 190-197.

Rickert, C., Sträter, R., Kaatsch, P., Wassmann, H., Jürgens, H., Dockhorn-Dworniczak, B. and Paulus, W. (2001) Pediatric High-Grade Astrocytomas Show Chromosomal Imbalances Distinct from Adult Cases. *The American Journal of Pathology*, 158(4), pp. 1525-1532.

Riggs, A.D. (1975) X inactivation, differentiation, and DNA methylation.*Cytogenetic and Genome Research*, *14*(1), pp.9-25.

Ritelli, M., Dordoni, C., Venturini, M., Chiarelli, N., Quinzani, S., Traversa, M., Zoppi, N., Vascellaro, A., Wischmeijer, A., Manfredini, E., Garavelli, L.,

Calzavara-Pinton, P. and Colombi, M. (2013) Clinical and molecular characterization of 40 patients with classic Ehlersâ€“Danlos syndrome: identification of 18 COL5A1 and 2 COL5A2 novel mutations. *Orphanet Journal of Rare Diseases*, 8(1), p. 58.

Rodríguez-Paredes, M. and Esteller, M. (2011) Cancer epigenetics reaches mainstream oncology.*Nature Medicine*, pp. 330-339.

Rosenfeld, A., Listernick, R., Charrow, J. and Goldman, S. (2009) Neurofibromatosis type 1 and high-grade tumors of the central nervous system. *Childs Nerv Syst*, 26(5), pp. 663-667.

Ross, D. and Perou, C. (2001) A Comparison of Gene Expression Signatures from Breast Tumors and Breast Tissue Derived Cell Lines. *Disease Markers*, 17(2), pp. 99-109.

Rothbart, S. and Strahl, B. (2014) Interpreting the language of histone and DNA modifications.*Biochimica et Biophysica Acta (BBA) - Gene Regulatory Mechanisms*, 1839(8), pp. 627-643.

Rowther, F., Kardooni, H. and Warr, T. (2012) TOUCH-UP Gradient Amplification Method. *J Biomol Tech*, 23(1), pp. 1-3.

Roy, B., Guittet, O., Beuneu, C., Lemaire, G. and Lepoivre, M. (2004) Depletion of deoxyribonucleoside triphosphate pools in tumor cells by nitric oxide. *Free Radical Biology and Medicine*, 36(4), pp. 507-516.

Ruderman, N., Kapeller, R., White, M. and Cantley, L. (1990) Activation of phosphatidylinositol 3-kinase by insulin. *Proceedings of the National Academy of Sciences*, 87(4), pp. 1411-1415.

Rusten, T., Haglund, K. and Stenmark, H. (2007) Aberrant Receptor Signaling and Trafficking as Mechanisms in Oncogenesis. *Crit Rev Oncog*, 13(1), pp. 39-74.

Rutnam, Z., Du, W., Yang, W., Yang, X. and Yang, B. (2014) The pseudogene TUSC2P promotes TUSC2 function by binding multiple microRNAs. *Nature Communications*, 5.

Sahin, U., Weskamp, G., Kelly, K., Zhou, H., Higashiyama, S., Peschon, J., Hartmann, D., Saftig, P. and Blobel, C. (2004) Distinct roles for ADAM10 and ADAM17 in ectodomain shedding of six EGFR ligands. *J Cell Biol*, 164(5), pp. 769-779.

Samuels, Y. (2004) High Frequency of Mutations of the PIK3CA Gene in Human Cancers. *Science*, 304(5670), pp. 554-554.

Sanders, R., Kocak, M., Burger, P., Merchant, T., Gajjar, A. and Broniscer, A. (2007) High-grade astrocytoma in very young children. *Pediatr. Blood Cancer*, 49(7), pp. 888-893.

Sandgren, J., Andersson, R., Rada-Iglesias, A., Enroth, S., Åkerström, G., Dumanski, J., Komorowski, J., Westin, G. and Wadelius, C. (2010) Integrative epigenomic and genomic analysis of malignant pheochromocytoma. *Experimental and Molecular Medicine*, 42(7), p. 484.

Sands, S., Zhou, T., O'Neil, S., Patel, S., Allen, J., McGuire Cullen, P., Kaleita, T., Noll, R., Sklar, C. and Finlay, J. (2012) Long-Term Follow-Up of Children Treated for High-Grade Gliomas: Children's Oncology Group L991 Final Study Report. *Journal of Clinical Oncology*, 30(9), pp. 943-949.

Saratsis, A., Kambhampati, M., Snyder, K., Yadavilli, S., Devaney, J., Harmon, B., Hall, J., Raabe, E., An, P., Weingart, M., Rood, B., Magge, S., MacDonald, T., Packer, R. and Nazarian, J. (2013) Comparative multidimensional molecular analyses of pediatric diffuse intrinsic pontine glioma reveals distinct molecular subtypes. *Acta Neuropathologica*, 127(6), pp. 881-895.

Sareen, D., McMillan, E., Ebert, A., Shelley, B., Johnson, J., Meisner, L. and Svendsen, C. (2009) Chromosome 7 and 19 Trisomy in Cultured Human Neural Progenitor Cells. *PLoS ONE*, 4(10), p. e7630.

Sasayama, T., Nishihara, M., Kondoh, T., Hosoda, K. and Kohmura, E. (2009) MicroRNA-10b is overexpressed in malignant glioma and associated with tumor invasive factors, uPAR and RhoC.*International Journal of Cancer*, 125(6), pp. 1407-1413.

Sato, N., Fukushima, N., Chang, R., Matsubayashi, H. and Goggins, M. (2006) Differential and Epigenetic Gene Expression Profiling Identifies Frequent Disruption of the RELN Pathway in Pancreatic Cancers. *Gastroenterology*, 130(2), pp. 548-565.

Schiffman, J., Lorimer, P., Rodic, V., Jahromi, M., Downie, J., Bayerl, M., Sanmann, J., Althof, P., Sanger, W., Barnette, P., Perkins, S. and Miles, R. (2011) Genome wide copy number analysis of paediatric Burkitt lymphoma using formalin-fixed tissues reveals a subset with gain of chromosome 13q and corresponding miRNA over expression. *British Journal of Haematology*, 155(4), pp. 477-486.

Schultz, S., Pinsky, G.S., Wu, N.C., Chamberlain, M.C., Rodrigo, A.S. and Martin, S.E. (2005) Fine needle aspiration diagnosis of extracranial glioblastoma multiforme: Case report and review of the literature. *CytoJournal*,*2*(1), p.19.

Schwartzentruber, J., Korshunov, A., Liu, X., Jones, D., Pfaff, E., Jacob, K., Sturm, D., Fontebasso, A., Quang, D., TÃ¶njes, M., Hovestadt, V., Albrecht, S., Kool, M., Nantel, A., Konermann, C., Lindroth, A., JÃ¤ger, N., Rausch, T., Ryzhova, M., Korbel, J., Hielscher, T., Hauser, P., Garami, M., Klekner, A., Bognar, L., Ebinger, M., Schuhmann, M., Scheurlen, W., Pekrun, A., FrÃ¼hwald, M., Roggendorf, W., Kramm, C., DÃ¼rken, M., Atkinson, J., Lepage, P., Montpetit, A., Zakrzewska, M., Zakrzewski, K., Liberski, P., Dong, Z., Siegel, P., Kulozik, A., Zapatka, M., Guha, A., Malkin, D., Felsberg, J., Reifenberger, G., von Deimling, A., Ichimura, K., Collins, V., Witt, H., Milde, T., Witt, O., Zhang, C., Castelo-Branco, P., Lichter, P., Faury, D., Tabori, U., Plass, C., Majewski, J., Pfister, S. and Jabado, N. (2012) Driver mutations in histone H3.3 and chromatin remodelling genes in paediatric glioblastoma. *Nature*, 482(7384), pp. 226-231.

Scott, L., Lamb, J., Smith, S. and Wheatley, D.N. (2000) Single amino acid (arginine) deprivation: rapid and selective death of cultured transformed and malignant cells. *British journal of cancer*, *83*(6), p.800.

Sethi, R., Allen, J., Donahue, B., Karajannis, M., Gardner, S., Wisoff, J., Kunnakkat, S., Mathew, J., Zagzag, D., Newman, K. and Narayana, A. (2010) Prospective neuraxis MRI surveillance reveals a high risk of leptomeningeal dissemination in diffuse intrinsic pontine glioma. *J Neurooncol*, 102(1), pp. 121-127.

Sharma, S., Kelly, T. and Jones, P. (2009) Epigenetics in cancer. *Carcinogenesis*, 31(1), pp. 27-36.

Shen, J., Wang, S., Siegel, A., Remotti, H., Wang, Q., Sirosh, I. and Santella, R. (2015) Genome-Wide Expression of MicroRNAs Is Regulated by DNA Methylation in Hepatocarcinogenesis.*Gastroenterology Research and Practice*, 2015, pp. 1-12.

Shi, Z., Park, H., Du, Y., Li, Z., Cheng, K., Sun, S., Li, Z., Fu, H. and Khuri, F. (2014) Cables1 Complex Couples Survival Signaling to the Cell Death Machinery. *Cancer Research*, 75(1), pp. 147-158.

Shih, B., Tassabehji, M., Watson, J. and Bayat, A. (2012) DNA Copy Number Variations at Chromosome 7p14.1 and Chromosome 14q11.2 Are Associated

with DupuytrenÊ¼s Disease. *Plastic and Reconstructive Surgery*, 129(4), pp. 921-932.

Shogren-Knaak, M., Ishii, H., Sun, J., Pazin, M., Davie, J. and Peterson, C. (2006) Histone H4-K16 Acetylation Controls Chromatin Structure and Protein Interactions. *Science*, 311(5762), pp. 844-847.

Shore, E. and Kaplan, F. (2010) Inherited human diseases of heterotopic bone formation. *Nat Rev Rheumatol*, 6(9), pp. 518-527.

Shostak, K., Zhang, X., Hubert, P., Göktuna, S., Jiang, Z., Klevernic, I., Hildebrand, J., Roncarati, P., Hennuy, B., Ladang, A., Somja, J., Gothot, A., Close, P., Delvenne, P. and Chariot, A. (2014) NF-κB-induced KIAA1199 promotes survival through EGFR signalling. *Nature Communications*, 5, p. 5232.

Shull, A., Latham-Schwark, A., Ramasamy, P., Leskoske, K., Oroian, D., Birtwistle, M. and Buckhaults, P. (2012) Novel Somatic Mutations to PI3K Pathway Genes in Metastatic Melanoma.*PLoS ONE*, 7(8), p. e43369.

Siegel, R., Miller, K. and Jemal, A. (2015) Cancer statistics, 2015. *CA: A Cancer Journal for Clinicians*, 65(1), pp. 5-29.

Sievert, A. and Fisher, M. (2009) Pediatric Low-Grade Gliomas. *Journal of Child Neurology*, 24(11), pp. 1397-1408.

Simanovsky, N., Rozovsky, K., Hiller, N., Weintraub, M. and Stepensky, P. (2016) Extending the Spectrum of Radiological Findings in Patients With Severe Osteopetrosis and Different Genetic Backgrounds. *Pediatric Blood & Cancer*, p. n/a-n/a.

Smith, D., Zhu, Y., McAvoy, S. and Kuhn, R. (2006) Common fragile sites, extremely large genes, neural development and cancer. *Cancer Letters*, 232(1), pp. 48-57.

Song, G., Kim, H., Woo, K., Baek, J., Kim, G., Choi, J. and Ryoo, H. (2010) Molecular Consequences of the ACVR1R206H Mutation of Fibrodysplasia Ossificans Progressiva. *Journal of Biological Chemistry*, 285(29), pp. 22542-22553.

Song, Y., Aglipay, J., Bernstein, J., Goswami, S. and Stanley, P. (2010) The Bisecting GlcNAc on N-Glycans Inhibits Growth Factor Signaling and Retards Mammary Tumor Progression. *Cancer Research*, 70(8), pp. 3361-3371.

Sottoriva, A., Spiteri, I., Piccirillo, S., Touloumis, A., Collins, V., Marioni, J., Curtis, C., Watts, C. and Tavare, S. (2013) Intratumor heterogeneity in human glioblastoma reflects cancer evolutionary dynamics. *Proceedings of the National Academy of Sciences*, 110(10), pp. 4009-4014.

Spostol, R., Ertel, I., Jenkin, R., Boesel, C., Venes, J., Ortega, J., Evans, A., Waral, W. and Hammond, D. (1989) The effectiveness of chemotherapy for treatment of high grade astrocytoma in children: Results of a randomized trial. *J Neuro-Oncol*, 7(2), pp. 165-177.

Stojcheva, N., Schechtmann, G., Sass, S., Roth, P., Florea, M., Stefanski, A., Stuhler, K., Wolter, M., Muller, N., Theis, F., Weller, M., Reifenberger, G. and Happold, C. (2016) MicroRNA-138 promotes acquired alkylator resistance in glioblastoma by targeting the Bcl-2-interacting mediator BIM. *Oncotarget*.

Stratton, M.R., Campbell, P.J. and Futreal, P.A. (2009) The cancer genome.*Nature*, *458*(7239), pp.719-724.

Stupp, R., Mason, W. and van den Bent, M. (2005) "Radiotherapy plus Concomitant and Adjuvant Temozolomide for Glioblastoma". *Oncology Times*, 27(9), pp. 15-16.

Sturm, D., Witt, H., Hovestadt, V., Khuong-Quang, D., Jones, D., Konermann, C., Pfaff, E., Tönjes, M., Sill, M., Bender, S., Kool, M., Zapatka, M., Becker, N., Zucknick, M., Hielscher, T., Liu, X., Fontebasso, A., Ryzhova, M., Albrecht, S., Jacob, K., Wolter, M., Ebinger, M., Schuhmann, M., van Meter, T., Frühwald, M., Hauch, H., Pekrun, A., Radlwimmer, B., Niehues, T., von Komorowski, G., Dürken, M., Kulozik, A., Madden, J., Donson, A., Foreman, N., Drissi, R., Fouladi, M., Scheurlen, W., von Deimling, A., Monoranu, C., Roggendorf, W., Herold-Mende, C., Unterberg, A., Kramm, C., Felsberg, J., Hartmann, C., Wiestler, B., Wick, W., Milde, T., Witt, O., Lindroth, A., Schwartzentruber, J., Faury, D., Fleming, A., Zakrzewska, M., Liberski, P., Zakrzewski, K., Hauser, P., Garami, M., Klekner, A., Bognar, L., Morrissy, S., Cavalli, F., Taylor, M., van Sluis, P., Koster, J., Versteeg, R., Volckmann, R., Mikkelsen, T., Aldape, K., Reifenberger, G., Collins, V., Majewski, J., Korshunov, A., Lichter, P., Plass, C., Jabado, N. and Pfister, S. (2012) Hotspot Mutations in H3F3A and IDH1 Define Distinct Epigenetic and Biological Subgroups of Glioblastoma. *Cancer Cell*, 22(4), pp. 425-437.

Sumazin, P., Califano, A., sheng Chiu, H. and Yang, X. (2011) Abstract 4186: An extensive microRNA-mediated network of RNA-RNA interactions regulates established oncogenic pathways in glioblastoma. *Cancer Research*, 72(8 Supplement), pp. 4186-4186.

Sun, L., Bian, G., Meng, Z., Dang, G., Shi, D. and Mi, S. (2015) MiR-144 Inhibits Uveal Melanoma Cell Proliferation and Invasion by Regulating c-Met Expression. *PLOS ONE*, 10(5), p. e0124428.

Sun, L., Li, M., Huang, X., Xu, J., Gao, Z. and Liu, C. (2014) High-resolution genome-wide analysis identified recurrent genetic alterations in NK/T-cell lymphoma, nasal type, which are associated with disease progression. *Medical Oncology*, 31(7).

Sun, Y., Deng, K., Wang, F., Zhang, J., Huang, X., Qiao, S. and Zhao, S. (2004) Two novel isoforms of Adam23 expressed in the developmental process of mouse and human brains. *Gene*, 325, pp. 171-178.

Sung, T., Miller, D., Hayes, R., Alonso, M., Yee, H. and Newcomb, E. (2000) Preferential Inactivation of the p53 Tumor Suppressor Pathway and Lack of EGFR Amplification Distinguishde novoHigh Grade Pediatric Astrocytomas fromde novoAdult Astrocytomas. *Brain Pathology*, 10(2), pp. 249-259.

Swartling, F., Ferletta, M., Kastemar, M., Weiss, W. and Westermark, B. (2009) Cyclic GMP-dependent protein kinase II inhibits cell proliferation, Sox9 expression and Akt phosphorylation in human glioma cell lines. *Oncogene*, 28(35), pp. 3121-3131.

Syed, N., Langer, J., Janczar, K., Singh, P., Lo Nigro, C., Lattanzio, L., Coley, H., Hatzimichael, E., Bomalaski, J., Szlosarek, P., Awad, M., O'Neil, K., Roncaroli, F. and Crook, T. (2013) Epigenetic status of argininosuccinate synthetase and argininosuccinate lyase modulates autophagy and cell death in glioblastoma. *Cell Death Dis*, 4(1), p. e458.

Sykulski, M., Gambin, T., Bartnik, M., DerwiÅ„ska, K., WiÅ›niowiecka-Kowalnik, B., Stankiewicz, P. and Gambin, A. (2013) Multiple samples aCGH analysis for rare CNVs detection. *J Clin Bioinformatics*, 3(1), p. 12.

Synakiewicz, A., Stachowicz-Stencel, T. and Adamkiewicz-Drozynska, E. (2014) The role of arginine and the modified arginine deiminase enzyme ADI-PEG 20 in cancer therapy with special emphasis on Phase I/II clinical trials. *Expert Opinion on Investigational Drugs*, 23(11), pp. 1517-1529.

Szlosarek, P., Klabatsa, A., Pallaska, A., Sheaff, M., Smith, P., Crook, T., Grimshaw, M., Steele, J., Rudd, R., Balkwill, F. and Fennell, D. (2006) In vivo Loss of Expression of Argininosuccinate Synthetase in Malignant Pleural Mesothelioma Is a Biomarker for Susceptibility to Arginine Depletion. *Clinical Cancer Research*, 12(23), pp. 7126-7131.

Szlosarek, P., Luong, P., Phillips, M., Baccarini, M., Ellis, S., Szyszko, T., Sheaff, M. and Avril, N. (2013) Metabolic Response to Pegylated Arginine Deiminase in Mesothelioma With Promoter Methylation of Argininosuccinate Synthetase. *Journal of Clinical Oncology*, 31(7), pp. e111-e113.

Tahiliani, M., Koh, K., Shen, Y., Pastor, W., Bandukwala, H., Brudno, Y., Agarwal, S., Iyer, L., Liu, D., Aravind, L. and Rao, A. (2009) Conversion of 5-Methylcytosine to 5-Hydroxymethylcytosine in Mammalian DNA by MLL Partner TET1. *Science*, 324(5929), pp. 930-935.

Takai, D. and Jones, P. (2002) Comprehensive analysis of CpG islands in human chromosomes 21 and 22. *Proceedings of the National Academy of Sciences*, 99(6), pp. 3740-3745.

Talbert, P. and Henikoff, S. (2010) Histone variants — ancient wrap artists of the epigenome. *Nature Reviews Molecular Cell Biology*, 11(4), pp. 264-275.

Tan, M., Luo, H., Lee, S., Jin, F., Yang, J., Montellier, E., Buchou, T., Cheng, Z., Rousseaux, S., Rajagopal, N., Lu, Z., Ye, Z., Zhu, Q., Wysocka, J., Ye, Y., Khochbin, S., Ren, B. and Zhao, Y. (2011) Identification of 67 Histone Marks and Histone Lysine Crotonylation as a New Type of Histone Modification. *Cell*, 146(6), pp. 1016-1028.

Tang, J., Wu, S., Liu, H., Stratt, R., Barak, O., Shiekhattar, R., Picketts, D. and Yang, X. (2004) A Novel Transcription Regulatory Complex Containing Death Domain-associated Protein and the ATR-X Syndrome Protein. *Journal of Biological Chemistry*, 279(19), pp. 20369-20377.

Tay, Y., Tan, S., Karreth, F., Lieberman, J. and Pandolfi, P. (2014) Characterization of Dual PTEN and p53-Targeting MicroRNAs Identifies MicroRNA-638/Dnm2 as a Two-Hit Oncogenic Locus. *Cell Reports*, 8(3), pp. 714-722.

Taylor, K., Mackay, A., Truffaux, N., Butterfield, Y., Morozova, O., Philippe, C., Castel, D., Grasso, C., Vinci, M., Carvalho, D., Carcaboso, A., de Torres, C., Cruz, O., Mora, J., Entz-Werle, N., Ingram, W., Monje, M., Hargrave, D., Bullock, A., Puget, S., Yip, S., Jones, C. and Grill, J. (2014) Recurrent activating ACVR1 mutations in diffuse intrinsic pontine glioma. *Nature Genetics*, 46(5), pp. 457-461.

Teixeira, C., Masachs, N., Muhaisen, A., Bosch, C., Pérez-Martínez, J., Howell, B. and Soriano, E. (2014) Transient Downregulation of Dab1 Protein Levels during Development Leads to Behavioral and Structural Deficits: Relevance for Psychiatric Disorders. *Neuropsychopharmacology*, 39(3), pp. 556-568.

Teodorczyk, M. and Schmidt, M. (2015) Notching on Cancer's Door: Notch Signaling in Brain Tumors.*Front. Oncol.*, 4.

Thedieck, K., Polak, P., Kim, M., Molle, K., Cohen, A., Jenö, P., Arrieumerlou, C. and Hall, M. (2007) PRAS40 and PRR5-Like Protein Are New mTOR Interactors that Regulate Apoptosis. *PLoS ONE*, 2(11), p. e1217.

Thomas, S., Thurn, K., Raha, P., Chen, S. and Munster, P. (2013) Efficacy of Histone Deacetylase and Estrogen Receptor Inhibition in Breast Cancer Cells Due to Concerted down Regulation of Akt.*PLoS ONE*, 8(7), p. e68973.

Thorpe, L., Yuzugullu, H. and Zhao, J. (2014) PI3K in cancer: divergent roles of isoforms, modes of activation and therapeutic targeting. *Nature Reviews Cancer*,

15(1), pp. 7-24.
Timp, W. and Feinberg, A. (2013) Cancer as a dysregulated epigenome allowing cellular growth advantage at the expense of the host. *Nature Reviews Cancer*, 13(7), pp. 497-510.
Toledano-Katchalski, H., Kraut, J., Sines, T., Granot-Attas, S., Shohat, G., Gil-Henn, H., Yung, Y. and Elson, A. (2003) Protein tyrosine phosphatase Epsilon inhibits signaling by mitogen-activated protein kinases. *Mol. Cancer Res.*, 1, pp. 541-550.
Tsai, H. and Baylin, S. (2011) Cancer epigenetics: linking basic biology to clinical medicine. *Cell Res*, 21(3), pp. 502-517.
Tukey, R. and Strassburg, C. (2000) Human UDP-Glucuronosyltransferases: Metabolism, Expression, and Disease. *Annu. Rev. Pharmacol. Toxicol.*, 40(1), pp. 581-616.
Tumilson, C., Lea, R., Alder, J. and Shaw, L. (2014) Circulating MicroRNA Biomarkers for Glioma and Predicting Response to Therapy. *Molecular Neurobiology*, 50(2), pp. 545-558.
Turtoi, A., Blomme, A., Bellahcene, A., Gilles, C., Hennequiere, V., Peixoto, P., Bianchi, E., Noel, A., De Pauw, E., Lifrange, E., Delvenne, P. and Castronovo, V. (2013) Myoferlin Is a Key Regulator of EGFR Activity in Breast Cancer. *Cancer Research*, 73(17), pp. 5438-5448.
UEDA, M., HUNG, Y., TERM, Y., KANDA, K., TAKEHARA, M., YAMASHITA, H., YAMAGUCHI, H., AKISE, D., YASUDA, M., NISHIYAMA, K. and UEKI, M. (2003) Glutathione S-Transferase GSTM1, GSTT1 and p53 Codon 72 Polymorphisms in Human Tumor Cells. *Human Cell*, 16(4), pp. 241-251.
Unoki, M., Nishidate, T. and Nakamura, Y. (2004) ICBP90, an E2F-1 target, recruits HDAC1 and binds to methyl-CpG through its SRA domain. *Oncogene*, 23(46), pp. 7601-7610.
Valladares-Ayerbes, M. (2011) Prognostic impact of disseminated tumor cells and microRNA-17-92 cluster deregulation in gastrointestinal cancer. *Int J Oncol*.
van de Wiel, M., Brosens, R., Eilers, P., Kumps, C., Meijer, G., Menten, B., Sistermans, E., Speleman, F., Timmerman, M. and Ylstra, B. (2009) Smoothing waves in array CGH tumor profiles.*Bioinformatics*, 25(9), pp. 1099-1104.
Vanan, M. and Eisenstat, D. (2015) DIPG in Children – What Can We Learn from the Past?. *Front. Oncol.*, 5.
Vander Heiden, M., Cantley, L. and Thompson, C. (2009) Understanding the Warburg Effect: The Metabolic Requirements of Cell Proliferation. *Science*, 324(5930), pp. 1029-1033.
Vanhaesebroeck, B., Stephens, L. and Hawkins, P. (2012) PI3K signalling: the path to discovery and understanding. *Nature Reviews Molecular Cell Biology*, 13(3), pp. 195-203.
Varela, I., Tarpey, P., Raine, K., Huang, D., Ong, C., Stephens, P., Davies, H., Jones, D., Lin, M., Teague, J., Bignell, G., Butler, A., Cho, J., Dalgliesh, G., Galappaththige, D., Greenman, C., Hardy, C., Jia, M., Latimer, C., Lau, K., Marshall, J., McLaren, S., Menzies, A., Mudie, L., Stebbings, L., Largaespada, D., Wessels, L., Richard, S., Kahnoski, R., Anema, J., A.Tuveson, D., Perez-Mancera, P., Mustonen, V., Fischer, A., Adams, D., Rust, A., Chan-on, W., Subimerb, C., Dykema, K., Furge, K., Campbell, P., Teh, B., Stratton, M. and Futreal, P. (2011) Exome sequencing identifies frequent mutation of the SWI/SNF complex gene PBRM1 in renal carcinoma. *Nature*, 469(7331), pp. 539-542.

Varley, J.M. (2003) Germline TP53 mutations and Li-Fraumeni syndrome.*Human mutation*, *21*(3), pp.313-320.

Varley, K., Gertz, J., Bowling, K., Parker, S., Reddy, T., Pauli-Behn, F., Cross, M., Williams, B., Stamatoyannopoulos, J., Crawford, G., Absher, D., Wold, B. and Myers, R. (2013) Dynamic DNA methylation across diverse human cell lines and tissues. *Genome Research*, 23(3), pp. 555-567.

Verhaak, R., Hoadley, K., Purdom, E., Wang, V., Qi, Y., Wilkerson, M., Miller, C., Ding, L., Golub, T., Mesirov, J., Alexe, G., Lawrence, M., O'Kelly, M., Tamayo, P., Weir, B., Gabriel, S., Winckler, W., Gupta, S., Jakkula, L., Feiler, H., Hodgson, J., James, C., Sarkaria, J., Brennan, C., Kahn, A., Spellman, P., Wilson, R., Speed, T., Gray, J., Meyerson, M., Getz, G., Perou, C. and Hayes, D. (2010) Integrated Genomic Analysis Identifies Clinically Relevant Subtypes of Glioblastoma Characterized by Abnormalities in PDGFRA, IDH1, EGFR, and NF1. *Cancer Cell*, 17(1), pp. 98-110.

Veringa, S., Biesmans, D., van Vuurden, D., Jansen, M., Wedekind, L., Horsman, I., Wesseling, P., Vandertop, W., Noske, D., Kaspers, G. and Hulleman, E. (2013) In Vitro Drug Response and Efflux Transporters Associated with Drug Resistance in Pediatric High Grade Glioma and Diffuse Intrinsic Pontine Glioma. *PLoS ONE*, 8(4), p. e61512.

Versteege, I., Sévenet, N., Lange, J., Rousseau-Merck, M., Ambros, P., Handgretinger, R., Aurias, A. and Delattre, O. (1998) Truncating mutations of hSNF5/INI1 in aggressive paediatric cancer.*Nature*, 394(6689), pp. 203-206.

Vidigal, J. and Ventura, A. (2015) The biological functions of miRNAs: lessons from in vivo studies.*Trends in Cell Biology*, 25(3), pp. 137-147.

Vincenzi, B., Iuliani, M., Zoccoli, A., Pantano, F., Fioramonti, M., Lisi, D., Frezza, A., Rabitti, C., Perrone, G., Onetti Muda, A., Russo, A., Giordano, A., Santini, D., Dei Tos, A. and Tonini, G. (2015) Deregulation of dicer and mir-155 expression in liposarcoma. *Oncotarget*, 6(12), pp. 10586-10591.

Vranova, V., NeCesalova, E., Kuglík, P., Cejpek, P., PeSakova, M., Budínska, E., Relichova, J. and Veselska, R. (2007) Screening of genomic imbalances in glioblastoma multiforme using high-resolution comparative genomic hybridization. *Oncology Reports*.

Vrba, L., Jensen, T., Garbe, J., Heimark, R., Cress, A., Dickinson, S., Stampfer, M. and Futscher, B. (2010) Role for DNA Methylation in the Regulation of miR-200c and miR-141 Expression in Normal and Cancer Cells. *PLoS ONE*, 5(1), p. e8697.

WABAKKEN, T., HAUGE, H., FINNE, E., WIEDLOCHA, A. and AASHEIM, H. (2002) Expression of Human Protein Tyrosine Phosphatase Epsilon in Leucocytes: a Potential ERK Pathway-Regulating Phosphatase. *Scandinavian Journal of Immunology*, 56(2), pp. 195-203.

Wagle, N., Grabiner, B., Van Allen, E., Hodis, E., Jacobus, S., Supko, J., Stewart, M., Choueiri, T., Gandhi, L., Cleary, J., Elfiky, A., Taplin, M., Stack, E., Signoretti, S., Loda, M., Shapiro, G., Sabatini, D., Lander, E., Gabriel, S., Kantoff, P., Garraway, L. and Rosenberg, J. (2014) Activating mTOR Mutations in a Patient with an Extraordinary Response on a Phase I Trial of Everolimus and Pazopanib. *Cancer Discovery*, 4(5), pp. 546-553.

Wang, G., Allis, C. and Chi, P. (2007) Chromatin remodeling and cancer, part II: ATP-dependent chromatin remodeling. *Trends in Molecular Medicine*, 13(9), pp. 373-380.

Wang, W., Zhao, L., Tan, Y., Ren, H. and Qi, Z. (2012) MiR-138 induces cell cycle arrest by targeting cyclin D3 in hepatocellular carcinoma. *Carcinogenesis*, 33(5), pp. 1113-1120.

Wang, Y., Sun, Y. and Qiao, S. (2012) ADAM23 knockdown promotes neuronal differentiation of P19 embryonal carcinoma cells by up-regulating P27KIP1 expression. *Cell. Biol. Int.*, 36(12), pp. 1275-1279.

Ward, B. and Gutmann, D. (2005) Neurofibromatosis 1: From lab bench to clinic. *Pediatric Neurology*, 32(4), pp. 221-228.

Warren, K. (2012) Diffuse intrinsic pontine glioma: poised for progress. *Front. Oncol.*, 2.

Warren, K. (2012) Diffuse intrinsic pontine glioma: poised for progress. *Front. Oncol.*, 2.

Waters, C., Saldivar, J., Amin, Z., Schrock, M. and Huebner, K. (2015) FHIT loss-induced DNA damage creates optimal APOBEC substrates: Insights into APOBEC-mediated mutagenesis.*Oncotarget*, 6(5), pp. 3409-3419.

Weller, M., Stupp, R., Reifenberger, G., Brandes, A., van den Bent, M., Wick, W. and Hegi, M. (2009) MGMT promoter methylation in malignant gliomas: ready for personalized medicine?. *Nature Reviews Neurology*, 6(1), pp. 39-51.

Wheatley, D.N. (1998) Dietary restriction, amino acid deprivation, and cancer.*Cancer J, 11*, pp.183-189.

Winter, J., Jung, S., Keller, S., Gregory, R. and Diederichs, S. (2009) Many roads to maturity: microRNA biogenesis pathways and their regulation. *Nature Cell Biology*, 11(3), pp. 228-234.

Wolff, J., Driever, P., Erdlenbruch, B., Kortmann, R., Rutkowski, S., Pietsch, T., Parker, C., Metz, M., Gnekow, A. and Kramm, C. (2010) Intensive chemotherapy improves survival in pediatric high-grade glioma after gross total resection: results of the HIT-GBM-C protocol. *Cancer*, 116(3), pp. 705-712.

Wolff, J.C.P. and Chastagner, P.A.S.C.A.L. (2004) Astrocytic Tumors, High Grade. *Brain and spinal tumors of childhood cancer. London: Arnold Health Sciences, Inc*, pp.277-290.

Wolfgang, C., Essand, M., Vincent, J., Lee, B. and Pastan, I. (2000) TARP: A nuclear protein expressed in prostate and breast cancer cells derived from an alternate reading frame of the T cell receptor gamma chain locus. *Proceedings of the National Academy of Sciences*, 97(17), pp. 9437-9442.

Wolfsberg, T. (1995) ADAM, a novel family of membrane proteins containing A Disintegrin And Metalloprotease domain: multipotential functions in cell-cell and cell- matrix interactions. *The Journal of Cell Biology*, 131(2), pp. 275-278.

Wong, A., Ruppert, J., Bigner, S., Grzeschik, C., Humphrey, P., Bigner, D. and Vogelstein, B. (1992) Structural alterations of the epidermal growth factor receptor gene in human gliomas. *Proceedings of the National Academy of Sciences*, 89(7), pp. 2965-2969.

Wong, K., Tsang, Y., Chang, Y., Su, J., Di Francesco, A., Meco, D., Riccardi, R., Perlaky, L., Dauser, R., Adesina, A., Bhattacharjee, M., Chintagumpala, M. and Lau, C. (2006) Genome-Wide Allelic Imbalance Analysis of Pediatric Gliomas by Single Nucleotide Polymorphic Allele Array. *Cancer Research*, 66(23), pp. 11172-11178.

Wu, A., Huang, Y., Zhang, L., Tian, G., Liao, Q. and Chen, S. (2016) MiR-572 prompted cell proliferation of human ovarian cancer cells by suppressing PPP2R2C expression. *Biomedicine & Pharmacotherapy*, 77, pp. 92-97.

Wu, G., Broniscer, A., McEachron, T., Lu, C., Paugh, B., Becksfort, J., Qu, C., Ding, L., Huether, R., Parker, M., Zhang, J., Gajjar, A., Dyer, M., Mullighan, C., Gilbertson, R., Mardis, E., Wilson, R., Downing, J., Ellison, D., Zhang, J. and Baker, S. (2012) Somatic histone H3 alterations in pediatric diffuse intrinsic pontine gliomas and non-brainstem glioblastomas. *Nature Genetics*, 44(3), pp. 251-253.

Wu, G., Diaz, A., Paugh, B., Rankin, S., Ju, B., Li, Y., Zhu, X., Qu, C., Chen, X., Zhang, J., Easton, J., Edmonson, M., Ma, X., Lu, C., Nagahawatte, P., Hedlund, E., Rusch, M., Pounds, S., Lin, T., Onar-Thomas, A., Huether, R., Kriwacki, R., Parker, M., Gupta, P., Becksfort, J., Wei, L., Mulder, H., Boggs, K., Vadodaria, B., Yergeau, D., Russell, J., Ochoa, K., Fulton, R., Fulton, L., Jones, C., Boop, F., Broniscer, A., Wetmore, C., Gajjar, A., Ding, L., Mardis, E., Wilson, R., Taylor, M., Downing, J., Ellison, D., Zhang, J. and Baker, S. (2014) The genomic landscape of diffuse intrinsic pontine glioma and pediatric non-brainstem high-grade glioma. *Nature Genetics*, 46(5), pp. 444-450.

Wu, G., Diaz, A., Paugh, B., Rankin, S., Ju, B., Li, Y., Zhu, X., Qu, C., Chen, X., Zhang, J., Easton, J., Edmonson, M., Ma, X., Lu, C., Nagahawatte, P., Hedlund, E., Rusch, M., Pounds, S., Lin, T., Onar-Thomas, A., Huether, R., Kriwacki, R., Parker, M., Gupta, P., Becksfort, J., Wei, L., Mulder, H., Boggs, K., Vadodaria, B., Yergeau, D., Russell, J., Ochoa, K., Fulton, R., Fulton, L., Jones, C., Boop, F., Broniscer, A., Wetmore, C., Gajjar, A., Ding, L., Mardis, E., Wilson, R., Taylor, M., Downing, J., Ellison, D., Zhang, J. and Baker, S. (2014) The genomic landscape of diffuse intrinsic pontine glioma and pediatric non-brainstem high-grade glioma. *Nature Genetics*, 46(5), pp. 444-450.

Xia, H., He, T., Liu, C., Cui, Y., Song, P., Jin, X. and Ma, X. (2009) MiR-125b Expression Affects the Proliferation and Apoptosis of Human Glioma Cells by Targeting Bmf. *Cellular Physiology and Biochemistry*, 23(4-6), pp. 347-358.

Xiao-Jie, L., Ai-Mei, G., Li-Juan, J. and Jiang, X. (2014) Pseudogene in cancer: real functions and promising signature. *Journal of Medical Genetics*, 52(1), pp. 17-24.

Xie, K. (2003) Contribution of nitric oxide-mediated apoptosis to cancer metastasis inefficiency. *Free Radical Biology and Medicine*, 34(8), pp. 969-986.

Xu, C., Liu, S., Fu, H., Li, S., Tie, Y., Zhu, J., Xing, R., Jin, Y., Sun, Z. and Zheng, X. (2010) MicroRNA-193b regulates proliferation, migration and invasion in human hepatocellular carcinoma cells. *European Journal of Cancer*, 46(15), pp. 2828-2836.

Xu, Y., He, J., Wang, Y., Zhu, X., Pan, Q., Xie, Q. and Sun, F. (2015) miR-889 promotes proliferation of esophageal squamous cell carcinomas through DAB2IP. *FEBS Letters*, 589(10), pp. 1127-1135.

Yamashita, N., Tokunaga, E., Kitao, H., Hitchins, M., Inoue, Y., Tanaka, K., Hisamatsu, Y., Taketani, K., Akiyoshi, S., Okada, S., Oda, Y., Saeki, H., Oki, E. and Maehara, Y. (2015) Epigenetic Inactivation of BRCA1 Through Promoter Hypermethylation and Its Clinical Importance in Triple-Negative Breast Cancer. *Clinical Breast Cancer*, 1

Yan, Y., Tsukamoto, O., Nakano, A., Kato, H., Kioka, H., Ito, N., Higo, S., Yamazaki, S., Shintani, Y., Matsuoka, K., Liao, Y., Asanuma, H., Asakura, M., Takafuji, K., Minamino, T., Asano, Y., Kitakaze, M. and Takashima, S. (2015) Augmented AMPK activity inhibits cell migration by phosphorylating the novel substrate Pdlim5. *Nature Communications*, 6, p. 6137.

Yanaihara, N., Caplen, N., Bowman, E., Seike, M., Kumamoto, K., Yi, M., Stephens, R., Okamoto, A., Yokota, J., Tanaka, T., Calin, G., Liu, C., Croce, C. and Harris, C. (2006) Unique microRNA molecular profiles in lung cancer diagnosis and prognosis. *Cancer Cell*, 9(3), pp. 189-198.

Yao, K., Yin, Y.L., Chu, W., Liu, Z., Deng, D., Li, T., Huang, R., Zhang, J., Tan, B., Wang, W. and Wu, G., (2008) Dietary arginine supplementation increases mTOR signaling activity in skeletal muscle of neonatal pigs. *The Journal of nutrition*, *138*(5), pp.867-872.

Yost, S., Pastorino, S., Rozenzhak, S., Smith, E., Chao, Y., Jiang, P., Kesari, S., Frazer, K. and Harismendy, O. (2013) High-Resolution Mutational Profiling Suggests the Genetic Validity of Glioblastoma Patient-Derived Pre-Clinical Models. *PLoS ONE*, 8(2), p. e56185.

You, J. and Jones, P. (2012) Cancer Genetics and Epigenetics: Two Sides of the Same Coin?. *Cancer Cell*, 22(1), pp. 9-20.

Young, B., Zhang, G., Koch, M. and Birk, D. (2002) The roles of types XII and XIV collagen in fibrillogenesis and matrix assembly in the developing cornea. *Journal of Cellular Biochemistry*, 87(2), pp. 208-220.

Yu, G., Yao, W., Gumireddy, K., Li, A., Wang, J., Xiao, W., Chen, K., Xiao, H., Li, H., Tang, K., Ye, Z., Huang, Q. and Xu, H. (2014) Pseudogene PTENP1 Functions as a Competing Endogenous RNA to Suppress Clear-Cell Renal Cell Carcinoma Progression. *Molecular Cancer Therapeutics*, 13(12), pp. 3086-3097.

Yuan, R., Primakoff, P. and Myles, D. (1997) A Role for the Disintegrin Domain of Cyritestin, a Sperm Surface Protein Belonging to the ADAM Family, in Mouse Sperm–Egg Plasma Membrane Adhesion and Fusion. *J Cell Biol*, 137(1), pp. 105-112.

Zarghooni, M., Bartels, U., Lee, E., Buczkowicz, P., Morrison, A., Huang, A., Bouffet, E. and Hawkins, C. (2010) Whole-Genome Profiling of Pediatric Diffuse Intrinsic Pontine Gliomas Highlights Platelet-Derived Growth Factor Receptor and Poly (ADP-ribose) Polymerase As Potential Therapeutic Targets. *Journal of Clinical Oncology*, 28(8), pp. 1337-1344.

Zhang, B., Pan, X., Cobb, G. and Anderson, T. (2007) microRNAs as oncogenes and tumor suppressors. *Developmental Biology*, 302(1), pp. 1-12.

Zhang, L., Ho-Fun Lee, V., Wong, A., Kwong, D., Zhu, Y., Dong, S., Kong, K., Chen, J., Tsao, S., Guan, X. and Fu, L. (2012) MicroRNA-144 promotes cell proliferation, migration and invasion in nasopharyngeal carcinoma through repression of PTEN. *Carcinogenesis*, 34(2), pp. 454-463.

Zhang, S., Shan, C., Kong, G., Du, Y., Ye, L. and Zhang, X. (2011) MicroRNA-520e suppresses growth of hepatoma cells by targeting the NF-κB-inducing kinase (NIK). *Oncogene*, 31(31), pp. 3607-3620.

Zhang, X., Liu, J., Zang, D., Wu, S., Liu, A., Zhu, J., Wu, G., Li, J. and Jiang, L. (2015) Upregulation of miR-572 transcriptionally suppresses SOCS1 and p21 and contributes to human ovarian cancer progression. *Oncotarget*, 6(17), pp. 15180-15193.

Zhang, Y. and Yang, J. (2013) Altered energy metabolism in cancer. *Cancer Biology & Therapy*, 14(2), pp. 81-89.

Zhang, Y.O.U.N.G.H.U.I., Shields, T., Crenshaw, T., Hao, Y., Moulton, T. and Tycko, B. (1993) Imprinting of human H19: allele-specific CpG methylation, loss of the active allele in Wilms tumor, and potential for somatic allele switching. *American journal of human genetics*, *53*(1), p.113.

Zhao, S., Liu, H., Liu, Y., Wu, J., Wang, C., Hou, X., Chen, X., Yang, G., Zhao, L., Che, H., Bi, Y., Wang, H., Peng, F. and Ai, J. (2013) miR-143 inhibits glycolysis and depletes stemness of glioblastoma stem-like cells. *Cancer Letters*, 333(2), pp. 253-260.

Zhao, Y., Takahashi, M., Gu, J., Miyoshi, E., Matsumoto, A., Kitazume, S. and Taniguchi, N. (2008) Functional roles of N-glycans in cell signaling and cell adhesion in cancer. *Cancer Science*, 99(7), pp. 1304-1310.

Zou, H., Osborn, N., Harrington, J., Klatt, K., Molina, J., Burgart, L. and Ahlquist, D. (2005) Frequent Methylation of Eyes Absent 4 Gene in Barrett's Esophagus and Esophageal Adenocarcinoma.*Cancer Epidemiology Biomarkers & Prevention*, 14(4), pp. 830-834.